COMPUTER SIMULATION OF SEDIMENTATION IN MEANDERING STREAMS

John S. Bridge

A Thesis Submitted for the Degree of PhD
at the
University of St Andrews

1973

COMPUTER SIMULATION OF SEDIMENTATION IN MEANDERING STREAMS

by

JOHN S. BRIDGE

Ph.D. thesis

St. Andrews, June 1973.

C E R T I F I C A T E

I hereby certify that JOHN S. BRIDGE has been engaged in research for 9 terms at the University of St. Andrews, that he has fulfilled the conditions of Ordinance No. 12 and Resolution of the University Court, 1967, No. 1, and that he is qualified to submit the accompanying thesis in application for the degree of Doctor of Philosophy.

I certify that the following thesis is of my own composition, that it is based on the results of research carried out by me, and that it has not previously been presented in application for a higher degree.

A B S T R A C T

A dynamic mathematical model has been constructed for the computer simulation of sedimentation in free meandering streams. The system is defined in terms of form and process, and component mathematical models (with mainly deterministic, but also probabilistic, characteristics) are formulated for the prediction of the following aspects of the system for a given physical situation and a single time increment: (1) The characteristics of the plan form of free meanders; (2) The movement of meanders in plan, and definition of cross sections across the meander in which erosion and deposition are considered in detail; (3) The hydraulic properties of the channel and the erosional and depositional activity within the channel as defined in specific cross sections; (4) Whether neck or chute cut off will occur; (5) A relative measure of the discharge during seasonal high water periods, which is used in (3) and (4); (5) Aggradation. The limitations, qualifications and validity of the component mathematical models are discussed during their development, as is the input required.

The overall model has been translated into a FORTRAN IV computer program and a set of experiments with selected input parameters has been performed. The results and their implications are fully documented and compared qualitatively with recent and ancient fluviatile sedimentation.

The shape of simulated pointbar sediments, as controlled by channel migration over floodplains of variable sediment type, agrees broadly with the natural situation. Sheet deposits cannot be simulated because large-scale meander-belt movements are not accounted for; this also inhibits generation of thick sequences of alluvial sediments. When channel migration is combined with a constant aggradation rate the model predicts a general slope (relative to the land surface) of facies boundaries and scoured

basal surfaces upward in the direction of channel movement. If aggradation sufficiently increases the thickness of fine grained overbank material, there is a channel stabilisation effect.

Epsilon cross-stratification, which represents the shape o a pointbar surface before falling-stage deposition (lateral and vertical), may be picked out in the simulated sediments. The epsilon unit thickness is that measured from bankfull stage down to the lowest channel position existing prior to deposition.

The model records the characteristic fining upwards of grain sizes in the pointbar, and the systematic distribution of sedimentary structures. Channel migration combined with seasonal scouring and filling across the channel produces a characteristic relief in the basal scoured surfaces and the grain size and sedimentary structure boundaries. A related lensing and inter-fingering of grain size and sedimentary structure facies may also b present. The model also records large-scale lateral changes in grain size and sedimentary structure associated with changes in the shape of developing meanders.

It is shown that a complete sequence of pointbar sediments capped by overbank sediments would rarely be preserved in the moving-phase situation. Such preservation only becomes likely when an aggrading section lies out of range of an eroding channel for a considerably longer time span than it takes a meander to move one half-wavelength downvalley. Deep channel-scours have a higher preservation potential than contemporary shallower ones.

Where appropriate field data exist the model can be used i the more accurate recognition of ancient fluviatile sediments. Inferences may be made about the erosion-deposition processes operating in the ancient channel system, and the geometry and hydraulics of the system can be alluded to. A representative application of the model to the quantitative interpretation of an ancient pointbar deposit is illustrated. There is reasonable agreement between the natural and the simulated deposits, and a broad quantitative picture of the palaeoenvironment of sedimentation is obtained.

A B S T R A C T

A dynamic mathematical model has been constructed for the computer simulation of sedimentation in free meandering streams. The system is defined in terms of form and process, and component mathematical models (with mainly deterministic, but also probabilistic, characteristics) are formulated for the prediction of the following aspects of the system for a given physical situation and a single time increment: (1) The characteristics of the plan form of free meanders; (2) The movement of meanders in plan, and definition of cross sections across the meander in which erosion and deposition are considered in detail; (3) The hydraulic properties of the channel and the erosional and depositional activity within the channel as defined in specific cross sections; (4) Whether neck or chute cut off will occur; (5) A relative measure of the discharge during seasonal high water periods, which is used in (3) and (4); (5) Aggradation. The limitations, qualifications and validity of the component mathematical models are discussed during their development, as is the input required.

The overall model has been translated into a FORTRAN IV computer program and a set of experiments with selected input parameters has been performed. The results and their implications are fully documented and compared qualitatively with recent and ancient fluviatile sedimentation.

The shape of simulated pointbar sediments, as controlled by channel migration over floodplains of variable sediment type, agrees broadly with the natural situation. Sheet deposits cannot be simulated because large-scale meander-belt movements are not accounted for; this also inhibits generation of thick sequences of alluvial sediments. When channel migration is combined with a constant aggradation rate the model predicts a general slope (relative to the land surface) of facies boundaries and scoured

basal surfaces upward in the direction of channel movement. If aggradation sufficiently increases the thickness of fine grained overbank material, there is a channel stabilisation effect.

Epsilon cross-stratification, which represents the shape of a pointbar surface before falling-stage deposition (lateral and vertical), may be picked out in the simulated sediments. The epsilon unit thickness is that measured from bankfull stage down to the lowest channel position existing prior to deposition.

The model records the characteristic fining upwards of grain sizes in the pointbar, and the systematic distribution of sedimentary structures. Channel migration combined with seasonal scouring and filling across the channel produces a characteristic relief in the basal scoured surfaces and the grain size and sedimentary structure boundaries. A related lensing and inter-fingering of grain size and sedimentary structure facies may also be present. The model also records large-scale lateral changes in grain size and sedimentary structure associated with changes in the shape of developing meanders.

It is shown that a complete sequence of pointbar sediments capped by overbank sediments would rarely be preserved in the moving-phase situation. Such preservation only becomes likely when an aggrading section lies out of range of an eroding channel for a considerably longer time span than it takes a meander to move one half-wavelength downvalley. Deep channel-scours have a higher preservation potential than contemporary shallower ones.

Where appropriate field data exist the model can be used in the more accurate recognition of ancient fluviatile sediments. Inferences may be made about the erosion-deposition processes operating in the ancient channel system, and the geometry and hydraulics of the system can be alluded to. A representative application of the model to the quantitative interpretation of an ancient pointbar deposit is illustrated. There is reasonable agreement between the natural and the simulated deposits, and a broad quantitative picture of the palaeoenvironment of sedimentation is obtained.

C O N T E N T S

	Page
CERTIFICATE	i
ABSTRACT	ii
PART 1 INTRODUCTION	1
PART 2 DEVELOPMENT OF MATHEMATICAL MODEL	
1. INTRODUCTION: ENERGY DISTRIBUTION IN RIVER SYSTEMS	7
2. PLANIMETRIC GEOMETRY OF MEANDERS	10
2.1. Theory of minimum variance	10
2.2. Geometric characteristics of 'sine-generated' curve	13
2.3. Validity of 'sine-generated' curve	17
2.4. Initial input required by planimetric geometry model	17
2.4.1. Floodplain sediments	17
2.4.2. Wavelength	18
2.4.3. Amplitude	20
2.4.4. Sinuosity	22
3. MEANDERS IN A DYNAMIC FRAMEWORK	25
4. CROSS SECTION DEFINITION	27
5. MODEL FOR DEPOSITION ON THE POINT BAR	33
Introduction	33
5.1. Qualitative features of a system involving lateral deposition	33
5.2. Shape of cross profile	35
5.3. Hydraulic properties of the system	36
5.4. Variation of grain size over the cross profile	43
5.5. Variation of bed form and internal structure over the cross profile	46
5.5.1. Allen's model	47
5.5.2. Alternative models	51
5.5.3. Alternative model no. 1	52
5.5.4. Alternative model no. 2	53

5.5.5. Alternative model no. 3 56

5.5.6. Other alternative models 66

5.6. Discussion of input parameters required in point bar model 68

5.6.1. Channel width and depth 68

5.6.2. Mean radius of curvature, longitudinal water surface slope, and valley slope 70

5.6.3. Resistance coefficients 71

5.6.4. Fluid viscosity, fluid and sediment density 74

5.6.5. Kennedy j factor 75

5.7. Experiments to show variation of grain size and sedimentary structure with different input parameters and alternative bed-form models proposed 76

5.8. Validity and limitations of point bar sedimentation model 79

6. MODEL FOR BANK EROSION 83

6.1. Factors affecting nature and rate of bank erosion 83

6.2. Mathematical model 86

6.3. Validity of models proposed 88

6.4. Input 89

7. BANK RECESSION AND BAR GROWTH 91

8. EROSION AND DEPOSITION DURING HIGH WATER PERIODS 94

9. SCOUR AND FILL 97

9.1. Preliminary discussion 97

9.2. Mathematical model for scour depth ... 100

9.3. Deposition on falling stages 102

9.4. Input 103

10. CUT OFF 104

10.1. Model for chute cut-off 104

10.2. Model for neck cut-off 105

10.3. Input 106

11. FLOOD PERIOD VOLUME 108

Introduction 108

11.1. Sequential generation of stream-flow data 108

11.2. Mathematical model of hydrologic time series 109

11.3. Input and experimentation with the model 113

12. CONSTRUCTION OF FLOODPLAINS 115

12.1. Overbank deposition 115

12.2. Aggradation 118

PART 3 THE COMPUTER PROGRAM

13. GENERAL REMARKS 125

14. DESCRIPTION OF MAIN PROGRAMS AND SUB-ROUTINES 128

14.1. Main program (no disc) 128

14.2. Main program (using disc storage) . 136

14.3. Subroutine BAR (with entry point BAR1) 138

14.4. Subroutine MEANDR (with entry point MEAND1) 139

14.5. Subroutine SIMINT (and FUNC2) 141

14.6. Subroutine RANSAM 141

14.7. Subroutine NEWRAP 142

14.8. Subroutines RNDMIN and RNDM 143

14.9. Subroutines PLOT and CHAR 143

15. INPUT REQUIREMENTS AND PROGRAM MODIFICATION INSTRUCTIONS 144

16. SAMPLE RUN 154

PART 4 EXPERIMENTATION AND RESULTS

INTRODUCTION 159

17. EXPERIMENT 1 - MEANDERS IN DYNAMIC EQUILIBRIUM 160

18. EXPERIMENT 2 - MEANDERS IN DYNAMIC EQUILIBRIUM 166

19. EXPERIMENT 4 - DEVELOPING MEANDERS 171

20. EXPERIMENT 5 - DEVELOPING MEANDERS 175

PART 5 DISCUSSION AND CONCLUSION

21. GENERAL REMARKS 177

22. COMPARISON WITH MODERN FREE MEANDERING STREAM DEPOSITS 179

22.1. Shape of pointbar deposits 179

22.2. Epsilon cross-stratification 181

22.3. Distribution of grain size and sedimentary structure 182

22.4. Times taken to cut off 186

23. COMPARISON WITH ANCIENT FLUVIATILE COARSE MEMBERS 187

24. PRESERVATION OF POINT BAR SEDIMENTS 191

25. APPLICATION OF MODEL TO QUANTITATIVE INTERPRETATION OF ANCIENT FLUVIATILE COARSE MEMBERS 192

26. CONCLUDING REMARKS 196

ACKNOWLEDGEMENTS 198

LIST OF SYMBOLS USED IN MATHEMATICAL MODEL 199

REFERENCES CITED 206

APPENDIX 1 - MATHEMATICAL METHODS A1

A1.1. Newton-Raphson iterative formula A1

A1.2. Simpson's rule A1

A1.3. Generation of random samples from specified theoretical distributions A2

APPENDIX 2 - STATISTICAL CURVE AND SURFACE FITTING.. A5

A2.1. Polynomial regression A5

A2.2. Polynomial surface fitting A5

APPENDIX 3 - DATA DECK SET UP FOR EXPERIMENTS A6

PART ONE

I N T R O D U C T I O N

INTRODUCTION

It is well known that meandering streams flowing between erodible banks sweep across their floodplains as their loops migrate downvalley and across the mean downvalley direction. Such migration involves erosion of the outer, steeply sloping bank of the inflected channel and concomitant accumulation of layers of sediment on the inner gently sloping bank. Such deposition lateral to the local current direction is sensibly termed lateral deposition. Lateral deposition is also important in tidal flats and estuaries, and is found to occur in comparatively straight channels with sinuous talwegs as well as those sinuous enough to be arbitrarily termed meandering. In all these cases the channel, or talweg, swings from one side to the other of the mean direction of fluid motion primarily because, at the high Reynolds numbers involved, the flow is unstable to centrifugal accelerations and is unable to assume a rectilinear path (Allen, 1970a).

It is known that lateral sedimentation leads, in both fluvial and tidal situations, to a sequence of deposits marked by systematic vertical changes of grain size and sedimentary structure. This knowledge has been obtained from studies of ancient strata as well as modern sediments. As regards fluviatile deposits, vertical patterning of grain size and sedimentary structure has an important place in the familiar concept of the fining upwards sedimentary cycle, where the lower, coarse member of the cycle is known or thought to have accumulated through processes of lateral deposition. The finer members of such cycles are thought to have accumulated dominantly by processes of overbank deposition.

As well as channel movements by erosion and lateral deposition in sinuous conduits, large-scale movements of a substantially discontinuous nature may occur in the form of cut-off (the abandonment of all or part of a meander loop) or avulsion (the abandonment and relocation of a section of the meander belt). When all these channel movements are combined with a gradual continuing net deposition within the floodplain, a complicated spatial distribution of lateral deposits, with a certain amount of overbank and channel fill deposits, will result within the preserved thickness of alluvium.

Although fining-upwards cyclothems have been widely recognised, our knowledge of them is still rather broad and unsupported by the detailed and comparative studies necessary for their full and correct interpretation. Several models of fluviatile sedimentation have been published and have formed a useful starting point in the recognition and interpretation of fining-upwards cycles (Allen, 1963c, 1964, 1965a, 1970a,b, 1971; Beerbower, 1964; Moody-Stuart, 1966; Potter, 1967; Potter and Blakely, 1967; Visher, 1965a,b). Most of these models are graphic and qualitative, and more than one of them embodies concepts that are physically suspect or oversimplified. Furthermore, they tend to be heavily biased towards study of single lateral deposits instead of including channel and overbank deposits within a three dimensional body of alluvium. Allen's (1970a,b, 1971) model of lateral deposition is the first quantitative approach to the interpretation of fining-upwards coarse members and, although static in nature, employs principles that may be extended for use in simple dynamic mathematical models.

The purpose of this study is to develop a dynamic mathematical model for computer simulation of the nature of erosion and deposition in free meandering streams. It is anticipated that such a study will enable more accurate recognition and quantitative interpretation of fining-upwards cycles than has hitherto been possible, as well as giving further insight into the processes involved in the natural system. The only previous attempt to simulate fluviatile sediments was by Potter and Blakely (1967). This study made extensive use of Markov processes to generate stratigraphic successions, and the starting point was essentially the transition matrix. Unfortunately it is of little use in the physical interpretation of ancient sediments, as it doesn't examine the processes at work.

The free meandering system under consideration is an open (in that it is being continually affected by external factors) system that is tending towards a steady state, or dynamic equilibrium (Leopold et al, 1964). The system must be arbitrarily defined by specifying its boundaries, its components and the structure of the inter-relationships among the components. A hierarchy of systems can be seen to exist here, with lesser systems nested within the overall framework of the free meandering river system, which is itself nested in the overall river system, and so on. Because the natural system consists of an assemblage of parts that are inter-related in a complex manner, it must be simplified conceptually before it can be represented by a model. Dynamic simulation is the operation of the model system in such a way that the behaviour of the real system is reproduced to some degree as the model moves through time.

The most powerful and flexible way of representing a system is with mathematical models, however one danger in their use is that a formal appearance may lend an unwarranted credibility. Basically development of the simulation model has necessitated the construction of component mathematical models, with mainly deterministic, but also probabilistic, characteristics, for the sequential prediction of various aspects of the system for a given physical situation and a single time increment. These are:-

1) The characteristics of the plan form of the meander within which erosion and lateral sedimentation are taking place.
2) The definition of sections across the meander in which erosion and deposition will be considered in detail, given modes and rates of meander movement in plan.
3) The hydraulic properties of the channel and the erosional and depositional activity within the channel in the bend, as defined in specific cross sections.
4) Whether neck or chute cut-off will occur.
5) A relative measure of the discharge during the seasonal high water periods, which is used in 3) and 4).
6) Long term depositional trends due to time persistent changes in the independent system variables, i.e. aggradation.

The system has been defined in detail in terms of form and process as the individual component mathematical models were developed, and their limitations, qualifications and validity are discussed, as is the input required. It will be seen that the simulation model emphasises lateral sedimentation. This is partly because of the lack of data sufficient to make up models for the complicated overbank erosional and depositional processes, and partly because of the greater importance of channel sedimentation compared with other modes of sedimentation and erosion within the system. Unfortunately most of the deterministic relations are empirical, and these are generally less versatile than theoretical ones. As the mechanisms of the processes must be well defined before they can be reduced to sets of algebraic equations and logic statements, the development of mathematical models leads to deep insight into the system, and it is interesting to look at the modes of sedimentation expected on the basis of the analysis.

A computer program of the mathematical model has been composed so that the model's behaviour can be reproduced with speed and ease with the progression of time. The programming language FORTRAN IV has proved sufficiently versatile for representation of the mathematical model and output from the program can easily be displayed in the form of graphs, tables and cross sections, using the line-printer and digital graph-plotter peripherals.

A fully comprehensive set of experiments with the program is not possible by virtue of the number of input variables involved, however examination of the expected behaviour of the system helped in designing a representative set of experiments. In supplying input variables, many are dependent system variables which must be mutually compatible in accordance with the natural system. The ideal situation would, of course, be to supply information only on the independent variables and be able to simulate the expected sedimentation and erosion patterns; such is not possible at present.

The set of experiments with selected input parameters has been fully documented. By matching the abundance of output with real-world observations the model can be evaluated and its ability to provide a useful analogue to the real system can be judged, in the light of approximating assumptions made in the mathematical model and the computer program. Difficulties exist in obtaining the comparative data from the real system; even when available, data may be sparse or unsuitable in form. Comparative studies are therefore, by necessity, only qualitative at present and concentrate on the broader implications of the model. The preservation potential of point bar and overbank sediments is discussed in the light of the model and a representative application of the model to the quantitative interpretation of an ancient point-bar deposit is performed.

In conclusion, the overall validity of the computer simulation model and its usefulness in the understanding and prediction of sedimentation aspects in meandering streams is discussed and suggestions are put forward for future development.

PART TWO

DEVELOPMENT OF MATHEMATICAL MODEL

1. INTRODUCTION: ENERGY DISTRIBUTION IN RIVER SYSTEMS

The river network as a whole is an open system tending towards a steady state (dynamic equilibrium) and within which several hydraulically related factors are mutually interacting and adjusting - specifically velocity, depth, width, hydraulic resistance and slope. These dependent variables adjust to the constraints applied by the independent variables of the system, that is, the quantity and character of runoff and sediment, valley slope and geological nature of the drainage basin.

The observed relationship between the dependent and the independent variables has been described using empirical equations of mean tendency, which are assumed to represent the channel form in dynamic equilibrium (e.g. Leopold and Maddock, 1953). A more desirable theoretical solution may be obtained by considering also the energy distribution in the system.

From its headwaters to its mouth a natural river channel essentially represents a system in which potential energy provided by quantities of water at given elevations is converted to kinetic energy of the flowing water and dissipated in friction created at the boundaries (Leopold et al, 1964). In analysing the behaviour of the channel system, primary interest lies not in the total energy in the system, but rather in the way in which energy is distributed throughout the system. This emphasis upon the distribution of energy within the system is in general analogous to a consideration of the entropy of thermodynamic systems (Leopold and Langbein, 1962; Scheidegger, 1970). From one point of view entropy may be said to be a measure of the energy in a system available for external work. The greater the entropy the less energy is available for external work. The natural process represented by the flow of water from the headwaters to the mouth of a river channel is an irreversible process in which energy is transformed with an increase in entropy.

Analogy with the thermodynamics of systems in a steady state led Leopold and Langbein (1962) to consider the way in which energy might be distributed and dissipated in the river system. They postulated the tendency toward minimum total rate of work in the system which is the same as uniform distribution, and minimum variance, of power expenditure per unit length. As discharge increases downstream this would tend to make the longitudinal profile concave upwards. They further postulated a tendency toward uniform distribution of power expenditure per unit bed area throughout the system, which tends to straighten the profile. The observed channel form is a 'quasi-equilibrium' state which, while fulfilling the usual hydraulic laws, represents the most probable state between these two opposing tendencies. These tendencies are promoted by erosion, deposition, variation in bed form, and related internal adjustments to energy utilisation (Langbein and Leopold, 1964). Langbein (1964) further showed that the adjustment in the hydraulic variables necessary to fulfil the energy and hydraulic requirements entails minimum variance among the components of stream power such that no single variable absorbs a disproportionate share of the required variation.

Theoretical solutions to the hydraulic geometry of fluvial systems, based on the above postulates, therefore represent the most probable behaviour of natural rivers satisfying the basic hydraulic equations. They are a measure of central tendency, therefore mutual adjustments of all the variables in every river system will not be expected to be the same, because of local physical constraints. The theoretical solutions agree well with the empirical mean measures of hydraulic geometry. The relevant application of these concepts to river meanders can be seen in the next and subsequent sections.

2. PLANIMETRIC GEOMETRY OF MEANDERS

2.1. Theory of Minimum Variance

Many authors have attempted to explain the processes involved in meander formation. None of these approaches, summarised by Leopold and Wolman (1960), Allen (1968, 1971), and Yang (1971b), can be used to calculate the characteristics of meander geometry adequately. Although various phenomena, particularly helicoidal flow, are known to be important in shaping meanders, there are many diverse effects involved. Although each of the individual effects is deterministic in itself their interactions are too numerous to treat in a deterministic way. These may, however be treated stochastically.

The striking similarity among meandering channels of various sizes in different settings is a result of certain geometric proportions apparently common to all. Based on a large number of flume and river data, Leopold and Wolman (1960) found a consistent correlation between meander length, 1, channel width, w, and mean radius of curvature, r_m, that is

$$1 = 10.9w^{1.01} = 4.7r_m^{0.98}. \qquad (2.1)$$

All terms used to describe meander geometry are defined in fig. 2.1. Assuming the exponents in the above equation to be unity they arrived at the relation

$$r_m/w = 2.3. \qquad (2.2)$$

These approximate mean relationships were considered to a great extent to be independent of bed and bank materials, and it was concluded that a general mechanical principle was responsible for the observed meander geometry. Bagnold (1960) found the value of r_m/w to be that at which flow resistance is a minimum within the channel, suggesting that some principle related to

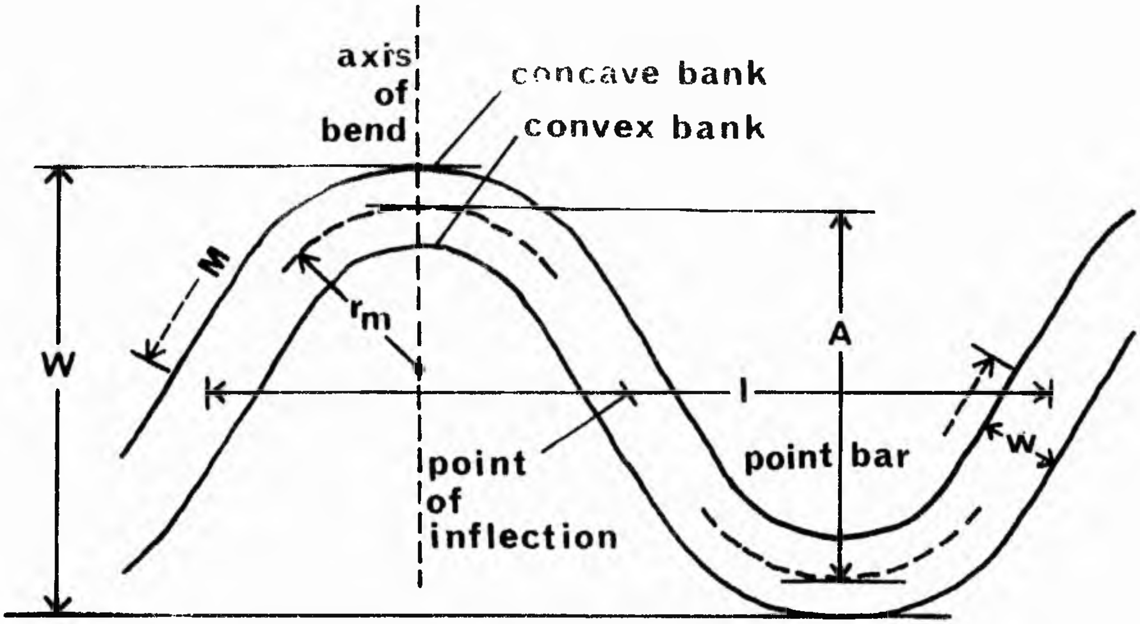

w	—	Channel Width
r_m	—	Mean Radius of Curvature
l	—	Wavelength
A	—	Amplitude
W	—	Meander Width
M	—	Length along channel in one wavelength

Fig. 2.1 Meander Geometry Definition.

energy conservation operates in the meander mechanism.

In 1966 the previously developed theories of minimum variance were introduced to river meanders where 'meanders are the result of erosion-deposition processes tending toward the most stable form in which the variability of certain essential properties is minimised' (Leopold and Langbein, 1966; Langbein and Leopold, 1966). This minimisation involves the adjustment of the planimetric geometry and the hydraulic factors of depth, velocity and local slope.

In the context of the entire river system a meandering segment, often but not always concentrated in the downstream rather than the upstream portions of the system, tends to provide a greater concavity by lengthening the downstream portion of the profile. Total work in the system is minimised therefore because, by increasing the concavity of the profile, the product of discharge and slope becomes more uniform along a stream that increases in flow downstream.

In the local context of a given segment of channel the average slope of the channel is fixed by the relation of that segment to the whole profile. Any change in the channel must maintain that average slope. Between any two points on the valley floor, however, a variety of paths are possible, any of which would maintain the same slope and thus the same length. This path is defined by a random walk model as follows.

A river has a finite probability, p, to deviate by an angle, $\Delta\phi$, from its previous direction in progressing an elemental distance, Δs, along its path. The probability distribution as a function of deviation angle is assumed normal. This has since been confirmed by Thakur and Scheidegger (1968). The actual meander path corresponds to the most probable river path proceeding between two points A and B, if the direction of

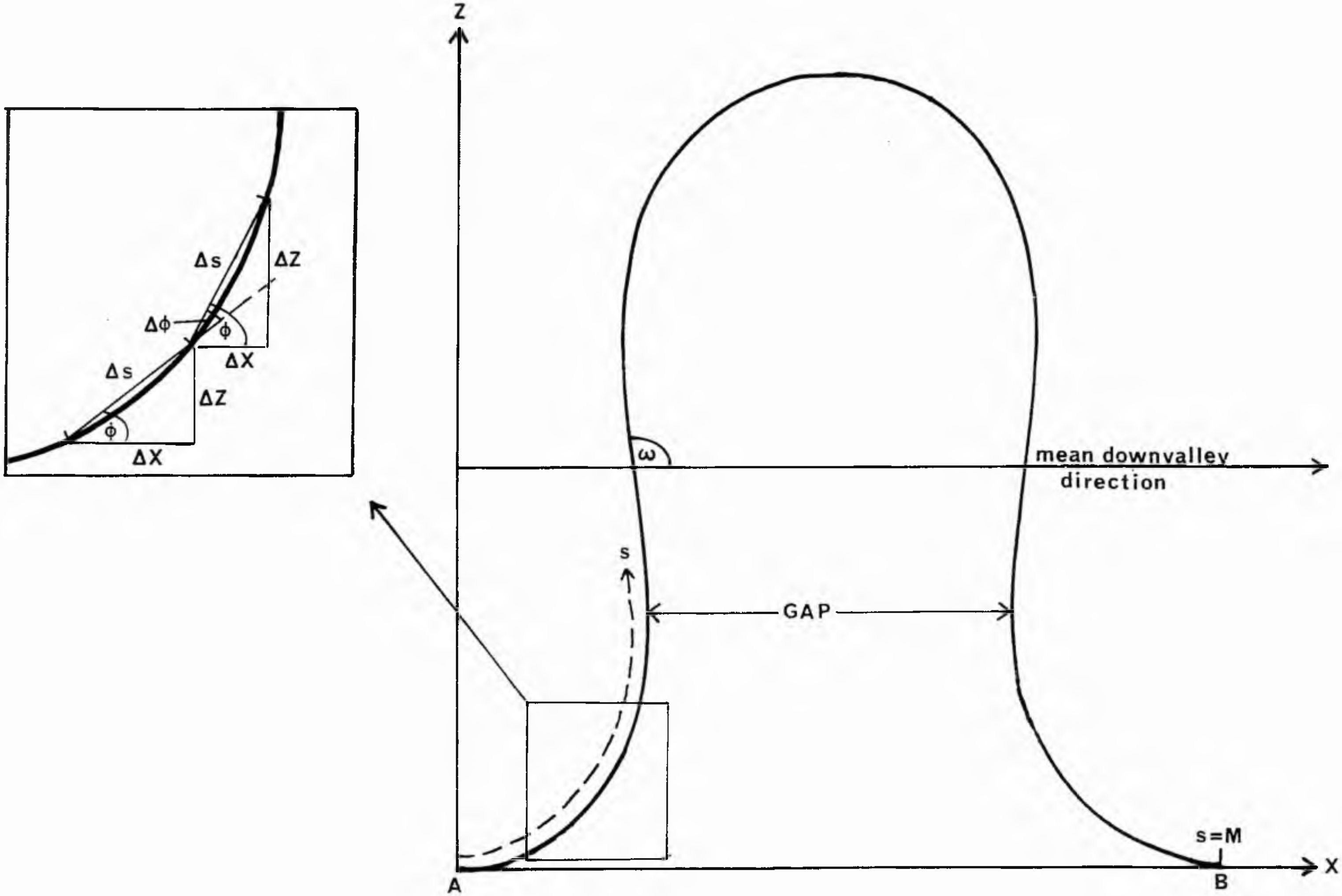

Fig. 2.2 Definition diagram for sine-generated curve.

flow at point A and the length of the path between A and B is fixed, and the probability of a change in direction is given by the probability distribution above. This formulation of the problem is identical to that of a class of random walk problems for which solutions have been derived (Von Schelling, 1951, 1964).

The exact solution is an elliptical integral but a sufficiently accurate approximation states that the most probable geometry for a river is one in which the angular direction of the channel at any point with respect to the mean downvalley direction is a sine function of the distance measured along the channel. The resulting curve minimises the sum of squares of the changes in direction in each unit length.

The equation of the 'sine-generated' curve is

$$\phi = \omega \sin\left(\frac{s}{M} 2\pi\right), \tag{2.3}$$

where ϕ is the deviation angle from the mean downvalley direction, ω is the maximum value of ϕ, s is the distance along the path, and M is the total path distance. The equation yields a meander shape typically present in regularly meandering rivers and flumes and has the characteristic that the ratio of meander length to mean radius of curvature is about 4.7. A definition diagram, fig. 2.2, shows the terms used in equation (2.3) and in the discussion of its development.

Furthermore, field observations have shown that depth, velocity and slope (the components of stream power) are adjusted so as to decrease the variance of shear and the friction factor compared to that of an otherwise comparable straight reach of the same river. This is manifested in the more uniform water surface slope at high stage in a meander, which signifies a more uniform expenditure of energy for each unit distance along the channel, after a slight correction for differences in velocity head (see fig. 5.4).

Since theory and observation indicate that meanders achieve the minimum variance postulated, it follows that for channels in which alternating pools and riffles occur, meandering is the most probable form of channel geometry and thus is more stable geometry than a nonmeandering reach. This has been independently demonstrated by Yang (1971a,b,c). Also using the thermodynamic analogy, he shows that the development of meanders, along with pools and riffles, fulfills the requirements of a natural stream evolving towards an equilibrium condition ; that is, minimum rate of potential energy expenditure per unit mass of water along its course. It should be noted that minimum variance adjustment describes the net river behaviour, not the processes.

2.2 Geometric characteristics of 'sine-generated' curve

Various geometric characteristics of the 'sine-generated' curve have been defined by Langbein and Leopold (1966). Inspection of equation (2.3) indicates that at a relative distance s/M equal to $\frac{1}{2}$ and 1, ϕ has a value of zero, or the channel is locally directed in the mean downvalley direction. At distance s/M equal to $\frac{1}{4}$ and $\frac{3}{4}$ the value of ϕ has its largest value ω. This is indicated in fig. 2.3a,b which shows the curve of equation (2.3) for $\omega = 110^{\circ}$ and also a plot of ϕ as a function of relative distance along the channel path. Furthermore, the distance between b and f is twice the distance between c and e measured along the mean downvalley direction as well as along the channel path. The tangent to the sine function at any point is $\Delta\phi / \Delta s$ which is the reciprocal of the local mean radius of curvature of the meander. The sine curve is nearly straight as it crosses the zero axis in fig. 2.3b, therefore the radius of curvature is nearly constant in a meander bend over two portions

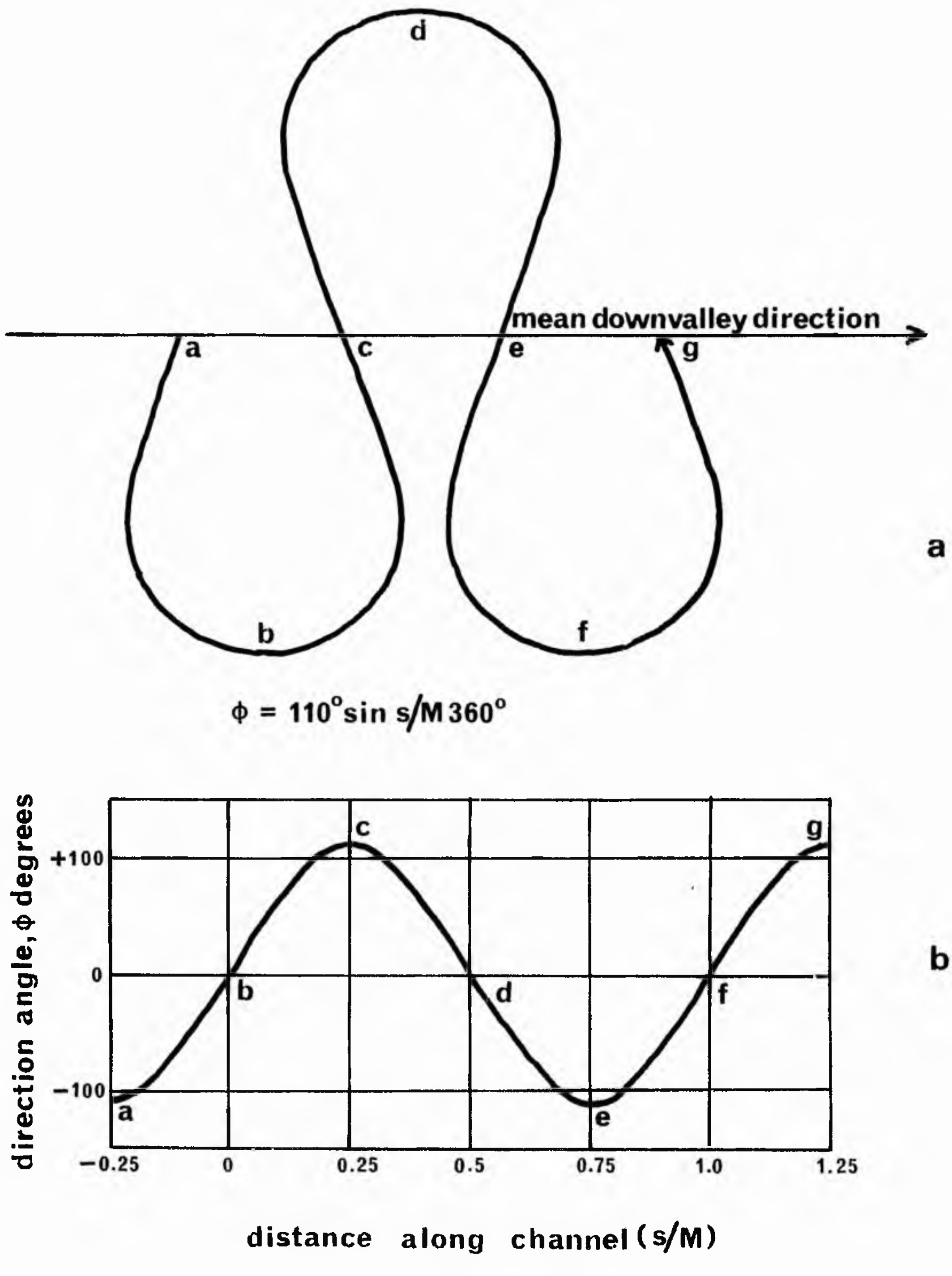

Fig. 2.3 Sine-generated curve (a) and a plot of its direction angle as a function of distance along the channel path (b). (after Langbein and Leopold, 1966).

covering fully a third of the length of each loop.

The angle ω is a unique function of sinuosity, sn, and an approximate algebraic expression is

$$\omega = 2.2\sqrt{\frac{sn-1}{sn}} \quad \text{or} \quad sn = 4.84/(4.84-\omega^2). \qquad (2.4)$$

Average bend radius is related to wavelength and sinuosity. Defined as before, as the average over the 1/6 of channel length for which ϕ is nearly linearly related to channel distance, bend radius is

$$r_m = \frac{1/6M}{\Delta\phi}.$$

Since ϕ ranges from $+0.5\omega$ to -0.5ω over this near linear range, $\Delta\phi=\omega$. As M=sn.1, after substituting for ω, we get

$$r_m = \frac{1}{13}\frac{(sn^{3/2})}{(\sqrt{sn-1})}. \qquad (2.5)$$

Differentiating r_m with respect to sn gives

$$\frac{dr_m}{dsn} = \frac{1}{13}\left[\frac{3}{2}\ sn^{1/2}(sn-1)^{-\frac{1}{2}} - \frac{1}{2}sn^{3/2}(sn-1)^{-3/2}\right].$$

At a turning point of the function $dr_m/dsn = 0$, therefore

$$\frac{3}{2}\left[\frac{sn}{sn-1}\right]^{\frac{1}{2}} = \frac{1}{2}\left[\frac{sn}{sn-1}\right]^{3/2},$$

which reduces to

$$(2sn-3)(4sn+3) = 0. \qquad (2.6)$$

The turning points are therefore at sn=1.5 and -3/4. The latter has no physical meaning, however, by inspection also of fig. 2.4 it can be seen that r_m has a minimum value at the turning point sn=1.5. The significance of this fact will become apparent later.

Other relations can also be derived that are important in the development of the model. By inspection of fig. 2.2, the following may be written,

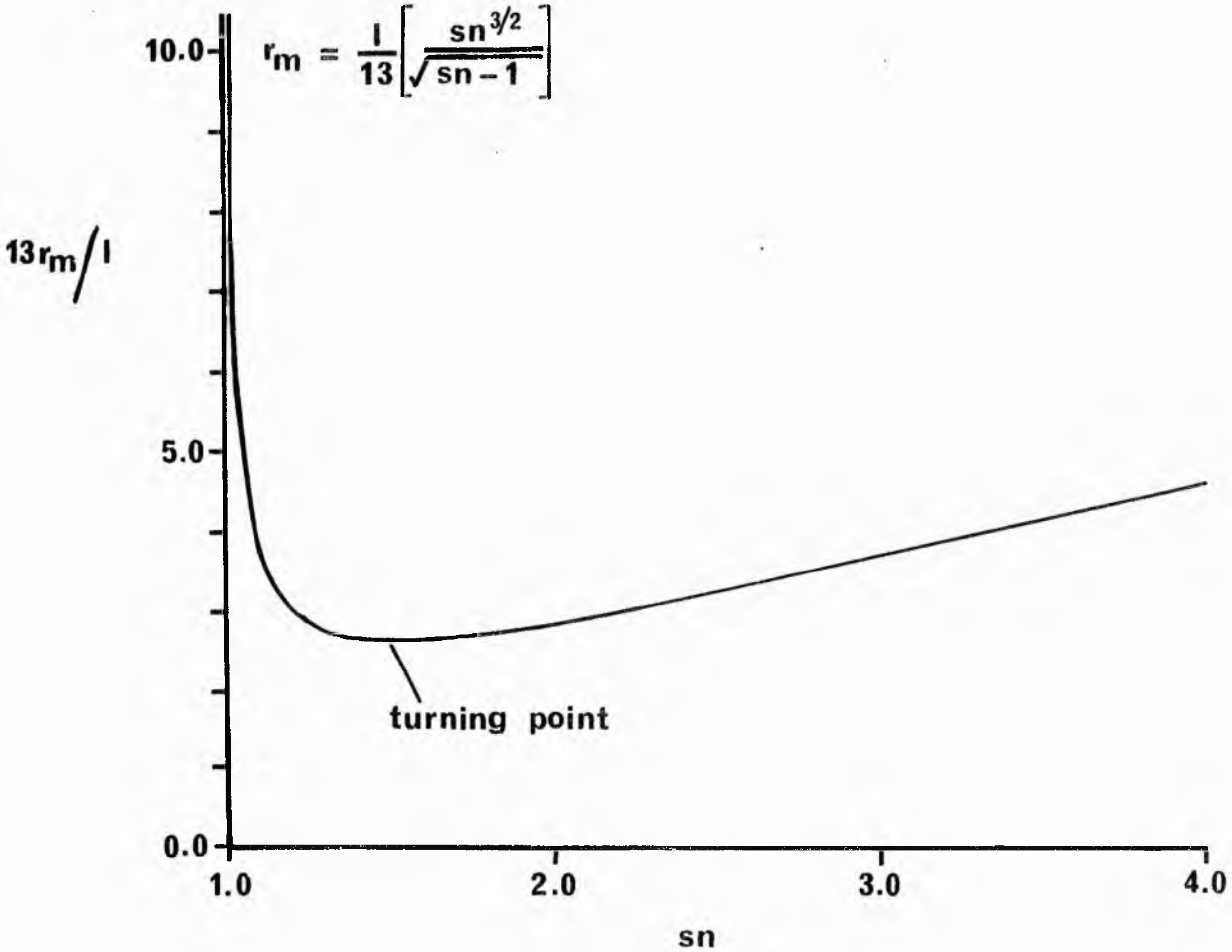

Fig. 2.4 Plot of sinuosity (sn) against dimensionless radius of curvature parameter.

$$X = \lim_{n \to \infty} \sum_{r=1}^{n} \Delta s.\cos\phi_r \tag{2.7a}$$

and

$$Z = \lim_{n \to \infty} \sum_{r=1}^{n} \Delta s.\sin\phi_r. \tag{2.7b}$$

This means that if a particular length of curve is divided into n equal parts, then as n tends to infinity, the projected length of the curve along the axis of abscissas, X, or the ordinate axis, Z, is given by the sums of the product of arc length, Δs, and a cosine or sine function of the direction angle for each interval. In terms of integral calculus

$$X = \int_0^{\phi} \cos\phi ds \quad \text{and} \quad Z = \int_0^{\phi} \sin\phi ds \tag{2.8}$$

To integrate these functions, ds must be expressed in terms of ϕ. Rearranging equation (2.3), we get

$$s = \frac{M}{2\pi} \sin^{-1} \left(\frac{\phi}{\omega}\right).$$

Differentiating with respect to ϕ,

$$ds = \frac{M}{2\pi} \frac{d\phi}{\sqrt{\omega^2 - \phi^2}}$$

Finally, substituting for M, the integrals may be written as,

$$X = \frac{sn.1}{2\pi} \int_0^{\phi} \frac{\cos\phi d\phi}{\sqrt{\omega^2 - \phi^2}} \tag{2.9a}$$

and

$$Z = \frac{sn.1}{2\pi} \int_0^{\phi} \frac{\sin\phi d\phi}{\sqrt{\omega^2 - \phi^2}} \tag{2.9b}$$

It is now easy to find expressions for meander amplitude, A, and the width of the meander neck, GAP, measured to channel centre lines. The last parameter is of course physically meaningless if ω is less than $\pi/2$. The expressions are

$$A = \frac{sn.1}{\pi} \int_0^{\omega} \frac{\sin\phi d\phi}{\sqrt{\omega^2-\phi^2}} \qquad (2.10)$$

and

$$GAP = 1\left\{1 - \frac{sn}{\pi}\right\} \int_0^{\pi/2} \frac{\cos\phi d\phi}{\sqrt{\omega^2-\phi^2}} \; . \qquad (2.11)$$

No analytical solutions are possible for these integrals and so approximate solutions are obtained numerically by Simpson's rule (see appendix 1 and program specifications).

An expression for sn(hence ω) in terms of amplitude and wavelength was obtained from equation (2.10) by evaluating the integral numerically over a range of sn(1.1 to 4.5) and performing a polynomial regression analysis with sn as the dependent variable and the ratio A/1 as the independent variable. The resulting best fit equation is

$$sn = 0.96 + 0.34 \left(\frac{A}{1}\right) + 1.67 \left(\frac{A}{1}\right)^2 - 0.43 \left(\frac{A}{1}\right)^3 \; . \qquad (2.12)$$

Full details of the analysis can be seen in appendix 2. As will be seen from fig. 2.5 and the analysis of variance table in appendix 2, the relation is almost linear, except for a small part of the curve at small values of sn.

It can be seen from the above expressions that by specifying any two of sinuosity, amplitude and wavelength, all of the other geometric parameters discussed can be derived. This is an important point in the analysis because, given only two geometric characteristics, much of the planimetric geometry can be defined - a definition which also implicitly specifies mutual internal adjustment of the dependent hydraulic variables to the independent system variables, according to the minimum variance theory previously outlined. A discussion of the dependence of wavelength, amplitude and sinuosity on the independent variables will follow later for the purposes of input to the model.

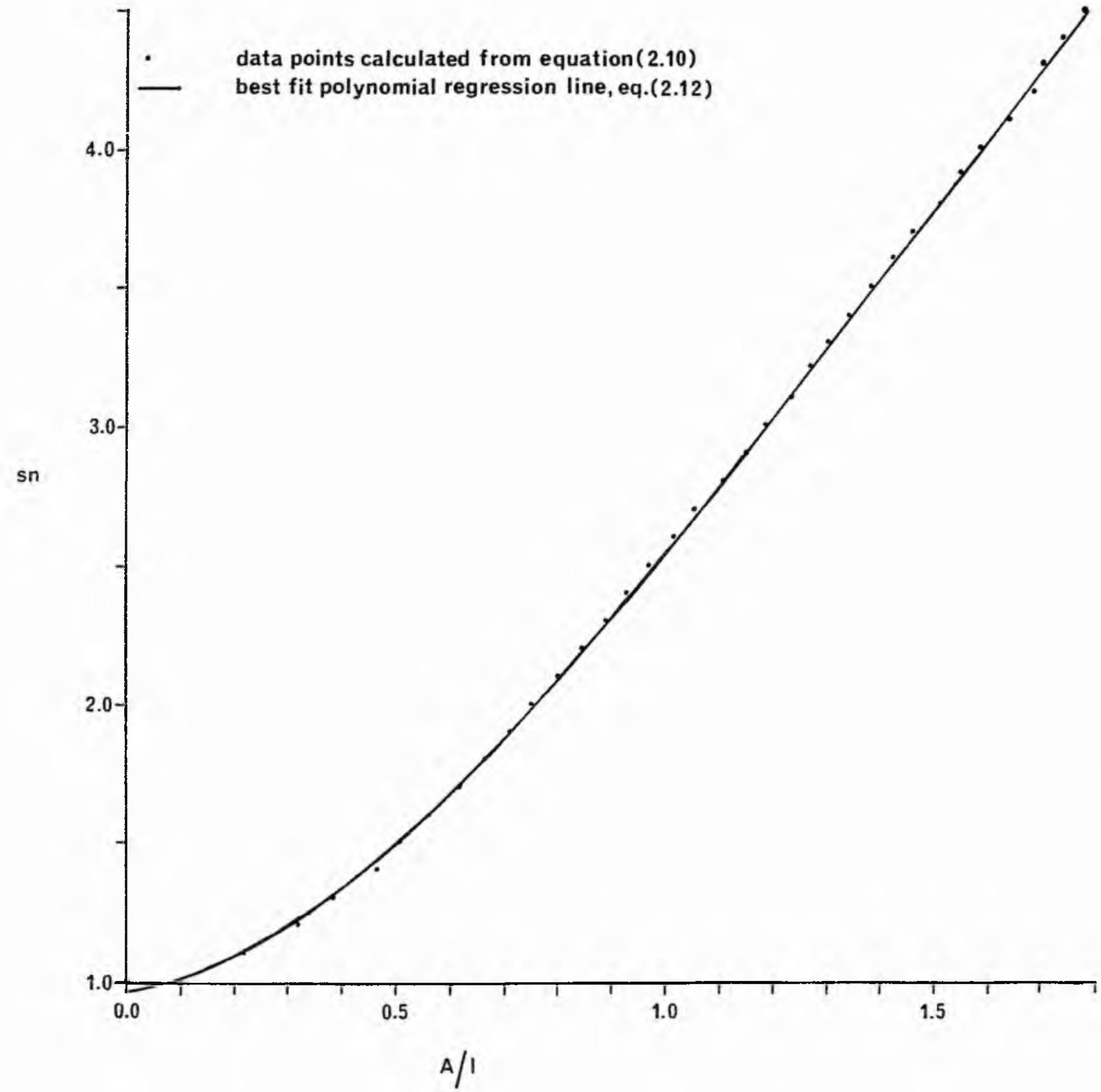

Fig. 2.5 Plot of polynomial regression between sinuosity(sn) and ratio of amplitude over wavelength (A/l).

2.3 Validity of the sine-generated curve

Scheidegger (1967, 1970) points out that the derivation of the sine generated curve is not in conformity with the commonly accepted principles of statistical mechanics. Usually the expected value of an observable is taken as its average over all the configurations of the ensemble in question, whereas in Langbein and Leopold's theory the characteristic pattern is taken as that pattern of the observable which occurs in the most probable configuration of the ensemble.

The curves are in general too regular to describe a whole system of river meanders, and the reason is sought in the fact that the most frequent are not the expected random walks. More recent studies have used models to generate constrained random walks whose expected paths cannot be distinguished statistically from the paths of natural meandering streams (Surkan and Van Kan, 1969; Thakur and Scheidegger, 1970; Ghosh and Scheidegger, 1971).

Although these studies may be more statistically rigourous and more authentic than Langbein and Leopold's model when applied to meandering reaches in general, the sine-generated curve has been shown, using empirical and theoretical considerations, to underlie the stable form of meanders and describes regular forms very well. As the present study may only treat regular shapes with definable geometric characteristics the sine-generated curve has been adopted, and will be used in the model to represent the channel centre line.

2.4. Initial input required by Planimetric Geometry model

2.4.1. Floodplain sediments

That actual meanders are often irregular is well known, and deviations from the idealised case are caused by heterogeneities in bank materials, structural controls, and other random actions causing varying flow.

In order that the model meanders conform to the minimum variance equations, it will be assumed that the bank materials are reasonably homogeneous laterally, and there are no random actions of any nature causing shifts from stable to unstable forms. The meanders will therefore be 'free' meanders. Lateral homogeneity in bank materials is built into the model, the vertical variation of sediments in the floodplain, however, will be specified as input.

2.4.2. Wavelength

Meander wavelength, like other form characteristics of stable alluvial channels, is a function of the independent variables. It has been recognised empirically for years by many authors that wavelength, l, increases with stream size according to

$$l = c_1 Q^N \tag{2.13}$$

in which stream size is measured by a discharge Q, c_1 is a coefficient and N is an exponent close to 0.5. Because channel width, w, and mean depth, d, depend on discharge relations can also be formed between w and l and d and l. It was shown in equation (2.1) that l and r_m are closely related.

As will be expanded in section 8, the precise interpretation of the discharge, or the range of discharges, that defines the channel form in natural streams is a major source of disagreement (Carlston, 1965; Ackers and Charlton, 1970c). This is not a problem under controlled laboratory studies with constant discharge. Although exponent N does not appreciably vary, c_1 varies considerably according to different authors depending on the data used, suggesting that one equation of the form given above cannot describe the wavelength of all free meandering streams. Indeed, discharge is but one of the independent variables and the control of wavelength is undoubtedly more complex than equation (2.13) would suggest.

The dependence of wavelength on some or all of the other independent variables has been empirically examined by many authors, often involving the arranging of the independent variables into dimensionless groups (e.g. Ackers and Charlton, 1970a,b; Carlston, 1965; Chang et al, 1971; Charlton and Benson, 1966; Freidkin, 1945; Kinosita, 1961; Schumm, 1967, 1969; Shahjahan, 1970). Theoretical studies of meandering have also yielded relationships for wavelength (e.g. Anderson, 1967; Callander, 1969; Engelund and Hansen, 1967; Fujiyoshi, 1950; Hansen, 1967). There appears to be some confusion and apparently conflicting views concerning the wavelength of meandering laboratory and natural streams of different sizes and types. It is clear that wavelength cannot be taken as uniquely related to discharge. Although the exponent in equation (2.13) appears to represent the effect of discharge fairly well when about 0.5, the coefficient c_1 obviously represents the net effect of the other independent variables. Although various investigators have attempted to account for the effects of some of these variables in their equations, valley slope has not been accounted for by any of them. None of the equations uniquely describes the effect of the independent variables, and even the theoretical studies require empirical information. It follows that in a natural stream, for a given discharge pattern, a number of different wavelengths may occur depending on the variation in the other dependent variables, either along the same stream or between different streams. The existence of a number of wavelengths in a given stream has been confirmed by Speight (1965a,b, 1967), Toebes and Chang (1967) and Chang and Toebes (1970).

In view of the aforesaid it appears that the theoretical or empirical relationships developed to date can only be used for an approximate estimate of the effect of the independent variables on wavelength. The problem of multiple wavelengths will not be encountered because of the choice of model conditions (see section 2.4.1). If l is being defined for input using one of the equations cited in the literature, estimates of empirical constants would necessarily be subjective. Furthermore, a time integral of the discharge hydrograph is more preferable than a single measure of discharge (see section 8). It will be seen later that channel width must be specified as input to the model. Leopold and Wolman's (1960) relation, that wavelength is approximately seven to ten times the channel width is a useful approximation linking these two parameters.

2.4.3 Amplitude

Freidkin (1945) showed in flume studies that in uniform material, at constant discharge, amplitude did not continue to increase nor did meander loops cut off as the meanders migrated downstream. After the initial development of the bends, the wavelength reached a limiting value, amplitude increased due to erosion at the concave banks but was checked by the formation of chutes when flow resistance was less over the bar than in the channel. After formation of a chute the bend formed a little further downstream, and again started to increase in amplitude to a limiting value, wavelength remaining constant, until another chute formed.

It is to be expected that this limiting amplitude, like wavelength, will be a function of the independent system variables. The variation of the limiting amplitudes (and the similar parameter, meander width) with the independent variables are best obtained from laboratory meanders that have been allowed to develop freely to a stable form (e.g. Shahjahan, 1970). However, the measured amplitude may not represent a stable limiting value in laboratory meanders that were not allowed to develop freely, or in natural rivers where meandering was developing, say, after cut off, and therefore not in dynamic equilibrium. A further problem in natural rivers is the variation of the independent variables along the length of the stream (i.e. tributaries, local variations in stream banks, etc.) which makes an objective measure of meander amplitude for a reach difficult to obtain. These points explain the poor correlations of amplitude separately with discharge, wavelength and channel width (Leopold and Wolman, 1960; Carlston, 1965; Ackers and Charlton, 1970a), and the poor multiple correlations, including various other hydraulic variables (Chitale, 1970).

One interesting study (Nagabhushanaiah, 1967) expresses meander width, W, of laboratory meanders in terms of discharge, critical discharge at which bed load movement begins, Q_c, mean diameter of bed material, D, bed slope, S_b, and time, t, i.e.

$$\frac{W}{D} = 0.76 \left(\frac{(QS_b^{\,2} - Q_c S_b^{\,2})t}{D^3} \right)^{0.5}. \qquad (2.14)$$

It is interesting to note that the time term describes the progressive development of the meander amplitudes from zero up to a limiting value (see fig. 2.6). The shapes of the curves broadly agree with the data on natural streams obtained by Handy (1972). Nagabhushanaiah further noted that the quantity and size of transported sediment increases with discharge and slope, and decreases with time; that is, in a developing meander, as amplitude increases, water surface slope decreases and rate of sediment transport decreases.

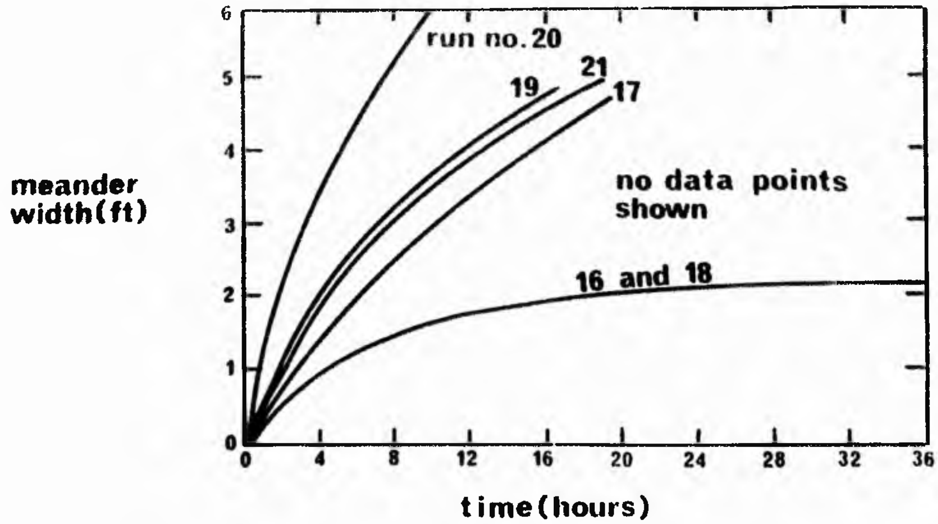

run no.	discharge(cfs)	initial bed slope
16	0.147	0.003
17	0.078	0.006
18	0.038	0.006
19	0.038	0.012
20	0.079	0.012
21	0.019	0.012

Fig.2.6 Variation of meander width with time. (after Nagabhushanaiah,1967).

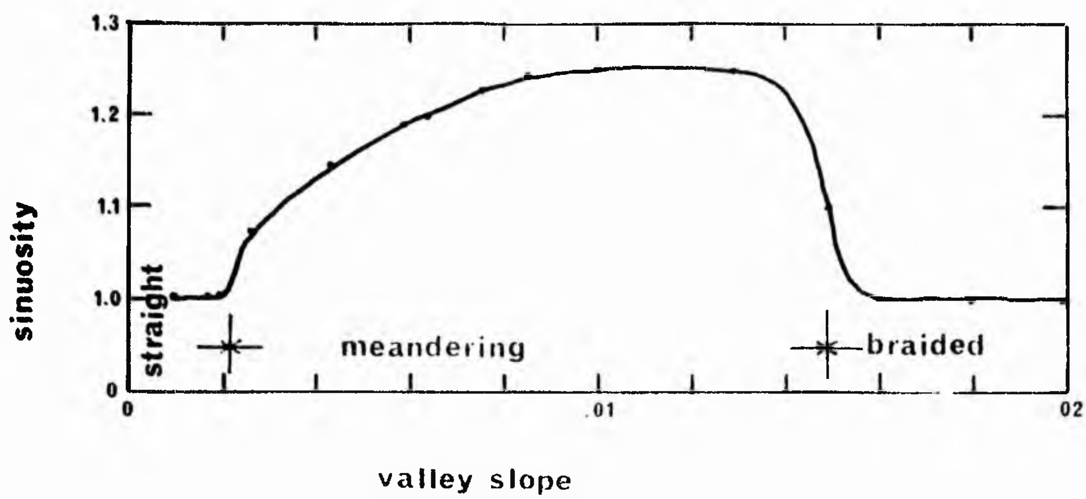

Fig.2.7 Relation between valley slope and sinuosity for experimental studies (after Schumm et al.,1972).

In general, limiting amplitude of meanders increases with increasing discharge, valley slope and sediment discharge, and decreases with increase in size of bed material. Some of the empirical derived relationships in the literature should be examined with caution as the values of amplitude used in their derivation may not be limiting values. Obviously the amplitude of a meander developing to a limiting value may have any value depending on the progression of time from any initial situation.

Amplitude is not actually required as physical input to the model, however its relationship with other dependent variables, notably l and sn in equation (2.12), is useful if a particular amplitude is required in the model.

2.4.4 Sinuosity

In this study sinuosity is defined as the ratio of length along the channel centre line to length along the valley axis. This definition is sometimes altered slightly by various authors to suit particular situations.

Schumm (1963, 1969) has shown, using data from natural streams, that sinuosity is related to width-depth (max.) ratio, F, and the weighted mean percentage of silt and clay in the perimeter of the channel, M, by the following regression equations

$$sn = 3.5\ F^{-0.27} \qquad (2.15)$$

$$sn = 0.94\ M^{0.25} \qquad (2.16)$$

where the lower limit of the sand sizes is defined as 0.074mm. M is considered as an index of the ratio of bed material load to sediment load, that is the type of sediment load moved through the channels. For channels in the Great Plains of the United States and the Riverine Plain of New South Wales, Australia, $M = 55/Q_t$ where Q_t is the total sediment load that is sand or bed load at mean annual discharge. Although the dimensions of meanders (wavelength, limiting amplitude, channel width, etc.) are related primarily to discharge, there is no significant relationship between sinuosity and discharge. However, a change in discharge may cause a modification through its effect on type of sediment load transported in the channel.

Valley slope has been found to control sinuosity (Freidkin, 1945; Ackers and Charlton, 1970a,d; Schumm, 1971; Schumm and Khan, 1972; Schumm et al., 1972), however some qualification is needed here. Fig. 2.7 relates to the experimental work of Schumm and Khan (1972). It should be noted that in this study the sediment load was increased to maintain a stable channel (nonscouring and nonaggrading) as valley slope was increased. If valley slope is too small or large for a given introduced sediment load general aggradation or degradation, respectively, will tend to occur, hence changing valley and channel slope (Ackers and Charlton, 1970a; Schumm and Khan, 1972). Sediment load and valley slope therefore cannot be viewed as mutually independent variables in this respect. Valley slope may be largely independent of sediment load when there are tectonic influences, that is, uplift, depression or tilting of the valley.

Fig. 2.7 shows sinuosity increasing with increasing valley slope (increase in sediment load is not shown). If, however, the valley slope is too steep for a given sediment discharge the river may either degrade in order to reduce the valley slope or reduce the channel gradient by increasing sinuosity (Schumm, 1971). The latter situation and fig. 2.7 therefore represent two apparently irreconcilable situations. The channel slope and sediment load in the latter situation must however be above that critical for the existence of meanders. There are obviously limits to the amount of degradation possible, and the relative amounts of adjustment will depend on the distribution of energy expenditure.

It should be noted that sinuosity in these relations, derived from natural streams, is that limiting sinuosity associated with a stable wavelength and limiting amplitude, i.e. in dynamic equilibrium. However sinuosity will vary somewhat with time about these measures of mean tendency depending on the occurrence of cut-offs and subsequent growth to a stable form. In the model limiting sinuosity and initial sinuosity are required as input. These will be synonymous if the meander is in a stable form. If the meander is developing to a stable form initial sinuosity may take any desired value.

3. MEANDERS IN A DYNAMIC FRAMEWORK

Although the meandering behaviour may be stable through time, meanders shift continuously in the mean downvalley and normal to the mean downvalley directions by the orderly erosion of the concave banks and deposition on point bars. The spatial and temporal distribution of erosion and deposition around a meander is determined by the interaction between the flow pattern and the sediment forming the perimeter of the channel. Inherent difficulty lies in expressing the magnitude and the direction of the forces involved at every point along the channel. These forces are discussed later in section 6.

Although theoretical studies make it possible to predict the flow around a channel bend given channel shape and discharge (e.g. Rozovskii, 1961; Yen, 1971), the flow may mould a loose sediment bed, which in turn will alter the flow pattern. The interactive relation between the shape of a loose sediment bed and the flow cannot be described adequately for every point in the bend. Difficulty also is experienced in describing the other forces acting on the bed and banks within the context of the whole meander. Furthermore, from a practical viewpoint, there would be severe limitations imposed by the availability of computer memory if the erosional and depositional activity of a meander was to be completely described and recorded in three spatial dimensions.

By using the sine-generated curve in a dynamic framework, however, the movement of meanders in plan can be referred to specific moving reference axes (see fig. 3.1). The net river behaviour can be described simply by looking at the movement of the reference axes and the changes in the shape of the sine generated curve relative to the reference axes.

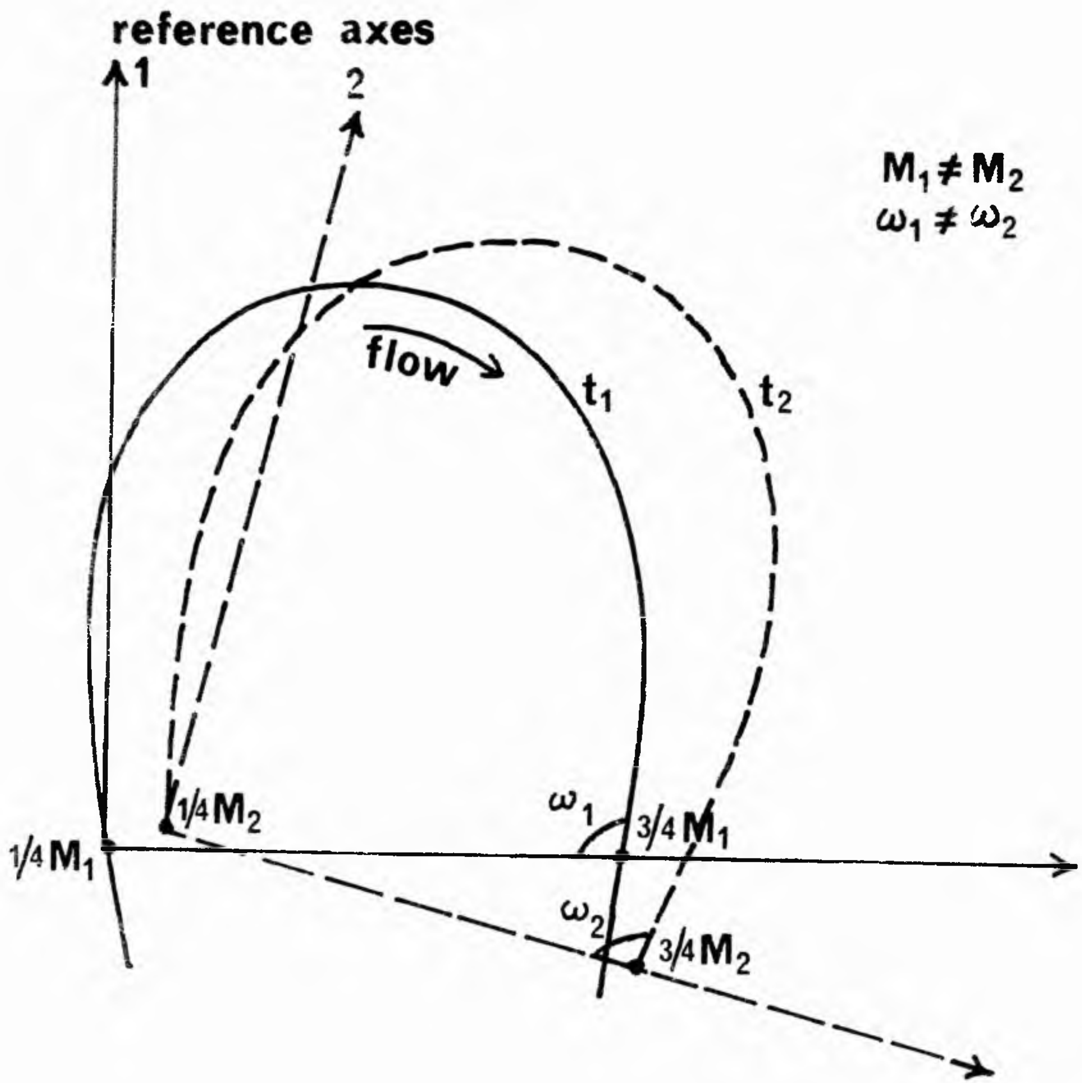

Fig. 3.1 General mechanism of meander loop movement.

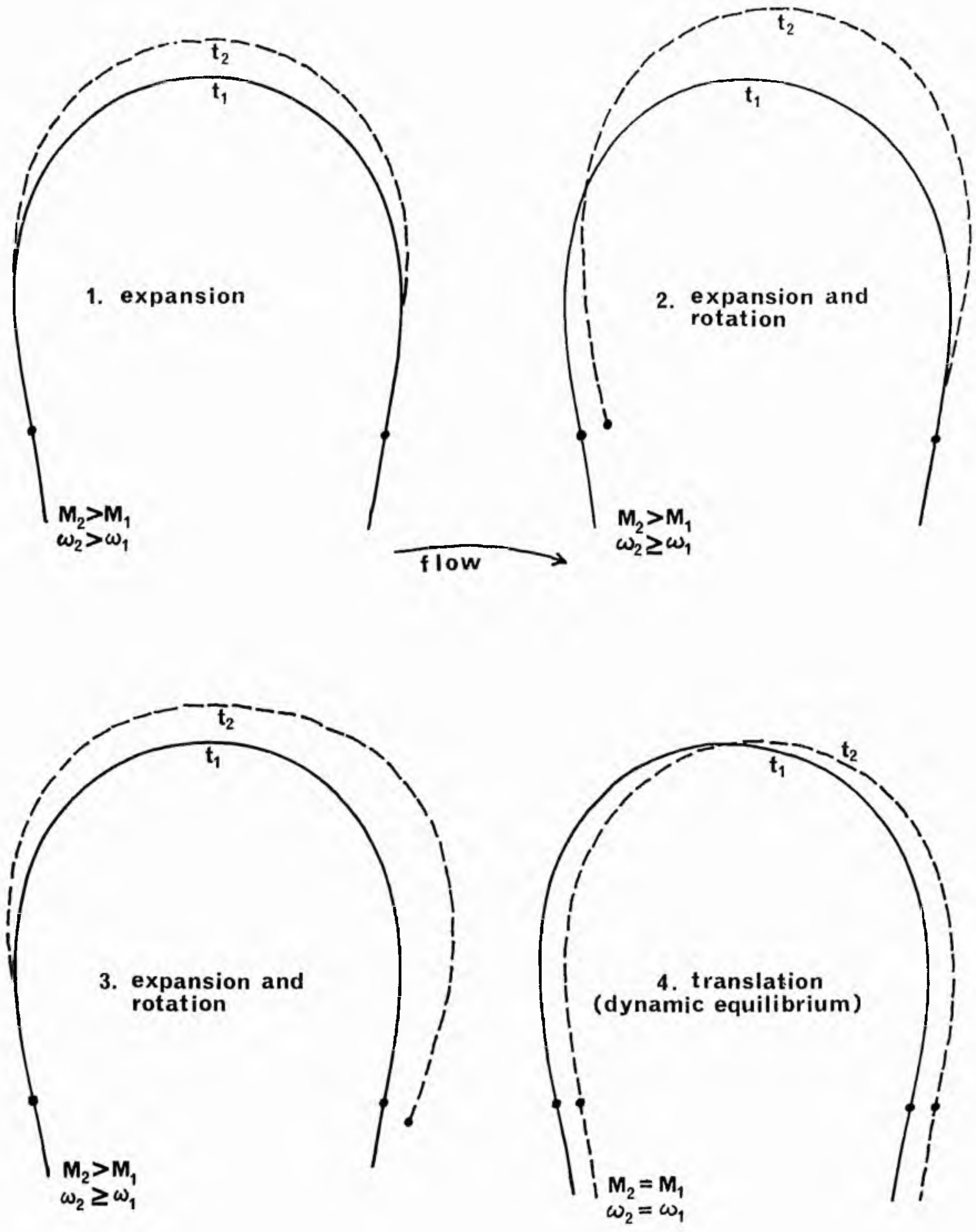

Fig. 3.2 Observed modes of movement in meander loops (modified from Daniel, 1971).

Daniel (1971) used this method in studying the movement of meandering streams in Indiana, and observed various modes of change, as shown in fig. 3.1 & 3.2. In the first case of fig. 3.2, the meander is developing to a stable limiting amplitude, the lack of downstream migration indicating a restriction to bank movement in the downvalley direction, perhaps due to clay plugs. In examples 2 and 3 the situation is essentially similar except one arm of the meander in each case is not having its downvalley migration hindered. Where erosion rates differ greatly within a loop in this way, rotation of the reference axes occurs and the meander wavelength changes. Example 4 represents the stable situation whereby path length is not increasing, wavelength, amplitude and sinuosity are constant and the meander is migrating downvalley. Daniel states that the three forms of movement, increasing path length, rotation, or translation, should have application to all forms of meanders, the dominance of any single mechanism depending on the local physical constraints. In natural streams the usual condition would be some combination of all three, as in fig. 3.1.

In the model, rotation will not occur because of the 'built in' lateral homogeneity of the bank materials. The only modes of movement will be (a) translation (downvalley migration of a meander in a stable form), fig. 3.2, example 4, and (b) translation and expansion together. The latter will be the situation in the case of a meander developing to a limiting stable form. During the development of free meandering from a straight natural or laboratory channel, the meander length remains essentially constant although the meander amplitude increases (Charlton and Benson, 1966; Ackers and Charlton, 1970a; Kinosita, 1961; Anderson, 1967). See fig. 3.3. In the model, therefore, meanders can be allowed to develop to a limiting sinuosity/ amplitude according to mode (b), while wavelength remains constant.

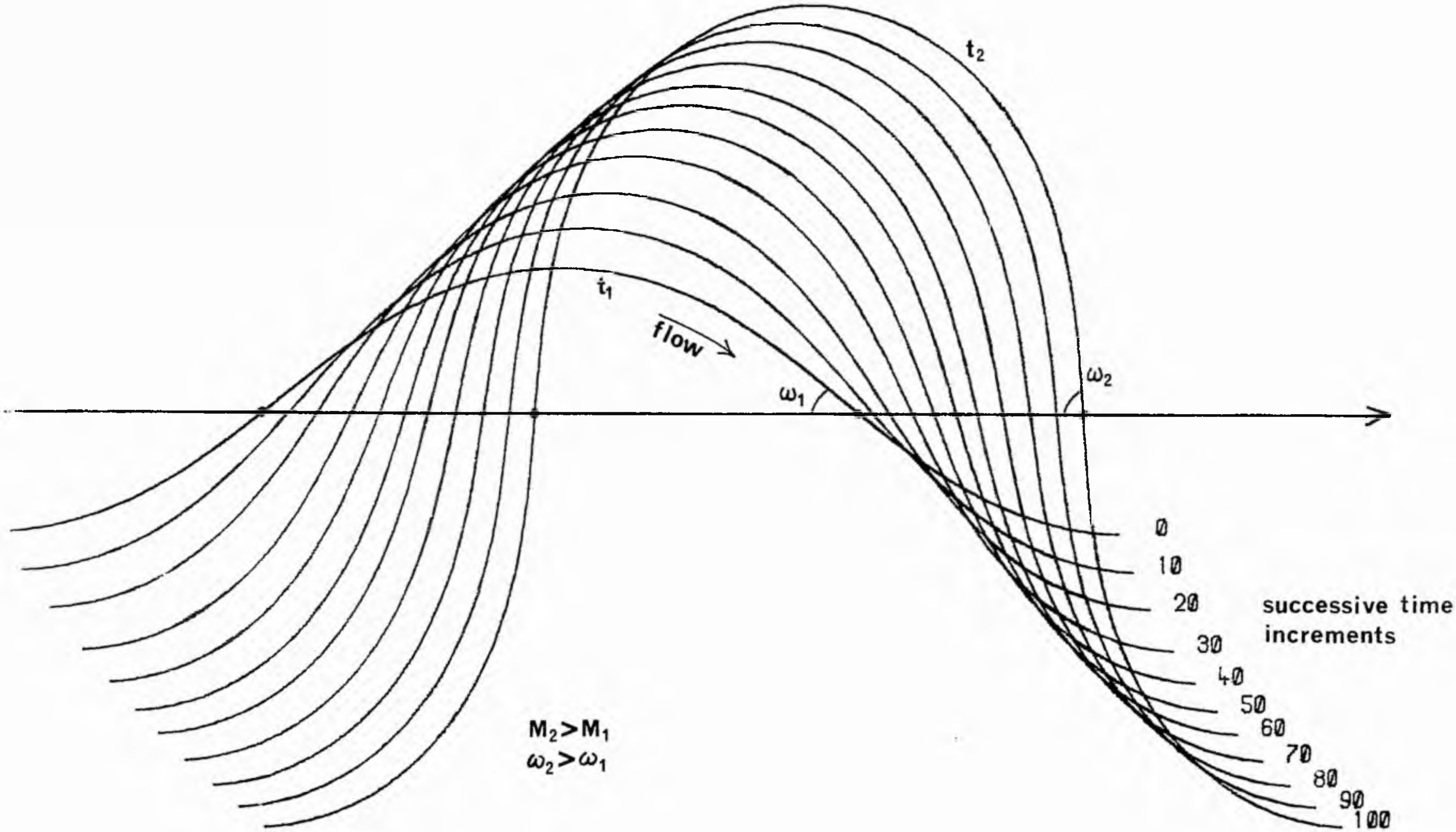

Fig.3.3 Meander loop migration by translation and expansion (developing meander).

Assuming these modes of movement, it can be seen that by specifying only the downvalley rate of bank migration and the rate of expansion (path length increase) of the meanders, the movement of the whole meander in plan form can be accounted for. Furthermore, as will be shown later, path length increase can be expressed readily in terms of rate of bank erosion in a direction through the axis of the bend.

4. CROSS SECTION DEFINITION

It has already been pointed out that it is not possible to analyse the detailed spatial and temporal distribution of erosion and deposition around the whole of a meander bend. This is quite possible, however, if dealing with specific cross sections across the channel. Because of the modes of movement of the meander in plan that are being considered, it it convenient to define cross sections across the channel in the downvalley direction and approximately normal to this direction.

In the model it is possible to look at the processes of erosion and sedimentation in three types of cross section. These are:-

(1) Through the axis of the bend at the inner (convex) bank in a direction approximately normal to the mean downvalley direction. The actual direction will depend on the successive positions of the bend axis at the inner bank as the meander migrates. This is the LATERAL section.

(2) In a direction parallel to the mean downvalley direction through one arm of the meander loop. This is the ONE-CHANNEL DOWNVALLEY section. In the case of a developing meander this section is located through the point of inflection of the meander limb.

(3) In a direction parallel to the mean downvalley direction through both arms of the meander, and located through the points of inflection of both meander limbs. This is the TWO-CHANNEL DOWNVALLEY section.

The best type of section to use will often depend largely on the type of migration that is occurring. In case (a) of section 3, downvalley migration of meanders in dynamic equilibrium, there is no point in using a lateral section as no deposition or erosion is occurring normal to the mean downvalley direction.

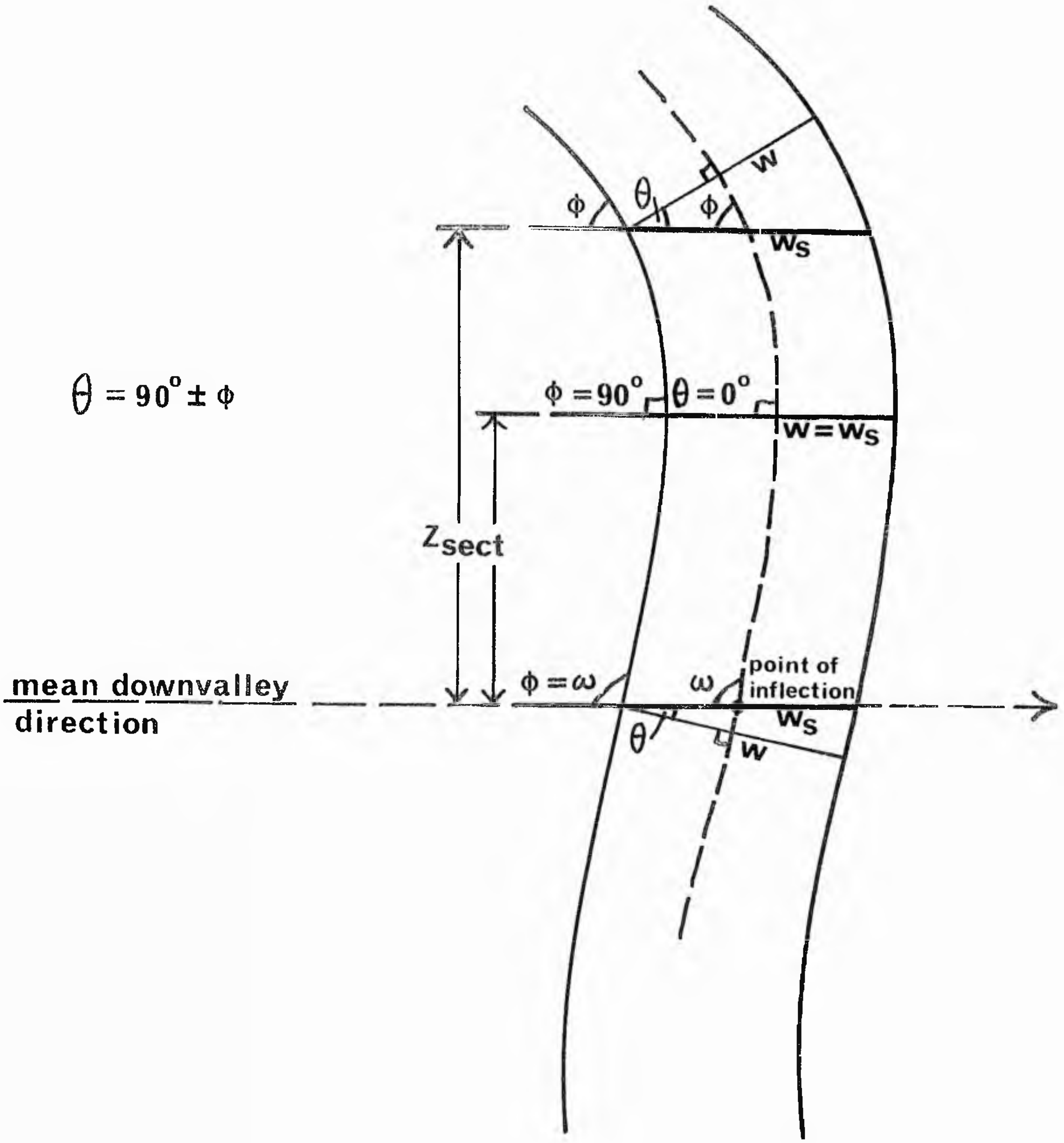

Fig. 4.1 Cross section definition – downvalley sections.

Cross section types 2 and 3 are the obvious choice. Type 2 could be located anywhere on a meander limb (except near the axis), however type 3 is always located through the points of inflection of the loop. This is largely because along this section the straight line distance between the channel centre lines can easily be calculated as half the wavelength.

It can be seen from fig. 4.1 that the angle the channel centre line makes with the mean downvalley direction, and hence the projection of the actual channel width in this direction, will depend on the distance of the cross section from the parallel line joining the points of inflection of the loop and, of course, the shape of the loop. In the model the width of the channel as represented in the chosen cross section must be adjusted with respect to the actual channel width. In this case of translation only, the adjusted channel width remains constant as migration proceeds, and the relation between actual width and width projected in the cross section, w_s, is given by

$$w_s = w/\sin\emptyset \qquad (4.1)$$

The value of the angle $\emptyset$ at a normal distance, Z_{sect}, from the line joining the points of inflection of the loop, is obtained using an equation of the form of equation (2.9b), i.e.

$$A/2.0 - Z_{sect} = \frac{sn.1}{2\pi} \int_0^{\emptyset} \frac{\sin\emptyset d\emptyset}{\sqrt{\omega^2 - \emptyset^2}} \qquad (4.2)$$

The integral in equation (4.2) was evaluated numerically by Simpson's rule for various values of $\omega (= f(sn))$ and $\emptyset$. Polynomial surfaces of degree 1,2 and 3 were then fitted by least squares to the values of sn, $\emptyset$, and the integral as the dependent variable. It was found that the cubic fit is statistically best, which yields the following equation.

$$\frac{\pi(A - 2Z_{sect})}{sn.1} = 0.2804\phi^3 - 0.1713sn\phi^2 + 0.1139\phi sn^2 - 0.0292sn^3 + 0.2244\phi^2 - 0.552\phi sn + 0.2123sn^2 + 0.8895\phi - 0.4651sn + 0.2668. \quad (4.3)$$

In the model, ϕ can be found, given A, sn, 1, and Z_{sect}, by solving equation (4.3) using the Newton-Raphson method (see appendix 1). A good initial estimate of ϕ, which is required by this method, is obtained using the equation of the fitted polynomial surface of degree 1 (plane surface). Full details of the trend surface fitting are given in appendix 2.

In case (b) of section 3, the developing meander, any type of cross section can be used, however the channel width projected in any of these cross sections does not remain constant as migration proceeds. Whichever of the three types of cross section is used, continual adjustment of channel width is necessary as outlined below.

In a developing meander the rate of downvalley migration must be referred to a specific axis, as each point in the meander is migrating downvalley at a different rate (see fig. 3.3). This reference axis is conveniently taken as the line joining the points of inflection of the loop. Cross section types 2 and 3 are therefore taken as lying along the line of this reference axis. Z_{sect} is therefore equal to zero, and the angle at which the channel centre line crosses the reference axis is of course ω. The width adjustment is given by

$$w_s = w/\sin\left\{2.2\sqrt{\frac{sn-1}{sn}}\right\}. \quad (4.4)$$

The lateral section is always defined through the inner bank at the axis of the bend. The direction therefore depends on the relative bank migration in the downvalley direction and normal to the downvalley direction (see fig. 4.2). The net amount of

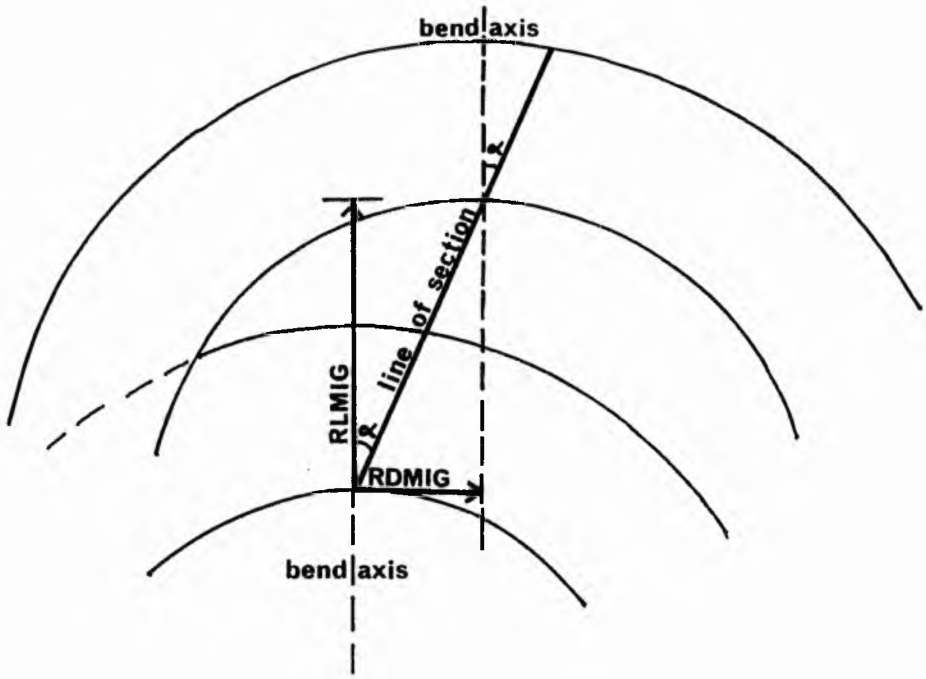

Fig.4.2 Definition of direction of line of section in a lateral section.

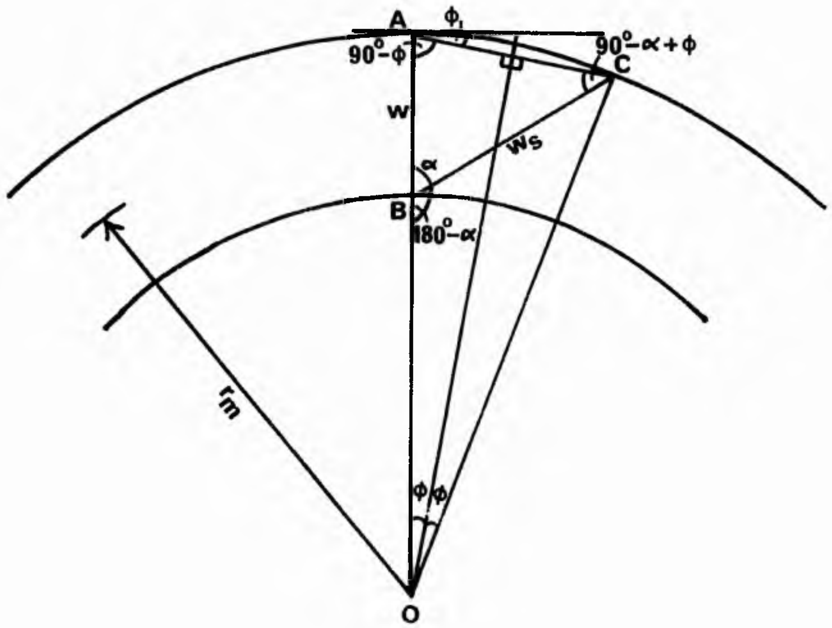

Fig.4.3 Definition of projected channel width (w_s) in a lateral section.

bank migration in this section, RMIG, is given by

$$RMIG = \sqrt{RLMIG^2 + RDMIG^2}\ , \qquad (4.5)$$

where RLMIG and RDMIG are the amounts of bank migration normal to and in the downvalley direction in any given time increment. The angle, α , that the line of section makes with the normal to the downvalley direction is given by

$$\alpha = \tan^{-1} \left(\frac{RDMIG}{RLMIG}\right). \qquad (4.6)$$

It can be seen that this angle will vary depending on the relative rates of bank migration. As in section types 2 and 3, the channel width represented in the section must be continuously adjusted as the meander develops. The adjustment formula is developed below.

By inspection of fig. 4.3, it can be seen that the sine rule applied to triangle OBC gives

$$\frac{OC}{\sin(180 - \alpha)} = \frac{w_s}{\sin 2\emptyset}$$

and for triangle ABC gives

$$\frac{w}{\sin(90 - \alpha + \emptyset)} = \frac{w_s}{\sin(90 - \emptyset)}$$

Eliminating w_s in the above equations, we obtain

$$\frac{OC\sin 2\emptyset}{\sin\alpha} = \frac{w\cos\emptyset}{\cos\alpha\cos\emptyset + \sin\alpha\sin\emptyset}$$

$$\therefore \quad \tan\alpha = \frac{OC\sin 2\emptyset}{w - 2OC\sin^2\emptyset}$$

As $1 + \cot^2\emptyset = \operatorname{cosec}^2\emptyset$ and $\sin 2\emptyset = \frac{2\tan\emptyset}{1+\tan^2\emptyset}$ we can write

$$\tan\alpha = OC\left(\frac{2\tan\emptyset}{1+\tan^2\emptyset}\right) \Big/ w - \frac{(2OC\tan^2\emptyset)}{(1+\tan^2\emptyset)}$$

$$\therefore \tan^2\phi\ (w - 2OC)\tan\alpha - \tan\phi\, 2OC + w\tan\alpha = 0$$

$$\therefore \tan\phi = \frac{OC \pm \sqrt{OC^2 - (w-2OC)w\tan^2\alpha}}{(w-2OC)\tan\alpha}$$

The physically meaningful value of $\tan\phi$ involves the negative of the square root term. Therefore ϕ is given by

$$\phi = \tan^{-1}\left[\frac{OC - \sqrt{OC^2 - (w-2OC)w\tan^2\alpha}}{(w-2OC)\tan\alpha}\right]$$

As $OC = r_m + w/2.0$

$$\phi = \tan^{-1}\left[\frac{r_m + w/2.0 - \sqrt{(r_m + w/2.0)^2 - 2r_m w\tan^2\alpha}}{2r_m\tan\alpha}\right] \qquad (4.7)$$

The projected width, w_s, is then given by

$$w_s = \frac{w\cos\phi}{\cos(\alpha - \phi)} \qquad (4.8)$$

If the rate of downvalley migration is large relative to the migration normal to this direction, the angle, α, is large and the width of the channel represented in the cross section will be considerably greater than the actual channel width. This will also depend on the radius of curvature of the bend. Furthermore, in this situation the point bar deposits produced in the cross section will very quickly be wiped out by the meander limb immediately upstream. Normally, in a developing meander, across valley migration of the channel will be several times greater than downvalley migration and angle α is small. But as the meander develops to its limiting amplitude, the across valley migration gradually slows down, while downstream migration remains about constant (see section 6). Therefore, unless cut off occurs before the rate of downvalley migration becomes large relative to the across valley migration, much of the deposit produced in type 1 section will be wiped out by the upstream meander limb. The model does not take account for the erosive effect of this upstream meander limb in section types 1 or 2, therefore care should be exercised when examining these sections.

5. MODEL FOR DEPOSITION ON THE POINT BAR

Introduction

The model adopted is based largely on Allen's (1970a,b) quantitative semi-empirical theory of lateral deposition which relates grain size and bed form across a curved channel to the existing flow conditions. If the changes across such a channel can be arrived at, the vertical variation within the sediment bar produced by lateral deposition at once becomes known. The term 'lateral deposition' here implies deposition lateral to the local mean downcurrent direction.

In the model it is assumed that the channel geometry is known and that the stream flow can be described by the conventional hydraulic equations, supplemented by a single additional relationship for the helicoidal secondary flow in the channel bend. It will be assumed that each type of bed form in the channel, leading to a distinctive type of sedimentary structure, is characterised by a unique value of the friction coefficient.

5.1 Qualitative features of a system involving lateral deposition

Figure 5.1 shows the main features of the physical situation in which lateral deposition occurs. The curved channel, containing a water stream powerful enough to entrain and transport sediment, is bounded by a steep outer bank and a gently inclined inner bank with a sigmoidal cross profile. The dimensions of the channel are discussed in section 5.6.1.

A water particle travelling along the channel follows a helicoidal spiral path taking it from inner to outer bank when close to the water surface, and from outer bank to inner bank when near the channel bed. The pitch of the spiral path taken by the particle is large even compared with the channel width,

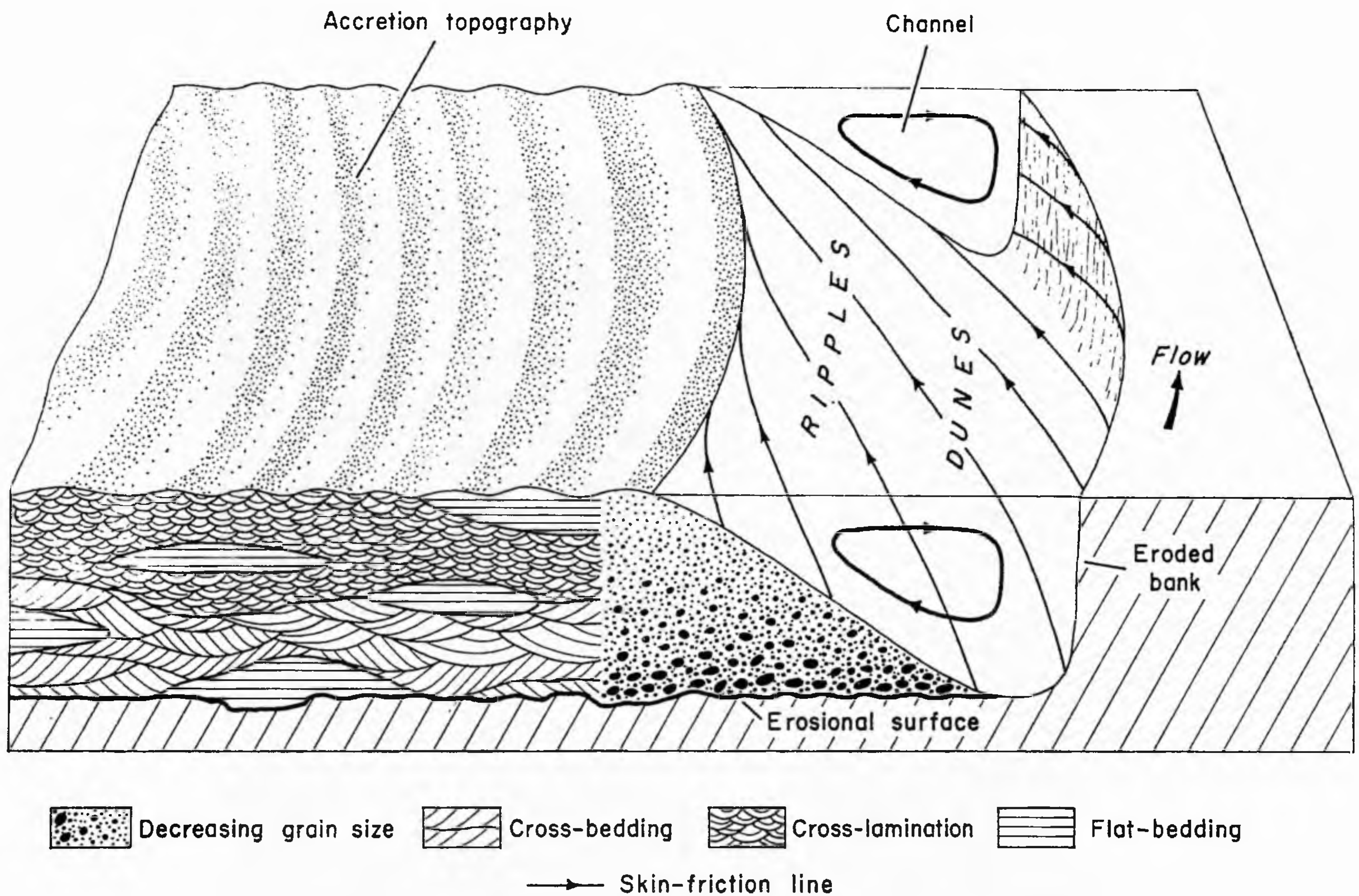

Fig. 5.1. Qualitative features of an ideal channel bend migrating by processes of lateral deposition. Vertical scale exaggerated. (from Allen, 1970a).

so that the transverse component of the particle velocity is small compared with the downstream component. The water particles moving exceedingly close to the channel bed can be represented by special limiting stream lines (skin friction lines) to which the bed shear vector is everywhere tangential. From the pattern of skin friction lines it can be seen why sediment accumulates on the inner bank rather than the outer, lateral deposition building up the inner bank of the channel to balance the erosional losses on the outer bank. Because of its migration in this way, the talweg of the channel sweeps out laterally an erosional surface on which is laid sediment deposited on the inner bank.

It is evident from the pattern of skin friction lines that the fluid flow must exert a component of bed shear stress directed tangentially up the slope of the cross profile. For equilibrium, this upslope force must be balanced by a force of equal magnitude acting tangentially down the slope of the cross profile. Allen (1970a,b) states that the balancing force is purely the body force associated with the sediment travelling over, and in substantially continuous contact with, the channel bed. However the work of Bagnold (1956, 1966) has established the existence also of a direct frictional opposition to the impulsion of the bed load, in the direction of motion, which is proportional to the excess weight of the sediment. The dynamic friction coefficient is defined as $\tan\theta$ and is of the same order as the static solid friction coefficient, not only when the grains are closely packed but also when they are considerably dispersed. In this dynamic condition when the mass of grains is under continuing shear, with mutual jostling motions in all directions, the angle θ is associated with the average angle of encounter between individual grains, and $\tan\theta$ is the ratio of the tangential to the normal components of grain momentum resulting from the encounters. By equating these forces, the way grain sizes of bed material varies over the cross profile may be predicted for equilibrium conditions.

When considering what bed form arises it is assumed that longitudinal slope of the water surface is constant over the cross profile, whence, from the conventional hydraulic equations, the bed shear stress and stream power must both in general decrease inwards from the talweg. Selection of the bed structure will be seen to follow, given empirical data on the hydraulic limits and friction coefficients of different bed forms.

5.2. Shape of cross profile

To describe the geometry of the cross profile it is assumed that the local flow depth varies as

$$\frac{y}{h} = \frac{1}{2}\left[\cos \pi \left(\frac{z}{w_1}\right)^{n_1} - 1\right], \ (z \leqslant w_1), \qquad (5.1)$$

where y is the flow depth, (measured positively downward from water surface), at any transverse distance z across the channel, h is the maximum flow depth measured above talweg, z is the perpendicular transverse distance across the water surface measured from edge of water at inner bank, and w_1 is the width of flow between inner bank and talweg (see fig. 5.2). The exponent n_1 prescribes the degree of concavity or convexity of the cross profile (see fig. 5.3). The cross profiles of natural channel bends are closely approximated by choosing n_1 similar to or a little larger than unity (Allen, 1970a).

The shape of the cross profile in bends has also been described using empirical expressions (e.g. Ripley, 1927), and theoretical expressions which attempt to describe the interactive effect between the loose sediment bed and the fluid flow (e.g. Yen, 1970; Ibade-Zade and Kiyasbeili, 1967; Pokhsraryan, 1957, 1958). An option will exist in the model to enable the use of an alternative expression to equation (5.1). However, a

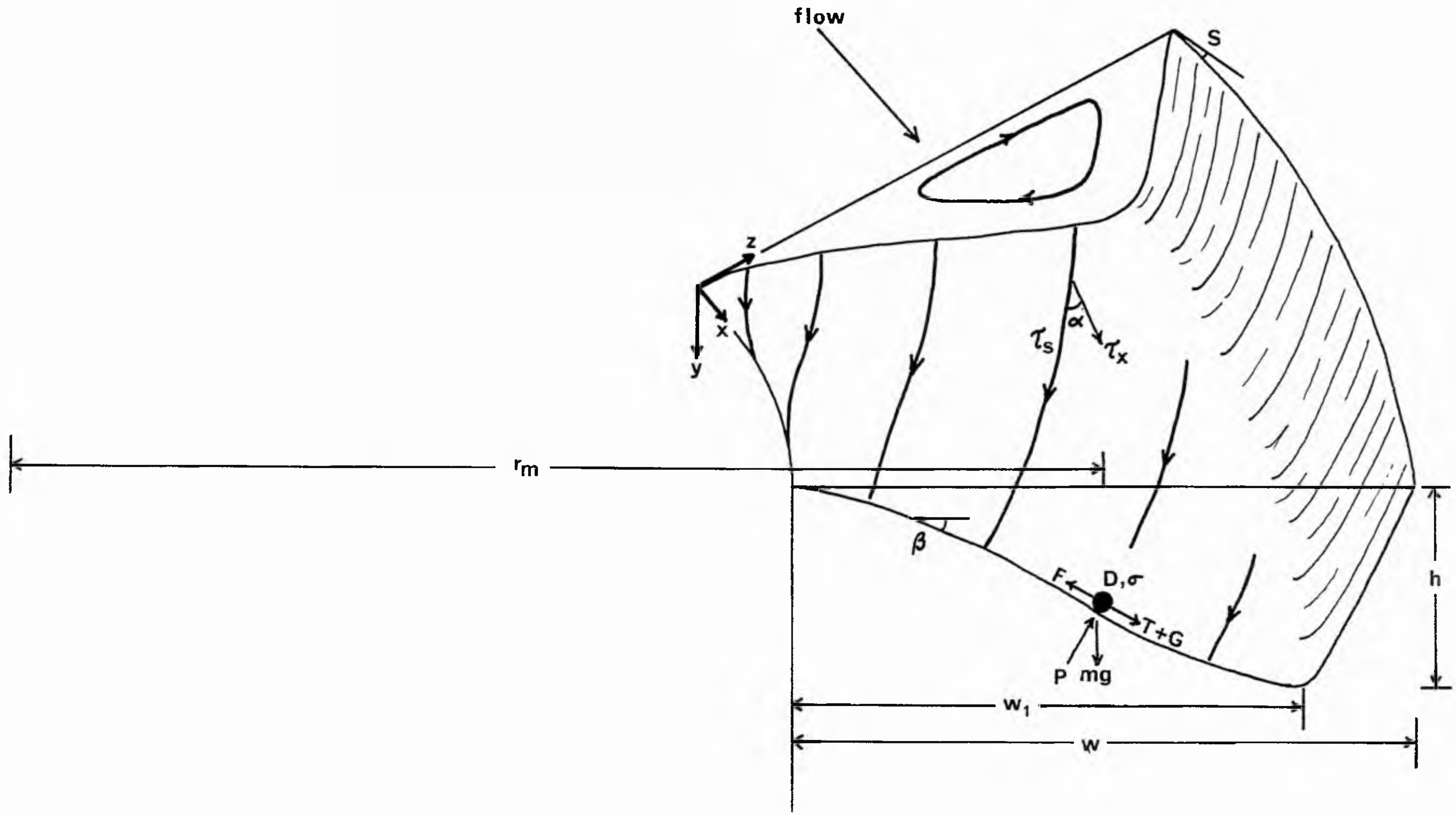

Fig. 5.2 Definition diagram for flow in an open channel bend. (modified after Allen,1970a).

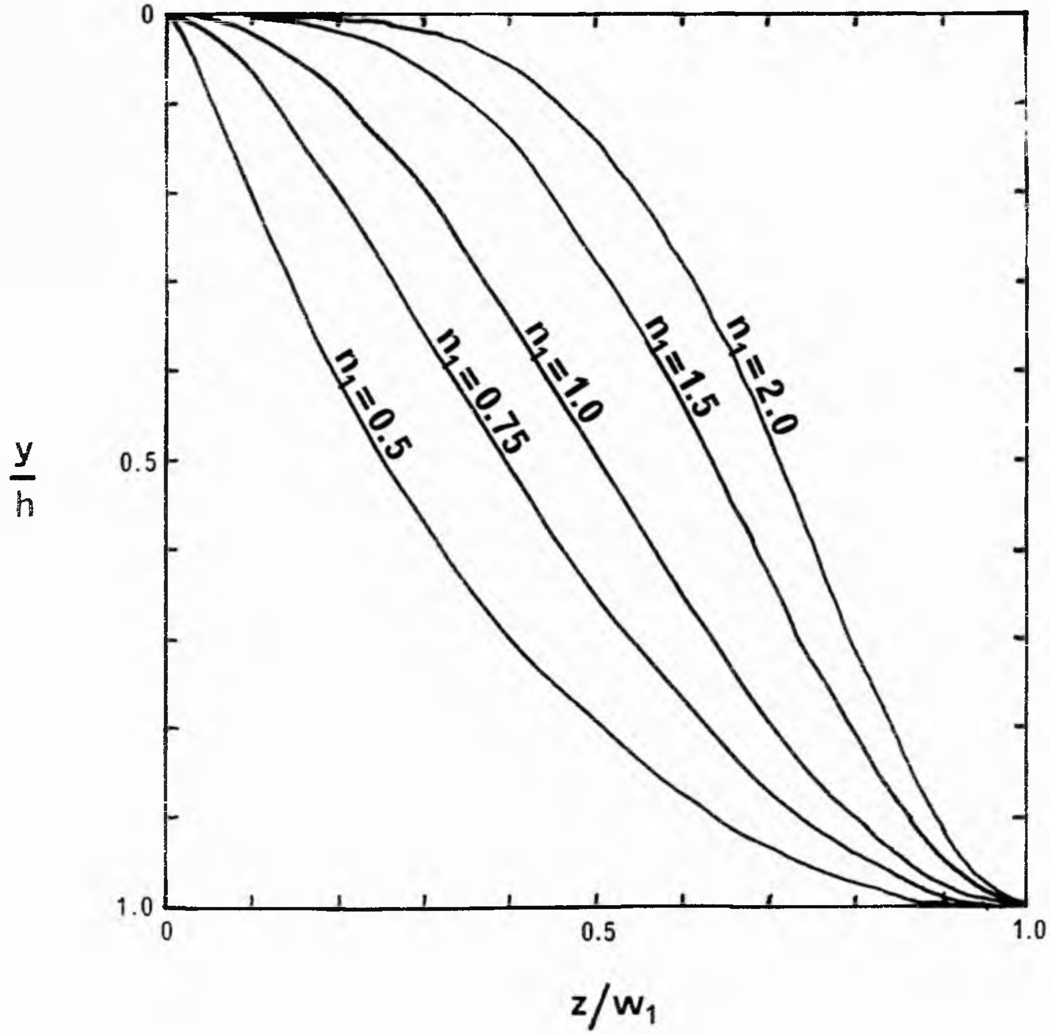

Fig. 5.3 **Dimensionless channel cross profiles, according to equation (5.1). (after Allen, 1970a).**

prerequisite of an alternative expression is that the value of dy/dz and any other defining parameters can be readily supplied. Some of the theoretical equations are unfortunately very cumbersome and others require parameters whose values cannot be readily obtained.

The above expression describes only the inner channel bank on which deposition takes place. An accurate description of the outer bank is not needed, but it is essential to relate channel width, w, to width measured outwards to the talweg. Thus

$$w_1 = k_1 w \tag{5.2}$$

where normally $0.70 \leqslant k_1 \leqslant 0.95$. In the model the shape of the outer bank is defined, for simplicity, with an equation of the form of equation (5.1) with the exponent assuming a value of unity.

5.3 Hydraulic properties of the system

The flow in the cross section of the channel bend can be described using the conventional hydraulic equations. At any transverse distance, z, the bed shear stress parallel to the x-direction (see fig.5.2) is

$$\tau_x = \rho g S y \cos\beta . \tag{5.3}$$

This reduces to

$$\tau_x = \rho g S y \tag{5.4}$$

since β is a small angle and $\cos\beta$ is near unity. Here the slope, S, in the general case represents the slope of the energy grade line. In the special case of uniform flow, the slope of the energy grade line is equal to the bed slope and the longitudinal water surface slope. In this study, S is actually taken as the longitudinal water surface slope, the rationale for which is discussed later.

The bed shear stress at any station z can also be expressed in a form which includes the fluid flow velocity averaged over the vertical at that station, thus

$$\tau_x = \tfrac{1}{8} f \rho V^2 , \qquad (5.5)$$

in which V is the mean fluid flow velocity parallel to the x-direction and f is the Darcy-Weisbach friction coefficient, both at the given station z. The value of f depends on the character of the bed and the flow and describes the flow resistance of the channel. The flow resistance in open channels is a complex problem. The shape of the channel in alluvium changes with flow conditions, bed features of various scales may form, and various degrees of channel sinuosity may develop. These changes affect the drag caused by the surface roughness and introduce form drag caused by bed features, as well as energy losses due to secondary currents. Furthermore, the fluid properties and turbulent characteristics of the flow are changed by moving sediment along the bed and in suspension (Raudkivi, 1967). A further discussion of flow resistance is warranted at this point.

Experimental investigations confirm the conclusions of dimensional reasoning that f is a function of Reynolds number and boundary roughness, as measured by the ratio of the size of roughness elements to the flow depth, or relative roughness. For fully turbulent open channel flow, f no longer depends on the flow Reynolds number, (Allen 1970c). However the application of the Darcy term 'friction coefficient' beyond the context within which it was developed (i.e. uniformly distributed wall friction in pipes) has tended to encourage the tacit assumption that flow resistance in open channels is due principally to friction associated with distributed boundary roughness. This simplified and traditional view of open channel resistance disregards the fact that the 'square law' resistance, described by f as in equation (5.5), may be appreciably increased by the distortion of the flow at discrete bends and other large scale channel irregularities. Also, such internal distortion is accompanied, inevitably, by some deformation of the free water surface, invalidating the required condition that the whole boundary remains fixed.

With steady, nonuniform flow, tangential accelerations occur when velocity is changed in magnitude, and normal accelerations when the velocity is changed in direction. These changes in velocity result in changes in momentum flux, which is accomplished only by pressures against the fluid in addition to pressures which would be associated with uniform flow (i.e. not a hydrostatic pressure distribution). When such changes in velocity occur, zones of separation and secondary flow (i.e. helicoidal flow) frequently result, and this consequently increases the shear and turbulence at the expense of the piezometric head. Hence head losses result. Since the foregoing changes in velocity and the resulting head losses are caused by nonuniform distribution of pressures on the boundary, the losses are termed form losses because of the pressure resistance and the associated changes, usually increases, in shear (Albertson and Simons, 1964).

The components of resistance to flow in a non-prismatic free boundary channel can therefore be stated as:-

(a) Surface resistance (due to grain roughness). Where surface resistance occurs, the flow does not separate from the macroboundary but does separate from the grains, or microroughness. This type of resistance occurs on a plane bed, on the back of dunes, and in antidune flow (Simons and Richardson, 1966).

(b) Pressure resistance (due to form roughness). On the smaller scale, flow separates from the macroboundary in the case of ripples, dunes, and, to a limited extent with antidunes. The result is a pressure reduction in the separation zones (form drag) and the generation of large scale eddies (Simons and Richardson, 1966). A further source of energy dissipation is associated with the nonuniform flow over backs of dunes, and when antidunes grow and subside. On a larger scale, nonuniform flow in meanders gives rise to pressure resistance due to changes in width and depth and changes in alignment, which set up helicoidal flow and sometimes eddies. As already stated pressure resistance normally involves increases in shear.

(c) Spill resistance (Leopold _et al._, 1960). Occurs locally at particular places in open channels under some conditions. Energy is dissipated by local waves and turbulence when a sudden reduction in velocity is forcibly imposed on the flow. Spill resistance is associated with local high velocities as when water backs up behind an obstruction and spills into lower velocity flow. This type of resistance occurs with breaking waves in chute and pool flow, and sometimes in antidune flow. Blocks of bank material slumped into a channel cause such spills as do some bends of sharp curvature.

If the types of resistances (a) and (b) are described in terms of a mean distributed boundary stress, ρgRS (where R is the hydraulic radius), they will vary as the square of the flow velocity (Leopold _et al._, 1960). However, when energy dissipation due to spill is introduced the equivalent distributed boundary stress can no longer be expected to vary as the square of the mean velocity because spill resistance in an open channel cannot exist at low velocities but must start increasing from zero at some finite mean velocity at which parts of the flow become locally supercritical. Such resistances cause foci of intense energy dissipation. Leopold et al. (1960) state that Froude numbers in natural streams show a distinct cut off below the critical value at which spill resistance occurs. They suggest that there exists some threshold beyond which processes operating in a natural channel alter the hydraulic relations at channel cross sections in such a way that the velocity depth ratio is reduced and thus the Froude number is limited.

Discussing the resistance to flow in terms of the Darcy-Weisbach friction coefficient, Ackers and Charlton (1970d) separated the overall friction coefficient, f, into that part representing form losses introduced due to the addition of bends, f_b, and another part representing the resistance due to bed friction of a comparable straight channel, f_s, thus

$$f = rf_s + f_b \quad , \qquad (5.6)$$

where r is a factor by which the straight channel friction factor would have to be multiplied to account for the change in relative roughness (arising from bed features) due to change in hydraulic radius with meandering. This subdivision is convenient for the present study, and the values of f_b, f_s and r to be used in the model are discussed in section 5.6.3.

Bearing in mind these points concerning flow resistance, we can proceed by combining equations (5.4) and (5.5) to give for each station z

$$V = \sqrt{(8gSy/f)} \quad . \qquad (5.7)$$

The Froude number, Fr, an important parameter describing open channel flow, is defined as

$$Fr = V/\sqrt{(gy)} \quad , \qquad (5.8)$$

whence from equation (5.7) the Froude number at each station becomes

$$Fr = \sqrt{(8S/f)} \ . \tag{5.9}$$

The stream power, a significant quantity determining the sediment transport rate and the existence of certain bed forms, is defined as

$$\omega = V\tau_x \ , \tag{5.10}$$

where ω is the stream power. From equations (5.4) and (5.7), we can write

$$\omega = \rho\sqrt{(8/f)}.(gSy)^{3/2} \ . \tag{5.11}$$

In the computations of velocity, Froude number, boundary shear stress and stream power, the longitudinal water surface will be used as an approximation for the required energy slope. In steady, uniform flow this is only approximately true. In the nonuniform flow associated with pools and riffles and horizontal bends, the water surface slope would be expected to vary along the length of the river, and not be parallel to the energy slope. Leopold et al. (1964) have shown, however, that in a meandering reach the energy slope and water surface slope at high stage are more uniform than in a comparable straight reach. The effect of the bend is to increase energy losses due to secondary circulation, thus locally increasing the slope, which would otherwise be lower than over the crossover. This tendency towards uniform distribution of energy expenditure is discussed earlier. Fig. 5.4 from Leopold et al. (1964) shows the uniform water surface slope and energy slope, also that they are practically parallel, the velocity heads being virtually constant along the reach in question.

Fig. 5.4. (from Leopold *et al.*, 1964).

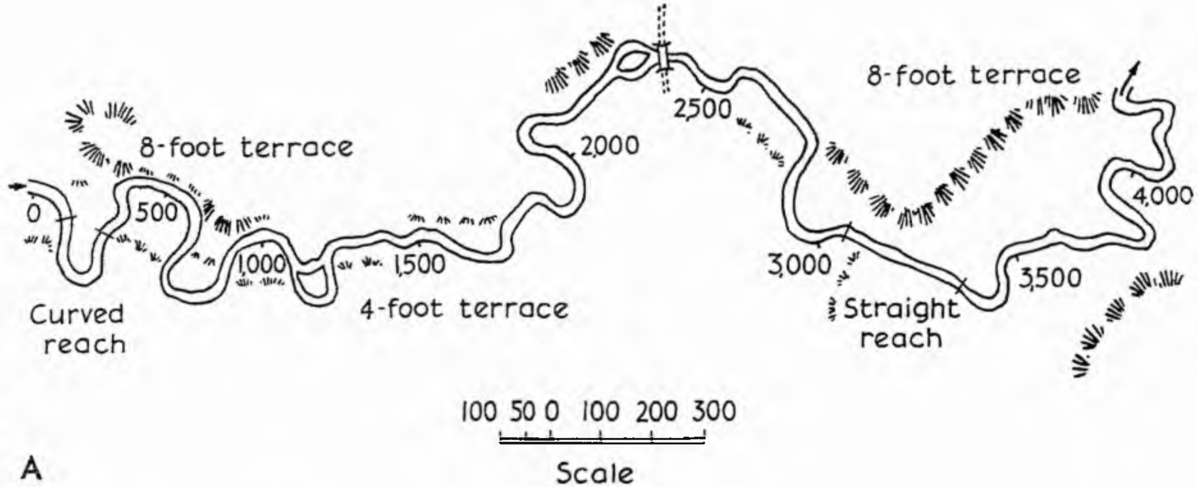

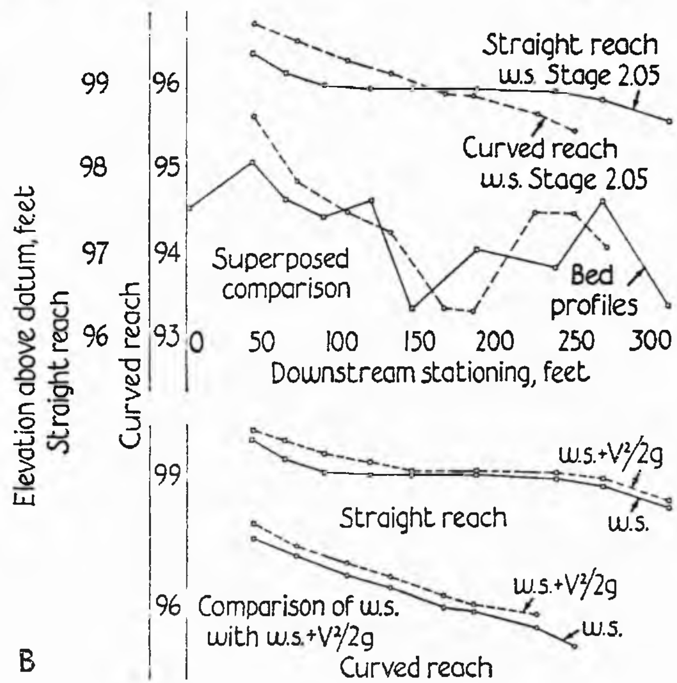

Plan view **(A)** *and profiles* **(B)** *of bed, water surface, and hydraulic grade line, for straight reach and meander reach. Baldwin Creek near Lander, Wyoming, June 12, 1959; flow is near bankfull stage.*

Leopold et al. (1960) comment that an appreciable part of the whole flow resistance ρgRS of an irregular channel is due to internal energy losses in eddies and vortices at local deflections, and therefore the friction slope is not equal to the energy slope. The stresses are probably borne by the projecting portions of the flow boundary. A considerable portion of this stress will consist of components normal to the local flow boundary and therefore of a nonerosive nature. As a result, the river bed on the whole must be relieved of a portion of the overall bed shear as given by ρgRS. This does not detract from the fact that shear is increased with nonuniform flow, as previously discussed, and that the maximum bed shear is higher in bends than in comparable straight reaches (Ippen and Drinker, 1962; Ackers and Charlton, 1970d). It should be noted, however, that increase in shear due to transverse circulation alone was not found to be very great by Shukry (1950) in his experiments. Rozovskii (1961) derives an expression for these losses.

Assuming that the longitudinal slope of the water surface ($\approx$ energy slope) is constant across the channel cross section we find that in a given cross section (a) local bed shear stress parallel to the channel centre line depends only on the local flow depth (b) the local mean flow velocity and stream power depend only on the local flow depth and the Darcy-Weisbach coefficient and (c) the local Froude number depends only on the local friction coefficient.

It remains necessary to account for the helicoidal motion of fluid particles carried through the channel bend and past a cross section of interest. We are chiefly concerned with the flow exceedingly close to the bed on the inner bank of the channel, that is, with the skin-friction lines, or limiting streamlines, of the motion. Rozovskii (1961) found theoretically and empirically that

$$\tan\alpha = 11y/r_1 \tag{5.12}$$

where α is the angle on the bed between the channel centre line and the skin friction line of the helicoidal flow, at any station z. Here, r_1 is the local radius of curvature. This expression will be found sufficient to take account of the helicoidal flow.

5.4 <u>Variation of grain size over the cross profile</u>

Because of the helicoidal flow in the channel, the fluid exerts a shear stress component directed upslope in the plane of the cross profile. However, a sediment particle moving over the bed in substantially continuous contact with it must be affected by the downslope component of the body force and the dynamic frictional stress due to shearing over other grains. Because the speed of lateral movement of the channel cross profile due to bank erosion and deposition is small compared with the speed of advance in the bed load layer of a slowly moving sediment particle, it can be supposed that equilibrium is achieved when the downslope force components are equal to the upslope component of the fluid force. The particle will then follow a path parallel to the channel centre line and, by equating the three force components, we can find the variation of particle size over a cross profile whose geometry is specified.

With the conventions of fig. 5.2, the body force component, G, acting on a particle of diameter D at a station on the cross profile is

$$G = \frac{4}{3}\pi\left(\frac{D}{2}\right)^3(\sigma-\rho)g\sin\beta \tag{5.13}$$

where β is the angle of slope of the cross profile, and σ and ρ are the sediment and fluid density respectively.

The frictional force opposing motion, T, in the plane of the cross profile is given by

$$\begin{aligned} T &= P\tan\theta \\ &= \frac{4}{3}\pi\left(\frac{D}{2}\right)^3(\sigma-\rho)g\cos\beta\tan\theta \end{aligned} \tag{5.14}$$

where P is the normal stress, and tanΘ is the dynamic friction coefficient of solid friction as previously described.

The upslope componenent of the fluid force is

$$F = \pi\left(\frac{D}{2}\right)^2 . \tau_s \sin\alpha = \pi\left(\frac{D}{2}\right)^2 . \tau_x \tan\alpha \qquad (5.15)$$

where τ_s is the bed shear stress measured tangentially to the skin friction line at the station considered. For equilibrium, F=T+G and

$$\sin\beta + \cos\beta \tan\Theta = \frac{3\tau_x \tan\alpha}{2(\sigma - \rho)gD} \qquad (5.16)$$

As β is very small, we may write $\sin\beta \approx \tan\beta$ and $\cos\beta \approx 1$, whence

$$\tan\beta = \frac{dy}{dz} = \frac{3\tau_x \tan\alpha}{2(\sigma - \rho)gD} - \tan\Theta \qquad (5.17)$$

A second expression for dy/dz is obtained by differentiating with respect to z the equation for the variation of local flow depth in the cross profile, y. If this is taken as equation (5.1), neglecting the negative sign, we obtain

$$\frac{dy}{dz} = \frac{n_1 z^{(n_1-1)}\pi h}{2w_1^{n_1}} \sin\pi\left(\frac{z}{w_1}\right)^{n_1}, \qquad (z \leqslant w_1). \quad (5.18)$$

Eliminating dy/dz between equations (5.17) and (5.18), and after substitutions from equations (5.4) and (5.12), an expression for D can be obtained as

$$D = \frac{33\rho S y^2 w_1^{n_1}}{r_1(\sigma-\rho)\left[n_1 z^{(n_1-1)} \pi h \sin\pi\left(\frac{z}{w_1}\right)^{n_1} + 2w_1^{n_1}\tan\Theta\right]}. \qquad (5.19)$$

Bagnold (1956) was able to define values of tanΘ under conditions in which the moving bed load solids are sufficiently numerous to interpose an effective flow boundary between the free fluid flow above and the stationary bed below. This critical stage is approximately when bed features disappear, or at least cease to create appreciable form drag. Above this critical stage experiments show $\tan\Theta$ to vary from 0.375 to 0.75 according to the conditions of shear owing to the variation of fluid-viscosity effects with variation of grain size and mass. Below this critical stage, Bagnold gives grounds for assuming values of $\tan\Theta$ over a similar range of values, depending on grain size only.

Grain size profiles were calculated using constant values of $\tan\Theta$ of 0.0, 0.3 and 0.6 for six separate cross sections in order to assess the importance of the dynamic frictional stress. The values of the other parameters used in equation (5.19) were conveniently taken from Allen (1970a). In reality the value of $\tan\Theta$ will vary over each profile with the conditions of shear, as defined by Bagnold (1956, 1966), however, by inspection of fig. 5.5 it can be seen that the effect of $\tan\Theta$ on the grain size distributions is so small that its variation over the cross profile can be ignored.

For simplicity, therefore, it is considered justifiable to omit the effect of $\tan\Theta$ and assume a value of zero. Equation (5.19) then becomes

$$D = \frac{33\,\rho\,S w_1^{\,n_1} y^2}{\pi n_1 (\sigma - \rho) r_1 \; h z^{(n_1 - 1)} \; \sin \pi \left(\frac{z}{w_1}\right)^{n_1}} \qquad (5.20)$$

Equation (5.20) has implications about the general calibre of the load that can be carried through a specified channel bend, as well as about the variation of particle size over a given cross profile in the bend. The general calibre of the load increases with ascending water surface slope, maximum channel depth, and channel width between the inner bank and the talweg. The general

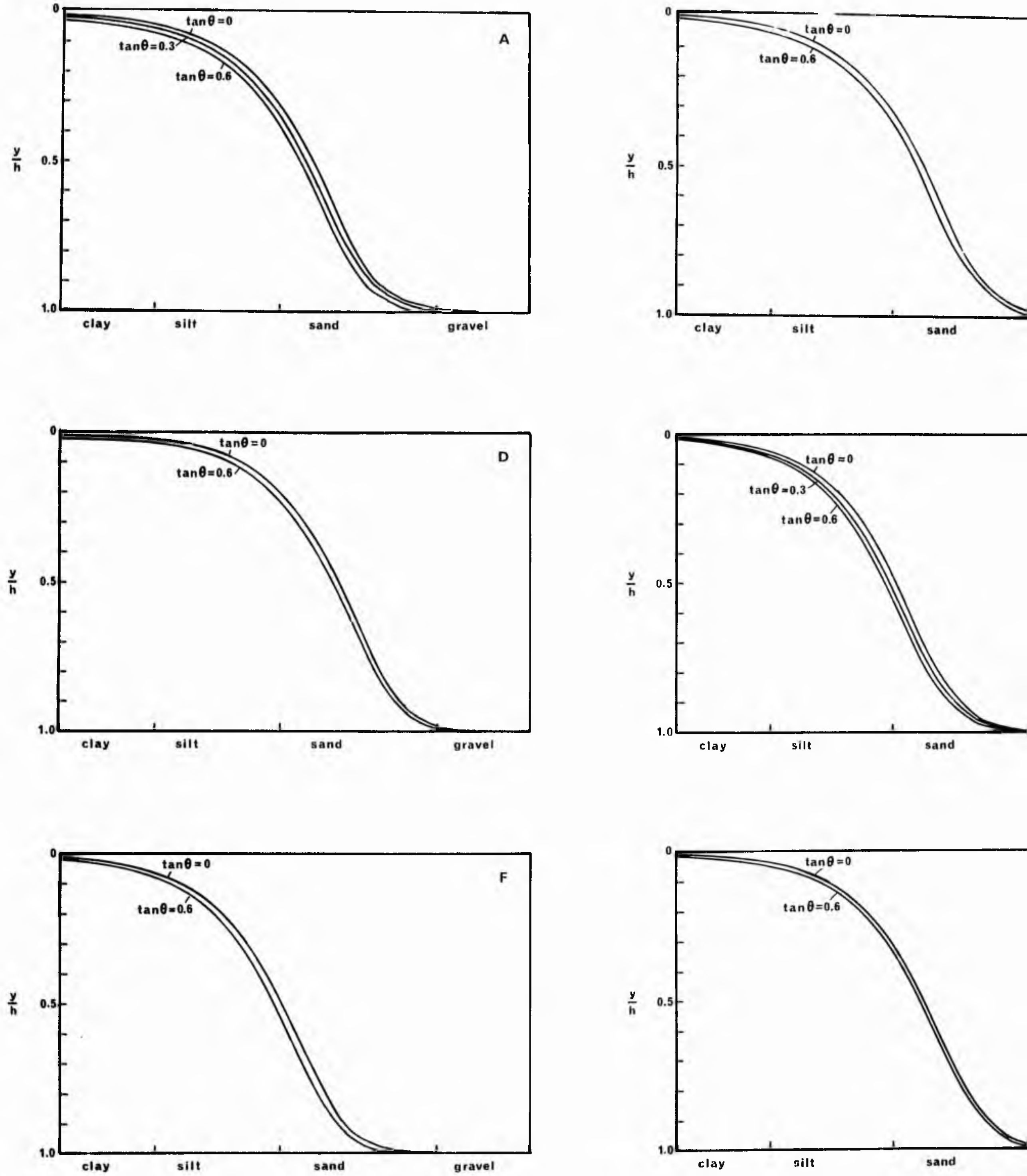

	h (metres)	w_1(metres)	r_m(metres)	S	
A	4.05	405.0	4050.0	0.000285	$n_1 = 2$
C	3.2	96.0	336.0	0.000125	$k_1 = 0.8$
D	4.4	110.0	228.8	0.0000973	$\sigma = 2.65$ gm/cm³
E	1.92	48.0	201.6	0.000124	$\rho = 1.0$ gm/cm³
F	3.2	80.0	300.0	0.0000666	
G	5.55	138.0	520.0	0.0000768	

FIG. 5.5 GRAIN SIZE PROFILES, ACCORDING TO EQUATION (5.19), C
FOR DIFFERENT VALUES OF DYNAMIC FRICTION COEFFICIE
OTHER INPUT PARAMETERS TAKEN FROM ALLEN, 1970a.

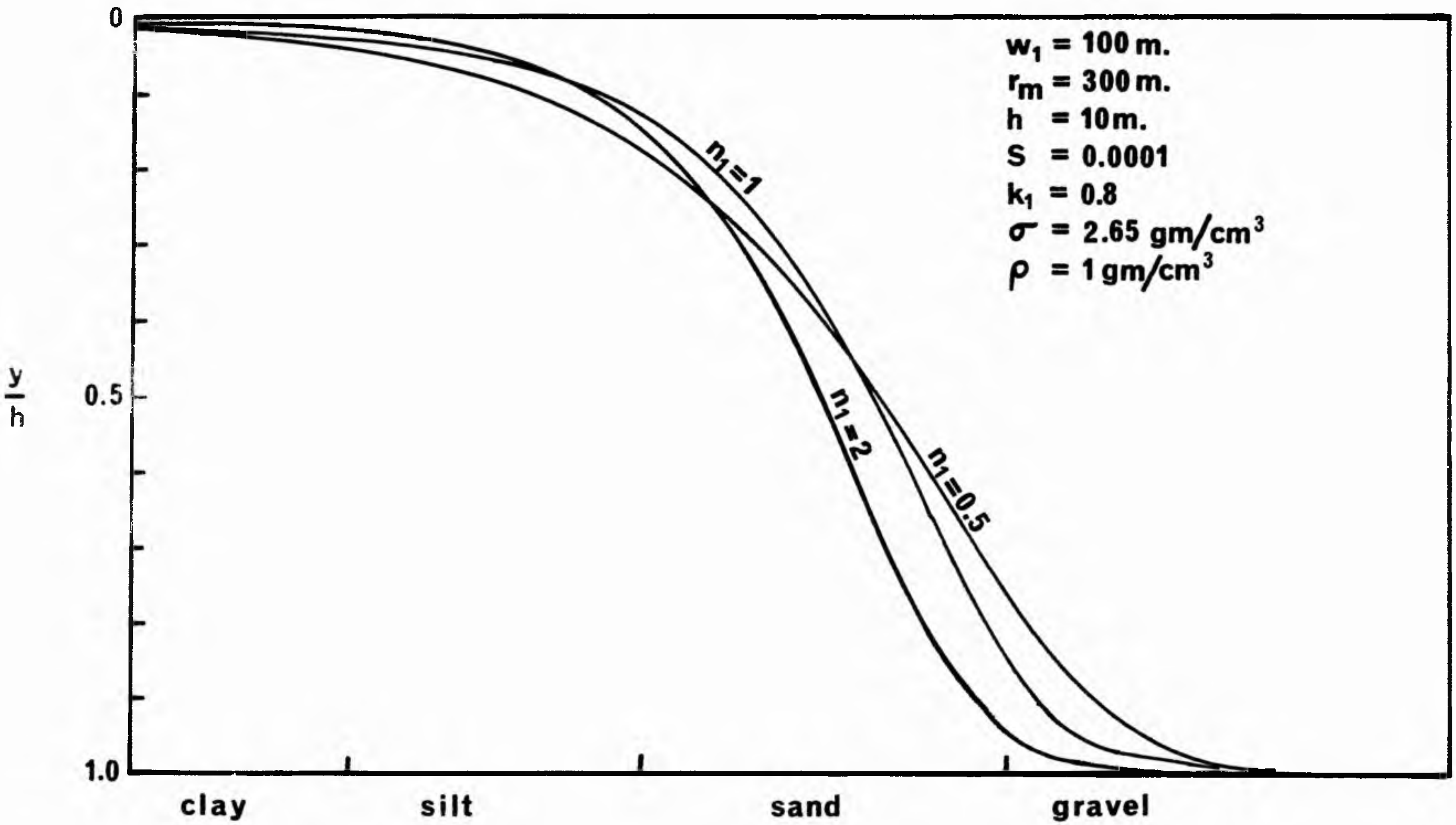

Fig. 5.6 Grain size profiles, according to equation (5.20), calculated for different values of n_1.

calibre decreases with increasing radius of curvature of the bend and convexity of the cross profile. As regards the cross profile, particle size increases from D=0 on the inner bank of the channel, to $D=\infty$ at the talweg. In practice D is not equal to infinity at the talweg, though it is commonly large, gravel being present. The steepness of the grainsize profile is very sensitive to changes in n_1 and fig. 5.6 illustrates some of the alternative grain size profiles obtained with different values of n_1.

5.5 Variation of bed form and internal structure over the cross profile

In the absence of large bars, the bed forms that occur in flume experiments and natural rivers (depending on flow, fluid, geometry and sediment characteristics) are ripples, ripples on dunes, dunes, plane beds, antidunes, and chutes and pools. These bed forms are classified into a lower flow regime, an intermediate transition zone, and an upper flow regime (Simons et al., 1961, 1965; Simons and Richardson, 1966, 1971). Classification is based on similarity of bed form, mode of sediment transport, and magnitude of resistance to flow (see fig. 5.7).

The primary sedimentary structures associated with ripples, dunes, flat beds and antidunes are respectively, cross lamination, cross bedding, flat bedding, and cross beds inclined at low angles upstream (Allen, 1968; Harms and Fahnestock, 1965). Although trough cross bedding is generally thought to be associated with dune migration, controversy exists over the exact nature of the sedimentation process and the type of dunes responsible (Allen, 1968). Tabular cross beds are thought to be associated with straight crested dunes, although flat topped transverse bars are probably responsible for some of the larger scale varieties (Allen, 1968).

Flow regime	Bed form	Bed Material concentrations (ppm)
Lower regime	Ripples	10–200
	Ripples on dunes	100–1,200
	Dunes	200–2,000
Transition	Washed out dunes	1,000–3,000
Upper regime	Plane beds	2,000–6,000
	Antidunes	2,000→
	Chutes and pools	2,000→

Fig. 5.7. Classification of flo

Mode of sediment transport	Type of roughness	Phase relation between bed and water surface
Discrete steps	Form roughness predominates	Out of phase
	Variable	
Continuous	Grain roughness predominates	In phase

w regime. (from Simons *et al.*, 1965).

5.5.1 Allen's model

To determine the variation of bed form, hence sedimentary structure over the cross profile, Allen (1970a,b) draws heavily on empirical information. The results of Guy et al. (1966) and Williams (1967) lead to fig. 5.8 showing that the occurrence of ripples, dunes and lower phase plane beds in quartz density sands is determined by stream power and calibre of load. It will be noted that a plane bed, and not ripples, is generated at conditions just a little more severe than the threshold of movement in the case of quartz density sands for which $D \geqslant 0.065$cm. If, in the case of a given flow, the flow conditions are made severe enough, a plane bed referable to an upper phase of such beds will appear. Upper phase plane beds depend for their appearance simply on a relationship between the bed shear stress and the body force exerted by the particles of the load, and not uniquely on stream power, as seen below.

Fig. 5.9 shows the variation of the Darcy-Weisbach friction coefficient with stream power and bed form, using the data of Guy et al. (1966). It can be seen that there is a well defined value of the stream power at which ripples or lower phase plane beds change to dunes for a given calibre of load, but that plane beds overlap with dunes as regards stream power. Under very severe flow conditions in an open channel, antidunes appear when the Froude number is in the neighbourhood of unity. These bed forms also are not uniquely determined by stream power.

Referring to fig. 5.9 it can be supposed that ripples and dunes are associated with a constant value of the friction coefficient. This will be designated as f_1 (=0.08 in fig. 5.9). It can also be supposed that plane beds of either phase and antidunes also take a constant value f_2(=0.02 in fig. 5.9). In practice, the friction coefficient for a given bed form is not

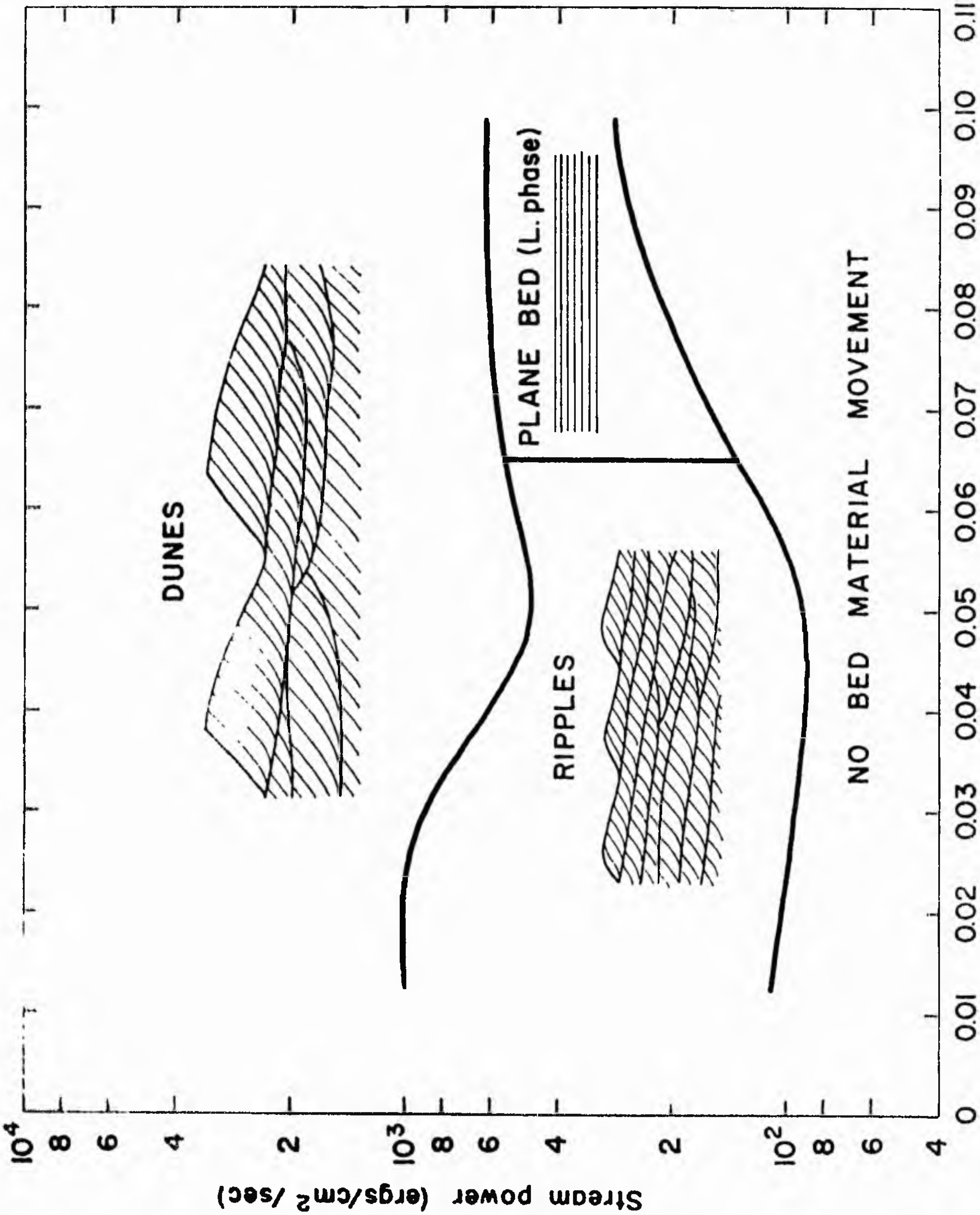

Fig. 5.8. Bed form as a function of stream power and calibre of load using data of Guy et al., 1966; Williams, 1967. (from Allen, 1970a).

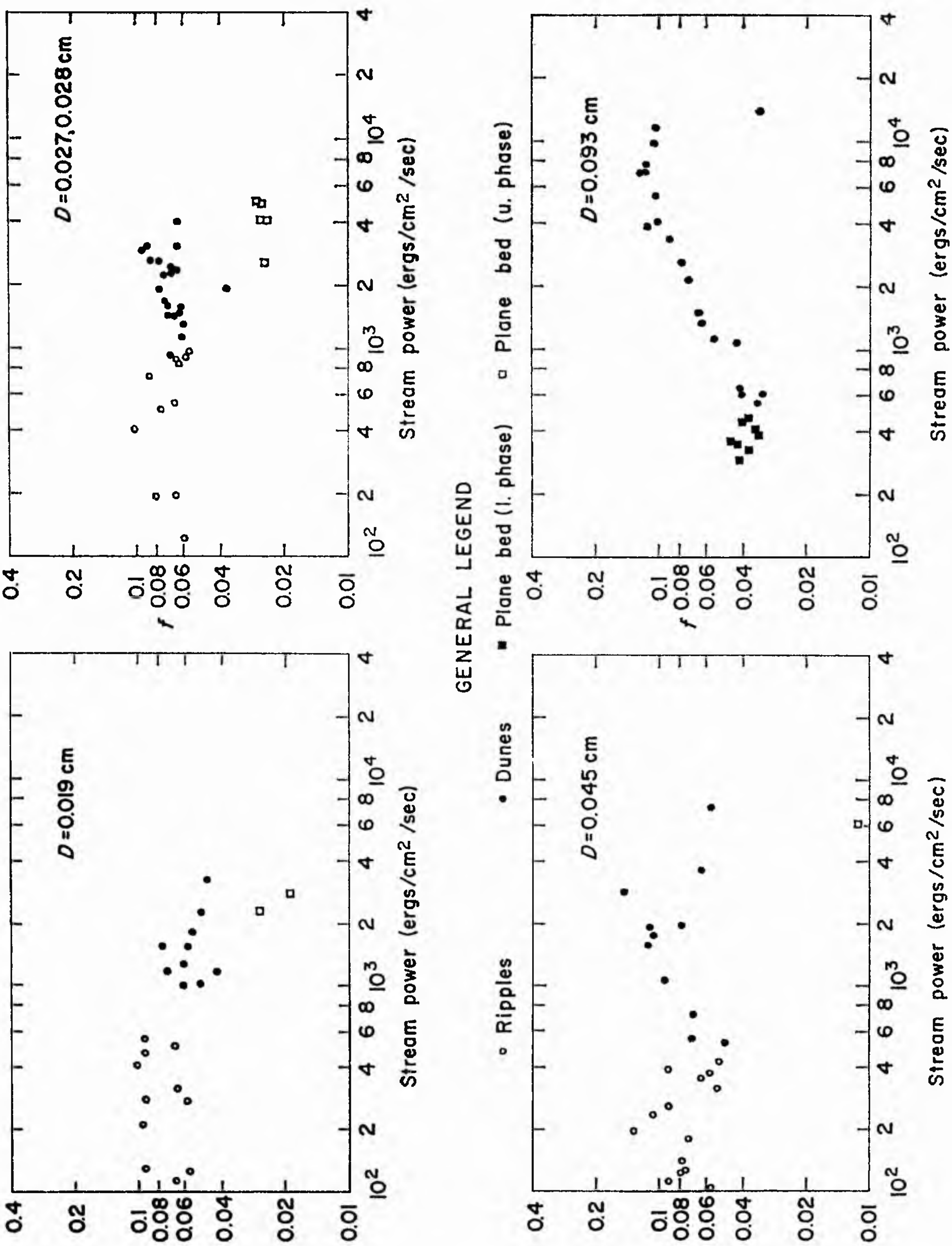

Fig. 5.9. Darcy-Weisbach friction coefficient as a function of bed forms, stream power and calibre of load using data of Guy et al., 1966. (from Allen, 1970a).

unique, being subject to a 20% variation or thereabouts in the diagram shown. Allen (1970a) considers the assumption of a constant value of the coefficient acceptable at the level of accuracy desired in the study. One further point is that diagram 5.9 refers to experiments in straight flumes, therefore the values of f_1 and f_2 quoted by Allen must be adjusted to account for the additional losses associated with bends, according to equation (5.6). This is discussed fully in section 5.6.3.

Kennedy (1963) showed that the minimum Froude number for the appearance of antidunes is Fr=0.844 and that the Froude number at which antidunes are the bed forms is insensitive to changing flow conditions. Therefore the bed form in the channel is antidunes if

$$Fr = \sqrt{(8S/f_2)} \geqslant 0.844 \qquad (5.21)$$

but is either a plane bed, dunes or ripples if

$$\sqrt{(8S/f_2)} < 0.844 \ . \qquad (5.22)$$

If the bed form is ripples or dunes by the inequality (equation (5.22)), then the friction coefficient f_1 is used in the calculation of actual mean flow velocity, Froude number and stream power.

In order to say whether a plane bed, dunes or ripples appear as the bed form at a given station, we first write for that station the dimensionless shear stress

$$\Theta = \tau_x / gD(\sigma - \rho) \qquad (5.23)$$

where Θ is the dimensionless shear stress and τ_x and D are the bed shear stress parallel to the channel centre line and the particle diameter, respectively, at the given station.

Bagnold (1966) and Hill (1966) showed theoretically, with an experimental justification, that granular solids driven over the bed of a fluid stream will exist as an upper phase plane bed provided that

$$\theta \geqslant \theta_{crit} \tag{5.24}$$

wherein θ_{crit} is the critical value of the dimensionless shear stress, dependent on particle size. When this inequality is not satisfied then either ripples, lower phase plane beds, or dunes will appear, depending on the local stream power.

Substituting for D from equation (5.20), equation (5.23) can be written as

$$\theta = \frac{\pi n_1 r_1 h z^{(n_1-1)} \quad \sin\pi\left(\frac{z}{w_1}\right)^{n_1}}{33 w_1^{\,n_1} y} \tag{5.25}$$

which, like equation (5.20) itself, depends strongly on exponent n_1.

Inspection of equation (5.25) will show that the value of θ for a channel bend increases in general magnitude with ascending radius of curvature, but decreases with increasing flow width. Thus large ratios of radius of curvature to channel width favour upper phase plane beds as the bed form, whereas small ratios favour ripples and dunes. There is, however, a critical range of values of the ratio which could permit upper phase plane beds at restricted levels in the channel cross profile, depending on values of the exponent n_1 (see fig. 5.10).

It remains explicitly to assign numerical values to θ_{crit}. According to the results of Bagnold (1954, 1966) these are, approximately

$$\theta_{crit} = 0.52 \quad (D < 0.025\text{cm.})$$

$$\theta_{crit} = (0.56 - 1.43D) \quad (0.025 \leqslant D \leqslant 0.20\text{cm.}) \tag{5.26}$$

$$\theta_{crit} = 0.27 \quad (D > 0.20\text{cm.})$$

for quartz density sands in water, depending primarily on how the grains behave when sheared in dense array over the stream bed, which was discussed previously in section 5.4.

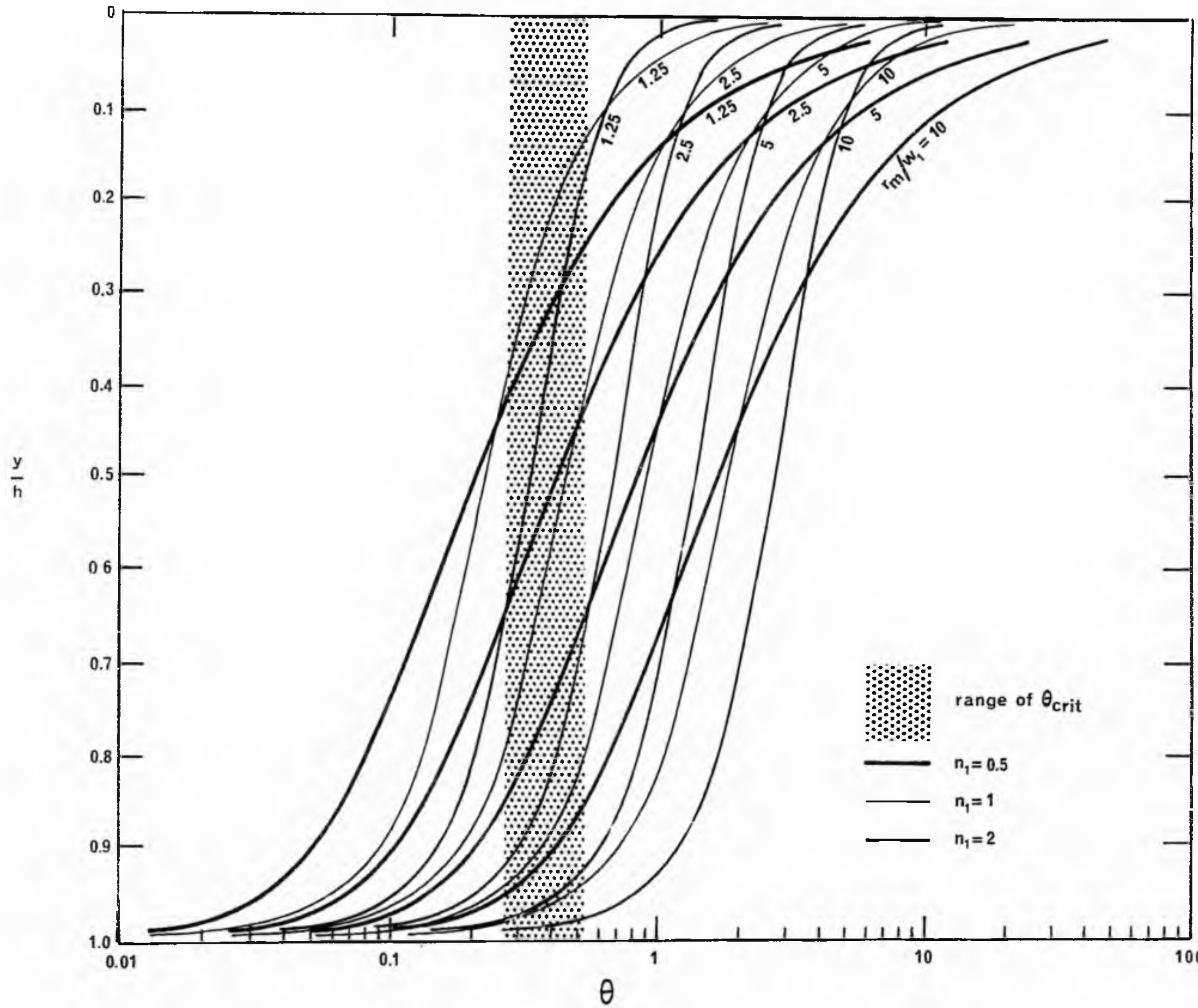

FIG. 5.10 PROFILES OF DIMENSIONLESS BED SHEAR STRESS AS A FUNCTION OF RATIO OF RADIUS OF CURVATURE TO CHANNEL WIDTH, ACCORDING TO EQUATION (5.25).

Either ripples, lower phase plane beds, or dunes are the bed form if the inequality, equation (5.24), is not satisfied. The choice may be made on the basis of the local stream power, for, as can be seen in figure 5.9, there is a definite value of the power for a given calibre of load at which ripples or lower phase plane beds give place to dunes. The bed form is dunes if

$$\omega \geqslant \omega_{crit} \tag{5.27}$$

where ω_{crit} is the critical power for the transition from ripples or lower phase plane beds to dunes, but ripples or lower phase plane beds if

$$\omega < \omega_{crit} \tag{5.28}$$

Values of ω_{crit} can be obtained from the experimental data summarised in fig. 5.9, thus

$$\begin{aligned}
\omega_{crit} &= 750 \quad (D \leqslant 0.023\text{cm.}) \\
\omega_{crit} &= 950 \quad (0.023 < D \leqslant 0.036\text{cm.}) \\
\omega_{crit} &= 475 \quad (0.036 < D \leqslant 0.069\text{cm.}) \\
\omega_{crit} &= 520 \quad (D > 0.069\text{cm.})
\end{aligned} \tag{5.29}$$

where ω_{crit} is in the units ergs $\text{cm.}^{-2}\text{sec.}^{-1}$.

If the inequality, equation (5.27), is not satisfied, then from fig. 5.8 ripples are the bed form if

$$D \leqslant D_{crit} \tag{5.30}$$

but lower phase plane beds appear when

$$D > D_{crit} \tag{5.31}$$

where D is the particle diameter of the local bed material and D_{crit} = 0.065cm.

Thus the bed form is selected by the application of a series of inequalities to stations on the channel cross profile.

Whether antidunes appear is determined by the Froude number, controlled primarily by the longitudinal slope of the water surface. It may be noted that since in the present model the slope is assumed constant in each cross section, antidunes either fill the whole channel width or do not appear at all. In the field, however, antidunes can occur in the same reach of the river as other bed forms (Kennedy, 1963). If the Froude number of flow is less than that required for antidunes, either plane beds, dunes or ripples may occur. Distinction between an upper phase plane bed and dunes, ripples or lower phase beds is made on the basis of an inequality involving the bed shear stress and the calibre of load combined in the form of a dimensionless stress. When the dimensionless stress falls below a critical value for an upper phase plane bed, either dunes, ripples or lower phase plane beds may be the bed form. The choice between the latter three is made using the knowledge that ripples or lower phase plane beds give place to dunes at a critical value of the stream power, and that ripples occur only when the calibre of the load material is less than a certain value.

5.5.2 <u>Alternative models</u>

Allen's (1970a,b) model for the prediction of bed form across the channel cross profile draws on the results of both theoretical and experimental work. Over the years many authors have attempted to predict the hydraulic limits for the existence of the various bed forms, and consequently a large body of experimental and field data exist. The predictive methods used have been by graphical or multivariate statistical analysis of empirical data, based on some theoretical reasoning, or by purely theoretical approaches. These methods are summarised, for example, in Allen (1968), Graf (1971), Raudkivi (1967), and Simons and Richardson (1971).

It is not intended here to go into the analysis of alluvial bed form mechanics (see, for instance, Allen (1968), Mercer (1971), Raudkivi (1967)), or perform a critical assessment of the many different approaches to the problem of bed form prediction. It is intended to describe some alternative models to that of Allen, which are thought to be equally acceptable in view of the prevailing state of knowledge. These alternative models inevitably contain certain elements in common with each other and with Allen's model. The differences that exist lie essentially in the prediction of the change from lower regime forms to upper regime forms.

5.5.3 Alternative model no. 1

In discussing the graphical method of prediction, Simons and Richardson (1971) point out its inability to consider all the variables involved in the problem, as opposed to the multivariate statistical technique. They point out the failures of some of the graphical methods proposed, and conclude that the relation between bed form, stream power, and median fall diameter of bed material fits the field and flume data fairly well. In fact the lower flow regime part of this relation is used in Allen's model previously discussed, with the substitution of median grain size for fall diameter.

Simons and Richardson (1971) also favour a Fr,R/D plot proposed by Athaullah and Simons (1970), however this plot only distinguishes between regimes rather than specific bed form types (see fig. 5.11). In this model, therefore, additional criteria are required to distinguish the different bed forms within the regimes. The delineation of the transition regime constitutes an improvement on Allen's model.

From fig. 5.11, the equations of the lines dividing the upper regime, transition and lower regime can be obtained. The line dividing the upper flow regime from the transition is given approximately by

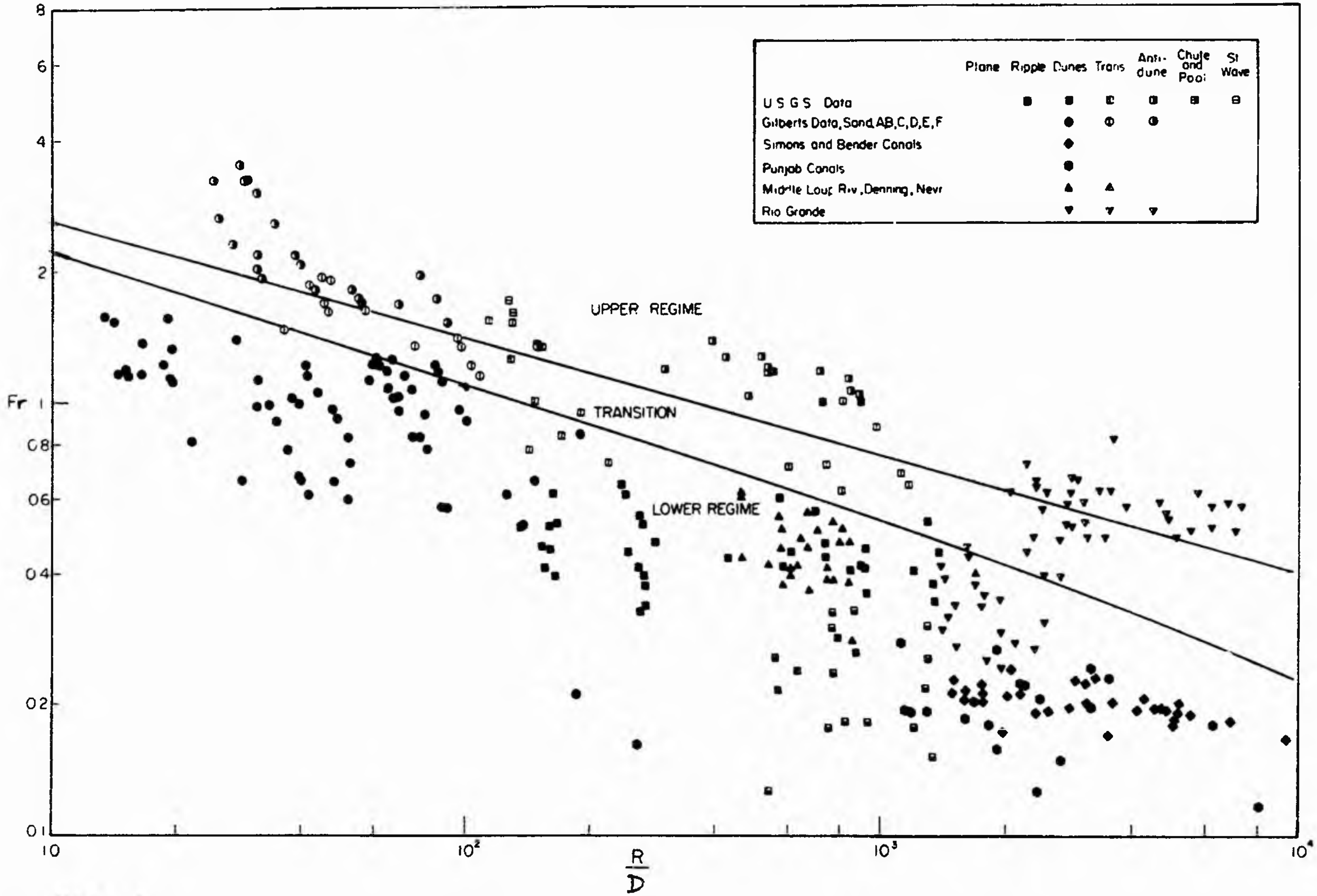

Fig. 5.11. Froude number, Fr, versus R/D criterion. (from Simons and Richardson, 1971).

$$\log_{10}Fr_u = 0.75 - 0.27 \log_{10}(R/D) \qquad (5.32)$$

where Fr_u is the Froude number at the change from transition to upper flow regime, R is the hydraulic radius and D is the particle diameter. Upper flow regime forms, upper phase plane beds or antidunes, will therefore form at a station if

$$\log_{10}Fr = \log_{10}(\sqrt{8S/f_2}) > \log_{10}Fr_u. \qquad (5.33)$$

In order to separate the antidunes and plane bed fields, the critical Froude number of 0.844 is used, as in Allen's model.

The line dividing the transition from the lower flow regime is given approximately by

$$\log_{10}Fr_t = 0.67 - 0.33 \log_{10}(R/D) \qquad (5.34)$$

where Fr_t is the Froude number at the change from lower flow regime to transition. Lower flow regime bed forms, dunes, ripples, or lower phase plane beds, will therefore form at a station if

$$\log_{10}Fr = \log_{10}(\sqrt{8S/f_1}) \leqslant \log_{10}Fr_t . \qquad (5.35)$$

The lower flow regime bed form fields will be separated by the stream power, median diameter of bed material criterion, fig. 5.8, as in Allen's model.

It should be noted here that extrapolation of boundary lines separating bed forms or regimes, outside the data fields to which they relate, is not strictly valid. This should be borne in mind when using equations (5.32) and (5.34) above, and in any other cases where a limited range of data points is used.

5.5.4 Alternative model no. 2

This model is the same as Allen's except that the existence of an upper phase plane bed instead of ripples or dunes is determined using the criteria proposed by Hill *et al.* (1969).

From dimensional analysis and theoretical considerations, they produce a general functional relationship applicable for the instability of an upper phase plane bed,

$$\frac{V_{*crit}D}{\nu} = f \left(\frac{gD^3}{\nu^2}\right) \qquad (5.36)$$

where V_{*crit} is the critical shear velocity for the instability and ν is the kinematic viscosity (cm^2/sec). Shear velocity, V_*, is defined here as $\sqrt{\tau_x/\rho}$, and has the dimensions of velocity. They further state that the two instabilities of upper phase plane bed to dunes and upper phase plane bed to ripples would represent two distinct functional relationships. Fig. 5.12 represents the stability diagram drawn from their own experimental data combined with that of other investigators, and demonstrates the existence of the two apparently distinct trends. The greater scatter of points shown by the data of 'other investigators' is due to the fact that the lowest observed values of shear on a plane bed were used. It should be realised that no transition regime is explicitly recognised in this model.

For high values of gD^3/ν^2 the plane bed is replaced by dunes while for low values the plane bed changes over to ripples. The authors explain this situation in terms of a dominant force at the particle level. The parameter gD^3/ν^2 can be looked upon as a ratio of the gravitational force to the viscous force on the particle. Then it simply follows that when the gravitational force dominates compared to the viscous force dunes result on the plane bed. On the other hand, if the viscous forces are more dominant than the gravitational forces, ripples seem to develop on the plane bed.

Hill et al. (1969) then tried to fit equations of the form

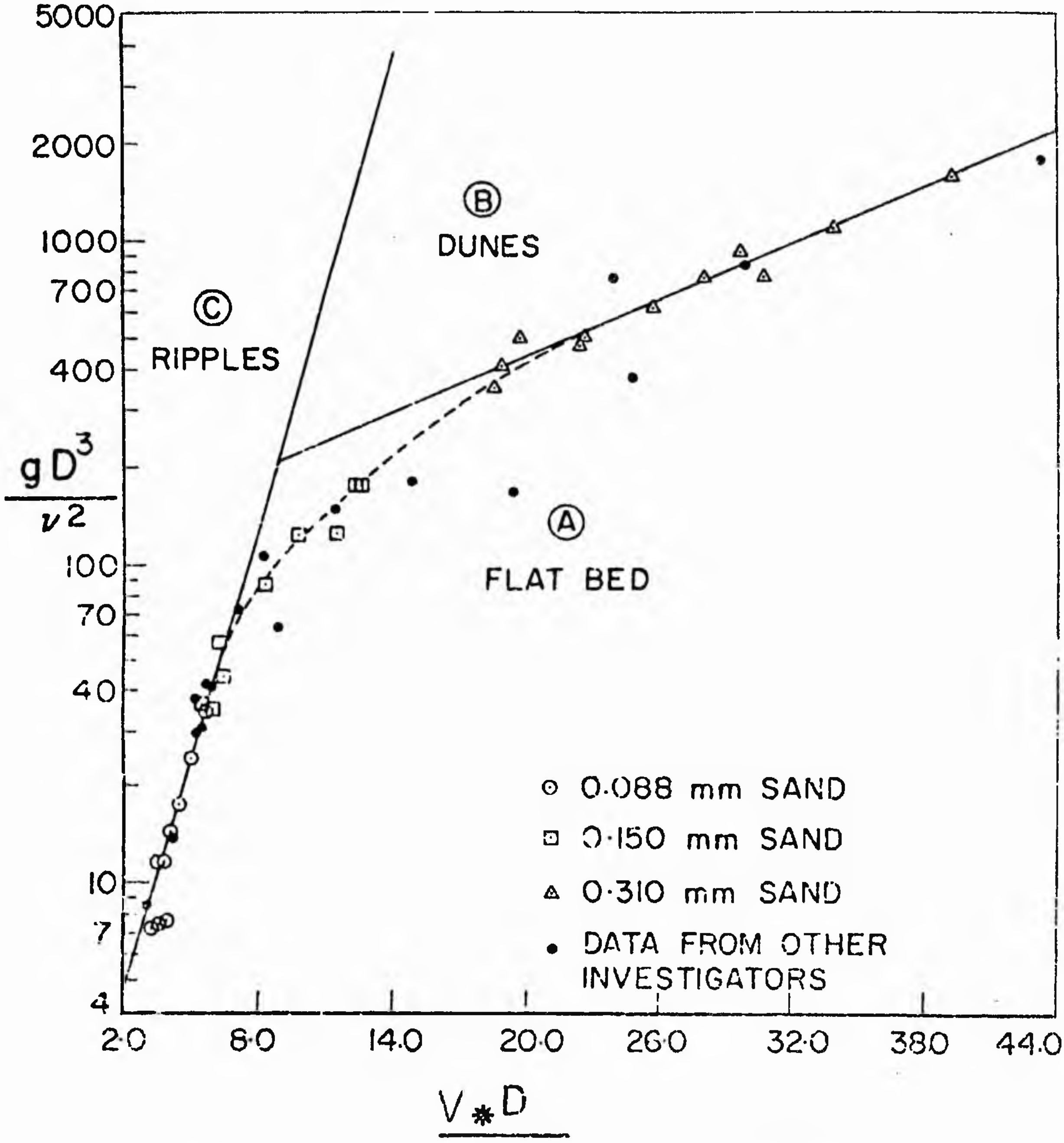

Fig. 5.12. Stability diagram from Hill et al., 1969: solid lines indicate limiting stability condition; broken lines indicate zone of transition.

$$\frac{V_{*crit}D}{\nu} = c_1\left(\frac{gD^3}{\nu^2}\right)^N + c_2 \qquad (5.37)$$

to the straight lines of fig. 5.12, where c_1 and c_2 are constants and N is an exponent. In general it is not possible to fit an equation of the form given above to straight lines drawn on semi-log scales. In fact subsequent examination has revealed that the best fit equations derived by the authors were fitted to all the data for each type of instability and not to the straight lines marked on fig. 5.12 (Hill, 1972, pers. comm.).

The intersection point of the equations derived by Hill et al. (1969) is at $V_{*crit}D/\nu \approx 6.6$, $gD^3/\nu^2 \approx 60.63$. As can be seen from fig. 5.12, this point is neither at the intersection of the two straight lines marked, nor at the point where the experimental data show the transition from one type of instability to the other, i.e. $V_{*crit}D/\nu \approx 10.63$, $gD^3/\nu^2 \approx 121.51$. The equations cannot be used therefore to determine when either type of instability will occur, because of this considerable inaccuracy in the 'transition' area. In order to overcome this difficulty, a polynomial regression analysis was performed for all the data points available, as the data appears to vary as a smooth function. The resulting best fit equation is

$$\frac{V_{*crit}D}{\nu} = 3.13+0.073\left(\frac{gD^3}{\nu^2}\right) - 0.92 \times 10^{-4} \left(\frac{gD^3}{\nu^2}\right)^2 \qquad (5.38)$$

$$+0.62\times10^{-7}\left(\frac{gD^3}{\nu^2}\right)^3 - 0.15\times10^{-10} \left(\frac{gD^3}{\nu^2}\right)^4 .$$

As can be seen from fig. 5.13, equation (5.38) describes the position of the transition between the two types of instabilities fairly well, and corresponds to a value of gD^3/ν^2 of about 120. Full details of the polynomial regression are given in appendix 2.

Thus, in the absence of antidunes, upper phase beds will form at a station if

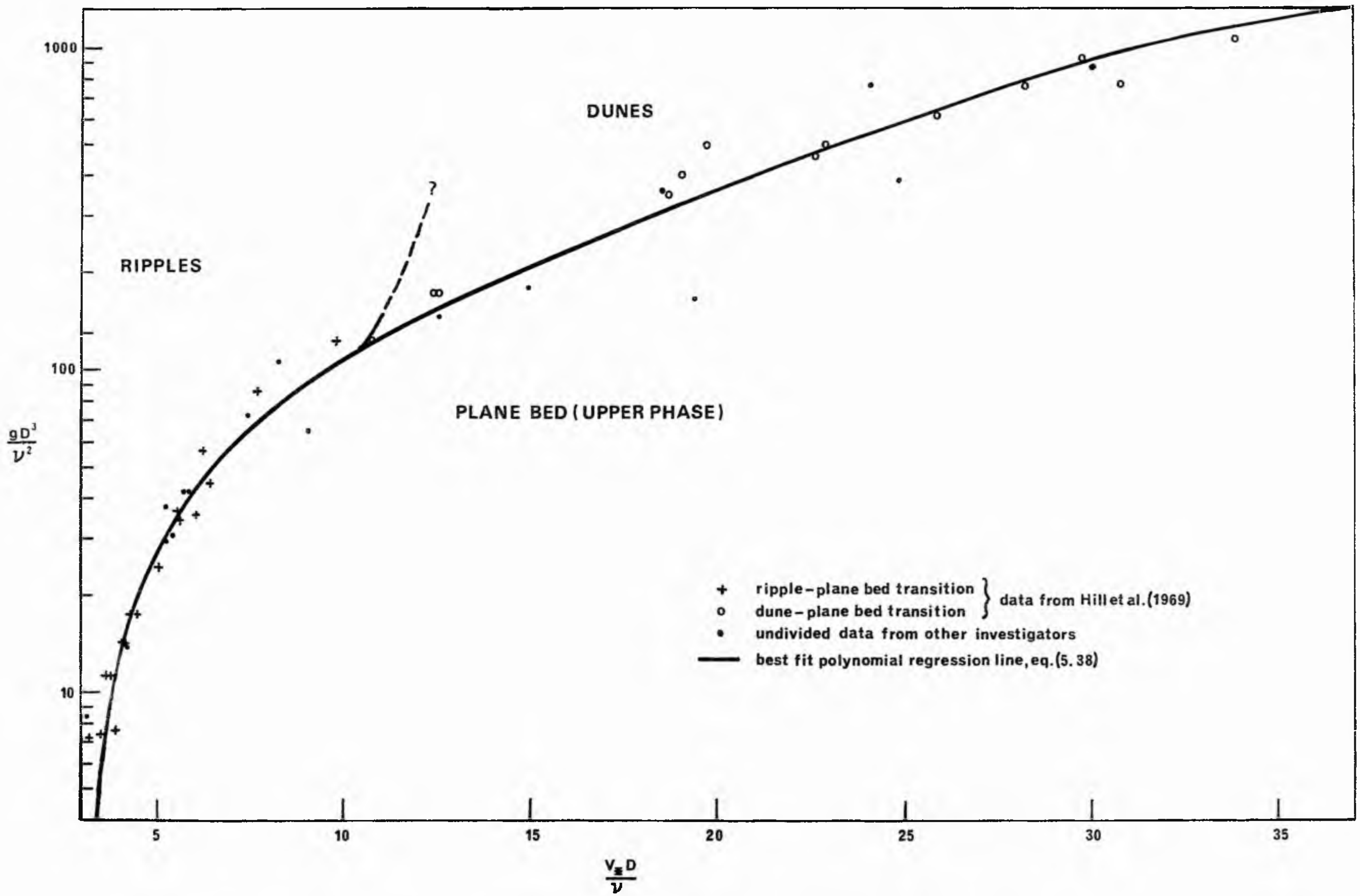

FIG. 5.13 STABILITY DIAGRAM FOR RIPPLES, DUNES AND UPPER PHASE PLANE BEDS, ACCORDING TO CRITERIA OF HILL ET AL., 1969. STABILITY BOUNDARY ACCORDING TO EQUATION (5.38).

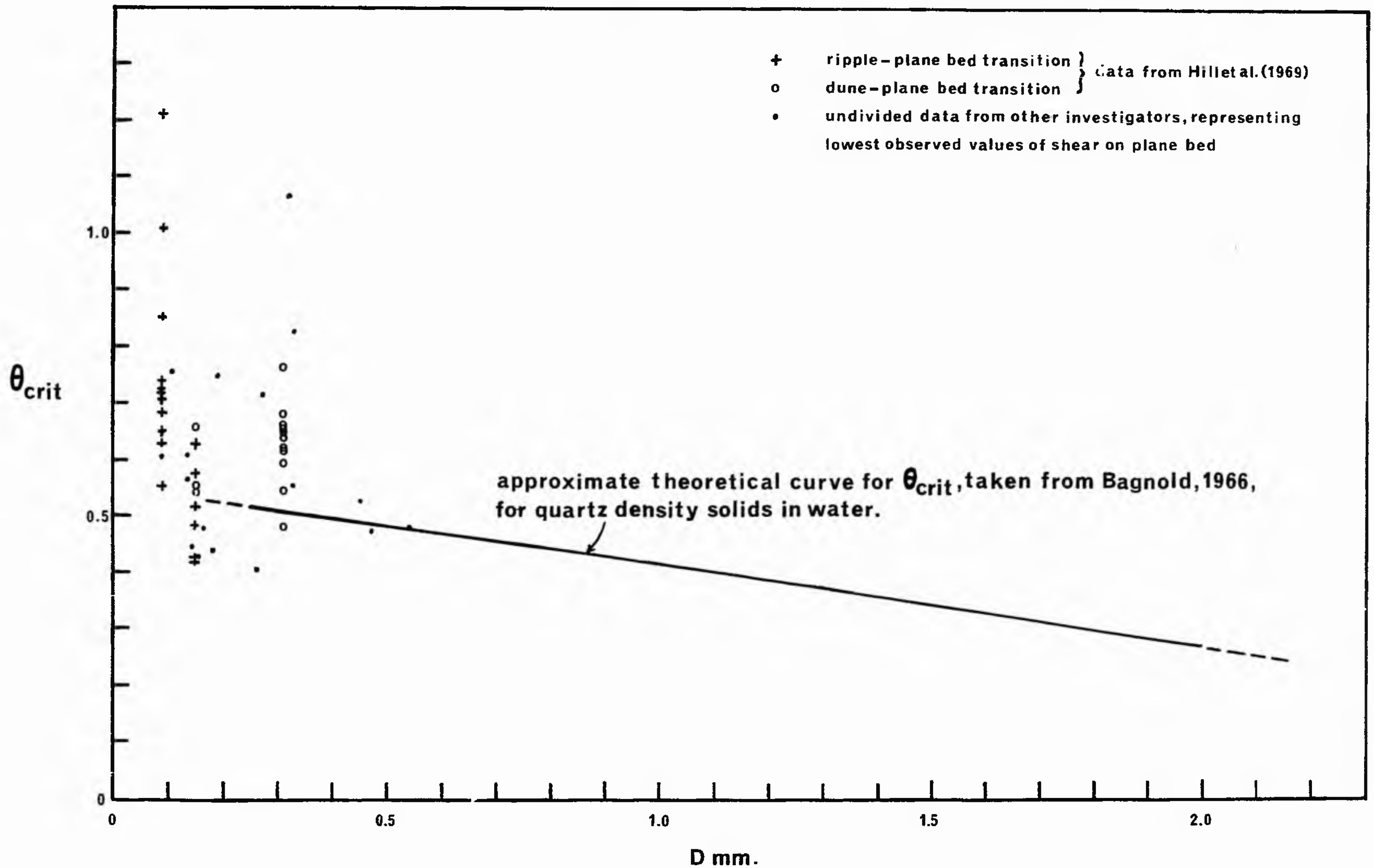

Fig. 5.14 Comparative plot of theoretical and empirical values of θ_{crit} against grain size.

$$\frac{V_* D}{\nu} > \frac{V_{*crit} D}{\nu} \qquad (5.39)$$

otherwise dunes or ripples will form, depending on whether gD^3/ν^2 is greater or less than 120, respectively.

By way of comparison of this method of prediction for upper phase plane beds and that used in Allen's model, we can rewrite $V_{*crit}D/\nu$ as follows

$$\frac{V_{*crit} D}{\nu} = \left(\frac{\tau_{crit}\ D^2}{\rho \nu^2}\right)^{\frac{1}{2}} = \left\{\frac{\theta_{crit}(\sigma - \rho)}{\rho}\right\} \cdot \left\{\frac{gD^3}{\nu^2}\right\}^{\frac{1}{2}} = f\left\{\frac{gD^3}{\nu^2}\right\} \qquad (5.40)$$

This is similar to the Bagnold criterion used in Allen's model except that, in addition, the viscosity of the fluid is taken into account. Fig. 5.14 shows θ_{crit} plotted against D, using the data from Hill et al's (1969) compilation and the values taken from Bagnold (1954, 1966) which Allen cites. It can be seen that the values of θ_{crit} used in Allen's model are not truly representative of the observed values for the range of D covered. The value of θ_{crit}, for a given D in this range should be higher than is shown, and clearly the excessive scatter of the data is an indication of the omission of important controlling factors. Indeed, Bagnold (1966) states '...though the value of θ is an approximate guide in default of a better one, it is not, as pointed out earlier, a precise criterion for either the disappearance of dune features on the bed of the change of trend in the transport rate versus power curves...' and '...dune features often persist at the higher flow stages...'.

5.5.5 Alternative model no. 3

One of the theoretical models that has received a lot of attention is that of Kennedy (1963, 1969). He made an elaborate stability analysis of the bed forms on lines similar to those adopted by Anderson (1953), but recognised phase differences between bed and surface waves. He also recognised that a change in the local transport rate might lag by a certain amount the causative change in the local fluid velocity.

Development of the model proceeds in the usual manner of fluid-stability analysis by tracing the development of sinesoidal shaped bed forms from a nearly flat bed on which there is an initial small sinesoidal disturbance. The flow over the developing bed forms is assumed to be two-dimensional, irrotational and incompressible, and the free surface is assumed to adjust itself continuously according to the requirements of the Bernoulli equation. The Bernoulli equation requires that the surface disturbance also be sinesoidal with the same wavelength as the bed form and have an amplitude given by

$$\frac{a(t)}{A(t)} = \left[1 - (1/Fr^2 kd) \tanh kd \right] \cosh kd \,, \qquad (5.41)$$

where a(t) and A(t) are the amplitudes of the bed and surface disturbances respectively, d is the mean depth of flow, Fr is the Froude number based on the velocity for mean depth, and k is the wave number.

Equation (5.41) can be used to show the conditions under which, theoretically, dunes and antidunes can form. For dunes, the bed wave and surface wave are 180° out of phase and a(t)/A(t) is less than zero; alternatively, for antidunes the two wave forms are in phase and a(t)/A(t) is greater than zero. Setting a(t)/A(t) to zero above gives

$$Fr^2 = \tanh kd \,/\, kd \qquad (5.42)$$

which is shown plotted in fig. 5.15 along with data accumulated by Kennedy (1963) from a number of sources. It does appear to separate the two types of bed forms successfully.

The sediment transport relation was then formulated, which relates transport rate to some power of the difference between flow

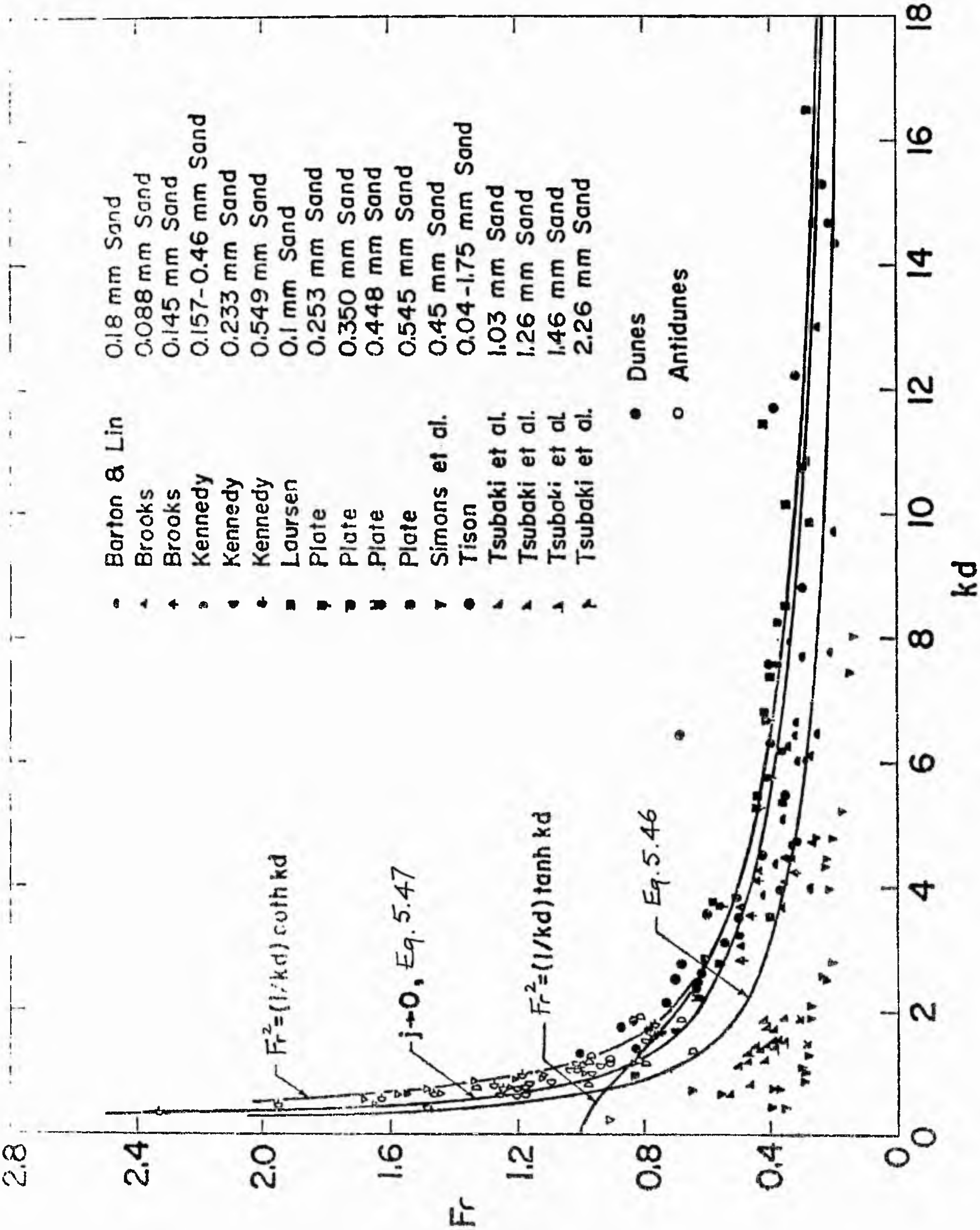

Fig. 5.15. Comparison of predicted and observed ranges of kd. (after Kennedy, 1969).

velocity and the critical velocity for the initiation of motion (Kennedy, 1969). The problem here is, if a simple bed load equation is used relating sediment transport to velocity alone, the transport of material will be symmetric about the crests and troughs so that the bed form will migrate but not grow. The asymmetry required for bed form growth is provided in Kennedy's model by introducing a lag distance δ whereby changes in bed load transport lag changes in velocity, as must be the case when particles at rest are picked up and accommodated in the main flow and moving particles are dropped and deposited in decelerating flow that can no longer move them (transport relaxation distance). Another factor contributing to δ is the phase shifts between the bed displacement and the longitudinal distributions of the local flow properties (Kennedy, 1969).

Using the sediment transport relations, the expressions for the velocity potential and the shape of the sinesoidal wave, and equation (5.42), given above, Kennedy (1969) derived the following relation for the bed form velocity

$$V_b = \bar{T}nk \cdot \frac{V}{V-V_c} \cdot \frac{1-Fr^2kd \tanh kd}{\tanh kd-Fr^2kd} \cos k\delta \qquad (5.43)$$

and for the bed amplitude

$$a(t)=A(0)(1/Fr^2kd)\cosh kd(Fr^2kd-\tanh kd). \qquad (5.44)$$

$$\exp\left\{tn\bar{T}k^2 \cdot \frac{V}{V-V_c} \cdot \frac{1-Fr^2kd \tanh kd}{Fr^2kd-\tanh kd} \sin k\delta\right\}$$

where V_b is the bed form velocity, V_c the critical velocity for initiation of motion, V the mean flow velocity, $\bar{T}$ is the net forward sediment transport rate for the whole stream, n is an exponent from Kennedy's transport law, and t is time.

Equation (5.44) shows that the amplitude of small bed waves on an otherwise flat bed caused by any arbitrary disturbance will increase exponentially with time provided that k and δ are such that the exponential term is positive. In reality, factors not accounted for in this linearised model must intervene and fix the equilibrium height of the bed forms. Table 5.1 summarises the various classes of bed forms predicted by equations (5.42), (5.43) and (5.44), and the conditions of occurrence of each. The configurations are classed as antidunes or as ripples or dunes according as the bed and surface waves are in phase or out of phase, as already discussed. The sign of the exponent in equation (5.44) constitutes the stability criterion: positive, zero and negative values of the exponent correspond to unstable, neutrally stable, and stable configurations respectively.

The possibility of an instability occurring at Froude numbers for which $Fr^2 kd.\tanh kd > 1$ was pointed out by Reynolds (1965). At these higher Froude numbers the horizontal component of the velocity perturbation changes sign between the bed and the free surface, whereas at lower values of Fr it retains the same sign over the full depth at each station. This high Froude number region is of little practical importance, as for a given Froude humber, values of kd less than that corresponding to $Fr^2 kd,\tanh kd=1$ have a greater initial growth and hence are dominant (Kennedy, 1969). The curve of $Fr^2 kd.\tanh kd=1$ is therefore the upper limit of two dimensional waves (Reynolds, 1965).

So far, no restrictions have been imposed on the wavelength. However, it is observed in both laboratory flumes and natural streams that flow-generated bed configurations have characteristic wavelengths and amplitudes that depend on the properties of the flow, fluid, and bed material. It is now assumed, as is customary in classical fluid stability analysis,

Case	Froude Number	Bed and Surface Profiles	$k\delta$
1	$Fr^2 kd > \tanh kd$	In phase	
1a	$Fr^2 kd \tanh kd < 1$	In phase	$0, 2\pi$
1b	$Fr^2 kd \tanh kd < 1$	In phase	$0 < k\delta < \pi/2$
1c	$Fr^2 kd \tanh kd < 1$	In phase	$\pi/2$
1d	$Fr^2 kd \tanh kd < 1$	In phase	$\pi/2 < k\delta < \pi$
1e	$Fr^2 kd \tanh kd < 1$	In phase	π
1f	$Fr^2 kd \tanh kd < 1$	In phase	$\pi < k\delta < 2\pi$
1g	$Fr^2 kd \tanh kd = 1$	In phase	—
1h	$Fr^2 kd \tanh kd > 1$	In phase	$0, 2\pi$
1i	$Fr^2 kd \tanh kd > 1$	In phase	$0 < k\delta < \pi$
1j	$Fr^2 kd \tanh kd > 1$	In phase	π
1k	$Fr^2 kd \tanh kd > 1$	In phase	$\pi < k\delta < 3\pi/2$
1l	$Fr^2 kd \tanh kd > 1$	In phase	$3\pi/2$
1m	$Fr^2 kd \tanh kd > 1$	In phase	$3\pi/2 < k\delta < 2\pi$
2	$Fr^2 kd = \tanh kd$	Indeterminate from potential formulation	
3	$Fr^2 kd < \tanh kd$	Out of phase	
3a	$Fr^2 kd < \tanh kd$	Out of phase	$0, 2\pi$
3b	$Fr^2 kd < \tanh kd$	Out of phase	$0 < k\delta < \pi$
3c	$Fr^2 kd < \tanh kd$	Out of phase	π
3d	$Fr^2 kd < \tanh kd$	Out of phase	$\pi < k\delta < 3\pi/2$
3e	$Fr^2 kd < \tanh kd$	Out of phase	$3\pi/2$
3f	$Fr^2 kd < \tanh kd$	Out of phase	$3\pi/2 < k\delta < 2\pi$

Table 5.1. Summary of conditions for occurre
Kennedy, 1969).

Bed Stability	Movement of Bed Forms	Bed Configuration
Neutral Unstable Unstable Unstable Neutral Stable	Upstream Upstream None Downstream Downstream —	Antidunes Antidunes Antidunes Antidunes Antidunes Flat bed
Neutral	None	Antidunes
Neutral Stable Neutral Unstable Unstable Unstable	Downstream — Upstream Upstream None Downstream	Antidunes Flat bed Antidunes Antidunes Antidunes Antidunes
	Indeterminate from potential formulation	Indeterminate from potential formulation
Neutral Stable Neutral Unstable Unstable Unstable	Downstream — Upstream Upstream None Downstream	Ripples or dunes Flat bed Ripples or dunes (Transition) " " Ripples or dunes

ence of various bed configurations (after that the characteristic or dominant wavelength is that for which the growth rate of the small amplitude disturbances is a maximum. The initial rate of amplification is obtained by differentiating equation (5.44) with respect to t, then putting t to zero, i.e.

$$a_t(0)=A(0)n\bar{T}k^2 \frac{V}{V-V_c} \left[(1/Fr^2kd)\cosh kd-\sinh kd \quad \sin k\delta\right] \tag{5.45}$$

Before the value of kd for which a_t (0) is a maximum can be determined it is necessary to refine the specification of the lag distance. As previously mentioned, at least two factors contribute to δ: the phase shifts between the bed displacement and the longitudinal distributions of the local flow properties, and the transport relaxation distance. The relative importance of each for a given flow cannot presently be assessed, however it is possible to examine the dominant wavelengths corresponding to the two limiting cases in which one or the other of these contributors to δ can be disregarded (Kennedy, 1969).

Where the lag distance results only from phase shifts between the local flow properties and bed displacements, δ can, as a first approximation, be treated as a constant multiple of the wavelength. Introducing $\delta = c_3 2\pi/k$ into equation (5.45) and equating to zero the derivative of $a_t(0)$ with respect to k gives

$$Fr^2 = \frac{\cosh^2 kd}{kd(\sinh kd+kd)} \tag{5.46}$$

In the other limiting case where the transport relaxation distance plays the predominant role, δ would be constant and independent of wavelength. It is then convenient to normalise by the flow depth and introduce $j= \delta/d$ into equation (5.45). Differentiating the resulting expression for a_t (0) with respect to k and equating to zero yields the following implicit equation for the dominant values of kd.

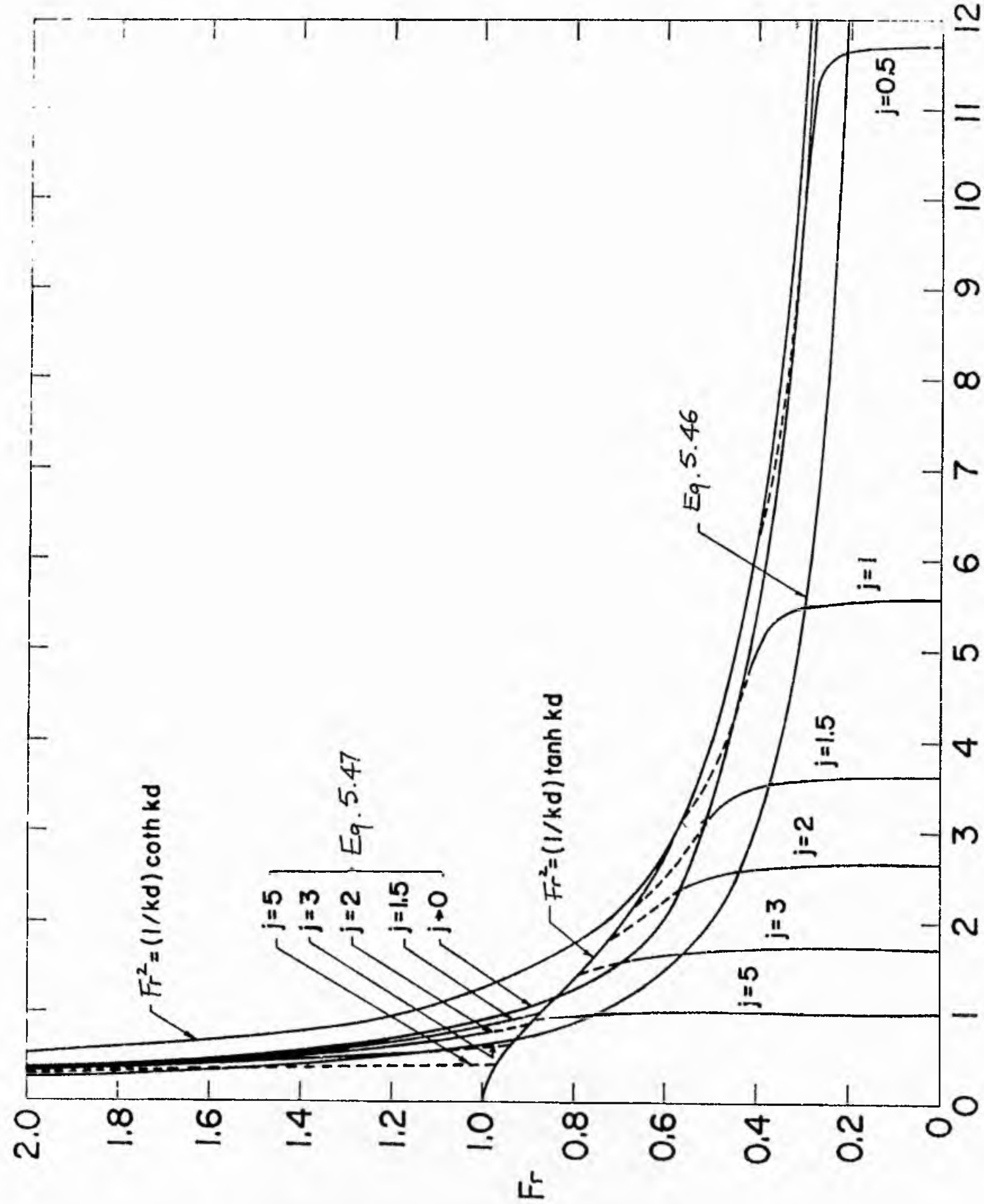

Fig. 5.16. Dominant kd given by equations (5.46) and (5.47), and regions of occurrence of various bed forms. The various configurations are identified by the character of the lines representing equation (5.47), except $j \to 0$, as follows. $Fr^2 kd < \tanh kd$: solid lines correspond to ripples and dunes, dashed lines to transition. $Fr^2 kd > \tanh kd$: solid lines correspond to antidunes moving upstream, dashed lines to antidunes moving downstream. (after Kennedy, 1969).

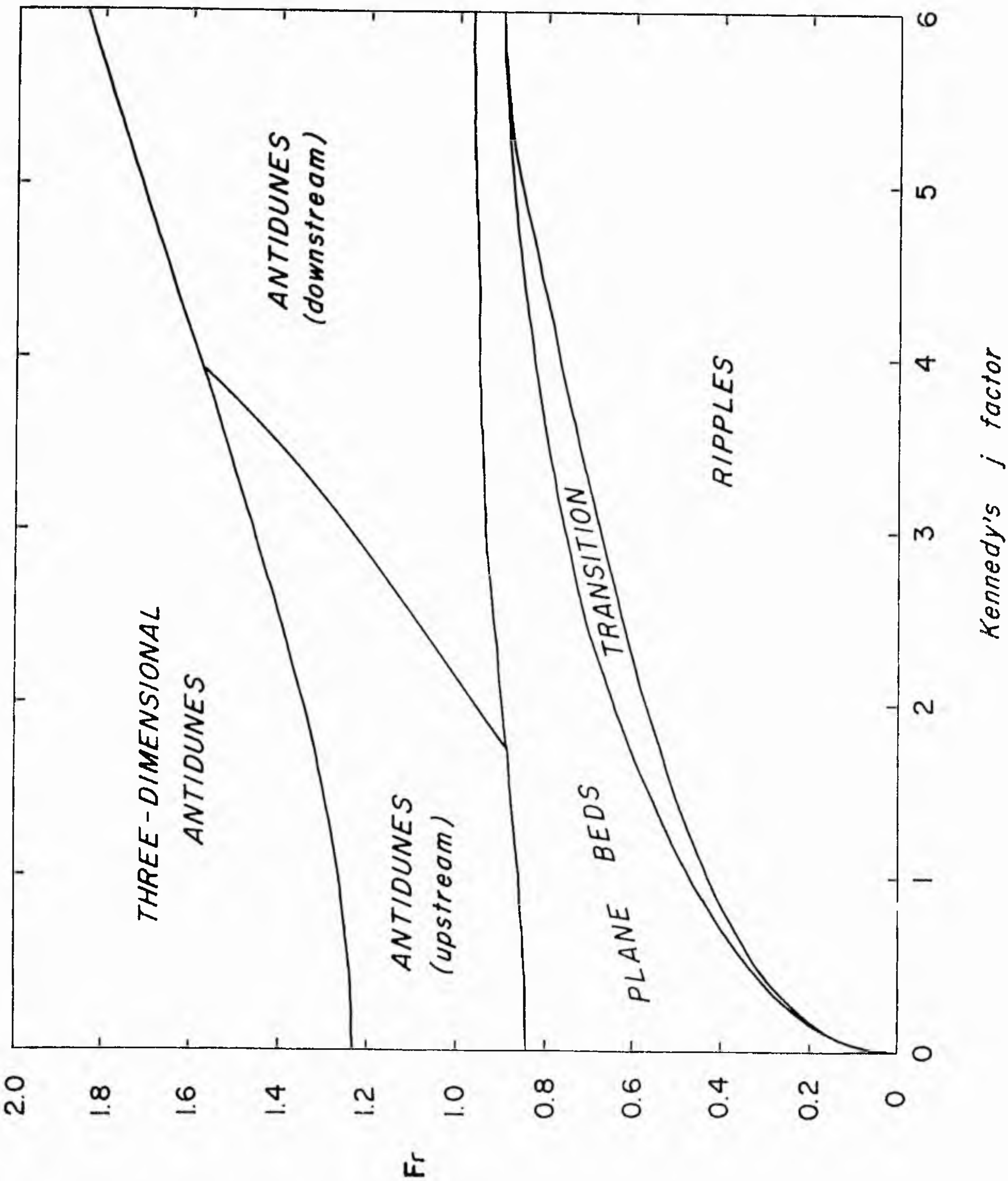

Fig. 5.17. Occurrence of bed forms according to analysis of J.F. Kennedy. Antidunes are distinguished according to whether they move upstream or downstream. (after Kennedy, 1963).

$$Fr^2 = \frac{1+kd\tanh kd + jkd\cot jkd}{(kd)^2+(2+jkd\cot jkd)kd\tanh kd} \quad (5.47)$$

Fig. 5.16 shows the relation between Fr and kd given by equations (5.46) and (5.47). Only the first two maxima of equation (5.44) are shown for each value of j; one each for $Fr^2 \lessgtr \tanh kd/kd$. Reynolds (1965) argues that some subsequent maxima actually have a higher growth rate, and hence should be retained. However, Kennedy (1969) states that it seems physically unlikely that the transport distribution over an individual bed form would be more strongly affected by more remote bed waves than by adjacent ones, and hence the higher harmonics are disregarded. As was noted above, all maxima of interest fall below the Froude number given by $Fr^2 kd\tanh kd=1$. The expected bed configurations summarised in table 5.1 are indicated by the character of the lines representing equation (5.47).

It is now therefore possible to define the conditions of occurrence of the various bed forms in table 5.1, for different values of Fr and j, by eliminating kd between equation (5.42) and (5.47), (thus assuming that δ is a constant rather than a function of k). An expression for the value of kd at the critical intersection of equation (5.42) and (5.47) is found to be the solution to

$$\sinh^2 kd - jkd\cot jkd = 1 \quad (5.48)$$

For any given j there are two solutions to equation (5.48) giving the two values of Fr which bound the plane bed field, as shown in fig. 5.17. In the model, antidunes will occur at a station if

$$Fr^2 = 8S/f_2 > Fr_a^2 = \tanh kd/kd, \text{ and } 0 < jkd < \pi \quad (5.49)$$

where Fr_a is the minimum Froude number for the formation of anti-dunes. The value of kd needed in this case by equation (5.49) cannot be easily obtained, as this involves finding the solutions to equation (5.48) numerically. The Newton-Raphson method breaks down here because the roots are very close at some values of j and an initial estimate of a root has to be very close to the actual root. To overcome this difficulty within the model, the roots of equation (5.48) were found by trial and error for various j values and a polynomial regression was performed with Fr_a as the dependent, and j as the independent, variable. The resulting best fit equation, which gives the value of Fr_a for use in the inequality (5.49), is

$$Fr_a=0.84+0.27j + 0.0047j^2 - 0.00089j^3 \qquad (5.50)$$

Full details of the analysis can be seen in appendix 2.

The plane bed configuration will therefore occur if the value of Fr lies below the curve of equation (5.50), for a given j, or lies above the curve which was obtained by performing a similar regression analysis using the lower Fr values (Fr_u), corresponding to the alternative roots of equation (5.48). The resulting polynomial regression equation of this lower boundary for plane beds is

$$Fr_u = 0.0049 + 072j-0.25j^2+0.04j^3-0.0024j^4. \qquad (5.51)$$

If Fr, as defined in inequality (5.49), is less than Fr_u given in the above equation, a transition regime will exist at a station, provided Fr is greater than Fr_1. Fr_1 is the maximum Froude number for the formation of dunes or ripples. Fr_1 is defined by substituting $jkd=3\pi/2$ in equation (5.47), thus

$$Fr_1^2 = \frac{1+\frac{3\pi}{2j}\tanh\frac{3\pi}{2j}}{(3\pi/2j)^2+(3\pi/j)\tanh\frac{3\pi}{2j}} \qquad (5.52)$$

As can be seen from fig. 5.17, there is no transition field above a value of j of 5.35.

Therefore, dunes or ripples will be the bed form if

$$Fr^2 = 8S/f_1 < Fr_1^2 \qquad (5.53)$$

which fulfills the requirements, shown in table 5.1, that $Fr^2 < \tanh kd/kd$ and $3\pi/2 < jkd < 2\pi$. To separate the fields of dunes, ripples and lower phase plane beds, the stream power and median diameter of bed material criteria are adopted, as used in Allen's model.

Fig. 5.15 presents a comparison of the experimental data summarised by Kennedy (1963) and the four reference curves shown in fig. 5.16. The agreement is seen to be very satisfactory. Practically all points fall below $Fr^2 kd \tanh kd=1$, which is taken as a justification for not including in figs. 5.16 and 5.17 case 1h to 1m of table 5.1 (Kennedy, 1969). A comparison of figs. 5.15 and 5.16 indicates that some dunes have values of j of five and greater. Such large values of δ seem very large for the bed load, but are readily conceivable for the suspended load, in which the transported material must settle significant distances to the bed as the flow decelerates, and be diffused upward as the local transport capacity increases. Accordingly, Kennedy (1969) argues here that dunes are formed by a perturbation of the longitudinal distribution of the suspended load transport, which has a relatively large value of δ , while ripples are formed by a perturbation of the bed load transport for which δ is much smaller. This would explain the simultaneous occurrence of ripples and dunes in some flows as resulting from two different modes of instability, the ripple instability associated with the bed load, and the dune instability with the suspended load.

In the model, the value of j, which depends on the depth and velocity of flow and the sediment and fluid properties, must be specified. However, nothing is really known about this parameter, upon which the appearance of the different bed forms depends. In this respect, a constant value of j is not really justifiable, but represents a best approximation for our present purposes. This problem is returned to in section 5.6.5. One further point is that, in Kennedy's formulation, the occurrence and effects of the separation zone when dunes and ripples occur is not accounted for.

Hayashi (1970) built upon Kennedy's model retaining his basic concepts and his results but mainly improving on the sediment transport flow relationship. Besides the lag distance δ, he introduced the local bed slope as a parameter influencing the sediment transport. The δ here is the distance by which the local sediment transport rate lags behind the local tractive force at the mean level of the bed. This will be a small distance and differs essentially from the quantity δ, in Kennedy's work. His analysis yields the following expression for the rate of growth of the waves.

$$a(t) = a(0) \exp\left[\frac{m g^2 c_4}{C} Fr^4 k^2 d^2 \left\{ C - 2Fr^2 kd \left(\frac{1 - Fr^2 kd \tanh kd}{\tanh kd - Fr^2 kd} \right) \right\} t \right] \quad (5.54)$$

where m is a dimensional coefficient in Hayashi's sediment transport relationship, c_4 is a constant and C is a dimensionless parameter defined by

$$\frac{c_4}{\delta} = C \frac{V^2}{2g} \quad (5.55)$$

Equation (5.54) shows that the amplitude of bed waves will increase with time when the sum in the parentheses is positive; in this case a flat bed is unstable. Putting $\Gamma = C - 2Fr^2 kd$.

$[1-Fr^2 kd\tanh kd)/(\tanh kd-Fr^2 kd)]$, $\Gamma>0$ gives the regions of occurrence of sand waves and $\Gamma<0$ gives the regions of flat bed. The limits of the regions of occurrence of sand waves are given by $\Gamma=0$ and $\tanh kd-Fr^2 kd=0$, and the limiting values are

$$Fr^2 = \begin{Bmatrix} Fr^2_2 \\ Fr^2_1 \end{Bmatrix} = \frac{1}{4kd\tanh kd}\left[C+2\pm\sqrt{(C+2)^2-8C\tanh^2 kd}\right] \qquad (5.56)$$

where Fr_1 is the maximum Fr for the formation of dunes, and Fr_2 is the maximum Fr for the formation of antidunes, and

$$Fr^2 = Fr^2_a = \tanh kd/kd \qquad (5.57)$$

which divides dunes from antidunes as in Kennedy's work.

The region of occurrence of dunes is delineated in the (Fr,kd) plane by $0<Fr<Fr_1$, that of antidunes by $Fr_a<Fr<Fr_2$, and the regions of flat beds are delineated by $Fr_1<Fr<Fr_a$ and $Fr_2<Fr$. It can be seen from equation (5.54) that in the case of C=0, instability occurs only in the region the limits of which are given by equation (5.57) and

$$Fr^2 = Fr^2_m = \coth kd/kd. \qquad (5.58)$$

It is to be noted that if C were zero, no dunes, only antidunes, would occur on erodible beds. As already mentioned, Reynolds (1965) argues that equation (5.58) marks the end of the region of instability of bed waves of small amplitude (antidunes) and the beginning of another region of instability. However, Hayashi's analysis indicates, in general, that equation (5.56) delineates the upper limits for antidunes, and beyond this flat beds will occur. Inspection of the dominant wave number in fig. 5.19 will indicate that Reynolds' (1965) criterion appears to be correct.

The magnitude of C has not been determined experimentally, nevertheless a comparison of experimental data summarised by Kennedy (1963) and the regions of occurrence of sand waves for the case C=2.0 provides the best agreement between theory and experimental data (Hayashi, 1970).

The initial rate of growth of sand waves is given, from equation (5.54), as

$$a_t(0)=a(0)(mg^2c_4/C)Fr^4k^2d^2\left\{C-\left[2Fr^2kd\left(\frac{1-Fr^2kd\tanh kd}{\tanh kd-Fr^2kd}\right)\right]\right\} \tag{5.58}$$

The initial rate of growth, normalised by $a(0)mg^2c_4/C$ for the case C=2.0 is plotted in Fig. 5.18 for different values of kd and Fr.

By way of explanation of Fig. 5.18, singularities have occurred in equation (5.58) for values of Fr from 0.5 to 0.9 at the resonant point, $Fr^2kd=\tanh kd$. Through the artifice of specifying the initial amplitude of the surface wave rather than that of the bed wave, the resonancy is replaced by a null point (see Kennedy, 1969). It can therefore be assumed, for practical purposes, that the maximum initial rates of growth in the dune field gradually decrease from Fr = 0.1 to zero at about Fr = 0.7. At and above about Fr = 1.0 the maximum initial rates of growth occupy the antidune field. As already stated, the dominant wavelength is that for which the initial rate of growth is a maximum. The maximum initial rates of growth are plotted on fig. 5.19, which indicates that dunes or ripples will exist as bed forms from Fr=0 to about Fr=0.7. Flat beds will exist from Fr $\approx$ 0.7 to Fr $\approx$ 1.0. Above Fr $\approx$ 1.0 antidunes are the stable bed form. It is worth noting that the line of maximum initial rates of growth is broadly similar to equation (5.46) of Kennedy, as previously cited. Furthermore, Hayashi's model for C=2.0 is consistent with fig. (5.17) and represents a value of j of about 2.5.

5.5.6 Other alternative models

As pointed out by Simons and Richardson (1971) the

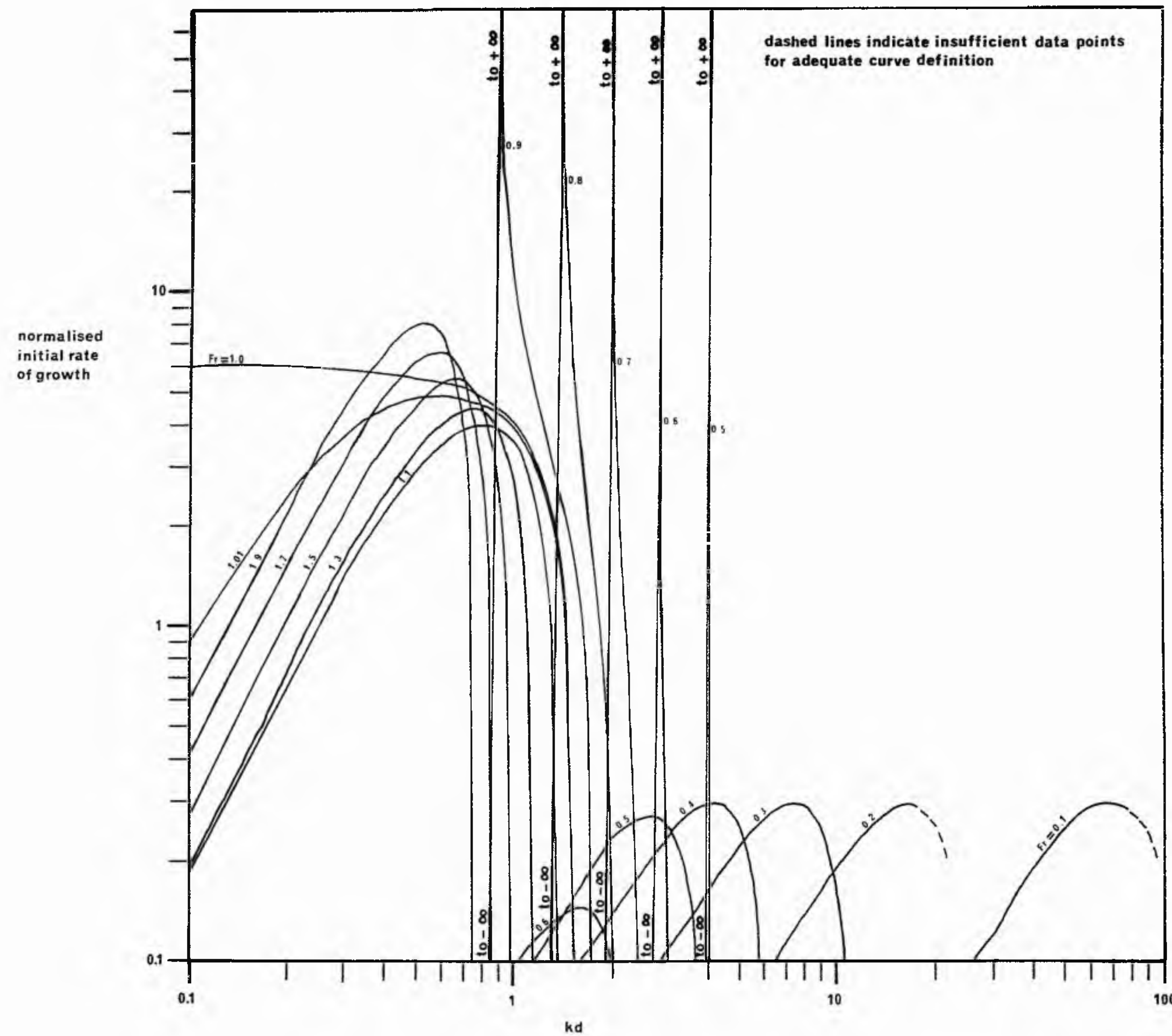

FIG. 5.18 INITIAL RATES OF GROWTH OF SAND WAVES FOR DIFFERENT VALUES OF Fr AND kd, ACCORDING TO EQUATION (5.58), FOR THE CASE C = 2.0.

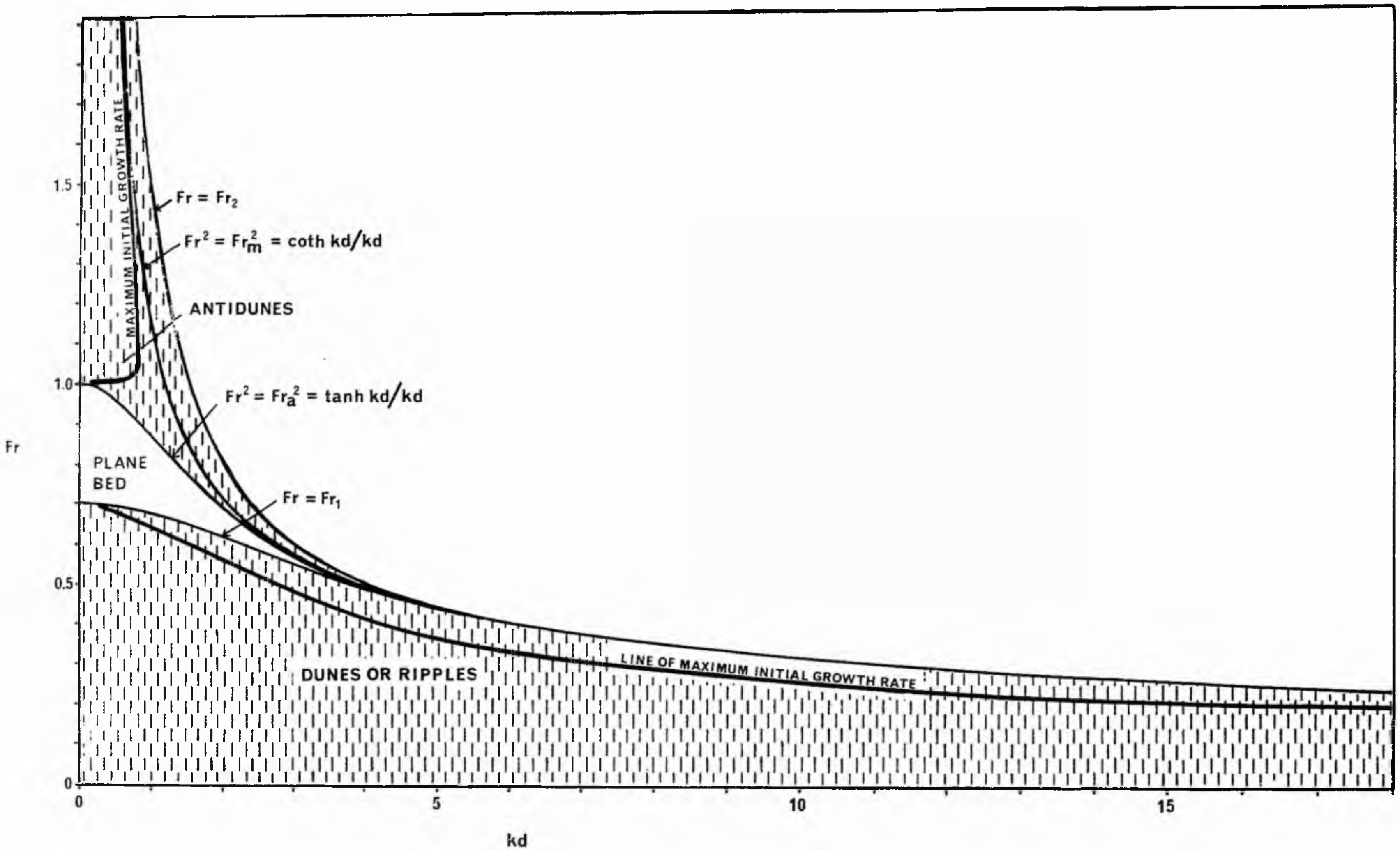

Fig. 5.19 Regions of occurrence of sand waves for the case C = 2, according to Hayashi (1970), with lines of maximum initial growth rate indicated.

multivariate statistical approach, specifically discriminant analysis, shows considerable promise in the field of bed form prediction. Its usefulness lies in its ability to consider the many variables which affect the existence of a particular bed form. Thus far, discriminant analysis has been used only to classify bed forms into lower, transition, or upper flow regimes based on four dimensionless hydraulic parameters that are assumed to control bed forms (Athaullah and Simons, 1970). Obviously considerable scope for development exists. For instance, Southard (1971) argues that dimensionless measures of depth, mean velocity, and sediment size (or these three parameters themselves) can be used as coordinates in three dimensional diagrams to characterise the various bed configurations. These have the property of one to one correspondence between possible bed configurations and points in the diagrams, thus eliminating overlapping fields in diagrams involving bed shear stress. Depth-velocity diagrams plotted primarily from the data of Guy et al. (1966) and Williams (1967, 1970) for five sediment sizes ranging from fine to very coarse sand show contiguous but nonoverlapping fields for the various bed forms. Discriminant analysis could be used to advantage here by classifying the bed forms according to the three parameters mentioned. Alternatively, examination of the boundaries between bed form fields in three dimensions could be analysed using multiple nonlinear regression.

With regard to theoretical approaches to bed form prediction, similar shear flow models to that of Kennedy (1963, 1969) have been developed (Reynolds, 1965; Gradowczyk, 1968), but the small additional information that they yield is obtained at the price of considerable analytical complexity (Kennedy, 1969). Engelund and Hansen (1966) developed a comprehensive stability theory based on the flow of a real fluid over a sinusoidal movable bed and were able to present stability diagrams for two and three dimensional bed waves. Improved account of the physical mechanisms involved in formation of bed waves in real fluid flow over movable beds has recently been made by Engelund (1970) and Engelund and Fredsoe (1971) with encouraging results. It is worth noting here that these two studies confirm Reynolds' (1965) upper stability limit for two dimensional bed waves (see equation (5.58)), but that the transition from antidunes to dunes from potential theory (see equation (5.42)) is a stability boundary marking the lower limit for antidunes.

5.6 Discussion of input parameters required in point bar model

5.6.1 Channel width and depth

The greater quantity of water that moves through a channel, the larger the cross section of that channel will be. Preceded by numerous studies of canal morphology and stability, Leopold and Maddock (1953) demonstrated that for most rivers the width and depth increase with mean annual discharge as

$$\begin{aligned} w &= c_5 Q_m^{0.5} \\ d &= c_6 Q_m^{0.4} \end{aligned} \qquad (5.59)$$

where c_5 and c_6 are coefficients and Q_m is mean annual discharge. The coefficients vary for each river, however, in some cases, with a downstream increase in discharge width or depth decreases. It is probable therefore that another independent variable is influencing channel dimensions, and this must be sediment load (Schumm, 1971). Analysis of data from the stable sand bed streams of the Great Plains of the United States and the Riverine Plains of New South Wales, Australia (Schumm, 1969, 1971) has produced the following relations

$$w = 2.3\, Q_m^{0.38}/M^{0.39}$$
$$d = 0.6\, Q_m^{0.29}\, M^{0.34} \qquad (5.60)$$

where M is Schumm's weighted mean percent silt and clay in the perimeter of the channel. The relation for channel width indicates that 88% of the variability of width can be accounted for by mean annual discharge and type of sediment load (M being an index of the latter), both being about equally important. The relationship for channel depth is not quite as good with about 81% of the variability of channel depth accounted for by discharge alone. Similar equations with equivalent correlation coefficients were obtained using mean annual flood discharge instead of mean annual discharge (Schumm, 1969).

When discharge is used with M to develop a multiple regression equation for width-depth ratio, that is

$$F = 56\, Q_m^{0.10}/M^{0.74} \qquad (5.61)$$

only a slight improvement over Schumm's earlier relation

$$F = 255M^{-1.08} \qquad (5.62)$$

is obtained.

Hence Schumm (1971) concludes that variations in channel dimensions with constant discharge are attributable to changes in sediment load. Local variations may be strongly affected by local variations in bank resistance, but the width-depth ratio of alluvial channels appears to be primarily determined by the nature of the sediment transported through the channel. This conclusion is supported by the observation of Leopold and Maddock (1953) that '...decreasing width at a constant velocity.... results in increased capacity for suspended load at constant discharge', and '..at constant velocity and discharge, an increase in width is associated with a decrease of suspended load and an increase in bed load transport'. Therefore a high width-depth ratio is associated with large bed material load.

It is to be expected that width and depth are significantly related to the other dependent morphological variables, which are also controlled by the independent system variables. Many authors have formed such relations. Some of the most useful ones in the present context are those linking wavelength and sinuosity with width and depth, i.e.

$$l = 10.9w^{1.01} \text{ from Leopold and Wolman (1960)} \quad (5.63)$$

$$l = 18F^{0.53}w^{0.69} \text{ from Schumm (1972)} \quad (5.64)$$

$$sn = 3.5F^{-0.27} \text{ from Schumm (1963)} \quad (5.65)$$

These equations can be used to define approximate relations between the dependent input variables, without making reference explicitly to the independent variables, specifically discharge and sediment load. An important point in this respect is that width and maximum depth (at specific cross sections) have to be defined in the model. It is well known that width and depth vary along the length of a meandering reach, as well as across the channel, with the alternating occurrence of pools and riffles. Averaged values of width and depth, either in the downstream direction or across the stream, will therefore not be truly representative of the channel dimensions at any specific cross section. Here, interest is centred around the pool areas, where width is normally less than over the riffles and maximum depth is normally greater.

Finally, another study of interest graphically relates depth-width ratio to various dependent and independent hydraulic variables. This work is summarised by Simons (1971).

5.6.2 Mean radius of curvature, longitudinal water surface slope and valley slope

Mean radius of curvature is defined in the planimetric geometry model, section 2.2, through its relationship with sinuosity and wavelength. Longitudinal water surface slope is obtained indirectly from the planimetric geometry model and is defined as valley slope divided by sinuosity. Valley slope is one of the substantially independent variables that is required as input to the model. The only specification restriction for the valley slope value is that, for a given discharge, the channel pattern is meandering. Straight, meandering and braided channels can be distinguished empirically in terms of slope and discharge (Leopold et al., 1964; Ackers and Charlton, 1970a,d; Schumm and Khan, 1972).

5.6.3 Resistance coefficients

As already stated, the Darcy-Weisbach friction coefficient can be conveniently separated into that part representing form losses introduced due to the addition of bends, f_b, and another part representing the resistance due to bed friction of a comparable straight channel, f_s. This subdivision involves the introduction of a factor, r, by which the straight channel friction factor must be multiplied to account for the change in relative roughness (arising from bed features) due to change in hydraulic radius with meandering.

Because of the large range of bed forms that may occur in an alluvial channel, the large variation of resistance to flow among the different bed forms, and the large number of interrelated independent variables affecting the bed form, it has not been possible to write a generalised function to predict resistance to flow or the velocity of flow (Simons and Richardson, 1966). As Simons and Richardson (1966) point out, 'A generalised function may not exist, because (1) more than one resistance to flow may occur for a given slope, depth, and bed material, (2) hysteresis exists in the change in bed configuration and resistance to flow depends on the preceding flow conditions, and (3) the bed configuration will oscillate between a dune bed and a plane bed for a given bed material at certain slopes and discharges. This problem is further complicated by three-dimensional flow, varying depth, varying bank roughness, and nonuniformity of flow in alluvial channels'. In this discussion of f_s only, however, we can assume that the complications due to the three dimensional helicoidal and nonuniform flow associated with meanders are accounted for in f_b, the discussion of which will follow.

In predicting the bed configuration present under different hydraulic conditions, it is necessary to know the value of f_s for the different bed forms that may exist. There are, in fact, various methods for estimating the resistance to flow under various conditions, and these are described in, for example, Graf (1971), Raudkivi (1967), Simons and Richardson (1966, 1971). Unfortunately, these methods normally require some information on the bed forms present, which precludes their general use in the model. With the appreciation that f_s varies for different bed forms and with the same bed form, due to the reasons outlined in Simons et al. (1965) and Simons and Richardson (1966, 1971), a single value of f_s may be assumed for each bed form as a reasonable first approximation. As mentioned in section 5.5.1, plane beds of either phase and antidunes take on one constant value, as do ripples and dunes. When these two constant values are multiplied by the factor r and combined with the component of the total coefficient which is due to the addition of bends, they become f_2 and f_1 respectively. Table 5.2 shows some of the observed ranges of f_s for different bed forms in flumes and natural rivers (in the absence of meanders).

Leopold et al. (1960) performed experiments in order to find the relative magnitudes of the resistance elements in straight and sinuous channels with fixed banks. The additional

Bedform	Range of f_s	
Lower phase plane bed	0.02-0.035[1]	0.019-0.14[5]
Ripples	0.052-0.13[1] 0.0693[2]	
Dunes	0.042-0.16[1] 0.056-0.099[3] 0.048-0.08[4]	
Upper phase plane bed	0.02-0.03[1] 0.014-0.022[3] 0.018-0.025[4]	0.011-0.034[5]
Antidunes	0.02-0.35[1] (standing waves 0.03-0.07[1] (breaking waves	

1. Simons and Richardson (1966)
2. Ackers and Charlton (1970d)
3. Nordin (1964)
4. Culbertson *et al* (1972)
5. Culbertson and Dawdy (1964)

Table 5.2. Some observed ranges of the friction coefficient in straight flumes and natural rivers.

losses due to bends were obtained using a constant cross section and boundary roughness in the straight and curved channels. In these experiments, therefore, there was no need to introduce the factor r, as there were no changes in relative roughness due to changes in hydraulic radius. In the straight channel the resistance to flow was wholly surface resistance, measurable by ρgRS. For a sinuous channel ρgRS no longer gives the surface resistance only but includes energy losses due to the addition of bends.

The experimental results confirmed their anticipated relation between resistances in the curved and straight channels and the square of the flow velocity (see fig. 5.20). In fig. 5.20 the overall resistance coefficient (=f/8) is given by the slope of the straight lines, except where spill resistance begins and resistance no longer varies as the square of the flow velocity.

The data indicate that the channel curvature alone can account for energy loss of the same order as that due to the surface resistance in straight channels in the absence of bed forms, and in tight curves may be double that quantity. Furthermore, Ackers and Charlton (1970d) find in their experiments on small meandering streams with rippled beds that some 60% of the head losses are due to bends and variations in cross section. Similar results were obtained by Allen (1939) and Allen and Shahwan (1954) from their model experiments and field studies.

Grave uncertainties exist in the relation between the extra 'square law' resistance introduced by channel bends and the geometric characteristics of the bends (Bagnold, 1960; Leopold et al, 1960; Shukry, 1950; Yen, 1965, 1971). Figure 5.21 shows the values of f_b, from the data of Ackers and Charlton (1970d), plus additional data on r_m from their records, and Leopold et al.

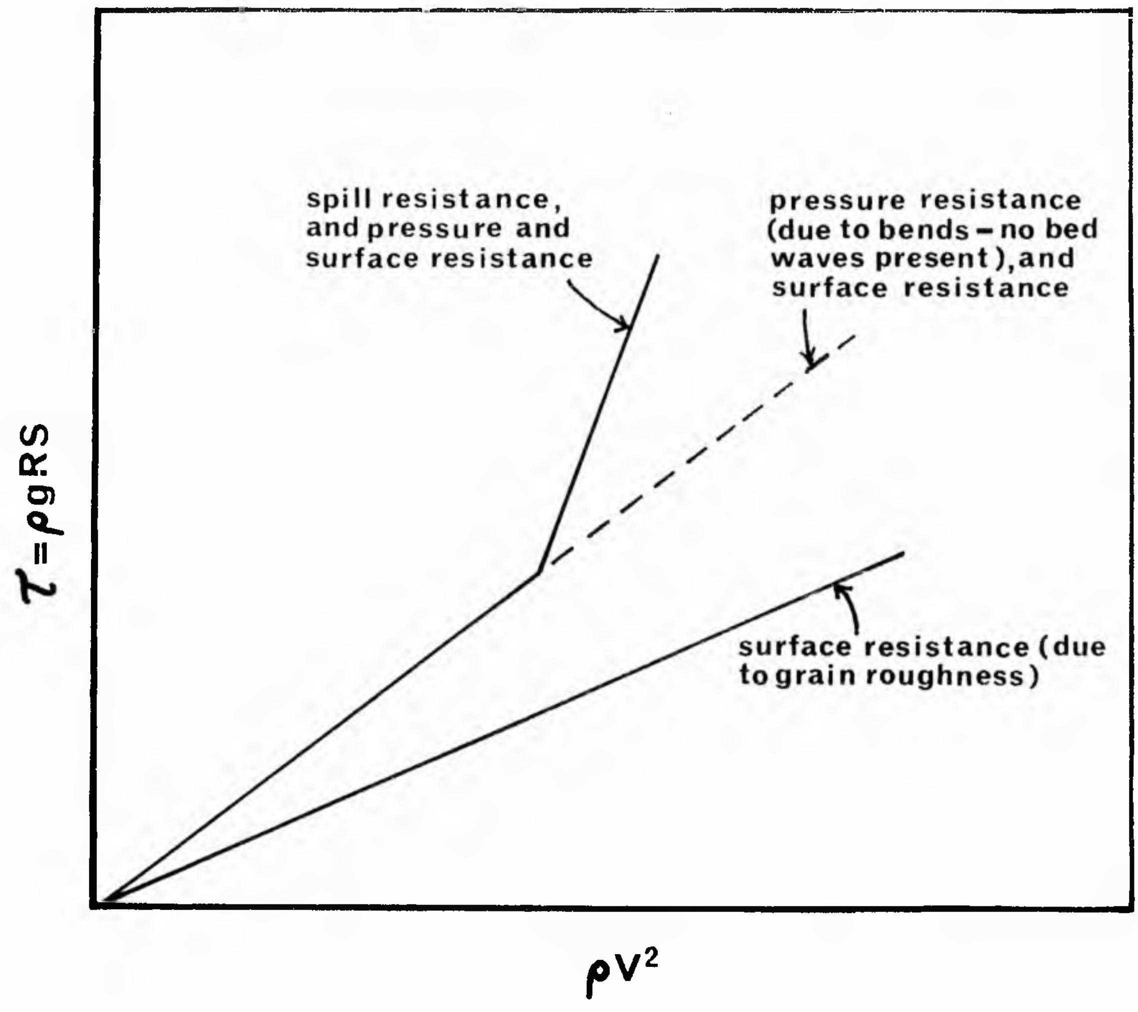

Fig. 5.20 Postulated relation of bed shear stress to square of flow velocity in sinuous fixed bed channel. (after Leopold et al.).

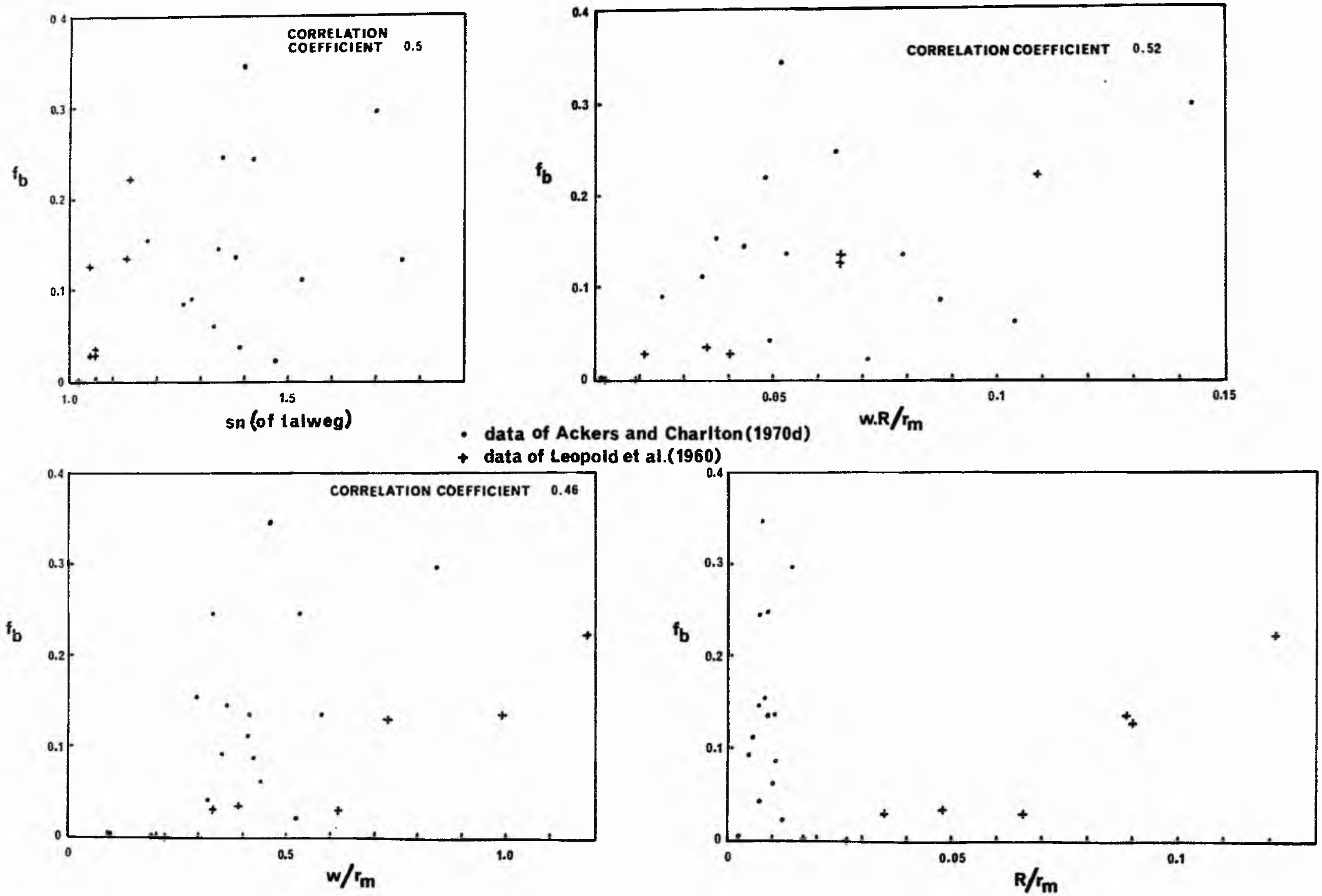

Fig. 5.21 Plots of f_b against various geometric proportions.

(1960), plotted against various geometric proportions. The values of f_b computed from the Ackers and Charlton data were derived by comparing the losses in the meanders at crossings with only one average straight reach with a corrected friction coefficient, rf_s, of 0.086. Due to the excessive scatter of the data available and the restricted range of experimental conditions, no general relation for the value of f_b is available. If the value of f_b is drawn from fig. 5.21 it must only be approximate, and there may be inherent danger in extrapolation based on these restricted data. Ackers and Charlton (1970d) used the following average values in their analysis based on small meandering streams; f_b=0.135; r=1.249; f_s=0.0693

5.6.4 Fluid viscosity, fluid and sediment density

A value of fluid viscosity is required for alternative model no.2 (section 5.5.4), and fig. 5.22 shows the effect of fine sediment (bentonite) and temperature on the apparent kinematic viscosity, ν (Simons and Richardson, 1971). This is an apparent viscosity because aqueous dispersions of fine sediment are non-Newtonian. The magnitude of the effect of the fine sediment on viscosity is large and depends on the chemical make-up of the fine sediment. The changes in fall velocity of the median diameter as a result of the changes in the viscosity and the fluid density can be noted in fig. 5.23 (see Simons and Richardson, 1971). Therefore, by specifying a particular value of ν (cm^2/sec units) in the model, implicit mention is made of the amount and nature of the suspended sediment concentration and the temperature of the fluid, which constitute substantially independent variables.

In addition to changing the viscosity, fine sediment

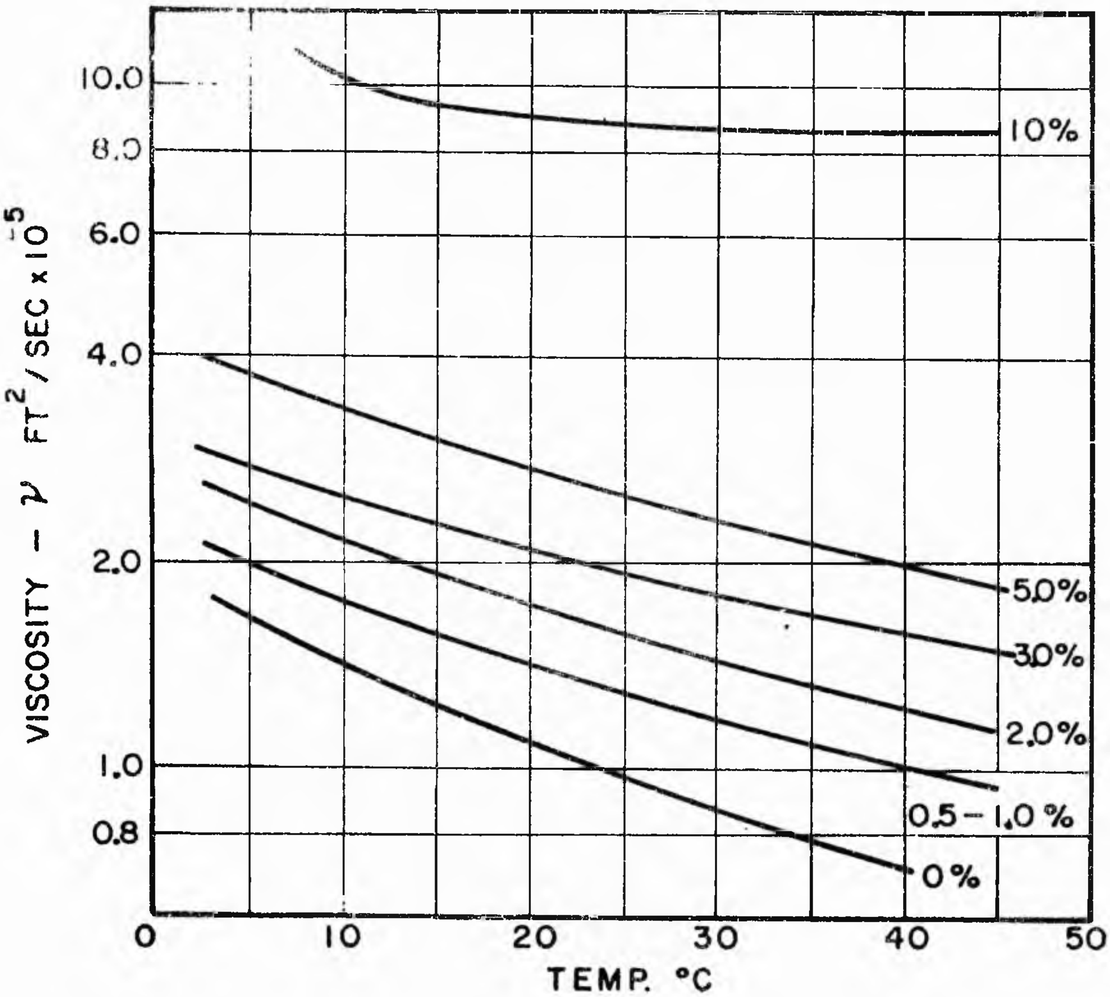

Fig. 5.22. Apparent kinematic viscosity of water-bentonite dispersions. (from Simons *et al.*, 1965).

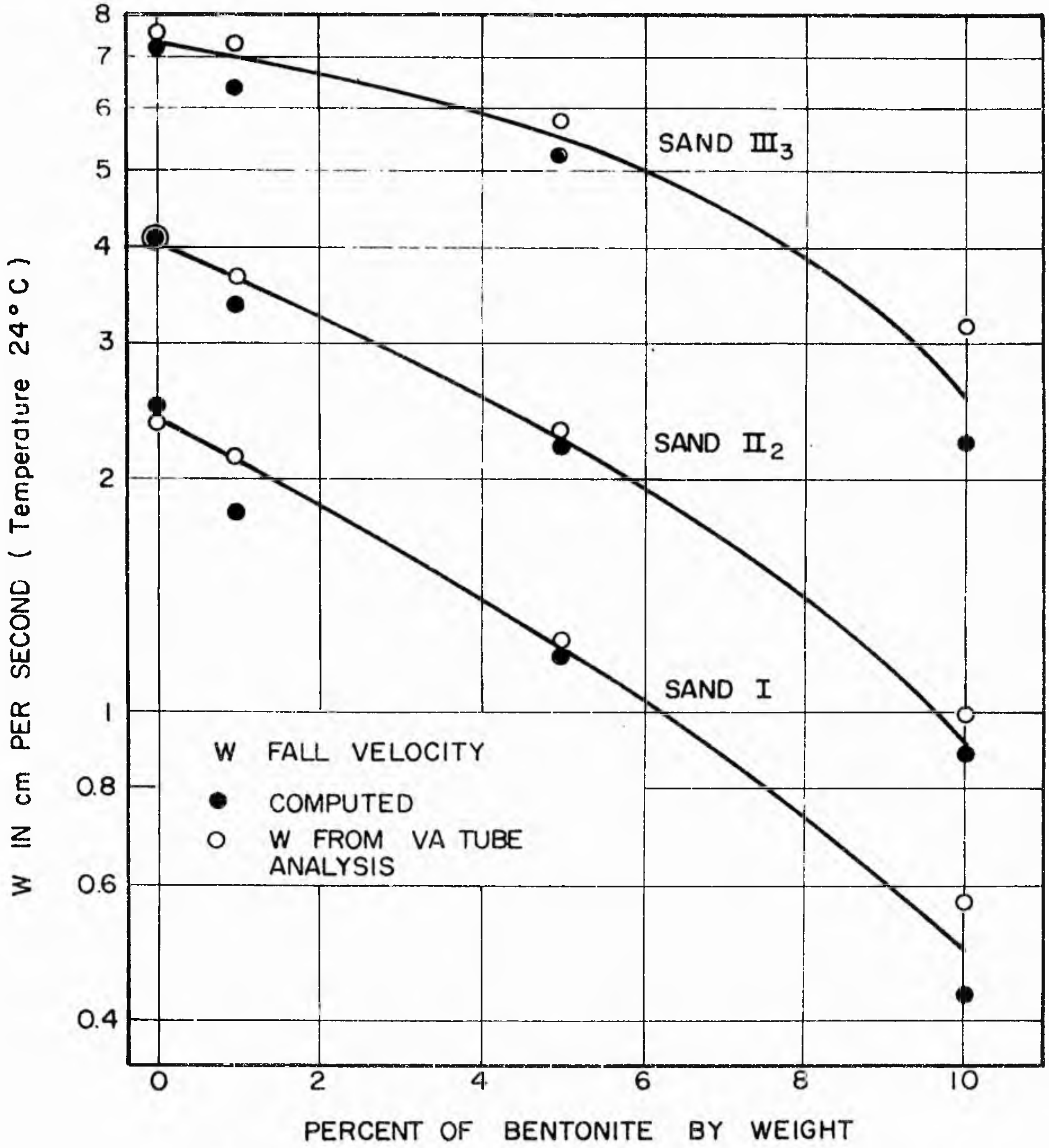

Fig. 5.23. Variation of fall velocity with percentage of bentonite in water. (from Simons et al., 1965).

suspended in water increases the mass density ρ of the mixture. The mass density of a water sediment mixture can be computed from

$$\rho = \frac{\rho_w \sigma_s}{\sigma_s - C_s(\sigma_s - \rho_w)} \qquad (5.66)$$

where ρ_w is the density of pure water, σ_s is the density of the suspended sediment, C_s is the suspended sediment concentration in % by weight (Simons and Richardson, 1971). As ρ_w = 1 gm./cm^3.,

$$\rho = \frac{\sigma_s}{\sigma_s - C_s(\sigma_s - 1)} \qquad (5.67)$$

The density of the sedimentary particles in the bed load is an independent system variable and is normally taken as the value for quartz grains, i.e. 2.65 gm./cm^3.

5.6.5 Kennedy j factor

It was pointed out in section 5.5.5 that the value of j depends on the depth and velocity of flow and the sediment and fluid properties, also that nothing is really known about the parameter. In alternative model no.3, it is required to specify a single value of j for the whole cross profile. This constitutes only a first approximation.

As there is no theoretical definition available for the value of j, it will be necessary to turn to the body of experimental data that exists. As an example, from the data of Guy *et al.* (1966), j appears to vary between about 2 and 3 for their finer sand grades.

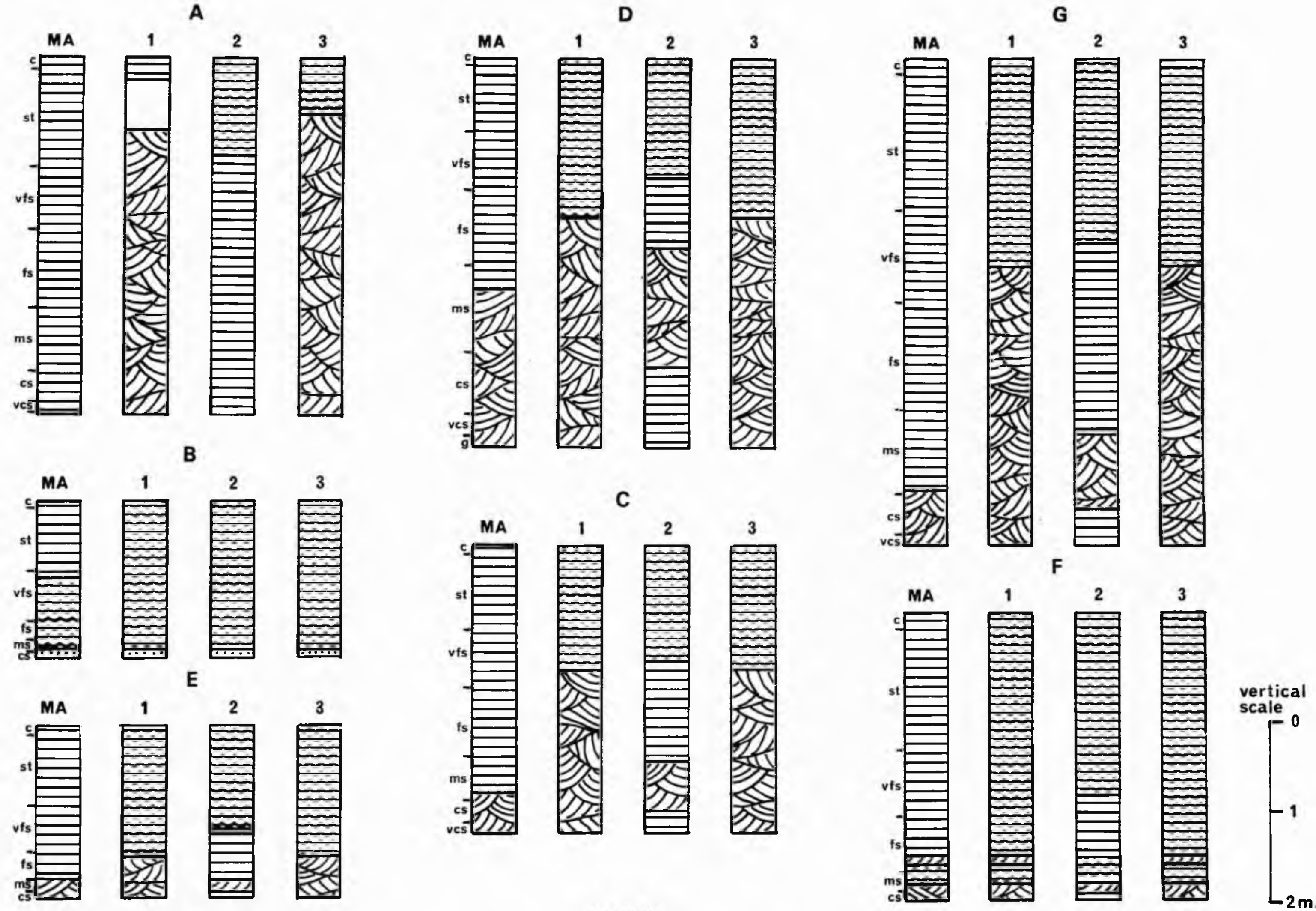

legend

	h(m)	w_1(m)	r_m (m)	S	
A	4.05	405.0	4050.0	0.000285	$n_1 = 2$
B	1.75	17.5	35.0	0.000065	$k_1 = 0.8$
C	3.2	96.0	336.0	0.000125	$\sigma = 2.65$ gm/cm^3
D	4.4	110.0	228.8	0.0000973	$\rho = 1$ gm/cm^3
E	1.92	48.0	201.6	0.000124	$f_1 = 0.08$
F	3.2	80.0	300.0	0.0000666	$f_2 = 0.02$
G	5.55	138.0	520.0	0.0000768	$\nu = 0.00929$ sq.cm/sec
					$j = 2$

c clay
st silt
vfs very fine sand
fs fine sand
ms medium sand
cs coarse sand
vcs very coarse sand
g gravel

flat bedding (lower plane bed)
cross lamination (ripples)
cross bedding (dunes)
transition
flat bedding (upper plane bed)

MA modified Allen model for grain size and bed form
1 alternative bed form model no.1
2 " " " " no. 2
3 " " " " no.3

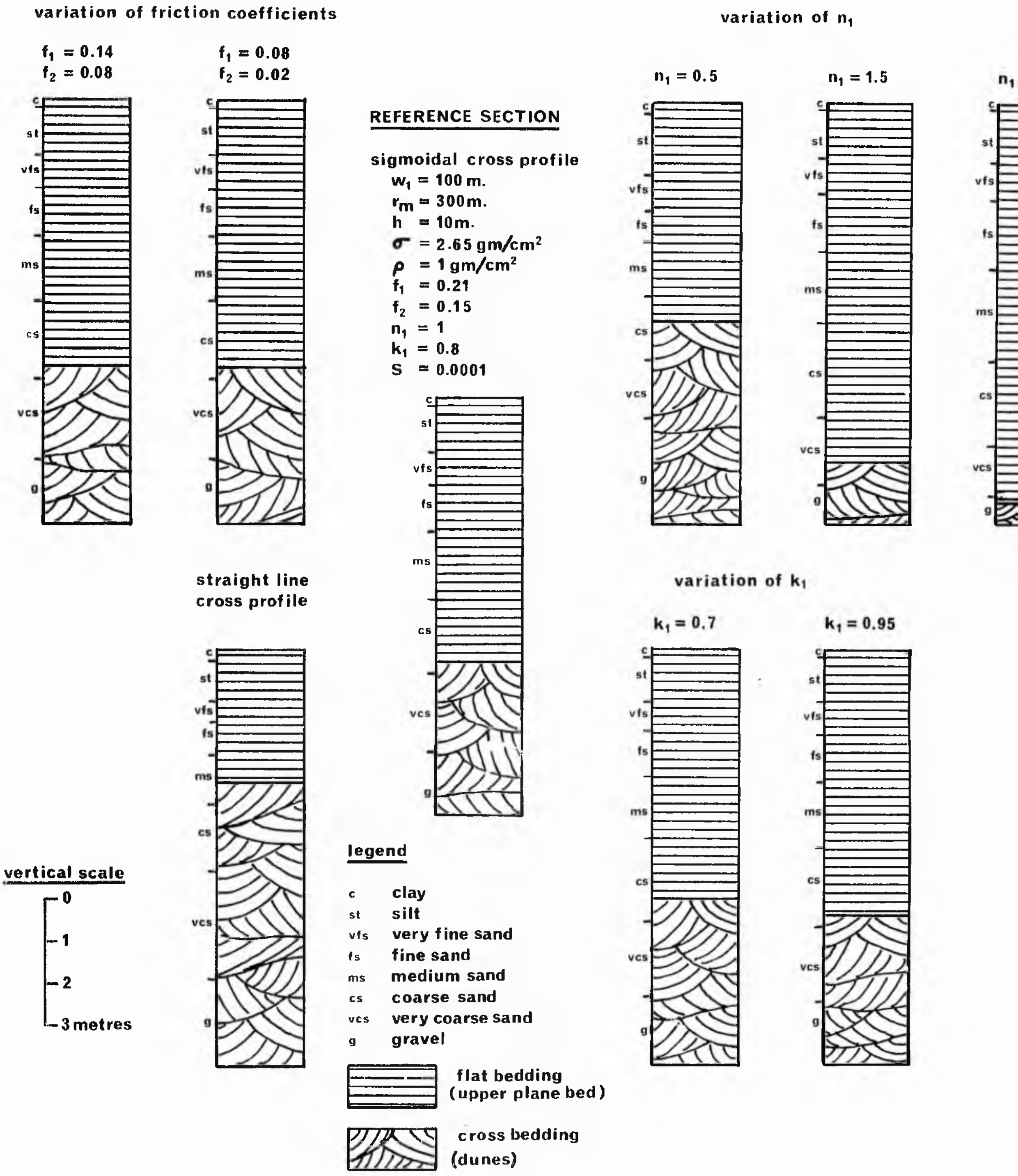

FIG. 5.24 VERTICAL VARIATION OF GRAIN SIZE AND SEDIMENTARY STRUCTURE WITHIN POINT BAR, ACC
TO MODIFIED ALLEN (1970a,b) MODEL, FOR SELECTED VARIABLE INPUT PARAMETERS.

5.7 Experiments to show variation of grain size and sedimentary structure with different input parameters and alternative bed-form models proposed

Fig. 5.24 shows the vertical variation of grain size and sedimentary structure within a point bar, calculated using Allen's bed-form model. The figure is designed to show the effect of variation of selected parameters on the sedimentary deposit over a point bar of constant dimensions. The sections shown should therefore be compared with the reference section in the centre of the figure. They all have the same input parameters listed except for the specific parameters which are being varied in each case.

The effect of variation of k_1, with all other input variables constant, is to vary the full width of the channel, which affects the local radius of curvature at a particular station. Increase in k_1 effectively increases the local radius of curvature. The effect on the grain size and sedimentary structure profiles is slight, but with an expected decrease in general calibre of the load as k_1 increases, and a slight downward extension of upper phase beds due to the decreased grain size.

Variation of the friction coefficients will obviously have no effect on the grain size, by virtue of the model used, however, in these particular cases, there is no effect on the sedimentary structure profiles either. This is by virtue of the criteria used to predict upper phase plane beds, and that the hydraulic conditions pertaining to the lower part of the profiles were not near the limiting conditions for the existence of ripples of lower plane beds. In the case of the hydraulic situation being near to these boundary conditions, dunes will be expected to occur at the expense of ripples or lower plane beds with decrease in the friction coefficients. The appropriate choice of friction coefficients for a particular meander is obviously an important consideration.

As already noted, the grain size profiles, and hence the sedimentary-structure profiles, are very sensitive to changes in the shape of the cross profile (e.g. fig. 5.6). Fig. 5.24 shows, as expected, a decrease in general calibre as the convexity, n_1, increases, also a steepening of the grain size profile. This variation in grain size has the effect of extending the upper phase plane bed field downwards, effectively doubling the thickness from $n_1=0.5$ to $n_1=2$. Substitution of a straight point-bar cross profile for the sigmoidal curve (equation (5.1)) has the effect of increasing the amount of coarse sediment grades relative to the finer grades, when compared with the reference section. This has the effect of upward extension of cross beds in the section at the expense of upper plane beds. In fact, with a straight profile, D varies approximately as the square of the local depth when r_m is large, but has an approximately linear relation when r_m is small.

Figure 5.25 is designed to show the effect of variation of the channel and meander dimensions on the grain size and sedimentary-structure profiles, and to compare the alternative bed-form models proposed. The parameters that were varied in fig. 5.24 are kept constant in this figure. The actual data used were taken from Allen (1970a).

From equation (5.20) it is expected that, apart from the effects of n_1, the general calibre of the load increases with longitudinal water-surface slope, maximum channel depth, and channel width between the inner bank and the talweg, but decreases with increasing radius of curvature. These constitute a sufficiently large number of variables such that the general calibre can be very similar for many different combinations.

However, fig. 5.25 does show, for instance, in the case of D that a generally high calibre of load exists due to a high ratio of w_1.h.S over r_1. Case F has a relatively low ratio and subsequently has a low general calibre.

The value of Θ given in equation (5.25) in Allen's bed-form model depends, apart from n_1, on the ratio of r_1 over w_1. The large ratio of r_1/w_1 in the case of A therefore gives a dominance of upper-phase plane beds, whereas low ratios in cases B and D give considerably less, as was expected.

The sedimentary structure profiles obtained using the different bed-form models are broadly in agreement, except Allen's model predicts more upper plane beds than the others. All of the alternative models concur fairly well in their prediction of the change from ripples to dunes or upper plane beds, however there is generally disagreement in the prediction of dunes or upper plane beds (except in the cases of models 1 and 3). Part of this disagreement may be due to the fact that the transition regime has been ignored in all the models except no.1. In the last case the sedimentary structures will be expected to be those resulting from washed-out dunes. Where only lower-regime forms are predicted, profiles will be the same, as the models differ fundamentally only in their prediction of the transition from lower-to upper-regime forms. It is worth noting that neither the grain size nor sedimentary structure can be assumed to be wholly correct at the top of the profiles where the grain-size model predicts fine silt and clay. The grain-size and bed-form models are based on a consideration of cohesionless particles and cannot take account of the cohesive forces involved with fine sediment. Nevertheless, although not theoretically correct, the profiles may be qualitatively acceptable in this range.

The alternative model no.3 is unfortunately limited by the lack of data on the variation of j, and in alternative no.2 the criterion for the change from dunes or ripples to upper plane beds is defined only for a small range of grain size ranging up to medium sand. Alternative no.1 appears to be generally applicable and has the advantage of being able to predict transitional bed forms. Allen's model is generally applicable and, although quoted values of θ_{crit} are only approximate, they cover a wide range of grain sizes. In default of a better one this model is most favourable because it combines a sound theoretical basis with a strong empirical justification. Allen's model has therefore been adopted in the simulation model, although any alternative may be easily incorporated if preferred.

5.8 Validity and limitations of the point-bar sedimentation model

The model is a considerable simplification of a physically complex natural situation and it contains a sufficiently large number of variables to produce closely corresponding deposits in a number of ways (Allen, 1970a). The only really independent variables are amount and character of fluid and sediment discharge and the valley slope. It has not been possible to produce a model which has only the independent variables as the starting point. Some of the input variables are system dependent, some are independent. For instance, the channel shape and dimensions are made 'independent' variables by specifying them as input, where they are in fact dependent. The bed sediment-size is treated as dependent where in fact it should be independent. Furthermore, availability of all size grades is assumed.

The dependent morphological variables to be specified as input (i.e. wavelength, width, depth, etc.) share an inter-dependency, as shown previously, because of their common link with the independent variables. These system dependent input variables must be mutually compatible, and, without specific reference to the independent variables, the relationships given by equations (5.63), (5.64) and (5.65) are the most useful way of monitoring the compatibility of the input variables.

Naturally the choice of any of the dependent variables has implications relating to the independent ones. Moreover, the amount and character of fluid and sediment discharge may be pre-defined explicitly in an approximate way by using the various relationships between the dependent and independent variables that exist in the literature and that have been mentioned hitherto.

The use of uniform-flow equations constitutes somewhat of a simplification, however uniform-flow formulae may be used for nonuniform flow if the flow is 'gradually varied' (Chow, 1959). As already stated, this involves using the energy slope in the computations, and assuming that the hydrostatic distribution of pressure prevails over the channel section. Yen (1965) has shown that the pressure distribution along any vertical is virtually hydrostatic as long as the ratio of depth to radius of curvature is small. The use of these formulae becomes increasingly suspect as the curvature of flow becomes more pronounced, producing non-hydrostatic-pressure distributions, separation zones, and a state of high turbulence (i.e. 'rapidly varied flow'). Yen (1965) and Rozovskii (1961) state that stream separation and eddy-zone formation is only encouraged at very sharp bends as depth increases relative to width, and particularly when the banks have gentler slopes; that is, the greater the influence of wall friction. An analysis of this problem does not therefore seem warranted.

Because of the secondary currents associated with flow in bends the subdivision of the channel cross-section into discrete subsections will likely result in the continuity principle being violated. However Yen (1965) has shown that the lateral discharge is very small compared with the downstream (longitudinal) discharge. It should be noted that the mean fluid velocity and bed stress calculated in the model, and used in the delineation of bed-form fields, are those measured in the longitudinal direction. Assumptions have been made about the uniqueness of the longitudinal water-surface slope and no account has been taken of the minor, yet characteristic superelevation of the transverse water surface. The substitution of the longitudinal water-surface slope for the energy slope was rationalised earlier.

Assumptions have also been made regarding the friction factors, hysteresis effects have not been analysed, and, in general, the effects of temperature and fine sediment on the development of bed-forms have been ignored. Subsequent refinements to the model may describe variations in the shape and dimensions of bed forms with hydraulic conditions. For instance, it is to be expected that, if present, dune height will vary with depth across the point-bar profile.

Only events at the bankfull stage of the stream have been considered, whereas in reality stage varies with time and deposition may occur over a range of stages. This is discussed more fully below (section 8). Associated with this is the fact that the model does not account for the deposition of 'clay drapes' during the late stages of the flood period, when suspended fines settle from the flow. This is seldom seen, however, because bar deposition is greatest when stage is high and scouring by successive floods may remove the mud drapes and much of the previous deposits. By virtue of the scales involved, and the fact that most deposition is assumed to occur around bankfull stage, much of this finer detail will be lost in the model.

Although the shape of the cross profile approximates the shape of sandy point bars described by many authors, others have noted distinct levels, particularly associated with chutes and chute bars. (McGowan and Garner, 1970; Bluck, 1971). The shape of the cross profile will be expected to vary along the length of the channel, not only due to chutes and chute bars if present, but with the natural occurrence of pools and riffles.

Despite the simplifications involved, Allen (1970a) shows the model to agree with the overall characteristics of known or inferred lateral deposits, and he goes on to make some generalisations based on the model. He points out that the abundance of erosional contacts between sedimentary units testifies to the incompleteness of the depositional record. The applicability of Allen's model as an entity is however limited to 'complete' point bar sections. It is anticipated that by embodying this component model in a real dynamic situation, and taking account of other important processes, that a fuller interpretation and understanding of lateral deposits will appear.

6 MODEL FOR BANK EROSION

6.1 Factors effecting the nature and rate of bank erosion

Recent work by Turnbull et al. (1966) on the Mississippi has shed much light on the detailed processes involved in bank erosion. During rising flood stages the river erodes a deep pool in its talweg. An oversteepening occurs at the toe of the concave bank slope, resulting in a subaqueous failure. Sometimes nothing further occurs but at other times the subaqueous bank failure triggers a further upper-bank failure. The upper-bank failures may be either by shear or by partial to complete liquefaction of the soil, resulting in a flow failure. The type of failure is determined by the type of sediment composing the river bank, but the initiating process was believed to be the same. The study indicates that when long spans of time are considered the subaqueous and upper-bank failures appear to be continuous. Within the period of a year bank failure is a discontinuous process which is seasonally controlled.

The accompanying diagrams, fig. 6.1, show the exact nature of bank failure in different types of exposed deposits, as the hydraulic and gravity forces acting are offered varying degrees of resistance to erosion. The nature of the applied and resisting forces are discussed below.

With regard to hydraulic forces, many authors describe the formation of a scour pool associated with the high velocities and bed shear stresses during high-water periods. Rozovskii (1961) has shown that the downward vertical component of velocity at the concave bank associated with the helicoidal flow is not very great, and so its erosive effect is not considered a dominant hydraulic factor. The impact of fluid on the concave bank is also considered unimportant (Kondratev, 1962).

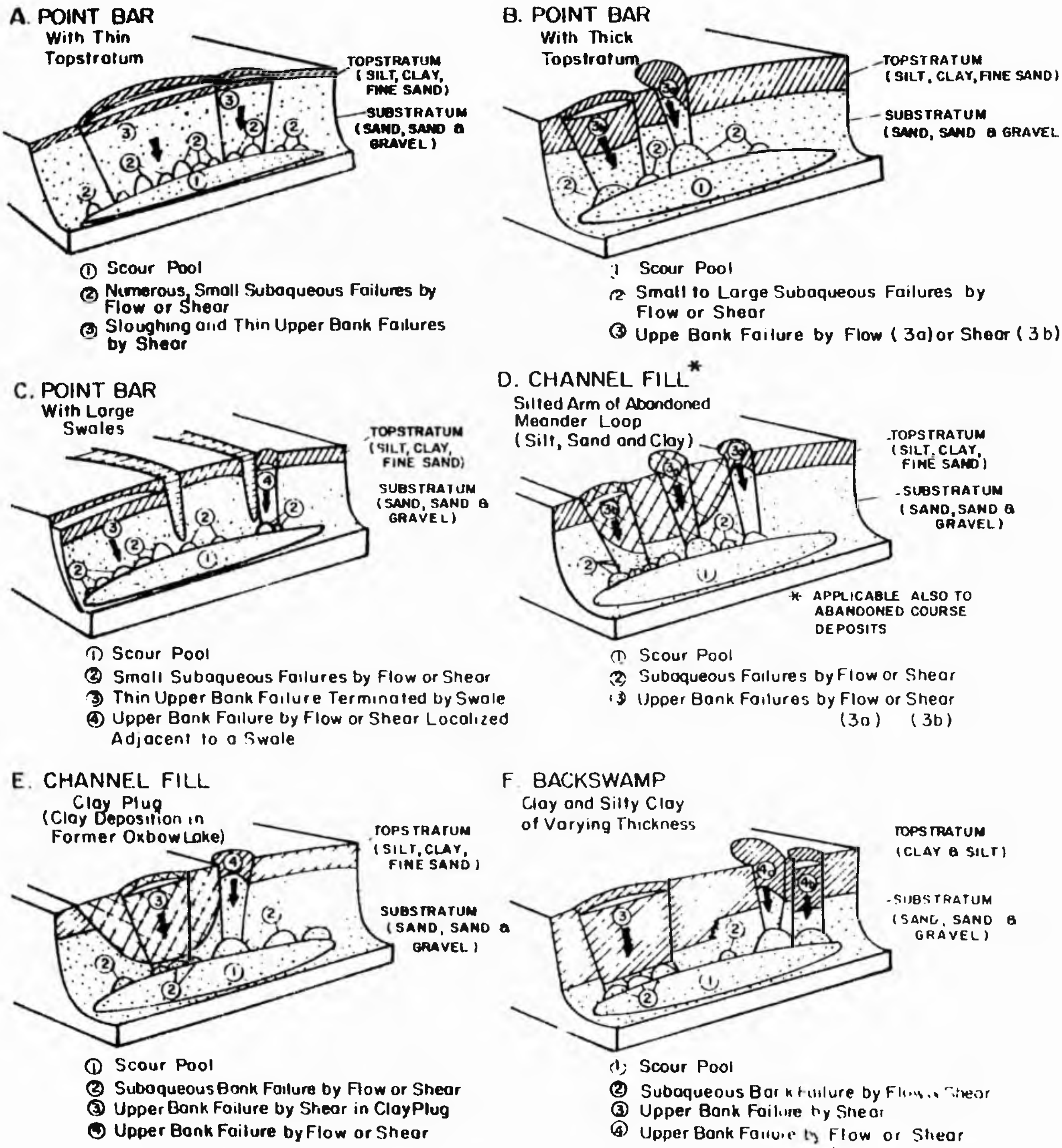

Fig. 6.1. General influences of the geology of river bank sediments on the mechanics of bank failure, according to Turnbull et al., 1966. (from Simons, 1971).

A substantial difference exists between cohesionless sands and gravels and cohesive silt and clay in their interaction with these flow-induced hydrodynamic forces. For the cohesionless sediment the resistance to erosion will depend on the submerged weight of the particles and their angle of repose. In the cohesive beds, surface forces and electrochemical forces control the resistance to erosion. These cohesive forces are only partially understood, however it is known that they are not constant forces but are functions of the fluid quality and have time-dependent strength properties (Partheniades and Paaswell, 1970). A large number of physico-chemical factors of cohesive soils control erosion resistance, and various gross soil properties have been used as indices of erodibility, i.e. shear strength, plasticity index, mean particle size, percent clay, Atterberg limits, dispersion ratio etc. Some of the indices are unsatisfactory for various reasons (e.g. not unique measures, do not accurately convey the state of the soil at the surface, etc.), and although single properties are probably undesirable in such a complex system, better indices may be surface moisture content, density, potential swell, or particle orientation. Unfortunately there is no quantitative standard of erodibility by running water yet developed (Leopold _et al._, 1964; Task committee on erosion of cohesive material, 1968; Partheniades and Paaswell, 1970; Partheniades, 1971).

In the talweg, the material is normally cohesionless sand or gravel, however the concave bank may have varying amounts of cohesive material exposed to the flow. Where the banks are noncohesive, sloughing (the continual and general movement of particles) occurs, as well as slumping. In cohesive sediment, although lumps of cohesive sediment are removed by direct action of fluid forces and impact of suspended sediment, the dominant mode of erosion here is slumping (Fisk, 1947).

The bank failures (slumping) by shear or flow are caused by gravitational instability, which has been shown to be a result of oversteepening of the bank due to the formation of a scour pool or due to undercutting of more easily erodible sediment deep on the eroded bank. Failures by flow or shear occur in the dominantly noncohesive point-bar deposits, and by shear in the thick backswamp clays and clay plugs (see fig. 6.1). Failure is greatly influenced by wetting of bank materials. Arroyos cut in fine-grained alluvium experience most bank cutting after, not during, flow, with wetting causing later slumping (Leopold and Miller, 1956). Wolman (1959) showed that a combination of thorough bank wetting and freeze and thaw promoted the greatest bank erosion in winter, despite large discharges in summer. Failure is also enhanced by the return seepage of water which infiltrates the banks during high flow. Upon lowering the stage the balancing pressure of the water in the channel is released and failure may occur (Jahns, 1947; Fisk, 1947; Inglis, 1949). The slumped blocks are broken up by the river and then subsequently become swept away and incorporated in the floodplain and channel deposits.

As far as slumping is concerned, therefore, the shear strength and permeability are important factors controlling erosion resistance, as are the spatial distribution of sediment types in the bank. Vegetation in the stream bank will inhibit sloughing and slumping, and Jahns (1947) cites the particular example of a vegetated slumped block on which trees re-established themselves at a lower level and severely inhibited erosion.

6.2 Mathematical model

Due to the complexity of the processes of bank erosion, an analytical treatment is not yet possible, however it is possible to look at bank erosion in the required directions using semi-empirical deterministic models. Rate of bank erosion in the direction normal to the mean downvalley direction is discussed first, followed by the development of an expression for downvalley migration.

Handy (1972) has shown that a first-order rate equation of the form

$$S/S_o = e^{-c_1 t} \qquad (6.1)$$

was found to describe the distance S of the channel at the bend axis from an assumed equilibrium position (i.e. from the position at limiting amplitude) as the meander was developing after cut off. S_o is the initial distance from equilibrium, and t is the time taken to get from S_o to S. The constant c_1 depends on the nature of the bank materials and the size of the river. From his analysis, the average rate of erosion at the bend axis, in a direction normal to the mean downvalley direction, can be expressed as

$$RLMIG = c_1 S \; . \qquad (6.2)$$

The equation describes the net river behaviour and indicates that in general the rate of erosion, RLMIG, will decrease as the meander amplitude increases. This is substantiated further by the flume study of Nagabhushanaiah (1967) discussed previously (see fig. 2.6). Although the equation (6.2) describes the gradual reduction in eroding ability in the direction normal to the mean downvalley direction, this will also vary on a different level as discharge varies with time, and as the erosion resistance varies with changes in bank materials.

As already mentioned, Daniel (1971) fitted the sine generated curve to successive meander shapes as the meanders migrated. He also correlated the increase in path length with flow volume, Q_{vol} (time integral over a year of all daily flows above mean annual flow), and percent of silt and clay in the banks. The flow volume showed a linear, and the grain size index a nonlinear, relation with increase in path length. It should be noted that the number of points used to define these relations was very small. Inspection of equation (2.12) and fig. 2.5 will show that path length (equals sn.1) increase has an approximate linear relation with amplitude increase, wavelength remaining constant. The erosion rate, RLMIG, will therefore also have a line relation with flow volume and a nonlinear relation with percent silt and clay. An expression for the erosion rate may therefore be written

$$RLMIG = Sk_2Q_{vol}/GSI^{n_2} \qquad (6.3)$$

where GSI is a grain size index (% silt and clay in the outer bank of the stream), n_2 is an exponent, and k_2 is a constant. Here the term k_2Q_{vol}/GSI^{n_2} replaces c_1 of equation (6.2). Q_{vol} will not be expected to vary very much because the annual flow volumes for days above average discharge are relatively constant (Daniel, 1971). A discussion of the variability of Q_{vol} is given in section 11.3. It may be possible to replace Q_{vol} by some measure of stage, as long as the relation with erosion rate is ascertained. This may, however, involve complications involved with discontinuities in the stage-discharge relation (shifts in rating).

Flume studies (e.g. Freidkin, 1945; Charlton and Benson, 1966; Ackers and Charlton, 1970a) and the field work of Handy (1972) have shown that the downvalley rate of meander migration is independent of the amplitude growth and development. Given lateral homogeneity in bank materials and a constant discharge pattern, therefore, the rate of downvalley migration (RDMIG) will be constant. A general expression for the rate of downvalley migration, of the same form of equation (6.3) is therefore

$$RDMIG = k_3 Q_{vol}/GSI^{n_2} \qquad (6.4)$$

By specifying the constants k_2 and k_3 in equations (6.3) and (6.4), the overall physical limitations to erosion are indicated, and the overall effects of the bank materials and variation in discharge pattern on bank erosion are accounted for. The exponent n_2 describes the nature of the variation in the 'bank materials term' with grain size. RLMIG and RDMIG refer to average erosion over the period of time covered in Q_{vol}.

6.3 Validity of models proposed

It has not been possible to construct generalised models which take account of the numerous controlling factors of bank erosion that have been described, particularly the specific distributions of bank materials that give rise to characteristic modes of bank failure. Instead a simplified view of the 'sub-system' has been taken, and a more practical empirical approach has been substituted for a more desirable, yet impracticable, analytical approach. Thus, the flood period volume has been used to account for the hydraulic forces acting. This may be assumed to account not only for direct fluid stress in the talweg and over the concave bank, but also the effect of the flood waters on the condition of the bank sediment and the return seepage of water on falling stages. A grain size index has been used as a measure of the resistance to erosion by direct fluid forces and failure due to gravitational instability. In reality, a number of different parameters of the sediment forming the banks will be expected to affect resistance to erosion, as previously discussed, and the spatial distribution of sediment types has been shown to be important. Furthermore, the effects of vegetation have not been accounted for explicitly.

The models do, however, maintain the general relationship that exists in natural streams, which is that bank erosion and recession is most rapid in the case of banks of loose sand and gravel and streams of large power, and is least rapid in the case of silt of clay and low powered streams (e.g. Jahns, 1947; Kolb, 1963; Allen, 1970c). Furthermore, equation (6.3) adequately accounts for the reduction in bank erosion normal to the mean downvalley direction as amplitude reaches a limiting value. The constants of proportionality, k_2 and k_3, and exponent n_2, give sufficient flexibility in the equations such that there is adequate representation of the controls of bank erosion in specific cases. As an example in this respect, a factor like vegetation may be accounted for implicitly by choosing the appropriate empirical constants.

6.4. Input

Actual rates of erosion in natural streams vary from a few decimetres to many tens of metres a year. Some of the observed rates of erosion are compiled by Wolman and Leopold (1957).

Fig. 6.2 shows the nature of the variation of bank migration rate, using equation (6.4), for various values of GSI, Q_{vol} and constants k_3 and n_2. Similar curves would be obtained for equation (6.3) with Sk_2Q_{vol} replacing k_3Q_{vol}.

No quantitative measure of n_2 is available, however, by inspection of fig. 6.2, a value close to 0.5 seems appropriate. Obviously more specific empirical data are required to define n_2 adequately. More empirical information is also required to define the relative rates of lateral and downvalley migration in the case of a developing meander, and thus to define the relative

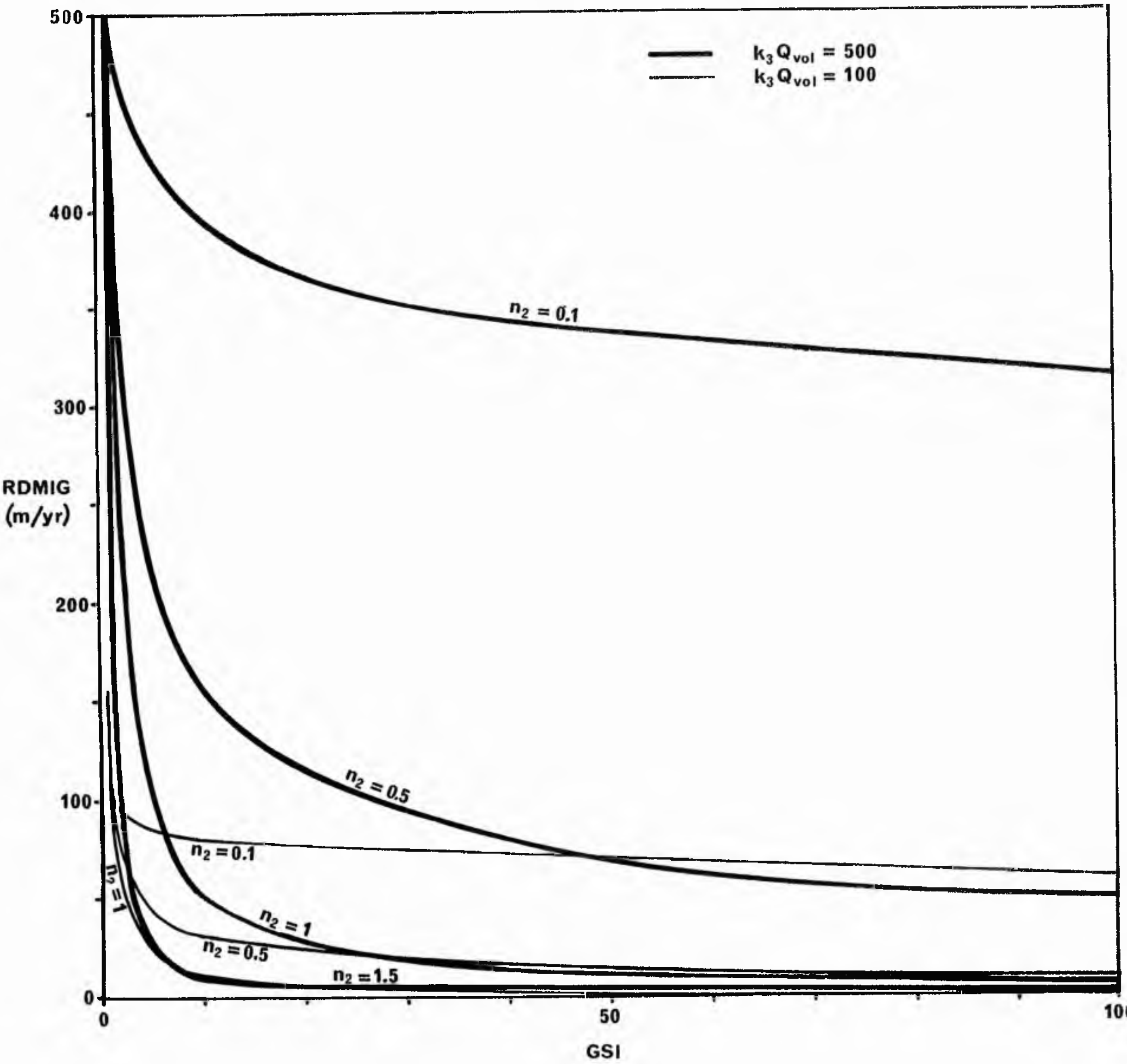

FIG. 6.2 PLOT OF BANK EROSION RATE AGAINST GRAIN SIZE INDEX, ACCORDING TO EQUATION (6.4), FOR DIFFERENT VALUES OF k_3Q_{vol} and n_2.

values of k_2 and k_3 given S and Q_{vol}. Handy's (1972) data suggest that the maximum lateral migration is more than three times the downvalley migration. The absolute values of k_2 and k_3 will depend on the values of Q_{vol}. In this respect, it should be noted that the absolute values and units of Q_{vol} for a particular channel are not explicitly specified (see section 11), therefore k_2 and k_3 assume the role of sealing constants.

7 BANK RECESSION AND BAR GROWTH

Bank erosion in the bend of a meander is usually counteracted by an approximately equal amount of deposition on the opposite bank, thus explaining why the width and cross sectional area remain about the same as the channel moves laterally across the floodplain (Wolman and Leopold, 1957; Leopold and Wolman, 1960; Leopold *et al.*, 1964). This is the basis for determining the amount of lateral sediment deposition in the model. However, certain important points must not be overlooked when using this simplified approach.

In the particular case of a meander developing to a stable form, under conditions where the independent variables are constant, the various dependent variables will be expected to change. The direction of the changes at a cross section may be discussed by examining the Darcy equation,

$$Q = a\sqrt{8gRS/f} \qquad (7.1)$$

where a is the cross sectional area of flow and Q is discharge. For the case of constancy in the independent variables of the channel, at bankfull stage, of a stable meander, all of the parameters on the right hand side of the equation (7.1) are constant (assuming that the 'friction' coefficient is the same for all occurrences of bankfull stage). However, as a meander increases in amplitude at constant wavelength, sinuosity increases and longitudinal water surface slope will decrease. Reference here is being made to development of meanders in which the initial water-surface slope is too steep for a given constant aqueous and sediment discharge (e.g. after the cut off or avulsion situations), and not the situation where water-surface slope is increasing during the development of meanders due to general aggradation which results from too high a sediment load for a given slope (see Ackers and Charlton, 1970). Involved with increase in sinuosity is a characteristic variation in the mean radius of curvature of the bend (see fig. 2.4). Radius of curvature decreases with sinuosity up to a value of 1.5; above this sinuosity, the radius of curvature gradually increases. To counteract the decrease in S on the right hand side of equation (7.1), f, a, and R may vary in any combination, however f has been shown to be intimately related to a, R and r_m.

In general, f_b and f_s will increase with sinuosity. With a and R constant, f_s will increase with decreasing bed shear stress and stream power and increase in the degree of form roughness with the lower flow regime. f_b has been shown to increase with sinuosity, however it also depends on the ratio r_m/w. With width constant, f_b will be expected to increase up to a sinuosity of 1.5, and then gradually decrease. This anomaly may be spurious but at the moment no further light can be thrown on the problem.

If it is assumed that f is increasing with development of the meander, a and/or R must increase. The effect of increasing R, keeping width constant, would be to increase the spiral motion (Yen, 1965; Rozovskii, 1961), thus increasing f_b. However f_s may be decreased due to relative roughness effects or increase in bed shear stress and flow power.

Increase in a, keeping R and the shape of the cross section constant, involves increasing width. The effect of increase in width on spiral flow appears to be somewhat confused in the literature. Yen (1965) infers that an increase in width at constant depth reduces the strength of the spiral flow; Shukry (1950) says the opposite but is dealing with channels of small width/depth ratio. Rozovskii (1961) says the losses due to spiral flow are independent of width.

As can be seen the relationship between f, a, R and r_m is very complex and is not properly understood. Furthermore, despite the difficulty in determining the direction of change in f,a and R, the relative amounts of change are indeterminate at present. Suffice it to say that there will be adjustments, however slight they may be, in the dimensions and resistance of the channel as the meander increases in sinuosity. Unfortunately these cannot be accounted for at present.

8 EROSION AND DEPOSITION DURING HIGH WATER PERIODS

It has been noted by many authors that most of the erosional and depositional activity of rivers is limited to periods of high water (Leopold et al., 1964), and the dimensions of various morphological characteristics of meandering rivers have been related to various measures of discharge that are considered to be 'dominant' discharge (e.g. equation (2.13)). Wolman (1959) states that 85% of observed erosion occurred during the winter floods, supporting Carlston's (1965) conclusions that the dominant deposition and erosion controlling meander wavelength occurred during flows that are equalled or exceeded 10-40% of the year. Schumm (1968, 1969) found that when average, bankfull, and mean annual flood discharge are each correlated with the percentage of silt and clay in the channel perimeter and the channel properties, the results are, to nearly equal degrees, significant explanations of meander wavelength and channel cross-section properties. Stall and Fok (1968) found that hydraulic geometry was best explained using the discharge that is exceeded 10% of the year. Recent work by Ackers and Charlton (1970c) supports some of the earlier workers in their contention that bankfull discharge determines meander pattern.

These facts show that no single measure of discharge can be assumed to control meander dimensions but that a range of discharges are involved. Indeed, Freidkin (1945) shows the position of the main velocity thread in a meander loop at varying discharge, and indicates that low flow, half-bankfull flow and bankfull flow, respectively, attack the upstream, mid, and downstream parts of the concave bank. At discharge greater than bankfull the meandering pattern is not lost, and vigorous erosional and depositional activity within the channel continues, however with a much more complicated flow field prevailing

(Toebes and Sooky, 1967).

Daniel (1971) submits evidence to support the assumption that channel formation will begin at just about the average discharge and continue for all higher discharges (not, however, making any distinction with respect to what part of this range will have the greatest effect). In the model this quantity, flood period volume, is calculated for every year and used in various computations involving erosional and depositional activity. For the reasons outlined above, this 'time integral' of the discharge hydrograph is much more preferable than an instantaneous measure of discharge (c.f. Allen, 1971).

Despite the range of discharges influencing channel formation much of the erosional and depositional activity is expected to occur at discharges closely associated with bankfull stage. This lends support to the study of events within the channel at bankfull stage only (see section 5.8). Bankfull stage recurs on average once or twice every year or so according to climatic regime (Leopold _et al._, 1964; Woodyer, 1968). It can be assumed, therefore that bankfull stage will be attained, or nearly attained, at least once a year, associated with the seasonal high water periods.

During the rising stages of a high water period, increase in velocity and bed shear stress bring about an increase in bed sediment transport and bank erosion. The outer concave bank, together with previously slumped material, is scoured outwards and normally net erosion will occur in the pool and over the point bar. Chutes may develop over the top of the bar and permanent chute or neck cut off may occur when certain limiting conditions exist. Avulsion is also a flood stage phenomenon.

On falling stages sediment is normally deposited on the bar and in the pool and, ultimately, approximately the same channel width and cross sectional area that existed before the flood period will be attained. The position of the bar will be different from that before the flood period, due to the recession of the outer bank. Bank caving following scouring in the pool is often a falling stage phenomenon (Matthes, 1941; Jahns, 1947; Inglis, 1947; Russell, 1967), and those caved blocks left after the end of the flood period will be swept away in subsequent flood periods. A detailed discussion of 'scour and fill' and cut-off follows.

9 SCOUR AND FILL

9.1 Preliminary discussion

Colby (1964) discusses two principles which are helpful in understanding scour and fill in sand bed streams. One is the principle of continuity of volume of bed material along a stream reach. This principle simply states that changes in the average elevation of a bed in a reach result from the difference in the rates at which sand enters and leaves the area. The second principle is that a relation exists between the discharge of sands and the characteristics of flow and available sediment (e.g. Bagnold, 1966). Therefore in the case of steady uniform flow the average sediment transport rate at a point remains constant with time and remains unchanged with distance along a streamline. In such a case there will be no progressive erosion or deposition of sediment and the stream bed elevation will remain constant. However, when the flow is unsteady and non-uniform, the ability to transport sediment varies and erosion and deposition can occur. For gradually changing flow, Allen (1970c) expressed the rate of erosion or deposition as

$$\text{rate of erosion or deposition} = \frac{\partial i}{\partial x} + \frac{1}{V}\frac{\partial i}{\partial t} \qquad (9.1)$$

where i is the sediment transport rate (immersed weight passed per unit width per unit time), V the mean fluid flow velocity, t is time, and x is the distance measured in the local downstream direction. The first term represents the contribution from the nonuniformity of flow and the second term the contribution from the unsteadiness. Whether erosion or deposition occurs depends on whether the right hand side is positive or negative respectively, which depends on the relative magnitudes and signs of the two terms. In fact, on further study of equation (9.1), it can be seen that the unsteady term indicates that erosion or deposition may occur at a point only because of changing transport rate at that point. This is not in agreement with Colby's principle of continuity of sediment movement and so in studies of scour and fill the meaningful use of this term is precluded.

The proviso of gradually varying flow is partly due to the lag between sediment transport rate and changes in flow. The quantities determining local sediment transport rate do not change instantaneously with changes in flow but instead, at any point, these quantities are strongly influenced by the flow conditions prevailing upstream from this location. Furthermore, a finite time and corresponding distance are required for the excess entrained sediment to settle to the bed as the flow power decreases, and for additional sediment to be entrained as flow power increases (Kennedy, 1963).

Study of the hydraulic geometry shows that, during the passing of a flood wave at a cross section, changes in water discharge and energy gradient will result in changes in flow resistance, width, depth, water surface slope, and velocity (Leopold *et al.*, 1964). In particular width, depth, slope and velocity generally increases. Flow resistance is affected by the changing concentration of fine sediment or, in a more discontinuous way, due to changing bed forms or overbank flow. Turbulence, fluid density and apparent viscosity, hence effective fall velocity of particles, are affected by changes in temperature and fine sediment concentration. This in turn affects bed configuration. The changes in hydraulic variables are inter-related in a complex way, however, in general, it can be said that sediment transport rate at a section increases with the flood wave.

The principles involved in scour and fill can be applied to meandering streams in two contexts; in terms of a reach and in terms of a single bend. In the first case, for simplicity, we will assume that there is no overbank flow and that the general characteristics of flow and available sediment are the same at each end of the reach. During a flood wave the hydrograph will lag a little from one end of the reach to the other, hence average sediment discharge will lag in a similar way. This will result in net deposition in the reach during the rising stages, i.e. $\partial i/\partial x$ is negative, and net erosion during the waning period, i.e. $\partial i/\partial x$ is positive. If however, for some reason, the inflow to the reach is stopped, scour over the distance required to entrain an equilibrium sediment load would occur at the beginning of the reach. Also, if the characteristics of flow and available sediment are not the same for both ends of the reach, perhaps due to differences in slope or flow resistance, then $\partial i/\partial x$ would not be zero and scour or deposition may occur.

Colby has shown that the thickness of sediment eroded or deposited in these cases is very small when averaged out over the stream bed. These points indicate that the average bed elevation in a reach, under the conditions specified, is usually fairly stable during the passage of a flood period, and that there is not general scouring and filling over the whole reach during rising and falling stages.

In the context of a single bend, the characteristics of flow and available sediment during the low water stages can be expected to be different between the pool and the riffle, and thus sediment transport rates will be different. However sediment transport rates will be very small at low discharges, so they warrant little attention. Lane and Borland (1954) have shown that as the water surface rises the cross sectional area of flow increases faster at the riffles than in the pools, and this is normally accompanied by changes in the hydraulic parameters in a different way in the pool from at the riffle. In general on rising stages $\partial i/\partial x$ becomes a positive number at the pool and scouring occurs in the pool. At the riffle $\partial i/\partial x$ becomes a negative quantity and deposition occurs on the riffle. On falling stages the opposite will happen (Freidkin, 1945; Sundborg, 1956; Kondratev, 1962). Such bed changes will be significantly more than in the cases previously mentioned (Colby, 1964). See fig. 9.1.

9.2 Mathematical model for scour depth

Scour and fill in a meander can be treated empirically on a deterministic basis with certain stochastic properties.

The average net scour (in terms of immersed weight per unit width) at a cross section in the pool, NS, can be written

$$NS = \int_0^T \frac{\partial i}{\partial x}(t)\, dt \qquad (9.2)$$

where $\partial i/\partial x(t)$ is the time varying rate of erosion or deposition at a particular section. T is the time from the beginning of appreciable sediment movement on rising stages ($\partial i/\partial x(t)$ may not necessarily be positive at this time) through the positive range of $\partial i/\partial x(t)$ until it becomes zero. $\partial i/\partial x(t)$ will then become negative and deposition will occur until it becomes zero again (see fig. 9.2).

It can be seen that the net scour (area A-B in fig. 9.2) will depend on T and the shape characteristics of the curve of $\partial i/\partial x(t)$ as t varies between 0 and T. The shape of the curve of $\partial i/\partial x(t)$ depends, as already indicated, mainly on (a) the hydraulic nature of the cross sections within the pool and riffle at a given stage, which controls the relative spatial and temporal distribution of sediment transport rates, together with (b) the time variation of the changes in stage. Fig. 9.1 shows a tendency for $\partial i/\partial x(t)$ to change from positive to negative

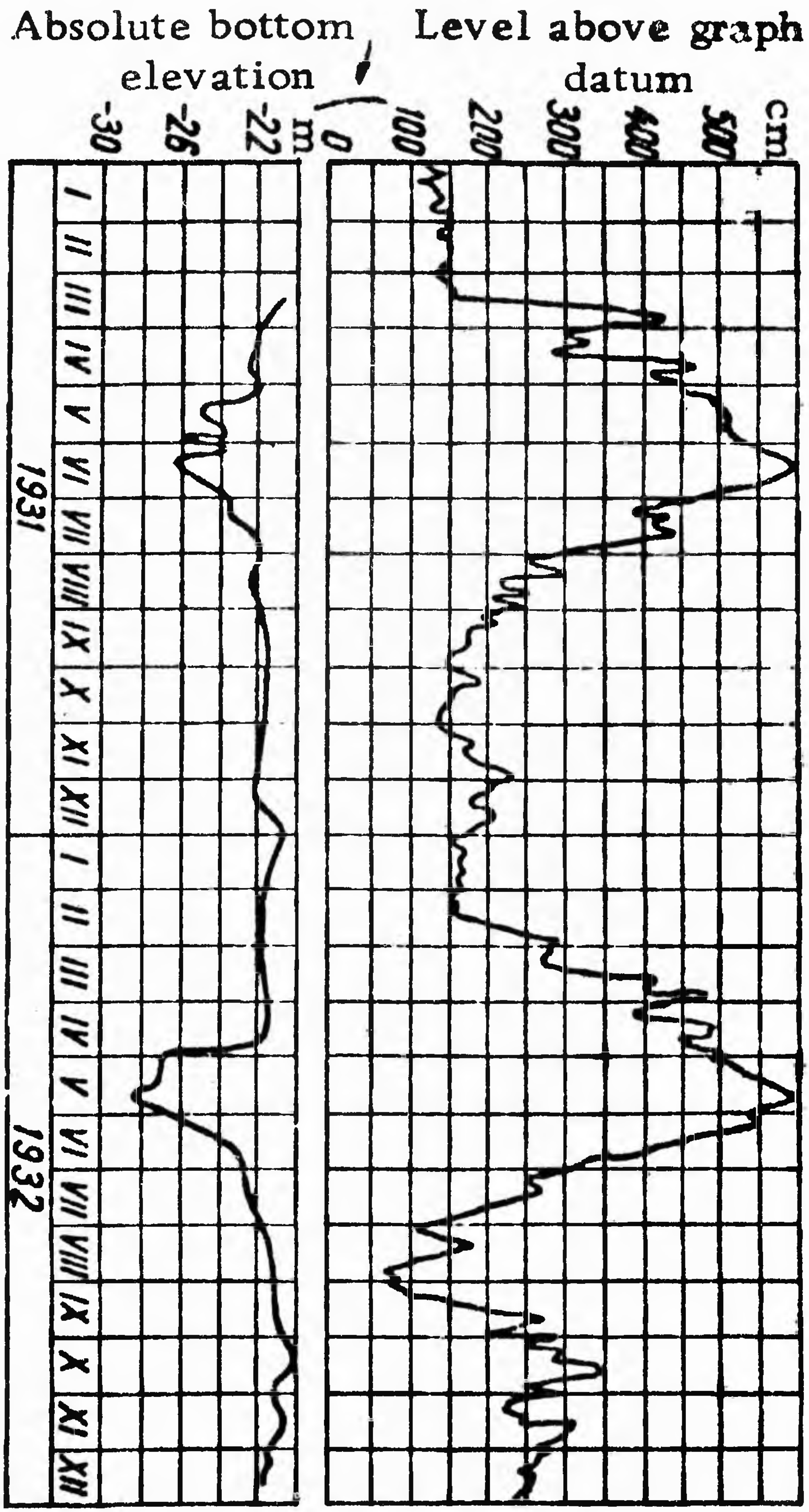

Fig. 9.1. Graph of daily water level and bed elevation in pools. (from Kondratev, 1962).

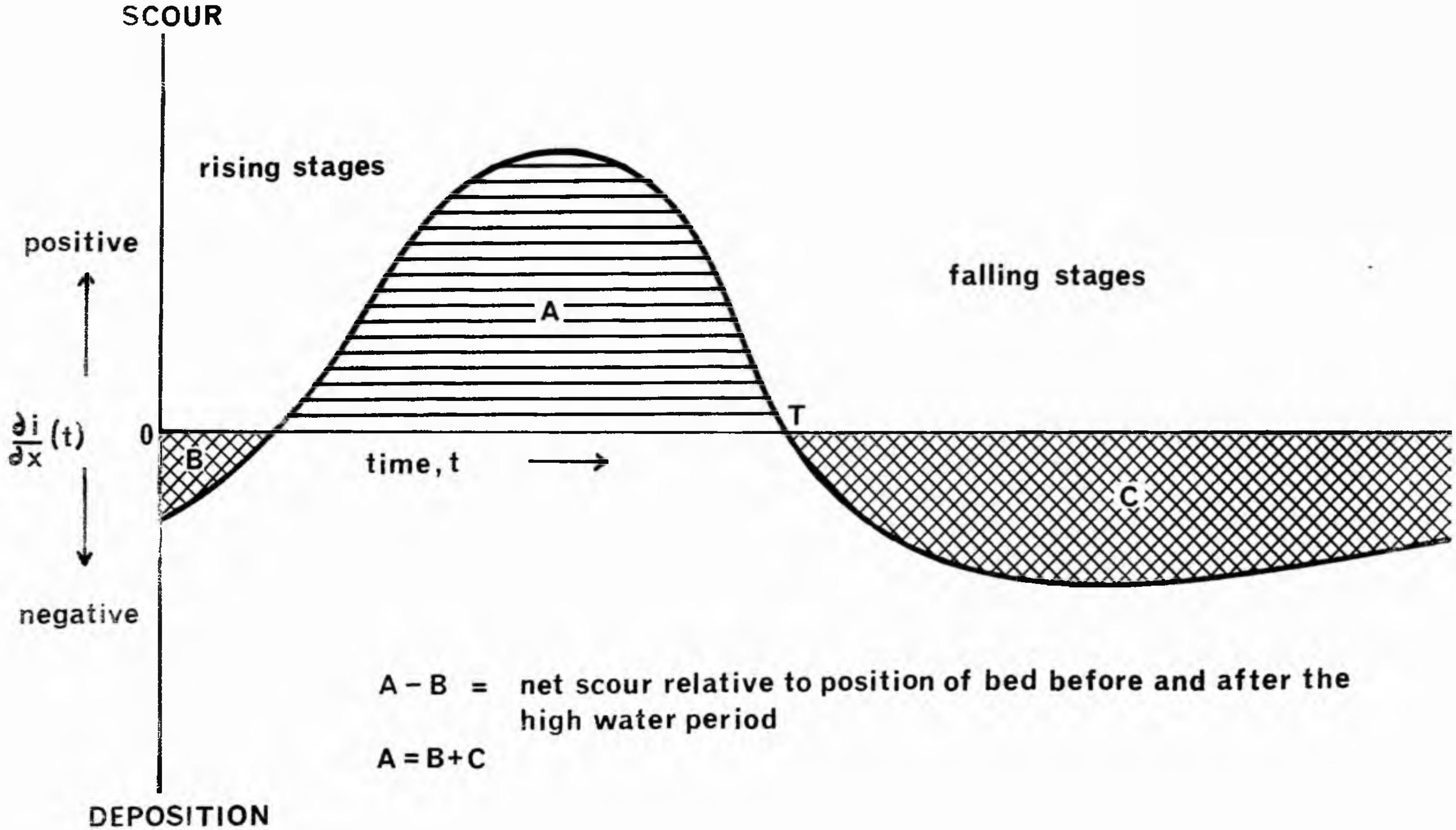

FIG. 9.2 IDEALISED VARIATION OF EROSION AND DEPOSITION AT A CROSS SECTION IN A CHANNEL BEND(POOL) WITH THE PASSING OF A HIGH WATER PERIOD.

(i.e. t=T) at about the peak stage for each flood period and that there is a tendency for a change from negative to positive (deposition to scouring) in the early rising stages. T is also expected to depend on (a) above, as well as the flood period hydrograph. The curve shown in fig. 9.2 is assumed to be smooth for simplicity, although by virtue of the controlling factors it would probably have fluctuations imposed on the general trend.

We may now say qualitatively that for any high water period, the average net scour at a cross section is a sole function of the cross section characteristics around the meander and the shape of the flood period hydrograph. An analytical representation of this functional relation cannot be determined at present; however a somewhat approximate relation will be determined for this study.

A measure of the flood period hydrograph can be obtained as the integral of the flood period discharges with respect to time, that is, the flood period volume, Q_{vol}, as defined earlier. It will now be assumed that the hydraulic nature of the cross sections within the pool and riffle at any given stage is constant for every flood period. This assumption may not be valid, especially when meander sinuosity and amplitude is increasing, however much further research is needed to test this assumption adequately. For the present the variation of NS can be described using an equation of the form

$$DSCR = k_4 (Q_{vol})^{n_3} \qquad (9.3)$$

where DSCR is a measure of NS and is the net depth of scour below the bed elevation before and after the flood period, measured at the talweg. The empirical values of the constants k_4 and n_3 for a particular cross section are imposed by the characteristics of the channel cross sections around the meander, for the range of Q_{vol} used. For a given value of Q_{vol} (with constant k_4 and n_3), NS (and DSCR) may vary for some combination of the following reasons; (a) Apart from the approximating assumption of using Q_{vol} as the only variable, approximations are also involved in the use of Q_{vol} as a parameter and effectively ignoring separate flood events within a flood period. (b) Local effects of scouring, i.e. in the lee of dunes. (c) General scouring or deposition affecting the whole reach as previously discussed.

It will therefore be assumed that all fluctuations about the mean curve (equation (9.3)) can be treated stochastically by introducing a term, er, which is a normally distributed random variable with mean 0 and standard deviation, stdvn, some function of the absolute limits of scour depth. Therefore, we write

$$DSCR = k_4(Q_{vol})^{n_3} + er\ (0,\ stdvn) \qquad (9.4)$$

Unfortunately, at present the general validity of equation (9.4) cannot be assessed, however it is sufficiently flexible to account for scouring in the specific case, as defined by the empirical input variables, k_4, n_3 and stdvn.

In the model the overall shape of the scour hollow is obtained by assuming no scour at the junction of the bankfull water surface and the inner bank. The scoured bed profile is then defined using the equation for the point bar profile (e.g. equation (5.1)) but, at the talweg, the bed is a distance DSCR below the original depth. This is illustrated in fig. 14.2. The shape of this scoured bed is purely heuristic, however inspection of fig. 9.3 lends a fair degree of credibility to the method used.

9.3 Deposition on falling stages

On falling stages, in the absence of any external disturbing factors, deposition will normally fill the bed to its original depth, however probably at a slower rate because the hydrograph is

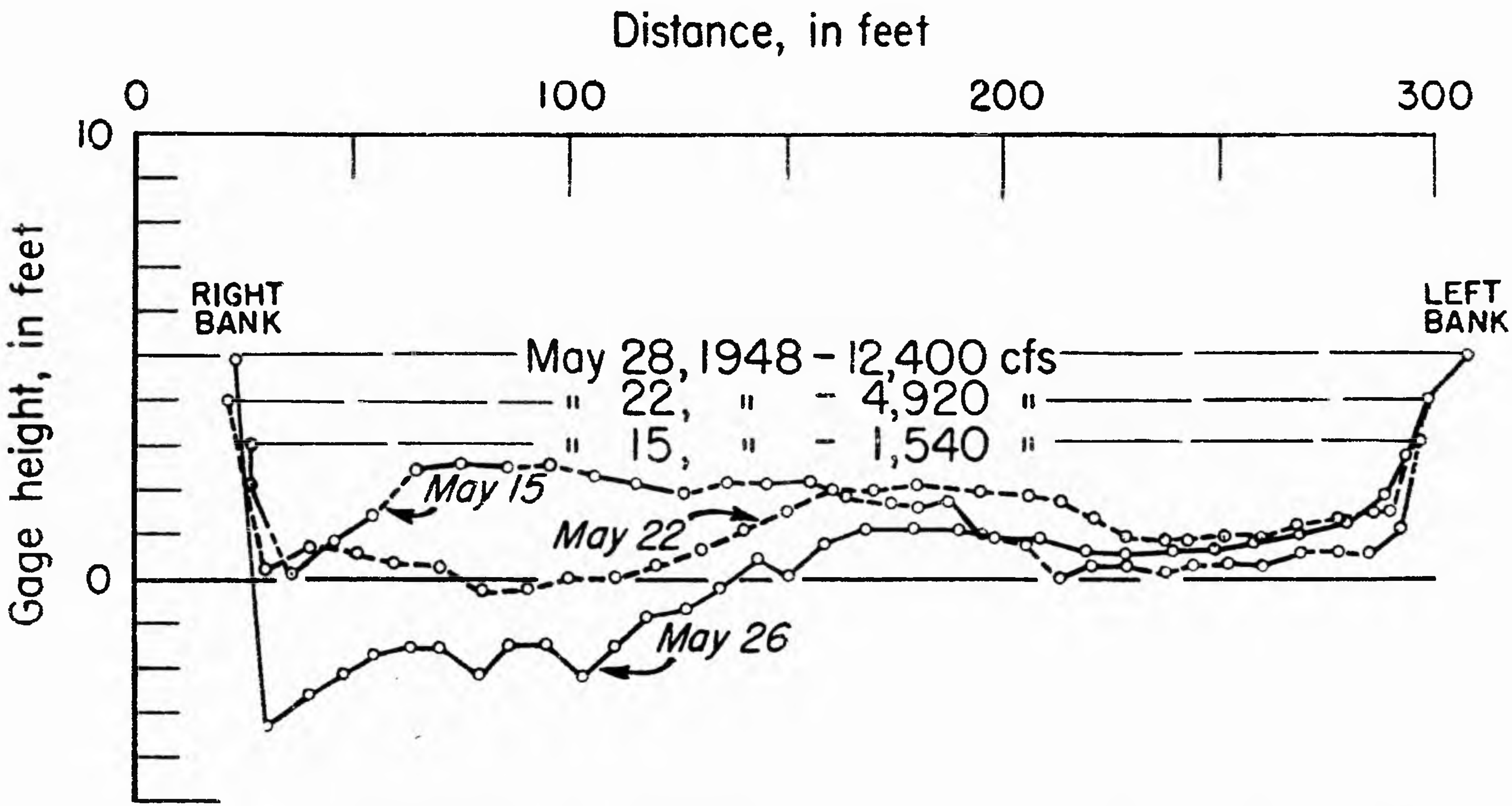

Fig. 9.3. Channel cross sections during progress of flood, May-June 1948, Rio Grande near Bernalillo, N. Mex. (from Leopold and Maddock, 1953).

not as steep on falling stages (see fig. 9.1). In the model it will be assumed that, after scour, most of the filling to the original bed profile is accomplished on falling stages, or at least before the next flood period. The scoured bed is filled by incrementally reducing the depth at the talweg and redefining the bed profile at each increment using the equation of the point bar profile. The grain size and sedimentary structure in the fill are obtained by repeated application of the point bar sediments model (section 5) across the profile as the depth is incrementally reduced to the original (see section 14 for details). It is therefore assumed that the 'equilibrium' bed forms, corresponding to the different flow conditions, have time to develop at each level of the bed as filling proceeds. Throughout this operation it is assumed that the water level and slope are constant at bankfull level. Thus, as in the point bar sediments model, it is assumed that all the depositional activity occurs at bankfull stage.

9.4 Input

The values chosen for k_4,n_3 and stdvn can only be heuristic at present, and they will be expected, because of their empirical nature, to be limited for use on any one specific cross section under discussion. As previously stated, the absolute values and units of Q_{vol} are not explicitly specified as they are only being used in empirical equations which are scaled by proportionality constants, in this case k_4. Having chosen the necessary empirical values, the variation of scour depth will be described, whilst also making a statement describing the limitations imposed on scouring by the whole hydraulic makeup of the meander in question. The shape of the curve of DSCR plotted against Q_{vol} is described by exponent n_3. It is expected to be a positive number but little else can be said at present. Stdvn is expected

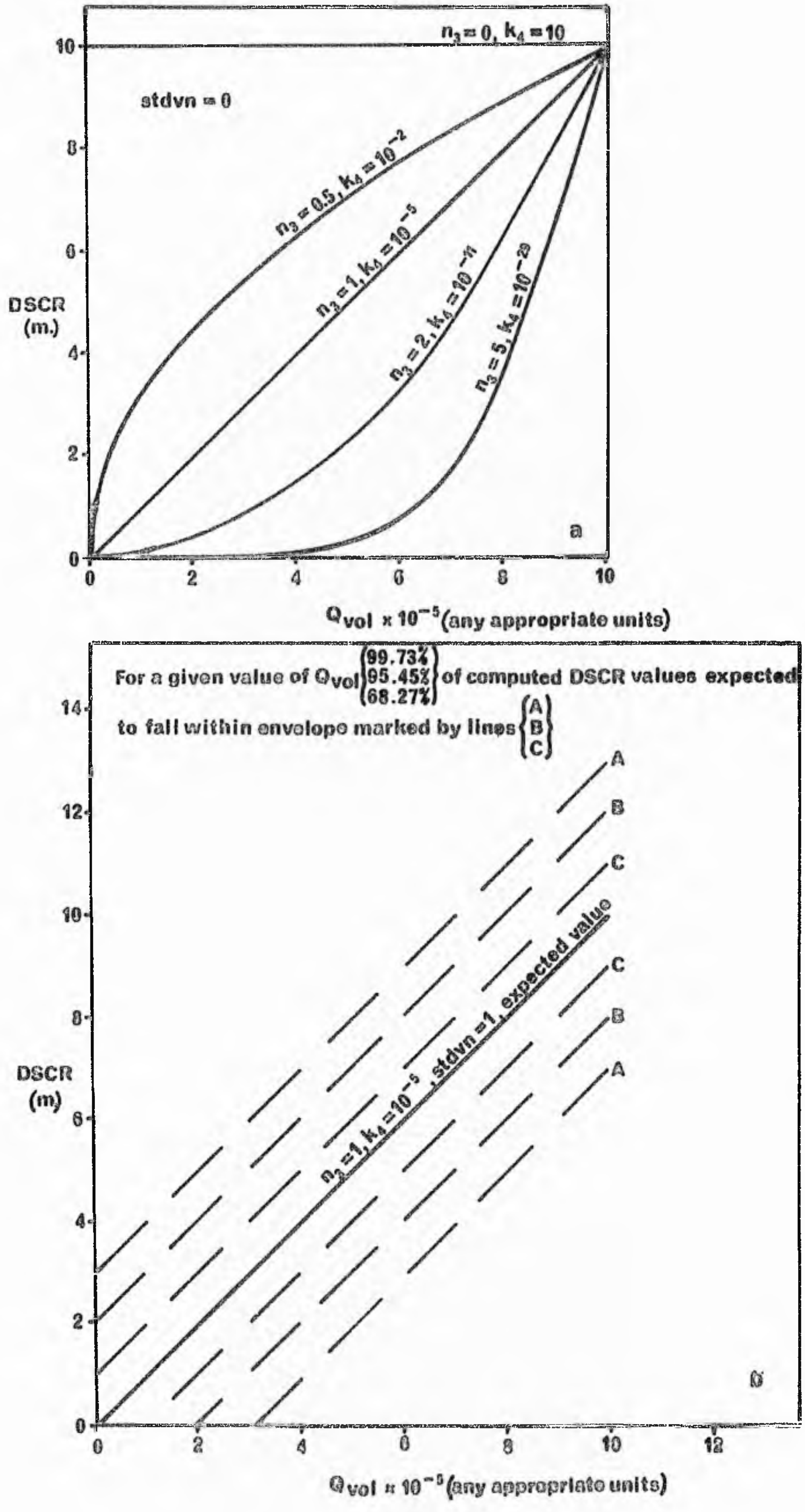

FIG. 8.4 VARIATION OF DSCR WITH Q_{vol} ACCORDING TO EQUATION (8.4) FOR (a) DIFFERENT VALUES OF n_3 AND k_4, WITH stdvn = 0, AND (b) CONSTANT n_3 AND k_4, AND stdvn = 1.

to be some fraction of the limiting scour depth. The value of k_4 for a given range of Q_{vol} can be alluded to by using as a general guide the fact that the bed commonly recedes about the same order of magnitude as the water surface rises (Leopold et al., 1964; Lane and Borland, 1954). Fig. 9.4 shows the variation of DSCR with Q_{vol} for various values of the parameters. It is to be noted here that if n_3 is required to be varied, for a given range of Q_{vol} and DSCR, k_4 must be adjusted also.

The phenomenon of scour and fill is characteristic of ephemeral sand bed streams and large rivers in semi-arid climates; it is less typical of rivers in humid areas or those in high mountains, presumably because perennial flow tends to winnow away the fine material and the bed becomes armoured with coarse materials (Leopold et al., 1964). In the sand bed streams of the present study scour and fill is to be expected, however an option will exist in the model if scour and fill is not required.

10 CUT-OFF

Cut-off occurs whenever the meandering stream can shorten its course and thus locally increase its slope, the frequency of cut-off increasing with channel sinuosity (Allen, 1965a).

10.1 Model for chute cut-off

As already stated, the formation of chutes is associated with a limiting sinuosity and amplitude to the extent that flow resistance is less over the bar than around the bend (Freidkin, 1945). An increase in amplitude and sinuosity towards limiting values, wavelength constant in the model, thus involves an increasing tendency for the formation of chutes. During flood stages, the directing of a greater part of the flow across the bar enhances the tendency for chute formation. Due to the assumed homogeneity of the bank materials, there will be no other cause of change in alignment of the flow upstream.

Permanent chute cut-off can therefore be treated as a probability function of the magnitude of the flood volume and the sinuosity, a higher probability of occurrence being associated with high floods and with a limiting value of sinuosity, thus

$$p(c) = (Q_{vol}/Q_{volmax})^{ec_1}(sn/sn_{lim})^{ec_2} \qquad (10.1)$$

where p(c) is the probability of chute cut off, sn_{lim} is the limiting sinuosity, and Q_{volmax} is the value of Q_{vol} at which cut off would be a certainty if sn is also equal to sn_{lim}. By increasing the empirical exponents ec_1 and ec_2, the probability of cut-off becomes very small unless Q_{vol} and sinuosity are close to their limiting values.

The occurrence of chute cut-off in the model is determined by generating a pseudorandom number in the range 0 to 1. This number is then compared with the value of p(c) for the particular high water period under consideration. If p(c) is greater than the number, chute cut-off will occur. In fact the process of chute cut-off takes place slowly because the angle of diversion of the water down the shorter course is small and the increase in flow is gradual (Fisk, 1947). The occurrence of chute cut-off is therefore defined as the beginning of the process which is assumed to go to its end point. The model will be stopped after the initiation of cut-off because of the complicated flow patterns that result, the inability to predict where the new channel will form, and the inability to account for the deposition in the old channel.

10.2 Model for neck cut-off

Neck cut-off will tend to occur when the meander neck, the shortest distance from the adjacent banks of closing meander limbs (therefore only defined in meanders in which the local downstream direction makes an angle greater than 90° with the mean downvalley direction), approaches close to a limiting width, necessarily a small quantity. Neck cut-off could occur if sinuosity could increase, wavelength remaining constant, to such a value that the meander neck, GAP, becomes very small. This is the situation in the meandering tidal creeks of the Niger Delta region (Nedeco, 1959). Decreasing wavelength of a meander due to a clay plug, and the associated distortion of the loop, will cause sinuosity to increase rapidly and the meander neck to become small. Neck cut-off in this situation is described by Fisk (1944, 1947) from the Lower Mississippi. Because of the conditions imposed in this study, the effects of clay plugs cannot be accounted for and the latter mechanism cannot be simulated. A probability function similar to that used for chute cut-off may be used for neck cut-off, i.e.

$$p(n) = (Q_{vol}/Q_{volmax})^{en_1}(GAP_{lim}/GAP)^{en_2} \qquad (10.2)$$

where GAP_{lim} is the limiting value of GAP, and en_1 and en_2 are empirical exponents. The occurrence of neck cut-off will be determined as outlined above, and the model will again be stopped after neck cut off has been initiated.

10.3 Input

The expressions given in equation (10.1) and (10.2) above are necessarily of a heuristic nature because of the lack of precise knowledge on the subject. The values of ec_1, ec_2, en_1 and en_2 will be intuitive and will be expected to be relatively large positive numbers. Their values can only be inferred by trial and error, and in this respect it is noteworthy that average times taken to cut-off from inception of a meander loop to cut-off are of the order of hundreds of years (see Handy, 1972; Lathrap, 1968). This will be expected to vary with the general hydraulic setting. Specifically, the time taken before cut-off is initiated will be expected to depend on the general calibre of sediment in the perimeter of the channel, which will influence the rate of lateral erosion relative to the size of the stream, the 'equilibrium' sinuosity, and the susceptibility to deep scouring. It will also depend on the variability of the flood period volume above that which exerts most control on the channel formation.

Examination of the maps produced by Fisk (1947) of the Mississippi Valley shows that natural chute cut-off occurs at sinuosities up to about 2.0, and before the angle between the local direction of the channel and the mean downvalley direction exceeds about 90°. If the value of the limiting sinuosity is greater than about 2.0 (approximately) chute cut-off will not normally be expected and mutual adjustments of the exponents may be required here.

The limiting value of sinuosity has been discussed earlier, and expected to depend on the grade of sediment in the meander and, related to this, the width/depth ratio of the channel. Fisk's maps further show that neck cut-off involves meanders with considerably greater sinuosity than 2.0, and the limiting value of the meander neck is expected to be very small relative to the dimensions of the meander.

The relationship between any Q_{vol} and the value of Q_{volmax} (presumably based on long period records) depends on the character of the river regime under consideration. Presumably adjustments in ec_1 and en_1 will be required as the variability of Q_{vol} varies.

11 FLOOD PERIOD VOLUME

Introduction

It is now necessary to compute the flood period volume, Q_{vol}, which is defined as the sum over a year of all daily flows above the mean daily flow for a particular hydrograph. This is done by sequential generation of daily streamflows using the apparatus of operational hydrology. The absolute values of daily flows, hence flood period volumes, are not important as they are used only in empirical equations which are scaled with proportionality constants. The important point therefore is the shapes of the hydrographs and not the absolute scales. It would in fact be difficult to find an absolutely rigorous discharge hydrograph (dimensionwise) to fit a particular channel section, as the discharge pattern, specifically bankfull discharge, is not explicitly defined. By virtue of model construction, discharge, an independent system variable, is made dependent by specifying the channel and meander dimensions.

11.1 Sequential generation of streamflow data

One approach to streamflow simulation involves analysis of the hydrological system in order to find the causal relation between streamflow and its controlling factors. Numerous deterministic methods have been proposed and developed to empirically relate one or more climatic and physiographic factors to the streamflow hydrograph or some other streamflow characteristic, with considerable variation in the number of factors used (see Chorley and Kennedy, 1971; Crawford and Linsley, 1966). Although such methods of streamflow generation may be useful in reconstructing the climatic and physiological characteristics of the basin to which a particular streamflow record is related, their use is precluded by the amount and nature of the input data required.

Other approaches seek only to analyse the observed streamflow record. The flood record is often analysed and fitted with a certain probability distribution to determine the recurrence intervals of the flood or the flood frequencies. This type of analysis cannot be used for sequential generation of streamflow data. Because the hydrologic process is stochastic (Chow, 1964, 1967) the streamflow hydrograph may be thought of as a continuous time series, and daily, monthly or annual discharges (or stages) represent discrete time series. A time series may be approximated by a mathematical generating model, the choice of which is based on how well the mathematical structure of the model fits the physical characteristics of the time series. Hydrological processes and time series are generally treated as stationary, sometimes after simple transformations on the original time series, in order to simplify the mathematics. Various mathematical models, or combinations of models have been used in hydrology, and, in order to decide which provides the best fit, the sample correlogram and power spectrum have been used (e.g. Chow and Kareliotis, 1970; Dawdy and Matalas, 1964; Quimpo, 1967, 1968a,b).

11.2 Mathematical model of hydrologic time series

In this study it is intended to generate a pattern of daily flows at a given stream section (absolute values being irrelevant) using the mathematical representation of the time series pertaining to that section. Such a series will be the combined effect of a deterministic component and a stochastic component. In general, the deterministic component may be composed of a trend and an oscillatory component. Trends may be removed from the time series by such methods as moving averages or polynomial regression, however, in this study the trend will, for simplicity, be assumed absent.

The mathematical model used is a combination of the sum of harmonics and autoregressive models (e.g. Roesner and Yevjevich, 1966; Quimpo, 1967, 1968a; Rodriguez-Iturbe, 1968; Adamowski, 1971). If X_t is a nonstationary time series of daily flows, that is assuming the observed value of each of the 365 days in the year is to be drawn from a different population, stationarity can be approximated and the components of X_t can be separated by the following transformation,

$$Z_t = (X_t - m_\tau)/s_\tau \tag{11.1}$$

where m_τ is the daily mean value of the day τ, s_τ is the standard deviation of day τ, and τ runs from 1 up to 365. The 'standardised series', Z_t, is second order stationary, being distributed with zero mean and standard deviation unity for all daily values.

Using Fourier analysis, a mathematical representation of the m_τ and the s_τ may be expressed as continuous functions, m_t and s_t, by the expressions

$$m_t = \bar{m}_\tau + \sum_k (A_k \cos \frac{2\pi k}{L} t + B_k \sin \frac{2\pi k}{L} t) \tag{11.2}$$

$$s_t = \bar{s}_\tau + \sum_k ({}_sA_k \cos \frac{2\pi k}{L} t + {}_sB_k \sin \frac{2\pi k}{L} t) \tag{11.3}$$

where $\bar{m}_\tau$ and $\bar{s}_\tau$ are the means of the m_τ and s_τ respectively, and $A_k, B_k, {}_sA_k$, and ${}_sB_k$ are Fourier coefficients. Experience shows that a plot of the expected daily values of the time series X_t over a number of years results in a periodic movement with a fundamental period of one year. L therefore becomes 365.

It should be noted that in order to fit the trigonometric functions of the Fourier series to the shape of the observed periodic movements, the number of harmonics required varies depending on the shape of the periodic movements in question.

For instance, physical considerations of hydrologic periodicities normally indicate a yearly cycle, often with a 6-month cycle as well. If the yearly periodic movement is far from a sine function, some or all of the other subharmonics may be needed, depending on their contribution to the observed variance. Thus, because of the method of analysis used, more harmonics than those corresponding to the basic astrononomical cycles may be required. In this study, no more than five subharmonics of the yearly cycle will be used, that is, k=1,2,..6.

If equation (11.1) is rewritten using the harmonic representation of m_τ and s_τ the resulting series

$$Y_t = (X_t - m_t)/s_t \qquad (11.4)$$

in the general case is no longer distributed with zero mean and standard deviation unity. A further transformation is necessary, i.e.

$$Z_t = \frac{Y_t - \bar{Y}}{s_y} = \frac{X_t - \bar{Y}s_t - m_t}{s_y s_t} \qquad (11.5)$$

where $\bar{Y}$ and s_y are the mean and standard deviation of Y_t, respectively. This is the 'standardised fitted series' or just 'fitted series'. It can be seen that Z_t may be described by equation (11.1 or (11.5), however the number of parameters required will always be much less using equation (11.5), thus making this expression more desirable.

Now that the periodic movement has been isolated, the residual series Z_t can be fitted with a mathematical model. The shape of the correlogram of Z_t will indicate the type of model to be used. If, on a given level of significance, it can be said that $E(r_L) = \rho_L = 0$, where r_L and ρ_L are the Lth order serial correlation coefficients of sample Z_t, and the population from which Z_t is drawn, respectively, then the time series Z_t may be considered as a sequence of stochastic variables which are independent among themselves. A significance test is available to test for independence.

It has been shown that in general the series Z_t for daily values cannot be represented by the independent model, but may be represented by a linear autoregressive (Markov) model of the second order (Quimpo, 1967, 1968a). The adequacy of the model is based on the fact that the computed variance of the model based on the estimated parameters agreed well with the computed residual variance. The model is given as

$$Z_t = a_1 Z_{t-1} + a_2 Z_{t-2} + \epsilon_t \quad (11.6)$$

Estimates of a_1 and a_2 are given as

$$a_1 = \frac{r_1(1-r_2)}{1-r_1^2} \qquad \text{and} \qquad a_2 = \frac{r_2 - r_1^2}{1-r_1^2}$$

The residual series ϵ_t is independent of Z_{t-1}, Z_{t-2}, and other ϵ's. For the model adopted

$$\epsilon_t = \frac{1+a_2}{1-a_2} \left\{ (1-a_2)^2 - a_1^2 \right\} \eta_t \quad (11.7)$$

where η_t is a standardised independent stochastic variable (the primary variable).

It is necessary to know the distribution of ϵ_t as this may be crucial if it contributes much of the variance of the whole series. However the model only accounts for second order stationarity in Z_t, therefore the frequency distribution of ϵ_t cannot be simply determined because the expected values of the central moments greater than two may not be constant. If they were constant, for instance if the residual series ϵ_t follows a Gaussian distribution, then Z_t would be strictly stationary. In practice the residual values are positively skewed because of the restraint imposed by a minimum flow of zero. Evaluation of the higher moments is unrealistic and so stationarity of order higher than two is best approximated by assuming that the residual series,

ϵ_t or η_t, is distributed with a positive skew, i.e. lognormal or gamma (Pearson type III) (Hamlin, 1971). Upon the determination of the probability distribution, a series X_t may be generated by generating random variables η_t with the appropriate distribution using Monte Carlo techniques (see appendix 1).

It is obviously important to know the relative influence of each component of the original time series in order to assign limits of accuracy when one or more of the components are neglected or approximated in a simplified synthesis of hydrologic data. In this study simplified models have been used at the cost of generality. The number of harmonics used to describe the periodicity has been limited to six, and the order of the auto-regressive model has not been tested beyond order three. Furthermore, the trend component, which may include a 'persistence' effect, has been ignored.

11.3 Input and experimentation with the model

Once the series of daily flows for a year has been generated it is a simple matter to find the flood period volume. The parameters used in the hydrology model adopted will depend on the shape of the hydrograph that is selected for use in the model, or the 'river regime' that is desired.

Fig. 11.1 represents the daily means and standard deviations about the means for selected rivers in the U.S.A., taken from Quimpo (1967). They are classified into different river regimes according to the classification given by Beckinsale (1969). Table 11.1 shows the values of the parameters used in the stochastic models of the daily river flows, as calculated by Quimpo (1967).

500 years of records were generated using the parameters given in table 11.1 for each station, using three different distributions for the primary variable η_t. The values of Q_{vol}

		BATTEN KILL R.	COWPASTURE R.	OCONTO R.	DELAWARE R.	NECHES R.	FALLS CREEK	BOISE R.
	$\bar{m}$	722.9	515.6	543.5	375.9	2385.2	141.2	1172.7
	$\bar{s}$	722.9	762.3	441.0	1617.7	3813.0	234.2	1458.6
	$\bar{Y}$	0.0	0.0	0.0	0.0	0.0	0.0	0.0
	s_y	1.0	1.0	1.0	1.0	1.0	1.0	1.0
	a_1	0.93028	0.71181	0.56671	0.62514	1.45329	0.92855	0.99132
	a_2	-0.16011	-0.08103	0.30560	-0.11192	-0.50655	-0.15132	-0.09326
k = 1 to 6	A_k	-503.1	-344.0	-200.3	-98.6	-2225.4	-133.0	-867.9
		193.6	79.0	145.4	-46.3	-33.0	-485.0	-228.3
		-192.8	-31.5	-85.5	56.8	418.9	62.4	422.2
		80.6	4.4	58.0	65.0	-342.1	-14.3	-145.5
		-47.6	-27.3	-39.8	-49.0	17.0	-7.1	-15.9
		15.5	13.2	7.4	-22.2	67.3	0.0	2.2
	B_k	71.1	147.8	-112.4	-252.4	477.0	-135.1	-1014.0
		199.8	-46.1	185.0	92.5	349.0	125.3	900.5
		-128.5	-12.2	-79.9	71.8	-218.5	-9.8	-180.1
		72.8	-9.1	65.6	-60.0	-96.0	-29.5	-113.0
		-57.6	16.9	-72.5	-77.9	188.2	1.0	36.6
		-5.5	11.2	27.8	63.2	-192.0	7.4	34.9
	sA_k	-269.3	-278.5	-123.3	-137.8	-1938.0	-49.5	-462.8
		78.8	77.2	141.6	-127.5	-167.5	-61.5	-133.6
		-142.3	-4.6	-66.4	107.7	373.2	9.9	142.2
		91.7	-23.4	75.5	199.1	-755.7	2.8	-1.5
		-18.3	-48.0	-47.2	-109.5	200.6	2.9	-11.8
		6.6	28.4	8.6	-75.1	90.6	1.8	-3.1
	sB_k	143.3	180.3	-85.6	-739.7	398.1	-47.6	-480.5
		67.0	-15.1	105.7	240.0	1179.0	81.1	455.7
		-10.8	-6.1	-46.2	199.7	-371.6	4.9	-92.2
		15.3	-27.2	31.7	-121.2	-116.5	-31.4	-48.9
		13.9	51.9	-43.2	-269.8	110.2	-10.2	-15.6
		-115.8	-6.4	4.3	138.5	-288.2	5.7	55.3

Table 11.1. Values of parameters, as calculated by Quimpo (1967), used in the stochastic models of daily river flows.

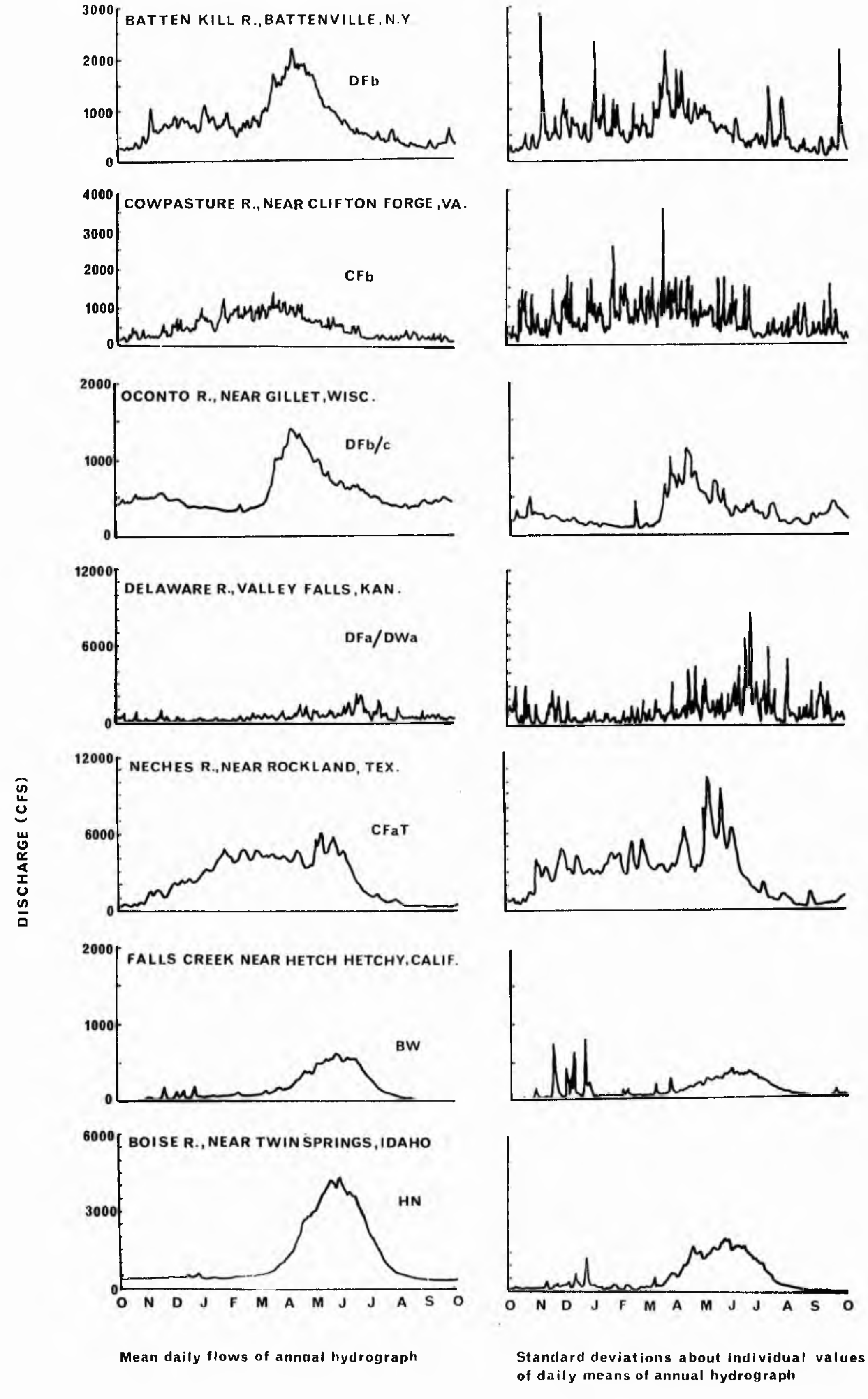

Fig. 11.1 Daily means and standard deviations about means for selected stream flows in the U.S.A.. (taken from Quimpo, 1967).

	coefficients of variation	variances explained by		
		periodic	autoregressive	primary series
BATTEN KILL RIVER	0.143(N) 0.151(G) 0.186(L)	0.2904	0.4627	0.2469
COWPASTURE RIVER	0.119(N) 0.132(G) 0.182(L)	0.1051	0.3912	0.5037
OCONTO RIVER	0.234(N) 0.245(G) 0.297(L)	0.3525	0.4514	0.1961
DELAWARE RIVER	0.116(N) 0.129(G) 0.195(L)	0.0216	0.3170	0.6614
NECHES RIVER*	0.271(N) 0.282(G) 0.332(L)	0.1969	0.7613	0.0418
FALLS CREEK	0.116(N) 0.119(G) 0.121(L)	0.5387	0.3035	0.1578
BOISE RIVER	0.235(N) 0.244(G) 0.285(L)	0.6725	0.2699	0.0576

N - Normal distributed primary variable

G - Gamma distributed primary variable, skewness=1

L - Lognormal distributed primary variable

* Not shown in fig. 11.2

Table 11.2. Coefficients of variation of Q_{vol} for simulated stream flows. Variances explained by different components of the stochastic generating model (taken from Quimpo, 1967).

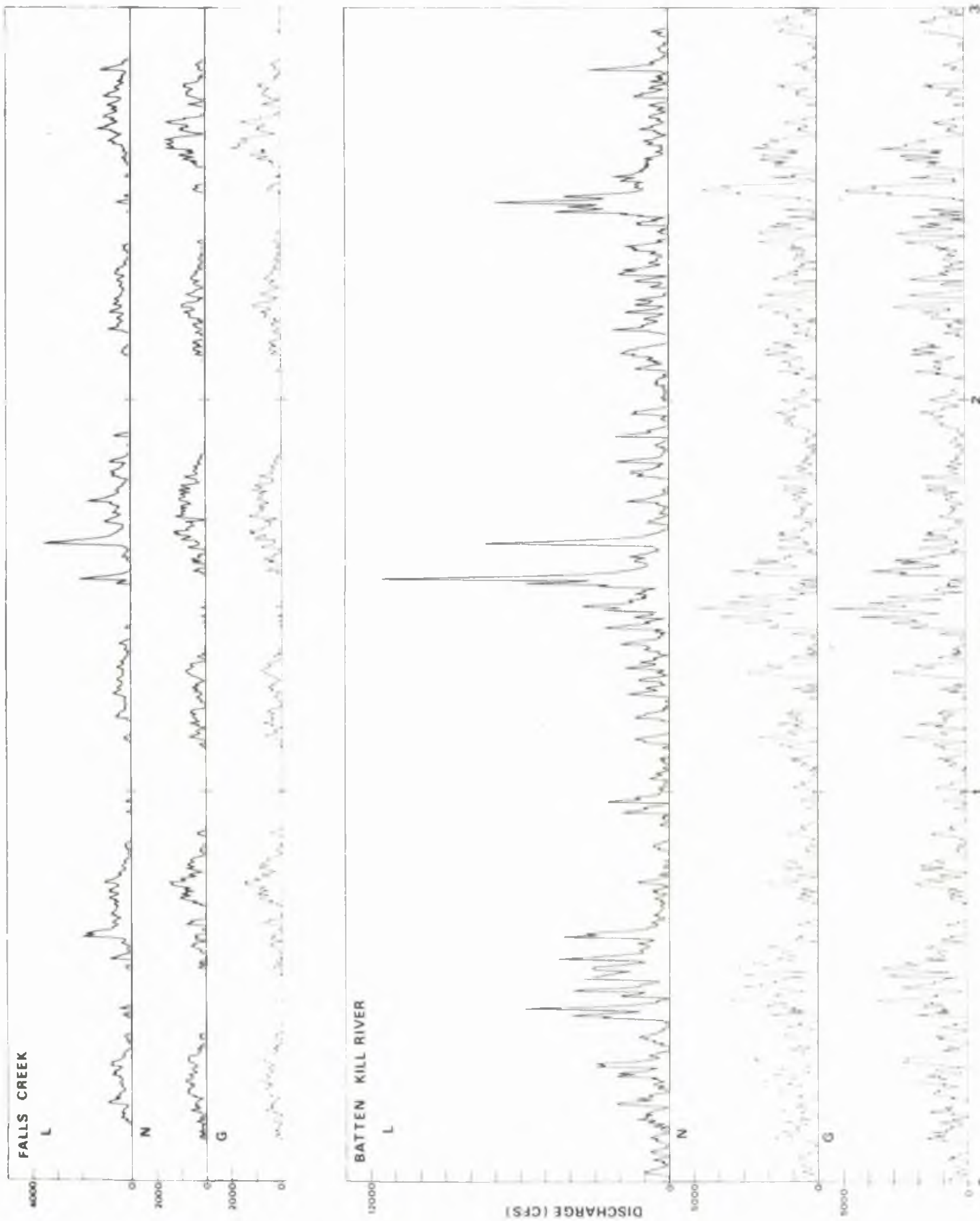

Fig. 11.2. Simulated daily river flows over a three year period, using data given in table 11.1.

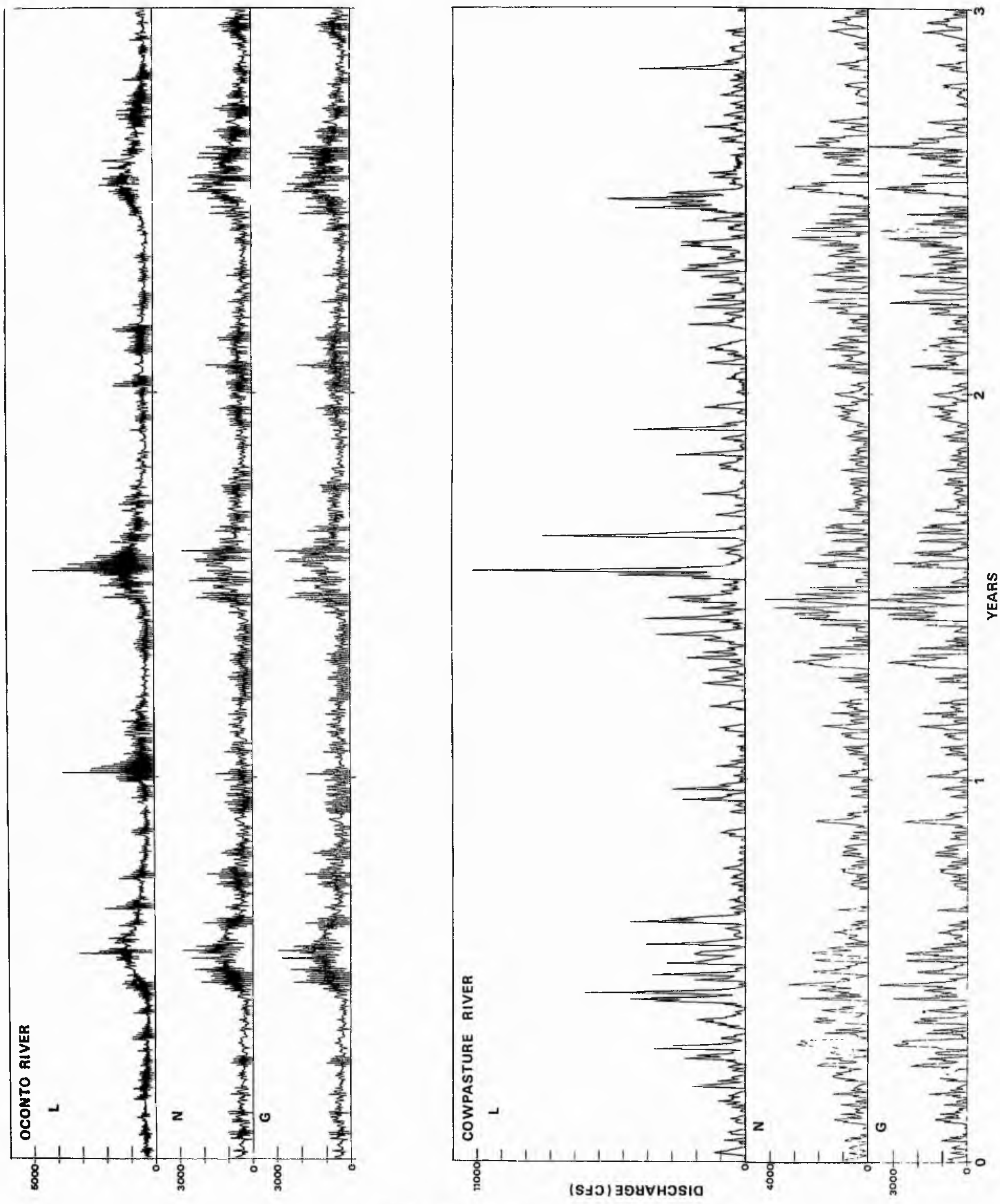

Fig. 11.2. - continued.

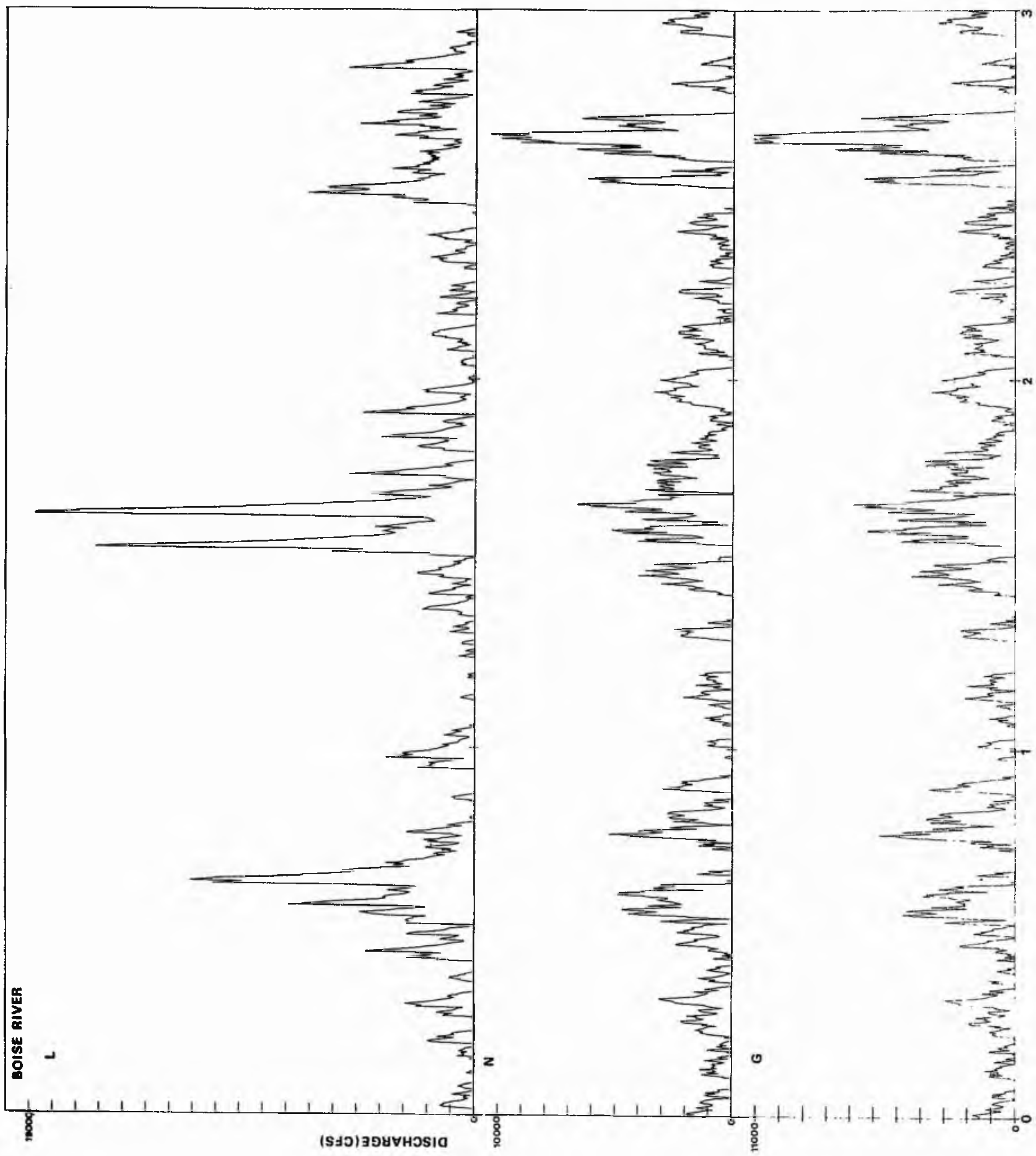

Fig. 11.2. - continued.

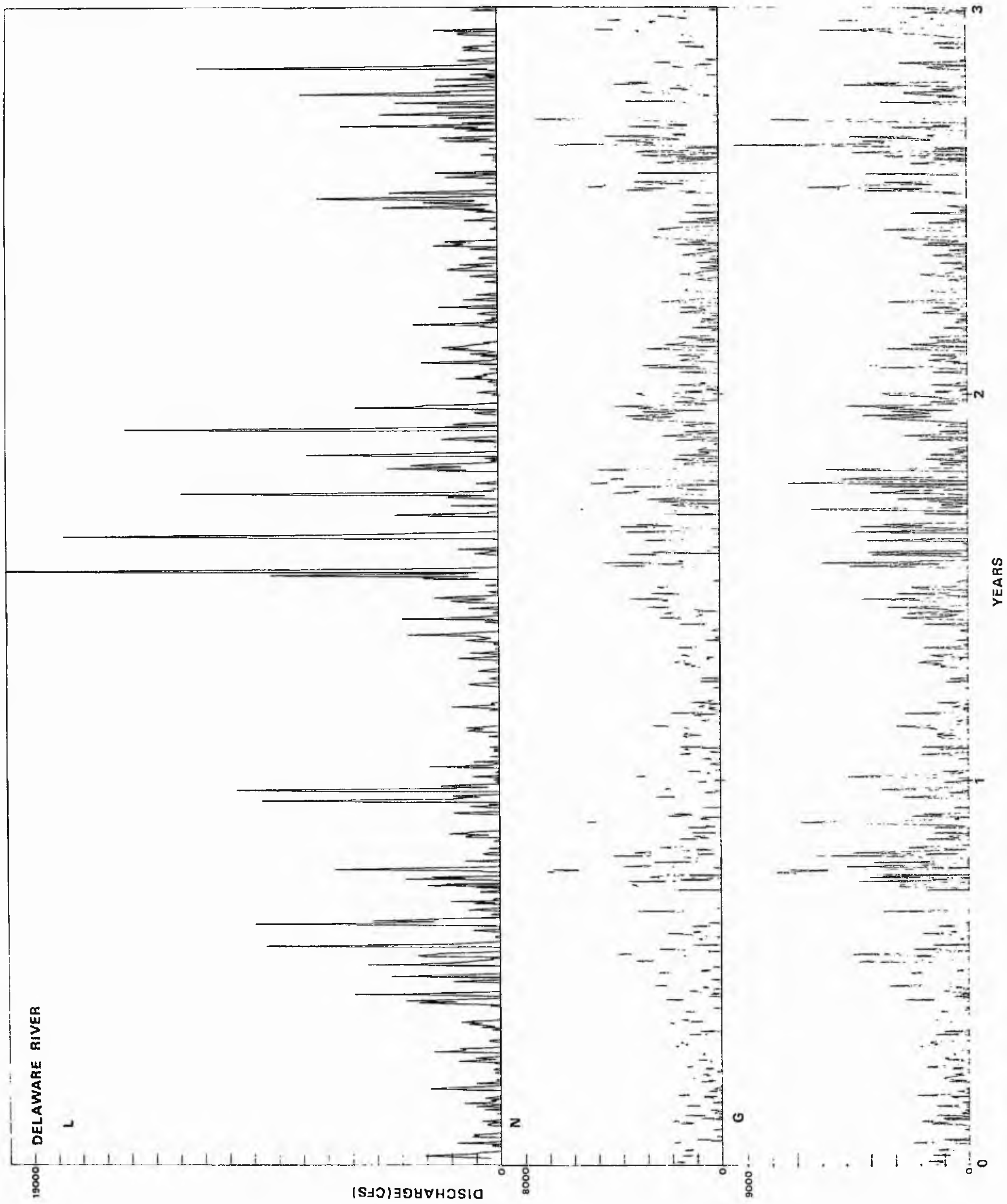

Fig. 11.2. - continued.

were calculated in each case, and the means, standard deviations and coefficients of variation over the period of 500 years were found. Figs. 11.2 show sample plots of the simulated flows over a three year period. Table 11.2 shows the coefficient of variation of Q_{vol} for each station and for each differently distributed primary variable. Also shown on the table are the variances explained, as fractions of unity, by the periodic and autoregressive components of the stochastic models adopted. As can be seen the coefficients of variation are closely dependent on the primary variable distribution. No obvious relation of the coefficients of variation with the other parameters in table 11.2 can be seen, however a detailed statistical analysis with additional data may yield one.

It is obvious that the variability of Q_{vol}, hence the variability of the processes it influences, is not only a function of the flow regime in question but also on the method of flow synthesis used.

12 CONSTRUCTION OF FLOODPLAINS

12.1 Overbank deposition

The annual high-water periods will equal or exceed the elevation of the floodplain just about every year. That the frequency of overbank flow is nearly the same in regions of very diverse runoff, from tropics to semi-arid regions, implies that the size of the river channel is appropriate to the quantity of flow provided by the drainage basin. It is also apparent, however that if overbank flooding by sediment-laden waters does occur, some deposition will in all likelihood be associated with it. If there were continuous deposition the channel would gradually appear to become depressed within its own alluvium. The regular frequency of flooding indicates that this is not the case, and hence some mechanisms must counteract this tendency (Wolman and Leopold, 1957; Leopold et al., 1964). It will be necessary to consider the nature of the deposits making up the flood plain and some possible explanations of the inferred lack of importance of overbank deposition in flood plain formation.

In their manner of construction and in the nature of the deposits which make them up, flood plain deposits form two fundamentally distinct groups (see Wolman and Leopold, 1957). Point bars, channel bars and alluvial islands result from the 'lateral' accretion of stream bed load on the sideways migration of channels. As a meandering stream shifts laterally, deposition on point bars is concomitant with erosion of the opposite concave bank. Wolman and Leopold (1957) further state that the surface of the material deposited approaches the level of the older part of the flood plain.

The 'vertical' accretion of suspended load after overbank flow leads to the construction of levees, crevasse splays, and floodbasins on top of lateral accretion deposits. Averaged thicknesses of sediment that have been deposited on flood plains by great floods is of the order of mm. and cm.. Observations show, however, that widespread deposition of sediment by overbank flows is not the case. In fact there is large variation in the thickness of deposits locally (with some deposits ranging up to metres in thickness); furthermore, velocities are often large enough to produce scour (see Wolman and Leopold, 1957; Wolman and Eiler, 1958; McKee _et al._, 1967).

Observations of Wolman and Leopold (1957) on U.S. rivers indicate that as much as 80-90% of a normal floodplain may be composed of deposits of lateral accretion, and the remaining 10-20% consists of overbank deposits. Whether significant vertical accretion occurs or not depends on internal factors, inherent in the stream regime, and on others external to the stream.

There are three 'internal' factors which help to explain the relative umimportance of overbank deposition in flood plains, and why the elevation of the surface of a flood plain remains stable relative to the level of the channel bed, despite frequent flooding (Wolman and Leopold, 1957). First, the highest discharges are often characterised by lower concentrations of suspended sediment than discharges of intermediate sizes. Second, periodic removal of the flood plain by lateral erosion helps to control its height. Third, velocities of the overbank flow may be high enough to move sediment of appreciable size.

Suspended sediment load is a substantially independent quantity within the floodplain system, and although correlated with discharge, is not a function of discharge itself. This explains the observations of Wolman and Leopold (1957) that many streams show a maximum concentration of suspended load at stages well below the bankfull and not, as might be expected, at the flood stage. Fisk (1947) refers the poor development of levees along certain Mississippi tributaries to small suspended loads.

The extent to which periodic removal and replacement is effective in limiting the height of the floodplain surface depends on the relative rates of channel migration and overbank accretion. Relatively steep braided streams with coarse loads are notorious for the rapidity with which their channels move across a floodplain, so keeping floodplain relief low and minimising the effect of overbank deposition. Many such streams are aggrading rapidly, although solely by net deposition following lateral accretion (e.g. Coleman, 1969). Meandering streams are also free to range and level their floodplains. It is noteworthy that with very sinuous streams, cut off and subsequent development of channel fills of fine sediment may lead to meander belt fixation, and an 'alluvial ridge' may form. Avulsion may occur, producing a surface of complex and appreciable relief. This will have the effect of hampering overbank flows in their movement downvalley, as well as inhibiting rapid channel migration.

When floodplain relief is kept low by the 'ploughing' action of shifting channels, overbank flows are able to move down the plains when floods occur. Wolman and Leopold (1957) report mean velocities of overbank flow in such situations to range between 0.15 and 2.7 ft/sec. and to average 1.6 ft./sec. McKee et al. (1967) compute mean velocities about five times greater than these. The downvalley slope may be considerably greater than that of the channel, and this higher gradient, together possibly with less roughness in the flood plain section, tends to keep the velocity high and reduces the probability of deposition of fine material on the flood plain. Indeed, widespread scouring has been observed.

The external factors include changes in stream base level and changes of land level due to subsidence (tectonic, compactional) or uplift (tectonic, isostatic). These are discussed more fully in the following section on aggradation.

Bearing in mind the aforesaid, it will be assumed in the model that the elevation of the surface of the floodplain remains stable relative to the general level of the channel bed. Also, sediment deposited on the point bar will extend up to the level of the floodplain, taken here obviously as the bankfull level of the channel. The surface of the flood plain will be assumed plane and horizontal in the direction normal to the mean down-valley direction. The relief of the floodplain surface will therefore be lost. The grain size of the pre-existing flood-plain sediments must be specified in the model, assuming that, at any level, they are laterally homogeneous. In this respect, it should be realised that a specified proportion of the total floodplain thickness may have the character of overbank deposits. Processes of overbank deposition will not be treated in the model because of (1) the negligible rates of erosion and deposition, (2) the complicated flow patterns within the channel and over the floodplain, which will partly determine the spatial and temporal distribution of erosion and deposition, (see Sellin, 1964; Toebes and Sooky, 1967), and (3) indeterminate concentrations of suspended sediment. The process of avulsion also cannot be treated at this stage.

12.2 Aggradation

There are various 'external' factors which influence the relative proportions of overbank and point-bar deposition within the floodplain. Variation of these external factors bring about persistent long term erosional and depositional trends over the floodplain. These are termed degradation and aggradation respectively. Degradation will not be considered here, as interest lies at present only in net deposition. By definition, progressive long term deposition both within the channel and on the floodplain is aggradation. Under these conditions overbank deposition may be expected to comprise a significant part of the floodplain deposits, but this will depend on the rate of channel migration relative to the rate of aggradation.

As already stated, the dimensions, shape, slope and pattern of stable alluvial streams are delicately adjusted to transport the amount of water and sediment supplied by the headwaters. Aggradation occurs when the production of sediment exceeds the amount that can be carried away by the processes of transportation (Leopold *et al.*, 1964). Up to this point we have considered meandering streams in the stable nonaggrading, nonscouring situation with the independent variables remaining constant. Various external factors can affect the independent system variables as defined previously, leading to aggradation in certain cases; that is, climatic changes and river diversions can modify the balance between sediment and water discharge. Also structural movements, sediment compaction, or eustatic sea level changes will cause valley slope to vary independently.

In the recent past the combination of subsidence and rising base level has led to deep alluviation by overloaded streams in the lower valley of the Mississippi (Fisk, 1944, 1947). Here the alluviation took place because rise in base level decreased the overall slope of the valley, which was reflected in the progressive upstream loss in carrying power. The gradational nature of the sediments throughout the valley and the occurrence of coarse clastics at depth at the present coastline indicate that aggradation kept pace with rise in sea level throughout most of the aggrading period. The constant general aggradation of the presently overloaded Brahmaputra causes the channel to become wider and shallower and to cause the main current to seek better gradients, new alignments and paths of least resistance (Coleman, 1969). Local faulting is partly responsible for these changes in direction. Slope oversteepening due to structural movements, with subsequent flattening due to aggradation, has also been recorded elsewhere (Leopold et al, 1964).

When changes in the independent factors cause aggradation the various dependent hydraulic variables may adjust in a wide variety of ways in order to maintain continuity of sediment and water transport. Schumm (1969, 1971) has formed generalised expressions relating water discharge and ratio of bed load to total load to various hydraulic variables, in order to illustrate expected directions of change of the dependent variables to changes in water and sediment discharge. Many other authors have noted changes in different hydraulic variables in response to changes in discharge and slope. However the precise form taken by the adjustments cannot be described quantitatively. They will probably be such that the rate of work expended in the system is minimised, the local conditions determining their exact nature.

Leopold et al. (1964) state that the tendency for the maintenance of quasi-equilibrium in stream channels is sufficiently pervasive that only slight deviations, if sustained for a long enough period of time, may account for aggradational features of considerable magnitude, but the deviation from equilibrium conditions necessary for the construction of such depositional features cannot be recognised or identified by any criteria now available. Stratigraphic studies of alluvial sequences indicate that large scale aggradation in valley systems results from processes which act relatively slowly. For example, during the aggradation of the Mississippi valley since late Wisconsin times the average valley slope has only changed on the order of 10^{-9} (10^{-3} of a percent).

It does not seem unrealistic, by virtue of the very small average changes in the hydraulic variables over the periods of time to be simulated in the model (up to the order of hundreds of years), to assume that the hydraulic parameters are constant during aggradation. Account cannot therefore be taken of large scale channel and flood plain changes due to sudden short-term variation in the independent variables, as happened, for example, in the Cimarron River of southwestern Kansas between 1914 and 1939 (Schumm and Lichty, 1963). Such changes in the independent variables are not persistent and the channel changes are not permanent.

Although the stability of the absolute elevation of the surfaces of most flood plains cannot be proven, evidence indicates that even during aggradation the difference in elevation between the river bed and surface of its floodplain does in many instances remain constant over long periods of time (Wolman and Leopold, 1957). Wolman and Leopold (1957) further state that 'In those cases where continual aggradation produced the valley fill, it is difficult to explain how the relative position of the channel to the floodplain remained fixed during aggradation if overbank deposition is considered the principle mechanism of laying down the valley fill. Rather, concomitant rise of both stream bed and floodplain surface appears to be best explained by attributing the bulk of the deposited material to the process of point bar formation'.

The uniform frequency of flooding of flood plains does not rule out the possibility that both the surface of the flood plain and the bed of the channel are being built simultaneously.

Gages on the Nile river, which provide the longest periods of record of any river in the world, indicate that both the bed and banks of the Nile are being raised at a rate of about one metre in 1000 years. The maximum thickness of recent valley alluvium in the Mississippi valley varies from about 200 ft. (av. 125 ft.) in the north to over 350 ft. (average 138 ft.) in the south, and this was deposited in 25,000-30,000 years (Fisk, 1944). Other data from Leopold *et al.* (1964) suggest comparable rates of aggradation.

In the model, it will be assumed that during aggradation the elevation of the surface of the floodplain remains stable relative to the level of the channel bed. As in the last section, the surface of the floodplain will be assumed plane and horizontal in the direction normal to the mean downvalley direction. It is not intended to look at the processes influencing aggradation, but to assume that the whole floodplain is aggrading at a specified constant rate due to one or more of the previously discussed factors, without taking account of them explicitly. The rate of aggradation will be specified as input and it will be assumed that progressive aggradation is continuing at this constant rate, without interruption, for the whole cross section represented in the model, irrespective of its direction. Due to the fact that the processes of overbank deposition in nonaggrading and aggrading situations are too complex to treat here, the nature and surface relief of the overbank deposit cannot be determined in detail. During aggradation much of the overbank deposit will be expected to be crevasse splay and levee deposit. However, by virtue of the observed rates of aggradation mentioned earlier, and the expected rates of channel migration, much of the total floodplain deposit is expected to be produced in the channel. In such an instance, relief will be kept low and the formation of 'alluvial

ERRATUM

There is no page number 122

ridges' would be inhibited. Movement across the floodplain of the meander belt continuously or discontinuously (avulsion) cannot be accounted for in the model. Avulsion and continuous meander belt migration may be expected to assume more importance in this aggrading situation with local slope oversteepening, perhaps due to tilting of the valley associated with tectonism, (e.g. Russell, 1954; Coleman, 1969). In the model, overbank deposits produced during aggradation will be separately designated, although their detailed structure and texture will be indeterminate. For the purpose of defining their erosion resistance in exposed cut banks they will be assumed to be predominantly silt and clay, although sand may be present also (e.g. Allen, 1965a).

PART THREE

THE COMPUTER PROGRAM

13. GENERAL REMARKS.

Once the structure of the mathematical model is established the next step is to develop a computer program that represents the various components and processes to be simulated. The programming language FORTRAN IV was found sufficiently versatile. Numerous texts deal with the definition and efficient use of the language (e.g. IBM, 1968; Cress et al, 1970; Kreitzberg and Shneiderman, 1972).

Flow of time is implicit in any dynamic system where all the processes are time dependent. In dealing with digital models, time can be moved forward in a series of discrete steps, the state of the system being altered by an increment at each step. Continuous time would be more closely approximated as the time increment is decreased. The choice of time increment of a year is purely for convenience, in that there is normally one major flood period a year during which most of the erosional and depositional activity takes place, ignoring the separate flood events that inevitably constitute a high water period. There may, however, be two flood periods (i.e. double equatorial maxima) where erosional and depositional activity are vigorous. This does not affect the model, as quantities involving the flood volume are defined bearing in mind that the time span involved is a year. For instance, in the case of scour and fill, if there were two equally important discrete flood periods in a year, then the net depth of scour for a given meander will be expected to be less for each one than for a single flood period with the same annual flood volume. If it is required to look at these flood periods within one year separately, it would be an easy matter to do so, as a mathematical model of the hydrograph has been made. By virtue of the model construction the time increment cannot be smaller than the length of time between the major seasonal periods of vigorous erosional and depositional activity which the model records.

Accompanying the examination of erosion and deposition in vertical cross sections arises the need to represent two dimensional space within the computer program. Not only is it required to locate a particular type of material (i.e. sand, water, dunes, etc.) in a cross section, but also discrete quantities of these materials must be transported to and from different locations within the section as erosion and deposition in the meander proceed. Because of the need to incorporate this accounting system space is represented by a fixed grid of rectangular (or square) cells. Two-dimensional FORTRAN arrays readily allow this, the accounting information is easy to handle, and can be displayed easily. The scale of the cells is a critical factor, which depends on the dimensions of the cross sections and the availability of computer time and storage. Clearly the greater the resolution required for a given cross section, the greater the number of cells are required, thus increasing computer time and storage requirements. In order to give the greatest number of cells possible the information in the two-dimensional FORTRAN arrays is accommodated in 'half length integer' form. Furthermore, two programs were written, one using only the addressable storage (core store) of the computer, and the other using additional disc storage.

Both programs have been run successfully many times on the IBM 360/44 computer in St. Andrews University Computing Laboratory. A CIL off-line graph plotter was used to plot channel-centre lines of meander planforms, but otherwise all output was produced on an IBM 1403 line printer. A disc is required by one of the programs. The maximum core store requirements depend on the number of cells, and whether a disc is used. With cross sections of 200 cells by 60 cells the program with a disc uses 78k bytes, and 129k bytes without a disc. The approximate running time (CPU time) depends on the number of time increments, the selection of various options within the program, and on the number of cells in the cross sections. When a disc is used the running time is considerably increased by the large number of input/output operations. Running times will accordingly be reported for the particular conditions of the individual experiments conducted.

14 DESCRIPTION OF MAIN PROGRAMS AND SUBROUTINES

The following descriptions are given in conjunction with the simplified flow diagrams, and the program listings. The programs are listed in tables 14.1 and 14.2. Table 14.1 lists the program that uses only core storage. The same subroutines listed here are required by the program using additional disc storage and are therefore omitted from table 14.2. In the following sections words in capital letters are FORTRAN variables, arrays or subroutine names.

14.1 Main Program (no disc)

1. Reads input parameters. The job is terminated if (a) NPRINT, NFPLOT, or NTPLOT equal zero, (b) the initial bankfull stage measured from the section base, WS, is greater than the section thickness, YTOT, (c) initial sinuosity, SN, is greater than the limiting sinuosity, SNLIM, (d) maximum unscoured flow depth measured above talweg, H, is greater than WS.

Some of the terms used within the program in the definition of the cross sections, and which are referred to above and subsequently, are shown in fig. 14.1.

2. Calls subroutine RNDMIN.
3. Finds cell depth (size in vertical direction), YCEL and cell width (size in the horizontal direction), ZCEL. If amount of aggradation per year, DWS, is greater than YCEL the job is terminated.
4. Finds bankfull stage relative to base of section, IWS, in cell depths/rows, and distance of inner bank of channel from left hand side of section, IBANK, in cell widths/columns. See fig. 14.1.
5. Finds initial amplitude, AMP, and the limiting amplitude, AMPLIM, by calling subroutine NEWRAP. Checks that a one-channel downvalley section is not located near the bend axis.

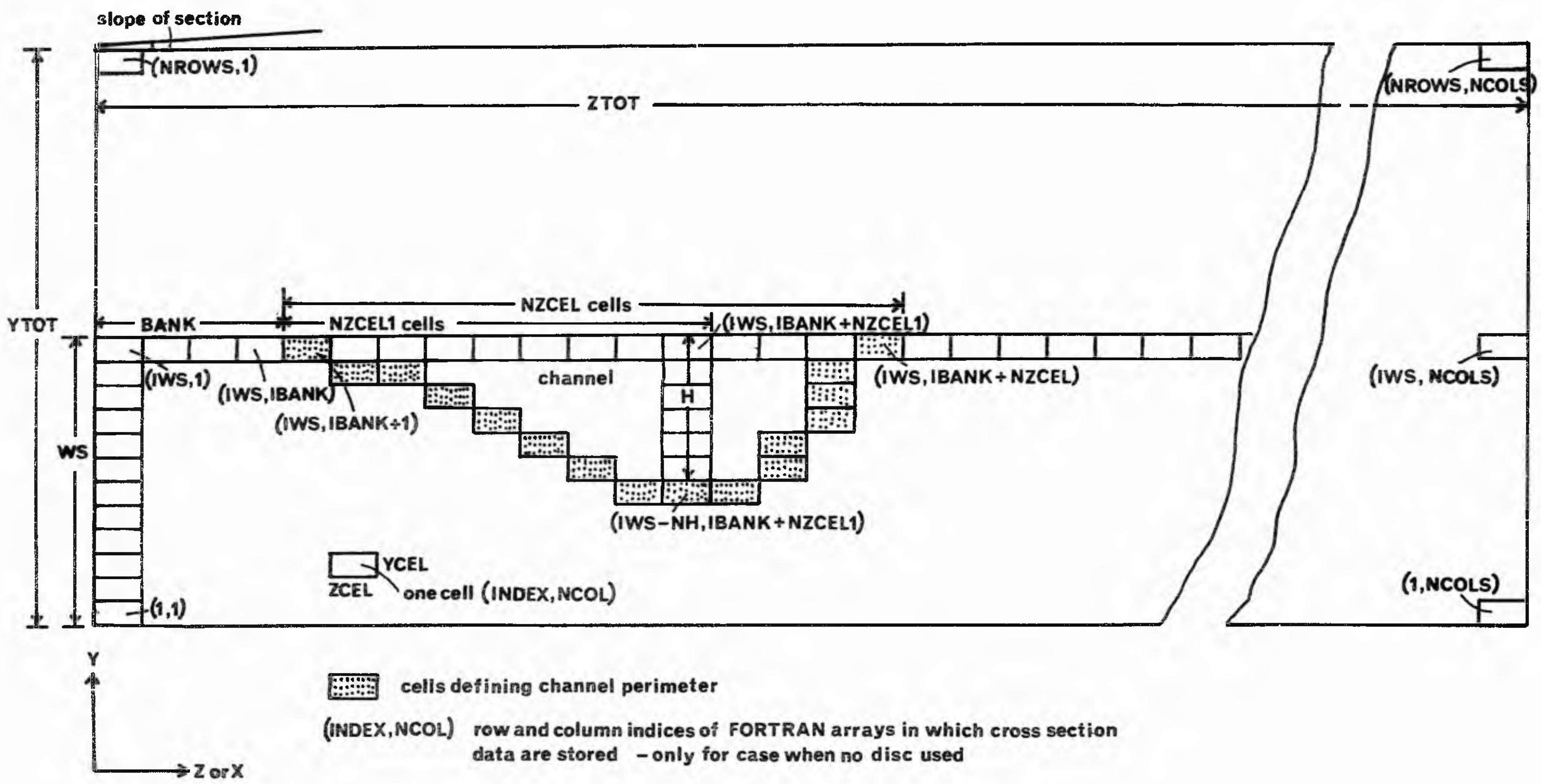

FIG. 14.1 Definition diagram for cross sections, in terms of FORTRAN variables.

That is, if the normal distance of the line of section from the line joining the points of inflection of the loop, ZSECT, is greater than the arbitrary value of AMP/3.0, the job is stopped. Finds initial distance of channel at the bend axis from the limiting amplitude position, SS. If SS$\leqslant$0.0, the indicator, LIM, is set to 1.

6. Alphameric characters are read into array SEDIN(I), and the arrays SEDGS(I,J) and SEDSTR(I,J), which hold the grain size and sedimentary structure cross sections respectively, are filled with alphameric characters. SEDGS is filled from the bottom of the section up to row IWS with the characters read into SEDIN(I), one character of this array specifying the character for one complete row, I, of SEDGS. The remaining rows are filled with blanks. Similarly, SEDSTR is filled with the old sediment character, OLDSED, and the array holding the time line cross section, TLPLOT(I,J), is filled with blanks.

7. Initialisation of synthetic hydrology parameters. Initialises parameters involving skewness, SKEW, the autoregressive model parameters, ZTM1, ZTM2, and COEFF (calling subroutine RANSAM), and stores the daily mean flow values and daily standard deviations of flow in FMSUM(NDAY) and FSSUM(NDAY), respectively, after evaluating them with the harmonic representation of equations (11.2) and (11.3).

8. Finds full width of flow between inner and outer banks, WW. Finds values of WW and the width of flow between inner bank and talweg, W, measured in cells, NZCEL and NZCEL1. NZCEL1 is also expressed in real mode, FLT2. Finds limiting width of meander neck measured from channel centre lines, GAPLIM. GAPLIM is initially read in as the limiting meander neck measured between immediately adjacent banks. Finds value of

H measured in cells, NH. Finds parameters used in subroutine MEANDR for use in calculating Froude numbers and for scaling the plot of the meander plan. Finds parameters used in subroutine BAR. Note VAR1 and EXNM1 are only required if the sigmoidal cross profile is used. The number of the time increment, NFLD, is set to 0, the time keeping devices, IPRINT and ITPLOT, are initialised, and the ratio YCEL/ZCEL is calculated.

9. Write scales and titles on graph containing traces of channel centre line. Calls subroutines CHAR and PLOT, for this operation.

10. Prints out cross section, channel, synthetic hydrology, bank migration, scour and fill, and cut-off control parameters. Prints out whether cross sections are lateral or downvalley sections, and the value of ZSECT for downvalley sections. Prints legend.

11. Calls subroutine MEANDR to calculate and plot initial planimetric form of the meander, and calculate other parameters for use in subroutine BAR.

12. Initial operations are performed concerning the projected channel widths in cross sections, including redefinition of NZCEL & NZCEL1. If a two-channel downvalley section is being used (i.e. if IFCOD6 = 2) the straight line distance between points of inflection of loop, NDAVA, is calculated. Then jumps to step 19 to initialise and print channel section using subroutine BAR.

All the above operations (1-12) are performed only once. Now begins the major loop of the program which is entered once every time increment. Steps 13 to 18 are omitted during initialisation (i.e. NFLD=0).

13. Reinitialises time keeping devices. If IPRINT and/or ITPLOT equal 0, printed output and/or a time line will be produced this time increment, NFLD.

14. Finds flood period volume, QVOL, by summing all daily flows, XT, in the year (generated using equation (11.5)) which are above the value of the mean daily flow, DM. Calls subroutine RANSAM for this operation.

15. Tests to see if the meander has a neck or chute cut-off during this year. Calls subroutine RNDM for these tests. If cut-off occurs (ICUT put to 2 or 3) various parameters are printed, the meander trace is plotted (MEANDR is called), and the job is terminated.

16. Finds amount of bank migration in downvalley direction, RDMIG, and normal to this direction, RLMIG. Finds respective total amounts of migration, TDMIG and TLMIG. RLMIG and TLMIG are not calculated if the limiting sinuosity has been reached (LIM=1). Prints various parameters if IPRINT=0.

17. Aggrades the flood plain if required. As amount of aggradation, AGG, fills the cells corresponding to a particular row, the row elements are allocated an alphameric character, FLOOD, for every column in the sedimentary structure and grain size cross sections. As the cells become filled, bankfull stage, IWS, is adjusted accordingly by adding 1. Thus although aggradation continues at a constant rate, the program represents it as a discontinuous process within the cross sections. However, a record is kept of AGG which is printed out if IPRINT=0.

18. Finds amount of bank migration in cross section represented, RMIG.

The following operations, as far as step 32, are involved with recording on SEDGS (INDEX, NCOL) and SEDSTR (INDEX, NCOL) the resulting erosion and deposition after this year's 'floods', and putting a time line on TLPLOT (INDEX, NCOL) if ITPLOT=0.

19. Adjusts channel width (in cells), NZCEL & NZCEL1, represented in the cross section, and related parameters, depending on type of cross section and changes in shape of the meander. The error due to smoothing in the amount of bank migration for the preceding time increment, DEV, is added to RMIG. DEV is then recalculated for the next time increment. The amount of concomitant point bar migration (in cells), NRMIG, is then defined depending on changes in channel width in the cross section represented.

20. Finds total number of cell widths/columns required for the channel section, NZCELT, and test to see if the right hand edge of the cross sections have been exceeded. If so, the job is terminated.

Scour and fill operations-if NFLD=0 or the scour and fill process is not required (IFCOD5=0), steps 21 to 24 are skipped.

21. Maximum depth of scour below unscoured depth measured above old talweg (i.e. position of talweg at end of last time increment), DSCR, is calculated using equation (9.4). Subroutine RANSAM is called during this operation. A test is made to ensure DSCR$\geqslant$0.0. If IPRINT=0, DSCR is printed out.

22. Maximum depth of water measured above the old talweg, HH, is calculated. If this exceeds the bottom of the specified section the job is terminated.

23. Every column of the inside bank of the channel section (IBANK+1 to IBANK+NZCEL1) is now filled to the original depth by successive recalculation of the transverse profile, the depth at the old talweg being progressively decreased by one cell depth/row until filling is complete. Subroutine BAR or BAR1 is called during these operations in order to fill the appropriate elements of SEDGS and SEDSTR with alphameric characters.

24. The area bounded by the position of the old talweg, the maximum scour depth below the old talweg, and the position of the new talweg (i.e. the base of the outer channel bank at the end of this time increment) is now filled by allocating for each row in this area the grain size and bed form symbols calculated for the row elements of the old talweg column, IBANK+NZCEL1, in step 23.

Fig. 14.2 illustrates the sequence of events in the scouring and filling operation described above. Steps 25 to 32 constitute a major loop and are concerned with erosion of the outer bank and deposition on the point bar. As a result of the erosion of the outer bank and changes in the projected channel width in the cross sections, the whole transverse profile is shifted accordingly, and the left hand side of the new point bar profile is started at column IBANK+NRMIG+1 of the cross section.

25. Parameters are initialised and if IPRINT=0 headings are written for the printed output from subroutine BAR.

For every column, NCOL, of the new point bar (up to IBANK + NZCEL1+NRMIG) steps 26 to 31 are executed.

26. The depth of water, sediment size and bed form are calculated by calling subroutine BAR or BAR1 and the appropriate elements of SEDGS (INDEX, NCOL) and SEDSTR (INDEX, NCOL) that describe the profile of the new point bar are filled with alphameric characters.

27. If the grain size at a particular station is silt or clay this is recorded.

28. The alphameric character for the time line is allocated to the appropriate element in TLPLOT (INDEX, NCOL) if ITPLOT=0.

29. The area between the old and new point bar is 'filled' by filling each row, INDEX, with the alphameric character as just allocated, in step 26, to the corresponding row of the new point bar profile. See fig. 14.2.

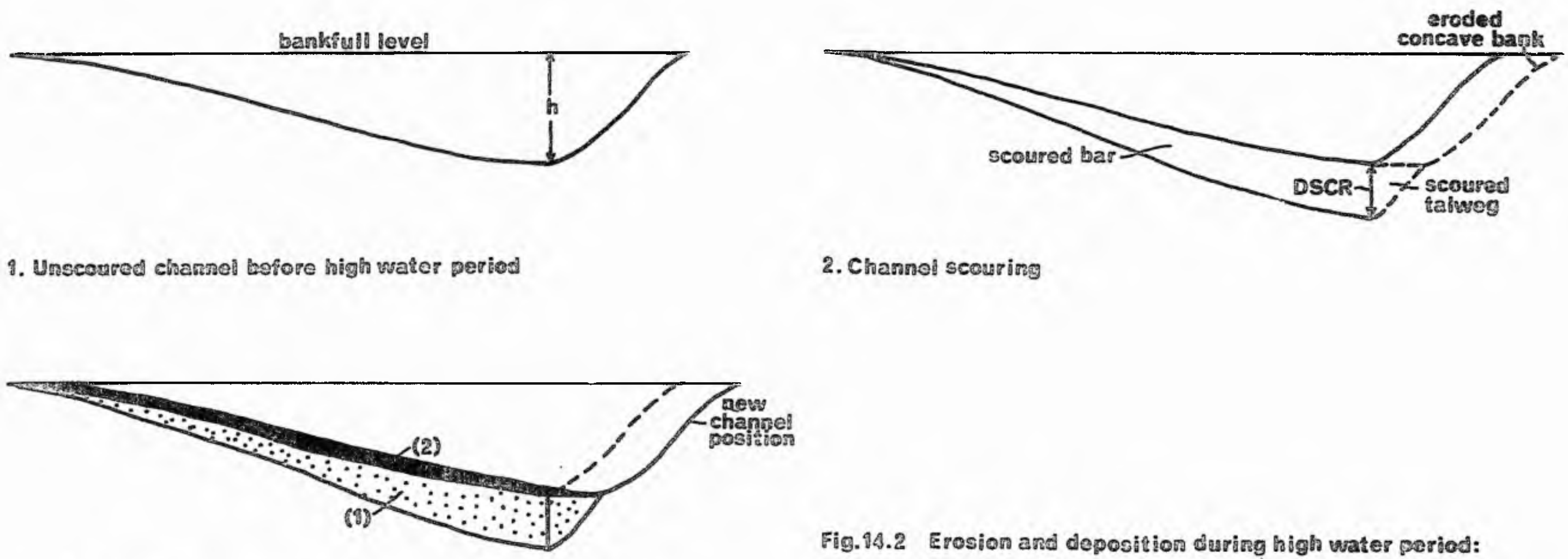

1. Unscoured channel before high water period

2. Channel scouring

3. Deposition – sequence: (1) fill scoured bar and talweg
(2) lateral deposition of new bar

Fig.14.2 Erosion and deposition during high water period: sequence of operations in computer program.

30. If the section scaling is such that not all of the rows in the point bar section had a character allocated in 26, the row(s) with 'missing' symbols is (are) filled with the same symbols as are on the next 'full' row beneath.

Steps 29 and 30 are omitted if there is no filling to be done.

31. Each column is finally filled with water.

For every column of the outer bank (IBANK+NZCEL1+NRMIG+1 up to IBANK+NXCELT) the following step is executed.

32. The depth is calculated using a similar equation to that of the sigmoidal profile of the point bar. The indices of the cells, (INDEX, NCOL), corresponding to the position of the bank are calculated and, if ITPLOT=0, alphameric characters for the time line are allocated to the appropriate elements in TLPLOT (INDEX, NCOL). The amount of exposed silt, clay, overbank deposit, and gravel are recorded by scanning each row in the outer bank. Each column is finally filled with water.

33. The weighted percentage of silt and clay (including overbank deposits) in the perimeter of the projected channel, SCHUMM, is calculated. This is not the same index as that used by Schumm (1960) which is calculated in a different way and uses 0.074 cm. as the lower limit of sand sizes.

34. Percentage of silt and clay in inner bank, BGSI, and the outer bank (including overbank deposits with the silt and clay), OBGSI, and the percentage of gravel, GRAVI, in the outer bank are calculated. If OBGSI=0 it is set to 1.0 for the purposes of equations (6.3) and (6.4). If GRAVI is greater than the limiting value, GRAVLM, the job is terminated.

35. If a two-channel downvalley section is being used, the channel section data just computed and stored in SEDGS, SEDSTR and

TLPLOT, are used to fill these arrays with the same information, NDAVA columns further on. NDAVA is the distance between the two channels measured in columns/cell widths along the valley axis.

36. If IPRINT=0 the cross sections showing grain size and sedimentary structure (bed form) distribution are printed out.

37. IBANK is incremented by NRMIG and a test is made to see if XMAX has been exceeded, before trying to plot the planimetric geometry with the graph plotter.

38. The new amplitude, AMP, and the distance of the channel at the bend axis from limiting amplitude, SS, are now calculated if the limiting sinuosity/amplitude has not already been reached, i.e. LIM=0. If LIM=0 subroutine MEANDR is called and a test is made to see if the two limbs of the meander have closed on each other. If the limiting sinuosity is just reached after the recalculation of AMP and SS, LIM is set to 1, AMP is set to AMPLIM, RLMIG and SS are set to 0.0, and MEANDR is called. Also a message is written saying that the limiting sinuosity/amplitude has been reached, and if a lateral section is represented the program is stopped. If LIM is already equal to 1, AMP and SS are left unaltered and MEAND1 is called, unless the downvalley migration is zero in which case neither MEANDR or MEAND1 are called.

39. NFLD is incremented by 1 and, if less than or equal to the number of required time increments, NTIM, control is transferred back to step 13.

The job is stopped either with an error message or due to the execution of the required number of time increments.

A simplified flow diagram of the main program is shown in fig. 14.3. This diagram relates to both main programs.

Fig. 14.3. Flow diagram for main programs.

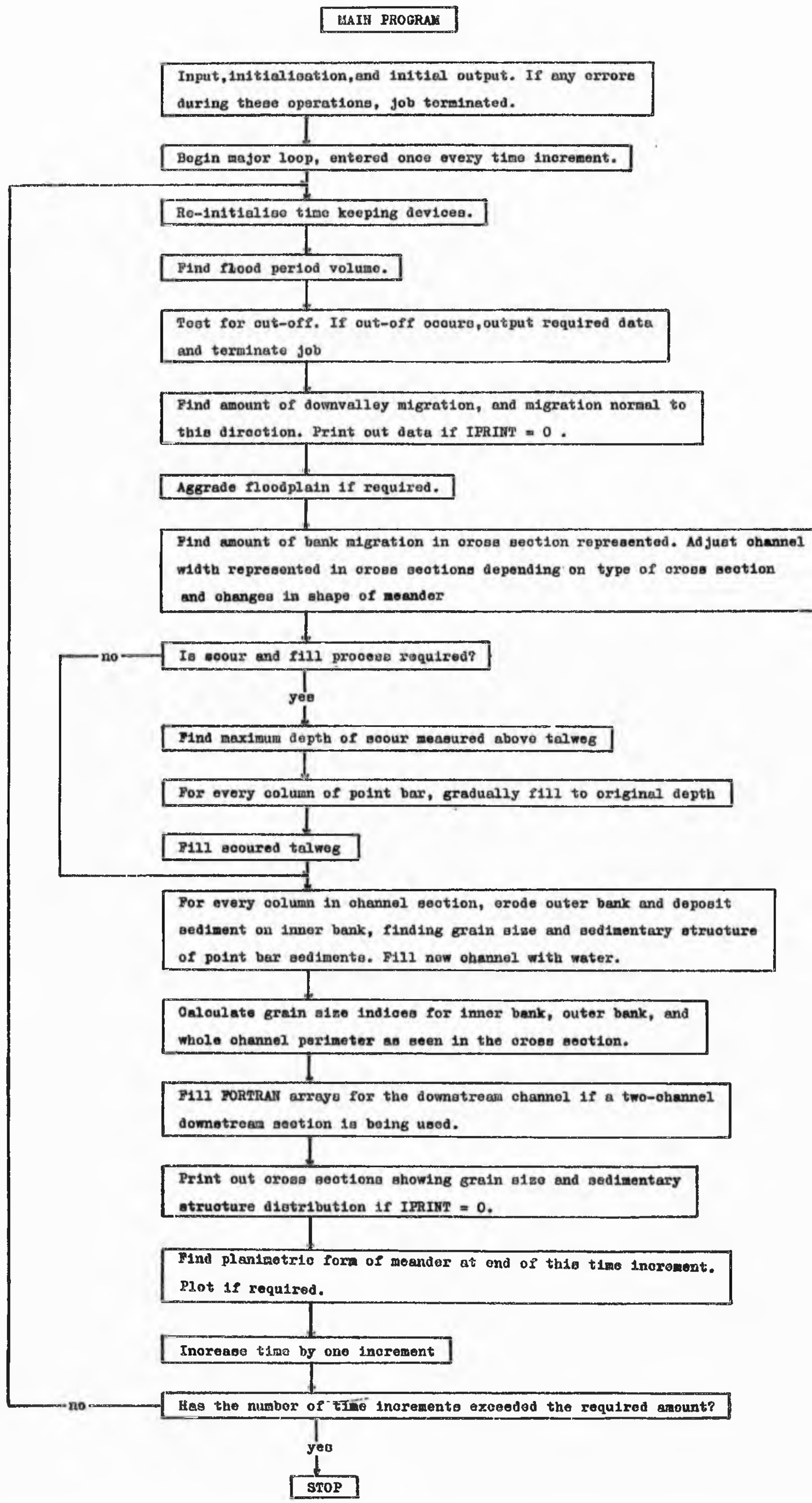

```
C
C CONTROL STATEMENTS
C
      REAL NEWRAP
      DIMENSION FMT4(5),A(6),B(6),SA(6),SB(6),FMSUM(365),FSSUM(365)
      INTEGER*2 SEDGS,SEDSTR,TLPLOT(60,200),GRAVEL,SAND,SILT,CLAY,UPPB,L
     1PPB,ANTIDN,RIPPLE,DUNES,OLDSED,WATER,DOT,BLANK,SEDIN(60),FLOOD
      COMMON/COM1/IPRINT,RINB,FROUD1,FROUD2,VAR2S,RC
      COMMON/COM2/INDEX,NCOL,W,EXN,IWS,Y,NYCEL,D,VAR1,EXNM1,YCEL,SIGRO,Z
     1,GRAVEL,SAND,SILT,CLAY,UPPB,LPPB,ANTIDN,RIPPLE,DUNES,SEDSTR(60,200
     2),SEDGS(60,200)
      COMMON/COM3/NFLD,TITLE(15),WVL,AMP,VS,GAP,NFPLOT,CHS,WW,R,RO,VAR2,
     1F28,F18,SS,TDMIG,SN
      COMMON/COM4/SKEW2,SKEW6,SKEW62
      DATA RMIG,TLMIG,AGG,DEV,NDAVA,LIM,MARK,ICUT/4*0.0,2*0,2*1/
C
C FORMAT STATEMENTS
C
    1 FORMAT(15A4,I10)
    2 FORMAT(I1,3F12.0,I1)
    3 FORMAT(4I4)
    4 FORMAT(3I4,6F8.0,5A4)
    5 FORMAT(80A1)
    6 FORMAT(6F12.0)
    7 FORMAT(8F8.0,I4)
   21 FORMAT(1H1,1X,15A4//1X,'CROSS SECTION PARAMETERS',49X,'METRES',5X,
     1'CELLS'//6X,'WIDTH OF SECTION',48X,F10.3,I10/6X,'THICKNESS OF SECT
     2ION',44X,F10.3,I10/6X,'INITIAL DISTANCE OF INNER CHANNEL BANK FROM
     3 L.H.S. OF SECTION',3X,F10.3,I10/6X,'INITIAL BANKFULL STAGE MEASUR
     4ED FROM SECTION BASE',15X,F10.3,I10/6X,'CELL SIZE IN VERTICAL(Y) D
     5IRECTION',30X,F10.3/6X,'CELL SIZE IN HORIZONTAL(Z OR X) DIRECTION'
     6,23X,F10.3///)
   23 FORMAT(1X,'CHANNEL PARAMETERS',55X,'METRES',5X,'CELLS'//6X,'TOTAL
     1WIDTH OF CHANNEL(W)',39X,F10.3,I10/6X,'WIDTH OF FLOW BETWEEN INNER
     2 BANK AND TALWEG(W1)',17X,F10.3,I10/6X,'RATIO OF W1 TO W',68X,F10.
     33/6X,'MAXIMUM FLOW DEPTH MEASURED ABOVE TALWEG',24X,F10.3/6X,'DENS
     4ITY OF SEDIMENTARY PARTICLES',52X,F10.3,' GM/CM3'/6X,'FLUID DENSIT
     5Y',71X,F10.3,' GM/CM3'/6X,'DARCY-WEISBACH FRICTION COEFFICIENT FOR
     6 DUNES AND RIPPLES',27X,F10.3/6X,'DARCY-WEISBACH FRICTION COEFFICI
     7ENT FOR PLANE BEDS AND ANTIDUNES',20X,F10.3/6X,'EXPONENT N1',73X,F
     810.3///)
   24 FORMAT(1X,'SYNTHETIC HYDROLOGY PARAMETERS(UNITS NOT NECESSARY)'//6
     1X,'MEAN OF ALL DAILY MEAN VALUES',25X,F10.3/6X,'STANDARD DEVIATION
     2 OF DAILY MEAN VALUES',15X,F10.3/6X,'MEAN OF YT SERIES',37X,F10.3/
     36X,'STANDARD DEVIATION OF YT SERIES',23X,F10.3/6X,'COEFFICIENTS IN
     4 AUTOREGRESSIVE MODEL',15X,'A1=',F10.3,7X,'A2=',F10.3/60X,'HARMONI
     5CS FROM 1 TO 6'/6X,'FOURIER COEFFICIENTS FOR DAILY MEANS(A)',15X,6
     6F10.3/42X,'(B)',15X,6F10.3/6X,'FOURIER COEFFICIENTS FOR DAILY STD
     7DEVIATIONS(SA)',5X,6F10.3/51X,'(SB)',5X,6F10.3/6X,'MAXIMUM VALUE O
     8F QVOL',33X,F10.3///)
   25 FORMAT(1X,'BANK MIGRATION PARAMETERS',/6X,'EXPONENT N2',53X,F10.3/
     16X,'VALUE OF CONSTANT IN LATERAL MIGRATION RELATION',14X,'K2=',E10
     2.3/6X,'VALUE OF CONSTANT IN DOWNVALLEY MIGRATION RELATION',11X,'K3
     3=',E10.3/6X,'LIMITING PERCENTAGE OF GRAVEL ALLOWABLE IN OUTER BANK
     4',11X,F10.3///)
   26 FORMAT(1X,'SCOUR AND FILL PARAMETERS'/6X,'CONSTANT K4',43X,E10.3/6
     1X,'EXPONENT N3',39X,F10.3/6X,'STANDARD DEVIATION OF ERROR TERM',18
     2X,F10.3///)
   27 FORMAT(1X,'LEGEND'//6X,'LOWER PHASE PLANE BED',5X,A1,7X,'GRAVEL',5
     1X,A1,8X,'OLD SEDIMENT',5X,A1/6X,'RIPPLES',19X,A1,7X,'SAND',7X,A1,8
     2X,'WATER',12X,A1/6X,'DUNES',21X,A1,7X,'SILT',7X,A1,8X,'TIME LINE',
     38X,5A1/6X,'UPPER PHASE PLANE BED',5X,A1,7X,'CLAY',7X,A1,8X,'AIR',1
     44X,'BLANK'/6X,'ANTIDUNES',17X,A1,7X,'OVERBANK',3X,A1/40X,'DEPOSITS
     5'//)
   28 FORMAT(1X,'CUT-OFF CONTROL PARAMETERS'/6X,'LIMITING WIDTH OF MEAND
     1ER NECK',24X,F10.3,' METRES'/6X,'EXPONENTS IN NECK CUT-OFF RELATIO
     2N',16X,'EN1=',F10.3,6X,'EN2=',F10.3/6X,'LIMITING SINUOSITY',36X,F1
     30.3/6X,'LIMITING AMPLITUDE',36X,F10.3,' METRES'/6X,'EXPONENTS IN C
     4HUTE CUT OFF RELATION',15X,'EC1=',F10.3,6X,'EC2=',F10.3///)
   29 FORMAT(1H1,1X,15A4,'TIME INCREMENT',I5//1X,'FLOOD PERIOD VOLUME FO
     1R THIS YEAR',26X,F10.3//1X,'OUTER BANK GRAINSIZE INDEX AT BEGINNIN
     2G OF YEAR',12X,F10.3//1X,'INNER BANK GRAINSIZE INDEX AT BEGINNING
     3OF YEAR',12X,F10.3//1X,'% SILT-CLAY IN CHANNEL PERIMETER AT BEGINN
     4ING OF YEAR',6X,F10.3//1X,'DISTANCE FROM LIMITING AMPLITUDE AT BEG
     5INNING OF YEAR',6X,F10.3,' METRES'//1X,'LATERAL MIGRATION DURING T
     6HIS YEAR',25X,F10.3,' METRES'//1X,'TOTAL LATERAL MIGRATION AT END
     7OF THIS YEAR',16X,F10.3,' METRES'//1X,'DOWNVALLEY MIGRATION DURING
     8 THIS YEAR',22X,F10.3,' METRES'//1X,'TOTAL DOWNVALLEY MIGRATION AT
```

Table 14.1. Listing of main program (no disc) and subroutines.

```
     9 END OF THIS YEAR',13X,F10.3,' METRES'//)
   30 FORMAT(1X,'TOTAL AGGRADATION AT END OF THIS YEAR',22X,F10.3,' METR
     1ES'//)
   31 FORMAT(///1X,'A DOWNVALLEY SECTION IS REPRESENTED IN THIS TEST'/1X
     1,'DISTANCE OF LINE OF SECTION FROM POINT OF INFLECTION OF LOOP IS'
     2,F10.3,' METRES'//)
   33 FORMAT(///1X,'A LATERAL SECTION IS REPRESENTED IN THIS TEST'//)
   35 FORMAT(1H1,1X,15A4,' TIME INCREMENT',I5//1X,'CROSS SECTION SHOWING
     1 DISTRIBUTION OF GRAIN SIZE ACROSS MEANDERING RIVER FLOOD PLAIN'//
     2/)
   36 FORMAT(1H1,1X,15A4,' TIME INCREMENT',I5//1X,'CROSS SECTION SHOWING
     1 DISTRIBUTION OF SEDIMENTARY STRUCTURE ACROSS MEANDERING RIVER FLO
     2OD PLAIN'///)
   39 FORMAT(1X,'THE SPECIFIED SECTION WIDTH HAS BEEN EXCEEDED-THE WIDTH
     1 MUST BE INCREASED IF MIGRATION IS TO PROCEED')
   41 FORMAT(1X,'DEPTH OF SCOUR AT TALWEG FOR THIS YEAR',21X,F10.3,' MET
     1RES'//)
   42 FORMAT(1H0,1X,15A4,' TIME INCREMENT',I5//1X,'VARIATION OF GRAINSIZ
     1E AND BED FORM OVER CHANNEL CROSS PROFILE'//7X,'DEPTH',3X,'GRAINSI
     2ZE',8X,'BED FORM',6X,'LOCAL MEAN',4X,'LOCAL',10X,'LOCAL STREAM',2X
     3,'LOCAL BED',5X,'LOCAL FROUDE'/7X,'(M)',5X,'(CM)',27X,'FLOW VELOCI
     4TY',1X,'DIMENSIONLESS',2X,'POWER',9X,'SHEAR STRESS',2X,'NUMBER'/46
     5X,'(CM/SEC)',6X,'SHEAR STRESS',1X,'(ERGS/CM2/SEC)',2X,'(DYN/CM2)'/
     6)
   43 FORMAT(1X,'UNFORTUNATELY THE PERCENTAGE OF GRAVEL IN THE OUTER BAN
     1K IS ',F10.3)
   45 FORMAT('SCALE-1 INCH TO',F10.2,' METRES',100X)
   47 FORMAT('MEANDER GEOMETRY',100X)
   49 FORMAT(////1X,'TIME INCREMENT ',I5,' LIMITING SINUOSITY/AMPLITUDE
     1HAS BEEN REACHED')
  972 FORMAT(///1X,' TIME INCREMENT ',I5,/1X,'LIMITING SINUOSITY/AMPLITU
     1DE REACHED IN A LATERAL SECTION - TEST TERMINATED')
  977 FORMAT(///1X,'INITIAL BANKFULL STAGE MEASURED FROM BASE OF SECTION
     1 EXCEEDS SPECIFIED SECTION THICKNESS - TEST TERMINATED')
  979 FORMAT(///1X,'ERROR IN SECOND DATA CARD - LAST THREE VARIABLES MUS
     1T BE NONZERO')
  981 FORMAT(1X,'THE LOWER BOUNDARY OF THE CROSS SECTION HAS BEEN EXCEED
     1ED -'/1X,'ADJUSTMENT IS REQUIRED IN EITHER INITIAL BANKFULL STAGE,
     2DEPTH AT TALWEG,OR SCOUR AND FILL PARAMETERS')
  983 FORMAT(1X,'INITIAL SINUOSITY IS OUTSIDE THE SPECIFIED LIMITS - TES
     1T TERMINATED')
  985 FORMAT(1X,'THE SPECIFIED SECTION THICKNESS HAS BEEN EXCEEDED - RES
     1CALING IS REQUIRED IF AGGRADATION IS TO CONTINUE')
  987 FORMAT(1X,'THE SPECIFIED LENGTH OF THE X-AXIS ON THE GRAPH PLOTTER
     1 HAS BEEN EXCEEDED - RESCALING IS REQUIRED')
  989 FORMAT(///1X,'RATE OF AGGRADATION PER FLOOD INCREMENT IS GREATER T
     1HAN ONE VERTICAL CELL - RESCALING IS REQUIRED')
  991 FORMAT(///1X,' TIME INCREMENT ',I5,' - TEST TERMINATED DUE TO CHUT
     1E CUT OFF')
  993 FORMAT(///1X,' TIME INCREMENT ',I5,' - TEST TERMINATED DUE TO NECK
     1 CUT OFF')
  995 FORMAT(///1X,'DEFINITION OF LINE OF SECTION IS IN ERROR - TEST TER
     1MINATED')
C
C READ INPUT PARAMETERS
C
      READ(5,1)TITLE,IX
      READ(5,3)NTIM,NPRINT,NFPLOT,NTPLOT
      IF(NPRINT.EQ.0.OR.NFPLOT.EQ.0.OR.NTPLOT.EQ.0)GO TO 978
      READ(5,4)NCOLS,NROWS,IFCOD6,ZTOT,YTOT,BANK,WS,DWS,ZSECT,FMT4
      IF(WS.GT.YTOT)GO TO 976
      READ(5,6)SN,WVL,VS,XMAX
      READ(5,6)C1,C2,E1,GRAVLM
      READ(5,6)EC1,EC2,EN1,EN2,GAPLIM,SNLIM
      IF(SN.GT.SNLIM)GO TO 982
      READ(5,7)W,H,EXN,C5,F1,F2,SIGMA,RO,IFCOD7
      IF(H.GT.WS)GO TO 980
      READ(5,5)GRAVEL,SAND,SILT,CLAY,UPPB,LPPB,ANTIDN,RIPPLE,DUNES,OLDSE
     1D,WATER,DOT,BLANK,FLOOD
      READ(5,2)IFCOD3,QVOLMX,SKEW
      READ(5,6)DM,DS,YM,YS,A1,A2,A,B,SA,SB
      READ(5,2)IFCOD5,C6,E2,STDVN,IFCOD1
C
C CALL RNDMIN
C
      CALL RNDMIN(IX)
C
C FIND CELL DIMENSIONS
```

```
C
      ZCEL=ZTOT/FLOAT(NCOLS)
      YCEL=YTOT/FLOAT(NROWS)
      IF(DWS.GT.YCEL)GO TO 988
C
C FIND BANKFULL STAGE RELATIVE TO BASE OF SECTION AND DISTANCE OF INNER
C BANK OF CHANNEL FROM LEFT HAND SIDE OF SECTION (IN CELLS)
C
      IBANK=BANK/ZCEL
      IWS=WS/YCEL
C
C FIND INITIAL AMPLITUDE
C
      AMP=WVL*NEWRAP(SN,0.0000001)
      IF(ZSECT.GT.(AMP/3.0))GO TO 994
C
C FIND LIMITING AMPLITUDE
C
      AMPLIM=WVL*NEWRAP(SNLIM,0.0000001)
C
C FIND INITIAL DISTANCE FROM LIMITING AMPLITUDE
C
      SS=(AMPLIM-AMP)/2.0
      IF(SS.LE.0.0)LIM=1
C
C INITIALISE CROSS SECTION ARRAYS
C
      READ(5,5)(SEDIN(I),I=1,IWS)
      DO 146 J=1,NCOLS
      DO 146 I=1,NROWS
      IF(I.GT.IWS)GO TO 145
      SEDGS(I,J)=SEDIN(I)
      SEDSTR(I,J)=OLDSED
      GO TO 146
  145 SEDGS(I,J)=BLANK
      SEDSTR(I,J)=BLANK
  146 TLPLOT(I,J)=BLANK
C
C INITIALISE SYNTHETIC HYDROLOGY PARAMETERS
C
C SKEWNESS PARAMETERS
C
      IF(SKEW.EQ.0.0)GO TO 162
      SKEW2=2.0/SKEW
      GO TO 163
  162 SKEW2=0.0
  163 SKEW6=SKEW/6.0
      SKEW62=SKEW6*SKEW6
C
C AUTOREGRESSIVE MODEL PARAMETERS
C
      ZTM1=RANSAM(IFCOD3)
      ZTM2=RANSAM(IFCOD3)
      COEFF=SQRT((1.0+A2)/(1.0-A2)*((1.0-A2)**2-A1**2))
C
C CALCULATE MEAN AND STANDARD DEVIATION OF FLOW FOR EACH DAY OF THE YEAR
C AND STORE IN ARRAYS
C
      DO 150 NDAY=1,365
      FSSUM(NDAY)=0.0
      FMSUM(NDAY)=0.0
      VAR=0.017211*FLOAT(NDAY)
      DO 149 K=1,6
      ARG=FLOAT(K)*VAR
      FMSUM(NDAY)=FMSUM(NDAY)+A(K)*COS(ARG)+B(K)*SIN(ARG)
  149 FSSUM(NDAY)=FSSUM(NDAY)+SA(K)*COS(ARG)+SB(K)*SIN(ARG)
  150 CONTINUE
C
C FIND FULL WIDTH OF FLOW BETWEEN INNER AND OUTER BANKS
C
      WW=W/C5
C
C FIND VALUES OF W AND WW IN CELLS
C
      NZCEL=WW/ZCEL
      NZCEL1=W/ZCEL
      FLT2=FLOAT(NZCEL1)
C
```

```
C FIND LIMITING WIDTH OF MEANDER NECK MEASURED FROM CHANNEL CENTRE LINES
C
      GAPLIM=GAPLIM+WW
C
C FIND VALUE OF H IN CELLS
C
      NH=H/YCEL
C
C PARAMETERS USED TO CALCULATE FROUDE NOS. IN MEANDR
C
      F18=8.0/F1
      F28=8.0/F2
C
C PARAMETERS USED IN BAR
C
      SIGRO=SIGMA-RO
      EXNM1=EXN-1.0
      VAR1=3.14*EXN/(200.0*W**EXN)
      VAR2=16.5*RO/SIGRO
C
C PARAMETERS FOR SCALING PLOT OF MEANDER GEOMETRY IN MEANDR
C
      SCALE=AMPLIM/9.0
      SCALE2=SCALE/2.0
      XL=XMAX/AMPLIM*9.0
      TDMIG=0.0
C
C INITIALISE TIME KEEPING DEVICES AND NFLD
C
      NFLD=0
      IPRINT=MOD(NFLD,NPRINT)
      ITPLOT=MOD(NFLD,NTPLOT)
C
C RATIO OF YCEL/ZCEL
C
      YCOZC=YCEL/ZCEL
C
C WRITE SCALES AND TITLES ON GRAPH
C
      CALL PLOT(1,0.0,XMAX,XL,XMAX,0.0,AMPLIM,9.0,AMPLIM)
      CALL PLOT(99)
      CALL PLOT(90,SCALE2,-SCALE2)
      WRITE(3,45)SCALE
      CALL CHAR(0.2,0)
      CALL PLOT(99)
      CALLPLOT(90,SCALE2,AMPLIM)
      WRITE(3,47)
      CALL CHAR(0.2,0)
      CALL PLOT(99)
C
C PRINT OUT CROSS SECTION PARAMETERS
C
      WRITE(6,21)TITLE,ZTOT,NCOLS,YTOT,NROWS,BANK,IBANK,WS,IWS,YCEL,ZCEL
C
C PRINT OUT CHANNEL PARAMETERS
C
      WRITE(6,23)WW,NZCEL,W,NZCEL1,C5,H,SIGMA,RO,F1,F2,EXN
C
C PRINT OUT SYNTHETIC HYDROLOGY PARAMETERS
C
      WRITE(6,24)DM,DS,YM,YS,A1,A2,A,B,SA,SB,QVOLMX
C
C PRINT OUT BANK MIGRATION PARAMETERS
C
      WRITE(6,25)E1,C1,C2,GRAVLM
C
C PRINT OUT SCOUR AND FILL PARAMETERS
C
      WRITE(6,26)C6,E2,STDVN
C
C PRINT OUT CUT OFF CONTROL PARAMETERS
C
      WRITE(6,28)GAPLIM,EN1,EN2,SNLIM,AMPLIM,EC1,EC2
C
C PRINT OUT TYPE OF SECTION
C
      IF(IFCOD6.GT.0)GO TO 167
      WRITE(6,33)
```

```
      GO TO 168
  167 WRITE(6,31)ZSECT
C
C PRINT LEGEND
C
  168 WRITE(6,27)LPPB,GRAVEL,OLDSED,RIPPLE,SAND,WATER,DUNES,SILT,DOT,DOT
     1,DOT,DOT,DOT,UPPB,CLAY,ANTIDN,FLOOD
C
C FIND AND PLOT INITIAL PLANIMETRIC FORM OF MEANDER
C
      CALL MEANDR
C
C INITIAL OPERATIONS CONCERNING CROSS SECTION DEFINITION - THEN BRANCH
C TO INITIALISE AND PRINT CHANNEL SECTION
C
      IF(IFCOD6-1)170,172,174
  170 NZCELO=NZCEL
      ZCEL1=ZCEL
      IF(LIM.EQ.1)GO TO 971
      GO TO 218
  172 IF(LIM.NE.1)GO TO 175
      PAR1=3.14159*(AMP-2.0*ZSECT)/(SN*WVL)
      PHI=(0.0505*SN+PAR1+0.0692)/0.6371
      PAR2=((-0.0292*SN+0.2132)*SN-0.4651)*SN-PAR1+0.2668
  130 FA=((PHI*0.2804+(0.2244-0.1713*SN))*PHI+((0.1139*SN-0.552)*SN+0.88
     195))*PHI+PAR2
      FB=(PHI*0.8412+(0.4488-0.3426*SN))*PHI+(0.1139*SN-0.552)*SN+0.8895
      PHIN=PHI-FA/FB
      IF(ABS(PHIN-PHI)-0.0001)140,140,135
  135 PHI=PHIN
      GO TO 130
  140 SINPHI=SIN(PHIN)
      GO TO 176
C
C STRAIGHT LINE DISTANCE BETWEEN POINTS OF INFLECTION OF LOOP
C
  174 NDAVA=WVL/(2.0*ZCEL)
  175 SINPHI=SIN(2.2*SQRT((SN-1.0)/SN))
  176 ZCEL1=SINPHI*ZCEL
      NZCEL=WW/ZCEL1
      NZCEL1=W/ZCEL1
      GO TO 216
C
C BEGIN MAJOR LOOP,ONCE THROUGH EVERY YEAR
C
C INITIALISE TIME KEEPING DEVICES
C
  169 IPRINT=MOD(NFLD,NPRINT)
      ITPLOT=MOD(NFLD,NTPLOT)
C
C FIND FLOOD PERIOD VOLUME
C
      QVOL=0.0
      DO 180 NDAY=1,365
      ZT=A1*ZTM1+A2*ZTM2+COEFF*RANSAM(IFCOD3)
      XT=DM+FMSUM(NDAY)+(DS+FSSUM(NDAY))*(YM+YS*ZT)
      IF(XT.GT.DM)QVOL=QVOL+XT
      ZTM2=ZTM1
  180 ZTM1=ZT
C
C TEST FOR CUT OFF
C
      PC=(QVOL/QVOLMX)**EC1*(SN/SNLIM)**EC2
      PN=(QVOL/QVOLMX)**EN1*(GAPLIM/GAP)**EN2
      X=RNDM(-1)
      IF(X.LE.PC)ICUT=2
      X=RNDM(-1)
      IF(X.LE.PN)ICUT=3
      IF(ICUT.EQ.1)GO TO 182
C
C CUT-OFF HAS OCCURRED - OUTPUT REQUIRED INFORMATION AND TERMINATE PROG.
C
      WRITE(6,29)TITLE,NFLD,QVOL,OBGSI,BGSI,SCHUMM,SS,RLMIG,TLMIG,RDMIG,
     1TDMIG
      WRITE(6,30)AGG
      IPRINT=0
      NFPLOT=NFLD
      CALL MEANDR
```

```
      GO TO 548
C
C FIND AMOUNT OF LATERAL AND DOWNSTREAM BANK MIGRATION
C
  182 IF(LIM.EQ.1)GO TO 185
      RLMIG=SS*C1*QVOL/OBGSI**E1
      TLMIG=TLMIG+RLMIG
  185 RDMIG=C2*QVOL/OBGSI**E1
      TDMIG=TDMIG+RDMIG
C
C PRINT OUT REQUIRED DATA FOR THIS TIME INCREMENT
C
      IF(IPRINT.EQ.0)WRITE(6,29)TITLE,NFLD,QVOL,OBGSI,BGSI,SCHUMM,SS,RLM
     1IG,TLMIG,RDMIG,TDMIG
C
C AGGRADE THE FLOODPLAIN IF REQUIRED
C
      AGG=AGG+DWS
C
C WRITE TOTAL AMOUNT OF AGGRADATION SO FAR
C
      IF(IPRINT.EQ.0)WRITE(6,30)AGG
      NAGG=AGG/YCEL
      IF(NAGG.LT.MARK)GO TO 210
C
C IF ROW OF CELLS IS FILLED,ADJUST BANKFULL STAGE AND FILL ROW WITH
C ALPHAMERIC CHARACTERS
C
      IWS=IWS+1
      IF(IWS.GT.NROWS)GO TO 984
      MARK=MARK+1
      DO 200 J=1,NCOLS
      SEDGS(IWS,J)=FLOOD
  200 SEDSTR(IWS,J)=FLOOD
C
C RECORD ON 2-D ARRAYS THE RESULTING EROSION AND DEPOSITION AFTER THIS
C YEAR
C
C FIND AMOUNT OF BANK MIGRATION IN CROSS SECTION REPRESENTED.ADJUST
C CHANNEL WIDTH(IN CELLS) REPRESENTED IN CROSS SECTION(AND RELATED
C PARAMETERS),DEPENDING ON TYPE OF CROSS SECTION AND CHANGES IN SHAPE
C OF MEANDER
C
  210 IF(IFCOD6.GT.0)GO TO 215
      RMIG=SQRT(RLMIG*RLMIG+RDMIG*RDMIG)
      AA=ATAN(RDMIG/RLMIG)
      TANA=RDMIG/RLMIG
      P=ATAN((R+WW/2.0-SQRT((R+WW/2.0)**2+2.0*R*WW*TANA*TANA))/(-2.0*R*T
     1ANA))
      ZCEL1=ZCEL*COS(AA-P)/COS(P)
      GO TO 216
  215 RMIG=RDMIG
      SINPHI=SIN(2.2*SQRT((SN-1.0)/SN))
      ZCEL1=ZCEL*SINPHI
  216 NZCELO=NZCEL
      NZCL1O=NZCEL1
      NZCEL=WW/ZCEL1
      NZCEL1=W/ZCEL1
      FLT2=FLOAT(NZCEL1)
      YZOZC=YCEL/ZCEL1
      IF(NZCEL1-NZCL1O)218,218,217
  217 NZDIF=NZCEL1-NZCL1O
      GO TO 225
  218 NZDIF=0
C
C ADD LAST YEAR'S SMOOTHING ERROR TO THIS YEAR'S BANK MIGRATION
C
  225 RMIG=RMIG+DEV
C
C FIND BANK MIGRATION(IN CELLS) IN CROSS SECTION,AND CALCULATE ERROR
C DUE TO SMOOTHING,DEV
C
      NRMIG=RMIG/ZCEL
      DEV=RMIG-ZCEL*FLOAT(NRMIG)
C
C DEFINE AMOUNT OF CONCOMITANT POINT BAR MIGRATION(IN CELLS),DEPENDING
C ON CHANGES IN CHANNEL WIDTH IN CROSS SECTION REPRESENTED
C
```

```
      IF(IFCOD6.EQ.0)GO TO 227
      NRMIG=NRMIG+NZCELO-NZCEL
      IF(NRMIG.LT.0)NRMIG=0
  227 FNRMIG=FLOAT(NRMIG)
C
C FIND TOTAL NUMBERS OF CELLS REQUIRED FOR CHANNEL SECTION AND CHECK
C THAT DOES NOT EXCEED SPECIFIED LIMITS
C
      NZCELT=NZCEL+NRMIG
      IF((IBANK+NZCELT+NDAVA).GT.NCOLS)GO TO 585
C
C IF NO SCOUR AND FILL GO TO 400
C
      IF(NFLD.EQ.0)GO TO 400
      IF(IFCOD5.NE.1)GO TO 400
C
C FIND MAXIMUM DEPTH OF SCOUR MEASURED ABOVE TALWEG
C
      DSCR=C6*QVOL**E2+RANSAM(IFCOD1)*STDVN
      IF(DSCR.LT.0.0)DSCR=0.0
      IF(IPRINT.EQ.0)WRITE(6,41)DSCR
      HH=H+DSCR
C
C IF MAX. CHANNEL DEPTH NOW EXCEEDS LOWER BOUNDARY OF SECTION - JOB ENDS
C
      IF(HH.GT.(FLOAT(IWS)*YCEL))GO TO 980
C
C FOR  EVERY COLUMN OF POINT BAR GRADUALLY FILL TO ORIGINAL DEPTH
C
  370 Z=ZCEL1
      DO 390 J=1,NZCEL1
      NCOL=J+IBANK
      IF(IFCOD7.EQ.0)GO TO 372
      CALL BAR1(0,HH)
      GO TO 373
  372 CALL BAR(0,HH)
  373 Z=Z+ZCEL1
  390 CONTINUE
      HH=HH-YCEL
      IF(HH.GE.H)GO TO 370
C
C FILL SCOURED TALWEG
C
      IF(NRMIG.LT.1)GO TO 400
      DO 380 J=1,NRMIG
      NCOL=IBANK+NZCEL1+J
      Y=-DSCR/2.0*(COS(3.14*(FLOAT(NRMIG-J)/FNRMIG))-1.0)
      NYCEL=(H+Y)/YCEL
      INDEX=IWS-NYCEL
  381 SEDGS(INDEX,NCOL)=SEDGS(INDEX,IBANK+NZCEL1)
      SEDSTR(INDEX,NCOL)=SEDSTR(INDEX,IBANK+NZCEL1)
      Y=Y-YCEL
      INDEX=INDEX+1
      IF(Y.GE.0.0)GO TO 381
  380 CONTINUE
C
C FOR EVERY COLUMN IN CHANNEL SECTION,FIND GRAINSIZE AND BEDFORM ACROSS
C INNER BANK AND ERODE OUTER BANK
C
C INITIALISE PARAMETERS AND WRITE HEADINGS
C
  400 Z=ZCEL1
      OBGS=0.0
      BGS=0.0
      GRAV=0.0
      NRMIG1=NRMIG+NZDIF+1
      INDEXK=IWS
      KOUNT=0
      INDEXO=IWS-NH+1
      IF(IPRINT.EQ.0)WRITE(6,42)TITLE,NFLD
C
C BEGIN MAJOR LOOP ENTERED ONCE FOR EVERY COLUMN OF CHANNEL SECTION
C
      DO 450 J=1,NZCEL
      NCOL=IBANK+J+NRMIG
      IF(J.LE.NZCEL1)GO TO 410
C
C ERODE OUTER BANK
```

```
C
      Y=-H/2.0*(COS(3.14*(WW-Z)/(WW-W))-1.0)
      NYCEL=Y/YCEL
      INDEX=IWS-NYCEL
      IF(ITPLOT.EQ.0)TLPLOT(INDEX,NCOL-1)=DOT
      INDEXK=INDEX
  405 IF(SEDGS(INDEX,NCOL).EQ.CLAY.OR.SEDGS(INDEX,NCOL).EQ.SILT.OR.SEDGS
     1(INDEX,NCOL).EQ.FLOOD)OBGS=OBGS+1.0
      IF(SEDGS(INDEX,NCOL).EQ.GRAVEL)GRAV=GRAV+1.0
      KOUNT=KOUNT+1
      INDEX=INDEX-1
      IF(INDEX.GT.INDEXO)GO TO 405
      INDEXO=INDEXK
      GO TO 440
C
C DEPOSIT SEDIMENT ON INNER BANK
C
  410 IF(IFCOD7.EQ.0)GO TO 411
      CALL BAR1(1,H)
      GO TO 412
  411 CALL BAR(1,H)
  412 IF(D.LE.0.00625)BGS=BGS+1.0
      IF(ITPLOT.EQ.0.AND.J.NE.NZCEL1)TLPLOT(INDEX,NCOL)=DOT
      IF(NFLD.EQ.0)GO TO 440
C
C 'FILL' POINT BAR
C
      IF(NRMIG1.LT.1)GO TO 440
      DO 415 JJJ=1,NRMIG1
      JJ=NCOL-JJJ
      IF(JJ.LT.1)GO TO 415
      IF(NZCEL1.LT.NZCL10.AND.IFCOD5.EQ.1)GO TO 413
      IF(SEDSTR(INDEX,JJ).NE.WATER.AND.SEDSTR(INDEX,JJ).NE.FLOOD.AND.SED
     1STR(INDEX,JJ).NE.OLDSED)GO TO 415
  413 SEDGS(INDEX,JJ)=SEDGS(INDEX,JJ+1)
      SEDSTR(INDEX,JJ)=SEDSTR(INDEX,JJ+1)
  415 CONTINUE
C
C FILL IN 'EMPTY' ROWS
C
  420 IF((INDEXK-INDEX).LT.2)GO TO 424
      INDEXK=INDEXK-1
      DO 422 JJ=1,NRMIG1
      NCOLK=NCOL-JJ
      IF(NCOLK.LT.1)GO TO 422
      IF(NZCEL1.LT.NZCL10.AND.IFCOD5.EQ.1)GO TO 421
      IF(SEDSTR(INDEXK,NCOLK).NE.WATER.AND.SEDSTR(INDEXK,NCOLK).NE.OLDSE
     1D)GO TO 422
  421 SEDGS(INDEXK,NCOLK)=SEDGS(INDEX,NCOLK)
      SEDSTR(INDEXK,NCOLK)=SEDSTR(INDEX,NCOLK)
  422 CONTINUE
      GO TO 420
  424 INDEXK=INDEX
C
C FILL NEW CHANNEL WITH WATER
C
  440 INDEX=IWS-NYCEL+1
      IF(NYCEL.EQ.0)GO TO 450
      DO 445 II=INDEX,IWS
      SEDSTR(II,NCOL)=WATER
  445 SEDGS(II,NCOL)=WATER
  450 Z=Z+ZCEL1
C
C CALCULATE PERCENT SILT-CLAY IN PERIMETER OF CHANNEL
C
      FLTK=FLOAT(KOUNT)
      SCHUMM=100.0*(BGS+OBGS*YCOZC)/(FLT2+YCOZC*FLTK)
C
C CALCULATE GRAIN SIZE INDICES FOR INNER AND OUTER BANKS
C
      BGSI=BGS/FLT2*100.0
      OBGSI=OBGS/FLTK*100.0
      IF(OBGSI.EQ.0.0)OBGSI=1.0
      GRAVI=GRAV/FLTK*100.0
      IF(GRAVI.GT.GRAVLM)GO TO 460
C
C FILL 2-D ARRAYS FOR THE SECOND CHANNEL IF A TWO CHANNEL DOWNVALLEY
C SECTION IS BEING USED
```

```
C
      IF(IFCOD6.NE.2)GO TO 548
      DO 545 J=1,NZCELT
      JJ=IBANK+J
      JJJ=JJ+NDAVA
      DO 545 I=1,IWS
      TLPLOT(I,JJJ)=TLPLOT(I,JJ)
      SEDGS(I,JJJ)=SEDGS(I,JJ)
  545 SEDSTR(I,JJJ)=SEDSTR(I,JJ)
  548 IF(IPRINT.NE.0)GO TO 570
C
C PRINT OUT CROSS SECTION SHOWING GRAIN SIZE DISTRIBUTION
C
      WRITE(6,35)TITLE,NFLD
      DO 550 J=1,NCOLS
  550 WRITE(6,FMT4)(SEDGS(I,J),I=1,NROWS),(TLPLOT(I,J),I=1,NROWS)
C
C PRINT OUT CROSS SECTION SHOWING SEDIMENTARY STRUCTURE DISTRIBUTION
C
      WRITE(6,36)TITLE,NFLD
      DO 560 J=1,NCOLS
  560 WRITE(6,FMT4)(SEDSTR(I,J),I=1,NROWS),(TLPLOT(I,J),I=1,NROWS)
      GO TO (570,990,992),ICUT
  570 IBANK=IBANK+NRMIG
C
C FIND PLANIMETRIC FORM OF MEANDER AT END OF THIS YEAR
C
      IF(NFLD.EQ.0)GO TO 575
      IF((TDMIG+WVL).GT.XMAX)GO TO 986
C
C FIND CHANGES IN AMPLITUDE
C
      IF(LIM.EQ.1)GO TO 572
      AMP=AMP+RLMIG*2.0
      SS=(AMPLIM-AMP)/2.0
      IF(SS.GT.0.0)GO TO 573
      LIM=1
      RLMIG=0.0
      AMP=AMPLIM
      SS=0.0
      CALL MEANDR
      IF(IFCOD6.LE.0)GO TO 971
      WRITE(6,49)NFLD
      GO TO 575
  572 IF(RDMIG.LE.0.0)GO TO 575
      CALL MEAND1
      GO TO 575
  573 CALL MEANDR
      IF(GAP.LE.WW)GO TO 992
  575 NFLD=NFLD+1
      IF(NFLD.LE.NTIM)GO TO 169
C
C ERROR MESSAGES
C
      GO TO 999
  460 WRITE(6,43)GRAVI
      GO TO 999
  585 WRITE(6,39)
      GO TO 999
  971 WRITE(6,972)NFLD
      GO TO 999
  976 WRITE(6,977)
      GO TO 1000
  978 WRITE(6,979)
      GO TO 1000
  980 WRITE(6,981)
      GO TO 1000
  982 WRITE(6,983)
      GO TO 1000
  984 WRITE(6,985)
      GO TO 999
  986 WRITE(6,987)
      GO TO 999
  988 WRITE(6,989)
      GO TO 1000
  990 WRITE(6,991)NFLD
      GO TO 999
  994 WRITE(6,995)
      GO TO 1000
  992 WRITE(6,993)NFLD
  999 CALL PLOT(7)
 1000 STOP
      END
```

```
C
C-----------------------------------------------------------------------
      SUBROUTINE MEANDR
C-----------------------------------------------------------------------
C
C CONTROL STATEMENTS
C
      EXTERNAL FUNC2
      DIMENSION COSPHI(50),SINPHI(50)
      COMMON/COM1/IPRINT,RINB,FROUD1,FROUD2,VAR2S,RC
      COMMON/COM3/NFLD,TITLE(15),WVL,AMP,VS,GAP,NFPLOT,CHS,WW,R,RO,VAR2,
     1F28,F18,SS,TDMIG,SN
C
C FORMAT STATEMENTS
C
    3 FORMAT(1X,'SELECTED GEOMETRIC RATIOS'//6X,'WAVELENGTH TO RADIUS OF
     1 CURVATURE',11X,F10.3/6X,'WAVELENGTH TO CHANNEL WIDTH',17X,F10.3/6
     2X,'RADIUS OF CURVATURE TO CHANNEL WIDTH',8X,F10.3/6X,'AMPLITUDE TO
     3 CHANNEL WIDTH',18X,F10.3///)
    4 FORMAT(1H1,1X,15A4,' TIME INCREMENT',I5//1X,'PLANIMETRIC FORM OF M
     1EANDER',26X,'METRES'//6X,'WAVELENGTH',34X,F10.3/6X,'AMPLITUDE',35X
     2,F10.3/6X,'SINUOSITY',45X,F10.3/6X,'RADIUS OF CURVATURE AT BEND AX
     3IS',12X,F10.3/6X,'WIDTH OF MEANDER NECK',23X,F10.3/6X,'CHANNEL LEN
     4GTH ALONG MEANDER',16X,F10.3/6X,'VALLEY SLOPE',42X,F10.8/6X,'LONGI
     5TUDINAL WATER SURFACE SLOPE',22X,F10.8///)
    6 FORMAT(I4,100X)
C
C REGRESSION EQUATION RELATING SINUOSITY TO AMPLITUDE/WAVELENGTH
C
      IF(NFLD.EQ.0)GO TO 5
      AOW=AMP/WVL
      SN=((-0.4301562*AOW+1.674662)*AOW+0.337086)*AOW+0.9634151
C
C CALCULATE CHL,CHS,AND R
C
    5 CHL=WVL*SN
      CHS=VS/SN
      R=WVL*(SN**1.5)/(13.0*SQRT(SN-1.0))
C
C CALCULATE MISCELLANEOUS PARAMETERS
C
      RINB=R-WW/2.0
      RC=RO*CHS
      VAR2S=VAR2*CHS
C
C CALCULATE FROUDE NUMBERS
C
      FROUD1=SQRT(CHS*F18)
      FROUD2=SQRT(CHS*F28)
C
C CALCULATE SELECTED RATIOS
C
      WVLR=WVL/R
      WVLWW=WVL/WW
      RWW=R/WW
      AMPWW=AMP/WW
C
C CALCULATE GAP
C
      OMEGA=2.2*SQRT((SN-1.0)/SN)
      IF(OMEGA.LE.1.57)GO TO 8
      CALL SIMINT(0.0,OMEGA,1.57,0.005,SIMP2,FUNC2)
      GAP=WVL*(1.0-SN/3.14*SIMP2)
      GO TO 9
    8 GAP=99999999.0
      ENTRY MEAND1
C
C PRINT GEOMETRIC PARAMETERS AND RATIOS IF REQUIRED
C
    9 IF(IPRINT.NE.0)GO TO 20
      WRITE(6,4)TITLE,NFLD,WVL,AMP,SN,R,GAP,CHL,VS,CHS
      WRITE(6,3)WVLR,WVLWW,RWW,AMPWW
C
C PARAMETER INITIALISATION FOR PLOTTING IF NFLD(MOD NFPLOT) EQUALS ZERO
C
   20 IF(MOD(NFLD,NFPLOT).NE.0)GO TO 55
      DSI=CHL/100.0
      S=DSI
```

```
      CHL2=CHL/2.0
      DZTOT=SS
      DXTOT=TDMIG
      CALL PLOT(90,DXTOT,DZTOT)
      I=1
C
C PLOT PLANIMETRIC FORM OF MEANDER IF NFLD(MOD NFPLOT) EQUALS ZERO
C
   10 PHI=OMEGA*SIN(S/CHL*6.28)
      COSPHI(I)=COS(PHI)
      SINPHI(I)=SIN(PHI)
   11 CALL PLOT(90,DXTOT,DZTOT)
      IF(I.LT.1)GO TO 44
      DX=DSI*COSPHI(I)
      DZ=DSI*SINPHI(I)
      DXTOT=DXTOT+DX
      IF(I.EQ.50)GO TO 41
      IF(S-CHL2)40,41,42
   40 DZTOT=DZTOT+DZ
      I=I+1
      S=S+DSI
      GO TO 10
   41 DZTOT=DZTOT+DZ
      S=S+DSI
      GO TO 43
   42 DZTOT=DZTOT-DZ
   43 I=I-1
      GO TO 11
C
C LABEL MEANDER TRACE
C
   44 WRITE(3,6)NFLD
      CALL CHAR(0.1,0)
      CALL PLOT(99)
   55 RETURN
      END


C
C-----------------------------------------------------------------------
      SUBROUTINE BAR(IFCOD4,H)
C-----------------------------------------------------------------------
C
      INTEGER*2 SEDGS,SEDSTR,GRAVEL,SAND,SILT,CLAY,UPPB,LPPB,ANTIDN,RIPP
     1LE,DUNES
      COMMON/COM1/IPRINT,RINB,FROUD1,FROUD2,VAR2S,RC
      COMMON/COM2/INDEX,NCOL,W,EXN,IWS,Y,NYCEL,D,VAR1,EXNM1,YCEL,SIGRO,Z
     1,GRAVEL,SAND,SILT,CLAY,UPPB,LPPB,ANTIDN,RIPPLE,DUNES,SEDSTR(60,200
     2),SEDGS(60,200)
   35 FORMAT(2F12.4,3X,A1,8X,A1,8X,5F14.4)
      ARG=3.14*(Z/W)**EXN
      Y=-H/2.0*(COS(ARG)-1.0)
      DYDZ=VAR1*H*Z**EXNM1*SIN(ARG)
      GO TO 10
      ENTRY BAR1(IFCOD4,H)
C
C INSERT ASSIGNMENT STATEMENT CARDS FOR Y AND DYDZ IMMEDIATELY BELOW IF
C USER SPECIFIED INNER BANK SHAPE IS REQUIRED.VALUE OF DYDZ MUST BE
C SCALED SUCH THAT UNITS OF D ARE CM.
C
      Y=Z*H/W
      DYDZ=H/(W*100.0)
   10 NYCEL=Y/YCEL
      INDEX=IWS-NYCEL
C
C FIND LOCAL RADIUS OF CURVATURE
C
      RL=RINB+Z
C
C FIND GRAIN SIZE
C
      D=VAR2S*Y*Y/(DYDZ*RL)
C
C FIND GRAIN SIZE CLASS
C
      IF(D.GT.0.00039)GO TO 15
      SEDGS(INDEX,NCOL)=CLAY
```

```
      GO TO 25
   15 IF(D.GT.0.00625)GO TO 17
      SEDGS(INDEX,NCOL)=SILT
      GO TO 25
   17 IF(D.GT.0.2)GO TO 19
      SEDGS(INDEX,NCOL)=SAND
      GO TO 25
   19 SEDGS(INDEX,NCOL)=GRAVEL
C
C FIND HYDRAULIC PARAMETERS
C
   25 YCM=100.0*Y
      YG=YCM*981.0
      VEL1=FROUD1*SQRT(YG)
      TX=RC*YG
      OMEGA1=VEL1*TX
      IF(D.EQ.0.0)GO TO 36
      THETA=RC*YCM/(D*SIGRO)
      GO TO 37
   36 THETA=0.0
C
C TEST FOR ANTIDUNES
C
   37 IF(FROUD2.GT.0.84)GO TO 70
C
C TEST FOR UPPER PHASE PLANE BED
C
      IF(D.GE.0.025)GO TO 90
      THETAC=0.52
      GO TO 94
   90 IF(D.GT.0.2)GO TO 92
      THETAC=0.56-1.43*D
      GO TO 94
   92 THETAC=0.27
   94 IF(THETA.GE.THETAC)GO TO 60
C
C TEST FOR DUNES
C
      IF(D.GT.0.023)GO TO 100
      OMEGAC=750.0
      GO TO 110
  100 IF(D.GT.0.036)GO TO 102
      OMEGAC=950.0
      GO TO 110
  102 IF(D.GT.0.069)GO TO 104
      OMEGAC=475.0
      GO TO 110
  104 OMEGAC=520.0
  110 IF(OMEGA1.GE.OMEGAC)GO TO 50
C
C TEST FOR RIPPLES
C
      IF(D.LE.0.065)GO TO 40
      SEDSTR(INDEX,NCOL)=LPPB
      GO TO 71
   40 SEDSTR(INDEX,NCOL)=RIPPLE
      GO TO 72
   50 SEDSTR(INDEX,NCOL)=DUNES
      GO TO 72
   60 SEDSTR(INDEX,NCOL)=UPPB
      GO TO 71
   70 SEDSTR(INDEX,NCOL)=ANTIDN
   71 IF(IFCOD4.EQ.0)GO TO 80
      VEL2=FROUD2*SQRT(YG)
      OMEGA2=TX*VEL2
      IF(IPRINT.EQ.0)WRITE(6,35)Y,D,SEDGS(INDEX,NCOL),SEDSTR(INDEX,NCOL)
     1,VEL2,THETA,OMEGA2,TX,FROUD2
      GO TO 80
   72 IF(IFCOD4.EQ.0)GO TO 80
      IF(IPRINT.EQ.0)WRITE(6,35)Y,D,SEDGS(INDEX,NCOL),SEDSTR(INDEX,NCOL)
     1,VEL1,THETA,OMEGA1,TX,FROUD1
   80 RETURN
      END
```

```
C
C------------------------------------------------------------------------
      SUBROUTINE SIMINT(A,OMEGA,B,E,SIMP,FUNC)
C------------------------------------------------------------------------
C
      H=(B-A)/2.0
      SM1=FUNC(A,OMEGA)+FUNC(B,OMEGA)
      SIMPO=0.0
      SM2=0.0
      R=A+H*2.0
   20 SM2=SM2+FUNC(R,OMEGA)
      R=R+H*2.0
      IF(R+H-B)20,70,30
   30 SM4=0.0
      R=A+H
   40 SM4=SM4+FUNC(R,OMEGA)
      R=R+H*2.0
      IF(R-B)40,70,50
   50 SIMP=H/3.0*(SM1+2.0*SM2+4.0*SM4)
      IF(ABS(SIMP-SIMPO)-E)70,70,60
   60 SM2=SM2+SM4
      SIMPO=SIMP
      H=H/2.0
      GO TO 30
   70 SIMP=SIMPO
      RETURN
      END
C
C------------------------------------------------------------------------
      FUNCTION FUNC2(X,OMEGA)
C------------------------------------------------------------------------
C
      FUNC2=COS(X)/SQRT(OMEGA*OMEGA-X*X)
      RETURN
      END

C
C------------------------------------------------------------------------
      REAL FUNCTION NEWRAP(SN,E)
C------------------------------------------------------------------------
C
      AOW=(SN-0.4529037)/2.186882
  130 FA=((-0.4301562*AOW+1.674662)*AOW+0.337086)*AOW+0.9634151-SN
      FB=(-1.2904686*AOW+3.349324)*AOW+0.337086
      AOWN=AOW-FA/FB
      IF(ABS(AOWN-AOW)-E)140,140,135
  135 AOW=AOWN
      GO TO 130
  140 NEWRAP=AOWN
      RETURN
      END
C
C------------------------------------------------------------------------
      FUNCTION RANSAM(IFCOD3)
C------------------------------------------------------------------------
C
      COMMON/COM4/SKEW2,SKEW6,SKEW62
      IF(IFCOD3.GT.2)GO TO 30
C
C RANDOM SAMPLE FROM USER SPECIFIED THEORETICAL DISTRIBUTION
C
      GO TO 41
   30 SUM=0.0
      DO 31 I=1,12
      X=RNDM(-1)
   31 SUM=SUM+X
      IF(IFCOD3-4)32,33,34
C
C RANDOM SAMPLE FROM NORMAL DISTRIBUTION
C
   32 RANSAM=SUM-6.0
      GO TO 41
C
C RANDOM SAMPLE FROM GAMMA DISTRIBUTION
C
   33 RANSAM=SKEW2*(1.0+SKEW6*(SUM-6.0)-SKEW62)**3-SKEW2
      GO TO 41
C
C RANDOM SAMPLE FROM LOGNORMAL DISTRIBUTION
C
   34 RANSAM=(EXP(SUM-6.0)-1.65)/2.15
   41 RETURN
      END
```

14.2 Main Program (using disc storage)

The structure of this program is essentially the same as the main program without a disc, therefore only those steps and comments which are not the same are listed below.

6. Alphameric characters are read into array SEDIN(I) and the grain size, sedimentary structure and time line cross sections are initialised and stored on disc. For every column of the cross sections the following operations are executed:- Array TEMPGS(I) is filled from the bottom of the section up to the row IWS with the grain size characters read into SEDIN, one character of SEDIN specifying the character for the complete row, I, of the grain size cross section. TEMPST(I) is filled up to IWS with the OLDSED character and the remaining rows in TEMPST and TEMPGS are filled with blanks. Every element in TEMPTL(I) is filled with blanks. Each set of three columns of data, one from each cross section, is then stored in one record on disc.
   Operations 19 to 32 are involved with recording on SEDGS (INDEX,NCOL) and SEDSTR (INDEX,NCOL) the resulting erosion and deposition after this years 'floods', and putting a time line on TLPLOT (INDEX,NCOL) if ITPLOT=0. These arrays are then stored on disc in the appropriate place.

20. Find total number of cell widths/columns, NZCELT, required for the channel section and corresponding array elements needed in the core store at once. If NZCELT exceeds the specified maximum number, MNCOLS, the job is terminated, as is the case if the right hand edge of the cross sections is exceeded. The necessary columns of the cross sections are read off disc into SEDGS (INDEX,NCOL), SEDSTR (INDEX,NCOL) and TLPLOT (INDEX,NCOL).

23. Every column of the inside bank of the channel section (1 to

NZCEL1) is now filled to the original depth by successive recalculation of the transverse profile, the depth at the old talweg being progressively decreased by one cell depth row until filling is complete. Subroutine BAR or BAR1 is called during these operations in order to fill the appropriate elements of SEDGS and SEDSTR with alphameric characters.

24. The area bounded by the position of the old talweg, the maximum scour depth below the old talweg, and the position of the new talweg is now filled by allocating for each row in this area the grain size and bed form symbols calculated for the row elements of the old talweg column, NZCEL1, in step 23.

Fig. 14.2 illustrates the sequence of events in the scouring and filling operation described above. Steps 25 to 32 constitute a major loop and are concerned with erosion of the outer bank and deposition on the point bar. As a result of the erosion of the outer bank and changes in the projected channel width in the cross sections, the whole transverse profile is shifted accordingly, and the left hand side of the new point bar profile is started at column NRMIG+1 of the cross section.

For every column, NCOL, of the new point bar (up to NZCEL1+NRMIG) steps 26 to 31 are executed.

For every column of the outer bank (NZCEL1+NRMIG+1 up to NZCELT) the following step is executed. (This is step 32).

35. The arrays SEDGS, SEDSTR, and TLPLOT containing the channel section data just computed, are written onto disc in the appropriate place with respect to the whole cross section. If a two-channel downvalley section is being used, this same information is also written on the disc, NDAVA records further on.

```
      C
      C CONTROL STATEMENTS
      C
0001        REAL NEWRAP
0002        DIMENSION FMT4(5),A(6),B(6),SA(6),SB(6),FMSUM(365),FSSUM(365)
0003        INTEGER*2 SEDGS,SEDSTR,TLPLOT(60,50),GRAVEL,SAND,SILT,CLAY,UPPB,LP
           1PB,ANTIDN,RIPPLE,DUNES,OLDSED,WATER,DOT,BLANK,SEDIN(60),TEMPGS(60)
           2,TEMPST(60),TEMPTL(60),FLOOD
0004        COMMON/COM1/IPRINT,RINB,FROUD1,FROUD2,VAR2S,RC
0005        COMMON/COM2/INDEX,NCOL,W,EXN,IWS,Y,NYCEL,D,VAR1,EXNM1,YCEL,SIGRO,Z
           1,GRAVEL,SAND,SILT,CLAY,UPPB,LPPB,ANTIDN,RIPPLE,DUNES,SEDSTR(60,50)
           2,SEDGS(60,50)
0006        COMMON/COM3/NFLD,TITLE(15),WVL,AMP,VS,GAP,NFPLOT,CHS,WW,R,RO,VAR2,
           1F28,F18,SS,TDMIG,SN
0007        COMMON/COM4/SKEW2,SKEW6,SKEW62
0008        DATA RMIG,TLMIG,AGG,DEV,NDAVA,LIM,MARK,ICUT/4*0.0,2*0,2*1/
0009        DEFINE FILE 4(200,360,L,ID)
      C
      C FORMAT STATEMENTS
      C
0010      1 FORMAT(15A4,I10,I2)
0011      2 FORMAT(I1,3F12.0,I1)
0012      3 FORMAT(4I4,5A4)
0013      5 FORMAT(80A1)
0014      6 FORMAT(6F12.0)
0015      7 FORMAT(8F8.0,I4)
0016     21 FORMAT(1H1,1X,15A4//1X,'CROSS SECTION PARAMETERS',49X,'METRES',5X,
           1'CELLS'//6X,'WIDTH OF SECTION',48X,F10.3,I10/6X,'THICKNESS OF SECT
           2ION',44X,F10.3,I10/6X,'INITIAL DISTANCE OF INNER CHANNEL BANK FROM
           3 L.H.S. OF SECTION',3X,F10.3,I10/6X,'INITIAL BANKFULL STAGE MEASUR
           4ED FROM SECTION BASE',15X,F10.3,I10/6X,'CELL SIZE IN VERTICAL(Y) D
           5IRECTION',30X,F10.3/6X,'CELL SIZE IN HORIZONTAL(Z OR X) DIRECTION'
           6,23X,F10.3///)
0017     23 FORMAT(1X,'CHANNEL PARAMETERS',55X,'METRES',5X,'CELLS'//6X,'TOTAL
           1WIDTH OF CHANNEL(W)',39X,F10.3,I10/6X,'WIDTH OF FLOW BETWEEN INNER
           2 BANK AND TALWEG(W1)',17X,F10.3,I10/6X,'RATIO OF W1 TO W',68X,F10.
           33/6X,'MAXIMUM FLOW DEPTH MEASURED ABOVE TALWEG',24X,F10.3/6X,'DENS
           4ITY OF SEDIMENTARY PARTICLES',52X,F10.3,' GM/CM3'/6X,'FLUID DENSIT
           5Y',71X,F10.3,' GM/CM3'/6X,'DARCY-WEISBACH FRICTION COEFFICIENT FOR
           6 DUNES AND RIPPLES',27X,F10.3/6X,'DARCY-WEISBACH FRICTION COEFFICI
           7ENT FOR PLANE BEDS AND ANTIDUNES',20X,F10.3/6X,'EXPONENT N1',73X,F
           810.3///)
0018     24 FORMAT(1X,'SYNTHETIC HYDROLOGY PARAMETERS(UNITS NOT NECESSARY)'//6
           1X,'MEAN OF ALL DAILY MEAN VALUES',25X,F10.3/6X,'STANDARD DEVIATION
           2 OF DAILY MEAN VALUES',15X,F10.3/6X,'MEAN OF YT SERIES',37X,F10.3/
           36X,'STANDARD DEVIATION OF YT SERIES',23X,F10.3/6X,'COEFFICIENTS IN
           4 AUTOREGRESSIVE MODEL',15X,'A1=',F10.3,7X,'A2=',F10.3/60X,'HARMONI
           5CS FROM 1 TO 6'/6X,'FOURIER COEFFICIENTS FOR DAILY MEANS(A)',15X,6
           6F10.3/42X,'(B)',15X,6F10.3/6X,'FOURIER COEFFICIENTS FOR DAILY STD
           7DEVIATIONS(SA)',5X,6F10.3/51X,'(SB)',5X,6F10.3/6X,'MAXIMUM VALUE O
           8F QVOL',33X,F10.3///)
0019     25 FORMAT(1X,'BANK MIGRATION PARAMETERS',/6X,'EXPONENT N2',53X,F10.3/
           16X,'VALUE OF CONSTANT IN LATERAL MIGRATION RELATION',14X,'K2=',E10
           2.3/6X,'VALUE OF CONSTANT IN DOWNVALLEY MIGRATION RELATION',11X,'K3
           3=',E10.3/6X,'LIMITING PERCENTAGE OF GRAVEL ALLOWABLE IN OUTER BANK
           4',11X,F10.3///)
0020     26 FORMAT(1X,'SCOUR AND FILL PARAMETERS'/6X,'CONSTANT K4',43X,E10.3/6
           1X,'EXPONENT N3',39X,F10.3/6X,'STANDARD DEVIATION OF ERROR TERM',18
           2X,F10.3///)
0021     27 FORMAT(1X,'LEGEND'//6X,'LOWER PHASE PLANE BED',5X,A1,7X,'GRAVEL',5
           1X,A1,8X,'OLD SEDIMENT',5X,A1/6X,'RIPPLES',19X,A1,7X,'SAND',7X,A1,8
           2X,'WATER',12X,A1/6X,'DUNES',21X,A1,7X,'SILT',7X,A1,8X,'TIME LINE',
           38X,5A1/6X,'UPPER PHASE PLANE BED',5X,A1,7X,'CLAY',7X,A1,8X,'AIR',1
           44X,'BLANK'/6X,'ANTIDUNES',17X,A1,7X,'OVERBANK',3X,A1/40X,'DEPOSITS
           5'//)
0022     28 FORMAT(1X,'CUT-OFF CONTROL PARAMETERS'/6X,'LIMITING WIDTH OF MEAND
           1ER NECK',24X,F10.3,' METRES'/6X,'EXPONENTS IN NECK CUT-OFF RELATIO
           2N',16X,'EN1=',F10.3,6X,'EN2=',F10.3/6X,'LIMITING SINUOSITY',36X,F1
           30.3/6X,'LIMITING AMPLITUDE',36X,F10.3,' METRES'/6X,'EXPONENTS IN C
           4HUTE CUT OFF RELATION',15X,'EC1=',F10.3,6X,'EC2=',F10.3///)
0023     29 FORMAT(1H1,1X,15A4,'TIME INCREMENT',I5//1X,'FLOOD PERIOD VOLUME FO
           1R THIS YEAR',26X,F10.3//1X,'OUTER BANK GRAINSIZE INDEX AT BEGINNIN
           2G OF YEAR',12X,F10.3//1X,'INNER BANK GRAINSIZE INDEX AT BEGINNING
           3OF YEAR',12X,F10.3//1X,'% SILT-CLAY IN CHANNEL PERIMETER AT BEGINN
           4ING OF YEAR',6X,F10.3//1X,'DISTANCE FROM LIMITING AMPLITUDE AT BEG
           5INNING OF YEAR',6X,F10.3,' METRES'//1X,'LATERAL MIGRATION DURING T
           6HIS YEAR',25X,F10.3,' METRES'//1X,'TOTAL LATERAL MIGRATION AT END
           7OF THIS YEAR',16X,F10.3,' METRES'//1X,'DOWNVALLEY MIGRATION DURING
```

Table 14.2. Listing of main program (using additional disc storage).

```
                    8 THIS YEAR',22X,F10.3,' METRES'//1X,'TOTAL DOWNVALLEY MIGRATION AT
                    9 END OF THIS YEAR',13X,F10.3,' METRES'//)
0024             30 FORMAT(1X,'TOTAL AGGRADATION AT END OF THIS YEAR',22X,F10.3,' METR
                    1ES'//)
0025             31 FORMAT(///1X,'A DOWNVALLEY SECTION IS REPRESENTED IN THIS TEST'/1X
                    1,'DISTANCE OF LINE OF SECTION FROM POINT OF INFLECTION OF LOOP IS'
                    2,F10.3,' METRES'//)
0026             33 FORMAT(///1X,'A LATERAL SECTION IS REPRESENTED IN THIS TEST'//)
0027             35 FORMAT(1H1,1X,15A4,' TIME INCREMENT',I5//1X,'CROSS SECTION SHOWING
                    1 DISTRIBUTION OF GRAIN SIZE ACROSS MEANDERING RIVER FLOOD PLAIN'//
                    2/)
0028             36 FORMAT(1H1,1X,15A4,' TIME INCREMENT',I5//1X,'CROSS SECTION SHOWING
                    1 DISTRIBUTION OF SEDIMENTARY STRUCTURE ACROSS MEANDERING RIVER FLO
                    2OD PLAIN'///)
0029             37 FORMAT(1X,'THE NUMBER OF COLUMNS REQUIRED FOR THE SPECIFIED CHANNE
                    1L WIDTH IS GREATER THAN'/1X,'THE CORE STORE WILL HOLD - RESCALING
                    2 IS REQUIRED')
0030             38 FORMAT(1X,'A DEVICE ERROR CONDITION WAS ENCOUNTERED DURING DATA TR
                    1ANSFER FROM DEVICE TO STORAGE')
0031             39 FORMAT(1X,'THE SPECIFIED SECTION WIDTH HAS BEEN EXCEEDED-THE WIDTH
                    1 MUST BE INCREASED IF MIGRATION IS TO PROCEED')
0032             41 FORMAT(1X,'DEPTH OF SCOUR AT TALWEG FOR THIS YEAR',21X,F10.3,' MET
                    1RES'//)
0033             42 FORMAT(1H0,1X,15A4,' TIME INCREMENT',I5//1X,'VARIATION OF GRAINSIZ
                    1E AND BED FORM OVER CHANNEL CROSS PROFILE'//7X,'DEPTH',3X,'GRAINSI
                    2ZE',8X,'BED FORM',6X,'LOCAL MEAN',4X,'LOCAL',10X,'LOCAL STREAM',2X
                    3,'LOCAL BED',5X,'LOCAL FROUDE'/7X,'(M)',5X,'(CM)',27X,'FLOW VELOCI
                    4TY',1X,'DIMENSIONLESS',2X,'POWER',9X,'SHEAR STRESS',2X,'NUMBER'/46
                    5X,'(CM/SEC)',6X,'SHEAR STRESS',1X,'(ERGS/CM2/SEC)',2X,'(DYN/CM2)'/
                    6)
0034             43 FORMAT(1X,'UNFORTUNATELY THE PERCENTAGE OF GRAVEL IN THE OUTER BAN
                    1K IS ',F10.3)
0035             45 FORMAT('SCALE-1 INCH TO',F10.2,' METRES',100X)
0036             47 FORMAT('MEANDER GEOMETRY',100X)
0037             49 FORMAT(////1X,'TIME INCREMENT ',I5,' LIMITING SINUOSITY/AMPLITUDE
                    1HAS BEEN REACHED')
0038            972 FORMAT(///1X,' TIME INCREMENT ',I5,/1X,'LIMITING SINUOSITY/AMPLITU
                    1DE REACHED IN A LATERAL SECTION - TEST TERMINATED')
0039            977 FORMAT(///1X,'INITIAL BANKFULL STAGE MEASURED FROM BASE OF SECTION
                    1 EXCEEDS SPECIFIED SECTION THICKNESS - TEST TERMINATED')
0040            979 FORMAT(///1X,'ERROR IN SECOND DATA CARD - LAST THREE VARIABLES MUS
                    1T BE NONZERO')
0041            981 FORMAT(1X,'THE LOWER BOUNDARY OF THE CROSS SECTION HAS BEEN EXCEED
                    1ED -'/1X,'ADJUSTMENT IS REQUIRED IN EITHER INITIAL BANKFULL STAGE,
                    2DEPTH AT TALWEG,OR SCOUR AND FILL PARAMETERS')
0042            983 FORMAT(1X,'INITIAL SINUOSITY IS OUTSIDE THE SPECIFIED LIMITS - TES
                    1T TERMINATED')
0043            985 FORMAT(1X,'THE SPECIFIED SECTION THICKNESS HAS BEEN EXCEEDED - RES
                    1CALING IS REQUIRED IF AGGRADATION IS TO CONTINUE')
0044            987 FORMAT(1X,'THE SPECIFIED LENGTH OF THE X-AXIS ON THE GRAPH PLOTTER
                    1 HAS BEEN EXCEEDED - RESCALING IS REQUIRED')
0045            989 FORMAT(///1X,'RATE OF AGGRADATION PER FLOOD INCREMENT IS GREATER T
                    1HAN ONE VERTICAL CELL - RESCALING IS REQUIRED')
0046            991 FORMAT(///1X,' TIME INCREMENT ',I5,' - TEST TERMINATED DUE TO CHUT
                    1E CUT OFF')
0047            993 FORMAT(///1X,' TIME INCREMENT ',I5,' - TEST TERMINATED DUE TO NECK
                    1 CUT OFF')
0048            995 FORMAT(///1X,'DEFINITION OF LINE OF SECTION IS IN ERROR - TEST TER
                    1MINATED')
              C
              C READ INPUT PARAMETERS
              C
0049                READ(5,1)TITLE,IX,IDISK
0050                READ(5,3)NTIM,NPRINT,NFPLOT,NTPLOT
0051                IF(NPRINT.EQ.0.OR.NFPLOT.EQ.0.OR.NTPLOT.EQ.0)GO TO 978
0052                READ(5,3)NCOLS,NROWS,MNCOLS,IFCOD6,FMT4
0053                READ(5,6)ZTOT,YTOT,BANK,WS,DWS,ZSECT
0054                IF(WS.GT.YTOT)GO TO 976
0055                READ(5,6)SN,WVL,VS,XMAX
0056                READ(5,6)C1,C2,E1,GRAVLM
0057                READ(5,6)EC1,EC2,EN1,EN2,GAPLIM,SNLIM
0058                IF(SN.GT.SNLIM)GO TO 982
0059                READ(5,7)W,H,EXN,C5,F1,F2,SIGMA,RO,IFCOD7
0060                IF(H.GT.WS)GO TO 980
0061                READ(5,5)GRAVEL,SAND,SILT,CLAY,UPPB,LPPB,ANTIDN,RIPPLE,DUNES,OLDSE
                   1D,WATER,DOT,BLANK,FLOOD
0062                READ(5,2)IFCOD3,QVOLMX,SKEW
0063                READ(5,6)DM,DS,YM,YS,A1,A2,A,B,SA,SB
```

```
      READ(5,2)IFCOD5,C6,E2,STDVN,IFCOD1
C
C CALL RNDMIN
C
      CALL RNDMIN(IX)
C
C FIND CELL DIMENSIONS
C
      ZCEL=ZTOT/FLOAT(NCOLS)
      YCEL=YTOT/FLOAT(NROWS)
      IF(DWS.GT.YCEL)GO TO 988
C
C FIND BANKFULL STAGE RELATIVE TO BASE OF SECTION AND DISTANCE OF INNER
C BANK OF CHANNEL FROM LEFT HAND SIDE OF SECTION (IN CELLS)
C
      IBANK=BANK/ZCEL
      IWS=WS/YCEL
C
C FIND INITIAL AMPLITUDE
C
      AMP=WVL*NEWRAP(SN,0.0000001)
      IF(ZSECT.GT.(AMP/3.0))GO TO 994
C
C FIND LIMITING AMPLITUDE
C
      AMPLIM=WVL*NEWRAP(SNLIM,0.0000001)
C
C FIND INITIAL DISTANCE FROM LIMITING AMPLITUDE
C
      SS=(AMPLIM-AMP)/2.0
      IF(SS.LE.0.0)LIM=1
C
C INITIALISE AND STORE SECTION DATA ON DISK
C
      READ(5,5)(SEDIN(I),I=1,IWS)
      ID=1
      DO 150 J=1,NCOLS
      DO 146 I=1,NROWS
      IF(I.GT.IWS)GO TO 145
      TEMPGS(I)=SEDIN(I)
      TEMPST(I)=OLDSED
      GO TO 146
  145 TEMPGS(I)=BLANK
      TEMPST(I)=BLANK
  146 TEMPTL(I)=BLANK
  150 WRITE(IDISK'ID)(TEMPGS(I),TEMPST(I),TEMPTL(I),I=1,NROWS)
C
C INITIALISE SYNTHETIC HYDROLOGY PARAMETERS
C
C SKEWNESS PARAMETERS
C
      IF(SKEW.EQ.0.0)GO TO 162
      SKEW2=2.0/SKEW
      GO TO 163
  162 SKEW2=0.0
  163 SKEW6=SKEW/6.0
      SKEW62=SKEW6*SKEW6
C
C AUTOREGRESSIVE MODEL PARAMETERS
C
      ZTM1=RANSAM(IFCOD3)
      ZTM2=RANSAM(IFCOD3)
      COEFF=SQRT((1.0+A2)/(1.0-A2)*((1.0-A2)**2-A1**2))
C
C CALCULATE MEAN AND STANDARD DEVIATION OF FLOW FOR EACH DAY OF THE YEAR
C AND STORE IN ARRAYS
C
      DO 165 NDAY=1,365
      FSSUM(NDAY)=0.0
      FMSUM(NDAY)=0.0
      VAR=0.017211*FLOAT(NDAY)
      DO 164 K=1,6
      ARG=FLOAT(K)*VAR
      FMSUM(NDAY)=FMSUM(NDAY)+A(K)*COS(ARG)+B(K)*SIN(ARG)
  164 FSSUM(NDAY)=FSSUM(NDAY)+SA(K)*COS(ARG)+SB(K)*SIN(ARG)
  165 CONTINUE
C
C FIND FULL WIDTH OF FLOW BETWEEN INNER AND OUTER BANKS
```

```
            C
0106              WW=W/C5
            C
            C FIND VALUES OF W AND WW IN CELLS
            C
0107              NZCEL=WW/ZCEL
0108              NZCEL1=W/ZCEL
0109              FLT2=FLOAT(NZCEL1)
            C
            C FIND LIMITING WIDTH OF MEANDER NECK MEASURED FROM CHANNEL CENTRE LINES
            C
0110              GAPLIM=GAPLIM+WW
            C
            C FIND VALUE OF H IN CELLS
            C
0111              NH=H/YCEL
            C
            C PARAMETERS USED TO CALCULATE FROUDE NOS. IN MEANDR
            C
0112              F18=8.0/F1
0113              F28=8.0/F2
            C
            C PARAMETERS USED IN BAR
            C
0114              SIGRO=SIGMA-RO
0115              EXNM1=EXN-1.0
0116              VAR1=3.14*EXN/(200.0*W**EXN)
0117              VAR2=16.5*RO/SIGRO
            C
            C PARAMETERS FOR SCALING PLOT OF MEANDER GEOMETRY IN MEANDR
            C
0118              SCALE=AMPLIM/9.0
0119              SCALE2=SCALE/2.0
0120              XL=XMAX/AMPLIM*9.0
0121              TDMIG=0.0
            C
            C INITIALISE TIME KEEPING DEVICES AND NFLD
            C
0122              NFLD=0
0123              IPRINT=MOD(NFLD,NPRINT)
0124              ITPLOT=MOD(NFLD,NTPLOT)
            C
            C RATIO OF YCEL/ZCEL
            C
0125              YCOZC=YCEL/ZCEL
            C
            C WRITE SCALES AND TITLES ON GRAPH
            C
0126              CALL PLOT(1,0.0,XMAX,XL,XMAX,0.0,AMPLIM,9.0,AMPLIM)
0127              CALL PLOT(99)
0128              CALL PLOT(90,SCALE2,-SCALE2)
0129              WRITE(3,45)SCALE
0130              CALL CHAR(0.2,0)
0131              CALL PLOT(99)
0132              CALLPLOT(90,SCALE2,AMPLIM)
0133              WRITE(3,47)
0134              CALL CHAR(0.2,0)
0135              CALL PLOT(99)
            C
            C PRINT OUT CROSS SECTION PARAMETERS
            C
0136              WRITE(6,21)TITLE,ZTOT,NCOLS,YTOT,NROWS,BANK,IBANK,WS,IWS,YCEL,ZCEL
            C
            C PRINT OUT CHANNEL PARAMETERS
            C
0137              WRITE(6,23)WW,NZCEL,W,NZCEL1,C5,H,SIGMA,RO,F1,F2,EXN
            C
            C PRINT OUT SYNTHETIC HYDROLOGY PARAMETERS
            C
0138              WRITE(6,24)DM,DS,YM,YS,A1,A2,A,B,SA,SB,QVOLMX
            C
            C PRINT OUT BANK MIGRATION PARAMETERS
            C
0139              WRITE(6,25)E1,C1,C2,GRAVLM
            C
            C PRINT OUT SCOUR AND FILL PARAMETERS
            C
0140              WRITE(6,26)C6,E2,STDVN
```

```
      C
      C PRINT OUT CUT OFF CONTROL PARAMETERS
      C
            WRITE(6,28)GAPLIM,EN1,EN2,SNLIM,AMPLIM,EC1,EC2
      C
      C PRINT OUT TYPE OF SECTION
      C
            IF(IFCOD6.GT.0)GO TO 167
            WRITE(6,33)
            GO TO 168
        167 WRITE(6,31)ZSECT
      C
      C PRINT LEGEND
      C
        168 WRITE(6,27)LPPB,GRAVEL,OLDSED,RIPPLE,SAND,WATER,DUNES,SILT,DOT,DOT
           1,DOT,DOT,DOT,UPPB,CLAY,ANTIDN,FLOOD
      C
      C FIND AND PLOT INITIAL PLANIMETRIC FORM OF MEANDER
      C
            CALL MEANDR
      C
      C INITIAL OPERATIONS CONCERNING CROSS SECTION DEFINITION - THEN BRANCH
      C TO INITIALISE AND PRINT CHANNEL SECTION
      C
            IF(IFCOD6-1)170,172,174
        170 NZCELO=NZCEL
            ZCEL1=ZCEL
            IF(LIM.EQ.1)GO TO 971
            GO TO 218
        172 IF(LIM.NE.1)GO TO 175
            PAR1=3.14159*(AMP-2.0*ZSECT)/(SN*WVL)
            PHI=(0.0505*SN+PAR1+0.0692)/0.6371
            PAR2=((-0.0292*SN+0.2132)*SN-0.4651)*SN-PAR1+0.2668
        130 FA=((PHI*0.2804+(0.2244-0.1713*SN))*PHI+((0.1139*SN-0.552)*SN+0.88
           195))*PHI+PAR2
            FB=(PHI*0.8412+(0.4488-0.3426*SN))*PHI+(0.1139*SN-0.552)*SN+0.8895
            PHIN=PHI-FA/FB
            IF(ABS(PHIN-PHI)-0.0001)140,140,135
        135 PHI=PHIN
            GO TO 130
        140 SINPHI=SIN(PHIN)
            GO TO 176
      C
      C STRAIGHT LINE DISTANCE BETWEEN POINTS OF INFLECTION OF LOOP
      C
        174 NDAVA=WVL/(2.0*ZCEL)
        175 SINPHI=SIN(2.2*SQRT((SN-1.0)/SN))
        176 ZCEL1=SINPHI*ZCEL
            NZCEL=WW/ZCEL1
            NZCEL1=W/ZCEL1
            GO TO 216
      C
      C BEGIN MAJOR LOOP,ONCE THROUGH EVERY YEAR
      C
      C INITIALISE TIME KEEPING DEVICES
      C
        169 IPRINT=MOD(NFLD,NPRINT)
            ITPLOT=MOD(NFLD,NTPLOT)
      C
      C FIND FLOOD PERIOD VOLUME
      C
            QVOL=0.0
            DO 180 NDAY=1,365
            ZT=A1*ZTM1+A2*ZTM2+COEFF*RANSAM(IFCOD3)
            XT=DM+FMSUM(NDAY)+(DS+FSSUM(NDAY))*(YM+YS*ZT)
            IF(XT.GT.DM)QVOL=QVOL+XT
            ZTM2=ZTM1
        180 ZTM1=ZT
      C
      C TEST FOR CUT OFF
      C
            PC=(QVOL/QVOLMX)**EC1*(SN/SNLIM)**EC2
            PN=(QVOL/QVOLMX)**EN1*(GAPLIM/GAP)**EN2
            X=RNDM(-1)
            IF(X.LE.PC)ICUT=2
            X=RNDM(-1)
            IF(X.LE.PN)ICUT=3
            IF(ICUT.EQ.1)GO TO 182
```

```
C
C CUT-OFF HAS OCCURRED - OUTPUT REQUIRED INFORMATION AND TERMINATE PROG.
C
      WRITE(6,29)TITLE,NFLD,QVOL,OBGSI,BGSI,SCHUMM,SS,RLMIG,TLMIG,RDMIG,
     1TDMIG
      WRITE(6,30)AGG
      IPRINT=0
      NFPLOT=NFLD
      CALL MEANDR
      GO TO 548
C
C FIND AMOUNT OF LATERAL AND DOWNSTREAM BANK MIGRATION
C
  182 IF(LIM.EQ.1)GO TO 185
      RLMIG=SS*C1*QVOL/OBGSI**E1
      TLMIG=TLMIG+RLMIG
  185 RDMIG=C2*QVOL/OBGSI**E1
      TDMIG=TDMIG+RDMIG
C
C PRINT OUT REQUIRED DATA FOR THIS TIME INCREMENT
C
      IF(IPRINT.EQ.0)WRITE(6,29)TITLE,NFLD,QVOL,OBGSI,BGSI,SCHUMM,SS,RLM
     1IG,TLMIG,RDMIG,TDMIG
C
C AGGRADE THE FLOODPLAIN IF REQUIRED
C
      AGG=AGG+DWS
C
C WRITE TOTAL AMOUNT OF AGGRADATION SO FAR
C
      IF(IPRINT.EQ.0)WRITE(6,30)AGG
      NAGG=AGG/YCEL
      IF(NAGG.LT.MARK)GO TO 210
C
C IF ROW OF CELLS IS FILLED,ADJUST BANKFULL STAGE AND FILL ROW WITH
C ALPHAMERIC CHARACTERS
C
      IWS=IWS+1
      IF(IWS.GT.NROWS)GO TO 984
      MARK=MARK+1
      ID=1
      DO 200 J=1,NCOLS
      READ(IDISK'ID)(TEMPGS(I),TEMPST(I),TEMPTL(I),I=1,NROWS)
      ID=J
      TEMPGS(IWS)=FLOOD
      TEMPST(IWS)=FLOOD
  200 WRITE(IDISK'ID)(TEMPGS(I),TEMPST(I),TEMPTL(I),I=1,NROWS)
C
C RECORD ON 2-D ARRAYS THE RESULTING EROSION AND DEPOSITION AFTER THIS
C YEAR - STORE ARRAYS ON DISK
C
C FIND AMOUNT OF BANK MIGRATION IN CROSS SECTION REPRESENTED.ADJUST
C CHANNEL WIDTH(IN CELLS) REPRESENTED IN CROSS SECTION(AND RELATED
C PARAMETERS),DEPENDING ON TYPE OF CROSS SECTION AND CHANGES IN SHAPE
C OF MEANDER
C
  210 IF(IFCOD6.GT.0)GO TO 215
      RMIG=SQRT(RLMIG*RLMIG+RDMIG*RDMIG)
      AA=ATAN(RDMIG/RLMIG)
      TANA=RDMIG/RLMIG
      P=ATAN((R+WW/2.0-SQRT((R+WW/2.0)**2+2.0*R*WW*TANA*TANA))/(-2.0*R*T
     1ANA))
      ZCEL1=ZCEL*COS(AA-P)/COS(P)
      GO TO 216
  215 RMIG=RDMIG
      SINPHI=SIN(2.2*SQRT((SN-1.0)/SN))
      ZCEL1=ZCEL*SINPHI
  216 NZCELO=NZCEL
      NZCL1O=NZCEL1
      NZCEL=WW/ZCEL1
      NZCEL1=W/ZCEL1
      FLT2=FLOAT(NZCEL1)
      YZOZC=YCEL/ZCEL1
      IF(NZCEL1-NZCL1O)218,218,217
  217 NZDIF=NZCEL1-NZCL1O
      GO TO 225
  218 NZDIF=0
C
```

```
C ADD LAST YEAR'S SMOOTHING ERROR TO THIS YEAR'S BANK MIGRATION
C
  225 RMIG=RMIG+DEV
C
C FIND BANK MIGRATION(IN CELLS) IN CROSS SECTION,AND CALCULATE ERROR
C DUE TO SMOOTHING,DEV
C
      NRMIG=RMIG/ZCEL
      DEV=RMIG-ZCEL*FLOAT(NRMIG)
C
C DEFINE AMOUNT OF CONCOMITANT POINT BAR MIGRATION(IN CELLS),DEPENDING
C ON CHANGES IN CHANNEL WIDTH IN CROSS SECTION REPRESENTED
C
      IF(IFCOD6.EQ.0)GO TO 227
      NRMIG=NRMIG+NZCELO-NZCEL
      IF(NRMIG.LT.0)NRMIG=0
  227 FNRMIG=FLOAT(NRMIG)
C
C FIND TOTAL NUMBERS OF CELLS REQUIRED FOR CHANNEL SECTION AND CHECK
C THAT DOES NOT EXCEED SPECIFIED LIMITS
C
      NZCELT=NZCEL+NRMIG
      IF(NZCELT.GT.MNCOLS)GO TO 580
      IF((IBANK+NZCELT+NDAVA).GT.NCOLS)GO TO 585
C
C READ APPROPRIATE COLUMNS FROM DISK
C
      ID=IBANK+1
      DO 230 J=1,NZCELT
  230 READ(IDISK'ID,ERR=590)(SEDGS(I,J),SEDSTR(I,J),TLPLOT(I,J),I=1,NROW
     1S)
C
C IF NO SCOUR AND FILL GO TO 400
C
      IF(NFLD.EQ.0)GO TO 400
      IF(IFCOD5.NE.1)GO TO 400
C
C FIND MAXIMUM DEPTH OF SCOUR MEASURED ABOVE TALWEG
C
      DSCR=C6*QVOL**E2+RANSAM(IFCOD1)*STDVN
      IF(DSCR.LT.0.0)DSCR=0.0
      IF(IPRINT.EQ.0)WRITE(6,41)DSCR
      HH=H+DSCR
C
C IF MAX. CHANNEL DEPTH NOW EXCEEDS LOWER BOUNDARY OF SECTION - JOB ENDS
C
      IF(HH.GT.(FLOAT(IWS)*YCEL))GO TO 980
C
C FOR  EVERY COLUMN OF POINT BAR GRADUALLY FILL TO ORIGINAL DEPTH
C
  370 Z=ZCEL1
      DO 390 NCOL=1,NZCEL1
      IF(IFCOD7.EQ.0)GO TO 372
      CALL BAR1(O,HH)
      GO TO 373
  372 CALL BAR(O,HH)
  373 Z=Z+ZCEL1
  390 CONTINUE
      HH=HH-YCEL
      IF(HH.GE.H)GO TO 370
C
C FILL SCOURED TALWEG
C
      IF(NRMIG.LT.1)GO TO 400
      DO 380 J=1,NRMIG
      NCOL=NZCEL1+J
      Y=-DSCR/2.0*(COS(3.14*(FLOAT(NRMIG-J)/FNRMIG))-1.0)
      NYCEL=(H+Y)/YCEL
      INDEX=IWS-NYCEL
  381 SEDGS(INDEX,NCOL)=SEDGS(INDEX,NZCEL1)
      SEDSTR(INDEX,NCOL)=SEDSTR(INDEX,NZCEL1)
      Y=Y-YCEL
      INDEX=INDEX+1
      IF(Y.GE.0.0)GO TO 381
  380 CONTINUE
C
C FOR EVERY COLUMN IN CHANNEL SECTION,FIND GRAINSIZE AND BEDFORM ACROSS
C INNER BANK AND ERODE OUTER BANK
```

```
C
C INITIALISE PARAMETERS AND WRITE HEADINGS
C
  400 Z=ZCEL1
      OBGS=0.0
      BGS=0.0
      GRAV=0.0
      NRMIG1=NRMIG+NZDIF+1
      INDEXK=IWS
      KOUNT=0
      INDEXO=IWS-NH+1
      IF(IPRINT.EQ.0)WRITE(6,42)TITLE,NFLD
C
C BEGIN MAJOR LOOP ENTERED ONCE FOR EVERY COLUMN OF CHANNEL SECTION
C
      DO 450 J=1,NZCEL
      NCOL=J+NRMIG
      IF(J.LE.NZCEL1)GO TO 410
C
C ERODE OUTER BANK
C
      Y=-H/2.0*(COS(3.14*(WW-Z)/(WW-W))-1.0)
      NYCEL=Y/YCEL
      INDEX=IWS-NYCEL
      IF(ITPLOT.EQ.0)TLPLOT(INDEX,NCOL-1)=DOT
      INDEXK=INDEX
  405 IF(SEDGS(INDEX,NCOL).EQ.CLAY.OR.SEDGS(INDEX,NCOL).EQ.SILT.OR.SEDGS
     1(INDEX,NCOL).EQ.FLOOD)OBGS=OBGS+1.0
      IF(SEDGS(INDEX,NCOL).EQ.GRAVEL)GRAV=GRAV+1.0
      KOUNT=KOUNT+1
      INDEX=INDEX-1
      IF(INDEX.GT.INDEXO)GO TO 405
      INDEXO=INDEXK
      GO TO 440
C
C DEPOSIT SEDIMENT ON INNER BANK
C
  410 IF(IFCOD7.EQ.0)GO TO 411
      CALL BAR1(1,H)
      GO TO 412
  411 CALL BAR(1,H)
  412 IF(D.LE.0.00625)BGS=BGS+1.0
      IF(ITPLOT.EQ.0.AND.J.NE.NZCEL1)TLPLOT(INDEX,NCOL)=DOT
      IF(NFLD.EQ.0)GO TO 440
C
C 'FILL' POINT BAR
C
      IF(NRMIG1.LT.1)GO TO 440
      DO 415 JJJ=1,NRMIG1
      JJ=NCOL-JJJ
      IF(JJ.LT.1)GO TO 415
      IF(NZCEL1.LT.NZCL10.AND.IFCOD5.EQ.1)GO TO 413
      IF(SEDSTR(INDEX,JJ).NE.WATER.AND.SEDSTR(INDEX,JJ).NE.FLOOD.AND.SED
     1STR(INDEX,JJ).NE.OLDSED)GO TO 415
  413 SEDGS(INDEX,JJ)=SEDGS(INDEX,JJ+1)
      SEDSTR(INDEX,JJ)=SEDSTR(INDEX,JJ+1)
  415 CONTINUE
C
C FILL IN 'EMPTY' ROWS
C
  420 IF((INDEXK-INDEX).LT.2)GO TO 424
      INDEXK=INDEXK-1
      DO 422 JJ=1,NRMIG1
      NCOLK=NCOL-JJ
      IF(NCOLK.LT.1)GO TO 422
      IF(NZCEL1.LT.NZCL10.AND.IFCOD5.EQ.1)GO TO 421
      IF(SEDSTR(INDEXK,NCOLK).NE.WATER.AND.SEDSTR(INDEXK,NCOLK).NE.OLDSE
     1D)GO TO 422
  421 SEDGS(INDEXK,NCOLK)=SEDGS(INDEX,NCOLK)
      SEDSTR(INDEXK,NCOLK)=SEDSTR(INDEX,NCOLK)
  422 CONTINUE
      GO TO 420
  424 INDEXK=INDEX
C
C FILL NEW CHANNEL WITH WATER
C
  440 INDEX=IWS-NYCEL+1
      IF(NYCEL.EQ.0)GO TO 450
```

```
      DO 445 II=INDEX,IWS
      SEDSTR(II,NCOL)=WATER
  445 SEDGS(II,NCOL)=WATER
  450 Z=Z+ZCEL1
C
C CALCULATE PERCENT SILT-CLAY IN PERIMETER OF CHANNEL
C
      FLTK=FLOAT(KOUNT)
      SCHUMM=100.0*(BGS+OBGS*YCOZC)/(FLT2+YCOZC*FLTK)
C
C CALCULATE GRAIN SIZE INDICES FOR INNER AND OUTER BANKS
C
      BGSI=BGS/FLT2*100.0
      OBGSI=OBGS/FLTK*100.0
      IF(OBGSI.EQ.0.0)OBGSI=1.0
      GRAVI=GRAV/FLTK*100.0
      IF(GRAVI.GT.GRAVLM)GO TO 460
C
C FILL 2-D ARRAYS FOR THE SECOND CHANNEL IF A TWO CHANNEL DOWNVALLEY
C SECTION IS BEING USED - STORE ON DISK
C
      ID=IBANK+1
      DO 540 J=1,NZCELT
  540 WRITE(IDISK'ID)(SEDGS(I,J),SEDSTR(I,J),TLPLOT(I,J),I=1,NROWS)
      IF(IFCOD6.NE.2)GO TO 548
      ID=IBANK+NDAVA+1
      DO 545 J=1,NZCELT
  545 WRITE(IDISK'ID)(SEDGS(I,J),SEDSTR(I,J),TLPLOT(I,J),I=1,NROWS)
  548 IF(IPRINT.NE.0)GO TO 570
C
C PRINT OUT CROSS SECTION SHOWING GRAIN SIZE DISTRIBUTION
C
      ID=1
      WRITE(6,35)TITLE,NFLD
      DO 550 J=1,NCOLS
      READ(IDISK'ID,ERR=590)(TEMPGS(I),TEMPST(I),TEMPTL(I),I=1,NROWS)
  550 WRITE(6,FMT4)(TEMPGS(I),I=1,NROWS),(TEMPTL(I),I=1,NROWS)
C
C PRINT OUT CROSS SECTION SHOWING SEDIMENTARY STRUCTURE DISTRIBUTION
C
      ID=1
      WRITE(6,36)TITLE,NFLD
      DO 560 J=1,NCOLS
      READ(IDISK'ID,ERR=590)(TEMPGS(I),TEMPST(I),TEMPTL(I),I=1,NROWS)
  560 WRITE(6,FMT4)(TEMPST(I),I=1,NROWS),(TEMPTL(I),I=1,NROWS)
      GO TO (570,990,992),ICUT
  570 IBANK=IBANK+NRMIG
C
C FIND PLANIMETRIC FORM OF MEANDER AT END OF THIS YEAR
C
      IF(NFLD.EQ.0)GO TO 575
      IF((TDMIG+WVL).GT.XMAX)GO TO 986
C
C FIND CHANGES IN AMPLITUDE
C
      IF(LIM.EQ.1)GO TO 572
      AMP=AMP+RLMIG*2.0
      SS=(AMPLIM-AMP)/2.0
      IF(SS.GT.0.0)GO TO 573
      LIM=1
      AMP=AMPLIM
      RLMIG=0.0
      SS=0.0
      CALL MEANDR
      IF(IFCOD6.LE.0)GO TO 971
      WRITE(6,49)NFLD
      GO TO 575
  572 IF(RDMIG.LE.0.0)GO TO 575
      CALL MEAND1
      GO TO 575
  573 CALL MEANDR
      IF(GAP.LE.WW)GO TO 992
  575 NFLD=NFLD+1
      IF(NFLD.LE.NTIM)GO TO 169
C
C ERROR MESSAGES
C
      GO TO 999
```

```
  460 WRITE(6,43)GRAVI
      GO TO 999
  580 WRITE(6,37)
      GO TO 999
  585 WRITE(6,39)
      GO TO 999
  590 WRITE(6,38)
      GO TO 999
  971 WRITE(6,972)NFLD
      GO TO 999
  976 WRITE(6,977)
      GO TO 1000
  978 WRITE(6,979)
      GO TO 1000
  980 WRITE(6,981)
      GO TO 1000
  982 WRITE(6,983)
      GO TO 1000
  984 WRITE(6,985)
      GO TO 999
  986 WRITE(6,987)
      GO TO 999
  988 WRITE(6,989)
      GO TO 1000
  990 WRITE(6,991)NFLD
      GO TO 999
  994 WRITE(6,995)
      GO TO 1000
  992 WRITE(6,993)NFLD
  999 CALL PLOT(7)
 1000 STUP
      END
```

36. If IPRINT=0 the contents of the disc data set corresponding to the cross sections are read and printed out as sections showing grain size and sedimentary structure distribution.

14.3 Subroutine BAR (with entry point BAR1)

This subroutine calculates the grain size and bed form present at a particular station on the point bar using the somewhat modified version of Allen's (1970a,b) model.

1. Calculates the argument, ARG, required in the SIN and COS functions of the next two operations.
2. Calculates depth of water, Y, at a station (column NCOL), using equation (5.1).
3. Calculates local transverse slope of point bar, DYDZ, using equation (5.18).

If a user specified transverse profile is required, the above operations are skipped by using entry point BAR1. Arithmetic assignment FORTRAN statements defining Y and DYDZ must be added immediately below the ENTRY BAR1 statement (see listing). The value of DYDZ must be scaled such that the units of D are cm. In this respect it should be noted that units of length are everywhere metres, except where otherwise specified, and VAR2S is dimensionless.

4. Finds row, INDEX, in the two-dimensional arrays corresponding to calculated depth.
5. Finds local radius of curvature, RL.
6. Calculates grain size, D, at the station, using equation (5.20). Units are in cm.
7. Allocate grain size to Wentworth scale division, clay, silt, sand or gravel, and fill appropriate element of SEDGS (INDEX, NCOL) with corresponding alphameric character. Changing the program to accommodate further subdivision of grain size classes would be a simple task if required.

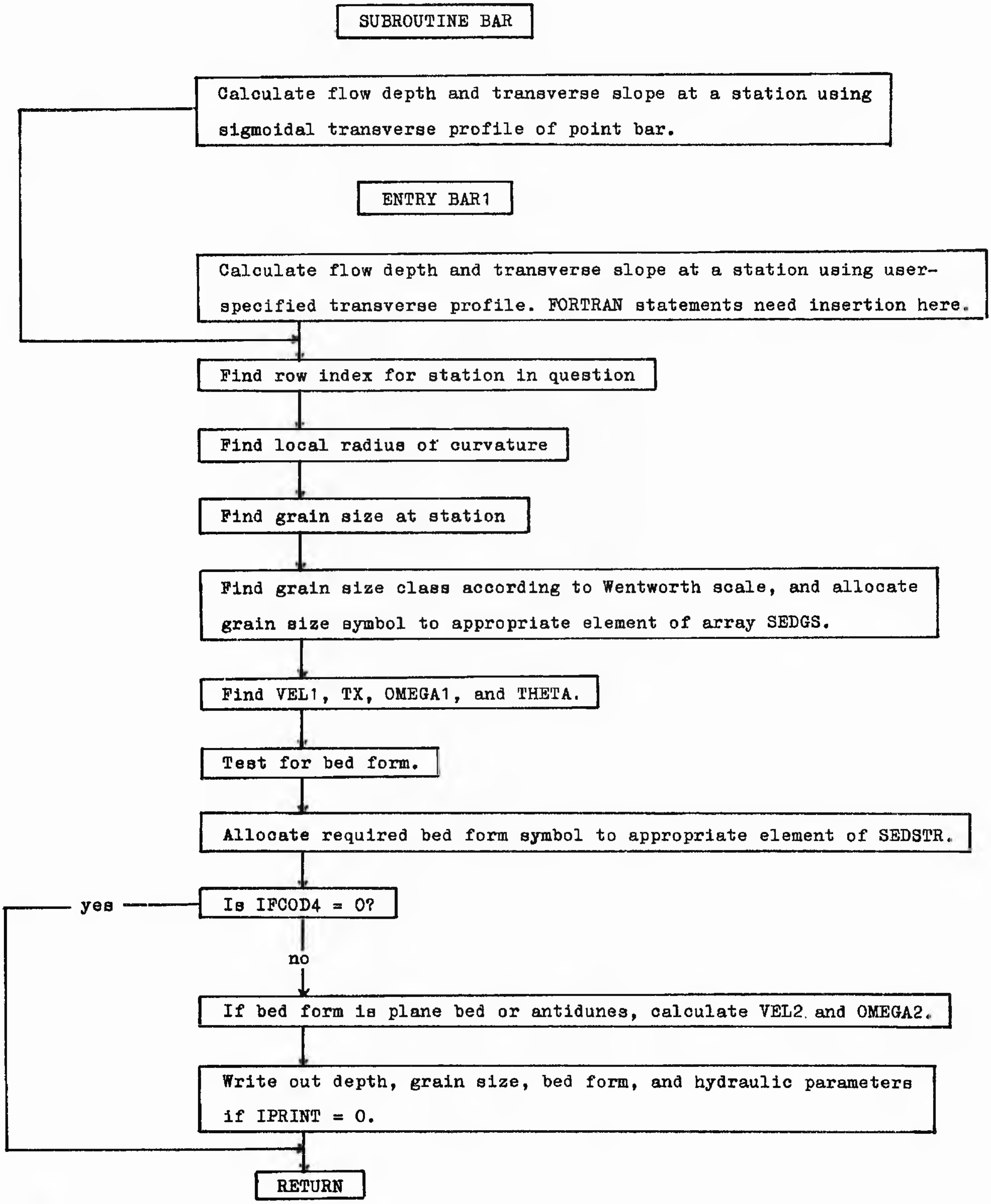

Fig. 14.4. Flow diagram for subroutine BAR.

8. Calculates local depth of water expressed in cm., YCM.
9. Calculates product of YCM and acceleration due to gravity, G, where the units of G are cm./sec/sec.
10. Calculates local mean flow velocity, VEL1, using equation and using the friction coefficient for dunes and ripples, F1 Units are cm/sec.
11. Calculates local bed shear stress parallel to the channel centre line, TX. Units are dynes/sq.cm.
12. Calculates local stream power, OMEGA1, as the product of TX and VEL1. Units are ergs/sq.cm./sec.
13. Calculates local dimensionless shear stress, THETA, using equation (5.23).
14. Tests to see if bed form is antidunes, upper phase plane bed, dunes, ripples, or lower phase plane beds by applying a series of inequalities, as in Allen's (1970a) model. The appropriate element of SEDSTR (INDEX, NCOL) is filled with an alphameric character corresponding to the bed form chosen.
15. If IPRINT=0 writes out grain size, bed form and other hydraulic variables, calculating VEL2 and OMEGA2 where necessary. VEL2 and OMEGA2 are the local mean flow velocity and stream power respectively, calculated using the friction coefficient for plane beds and antidunes, F2. If IFCOD4=0 step 15 is skipped, as BAR is being called during a scour and fill operation.

A simplified flow diagram for subroutine BAR is given in fig. 14.4.

14.4 Subroutine MEANDR (with entry point MEAND1)

This subroutine calculates the planimetric geometry of the meander for every time increment and plots a trace of the channel centre line whenever required. If entry point MEAND1 is used, the planimetric geometry is not calculated.

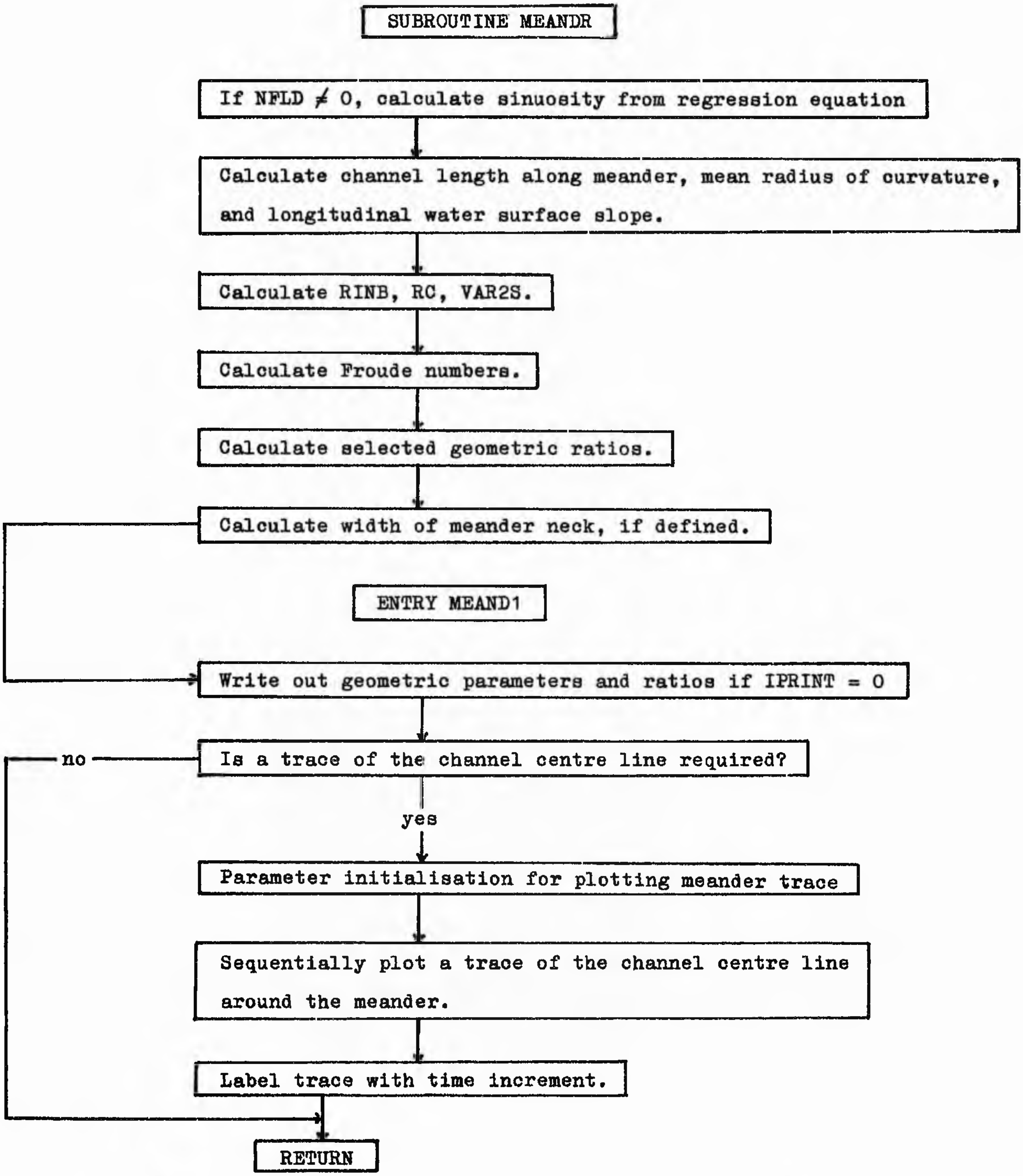

Fig. 14.5. Flow diagram for subroutine MEANDR.

1. Sinuosity, SN, is calculated, given amplitude, AMP, and wavelength, WVL, using the regression equation (2.12). If NFLD=0 this step is omitted as SN is read initially as input data.
2. Channel length along the meander centre line, CHL, is calculated as the product of WVL and SN.
3. Longitudinal water surface slope, CHS, is calculated as valley slope, VS, divided by SN.
4. Radius of curvature of the channel centre line at the bend axis, R, is calculated from equation (2.5).
5. Radius of curvature of the inner bank at the bend axis, RINB, is calculated for use in subroutine BAR.
6. Calculates product of fluid density, RO, and CHS for use in subroutine BAR. Units in gm./cu.cm.
7. Calculates product, VAR2S, of VAR2 and CHS for use in BAR. Dimensionless variables.
8. Calculates Froude numbers, FROUD1 and FROUD2 (calculated using friction coefficients F1 and F2, respectively), for use in BAR.
9. Calculates selected geometric ratios.
10. Calculates the maximum angle (radians) that the path of the channel centre line makes with the mean downvalley direction, OMEGA, using equation (2.4). If OMEGA is less than $\pi/2$, the width of the meander neck, GAP, is set to a very large number as an indication of being undefined, and the next step is omitted.
11. Calculates width of meander neck measured to channel centre lines, GAP, after solving the necessary integral by calling subroutine SIMINT (and FUNC2).

The preceding operations are skipped, by using entry point MEAND1, if amplitude growth of the meander has ceased, the variables above remaining unchanged. The following operation is skipped if no printed output is required.

12. If IPRINT=0 write out planimetric geometry parameters and selected geometric ratios.

The following operations are skipped if no trace of the channel centre line is to be plotted.

13. Divides CHL into 100 incremental lengths and, by calculating the deviation angle, PHI, from the downvalley direction (using equation (2.3)) for each incremental length, sequentially plots the meander trace. The sines and cosines of the deviation angles for the first half of the bend (50 of each) are stored in COSPHI (50) and SINPHI (50) and then used for plotting the second half. Subroutine PLOT is used during this step.

14. Labels the trace with the appropriate time increment. Subroutines PLOT and CHAR are called here.

All units of length are metres unless otherwise specified. A flow diagram of subroutine MEANDR is shown in fig. 14.5.

14.5 Subroutine SIMINT (and FUNC2)

This subroutine is called by MEANDR and evaluates integrals numerically using Simpson's rule. The interval is successively halved until estimates of the integral do not differ by more than the specified limit, E. This is set to 0.005. The function to be integrated, given in equation (2.11) is specified in a FUNCTION subroutine FUNC2, which is called by SIMINT. See appendix 1 for description of Simpson's rule.

14.6 Subroutine RANSAM

This FUNCTION subroutine returns random samples from specified frequency distributions. It is called by the main program, and is used when finding the flood period volume, also in the scour and fill relation, equation (9.4). A flow diagram is shown in fig. 14.6.

1. If IFCOD3 equals 3,4 or 5, twelve pseudorandom numbers are

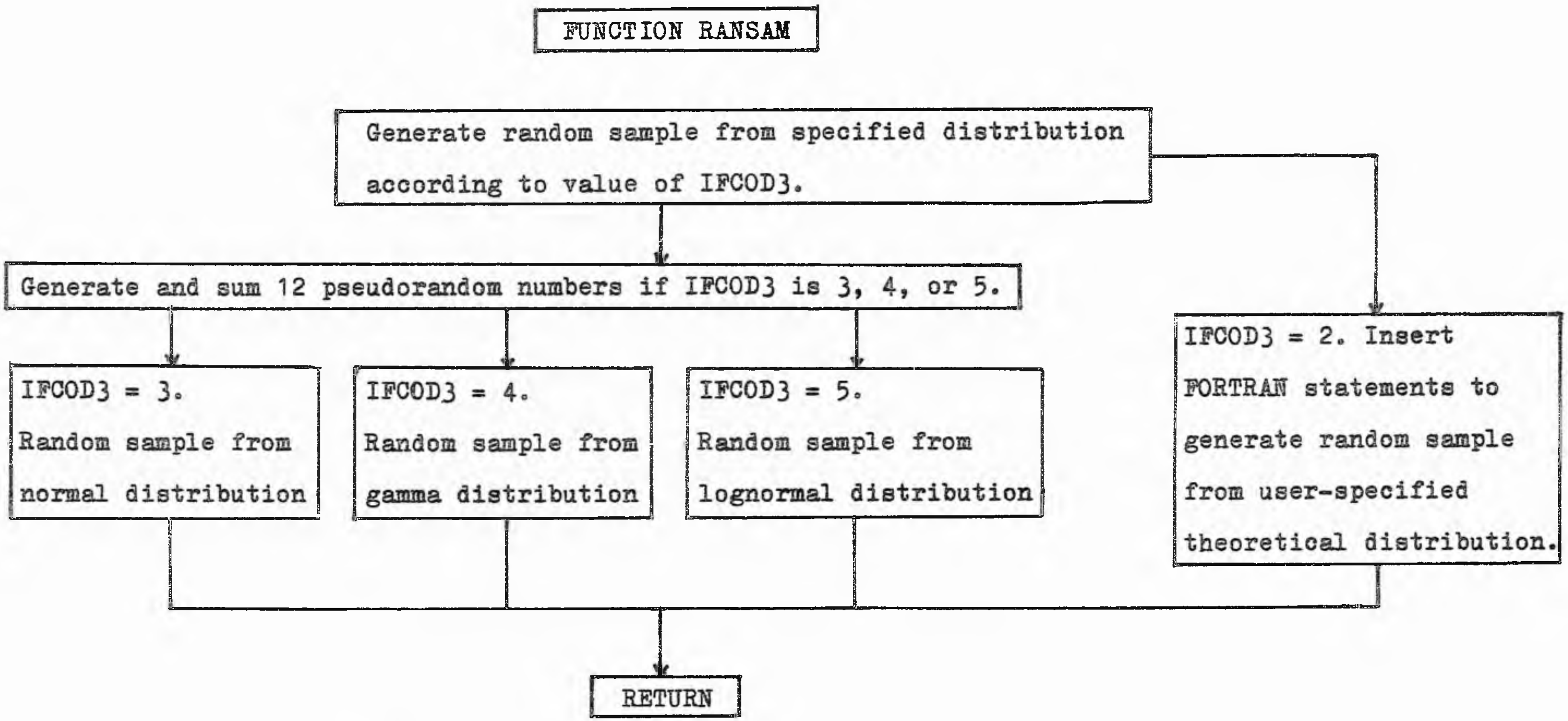

Fig. 14.6. Flow diagram for subroutine RANSAM.

generated, using subroutine RNDM, and summed.

2. This sum is then converted to a normally distributed random variable, using equation (A1.2). If IFCOD3=3 this variable is returned, but may be further converted to a gamma distributed (see equation (A1.7)) or a lognormally distributed (see equation (A1.6)) random variable, if IFCOD3 equals 4 or 5, respectively. These random samples are distributed with zero mean and standard deviation unity.

If a random sample from a user specified distribution is required, FORTRAN statements must be added immediately after the appropriate comment card (see listing). This is before step 1. Additional data will be required if more than the first three moments or any other parameters are required to describe the distribution.

14.7 Subroutine NEWRAP

This REAL FUNCTION subroutine is called by the main program during initialisation, and evaluates a root of the polynomial, given in equation (2.12), by the Newton-Raphson iteration procedure (see appendix 1). It is required to find a particular value of AMP/WVL, which satisfies the equation. Whence AMP is found given the initial value of SN and WVL as input.

The initial estimate of the root required is given by the linear approximation of the third degree polynomial, given in appendix 2. The estimate is sufficiently close to the required root, compared with other roots, to avoid any complications in the iteration procedure. The iteration continues until successive estimates differ by less than or equal to the specified amount, E. This is set to 0.0000001. Only a few iterations are required as the convergence is fairly rapid.

14.8 Subroutines RNDMIN and RNDM

These subroutines are involved in the generation of pseudorandom numbers (i.e. practically uniformly distributed random numbers). The purpose of RNDMIN is to read a starting variable, IX, an integer preferably 9 or less digits, on which the random floating point number generation will be based. RNDM does the actual random floating point number generation using the number declared above. It uses the same generating sequence as RANDU, in the IBM Scientific Subroutine Package (1971, p.77), to produce numbers between 0.0 and 1.0. RNDMIN and RNDM are automatically available on the IBM 360/44 system libraries.

14.9 Subroutines PLOT and CHAR

These are subroutines used for controlling the CIL graph plotter. PLOT is used for drawing and scaling of graph axes, and the actual plotting of the graph. CHAR is used for annotation. PLOT and CHAR are specific to the installation, and are automatically available in the system libraries of St. Andrews University Computing Laboratory. Different installations will be expected to use different graph plotter routines.

15 INPUT REQUIREMENTS AND PROGRAM MODIFICATION INSTRUCTIONS

FORTRAN 'FORMAT' codes are given for each variable to be read. With the I code all numbers must be right justified in the specified fields. With the F code, numbers can be anywhere in the specified field as long as a decimal point is present. In this program F codes have been used such that a decimal point is always required unless no places of decimals are needed, in which case the numbers must be right justified. Input requirements are given first for the program which uses no disc, and subsequently, those data cards which are different when using a disc are described.

1. Title Card

Column		
1-60	TITLE	Alphameric title (15A4). Can be placed anywhere in this 60 column field.
61-70	IX	Starting number for pseudorandom number generator, preferably large. (I10).

2. Time and output control card

Column		
1-4	NTIM	Number of time increments (I4).
6-8	NPRINT	Line printer output is printed every NPRINT-th time increment (I4).
9-12	NFPLOT	Graph plotter output is every NFPLOT-th time increment (I4).
13-16	NTPLOT	A time line is plotted on the cross sections every NTPLOT-th time increment (I4).

The last three variables must not be set to zero.

3. <u>Cross section control card</u> (see fig. 14.1)

Column

1-4	NCOLS	Number of columns in a cross section (I4). If this if greater than 200 the dimensional information given in the INTEGER*2 and the labelled COMMON/COM2 statements must be changed.
5-8	NROWS	Number of rows (I4). If this is greater than 60 the dimensional information given in the INTEGER*2 the labelled COMMON/COM2 statements must be changed.

The maximum possible sizes of NCOLS and NROWS will depend on the addressable storage (core store) available at a particular installation. If a reduction in the amount of core store used in the listed program is required, the same adjustments as outlined above apply. The physical size of the line printer will also limit NROWS (i.e. 132 in IBM 1403).

9-12	IFCOD6	Condition code to determine type of cross section represented (I4). That is, 0 - Lateral section 1 - One-channel downvalley section 2 - Two-channel downvalley section.
13-20	ZTOT	Width of section, in metres (F8.0)
21-38	YTOT	Thickness of section, in metres (F8.0).
29-36	BANK	Initial distance of inner channel bank from left hand side of section, in metres (F8.0).
37-44	WS	Initial bankfull stage measured from section base, in metres (F8.0). Must not exceed YTOT.
45-52	DWS	Rate of aggradation, in metres per year (F8.0). Value must not be greater than the cell depth, given by YTOT/NROWS.
53-60	ZSECT	Normal distance of line of section from line joining points of inflection of loop (F8.0). Applies only to one-channel downvalley section, therefore if

		IFCOD6≠1, leave blank. Must not exceed AMP/3.0.
61-80	FMT4	Object time FORMAT code used for printing out cross sections (5A4). Must be of the form (1X,nA1) where n equals NROWS

4. <u>Meander Geometry card</u>

Column		
1-12	SN	Initial sinuosity (F12.0). Must not exceed limiting sinuosity, SNLIM, which is read from card 6.
13-24	WVL	Meander wavelength, in metres (F12.0).
25-36	VS	Valley slope (F12.0).
37-48	XMAX	Maximum length in the X (downvalley) direction required for plotting the plan form of the meander as it migrates downvalley, in metres (F12.0). XMAX must not be less than WVL+total amount of downvalley migration.

5. <u>Bank migration card</u>

Column		
1-12	C1	Constant k_2 in bank migration relation, equation (6.3). (F12.0).
13-24	C2	Constant k_3 in bank migration relation, equation (6.4). (F12.0).
25-36	E1	Exponent n_2 in bank migration relations above. (F12.0).
37-48	GRAVLM	Limiting percentage of gravel (grain diameter 2mm.+) allowable in outer bank (F12.0). Measured as amount of areal exposure.

6. <u>Cut-off control card</u>

Column		
1-12	EC1	Exponent ec_1 in chute cut-off relation, equation (10.1) (F12.0).
13-24	EC2	Exponent ec_2 in chute cut-off relation (F12.0).

25-36	EN1	Exponent en_1 in neck cut-off relation, equation (10.2) (F12.0).
37-48	EN2	Exponent en_2 in neck cut-off relation (F12.0).
49-60	GAPLIM	Limiting width of meander neck, in metres, measured as the shortest distance between the adjacent banks of each meander limb (F12.0).
61-72	SNLIM	Limiting sinuosity (F12.0).

7. <u>Channel parameter card</u>

Column		
1-8	W	Width of flow between inner bank and talweg, w_1, in metres (F8.0).
9-16	H	Maximum unscoured depth of flow measured above talweg, h, in metres (F8.0). Must be less than or equal to WS, as specified in card 3.
17-24	EXN	Exponent n_1 in transverse profile equation (5.1) (F8.0).
25-32	C5	Ratio of w_1 to full width, w (constant k_1 in equation (5.2)) (F8.0).
33-40	F1	Darcy-Weisbach friction coefficient for dunes and ripples, f_1 (F8.0).
41-48	F2	Darcy-Weisbach friction coefficient for plane beds and antidunes, f_2(F8.0).
49-56	SIGMA	Density of sedimentary particles, in gm/cu.cm. (F8.0).
57-64	RO	Fluid density, in gm/cu.cm. (F8.0).
65-70	IFCOD7	Condition code to determine type of transverse profile of point bar (I4). That is, 0 - sigmoidal profile as given by equation (5.1). 1 - user specified profile. Extra parameters may be required to describe this.

8. Symbols card

Column

1 GRAVEL Alphameric character used in line printer output to represent gravel (A1).

2 SAND Character for sand (A1).

3 SILT Character for silt (A1).

4 CLAY Character for clay (A1).

5 UPPB Character for upper phase plane bed (A1).

6 LPPB Character for lower phase plane bed (A1).

7 ANTIDN Character for antidunes (A1).

8 RIPPLE Character for ripples (A1).

9 DUNES Character for dunes (A1).

10 OLDSED Character for old sediment (A1).

11 WATER Character for water (A1).

12 DOT Character used for plotting time lines (A1). Should ideally be a full stop.

13 BLANK Blank space.

14 FLOOD Character used for overbank sediments, produced with aggradation (A1).

9. Synthetic hydrology cards - any units allowable as long as they are consistent

Card 9a

Column

1 IFCOD3 Condition code used to determine the frequency distribution of the independent residual series, as given in equation (11.7) (I1). That is,

2 - User specified theoretical

3 - Normal

4 - Gamma

5 - Lognormal

2-13 QVOLMX A maximum value of Q_{vol}, to be used in the cut-off tests (F12.0).

14-25	SKEW	Skewness of gamma distribution (or user specified distribution) if condition code in column 1 is appropriate. Otherwise leave blank (F12.0).

<u>Card 9b</u>

Column

1-12	DM	Mean of all daily flow values (F12.0).
13-24	DS	Standard deviation of all daily flow values (F12.0).
25-36	YM	Mean of Y_t series (F12.0).
37-48	YS	Standard deviation of Y_t series (F12.0).
49-60	A1	Coefficient a_1 in autoregressive model (F12.0).
61-72	A2	Coefficient a_2 in autoregressive model (F12.0).

<u>Card 9c</u>

Column

1-72	A(6)	Array of Fourier coefficients, A_k, for the cosine terms of the harmonic representation of the daily means. Six coefficients corresponding to the first through to the sixth harmonic (k=1,6), each having (F12.0).

<u>Card 9d</u>

Column

1-72	B(6)	Array of Fourier coefficients, B_k, for the sine terms of the harmonic representation of the daily means. Six coefficients corresponding to the first through to the sixth harmonic (6F12.0).

<u>Card 9e</u>

Column

1-72	SA(6)	Array of Fourier coefficients ${}_sA_k$ for the cosine terms of the harmonic representation of the daily standard deviations. Six coefficients corresponding to the first through to the sixth harmonic (6F12.0).

<u>Card 9f</u>

Column

1-72	SB(6)	Array of Fourier coefficients, ${}_sB_k$, for the sine terms of the harmonic representation of the daily standard deviations. Six coefficients corresponding to the first through to the sixth harmonic (6F12.0).

10. Scour and fill card

Column		
1	IFCOD5	Condition code to determine whether scour and fill process is required. If 1, the process is required. If 0, the process is not required and the whole card may be left blank.
2-13	C6	Constant k_4 in scour and fill relation, equation (9.4) (F12.0).
14-25	E2	Exponent n_3 in scour sand fill relation (F12.0).
26-37	STDVN	Standard deviation of error term in scour and fill relation (F12.0).
38	IFCOD1	Condition code to determine frequency distribution of error term in scour and fill relation (I1). The codes available are as for IFCOD3 on card 9a.

11. Flood plain sediments card(s)

Column		
1-IWS	SEDIN(60)	Array containing alphameric characters to specify the initial grain size distribution in the cross section. One symbol for each row according to the symbols read from card 8, each in (A1) format. There will be IWS symbols, where IWS is the integer part of WS x NROWS/YTOT. The symbol in column 1 is allocated to the base of the section, and then successively up the section until the last character is read into row IWS. If IWS is greater than 60 the dimensional information given in the INTEGER*2 statement must be changed. If IWS is greater than 80 the data must be continued onto another card using the same format.

If a disc is being used a slightly different data input is required. The title card (1) and the cross section control card (3) must be replaced, the latter with two cards (3a and 3b). These replacement cards are as follows:

1. Title card

Column		
1-60	TITLE	Alphameric title (15A4). Can be placed anywhere in this 60 column field.
61-70	IX	Starting number for pseudorandom number generator, preferably large (I10).
71-72	IDISK	Data set reference number for disc data set (I2). The number will depend on the programming system, and whether a system or private disc is being used. If not equal to 4, the DEFINE FILE statement in the main program must be changed.

3. Cross section control cards

Card 3a

Column		
1-4	NCOLS	Number of columns (I4). If this is greater than 200 the number of records in the DEFINE FILE statement in the main program must be changed. NCOLS records must be stored on the disc data set.
5-8	NROWS	Number of rows (I4). If this is greater than 60 the dimensional information given in the INTEGER*2 and the labelled COMMON/COM2 statements must be changed. This will also entail changing the record size in the DEFINE FILE statement. The size of one record is NROWS x 6 bytes.
9-12	MNCOLS	Maximum number of columns that can be held in the core store at any one time (I4). If more than 50 dimensional information given in the INTEGER*2 and the labelled COMMON/COM2 statement must be changed.

The actual maximum number of columns required in the program will depend on the cell width, given by ZTOT/NCOLS, the channel width and the maximum rate of bank migration in the cross section represented (see fig. 14.1).

The maximum possible sizes of NROWS and MNCOLS will depend on the addressable (core) storage at a particular installation. If a reduction in the amount of core store in the listed program is required, the same adjustments as outlined above apply. NROWS will also be limited by the physical size of the line printer.

13-15	IFCOD6	Condition code to determine type of cross section represented (I4). That is, 0 - Lateral section 1 - One channel downvalley section 2 - Two channel downvalley section.
17-37	FMT4	Object time FORMAT code used for printing out cross sections (5A4). Must be of the form (1X, nA1) where n equals NROWS.

<u>Card 3b</u>

Column

1-12	ZTOT	Width of section, in metres (F12.0).
13-24	YTOT	Thickness of section, in metres (F12.0).
25-36	BANK	Initial distance of inner channel bank from left hand side of section, in metres (F12.0).
37-48	WS	Initial bankfull stage measured from section base, in metres, (F12.0). Must not exceed YTOT.
49-60	DWS	Rate of aggradation, in metres per year (F12.0). Value must not be greater than the cell depth given by YTOT/NROWS.
61-72	ZSECT	Normal distance of line of section from line joining points of inflection of loop (F12.0).

Applies only to one-channel downvalley section, therefore if IFCOD6$\neq$1, leave blank. Must not exceed AMP/3.0.

16. SAMPLE RUN

Table 16.1 contains the data input for an illustrative sample run of the program. Output is the same with or without the use of a disc. Tables 16.2 to 16.5 and figs. 16.1 to 16.3 illustrate the output from this run as follows.

Table 16.2 shows data which is output once for each separate run of the program, and this precedes all subsequent output for the run. The information given is partly that supplied as input and partly computed during initialisation. The notation used is as used in the development of the mathematical model, part 2. The cross section parameters listed are shown in fig. 14.1, and some of the channel parameters listed are shown in fig. 5.2. As already stated the synthetic hydrology parameters require no units to be specified. The data used in this case are taken from the data of Quimpo (1967) for the Oconto River as listed in table 11.1, and the maximum value of Q_{vol} was inferred from inspection of 500 years of simulated streamflows. With respect to the bank migration parameters, the word 'lateral' here refers to bank migration in the direction normal to the mean downvalley direction. This word is normally reserved for erosion or deposition 'lateral' to the local mean current direction. Limiting width of the meander neck specified here is the distance measured between channel centre lines, and therefore not as originally input. The legend refers to symbols used in the cross sections. It should be noted here that any number of symbols could be used (within the limitations of the line printer) and an increase in the number of the qualities (i.e. grain sizes, bed forms, etc.) used in the program would entail simple and straightforward modifications. The symbols used, however, are considered sufficient for present purposes.

```
FLUVIATILE PROCESS SIMULATICN  EXPERIMENT 2                         81241913
1CC   20   2C   20
35C   60    2  175C.0    60.0     0.0     30.0      C.1          (1X,6CA1)
          2.C       1CC0.0      0.0001      2C00.0
   0.COCCO1      0.CC01          0.5         3C.0
       1CO.C        1CC.0        10.0        10.0           0.0            2.C
  1CO.0     20.0      1.C      0.8     0.21     0.15     2.65      1.C


GCS-ULARDXI. F
4     13CCCO.0          1.0
543.5         441.0                     1.0            0.56671       0.3056C
-2CC.3        145.4         -85.5       58.0           -39.8         7.4
-112.4        185.C         -79.9       65.6           -72.5         27.8
-123.3        141.6         -66.4       75.7           -47.2         8.6
-85.6         105.7         -46.2       31.7           -43.2         4.3

OCCCCCCCCCCCCCCCCCCCCCCCCCCCCCSS
```

Table 16.1. Data input for sample run.

```
FLUVIATILE PROCESS SIMULATION  EXPERIMENT 2

CROSS SECTION PARAMETERS                                                        METRES      CELLS

      WIDTH OF SECTION                                                         1750.000      350
      THICKNESS OF SECTION                                                       60.000       60
      INITIAL DISTANCE OF INNER CHANNEL BANK FROM L.H.S. OF SECTION               0.0          0
      INITIAL BANKFULL STAGE MEASURED FROM SECTION BASE                          30.000       30
      CELL SIZE IN VERTICAL(Y) DIRECTION                                          1.000
      CELL SIZE IN HORIZONTAL(Z OR X) DIRECTION                                   5.000


CHANNEL PARAMETERS                                                              METRES      CELLS

      TOTAL WIDTH OF CHANNEL(W)                                                 125.000       25
      WIDTH OF FLOW BETWEEN INNER BANK AND TALWEG(W1)                           100.000       20
      RATIO OF W1 TO W                                                                                 0.800
      MAXIMUM FLOW DEPTH MEASURED ABOVE TALWEG                                   20.000
      DENSITY OF SEDIMENTARY PARTICLES                                                                 2.650 GM/CM3
      FLUID DENSITY                                                                                    1.000 GM/CM3
      DARCY-WEISBACH FRICTION COEFFICIENT FOR DUNES AND RIPPLES                                        0.210
      DARCY-WEISBACH FRICTION COEFFICIENT FOR PLANE BEDS AND ANTIDUNES                                 0.150
      EXPONENT N1                                                                                      1.000


SYNTHETIC HYDROLOGY PARAMETERS(UNITS NOT NECESSARY)

      MEAN OF ALL DAILY MEAN VALUES                                    543.500
      STANDARD DEVIATION OF DAILY MEAN VALUES                          441.000
      MEAN OF YT SERIES                                                  0.0
      STANDARD DEVIATION OF YT SERIES                                    1.000
      COEFFICIENTS IN AUTOREGRESSIVE MODEL                      A1=      0.567       A2=       0.306
                                                                  HARMONICS FROM 1 TO 6
      FOURIER COEFFICIENTS FOR DAILY MEANS(A)                         -200.300    145.400    -85.500     58.000    -39.800      7.400
                                           (B)                        -112.400    185.000    -79.900     65.600    -72.500     27.800
      FOURIER COEFFICIENTS FOR DAILY STD DEVIATIONS(SA)               -123.300    141.600    -66.400     75.700    -47.200      8.600
                                                   (SB)                -85.600    105.700    -46.200     31.700    -43.200      4.300
      MAXIMUM VALUE OF QVOL                                         130000.000


BANK MIGRATION PARAMETERS
      EXPONENT N2                                                                0.500
      VALUE OF CONSTANT IN LATERAL MIGRATION RELATION                      K2= 0.100E-05
      VALUE OF CONSTANT IN DOWNVALLEY MIGRATION RELATION                   K3= 0.100E-03
      LIMITING PERCENTAGE OF GRAVEL ALLOWABLE IN OUTER BANK                     30.000


SCOUR AND FILL PARAMETERS
      CONSTANT K4                                                  0.0
      EXPONENT N3                                                  0.0
      STANDARD DEVIATION OF ERROR TERM                             0.0


CUT-OFF CONTROL PARAMETERS
      LIMITING WIDTH OF MEANDER NECK                                   125.000 METRES
      EXPONENTS IN NECK CUT-OFF RELATION                      EN1=      10.000       EN2=      10.000
      LIMITING SINUOSITY                                                 2.000
      LIMITING AMPLITUDE                                               760.909 METRES
      EXPONENTS IN CHUTE CUT OFF RELATION                     EC1=     100.000       EC2=     100.000


A DOWNVALLEY SECTION IS REPRESENTED IN THIS TEST
DISTANCE OF LINE OF SECTION FROM POINT OF INFLECTION OF LOOP IS      0.0    METRES

LEGEND

      LOWER PHASE PLANE BED       L        GRAVEL       G        OLD SEDIMENT       X
      RIPPLES                     R        SAND         C        WATER              I
      DUNES                       D        SILT         S        TIME LINE          *****
      UPPER PHASE PLANE BED       U        CLAY         -        AIR                BLANK
      ANTIDUNES                   A        OVERBANK     F
                                           DEPOSITS
```

Table 16.2. Sample output from main program during initialisation.

Table 16.4. Sample output from subroutine MEANDR.

FLUVIATILE PROCESS SIMULATION EXPERIMENT 2 TIME INCREMENT 0

PLANIMETRIC FORM OF MEANDER

	METRES	
WAVELENGTH	1000.000	
AMPLITUDE	760.909	
SINUOSITY		2.000
RADIUS OF CURVATURE AT BEND AXIS	217.571	
WIDTH OF MEANDER NECK	**********	
CHANNEL LENGTH ALONG MEANDER	2000.000	
VALLEY SLOPE		0.00010000
LONGITUDINAL WATER SURFACE SLOPE		0.00005000

SELECTED GEOMETRIC RATIOS

WAVELENGTH TO RADIUS OF CURVATURE	4.596
WAVELENGTH TO CHANNEL WIDTH	8.000
RADIUS OF CURVATURE TO CHANNEL WIDTH	1.741
AMPLITUDE TO CHANNEL WIDTH	6.087

Table 16.3. Sample output from subroutine BAR.

FLUVIATILE PROCESS SIMULATION EXPERIMENT 2 TIME INCREMENT 0

VARIATION OF GRAINSIZE AND BED FORM OVER CHANNEL CROSS PROFILE

DEPTH (M)	GRAINSIZE (CM)		BED FORM	LOCAL MEAN FLOW VELOCITY (CM/SEC)	LOCAL DIMENSIONLESS SHEAR STRESS	LOCAL STREAM POWER (ERGS/CM2/SEC)	LOCAL BED SHEAR STRESS (DYN/CM2)	LOCAL FROUDE NUMBER
0.1230	0.0001	-	U	5.6716	3.8730	3.4207	0.6031	0.0516
0.4888	0.0007	S	U	11.3083	1.9846	27.1140	2.3977	0.0516
1.0886	0.0024	S	U	16.8754	1.3490	90.1076	5.3396	0.0516
1.9075	0.0056	S	U	22.3385	1.0260	209.0086	9.3564	0.0516
2.9255	0.0107	O	U	27.6641	0.8279	396.9644	14.3494	0.0516
4.1174	0.0180	O	U	32.8194	0.6917	662.8142	20.1958	0.0516
5.4540	0.0280	O	U	37.7725	0.5907	1010.4846	26.7518	0.0516
6.9024	0.0409	O	U	42.4931	0.5114	1438.6509	33.8561	0.0516
8.4270	0.0572	O	D	39.6817	0.4462	1640.2112	41.3342	0.0436
9.9902	0.0775	O	D	43.2058	0.3906	2117.1675	49.0020	0.0436
11.5537	0.1024	O	D	46.4639	0.3418	2633.1475	56.6709	0.0436
13.0790	0.1331	O	D	49.4358	0.2977	3171.4243	64.1524	0.0436
14.5286	0.1713	O	D	52.1034	0.2570	3713.0173	71.2625	0.0436
15.8668	0.2199	G	D	54.4501	0.2186	4237.6523	77.8264	0.0436
17.0607	0.2845	G	D	56.4615	0.1817	4724.8398	83.6825	0.0436
18.0809	0.3760	G	D	58.1253	0.1457	5154.9531	88.6870	0.0436
18.9025	0.5203	G	D	59.4311	0.1101	5510.2500	92.7166	0.0436
19.5051	0.7957	G	D	60.3710	0.0743	5775.8398	95.6724	0.0436
19.8739	1.5891	G	D	60.9392	0.0379	5940.4531	97.4817	0.0436
20.0000	127.5659	G	D	61.1321	0.0005	5997.0430	98.0998	0.0436

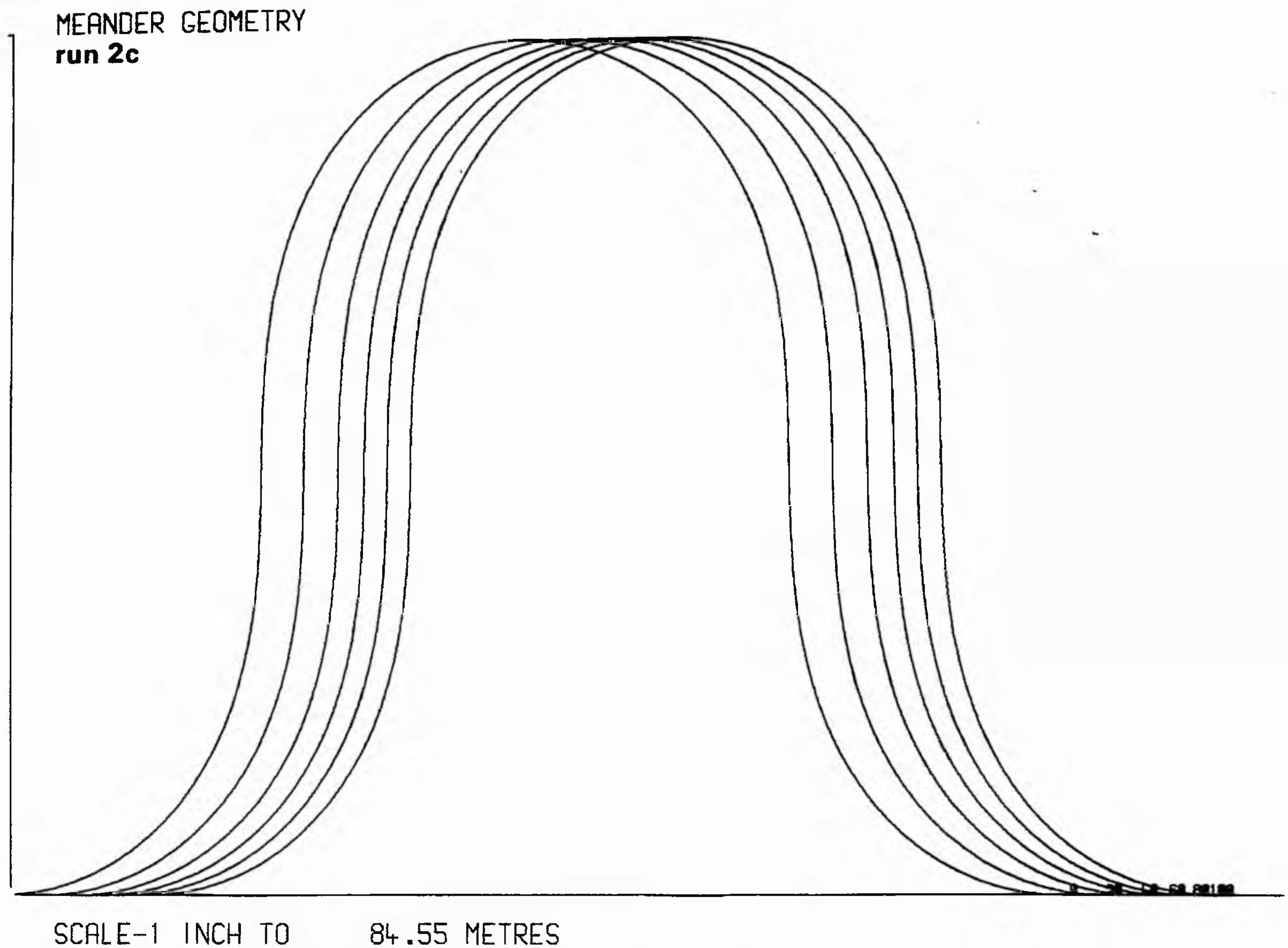

Fig. 16.1. Example of graph plotter output from subroutine MEANDR.

Tables 16.3 and 16.4 are printed at the beginning of the run and every NPRINT-th time increment. Table 16.3 represents an example of output from subroutine BAR and shows the computed grain size, bed form and various hydraulic parameters (measured parallel to the x direction) for selected depths over the point bar profile. These depths correspond to stations located one cell width apart over the profile, from the top of the profile (starting at a distance of one cell width from the inner bank) down to the talweg. The profiles pertain to the unscoured channel which exists before and after scouring and filling, and before slope adjustments are made (in the case of a developing meander). The depth at the talweg is therefore h. The symbols shown for grain size and bedform at a given depth are allocated to the cross sections in the appropriate place. The actual depth, grain size and bedform for a station, as seen approximately in the cross sections, correspond to the right hand edge of the appropriate cell. As previously mentioned, the very top parts of these profiles, where clay is predicted, may not be theoretically correct, but should be qualitatively acceptable.

Table 16.4 is an example of output from the subroutine MEANDR and refers to the planimetric form of the meander after a high water period, that is, at the end of the time increment in question. Similar information is also printed out at the beginning of the run during initialisation. If the width of the meander neck is not defined, asterisks are printed to indicate this. The longitudinal water surface slope is assumed constant all round the meander, as well as across the channel, during the water stages being considered. Fig. 16.1 shows an example of the graph plotter output from MEANDR. A trace of the channel centre line is produced during initialisation (and labelled with a zero), and subsequently every NFPLOT-th time increment. Each trace is

```
  FLUVIATILE PROCESS SIMULATION  EXPERIMENT 2             TIME INCREMENT   80

FLOOD PERIOD VOLUME FOR THIS YEAR                         79633.688

OUTER BANK GRAINSIZE INDEX AT BEGINNING OF YEAR              47.368

INNER BANK GRAINSIZE INDEX AT BEGINNING OF YEAR              20.000

% SILT-CLAY IN CHANNEL PERIMETER AT BEGINNING OF YEAR        24.370

DISTANCE FROM LIMITING AMPLITUDE AT BEGINNING OF YEAR         0.0   METRES

LATERAL MIGRATION DURING THIS YEAR                            0.0   METRES

TOTAL LATERAL MIGRATION AT END OF THIS YEAR                   0.0   METRES

DOWNVALLEY MIGRATION DURING THIS YEAR                         1.157 METRES

TOTAL DOWNVALLEY MIGRATION AT END OF THIS YEAR              115.491 METRES


TOTAL AGGRADATION AT END OF THIS YEAR                         8.000 METRES
```

Table 16.5. Sample output from main program.

annotated with the appropriate time increment, and represents the position at the end of the time increment. When an experimental run was stopped due to cut-off, the appropriate cut-off information has been added to these planform figures. The run numbers are also added. The scales shown at the bottom of these figures are those of the original graph plotter output and are not appropriate for the figures reproduced here. As the dimensions of the meander plans are specified in the text, the scales of the reproduced figures can be obtained.

Table 16.5 is printed every NPRINT-th time increment but not during initialisation. The grain size indices and the total percent of silt and clay (including overbank deposits) in the channel perimeter represent actual percent areal exposure in the cross section defined, not necessarily in the transverse profile defined at right angles to the local mean current direction. As already stated, the percent silt and clay in the channel perimeter is not the same as that used by Schumm (1960). The distance from the limiting amplitude at beginning of year refers to the distance normal to the mean downvalley direction measured from the channel centre line at the bend axis. Again, 'lateral' migration refers here to bank migration in the direction normal to the mean downvalley direction.

Fig. 16.2 and fig. 16.3, respectively, show representative parts of the grain size and bed form distribution cross sections produced after a certain number of time increments of this sample run. Each symbol marked (except for the time line dots) occupies one cell, the dimensions of which are given in table 16.2. The past positions of the unscoured channel bed are picked out with the dots of the time lines. These are plotted for the initial position, and subsequently every NTPLOT-th time increment, and they represent the situation at the end of the time increment. In the forthcoming experiments these time lines are annotated

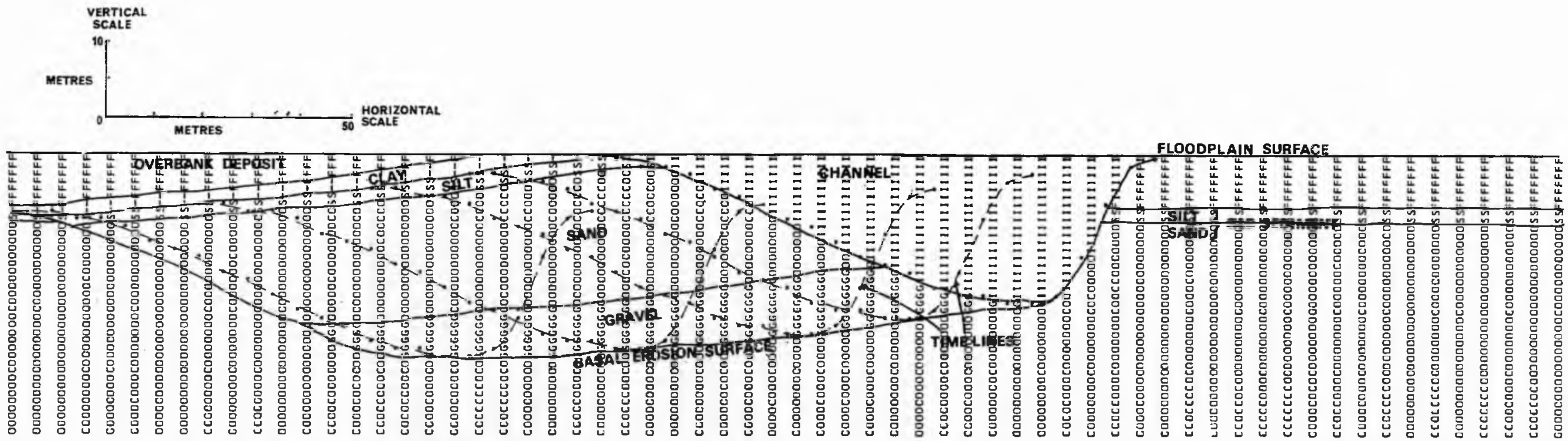

Fig. 16.2. Cross section showing grain size distribution.

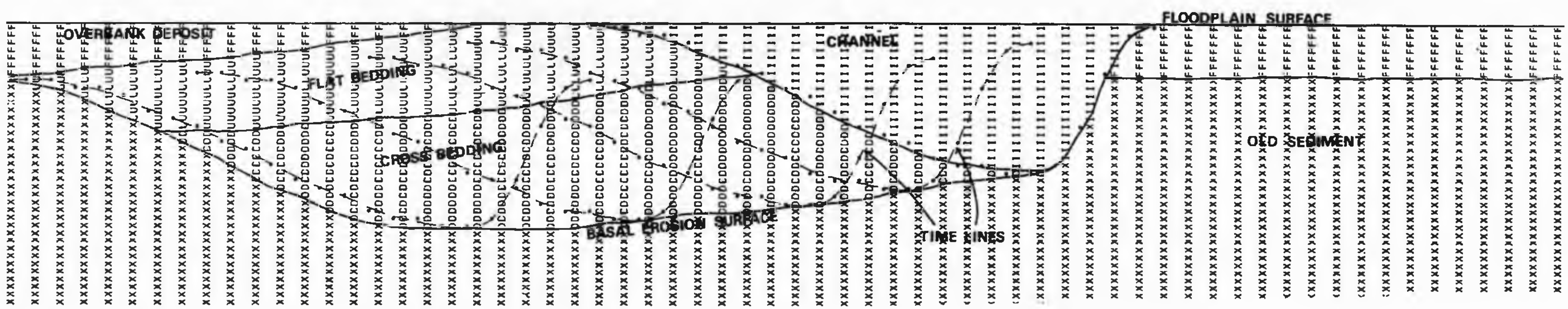

Fig. 16.3. Cross section showing distribution of bed form and sedimentary structure.

with the appropriate time.

Clearly the cross sections only record the response of the model to the processes as simplified from the real world system. However, an increasing degree of accuracy in the cross sections, within the simplified model system as it stands, could be obtained, for instance, by increasing the number of grain size divisions or decreasing the cell size. The symbols for dunes and ripples should be assumed to represent cross bedding and cross lamination respectively, and those for upper and lower phase beds to represent flat bedding. The symbol for overbank deposits must be thought of as being internally variable in both grain size and sedimentary structure, probably with some characteristics similar to the immediately underlying point bar sediments (particularly the grain sizes).

In the originals of cross sections shown and in subsequent sections produced in the experiments (except fig. 25.1), the vertical and horizontal scales were 1 cm. to YCEL/0.25 metres and ZCEL/0.85 metres, respectively. YCEL and ZCEL are the depth (size in vertical direction) and width (size in horizontal direction) of the cells, and in these cases their values are 1.0 and 5.0 metres respectively. The vertical exaggeration is therefore (ZCEL/0.85) x (0.25/YCEL), which equals 1.47. These scales only apply to the original line printer output (produced on IBM 1403). Other line printers may have different spacing and size of characters. During reproduction the cross sections were reduced. The horizontal and vertical scales are therefore calculated as, respectively, physical width of one cell (units) to ZCEL metres, and physical depth of one cell (units) to YCEL metres. The vertical exaggeration remains unchanged. This vertical exaggeration implies that the relief of any of the grain size, sedimentary structure, or sediment-water boundaries will be exaggerated.

Associated with the use of discrete cells which are filled with a particular quality, is a smoothing error, as all lengths in the cross section are rounded down to the nearest number of cell units. As a result of this, the positioning of any quality is only within an accuracy of one cell. Confidence should not be placed, therefore, in, say, irregularity in facies boundaries with only one cell relief.

It should be noticed that in neither lateral nor down-valley sections is the valley slope explicitly accounted for in the cross sections. This is largely due to the negligible slopes compared to the scales of the cross sections. It is a simple matter, however, in the case of the downvalley sections, to tilt the cross sections the required amount, as the bankfull level of the cross sections corresponds to the land surface. Also, no control is made of the erosive effect of an upstream channel, which will be present in all sections. It is therefore necessary to look at the plots of the channel centre lines to discover how much of the deposits to the left of the current channel in the cross sections can be sensibly assumed correct.

All lines separating different symbols or joining time line dots are added by hand, thus subjectivity in the positioning of such lines are the responsibility of the individual. In future, lines separating different grain size classes, sedimentary structures, etc., will be termed 'facies boundaries'.

PART FOUR

EXPERIMENTATION AND RESULTS

INTRODUCTION

The development of the overall mathematical model gives a more intimate insight into the natural system to be simulated, and it is interesting to look at the modes of sedimentation expected under particular conditions on the basis of this insight. Such an insight has also been important in the designing of selected experiments with the computer program, without the necessity of experimenting with every possible combination of variables. Broadly the experiments fall into two categories; those where the meandering is developing to a stable form and those already in dynamic equilibrium. Data input is such that all dependent and independent variables are in conformity with those found in natural situations, as far as these are known. This aspect was discussed in part 2.

17 EXPERIMENT 1 - MEANDERS IN DYNAMIC EQUILIBRIUM

It was noted that over a high-water period the bed in the pool of a meander characteristically scours and subsequently fills to the same position as existed before the high stages. When such changes occur in the channel bed, together with lateral movement associated with bank recession, it is expected that some degree of relief will exist in the grain size and sedimentary structure boundaries and in the basal erosion surface. This experiment is therefore designed to examine the nature of sedimentation as the rates of bank migration and depth of scour vary.

The experiment consists of nine runs of the program corresponding to all possible combinations of three different average rates of downvalley bank migration and three different average depths of scour at the talweg. The input data varied for each run are shown in table 17.1, and these correspond to average rates of bank migration of about 2.4, 12 and 48 metres per year (or, more precisely, per time increment), and average net depths of scour at the talweg of about 0.78, 7.8 and 15.6 metres. All other parameters, shown in table 17.2 and 17.1, are constant for all runs. The meanders are assumed in dynamic equilibrium with a sinuosity of 2.0, the meander and channel geometry being constant for all runs. Table 17.3 shows the variation of grain size, bed form and hydraulic parameters over the point bar profile (at bankfull stage) before and after the scouring and filling of the bed. This profile and the cross sections produced were defined in the mean downvalley direction. The input data deck set-up is listed in appendix 3. In this experiment a disc was used, the cross sections were made up of 200 by 60 cells, and 78k bytes of core store were required. Average running times (CPU times) were 10 seconds per time increment.

Table 17.1.

Run no.	1a	1b	1c	1d	1e	1f	1g	1h	1i
Average downvalley migration rate (metres/year)		2.4			12			48	
Mean scour depth (m.)	0.78	7.8	15.6	0.78	7.8	15.6	0.78	7.8	15.6
BANK MIGRATION PARAMETERS									
exponent n_2				constant at 0.5					
constant k_2	0.1E-05			0.5E-05			0.2E-04		
constant k_3	0.1E-03			0.5E-03			0.2E-02		
SCOUR AND FILL PARAMETERS									
constant k_4	0.1E-04	0.1E-03	0.2E-03	0.1E-04	0.1E-03	0.2E-03	0.1E-04	0.1E-03	0.2E-03
exponent n_3				constant at 1.0					
Standard deviation of error term	0.1	1.0	2.0	0.1	1.0	2.0	0.1	1.0	2.0

```
  FLUVIATILE PROCESS SIMULATION   EXPERIMENT 1

CROSS SECTION PARAMETERS                                                   METRES      CELLS

      WIDTH OF SECTION                                                   1000.000       200
      THICKNESS OF SECTION                                                 60.000        60
      INITIAL DISTANCE OF INNER CHANNEL BANK FROM L.H.S. OF SECTION        0.0            0
      INITIAL BANKFULL STAGE MEASURED FROM SECTION BASE                    60.000        60
      CELL SIZE IN VERTICAL(Y) DIRECTION                                    1.000
      CELL SIZE IN HORIZONTAL(Z OR X) DIRECTION                             5.000


CHANNEL PARAMETERS                                                         METRES      CELLS

      TOTAL WIDTH OF CHANNEL(W)                                           125.000        25
      WIDTH OF FLOW BETWEEN INNER BANK AND TALWEG(W1)                     100.000        20
      RATIO OF W1 TO W                                                                          0.800
      MAXIMUM FLOW DEPTH MEASURED ABOVE TALWEG                             20.000
      DENSITY OF SEDIMENTARY PARTICLES                                                          2.650 GM/CM3
      FLUID DENSITY                                                                             1.000 GM/CM3
      DARCY-WEISBACH FRICTION COEFFICIENT FOR DUNES AND RIPPLES                                 0.210
      DARCY-WEISBACH FRICTION COEFFICIENT FOR PLANE BEDS AND ANTIDUNES                          0.150
      EXPONENT N1                                                                               1.000


SYNTHETIC HYDROLOGY PARAMETERS(UNITS NOT NECESSARY)

      MEAN OF ALL DAILY MEAN VALUES                              141.200
      STANDARD DEVIATION OF DAILY MEAN VALUES                    234.200
      MEAN OF YT SERIES                                            0.0
      STANDARD DEVIATION OF YT SERIES                              1.000
      COEFFICIENTS IN AUTOREGRESSIVE MODEL              A1=        0.929       A2=     -0.151
                                                         HARMONICS FROM 1 TO 6
      FOURIER COEFFICIENTS FOR DAILY MEANS(A)                   -133.000  -485.000     62.400    -14.300     -7.100      0.0
                                         (B)                    -135.100   125.300     -9.800    -29.500      1.000      7.400
      FOURIER COEFFICIENTS FOR DAILY STD DEVIATIONS(SA)          -49.500   -61.500      9.900      2.800      2.900      1.800
                                                   (SB)          -47.600    81.100      4.900    -31.400    -10.200      5.700
      MAXIMUM VALUE OF QVOL                                     90000 000


CUT-OFF CONTROL PARAMETERS
      LIMITING WIDTH OF MEANDER NECK                             125.000 METRES
      EXPONENTS IN NECK CUT-OFF RELATION                EN1=      10.000       EN2=     10.000
      LIMITING SINUOSITY                                           2.000
      LIMITING AMPLITUDE                                         760.909 METRES
      EXPONENTS IN CHUTE CUT OFF RELATION               EC1=      50.000       EC2=     50.000



A DOWNVALLEY SECTION IS REPRESENTED IN THIS TEST
DISTANCE OF LINE OF SECTION FROM POINT OF INFLECTION OF LOOP IS      0.0    METRES


LEGEND

      LOWER PHASE PLANE BED      L       GRAVEL      G        OLD SEDIMENT      X
      RIPPLES                    R       SAND        O        WATER             I
      DUNES                      D       SILT        S        TIME LINE         .....
      UPPER PHASE PLANE BED      U       CLAY        -        AIR               BLANK
      ANTIDUNES                  A       OVERBANK    F
                                         DEPOSITS

PLANIMETRIC FORM OF MEANDER                        METRES

      WAVELENGTH                                  1000.000
      AMPLITUDE                                    760.909
      SINUOSITY                                                 2.000
      RADIUS OF CURVATURE AT BEND AXIS             217.571
      WIDTH OF MEANDER NECK                     **********
      CHANNEL LENGTH ALONG MEANDER                2000.000
      VALLEY SLOPE                                          0.00010000
      LONGITUDINAL WATER SURFACE SLOPE                      0.00005000


SELECTED GEOMETRIC RATIOS

      WAVELENGTH TO RADIUS OF CURVATURE              4.596
      WAVELENGTH TO CHANNEL WIDTH                    8.000
      RADIUS OF CURVATURE TO CHANNEL WIDTH           1.741
      AMPLITUDE TO CHANNEL WIDTH                     6.087
```

Table 17.2. Initial data for experiment 1.

FLUVIATILE PROCESS SIMULATION EXPERIMENT 1 TIME INCREMENT 0

VARIATION OF GRAINSIZE AND BED FORM OVER CHANNEL CROSS PROFILE

DEPTH (M)	GRAINSIZE (CM)		BED FORM	LOCAL MEAN FLOW VELOCITY (CM/SEC)	LOCAL DIMENSIONLESS SHEAR STRESS	LOCAL STREAM POWER (ERGS/CM2/SEC)	LOCAL BED SHEAR STRESS (DYN/CM2)	LOCAL FROUDE NUMBER
0.1229	0.CC01	-	U	5.6692	3.8746	3.4163	0.6026	0.0516
0.4884	0.0007	S	U	11.3035	1.9854	27.0793	2.3957	0.0516
1.0877	0.0024	S	U	16.8682	1.3495	89.9935	5.3351	0.0516
1.9059	0.0056	S	U	22.3292	1.0265	208.7475	9.3486	0.0516
2.9231	0.0107	O	U	27.6528	0.8282	396.4780	14.3377	0.0516
4.1141	0.0180	O	U	32.8063	0.6920	662.0220	20.1797	0.0516
5.4498	0.0279	O	U	37.7579	0.5910	1009.3118	26.7311	0.0516
6.8972	0.0409	O	U	42.4772	0.5116	1437.0444	33.8309	0.0516
8.4209	0.0572	O	D	39.6675	0.4464	1638.4565	41.3047	0.0436
9.9834	0.0774	O	D	43.1912	0.3909	2115.0190	48.9688	0.0436
11.5464	0.1023	O	D	46.4491	0.3420	2630.6348	56.6348	0.0436
13.0713	0.1329	O	D	49.4212	0.2979	3168.6182	64.1145	0.0436
14.5207	0.1711	O	D	52.0893	0.2572	3710.0164	71.2241	0.0436
15.8591	0.2196	G	D	54.4369	0.2188	4234.5820	77.7888	0.0436
17.0535	0.2840	G	D	56.4496	0.1820	4721.8594	83.6473	0.0436
18.0746	0.3752	G	D	58.1151	0.1460	5152.2305	88.6557	0.0436
18.8972	0.5190	G	D	59.4229	0.1103	5507.9609	92.6909	0.0436
19.5013	0.7925	G	D	60.3652	0.0746	5774.1602	95.6539	0.0436
19.8719	1.5764	G	D	60.9361	0.0382	5939.5352	97.4716	0.0436
19.9999	75.4812	G	D	61.1321	0.0008	5997.0352	98.0997	0.0436

Table 17.3. Experiment 1. Variation of grain size, bedform and hydraulic variables over unscoured channel cross profile.

With regard to the simulated cross sections, the errors involved due to smoothing (section 16) and the vertical exaggeration should be borne in mind. Unfortunately the cross sections do not record the position of the scoured bar profile for each time increment. These profiles may be thought of as representing the boundaries of sigmoidal units which will subsequently be termed epsilon units. Each unit marks the deposition during one flood period. In the case of no scouring and filling the time lines give the shape of these units. Where possible, however, profiles of the scoured bar for a number of time increments, have been added to the cross sections in order to show the variable distribution of grain size and sedimentary structure within and between the units.

The grain size distribution cross sections of runs 1 a,b and c, average downvalley bank migration about 2.4 m./year, show very little relief in the facies boundaries separating clay,silt and sand sizes (fig. 17.1). The sand-gravel facies boundary and the scoured basal surface, however, show increasing degrees of relief as the scour depth increases. A relief corresponding to up to about 5% of the unscoured talweg depth of the channel does not seem unrealistic for those channels that scour to the degree suggested in the literature. The scoured bar profiles for the final time increment are shown in the sections, and an interesting feature is the sloping of all facies boundaries up to the contemporary point bar surface. The upward slope represents the effect of filling of the scoured bar for the final time-increment with only a small amount of lateral migration. This feature is, of course, the basis for the relief of facies boundaries within the bar. If the channel is abandoned after cut-off or avulsion fairly rapidly such a feature may be preserved. It is interesting to note that the grain-size facies boundaries do not slope <u>down</u> into the talweg as filling and migration proceed. This is a function of the

RUN 1a

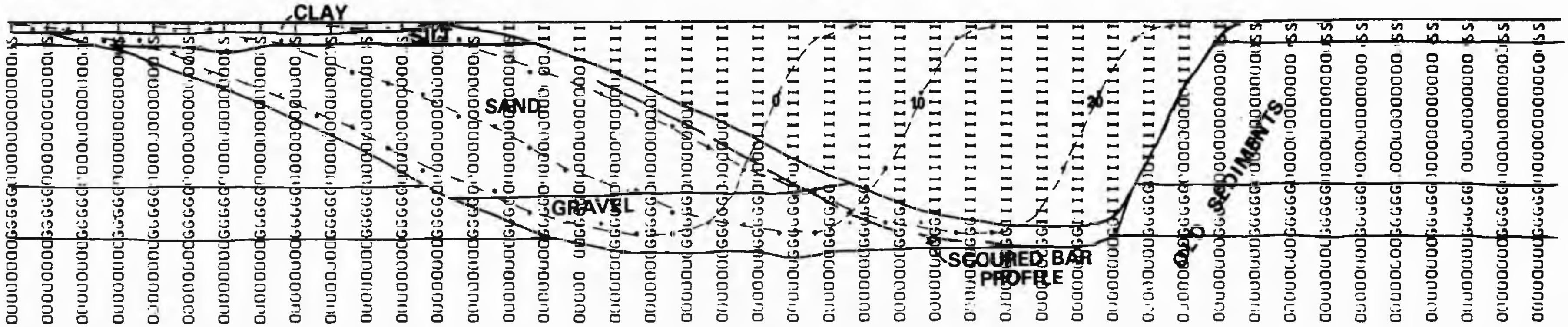

RUN 1b

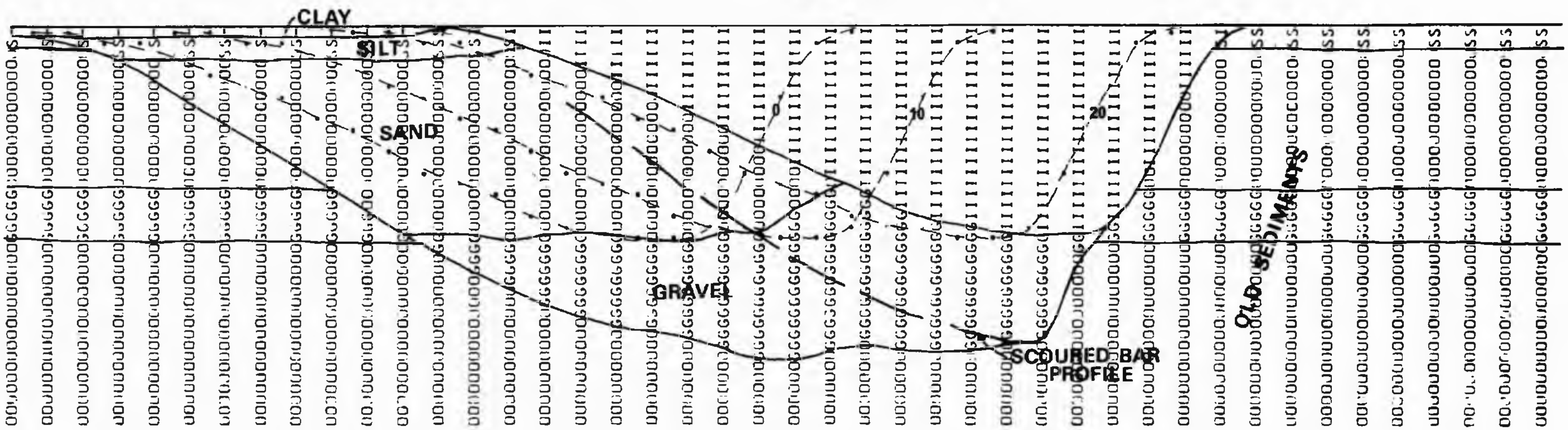

RUN 1c

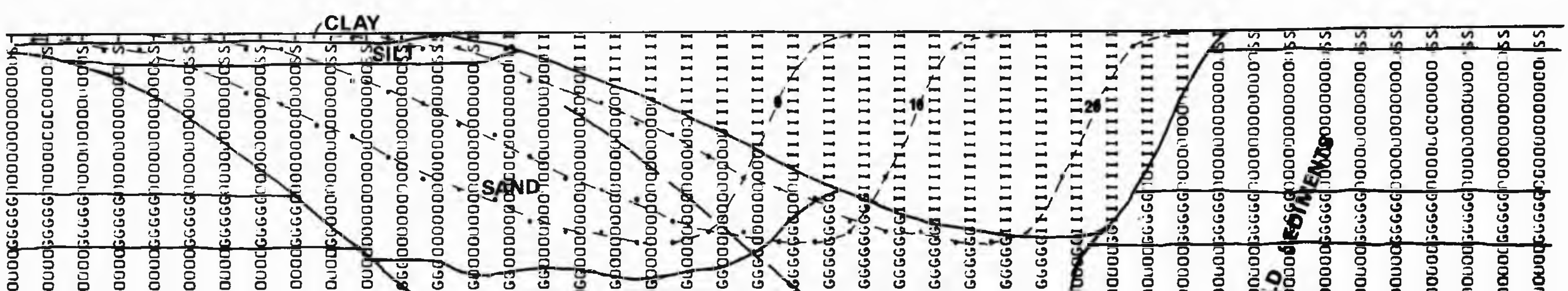

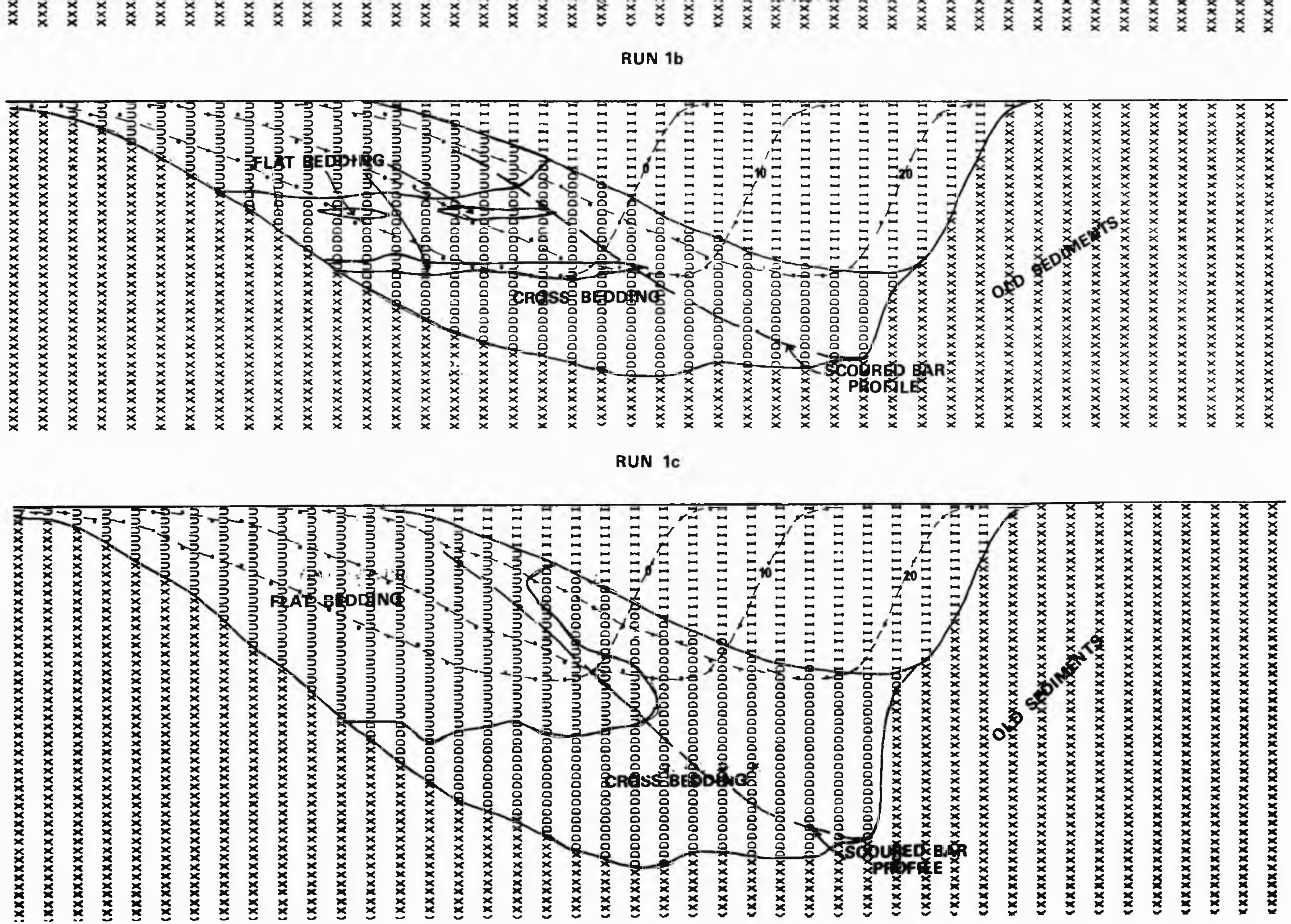

Fig. 17.2. Sedimentary structure sections for runs la, b and c.

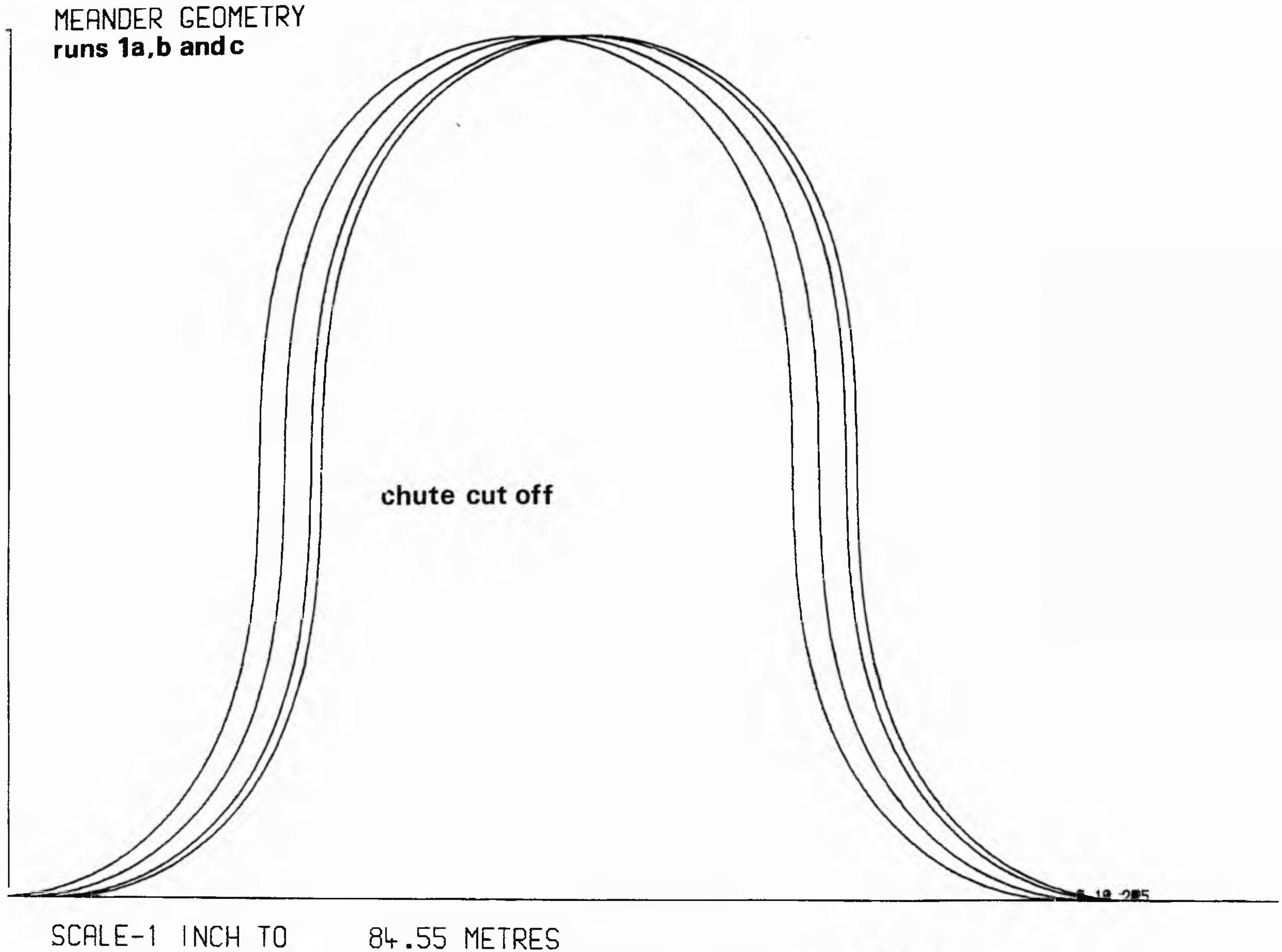

Fig. 17.3. Meander plan forms for runs 1a, b and c.

construction of the model and must be viewed in the light of approximations made. This point is returned to in part 5. Increasing scour depth has the effect of increasing the thicknesses of silt and sand, but increasing gravel thickness to a relatively greater extent.

The effect of increasing the depth of scour is more marked on the sedimentary structure sections for runs 1a, b and c, fig. 17.2. The relief of the facies boundaries separating flat bedding and cross bedding is again very small with little scouring. As scour depth increases the relief of the boundary becomes as much as 10% of the channel talweg depth. The tendency for development of lenses of flat bedding within the cross bedding is apparent in fig. 17.2, run 1b. As well as thickening the deposit, increasing scour depth has the effect of increasing total thickness of flat beds at the expense of cross bedding. Hence the sloping of the facies boundary up to the latest point bar surface is present to such an extent in run 1c that flat beds effectively interfinger with cross beds. Fig. 17.3 shows the meander movement in plan which produced the deposits in figs. 17.1 and 17.2.

In the grain-size distribution cross-sections of 1d, e and f, (fig. 17.4; corresponding to an average downvalley bank migration rate of about 12 m./year) the sand-gravel boundary and the basal scoured surface again show increasing relief as scour depth increases. With the basal scoured surface the relief ranges from virtually planar to about 20-30% of the unscoured talweg depth as the scour depth increases, while the relief of the gravel-sand facies boundary increases from a few to 20% of the unscoured talweg depth. Furthermore, in 1e and 1f the basal scoured surface is not regularly undulating, but has stretches several tens of metres in length where there is no appreciable change in relief. The relief of the clay-silt boundary does not vary and the regularly undulating relief is up to a few percent of the unscoured

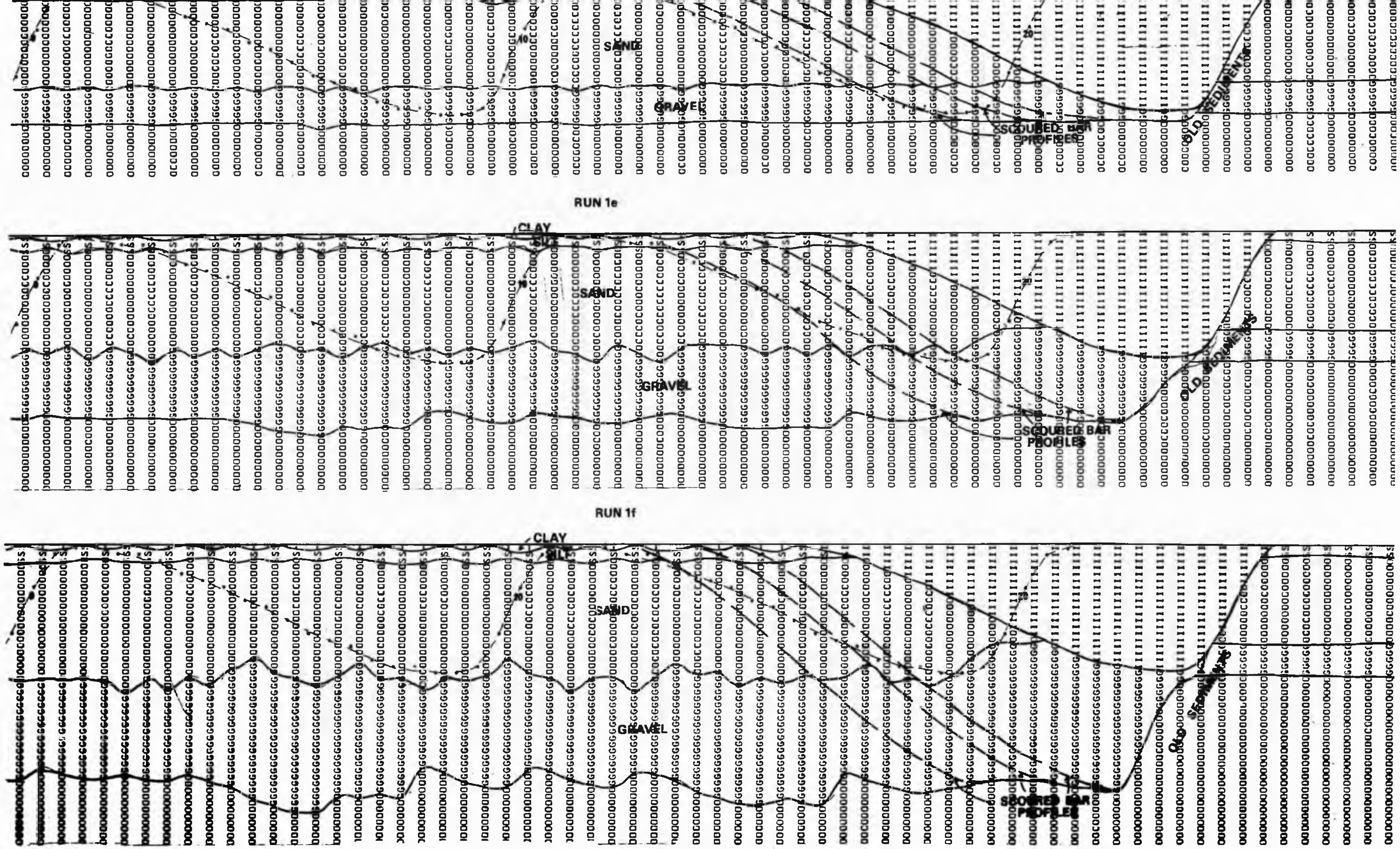

Fig. 17.4. Grain size sections for runs 1d, e and f.

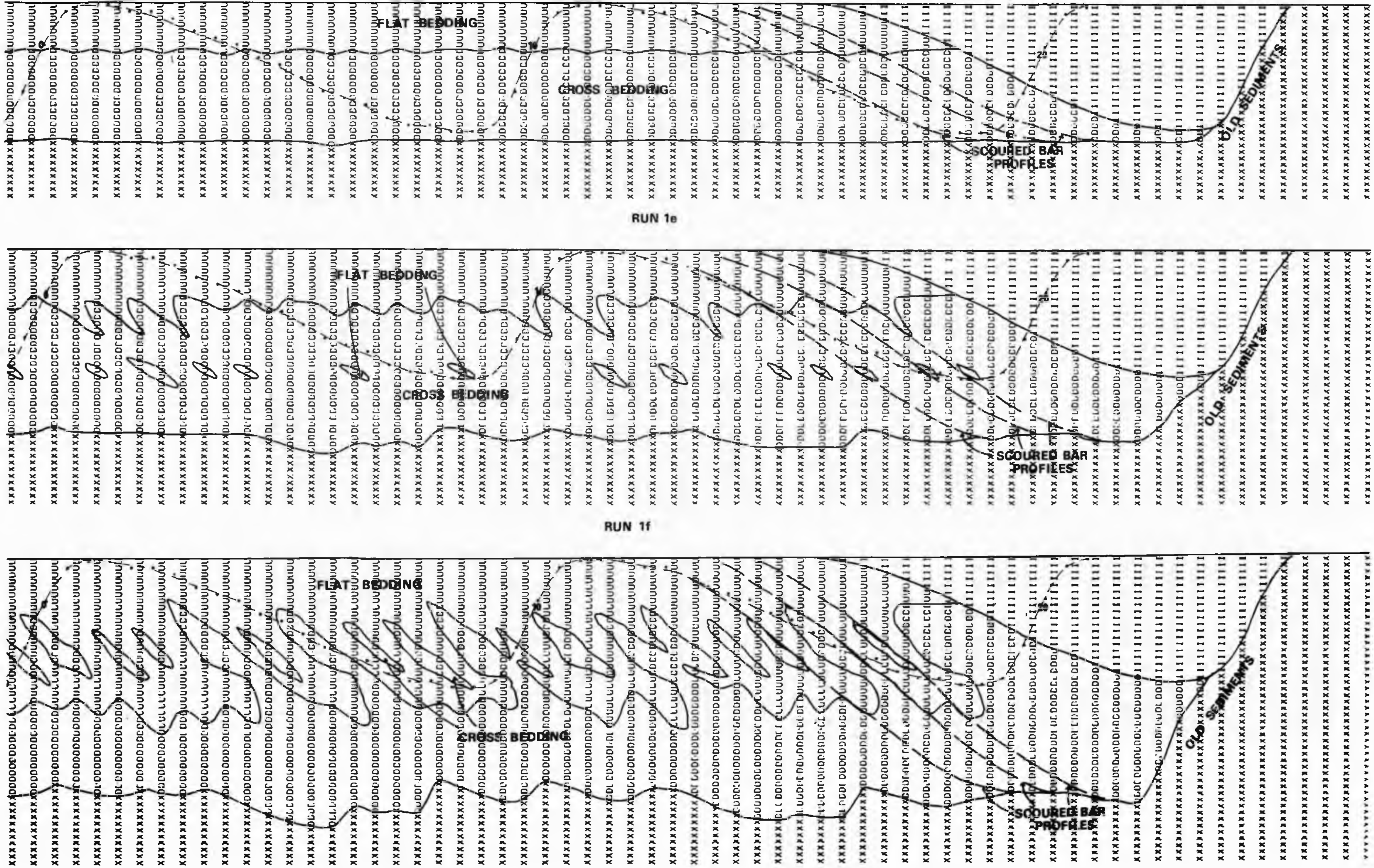

Fig. 17.5. Sedimentary structure sections for runs 1d, e and f.

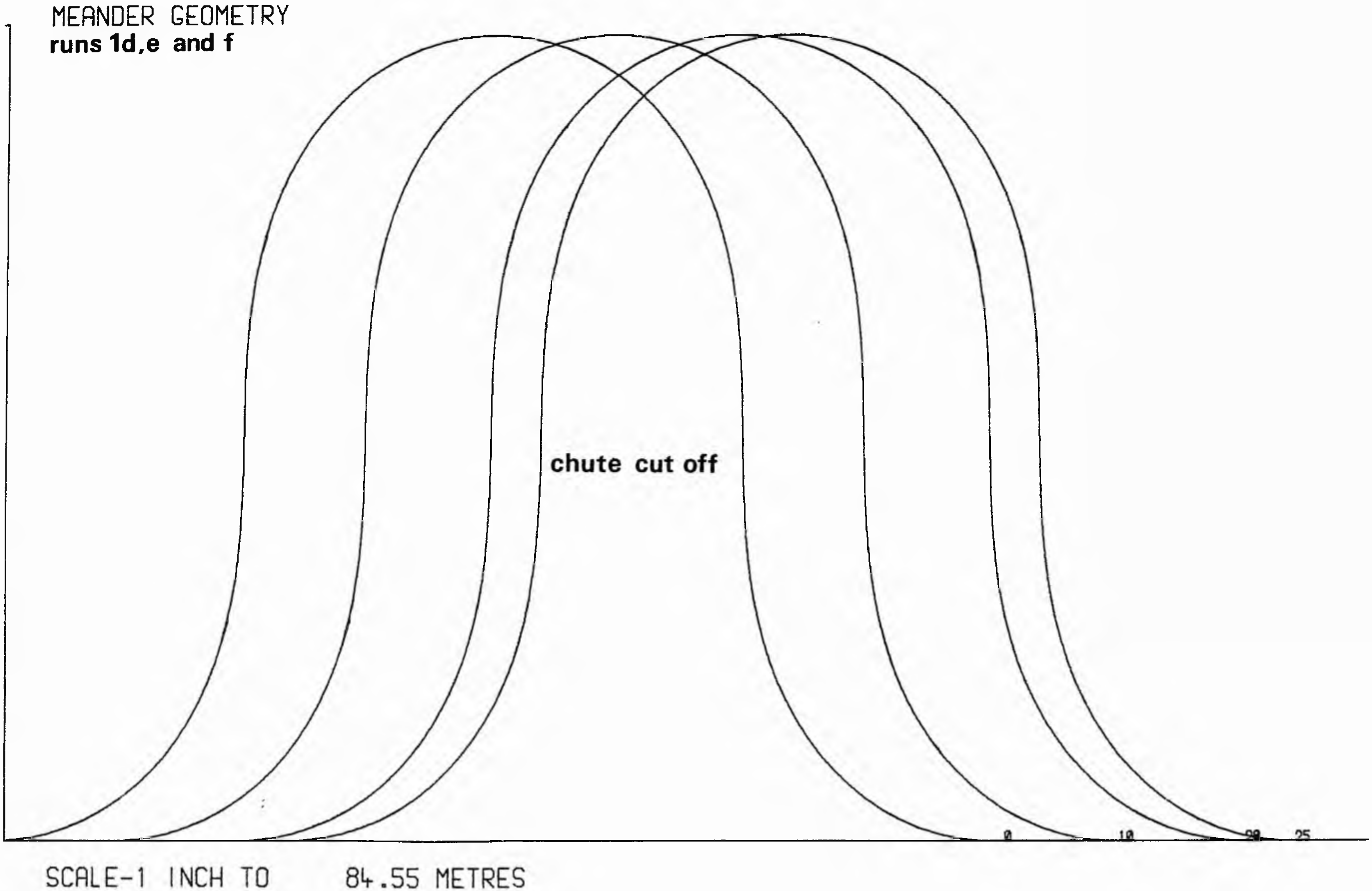

Fig. 17.6. Meander plan forms for runs 1d, e and f.

talweg depth. Similarly with the sand-silt boundary, except in case 1d where there is very little relief at all. In some cases, each separate undulation may mark the separate successive flood periods, particularly in the case of silt-clay and sand-gravel boundaries. As before, increasing scour depth involves increasing the thickness of sand and silt, with gravel thickening a relatively greater amount than the sand and silt.

The sedimentary-structure sections for runs 1d, e and f show a very marked variation in the flat bedding-cross bedding facies boundary with scour depth (fig. 17.5). In case 1d the relief is only a few percent of the unscoured talweg depth, but as scour depth increases, the relief increases until a complex system of interfingering and associated lensing becomes evident. The scale of the interfingering in case 1f is comparable with the maximum unscoured channel depth. The trend of the lensing and interfingering is associated with the scoured bar profiles. The relief and degree of lensing and interfingering is probably exaggerated a certain amount due to approximations involved in the mathematical model and computer program. However it seems likely that under similar conditions in the natural situation a noteworthy degree of scoured basal surface and facies boundary relief would be present, with associated facies lensing and interfingering. Such features would be associated with discrete seasonal periods of erosional and depositional activity. The thickness of flat bedding increases relative to cross bedding as scour depth increases. Fig. 17.6 shows the meander movement in plan relating to these sections.

The grain-size distribution cross-sections of 1g, h and i, shown in fig. 17.7, correspond to the cases with average downvalley bank migration of about 48 m./year. The basal scoured surface and sand-gravel facies boundary increase in relief from virtually nil up to about 35% of the unscoured talweg depth, with increase

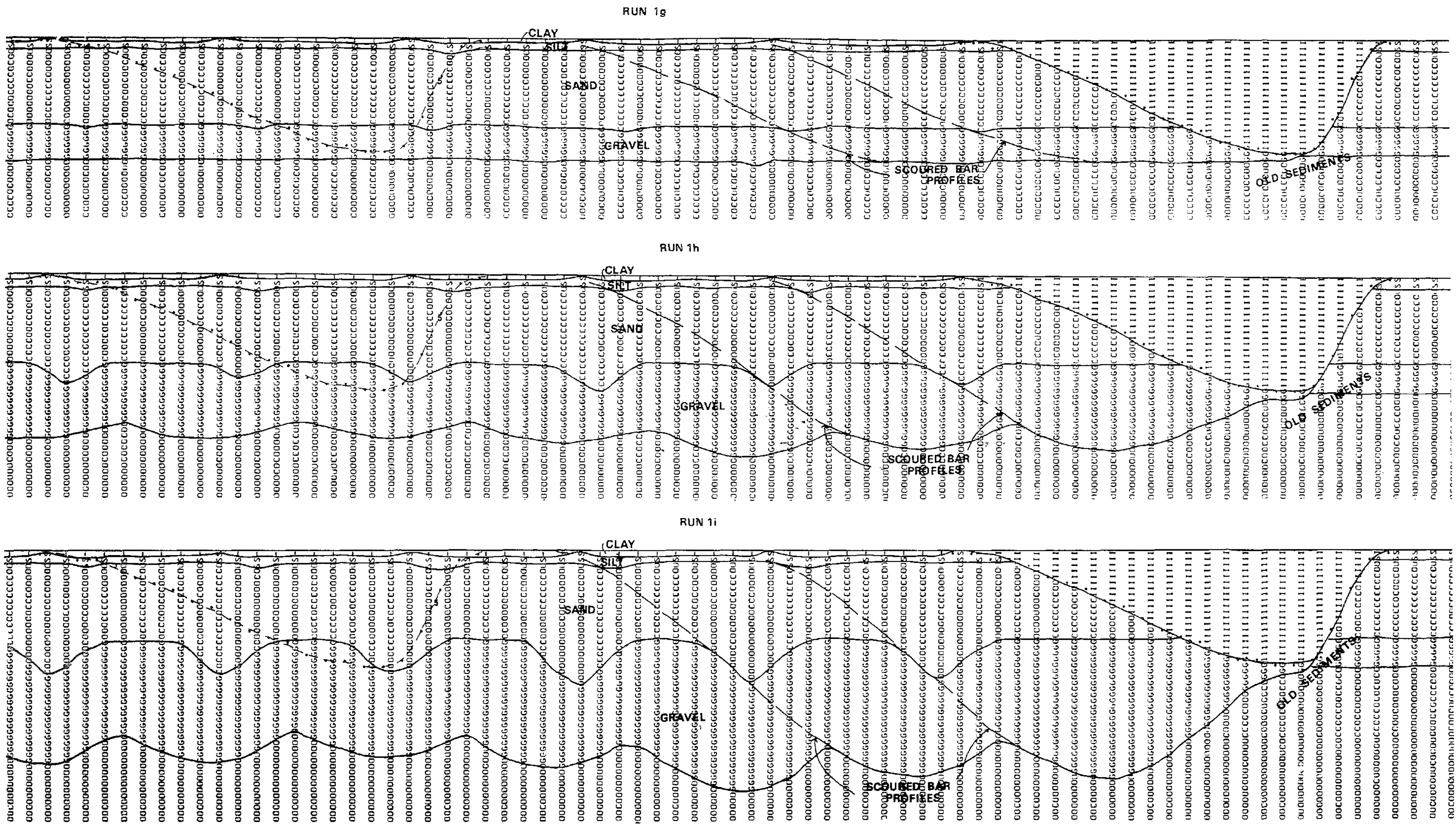

Fig. 17.7. Grain size sections for runs 1g, h and i.

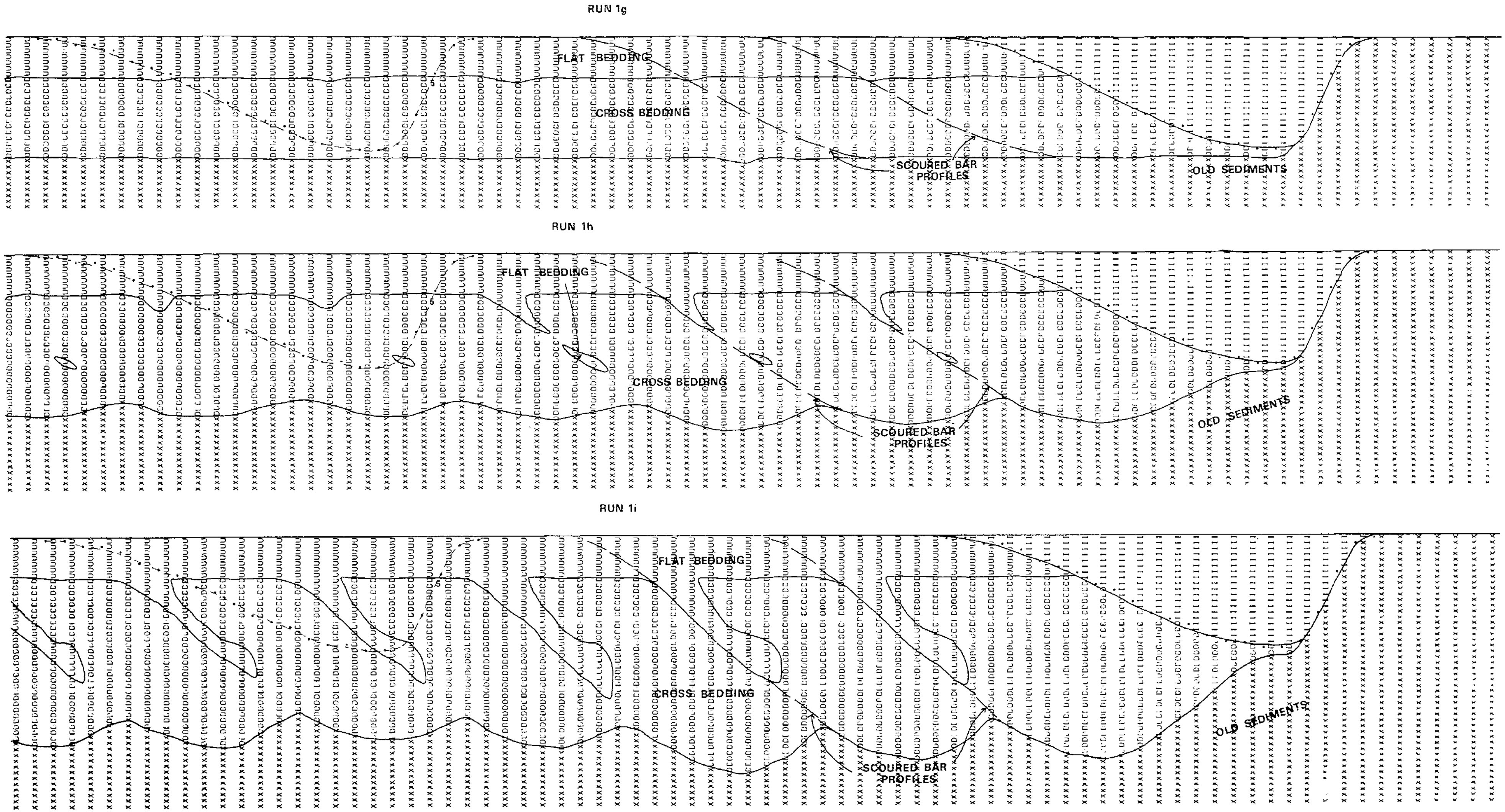

Fig.17.8. Sedimentary structure sections for runs 1g, h and i.

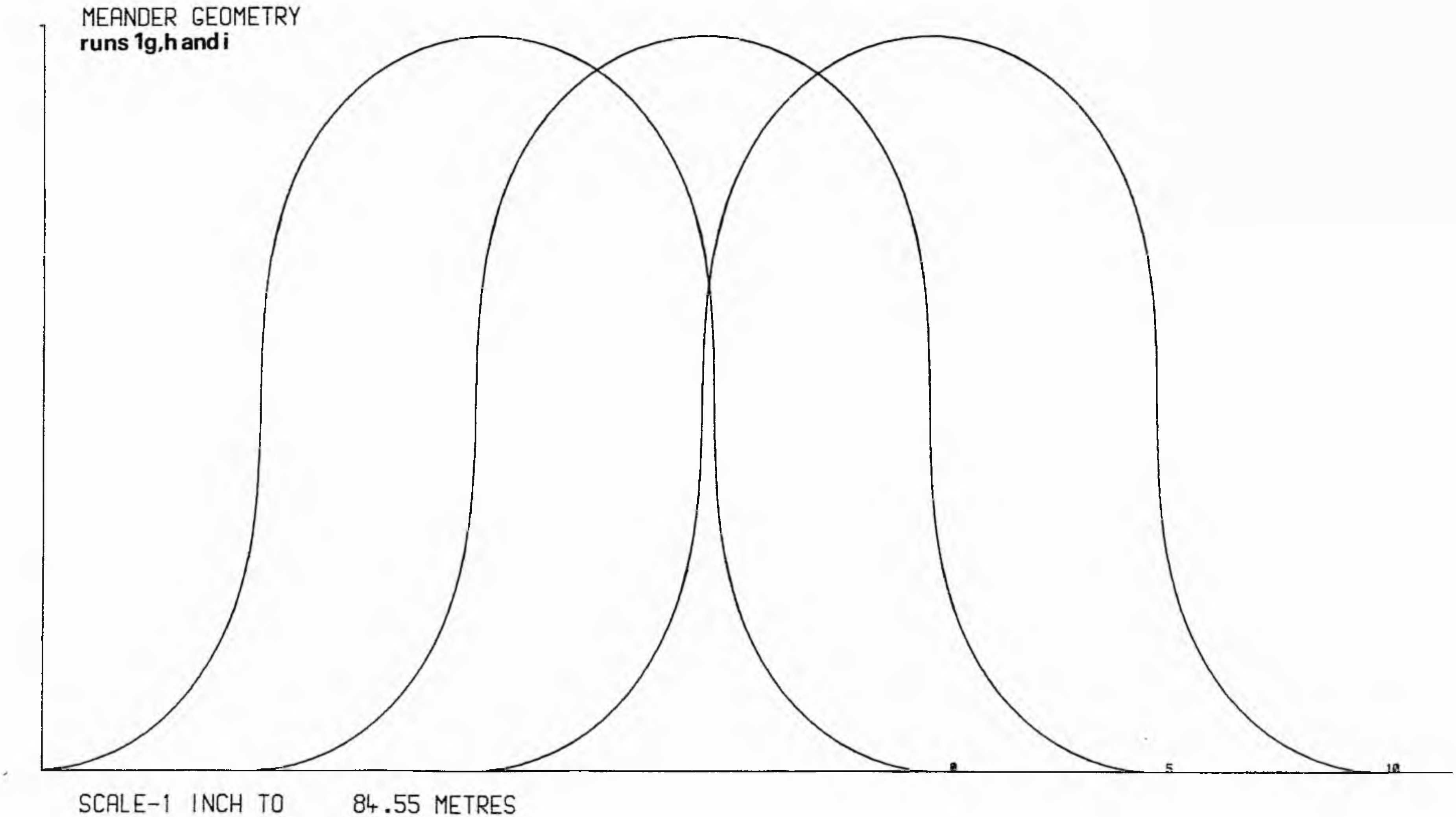

Fig. 17.9. Meander plan forms for runs 1g, h and i.

in scour depth. The relief of the clay-silt boundary does not vary and the regularly undulating relief is up to about 5% of the unscoured talweg depth. Similarly, with the sand-silt boundary, except in the case 1g where the boundary is essentially planar. Where any relief is developed it is of considerably greater wavelength than in the previous sections discussed, and each complete wave corresponds to a discrete flood period. It is noteworthy here that the peakedness of the depressions in facies boundaries is probably exaggerated due to the construction of the computer program, and becomes more so as the rate of migration increases. They should probably be more asymmetrical with less steep riverward sides. Thus, in general, the degree of relief will not be quite as marked as shown. It is expected, nevertheless, that regular long wavelength undulations of grain-size boundaries and scoured basal surfaces will be present where bank migration is very rapid, each complete wavelength corresponding to a discrete period of erosional and depositional activity. By virtue of the scale of the undulations, these surfaces may appear broadly planar when seen only in limited lateral extent.

As scour depth increases in the sedimentary structure cross sections for runs 1g, h and i, the flat bedding-cross bedding boundary develops from virtually planar to an undulating pattern with interfingering and lensing until, finally, large scale interfingering is present on a scale comparable with the maximum unscoured channel depth (fig. 17.8). The disturbances in this boundary are again associated with seasonal floods, their trend corresponding to the scoured bar profile. The degrees of interfingering and undulation are again exaggerated, and in particular the upper, riverward boundaries of the interfingering flat-bedded areas are expected to expand riverward at the expense of the cross bedding. Nevertheless, a marked degree of undulation, interfingering and lensing is expected under similar conditions in the natural situation, despite the approximations made. Silt, sand and gravel thicknesses increase as in the previous runs with increase in scour depth, and, in general, cross bedding thickens at the expense of the flat beds. Fig. 17.9 shows meander movement in plan associated with sections 1g, h and i.

Experiment 1 demonstrates that the relief and nature of the facies boundaries and erosion surfaces are dependent on the rate of bank migration relative to the depth of scour.

18. EXPERIMENT 2 - MEANDERS IN DYNAMIC EQUILIBRIUM

As meanders migrate systematically downstream, point bar and overbank deposits are eroded by the channel of the upstream meander limb. If there is no net vertical deposition there will obviously be no preservation of sediment. If there is continuing net deposition (aggradation) the level of the upstream channel will be above the basal erosion surface of the bar sequence it is truncating. Whether the land surface is being raised during aggradation or whether net vertical deposition is being accommodated by subsidence with land level remaining constant, or a combination of both, is not relevant here. It is only necessary to know the relative levels of the basal erosion surfaces being considered. Bluck (1971) has indicated that an inordinate amount of aggradation would be required to preserve a complete point bar sequence between erosion surfaces, but that it is possible for a small part of the sequence to be preserved. Furthermore, during aggradation, sediment deposited outside the channel is expected to be characteristically fine-grained silts, clays and some fine sands. As aggradation proceeds, therefore, the proportion of fine-grained alluvium exposed in the cut bank may increase, thus reducing the rate of channel migration calculated in the model. Experiment 2 is designed to examine the nature of the sedimentation in this 'moving phase' situation as the rates of downvalley migration and aggradation vary.

The experiment consists of nine runs of the program corresponding to all possible combinations of three different average rates of downvalley bank migration and three different rates of aggradation. The input data that are different for each run are shown in table 18.1, and correspond to average rates of bank migration of about 2, 10 and 42 m./year, and rates of aggradation of 0.001,0.01 and 0.1 m./year. All other parameters, shown in table 18.2 and 18.1, are constant for all runs. The meanders are

Table 18.1.

Run no.	2a	2b	2c	2d	2e	2f	2g	2h	2i
Average downvalley migration rate (metres/year)	2			10			42		
BANK MIGRATION PARAMETERS									
exponent n_2	Constant at 0.5								
constant k_2	0.1E-05			0.5E-05			0.2E-04		
constant k_3	0.1E-03			0.5E-03			0.2E-02		
Aggradation rate (metres/year)	0.001	0.01	0.1	0.001	0.01	0.1	0.001	0.01	0.1

FLUVIATILE PROCESS SIMULATION EXPERIMENT 2

CROSS SECTION PARAMETERS	METRES	CELLS
WIDTH OF SECTION	1750.000	350
THICKNESS OF SECTION	60.000	60
INITIAL DISTANCE OF INNER CHANNEL BANK FROM L.H.S. OF SECTION	0.0	0
INITIAL BANKFULL STAGE MEASURED FROM SECTION BASE	30.000	30
CELL SIZE IN VERTICAL(Y) DIRECTION	1.000	
CELL SIZE IN HORIZONTAL(Z OR X) DIRECTION	5.000	

CHANNEL PARAMETERS	METRES	CELLS	
TOTAL WIDTH OF CHANNEL(W)	125.000	25	
WIDTH OF FLOW BETWEEN INNER BANK AND TALWEG(W1)	100.000	20	
RATIO OF W1 TO W			0.800
MAXIMUM FLOW DEPTH MEASURED ABOVE TALWEG	20.000		
DENSITY OF SEDIMENTARY PARTICLES			2.650 GM/CM3
FLUID DENSITY			1.000 GM/CM3
DARCY-WEISBACH FRICTION COEFFICIENT FOR DUNES AND RIPPLES			0.210
DARCY-WEISBACH FRICTION COEFFICIENT FOR PLANE BEDS AND ANTIDUNES			0.150
EXPONENT N1			1.000

SYNTHETIC HYDROLOGY PARAMETERS(UNITS NOT NECESSARY)

MEAN OF ALL DAILY MEAN VALUES		543.500					
STANDARD DEVIATION OF DAILY MEAN VALUES		441.000					
MEAN OF YT SERIES		0.0					
STANDARD DEVIATION OF YT SERIES		1.000					
COEFFICIENTS IN AUTOREGRESSIVE MODEL	A1=	0.567	A2=	0.306			
		HARMONICS FROM 1 TO 6					
FOURIER COEFFICIENTS FOR DAILY MEANS(A)		-200.300	145.400	-85.500	58.000	-39.800	7.400
(B)		-112.400	185.000	-79.900	65.600	-72.500	27.800
FOURIER COEFFICIENTS FOR DAILY STD DEVIATIONS(SA)		-123.300	141.600	-66.400	75.700	-47.200	8.600
(SB)		-85.600	105.700	-46.200	31.700	-43.200	4.300
MAXIMUM VALUE OF QVOL		130000.000					

SCOUR AND FILL PARAMETERS	
CONSTANT K4	0.0
EXPONENT N3	0.0
STANDARD DEVIATION OF ERROR TERM	0.0

CUT-OFF CONTROL PARAMETERS				
LIMITING WIDTH OF MEANDER NECK		125.000 METRES		
EXPONENTS IN NECK CUT-OFF RELATION	EN1=	10.000	EN2=	10.000
LIMITING SINUOSITY		2.000		
LIMITING AMPLITUDE		760.909 METRES		
EXPONENTS IN CHUTE CUT OFF RELATION	EC1=	100.000	EC2=	100.000

A DOWNVALLEY SECTION IS REPRESENTED IN THIS TEST
DISTANCE OF LINE OF SECTION FROM POINT OF INFLECTION OF LOOP IS 0.0 METRES

LEGEND

LOWER PHASE PLANE BED	L	GRAVEL	G	OLD SEDIMENT	X
RIPPLES	R	SAND	C	WATER	I
DUNES	D	SILT	S	TIME LINE	.....
UPPER PHASE PLANE BED	U	CLAY	-	AIR	BLANK
ANTIDUNES	A	OVERBANK DEPOSITS	F		

PLANIMETRIC FORM OF MEANDER	METRES	
WAVELENGTH	1000.000	
AMPLITUDE	760.909	
SINUOSITY		2.000
RADIUS OF CURVATURE AT BEND AXIS	217.571	
WIDTH OF MEANDER NECK	**********	
CHANNEL LENGTH ALONG MEANDER	2000.000	
VALLEY SLOPE		0.00010000
LONGITUDINAL WATER SURFACE SLOPE		0.00005000

SELECTED GEOMETRIC RATIOS	
WAVELENGTH TO RADIUS OF CURVATURE	4.596
WAVELENGTH TO CHANNEL WIDTH	8.000
RADIUS OF CURVATURE TO CHANNEL WIDTH	1.741
AMPLITUDE TO CHANNEL WIDTH	6.087

Table 18.2. Initial data for experiment 2.

assumed in dynamic equilibrium with a sinuosity of 2.0. No scouring and filling was assumed in order to simplify examination of the cross sections. The cross sections were defined in the downvalley direction (TWO-CHANNEL DOWNVALLEY SECTIONS). In this experiment no disc was used, the cross sections were made up of 350 by 60 cells, and 182k bytes of core store were required. Average running times were 2-3 seconds/time increment.

Unfortunately the model does not explicitly record basal erosion surfaces in the cross sections. These are normally inferred by cross cutting of previously specified floodplain deposits by the simulated point bar sediments. This may not be obvious when the channel is cutting across sediment of a similar type, especially in the case where the channel is truncating previously deposited point bar sediments. With the simplification of no scour and fill the basal erosion surfaces, if not already obvious after inspection of the sections, can be drawn as straight lines joining successive positions of the channel bed at the talweg, as picked out with time lines. Where scouring and filling is present the nature of the cross cutting would be more difficult to infer.

Runs 2a, b and c refer to average downvalley migration of 2 m./year. After 100 years of simulation the channels have not moved through half a wavelength and therefore the upstream channel has not 'caught up' with the recent deposits of the channel immediately downstream (see fig. 18.1). Another 100 years or so would suffice. Vertical accretion over this period of time is 0.1, 1.0 and 10 metres respectively for runs 2a, b and c. Projecting these rates of movement and aggradation in time, it is seen that about 0.2,2 and 20 metres of sediment would be preserved between erosion surfaces. The two smaller rates of aggradation are not sufficiently great after 100 years to be recorded as vertical sedimentation on the simulated cross sections, figs. 18.2

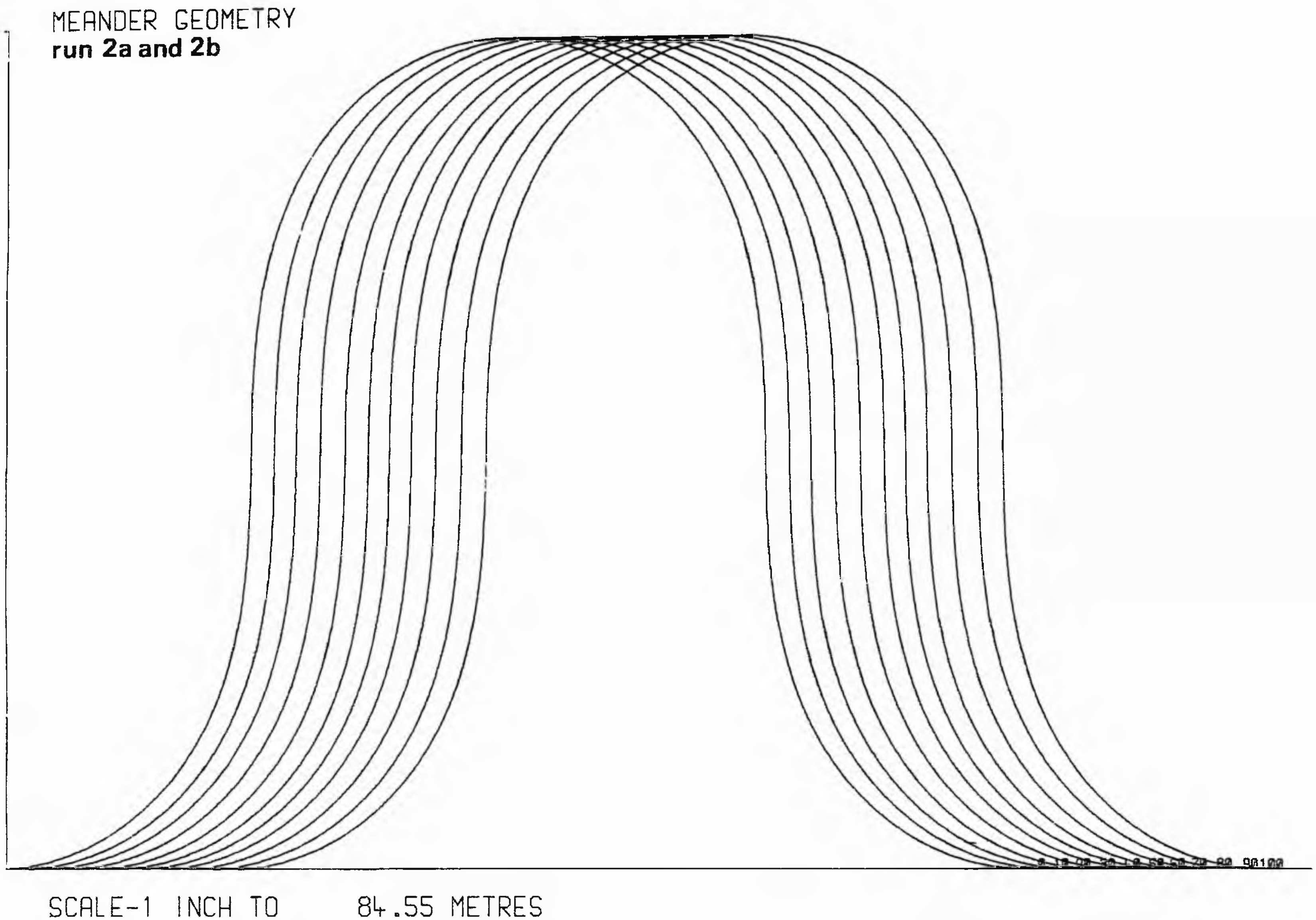

Fig. 18.1. Meander plan forms for runs 2a, b and c.

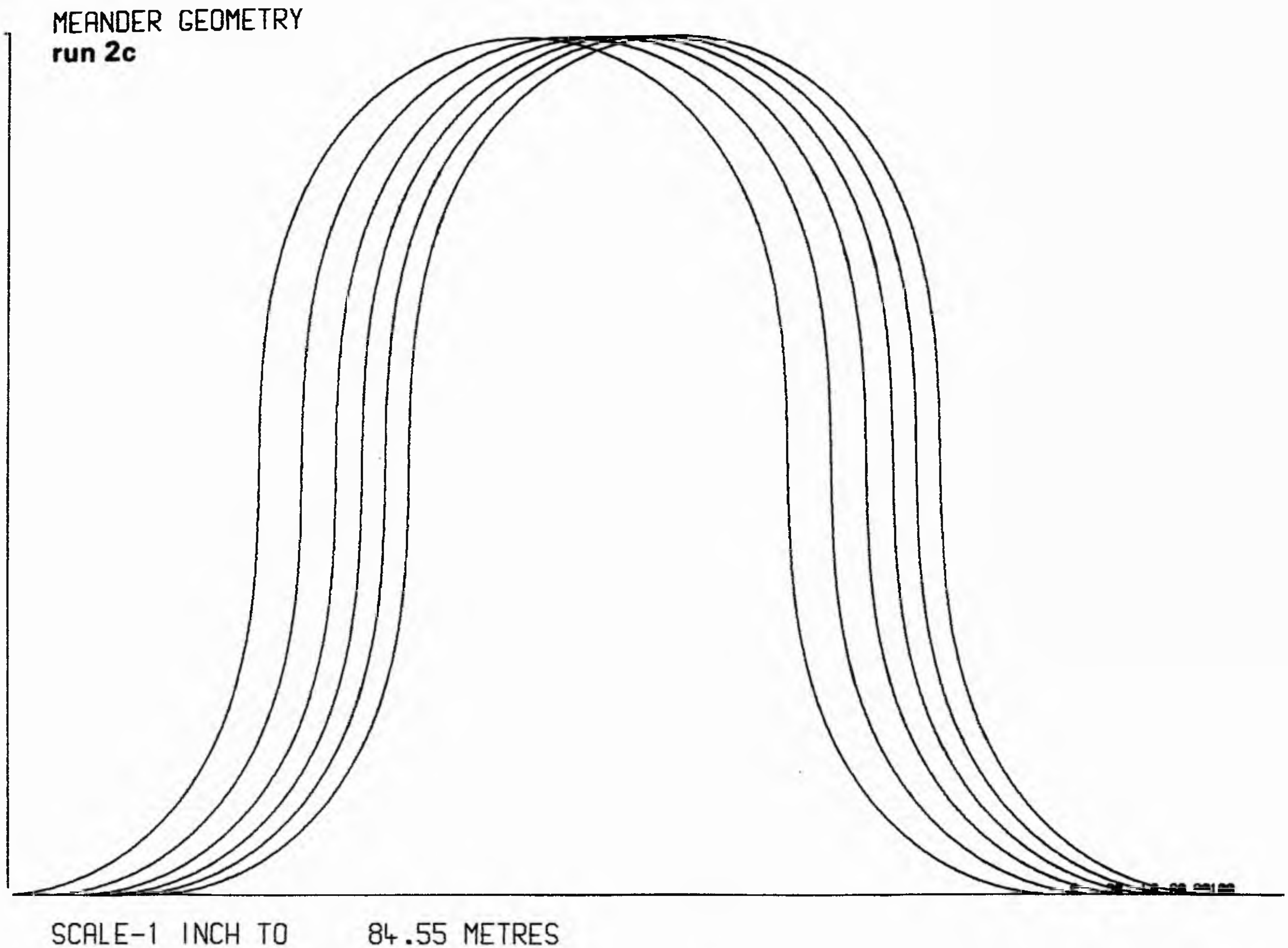

Fig. 18.1. - continued.

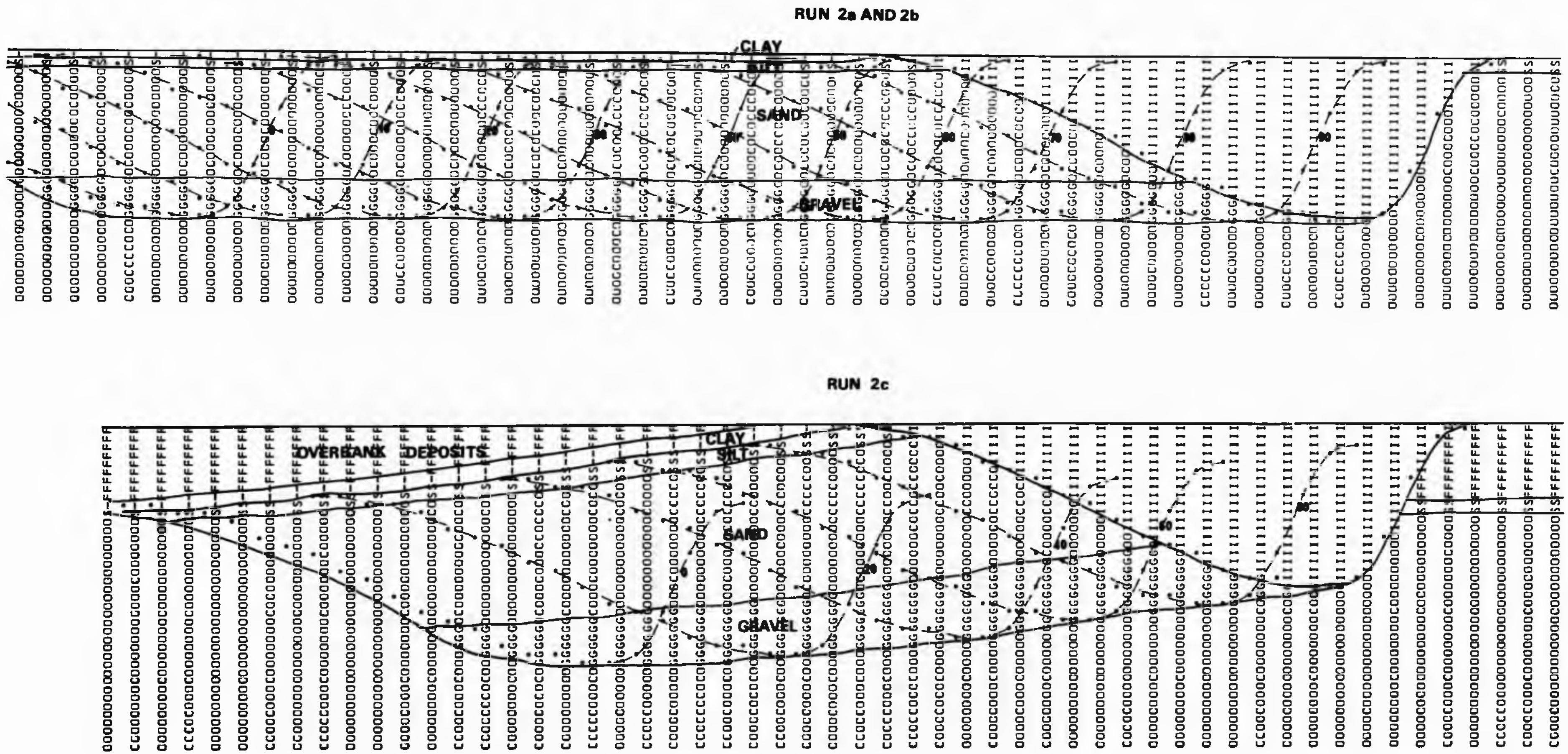

Fig. 18.2. Grain size sections for runs 2a, b and c.

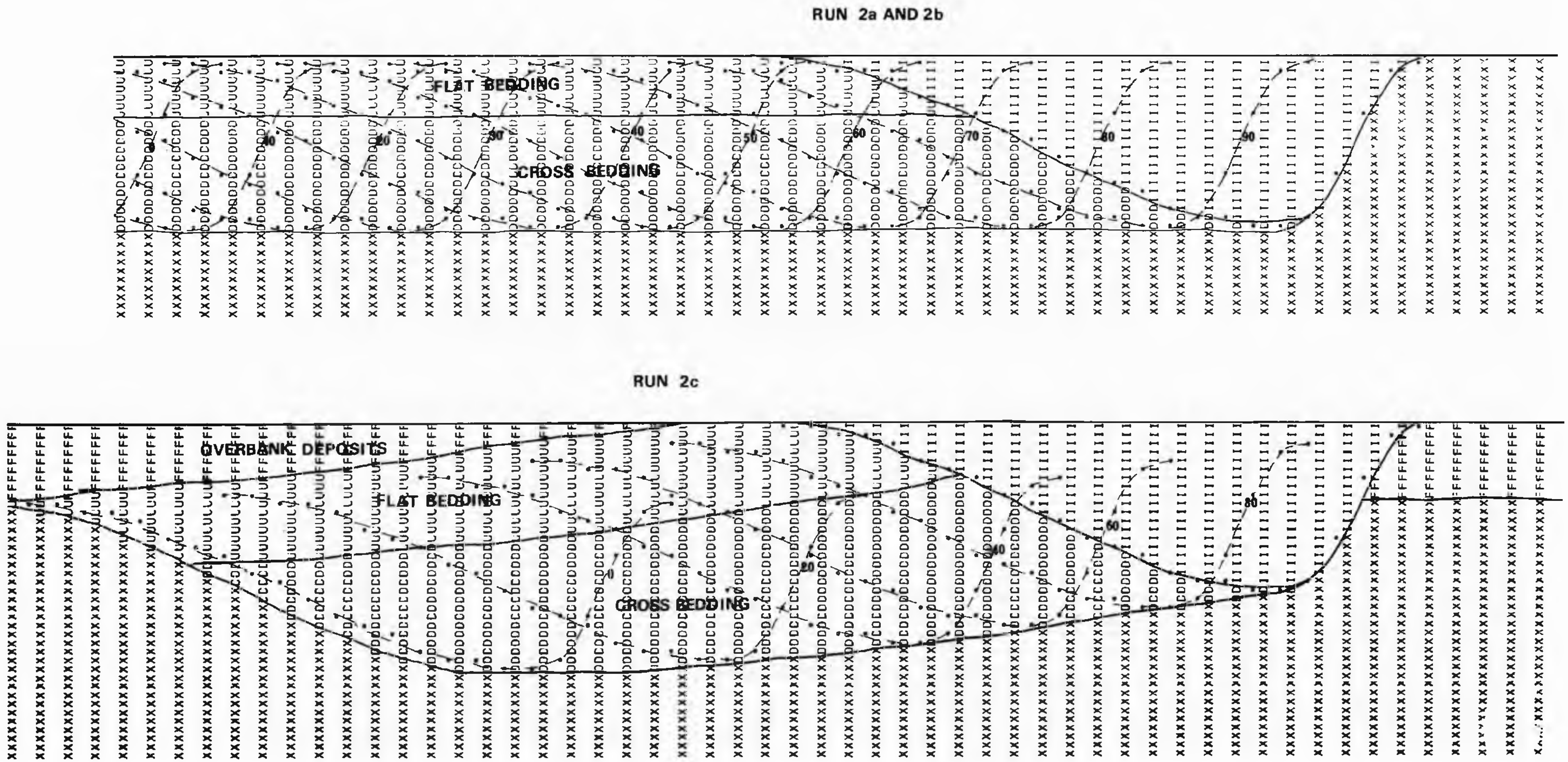

Fig. 18.3. Sedimentary structure sections for runs 2a, b and c.

and 18.3,because of the scale of an individual cell. All grain size and sedimentary structure facies boundaries and basal erosion surfaces on these particular sections appear as level, despite a very slight slope, and the effect of overbank deposits on rate of migration is negligible for this time span. With the largest aggradation rate (0.1 m./year) the overbank deposits can be seen as wedges of sediment, and all boundaries in the grain size and sedimentary structure sections are seen to slope up in the direction of migration. With this appreciable aggradation the rate of channel migration has slowed down (see fig. 18.1) and the slope of the facies boundaries and basal erosion surfaces increases with time. Thus in run 2c more than 20m. of sediment could be preserved, giving a complete point bar and some overbank deposits on top. Such rates of continuing aggradation are not common (see section 12.2) and the smaller rates are much more realistic. Clearly with scouring and filling acting as well, the pattern of sedimentation would be very complex at the base of the bar sequences.

Runs 2d, e and f correspond to an average downvalley migration of about 10m./year. With rates of aggradation of 0.001 and 0.01m./year (runs 2d and 2e), about 0.04 and 0.4 metres of sediment, respectively, are preserved between the erosion surfaces as the time taken to move through half a wavelength is a little over 40 years (see fig. 18.4). The thicknesses deposited vertically were not great enough to appear in the cross sections for the time span considered, and there is no effect of these extensive thin sheets of overbank alluvium on bank migration rates. With an aggradation rate of 0.1m./year, run 2f (figs. 18.5 and 18.6), the thickness preserved is between 6 and 7 metres, as the slowing down of bank migration, due to increasing thicknesses of overbank deposit, has increased the time span to over 60 years for movement of a half meander wavelength. The wedging of the overbank deposits

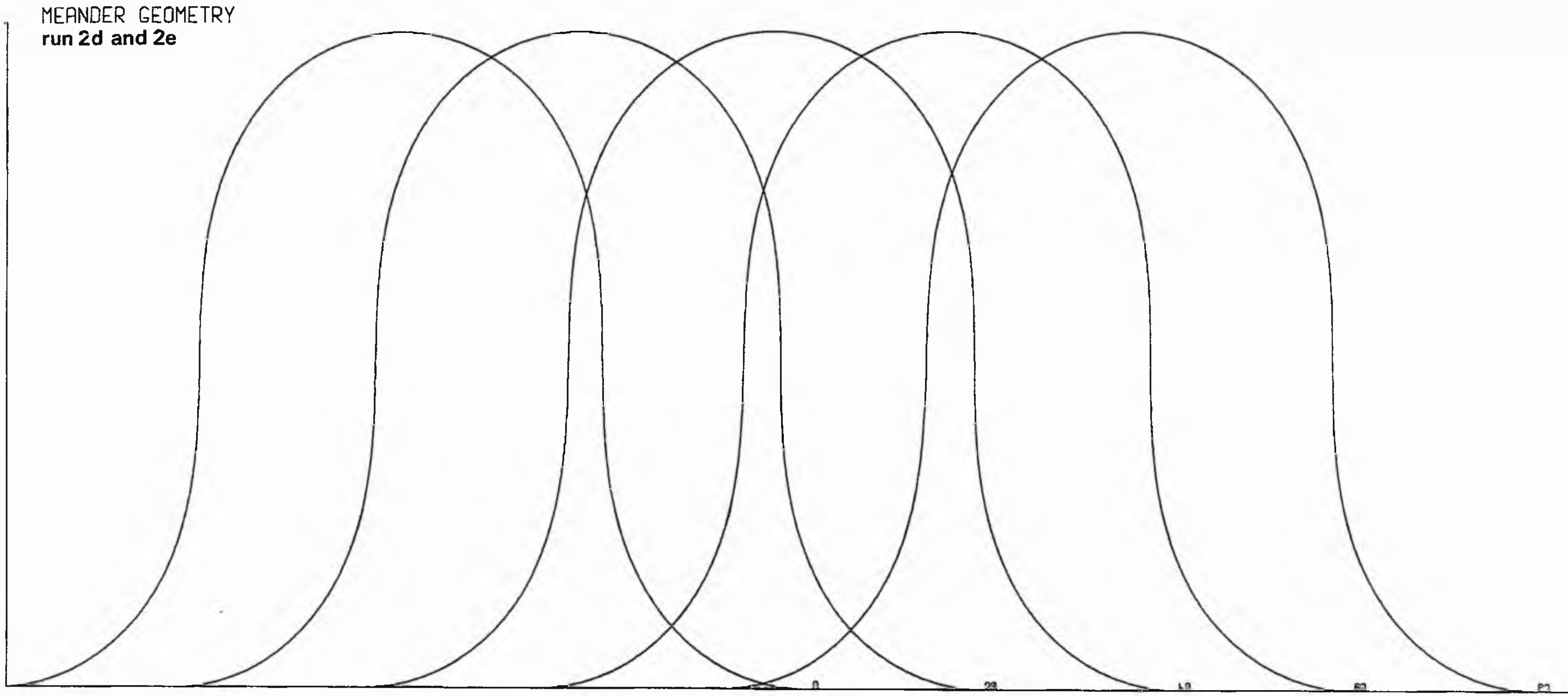

SCALE-1 INCH TO 84.55 METRES

Fig. 18.4. Meander plan forms for runs 2d, e and f.

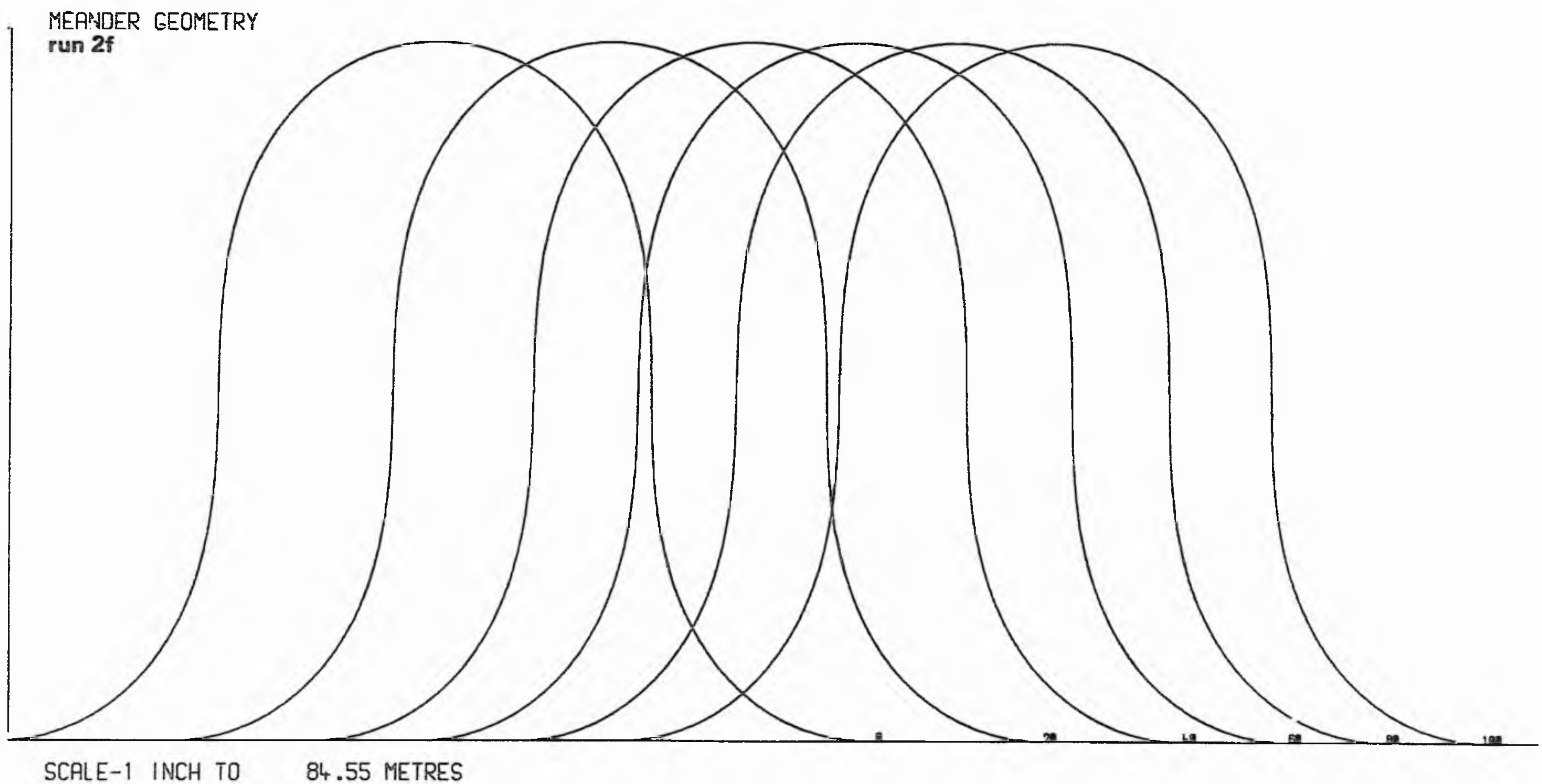

Fig. 18.4. - continued.

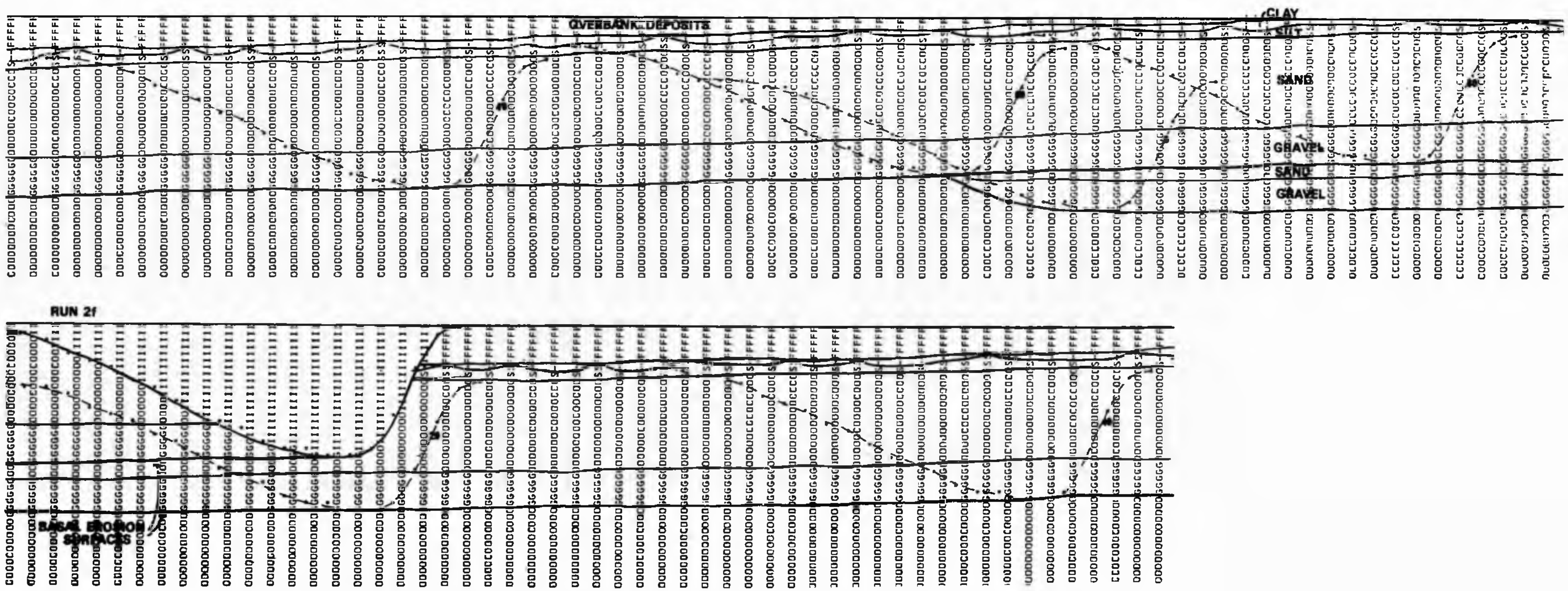

Fig. 18.5. Grain size section for run 2f.

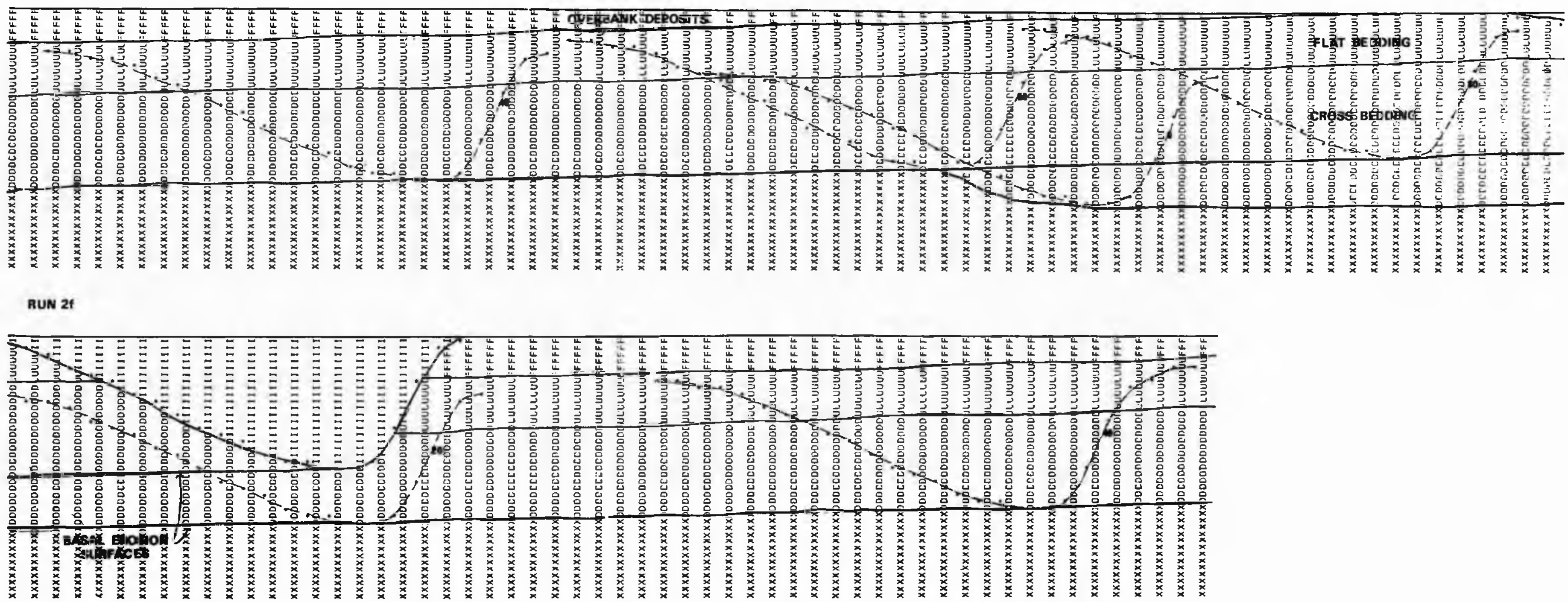

Fig. 18.6. Sedimentary structure section for run 2f.

and the upward sloping of the facies boundaries and basal erosion surfaces in the downvalley direction can be seen as in run 2c but with a less steep slope. However the gradual increase in the slope of these surfaces with time as the bank migration rate is reduced is not easily seen. Noteworthy is the sequence produced in this moving phase situation, gravel-sand-gravel-sand-silt-(clay)-overbank sediment. Again it should be noted that an aggradation rate of 0.1 m./year is very rapid and rather improbable, also that scouring and filling would obscure the simple patterns shown in figs. 18.5 and 18.6.

Runs 2g, h and i correspond to an average downvalley migration of about 42m./year. The time taken to move half a wavelength is a little over 10 years (see fig. 18.7), therefore there is about 0.01, 0.1 and 1 metres of sediment preserved between erosion surfaces, respectively with aggradation rates of 0.001, 0.01 and 0.1 metres/year. The aggraded thicknesses are not great enough to appear in the cross sections for 2g and 2h, and the effect of aggradation on bank migration rate is negligible. The grain size and sedimentary structure cross sections for the greatest rate of aggradation are shown in fig. 18.8 and fig. 18.9 respectively. The general features are similar to runs 2c and 2f, however, even in this extreme case, the slopes of the facies boundaries and basal erosion surfaces are not particularly marked.

The dependence of the shape of the wedge of overbank deposits and the upward slopes in the downvalley direction of the facies boundaries and basal erosion surfaces on the relative rates of bank migration and aggradation have been illustrated. The general upward slope in the downvalley direction of the facies boundaries and basal erosion surfaces (in the cross sections) is naturally equal to rate of aggradation divided by rate of down-valley migration; this slope must be corrected for valley slope, if an absolute value is required. It is expected, given the

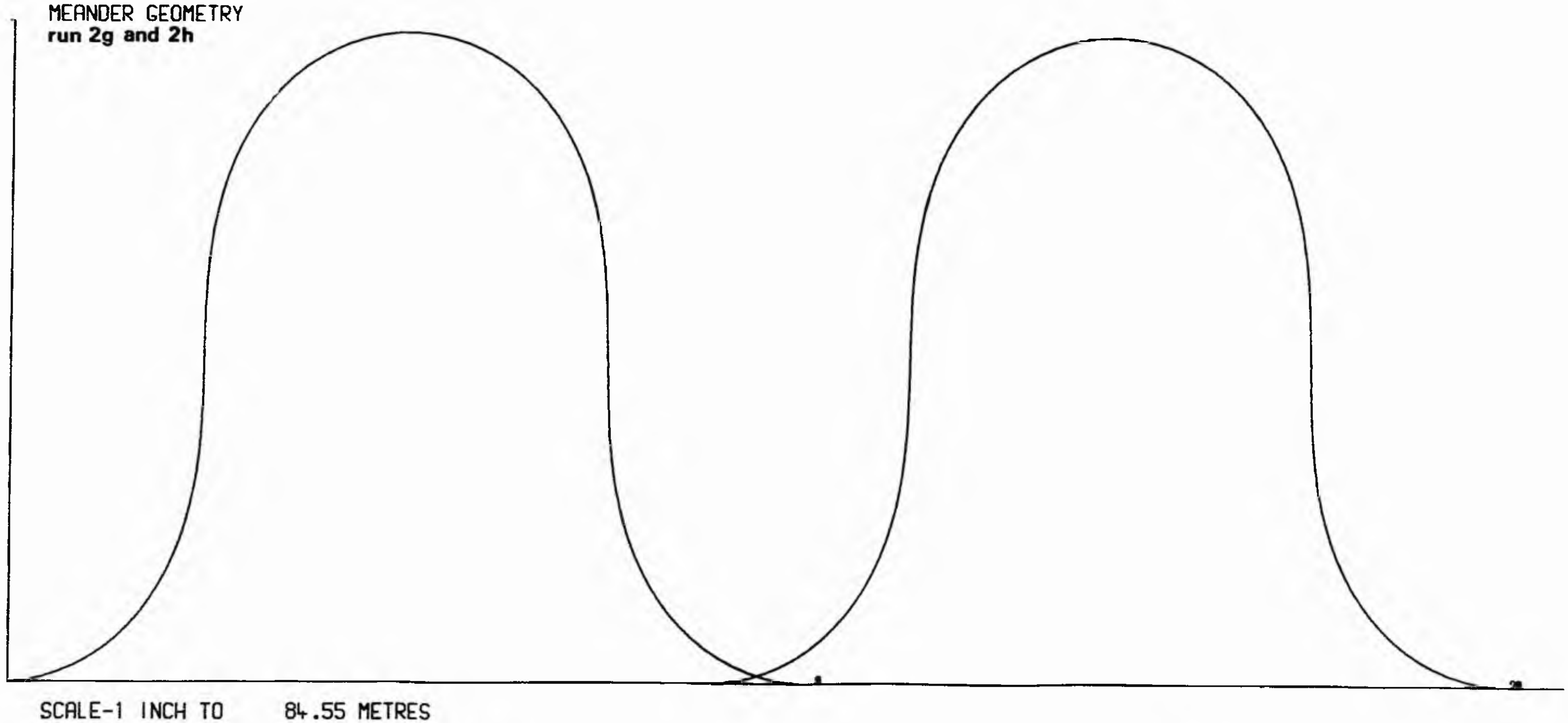

Fig. 18.7. Meander plan forms for runs 2g, h and i.

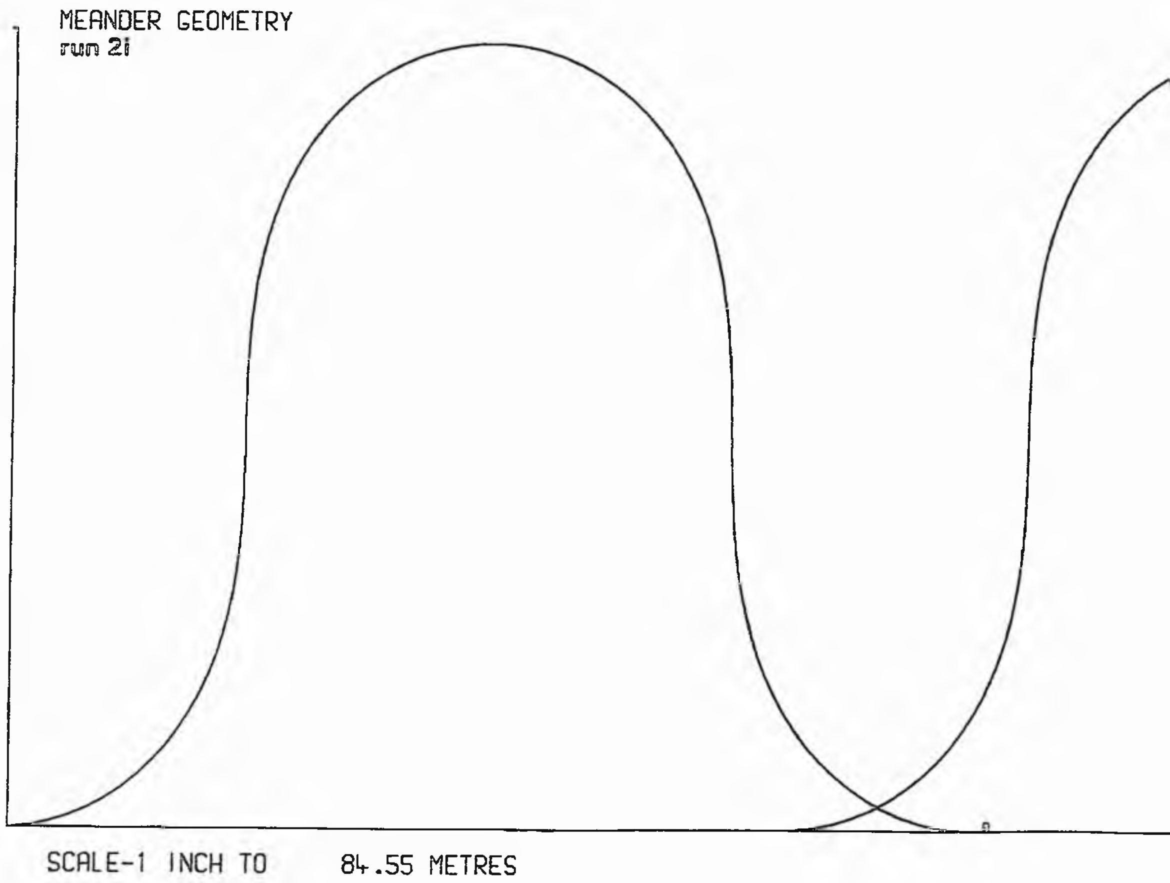

Fig, 18.7. - continued.

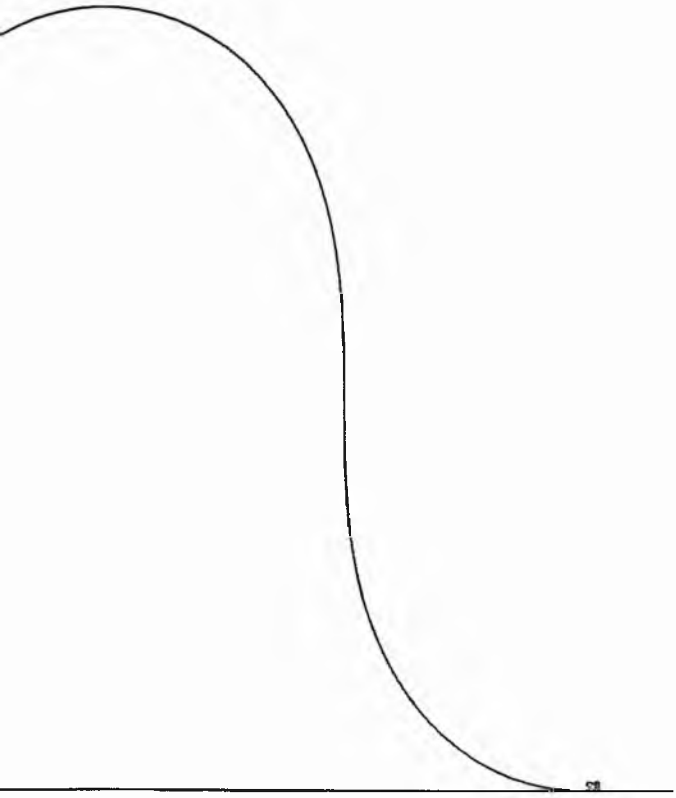

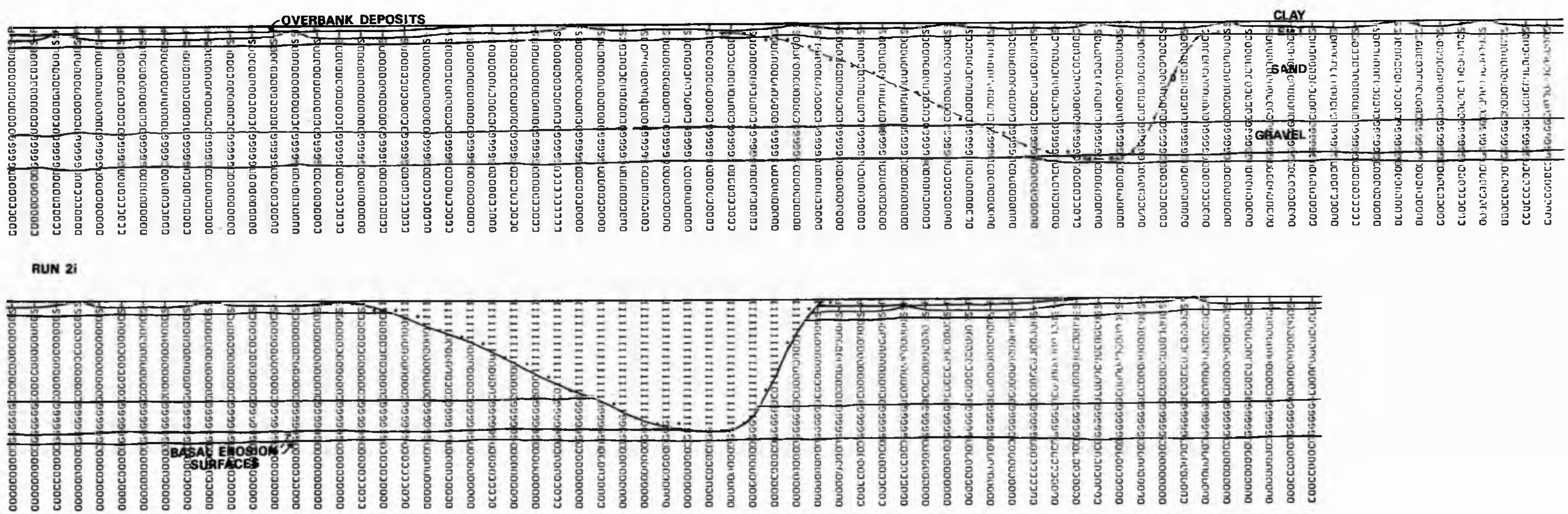

Fig. 18.8. Grain size section for run 2i.

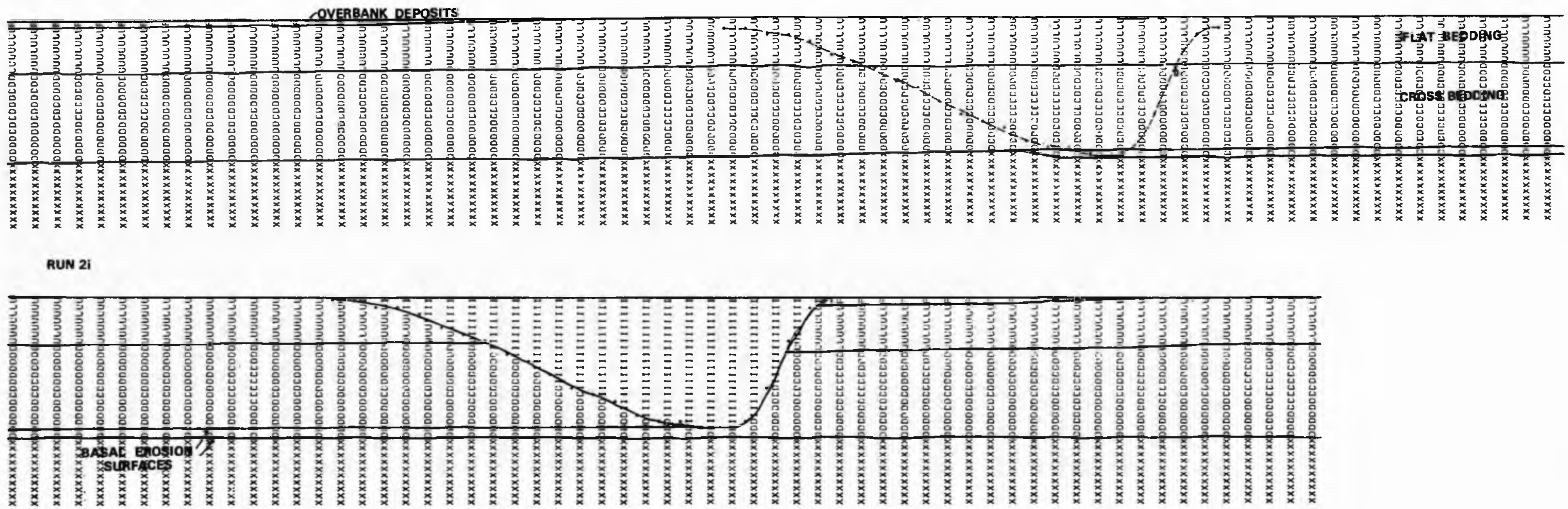

Fig. 18.9. Sedimentary structure section for run 2i.

natural observed rates of aggradation, that in the moving phase situation the thin overbank deposits will probably appear virtually constant in thickness (on the larger scale) although basically wedge shaped. Facies boundary slopes on the large scale will also be negligible. Smaller scale complications are introduced when considering scouring and filling, or if the relief of the flood-plain and variability of overbank sedimentation and erosion were accounted for.

The thickness of the deposit preserved in a moving phase situation, in these cross sections, follows the simple algorithm,

$$\text{thickness of deposit} = \frac{1}{2}\,\frac{\text{aggradation rate}}{\text{migration rate}},$$

although this is only approximate as there may be scouring and filling to complicate matters. Preserved thicknesses of sediment are expected to be only fractions of the total point bar thickness in the moving phase situation, and Bluck (1971) notes that many sequences of believed fluvial origin have many erosion surfaces at their base. Clearly greater thicknesses or complete sequences may be built up if the eroding medium does not act on the sediments for a long interval of time with respect to the aggradation rate. This may apply in the case of the avulsion situation or in the case of a cut-off which lies out of range of the main channel for a sufficient length of time, as discussed by Bluck (1971). It would appear that if the general slope of facies boundaries or basal erosion surfaces relative to the land surface is not great and complete bar sequences are preserved, then a process other than purely moving phase must be responsible.

19 EXPERIMENT 4 - DEVELOPING MEANDERS

According to the model, as meanders increase in amplitude and sinuosity, wavelength remaining constant, both longitudinal water surface slope and radius of curvature will change. In natural rivers with the independent variables unchanging, width, depth at the talweg, the friction coefficients, and the value of n_1 may be expected to vary to some extent, although such variation cannot be accounted for and is assumed absent for our present purposes. There may also be a systematic variation in the average scour depth as the meander develops, which is also not accounted for in the model. By inspection of equation 5.20, the model would predict a general decrease in the calibre of load as sinuosity exceeds 1.5. Up to a sinuosity of 1.5, depending on the relative changes in S and r_1, the general calibre could increase, decrease or remain about constant. It is noteworthy that increasing depth or width would always tend to increase general calibre of load.

In general, stream power will decrease as slope decreases at constant discharge (Bagnold, 1966, p. 15) and the dimensionless shear stress will vary with the ratio r_m/w (see equation 5.25). Such variation, combined with variation in D, will be expected to affect the distribution of bed form and sedimentary structures over the bar as the meander develops. In general, lower flow-regime forms are expected to increase at the expense of upper plane beds as sinuosity increases.

As the meander develops, the angle at which the mean channel direction cuts the line of section (lateral or downvalley) will cause the projected channel width to vary. This will be expected to affect the facies patterns within the bar in the cross sections represented in this experiment. An interesting point in this respect is that field sections of fluvial sedimentary rocks may suggest different channel widths due to varying channel direction

Table 19.1.

Run number	4A/a and 4B/a	4A/b and 4B/b	4A/c and 4B/c
Average initial rate of migration normal to mean downvalley direction (Metres/year)	3	9	30
BANK MIGRATION PARAMETERS			
exponent n_2		0.5	
constant k_2	0.3E-06	0.9E-06	0.3E-05
constant k_3		0.1E-03	

Same parameters for experiment 4A (downvalley section) and experiment 4B (lateral section).

FLUVIATILE PROCESS SIMULATION   EXPERIMENT 4B

CROSS SECTION PARAMETERS	METRES	CELLS
WIDTH OF SECTION	1000.000	200
THICKNESS OF SECTION	60.000	60
INITIAL DISTANCE OF INNER CHANNEL BANK FROM L.H.S. OF SECTION	0.0	0
INITIAL BANKFULL STAGE MEASURED FROM SECTION BASE	60.000	60
CELL SIZE IN VERTICAL(Y) DIRECTION	1.000	
CELL SIZE IN HORIZONTAL(Z OR X) DIRECTION	5.000	

CHANNEL PARAMETERS	METRES	CELLS	
TOTAL WIDTH OF CHANNEL(W)	125.000	25	
WIDTH OF FLOW BETWEEN INNER BANK AND TALWEG(W1)	100.000	20	
RATIO OF W1 TO W			0.800
MAXIMUM FLOW DEPTH MEASURED ABOVE TALWEG	20.000		
DENSITY OF SEDIMENTARY PARTICLES			2.650 GM/CM3
FLUID DENSITY			1.000 GM/CM3
DARCY-WEISBACH FRICTION COEFFICIENT FOR DUNES AND RIPPLES			0.210
DARCY-WEISBACH FRICTION COEFFICIENT FOR PLANE BEDS AND ANTIDUNES			0.150
EXPONENT N1			1.000

SYNTHETIC HYDROLOGY PARAMETERS(UNITS NOT NECESSARY)

MEAN OF ALL DAILY MEAN VALUES	543.500						
STANDARD DEVIATION OF DAILY MEAN VALUES	441.000						
MEAN OF YT SERIES	0.0						
STANDARD DEVIATION OF YT SERIES	1.000						
COEFFICIENTS IN AUTOREGRESSIVE MODEL	A1= 0.567	A2=	C.306				
	HARMONICS FROM 1 TO 6						
FOURIER COEFFICIENTS FOR DAILY MEANS(A)	-200.300	145.400	-85.500	58.000	-39.800	7.400
(B)	-112.400	185.000	-79.900	65.600	-72.500	27.800
FOURIER COEFFICIENTS FOR DAILY STD DEVIATIONS(SA)	-123.300	141.600	-66.400	75.700	-47.200	8.600
(SB)	-85.600	105.700	-46.200	31.700	-43.200	4.300
MAXIMUM VALUE OF QVOL	110000.000						

SCOUR AND FILL PARAMETERS	
CONSTANT K4	0.100E-03
EXPONENT N3	1.000
STANDARD DEVIATION OF ERROR TERM	1.000

CUT-OFF CONTROL PARAMETERS				
LIMITING WIDTH OF MEANDER NECK		225.000 METRES		
EXPONENTS IN NECK CUT-OFF RELATION	EN1=	5.000	EN2=	5.000
LIMITING SINUOSITY		3.000		
LIMITING AMPLITUDE		1185.529 METRES		
EXPONENTS IN CHUTE CUT OFF RELATION	EC1=	20.000	EC2=	20.000

LEGEND

LOWER PHASE PLANE BED	L	GRAVEL	G	OLD SEDIMENT	X
RIPPLES	R	SAND	O	WATER	I
DUNES	D	SILT	S	TIME LINE	.....
UPPER PHASE PLANE BED	U	CLAY	-	AIR	BLANK
ANTIDUNES	A	OVERBANK DEPOSITS	F		

PLANIMETRIC FORM OF MEANDER	METRES	
WAVELENGTH	1000.000	
AMPLITUDE	205.834	
SINUOSITY		1.100
RADIUS OF CURVATURE AT BEND AXIS	280.638	
WIDTH OF MEANDER NECK	**********	
CHANNEL LENGTH ALONG MEANDER	1099.999	
VALLEY SLOPE		0.00010000
LONGITUDINAL WATER SURFACE SLOPE		0.00009091

SELECTED GEOMETRIC RATIOS	
WAVELENGTH TO RADIUS OF CURVATURE	3.563
WAVELENGTH TO CHANNEL WIDTH	8.000
RADIUS OF CURVATURE TO CHANNEL WIDTH	2.245
AMPLITUDE TO CHANNEL WIDTH	1.647

Table 19.2. Initial data for experiment 4A and 4B.

relative to the plane of the section. Furthermore, in lateral sections only, the effect of slowing down of bank migration normal to the mean downvalley direction will be expected to influence the sedimentary facies patterns.

The experiment consists of three runs of the program using a lateral section and another three similar runs using a down-valley section. The three separate runs for each type of section correspond to three different average initial rates of bank migration normal to the mean downvalley direction as the meander develops from a sinuosity of 1.1 to a limiting value of 3.0. The average downvalley migration rate is constant for all runs (about 2.3 m./year), as is the selected average depth of scour. The input data that are different for each run are shown in table 19.1, and these correspond to average initial rates of about 3,9 and 30 metres per year. All other input parameters, shown in table 19.2 and 19.1, are the same for all runs. Fig. 19.1 shows the meander movement simulated which are responsible for the sedimentary deposits in the forthcoming cross sections. The data deck set-up for all six runs is listed in appendix 3.

In runs 4A and 4B the cross sections were comprised of 200 by 60 cells. In 4A a disc was used, 78k bytes of core store were required, and approximate running times were 7½ seconds per time increment. In 4B no disc was used, 129k bytes of core store were required, and approximate running times were 3 seconds per time increment.

Fig. 19.2 shows the variation of hydraulic parameters, at a specific station, as the meander develops, for the three separate input conditions. The station corresponds to a depth of 10 metres, or half the maximum unscoured talweg depth. The curves for D indicate a general increasing calibre of load followed by a more substantial decrease in calibre. The turning point here

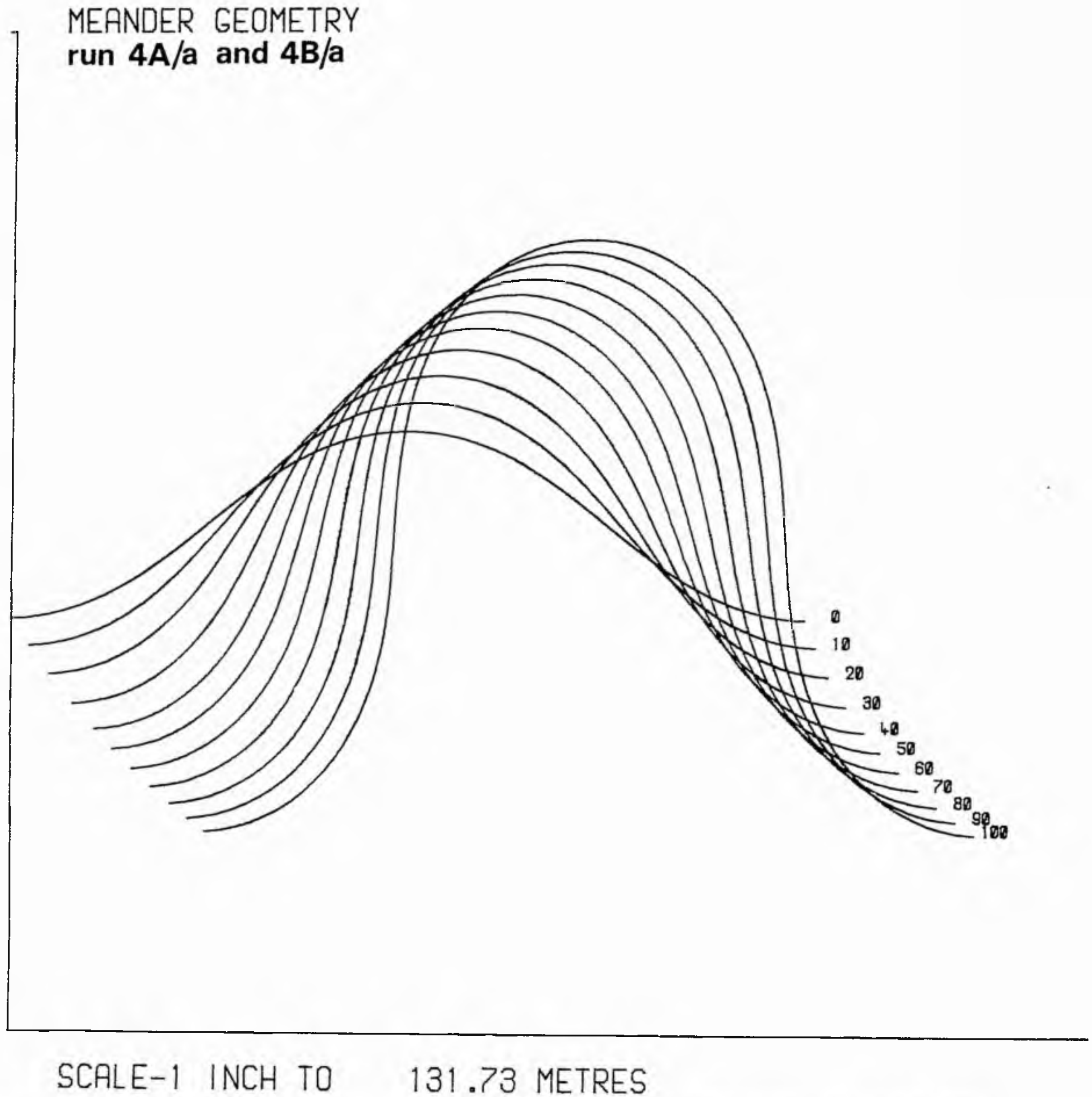

Fig. 19.1. Meander plan forms for experiments 4A and 4B.

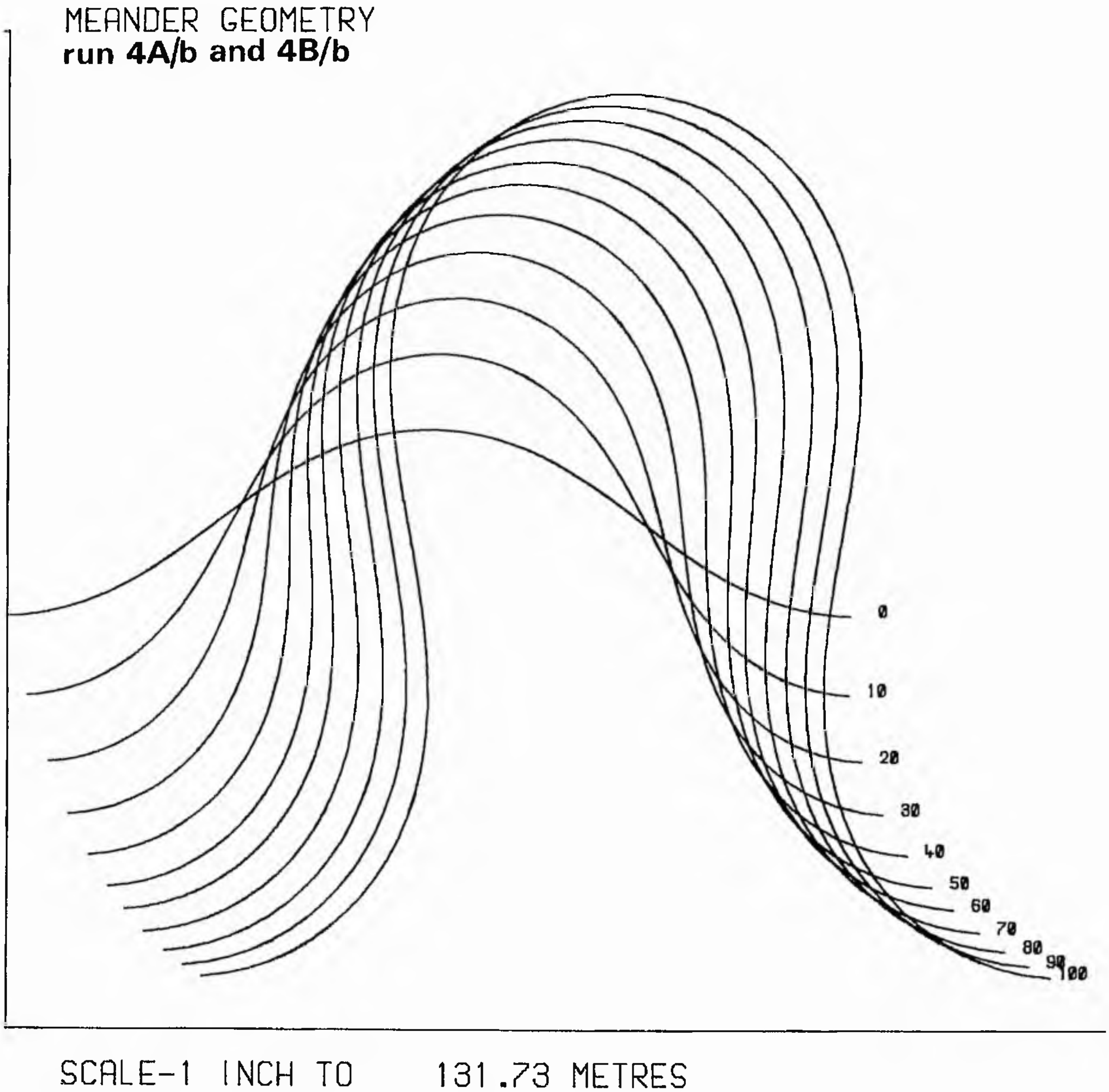

Fig. 19.1. - continued.

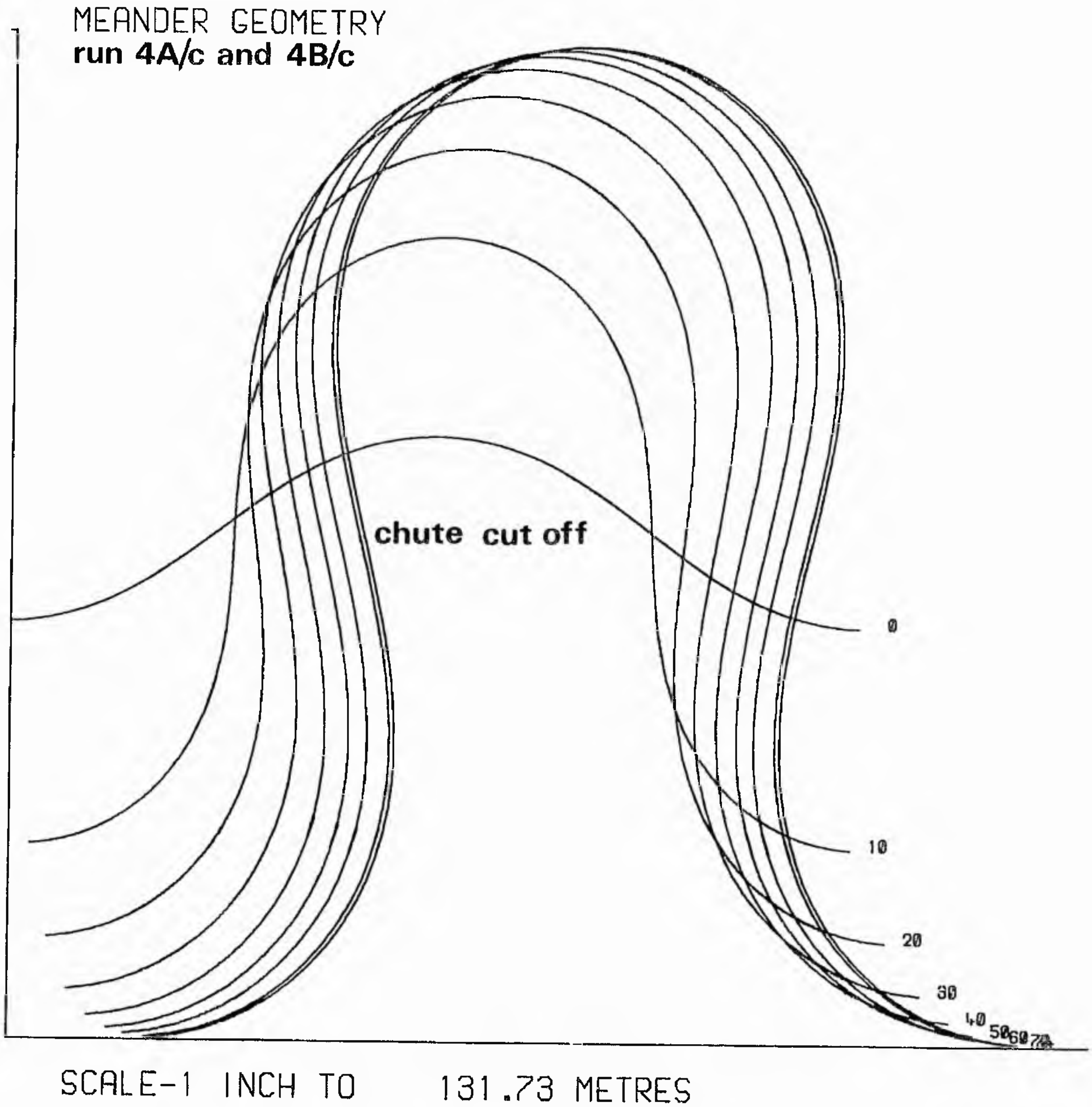

Fig. 19.1. - continued.

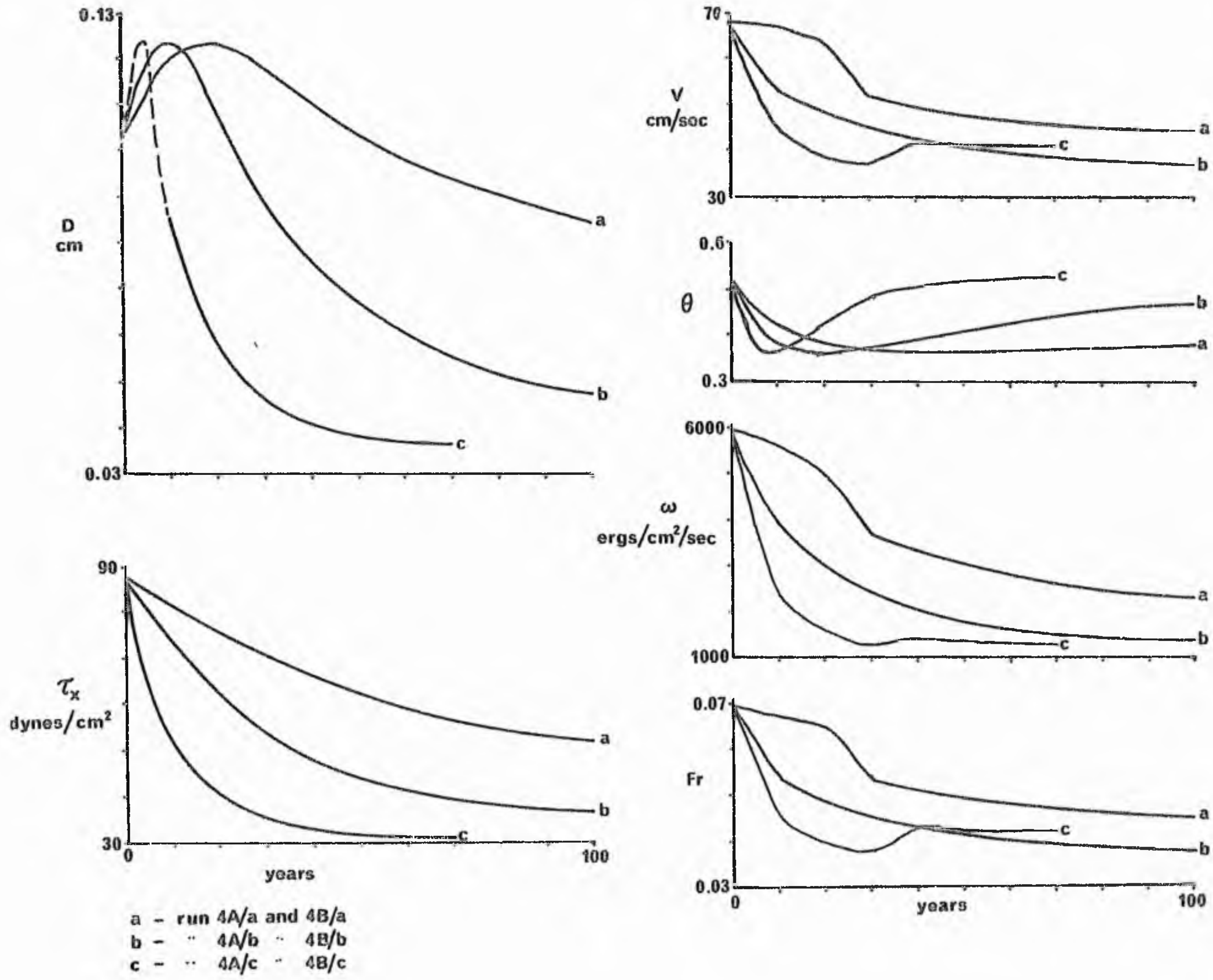

FIG. 10.2 VARIATION OF HYDRAULIC PARAMETERS AT A GIVEN DEPTH (10 METRES) FOR A DEVELOPING MEANDER WITH THREE DIFFERENT RATES OF AMPLITUDE GROWTH.

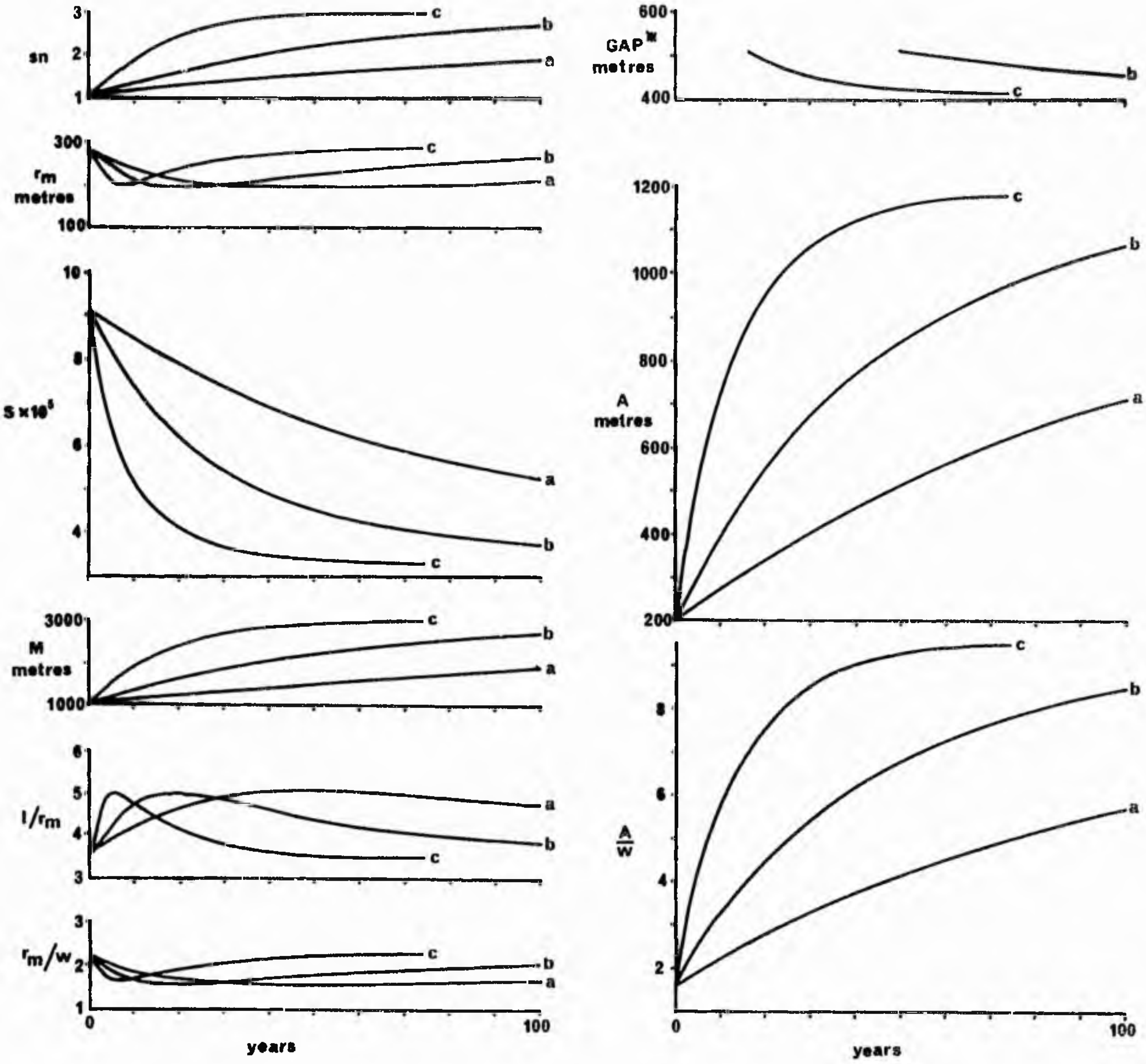

a – run 4A/a and 4B/a
b – " 4A/b " 4B/b
c – " 4A/c " 4B/c

* GAP is measured between channel centre lines here

FIG. 10.3 VARIATION OF GEOMETRIC PARAMETERS FOR DEVELOPING MEANDER WITH THREE DIFFERENT RATES OF AMPLITUDE GROWTH.

corresponds to a sinuosity of about 1.3. The curves for D would be expected to be influenced slightly by changes in width, depth at talweg and n_1. The curves of τ_x show a systematic decreasing trend, and these, being defined for a given depth of 10m., will remain independent of variation in width, depth at talweg, friction factors and n_1. Curves for θ show the expected trend as they depend on the ratio r_m/w (see fig. 19.3). Changes in width or n_1 will influence these curves. The curves of ω, V and Fr are all generally decreasing, the 'kinks' being the result of change in bed form from upper phase plane beds to dunes. These curves will only be influenced by changes in f.

Fig. 19.3 shows the variation of certain geometric parameters as the meander develops for the three separate input conditions. Parameters involving r_m show the characteristic turning point at sinuosity of 1.5. Those involving amplitude show the effect of the gradually decreasing rate of amplitude growth. The width of the meander neck here refers to the distance between channel centre lines, not adjacent banks.

Runs 4A/a,b and c, figs. 19.4 and 19.5, are downvalley sections, with the average rate of downvalley migration being constant at about 2.3 m./year. The main feature of the grain size sections is the gradual lateral decrease in thickness of gravel and increase in sand, silt and clay thicknesses, after a small initial increase in general calibre (as indicated in fig. 19.2). The degree of lateral change increases from section 4A/a to 4A/c as the initial rates of amplitude growth increase. Section 4A/c shows a tendency for interfingering to develop. The previous channel positions in all sections show the changes in the projected channel width in the cross sections as the meander develops. The relief of the basal scoured surfaces and facies boundaries were discussed earlier.

The main feature of the sedimentary structure cross sections

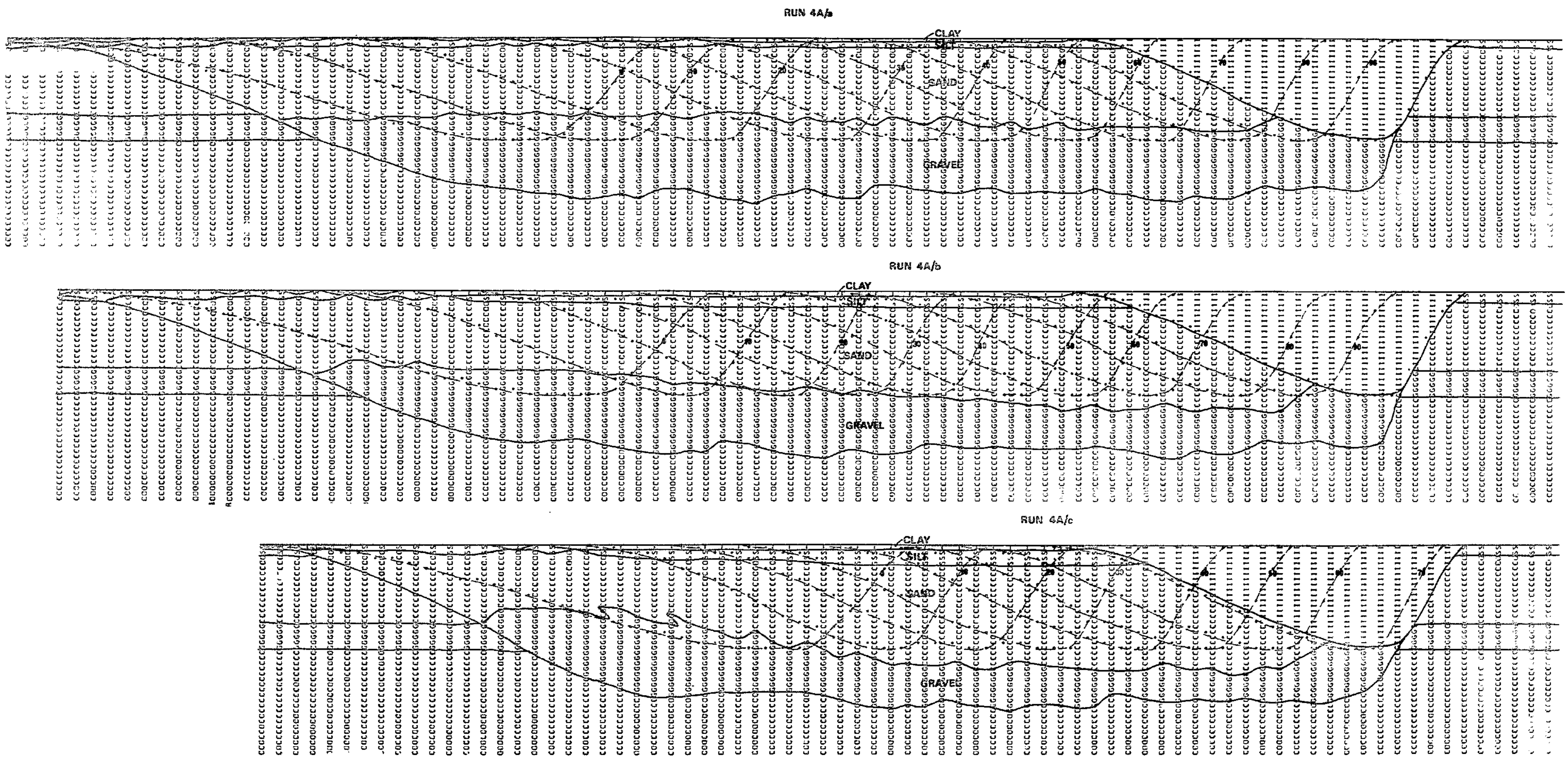

Fig. 19.4. Grain size sections for experiment 4A.

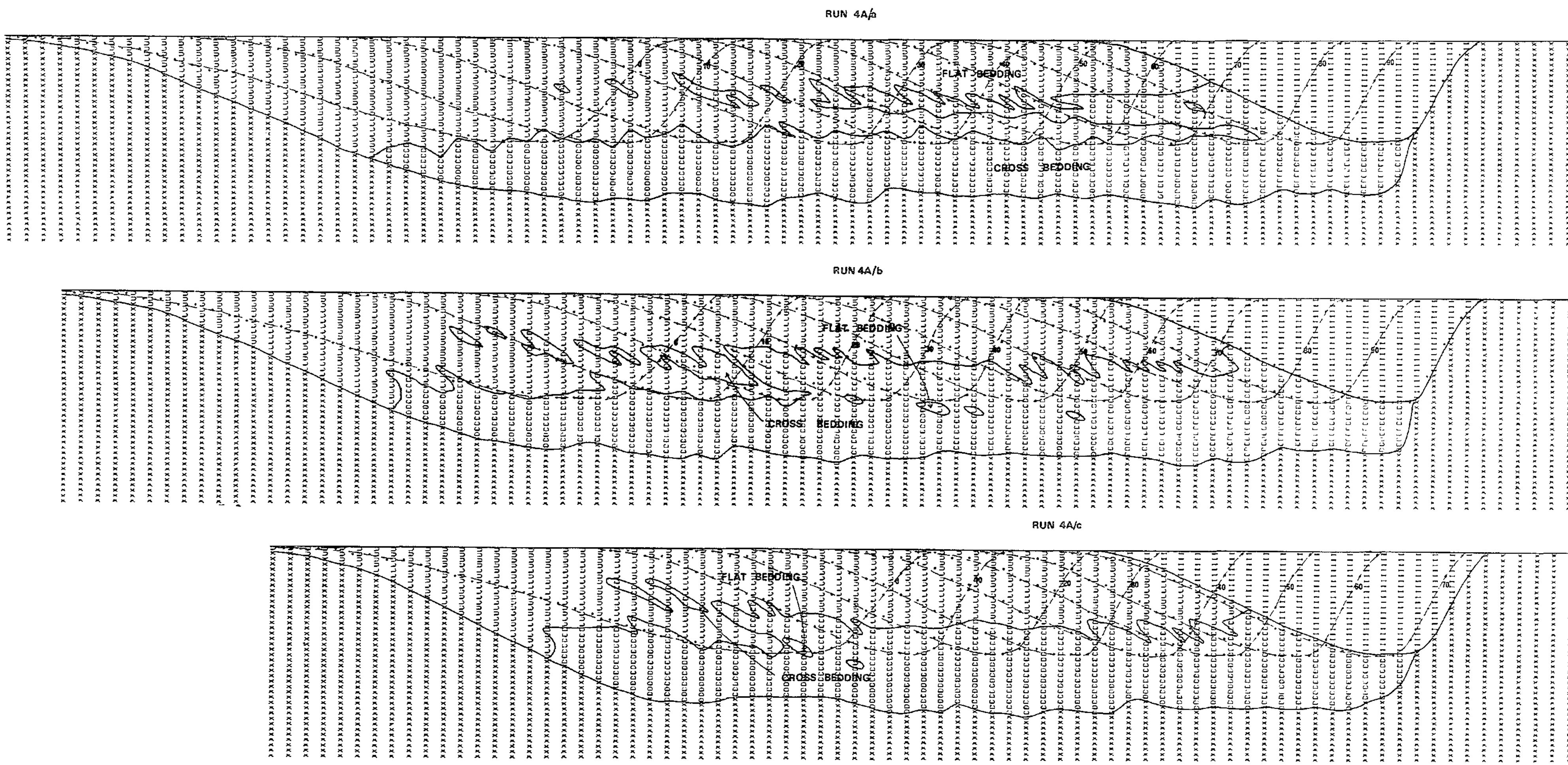

Fig. 19.5. Sedimentary structure sections for experiment 4A.

of 4A/a,b and c is the lateral increase of cross bedding at the expense of flat bedding. With gradual increase in the amount of cross bedding there is a transition area of considerable lateral extent which is a large-scale interfingering of flat beds and cross beds. The interfingering wedges of flat bedding or cross bedding break down laterally into lenses. The lateral extent of the transitional area decreases as the rate of amplitude growth increases. The smaller scale relief of the flat-bedding-cross-bedding boundary has been discussed elsewhere. It is noteworthy that such large scale interfingering produces a cyclical vertical sequence of cross-flat-cross-flat bedding continuously for a considerable lateral extent.

Runs 4B/a,b and c, figs. 19.6 and 19.7, are lateral sections, and therefore, by virtue of their definition, the projected channel widths are gradually increasing as the meander develops (as opposed to runs 4A). The grain size distribution cross sections are broadly similar to runs 4A except the same changes in grain size as occurred in 4A have in general occupied a greater lateral extent. The different rates of channel migration in these sections have also affected the smaller scale relief of the grain size facies boundaries, as opposed to 4A where channel migration is identical for each section. In these cases, therefore, the overall thinning or thickening of the various grain-size units may be overshadowed in field sections by local variation in thickness, the general trend only appearing over sections with large lateral extent.

Similar comments can be made with regard to the comparison of the sedimentary structure cross sections of 4B with 4A. In particular, the transition involved with the increase in cross bedding extends laterally for a greater extent, and the different migration rates have affected the smaller scale relief of the flat-cross bedding boundary.

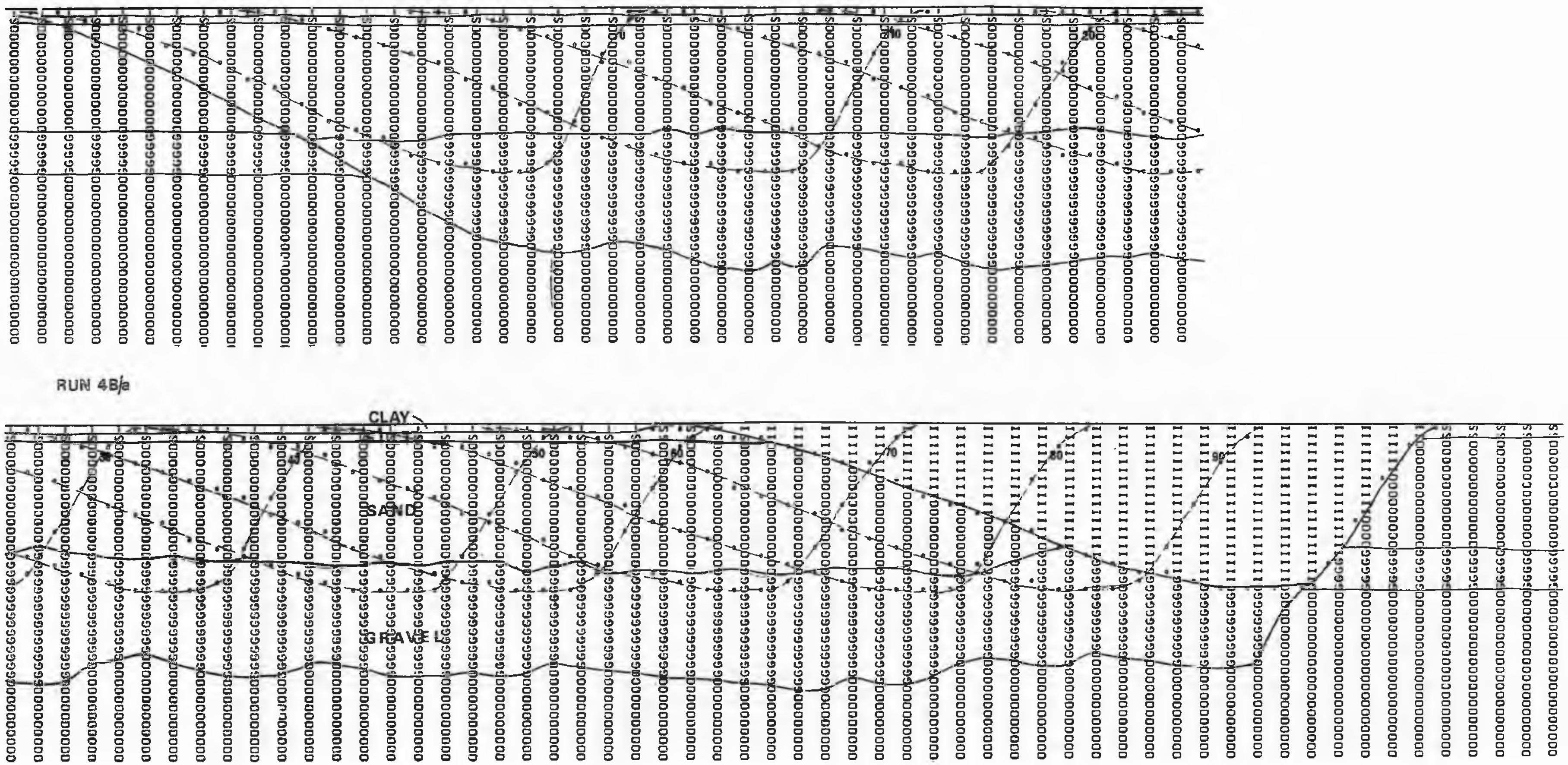

Fig. 19.6. Grain size sections for experiment 4B.

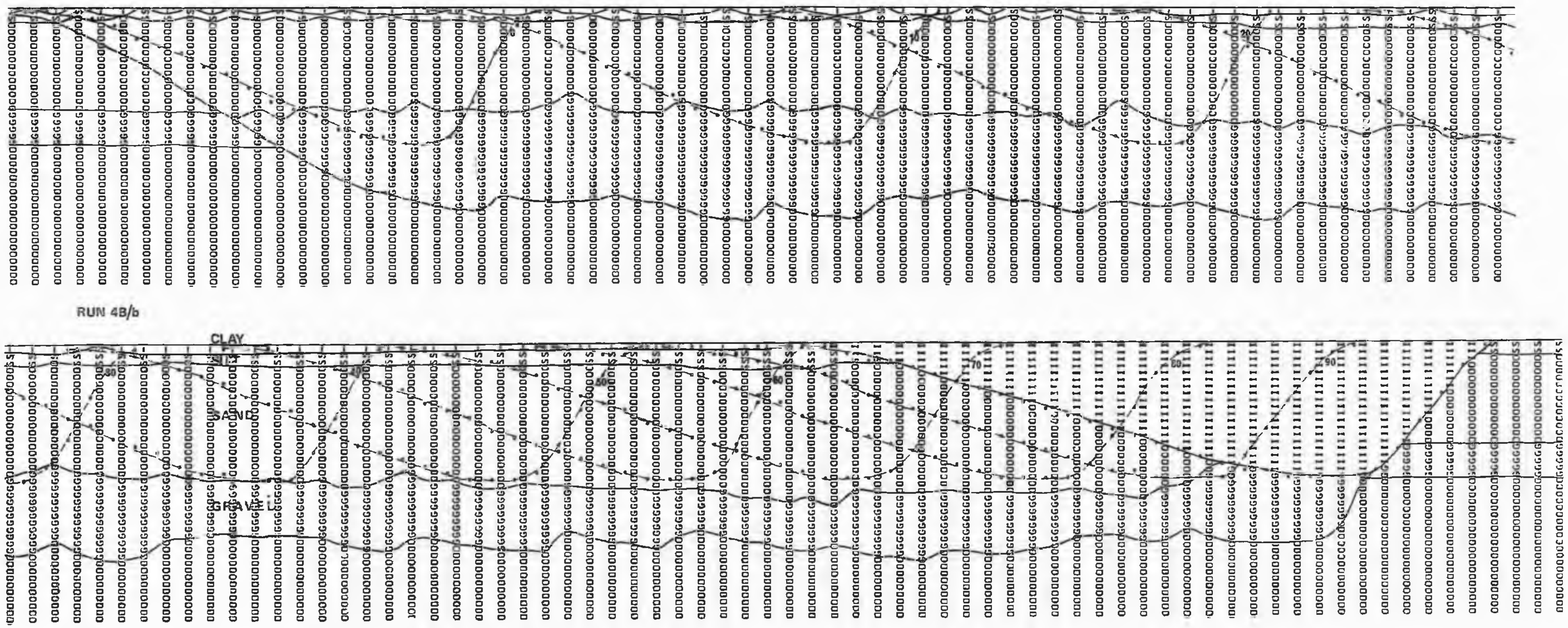

Fig. 19.6. - continued.

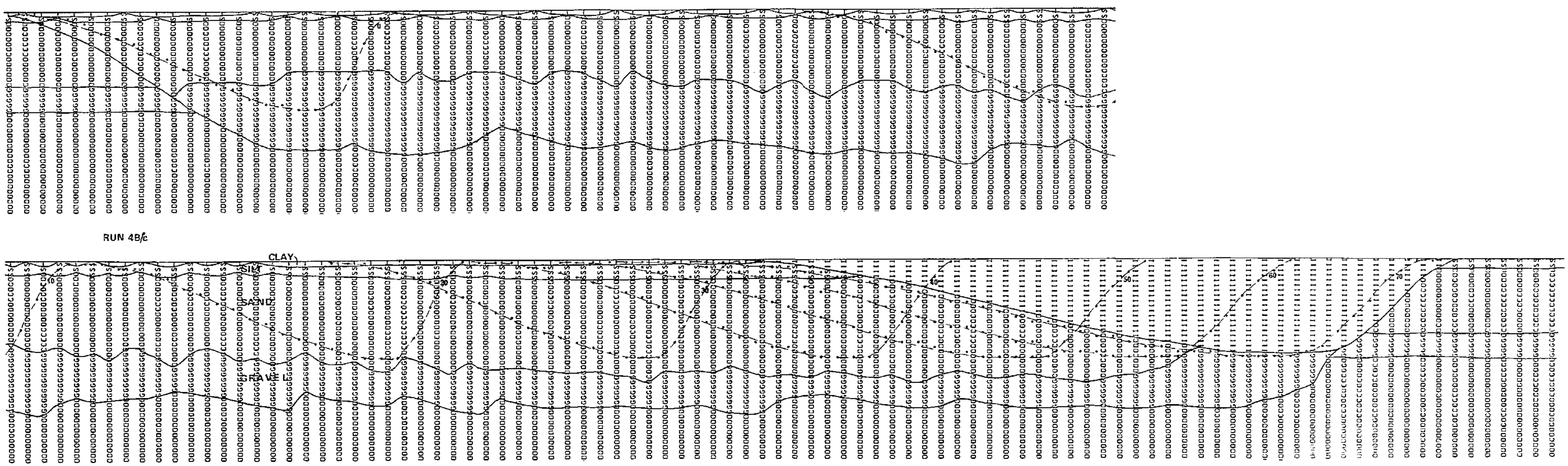

Fig. 19.6. - continued.

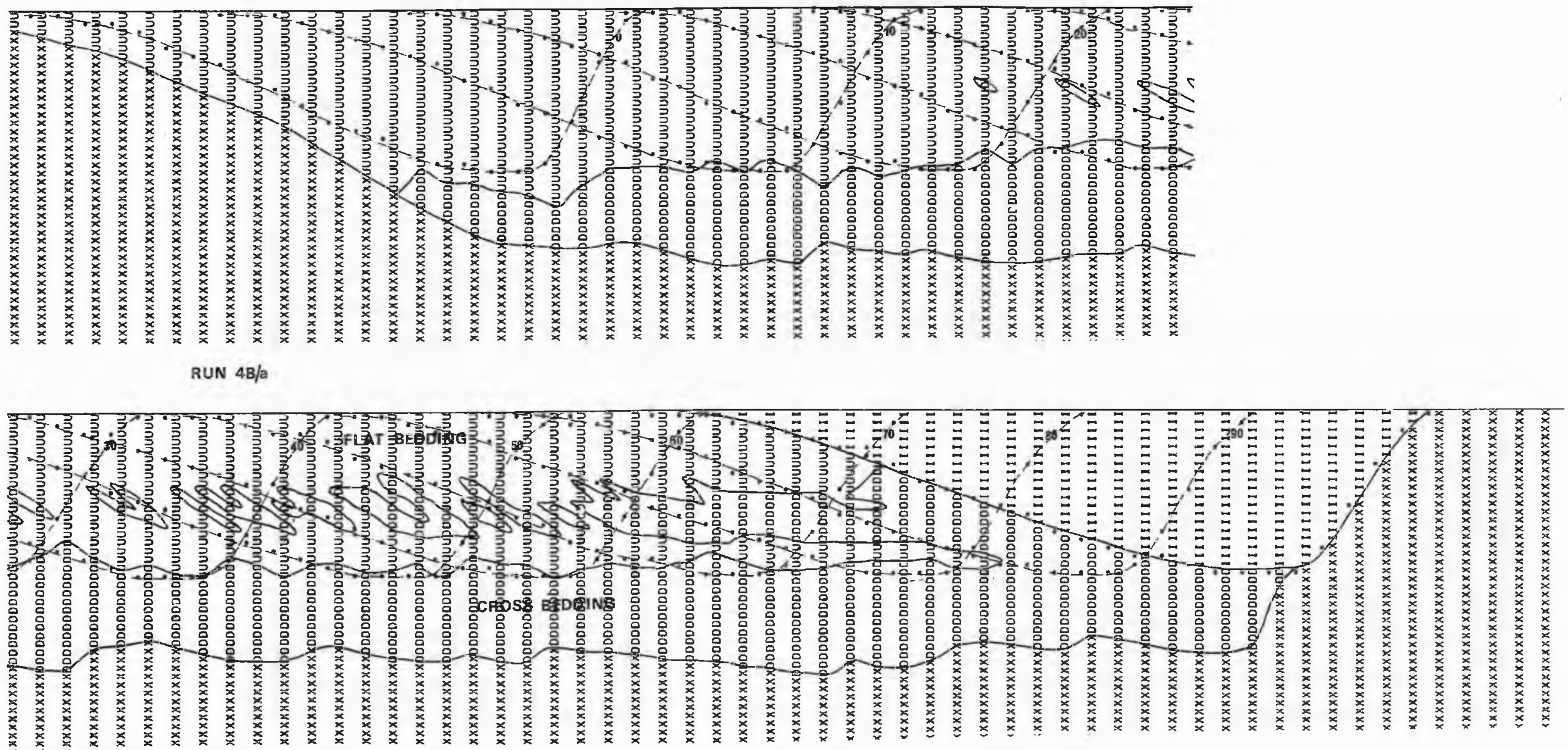

Fig. 19.7. Sedimentary structure sections for experiment 4B.

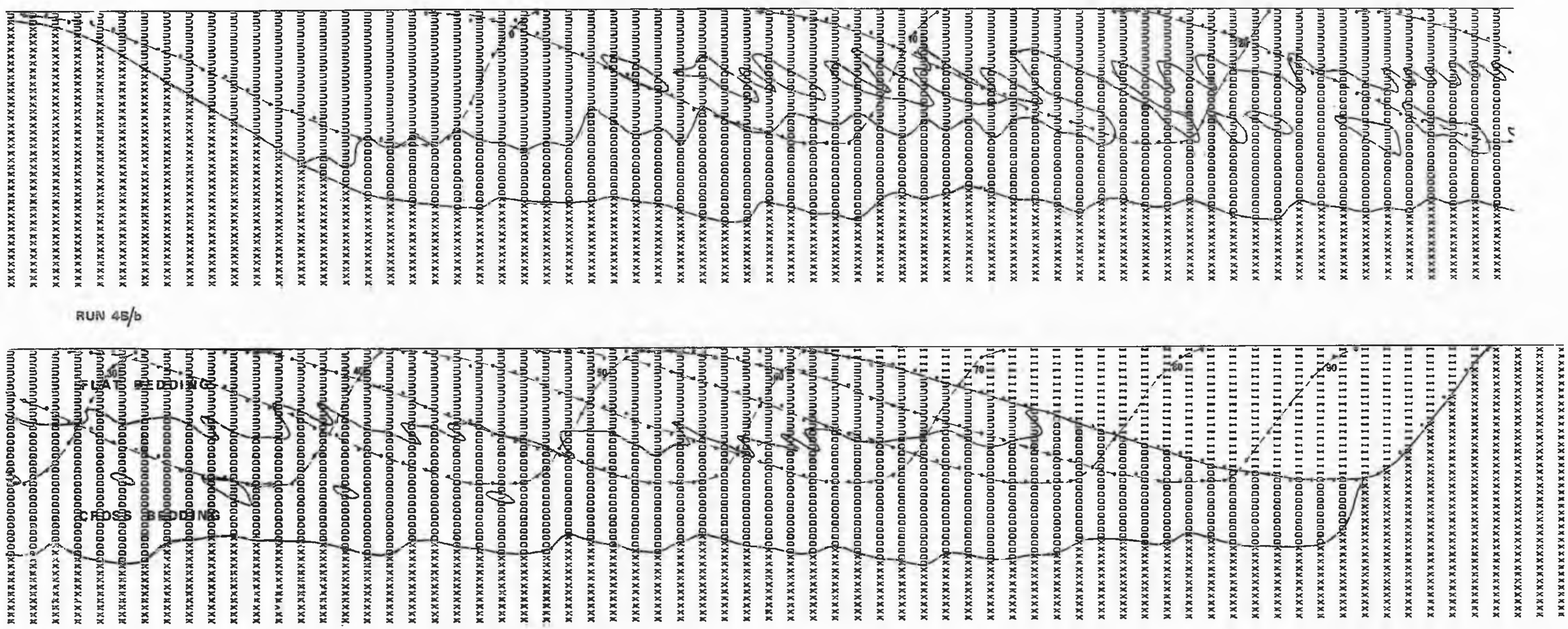

Fig. 19.7. - continued.

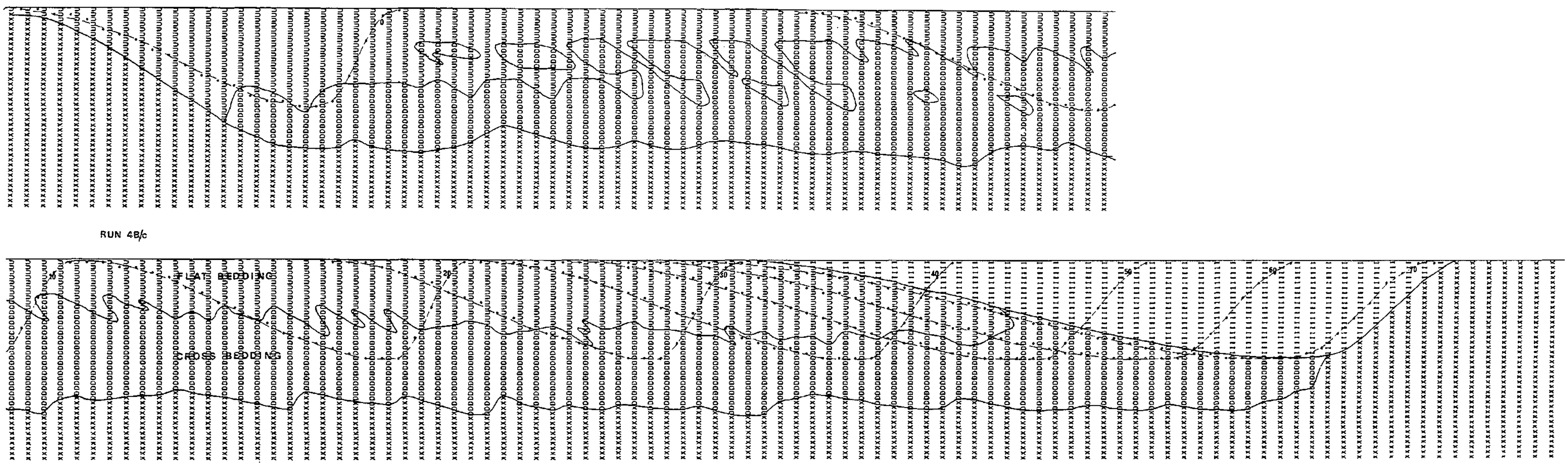

Fig. 19.7. - continued.

20 EXPERIMENT 5 - DEVELOPING MEANDERS

Experiment 5 is designed to illustrate the sedimentation patterns associated with aggradation as meanders are developing from a sinuosity of 1.1 to a limiting sinuosity. A lateral section is used for each of nine runs of the program, which correspond to all combinations of three different rates of aggradation (0.001,0.01, and 0.1 metres/year) and three different modes of meander migration. In this experiment the downvalley migration rates are not constant for all runs. The data which are different for each run are shown in table 20.1, and the bank migration parameters correspond to average initial rates of movement normal to the mean downvalley direction, and average downvalley migration, of about 3 and 2.2 m./year, 9 and 2.2 m./year, and 30 and 7 m./year, respectively, for the three different modes of meander movement. All other input parameters, shown in table 20.2, and 20.1, are the same for all nine runs. No scouring and filling is assumed, as in experiment 2, in order to simplify examination of the cross sections. Again, therefore, the sedimentary structure and grain size cross sections should be viewed bearing in mind all the simplifications and approximations involved. The data deck set-up for all nine runs is listed in the appendix 3. This experiment used no disc, the cross sections comprised 200 by 60 cells, and 129k of core store were required. The approximate running times were 2 seconds per time increment.

The simulated point-bar deposits, as shown in figs. 20.1 and 20.2, show essentially the same features as in experiment 4. The main points are the gradual lateral decrease in the general calibre of sediment, after an initial increase, and the lateral increase in cross bedding at the expense of flat bedding, with a large scale interfingering within a transition zone. The grain size and sedimentary-structure facies boundaries and basal erosion surfaces are more simplified, however, because of the lack of

Run number	5a	5b
Average initial migration rate normal to mean downvalley direction (metres/year)	3	
Average downvalley migration rate (metres/year)	2.2	
BANK MIGRATION PARAMETERS		
exponent n_2		
Constant k_2	0.3E-06	
Constant k_3		
Aggradation rate (metres/year)	0.001	0.01

Table 20.1

	5c	5d	5e	5f	5g	5h	5i
			9			30	
			2.2		7		
			0.5				
			0.9E-06		0.3E-05		
	0.1E-03				0.3E-03		
	0.1	0.001	0.01	0.1	0.001	0.01	0.1

FLUVIATILE PROCESS SIMULATION EXPERIMENT 5

CROSS SECTION PARAMETERS	METRES	CELLS
WIDTH OF SECTION	1000.000	200
THICKNESS OF SECTION	60.000	60
INITIAL DISTANCE OF INNER CHANNEL BANK FROM L.H.S. OF SECTION	0.0	0
INITIAL BANKFULL STAGE MEASURED FROM SECTION BASE	30.000	30
CELL SIZE IN VERTICAL(Y) DIRECTION	1.000	
CELL SIZE IN HORIZONTAL(Z OR X) DIRECTION	5.000	

CHANNEL PARAMETERS	METRES	CELLS	
TOTAL WIDTH OF CHANNEL(W)	125.000	25	
WIDTH OF FLOW BETWEEN INNER BANK AND TALWEG(W1)	100.000	20	
RATIO OF W1 TO W			0.800
MAXIMUM FLOW DEPTH MEASURED ABOVE TALWEG	20.000		
DENSITY OF SEDIMENTARY PARTICLES			2.650 GM/CM3
FLUID DENSITY			1.000 GM/CM3
DARCY-WEISBACH FRICTION COEFFICIENT FOR DUNES AND RIPPLES			0.210
DARCY-WEISBACH FRICTION COEFFICIENT FOR PLANE BEDS AND ANTIDUNES			0.150
EXPONENT N1			1.000

SYNTHETIC HYDROLOGY PARAMETERS(UNITS NOT NECESSARY)

MEAN OF ALL DAILY MEAN VALUES		543.500					
STANDARD DEVIATION OF DAILY MEAN VALUES		441.000					
MEAN OF YT SERIES		0.0					
STANDARD DEVIATION OF YT SERIES		1.000					
COEFFICIENTS IN AUTOREGRESSIVE MODEL	A1=	0.567	A2=	0.306			
		HARMONICS FROM 1 TO 6					
FOURIER COEFFICIENTS FOR DAILY MEANS(A)		-200.300	145.400	-85.500	58.000	-39.800	7.400
(B)		-112.400	185.000	-79.900	65.600	-72.500	27.800
FOURIER COEFFICIENTS FOR DAILY STD DEVIATIONS(SA)		-123.300	141.600	-66.400	75.700	-47.200	8.600
(SB)		-85.600	105.700	-46.200	31.700	-43.200	4.300
MAXIMUM VALUE OF QVOL		120000.000					

SCOUR AND FILL PARAMETERS	
CONSTANT K4	0.0
EXPONENT N3	0.0
STANDARD DEVIATION OF ERROR TERM	0.0

CUT-OFF CONTROL PARAMETERS				
LIMITING WIDTH OF MEANDER NECK		225.000 METRES		
EXPONENTS IN NECK CUT-OFF RELATION	EN1=	5.000	EN2=	5.000
LIMITING SINUOSITY		3.000		
LIMITING AMPLITUDE		1185.529 METRES		
EXPONENTS IN CHUTE CUT OFF RELATION	EC1=	50.000	EC2=	50.000

A LATERAL SECTION IS REPRESENTED IN THIS TEST

LEGEND

LOWER PHASE PLANE BED	L	GRAVEL	G	OLD SEDIMENT	X
RIPPLES	R	SAND	C	WATER	I
DUNES	D	SILT	S	TIME LINE	.....
UPPER PHASE PLANE BED	U	CLAY	-	AIR	BLANK
ANTIDUNES	A	OVERBANK DEPOSITS	F		

PLANIMETRIC FORM OF MEANDER	METRES	
WAVELENGTH	1000.000	
AMPLITUDE	205.834	
SINUOSITY		1.100
RADIUS OF CURVATURE AT BEND AXIS	280.638	
WIDTH OF MEANDER NECK	**********	
CHANNEL LENGTH ALONG MEANDER	1099.999	
VALLEY SLOPE		0.00010000
LONGITUDINAL WATER SURFACE SLOPE		0.00009091

SELECTED GEOMETRIC RATIOS	
WAVELENGTH TO RADIUS OF CURVATURE	3.563
WAVELENGTH TO CHANNEL WIDTH	8.000
RADIUS OF CURVATURE TO CHANNEL WIDTH	2.245
AMPLITUDE TO CHANNEL WIDTH	1.647

Table 20.2. Initial data for experiment 5.

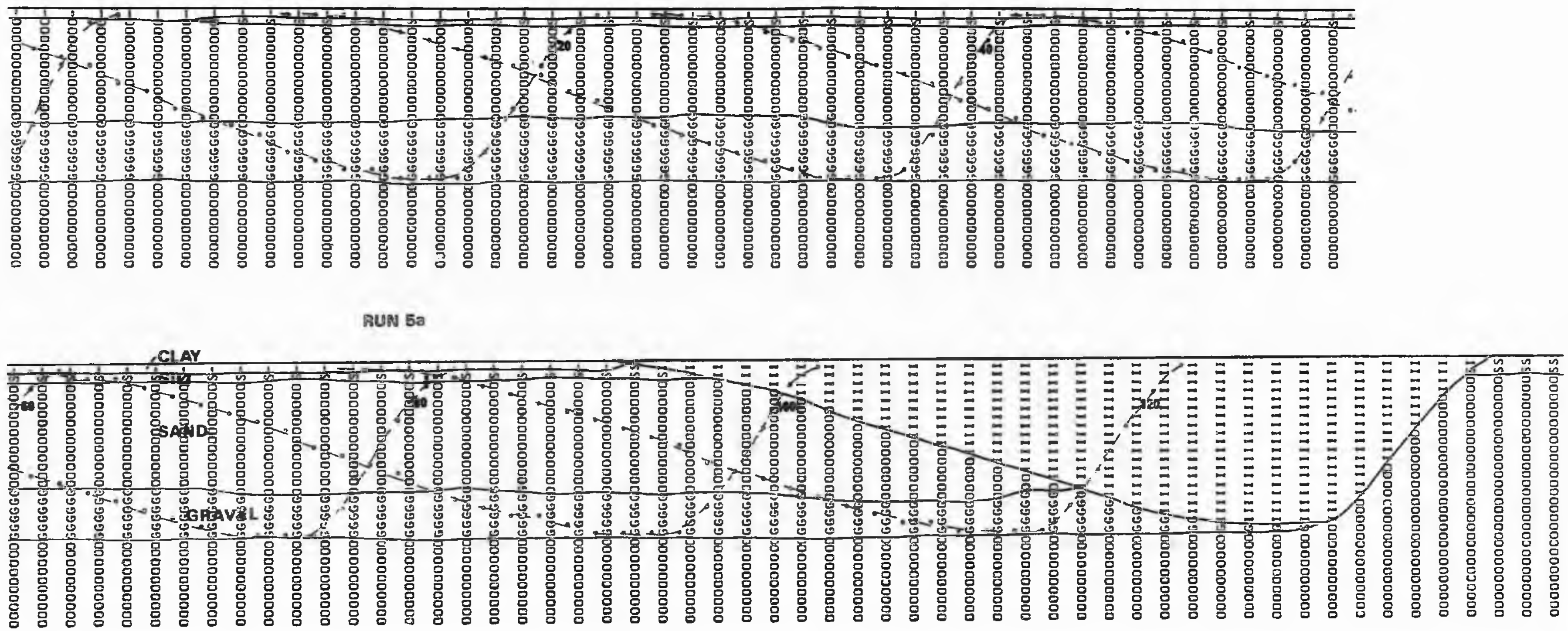

Fig. 20.1. Grain size sections for experiment 5.

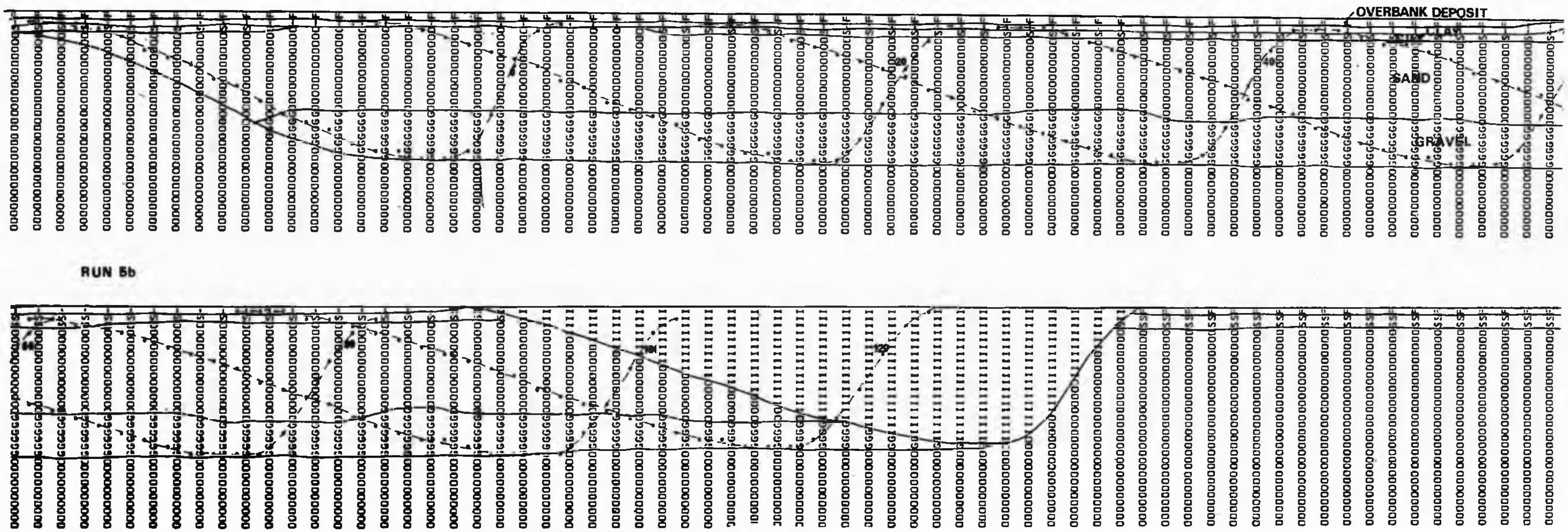

Fig. 20.1. - continued.

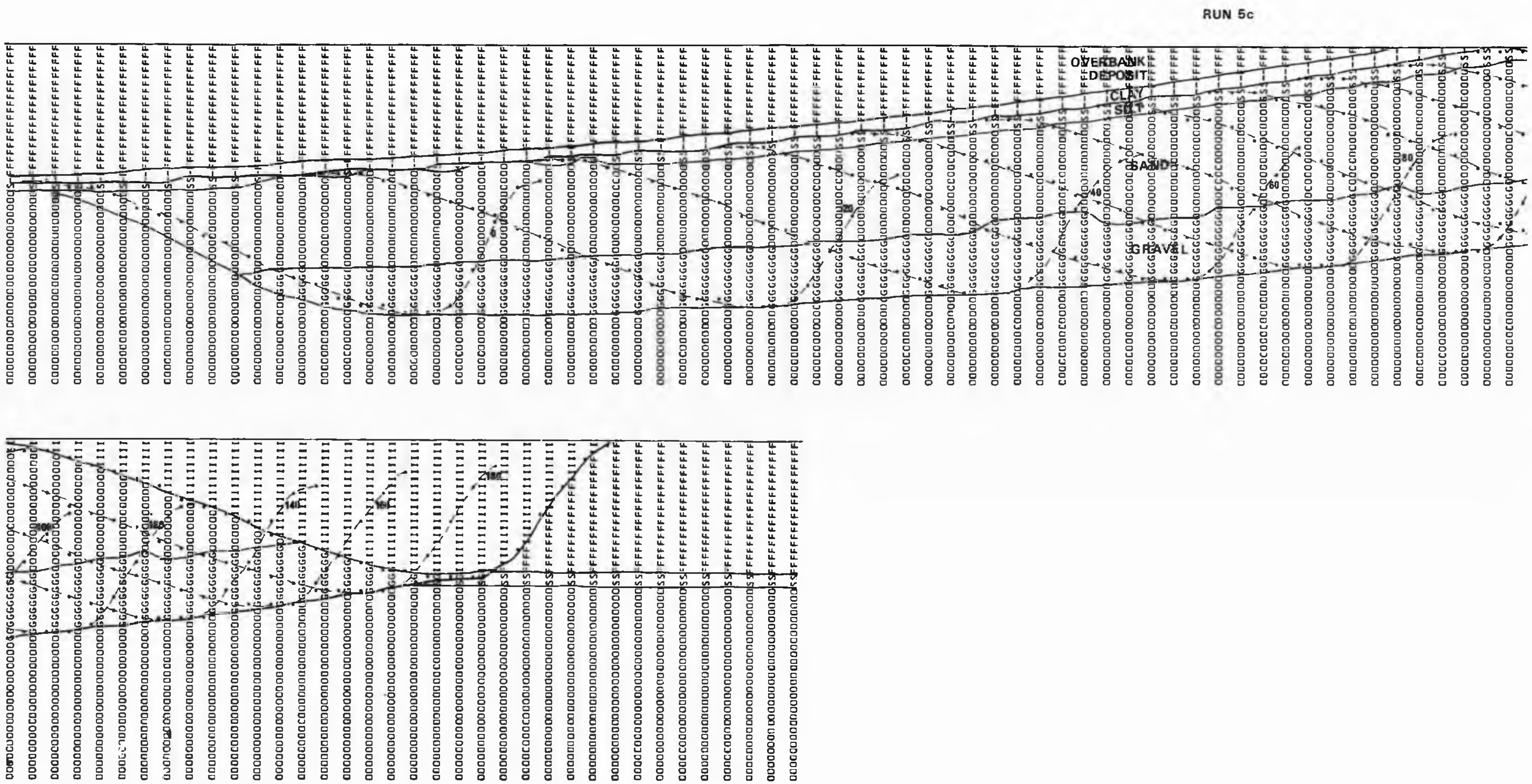

Fig. 20.1. - continued.

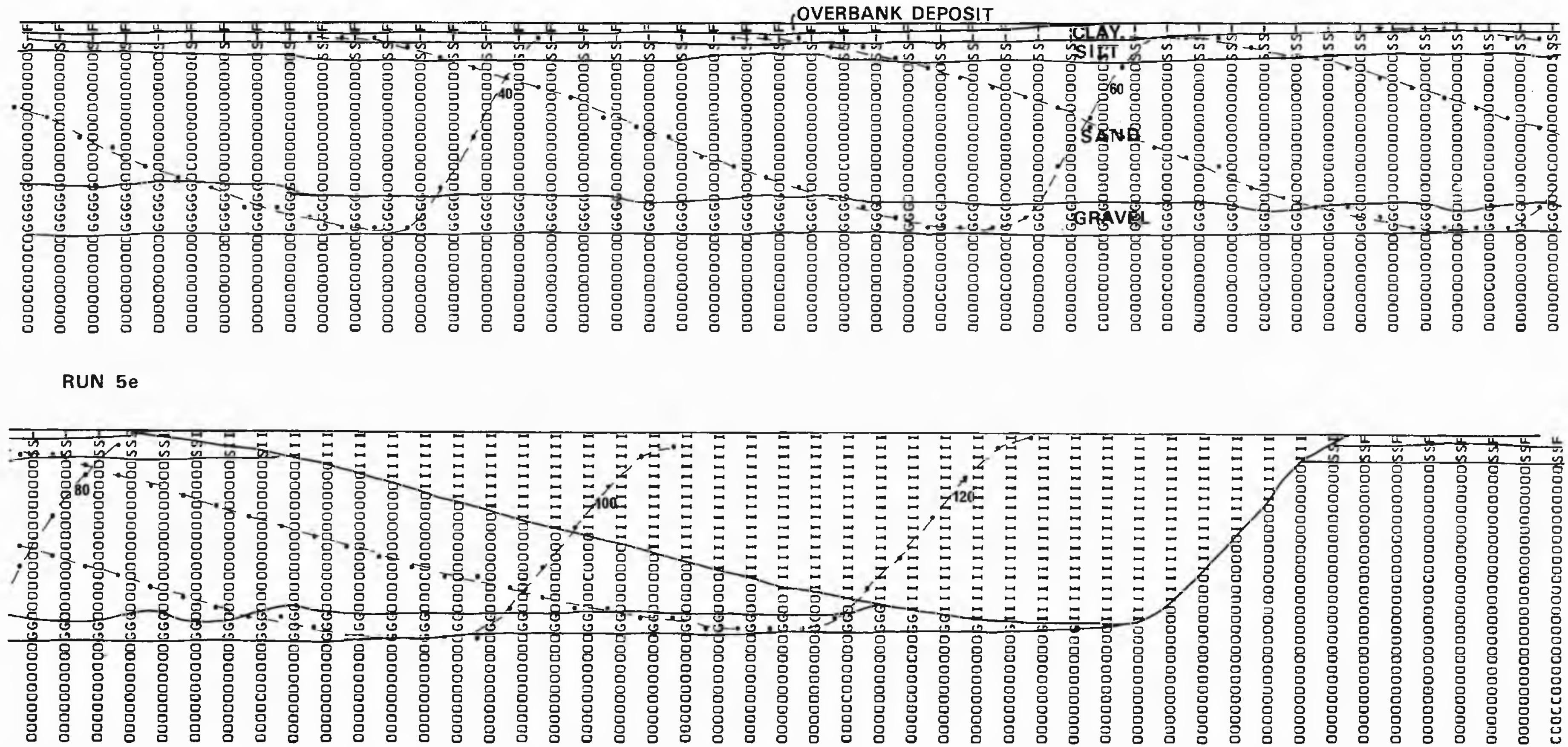

Fig. 20.1. - continued.

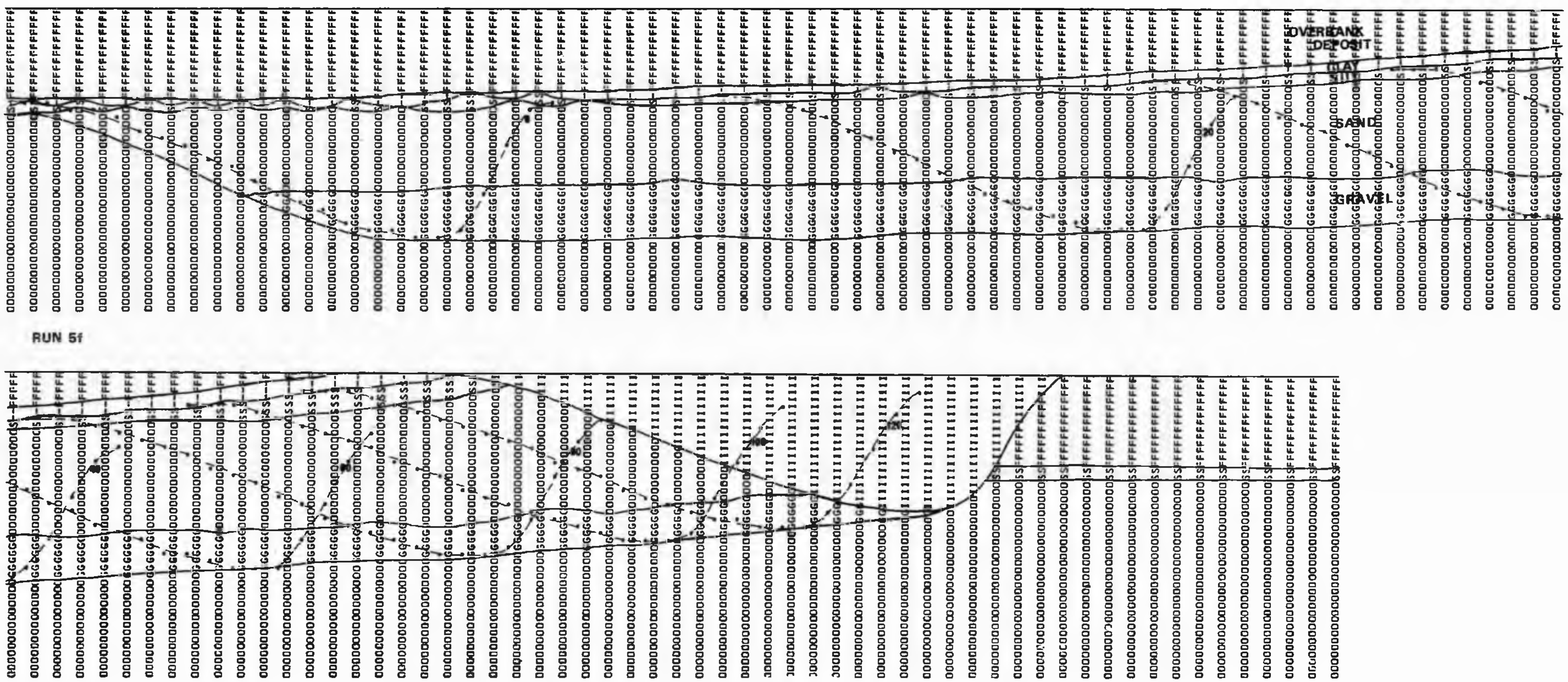

Fig. 20.1. - continued.

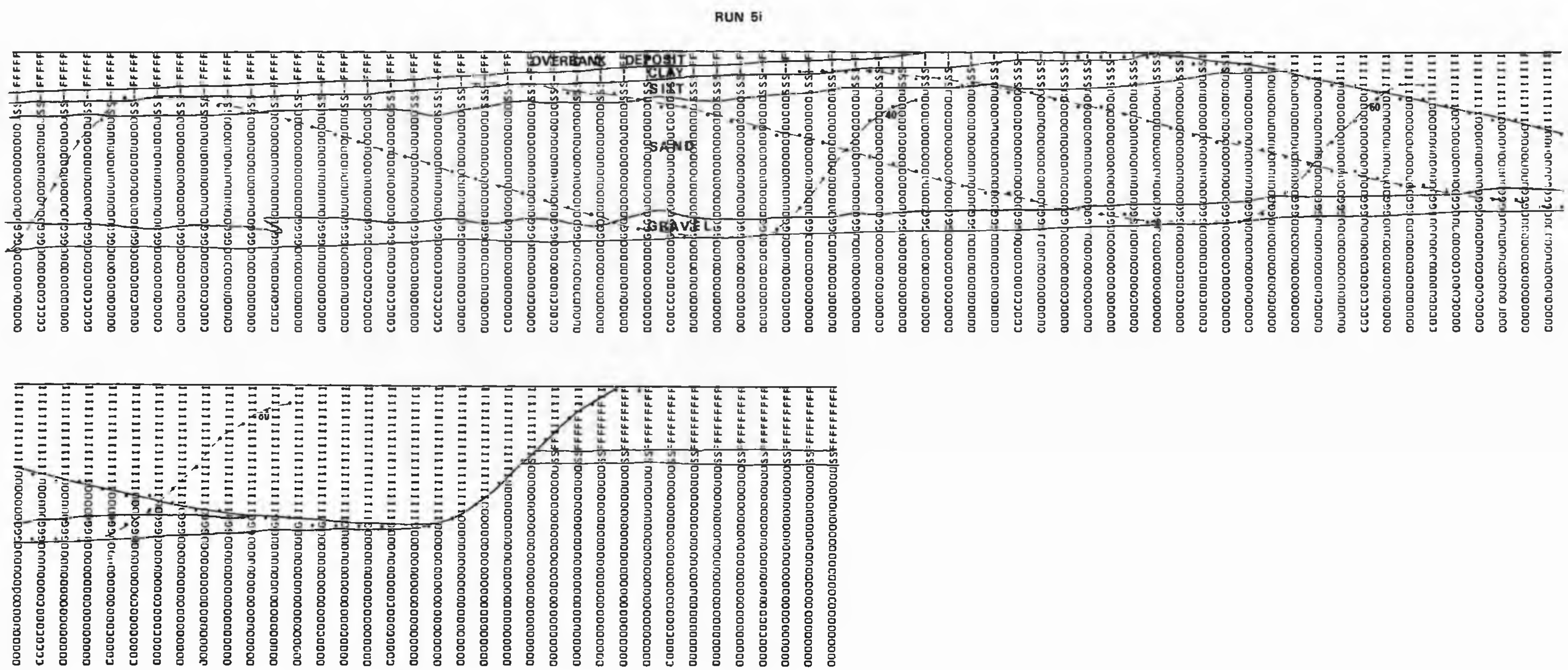

Fig. 20.1. - continued.

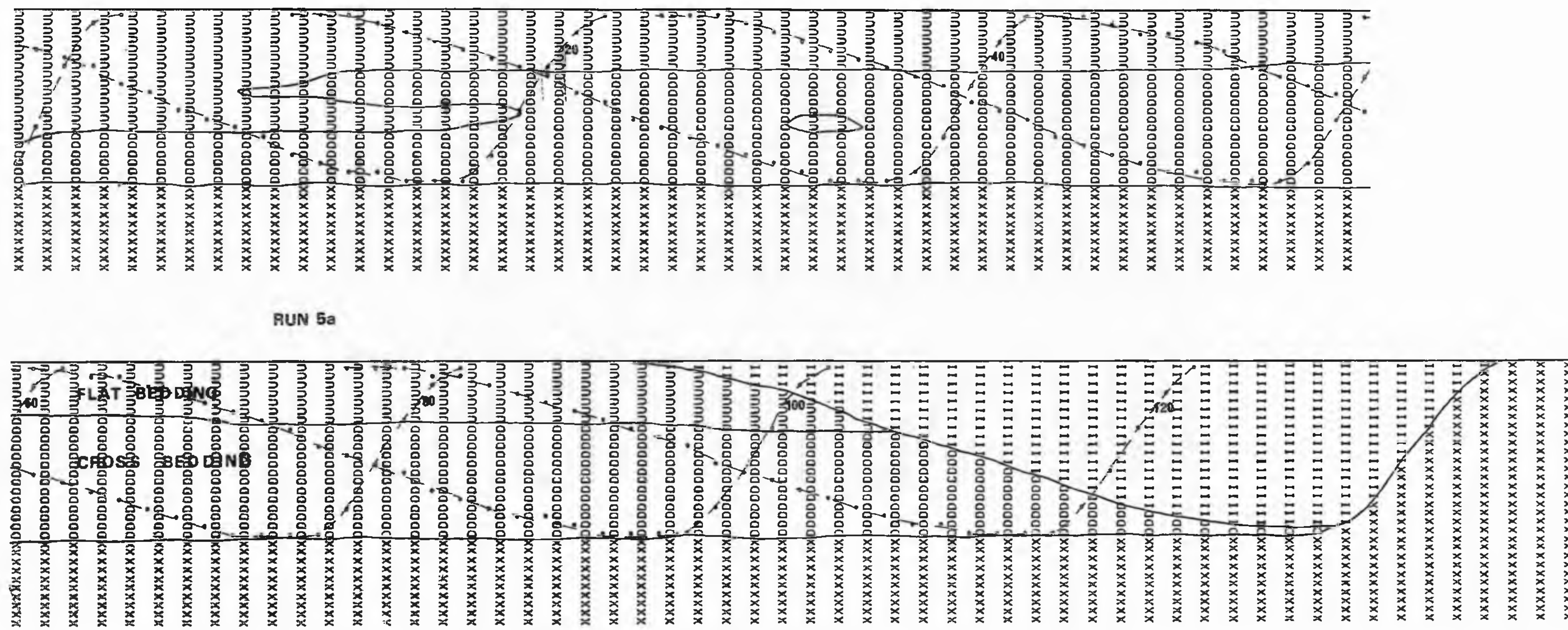

Fig. 20.2. Sedimentary structure sections for experiment 5.

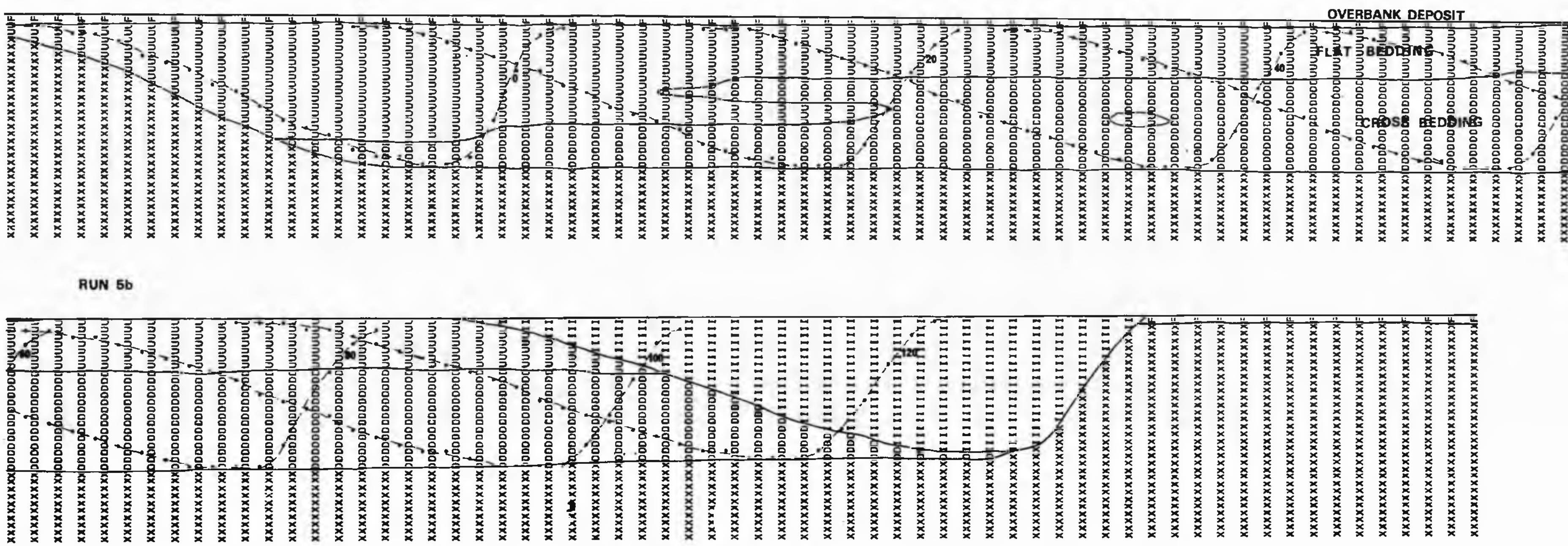

Fig. 20.2. - continued.

RUN 5c

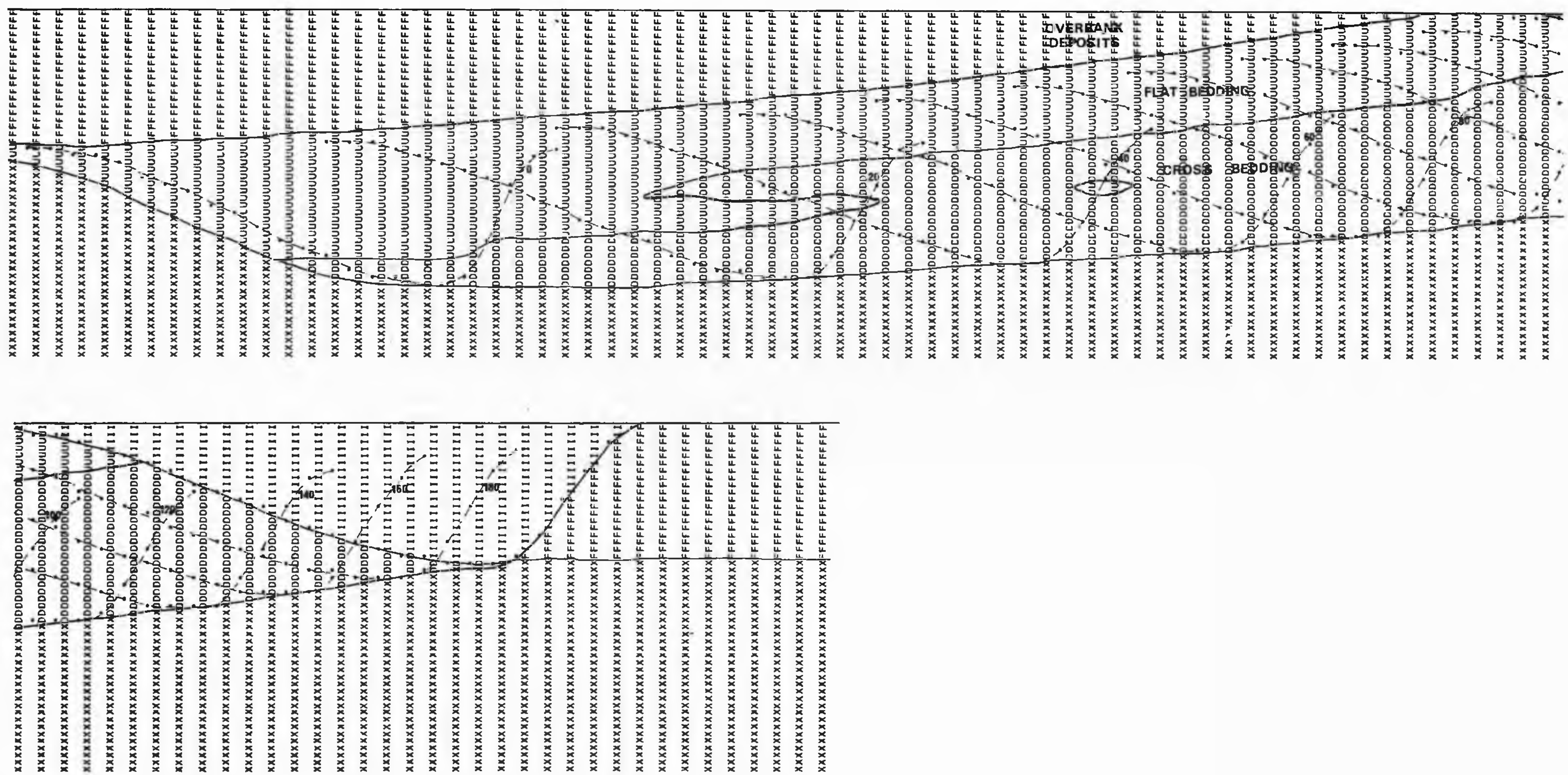

Fig. 20.2. - continued.

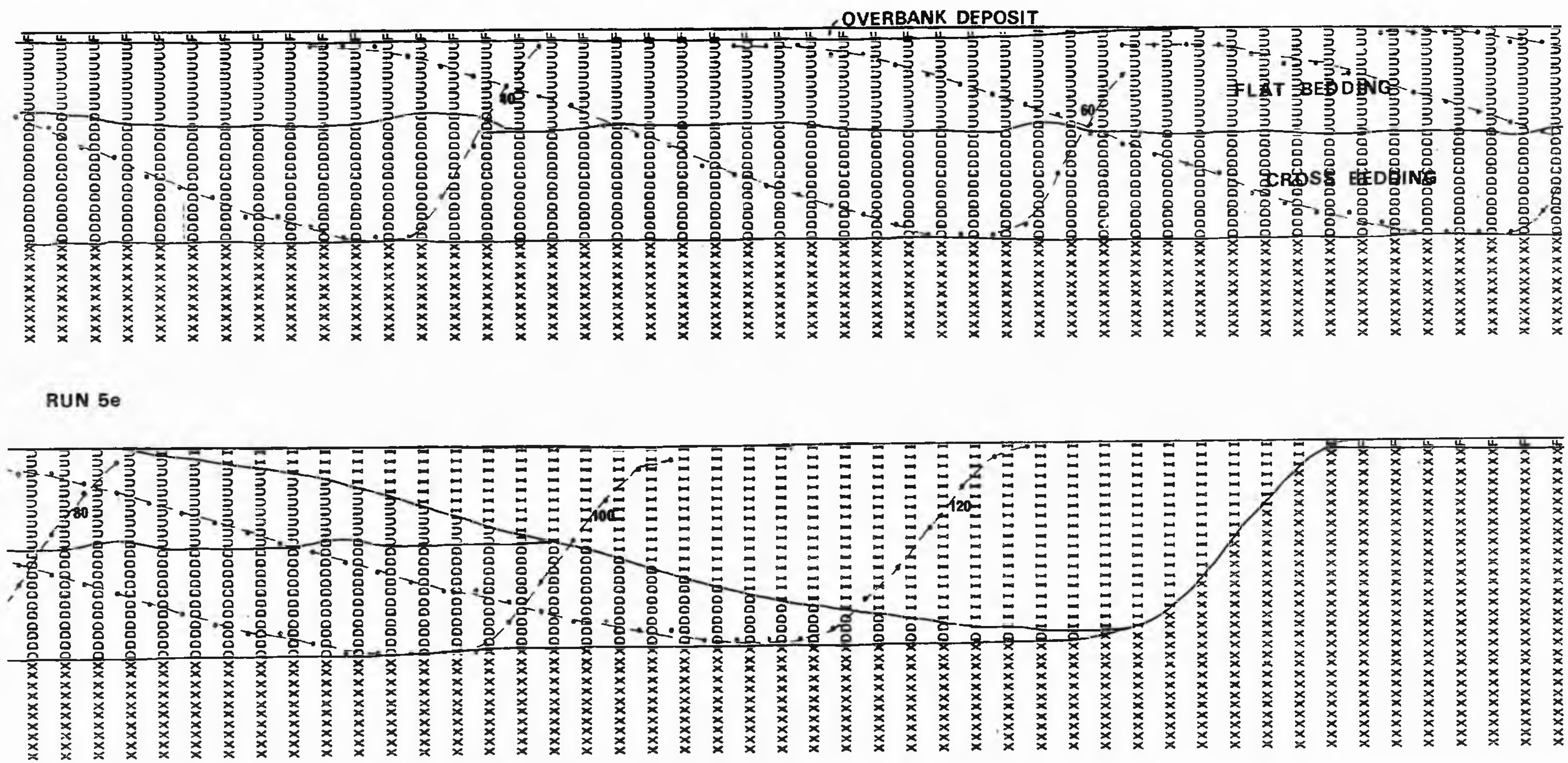

Fig. 20.2. - continued.

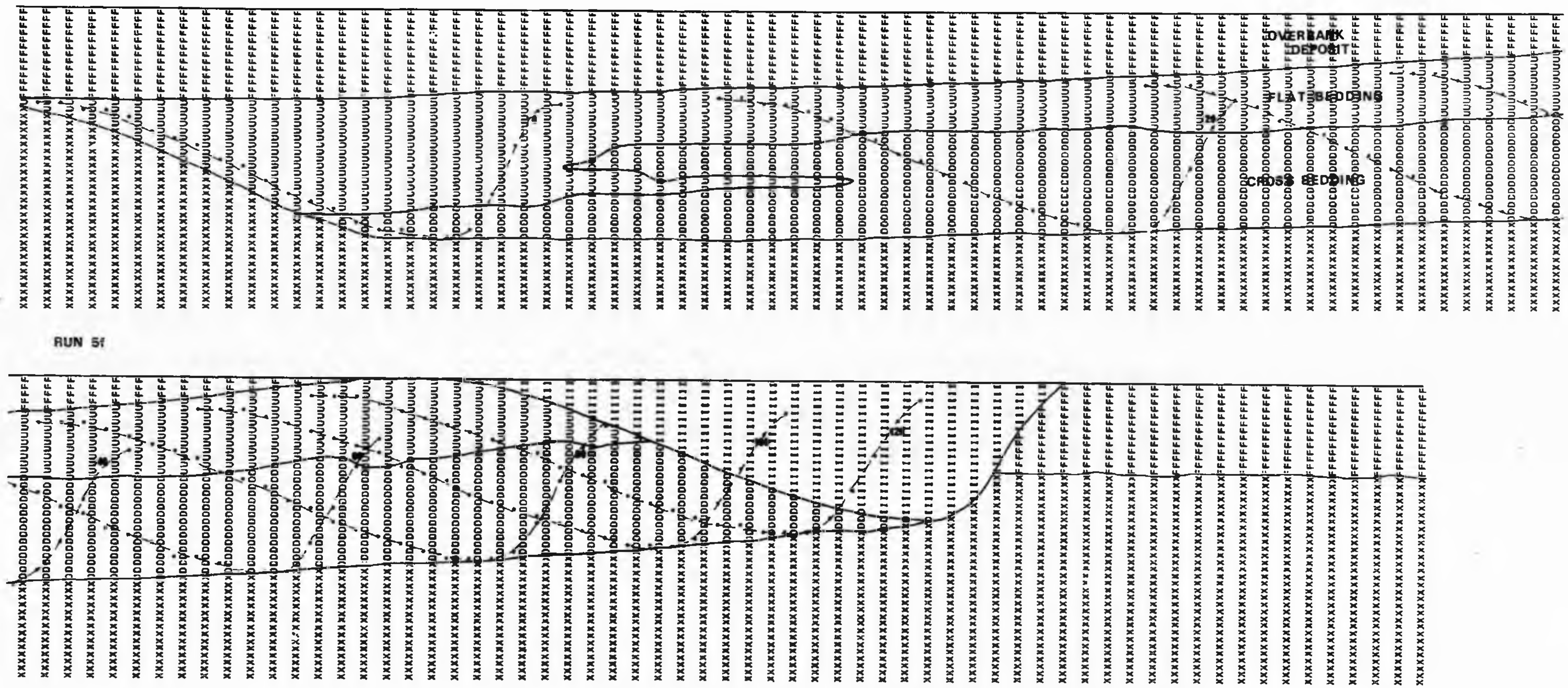

Fig. 20.2. - continued.

RUN 5i

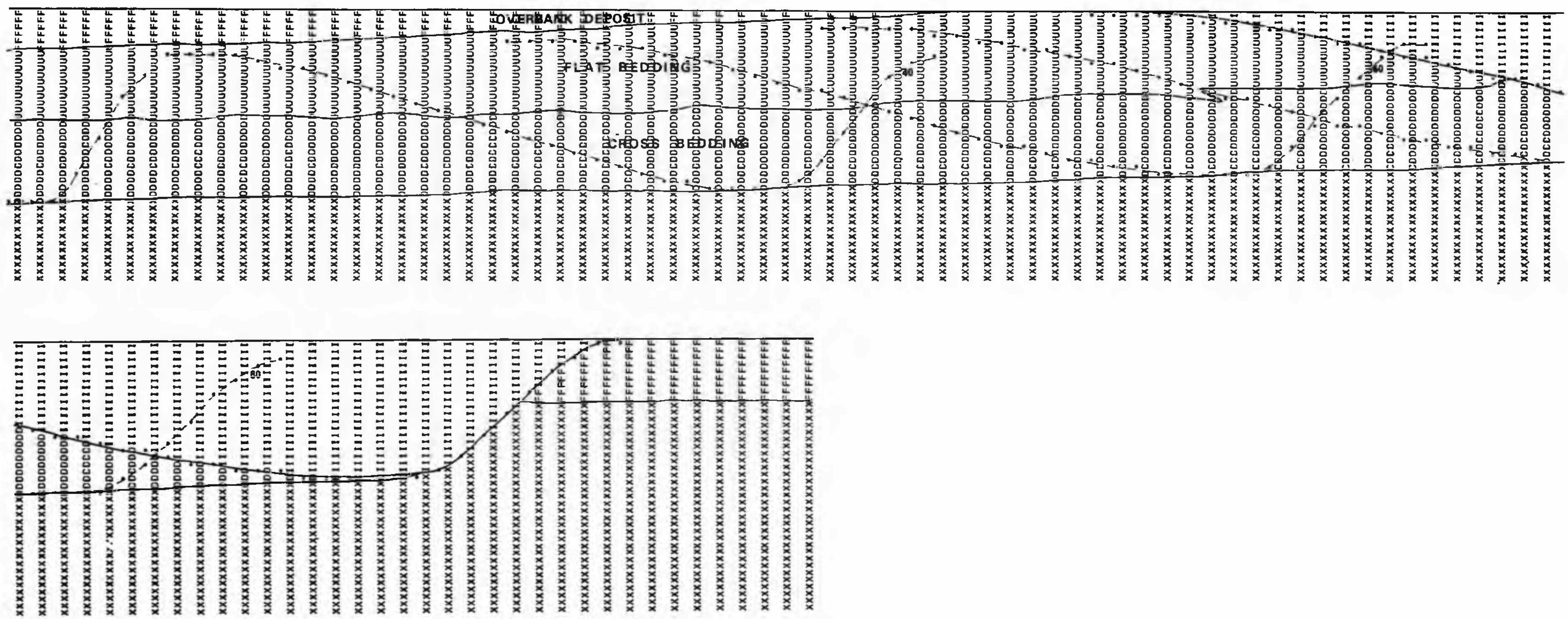

Fig. 20.2. - continued.

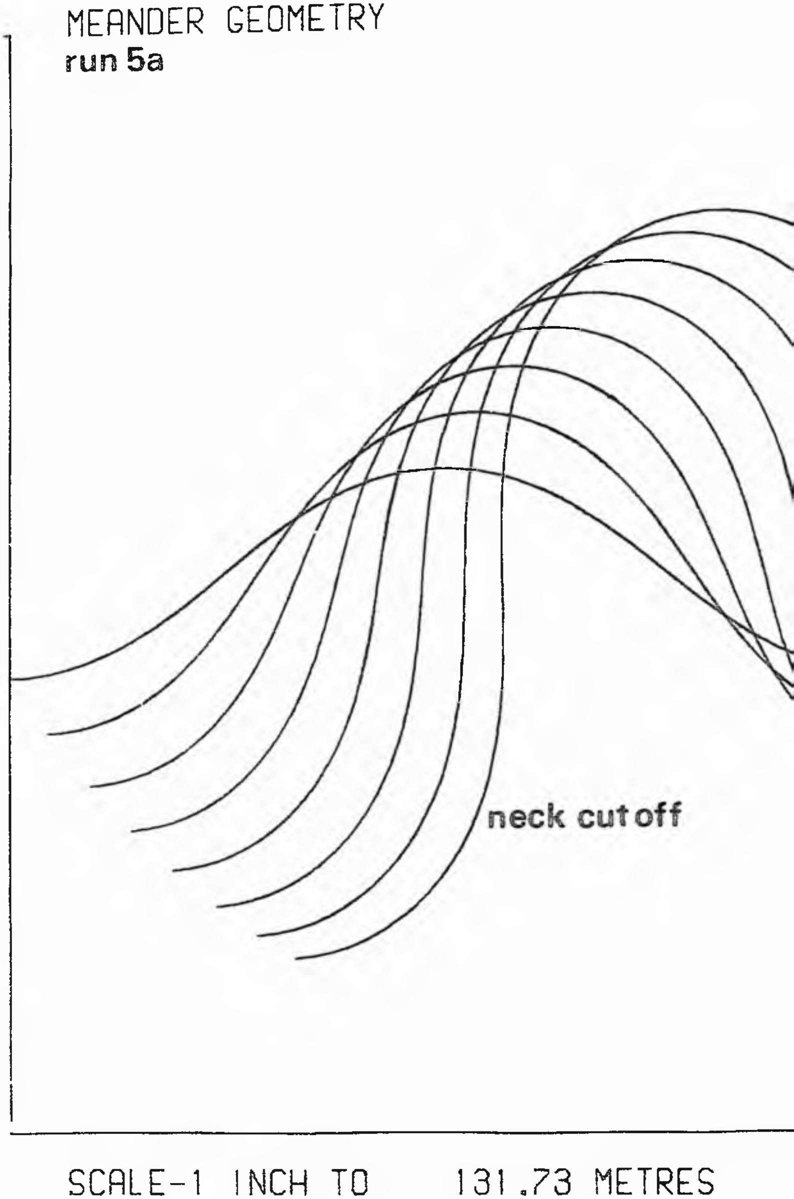

Fig. 20.3. Meander plan forms for experiment 5.

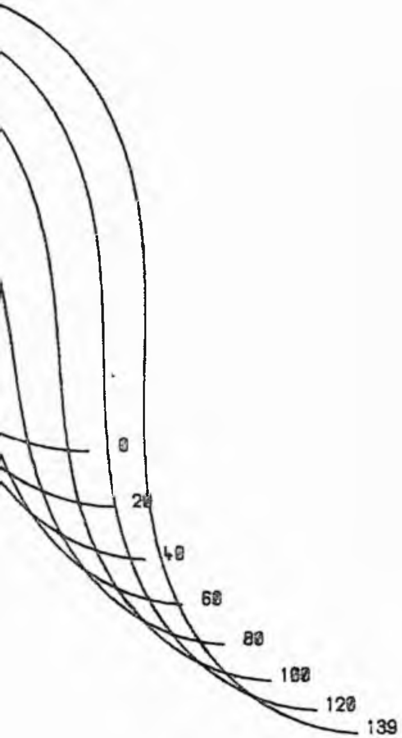

0
20
40
60
80
100
120
139

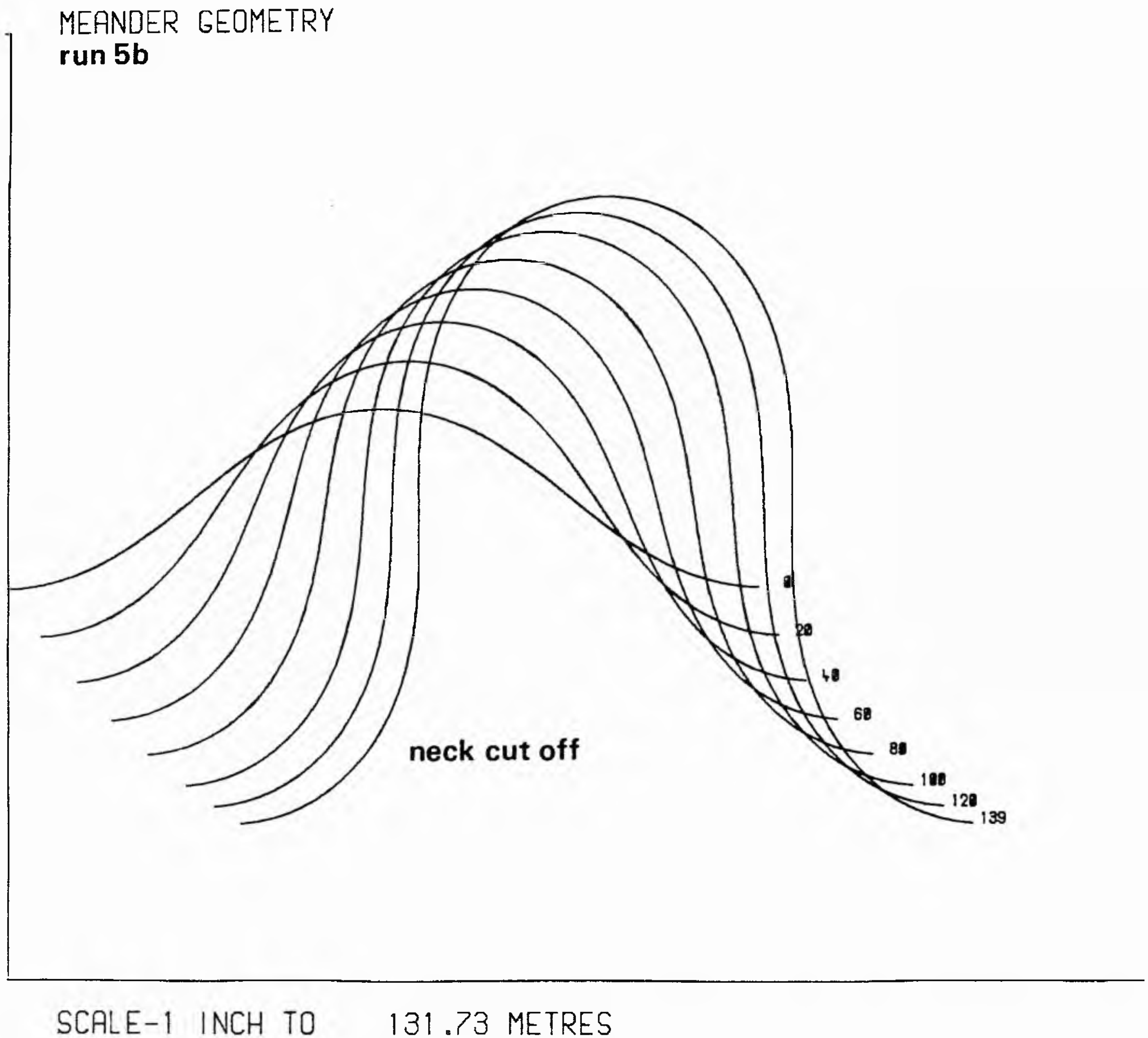

Fig. 20.3. - continued.

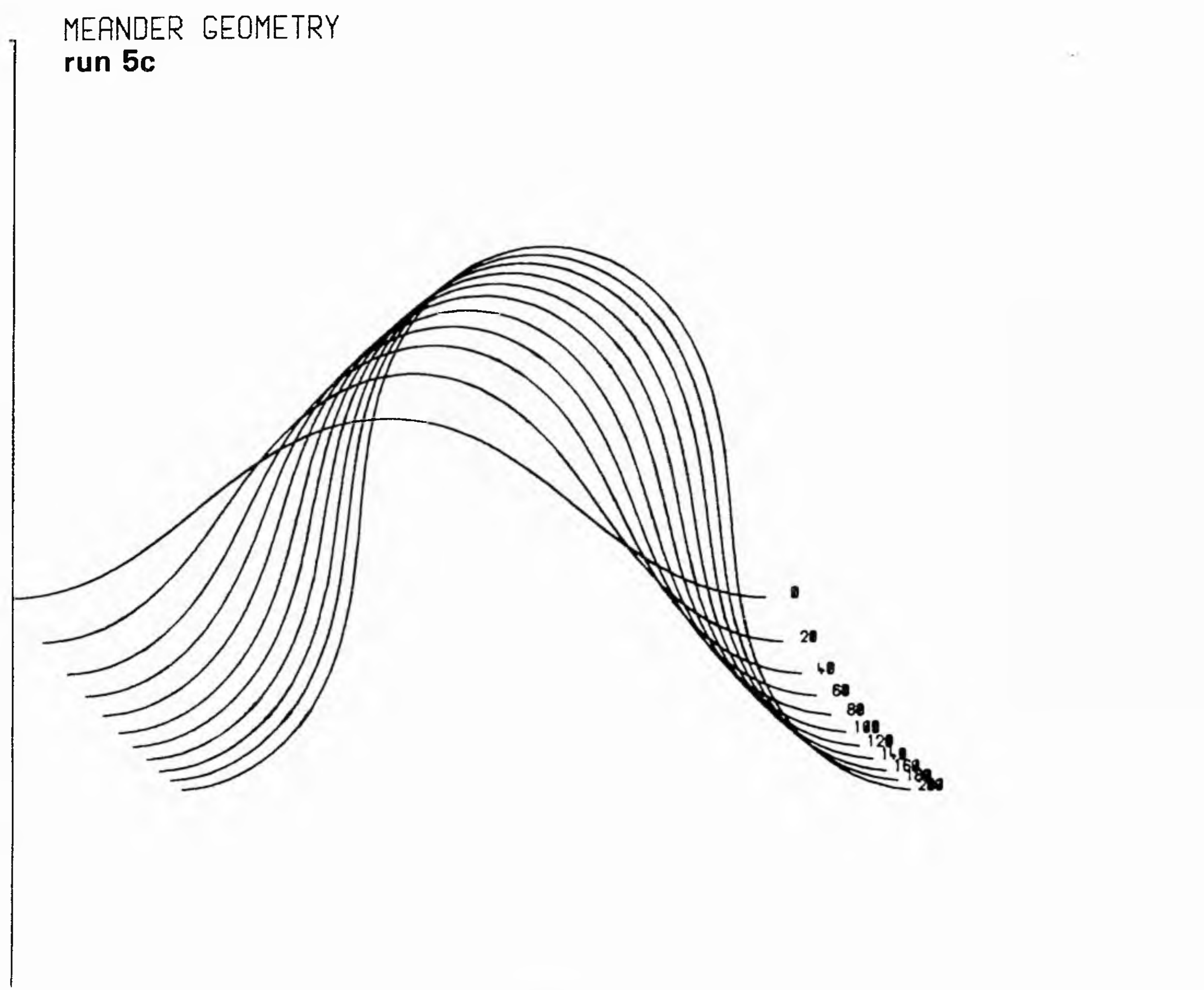

SCALE-1 INCH TO 131.73 METRES

Fig. 20.3. - continued.

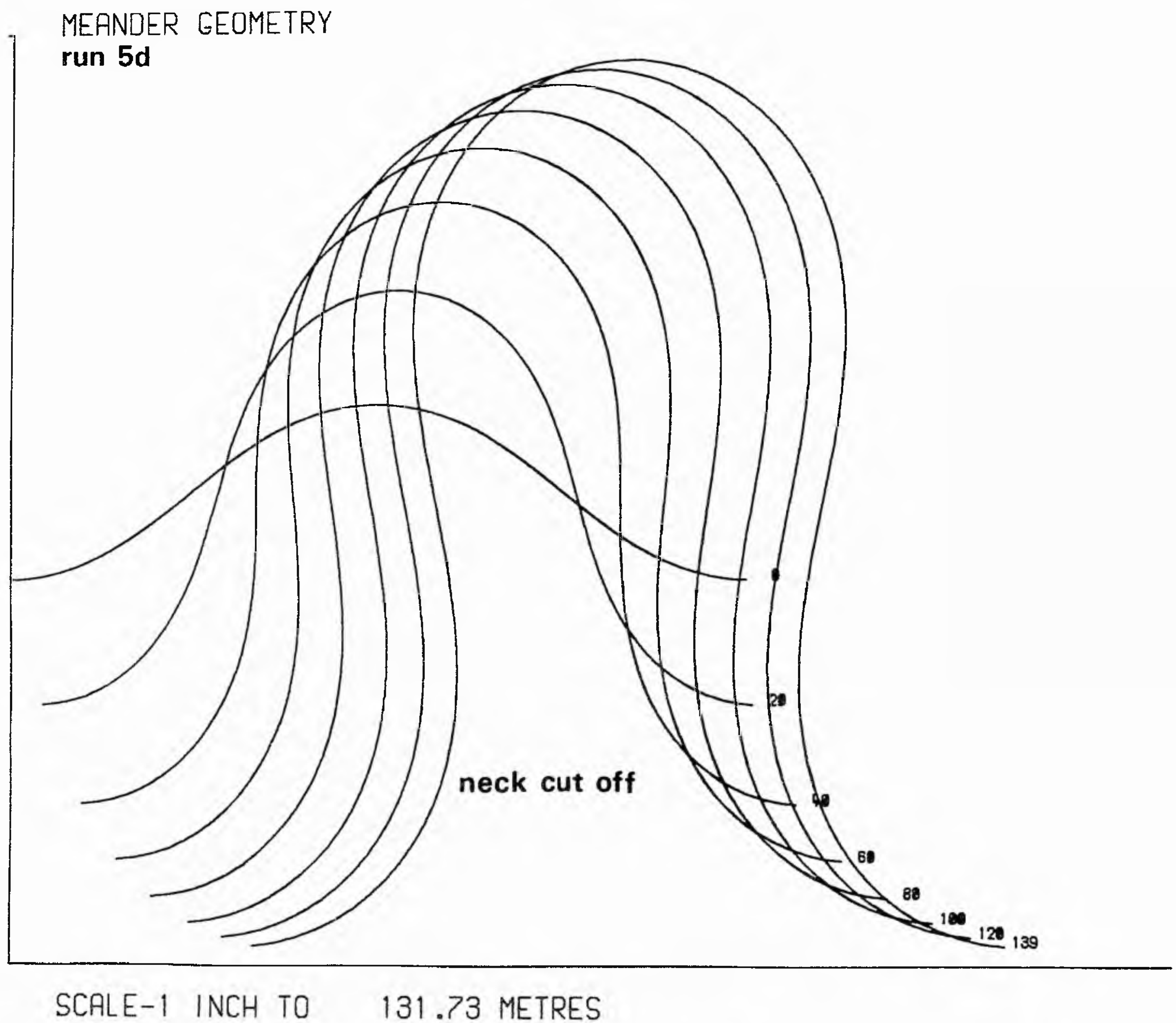

Fig. 20.3. - continued.

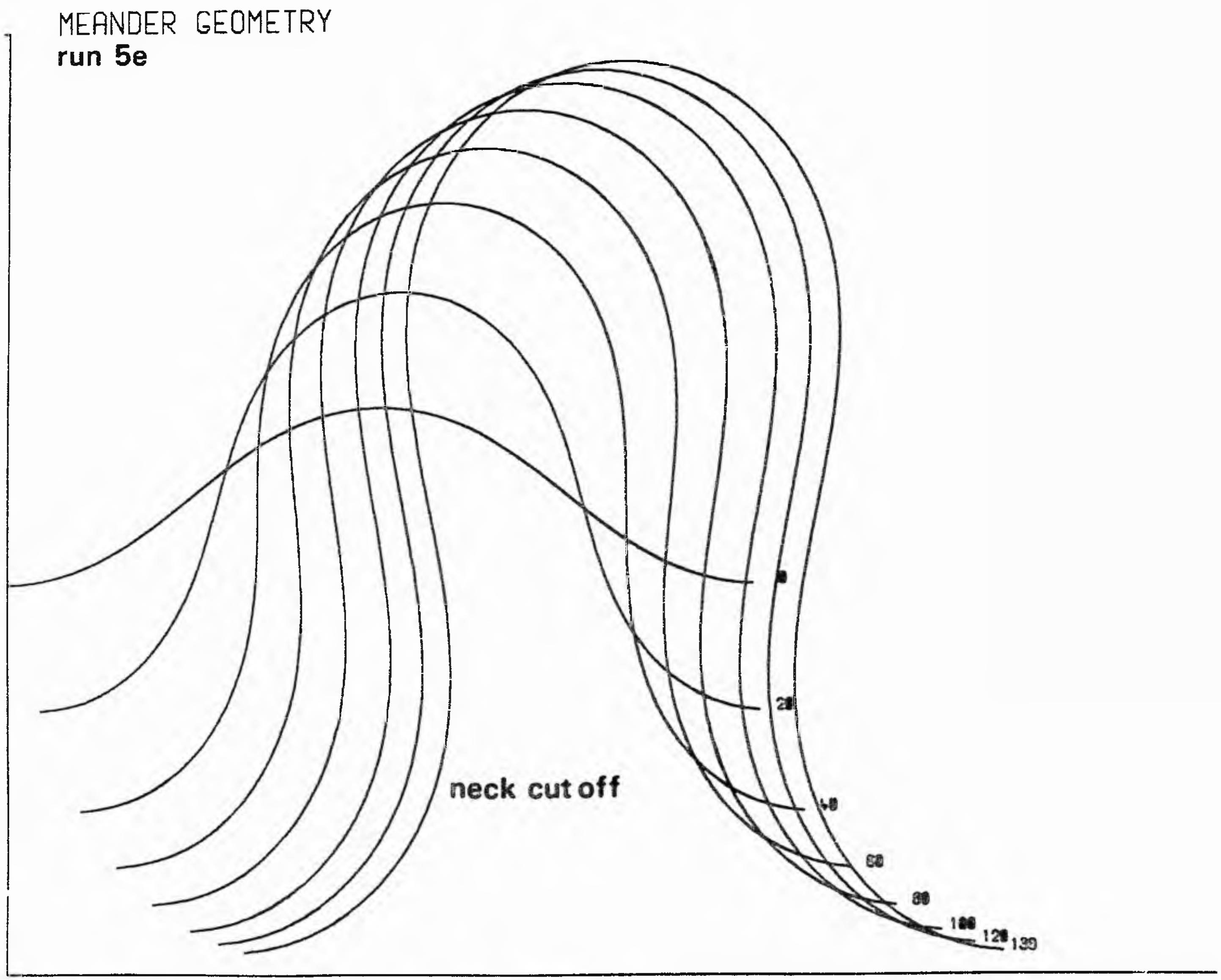

SCALE-1 INCH TO 131.73 METRES

Fig. 20.3. - continued.

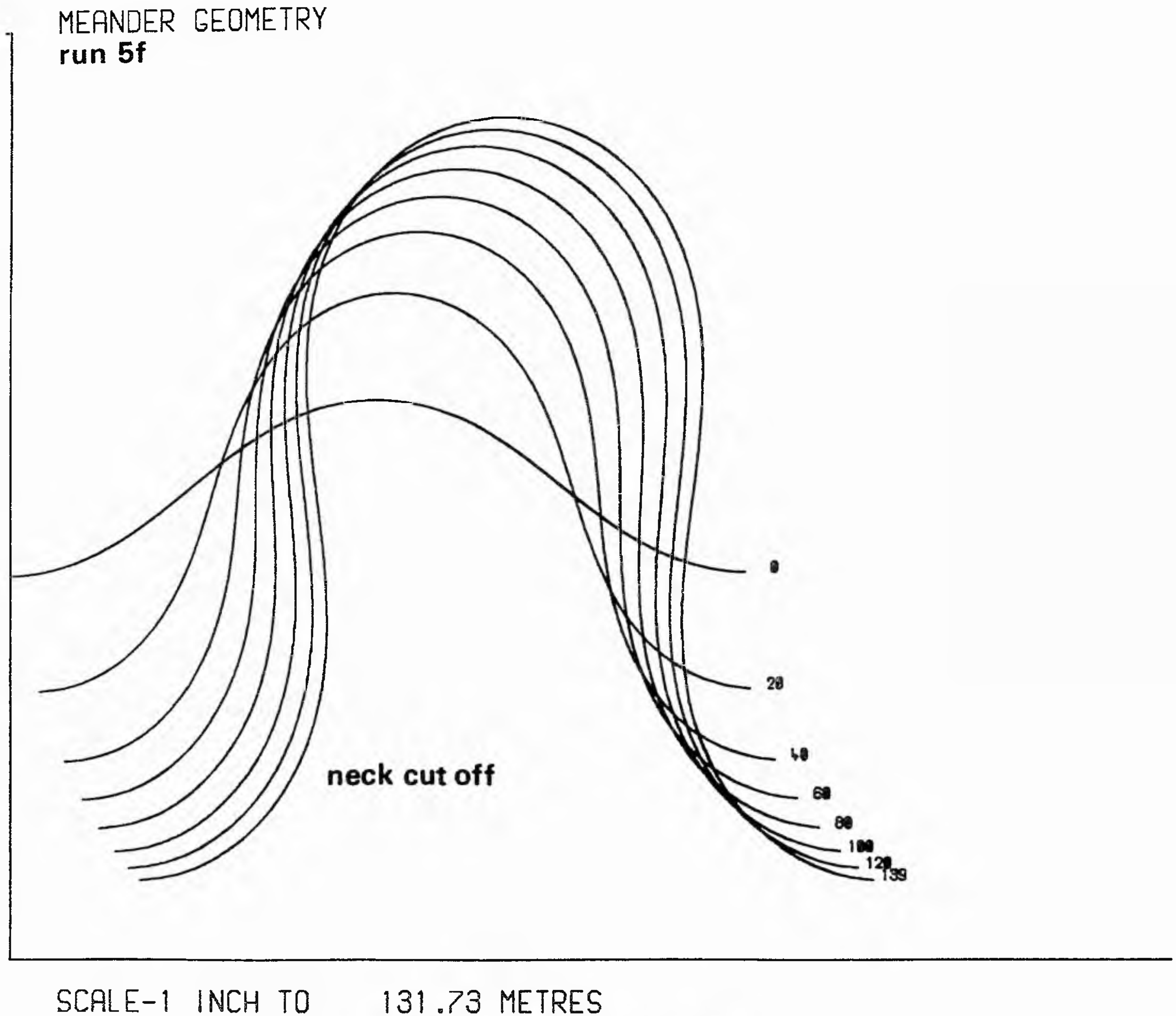

Fig. 20.3. - continued.

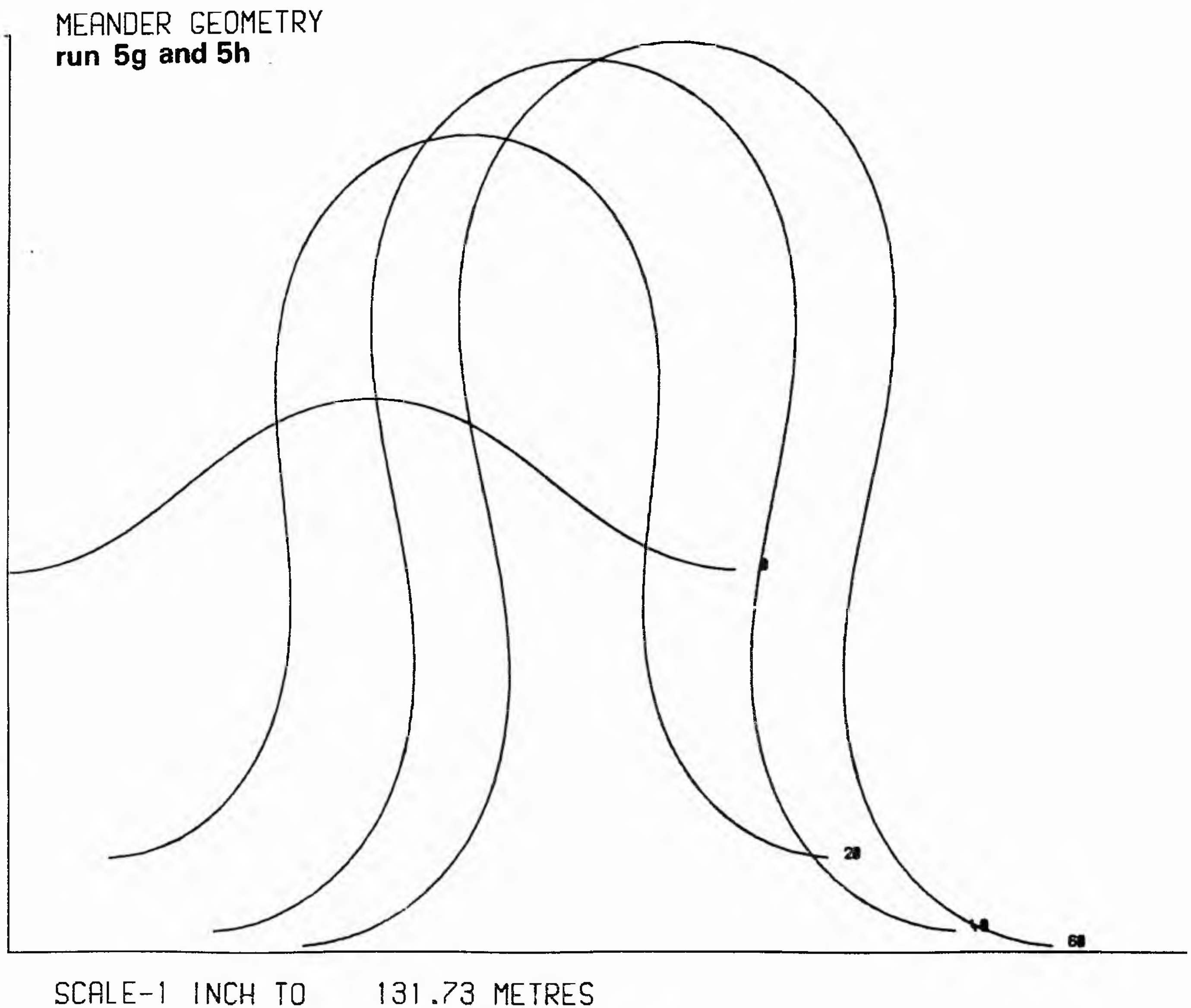

Fig. 20.3. - continued.

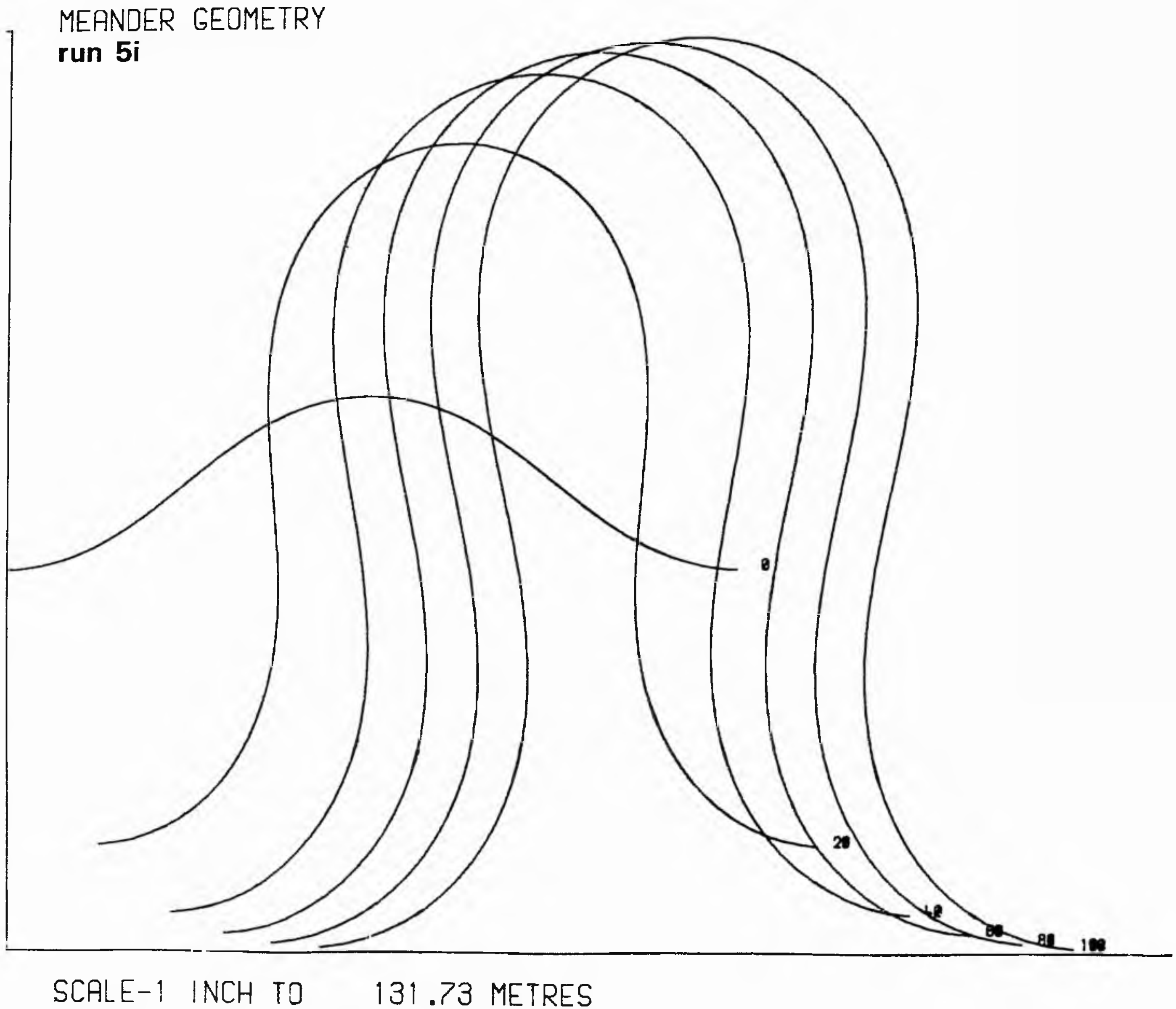

Fig. 20.3. - continued.

scouring and filling.

The overbank deposit wedges and the upward sloping of facies boundaries and basal erosion surfaces in the direction of migration are similar to those in experiment 2. The slowing down of bank migration rates due to the present overbank fines, with increasing aggradation rate, is enhanced by the slowing down of the amplitude growth anyway (see figs. 20.3). Thus the increase in slope of the facies boundaries and basal erosion surfaces is more marked than in experiment 2, as demonstrated particularly in the sections with an aggradation rate of 0.1 metres per year. In this simple moving phase situation the greatest thicknesses of overbank deposits, if preserved, will occur as aggradation rate increases relative to channel migration, as in experiment 2.

Some of the sections with the more realistic slower aggradation rates are not shown because there is not enough vertical deposition to be visually recorded on the sections. The maximum accumulated thicknesses of overbank deposit can easily be calculated for the different aggradation rates. Figs. 20.3 show that, by virtue of the direction of definition of the lateral sections, the deposits are soon obliterated by the meander limb immediately upstream from the bend axis. This is particularly marked where the rate of amplitude growth is small, or becomes small relative to the downvalley migration rate. As a result, there is, in general, less chance of preservation of deposits in this part of the bend than other parts, perhaps leading to a bias in current directions represented in preserved deposits, notably lacking in directions around the mean downvalley direction. The occurrence of cut-off will probably increase the preservation of point bar and overbank deposits produced in these sections. Some of the cross sections in figs. 20.1 and 20.2 are roughly 'edited' to account for truncation by the upstream limb. Unfortunately, the model cannot do this automatically.

PART FIVE

DISCUSSION AND CONCLUSION

21 GENERAL REMARKS

The computer simulation model yields an abundance of information. By matching this output with field observations the overall model can be evaluated, and its ability to provide a useful analogue to the real system can be judged. The closeness of the model to the real system will inevitably depend on whether important processes observed in nature have been accounted for and the adequacy of their treatment in mathematical and logical terms. The validity of the component mathematical models, and the approximations made, have been discussed in part 2. Approximations involving the representation of space in discrete form have been discussed in part 3. It is noteworthy that the development of the component mathematical models was based on observation, and subsequent theory, on natural meandering streams and scale model experiments. Purely theoretical models are therefore considerably subordinate to empirical relationships. Data input is supplied bearing in mind the restrictions and mutual compatibilities of the system variables as imposed by the overall natural system.

The necessary first step is to compare the output with information from modern free meandering stream systems, and subsequently apply the model to the understanding and prediction of modern erosion and deposition, and the interpretation of ancient fluvial systems. There are, however, inherent difficulties in obtaining data from many geological dynamic systems and, even if available, data may be sparse or unsuitable in form. The output from the model is conveniently in the form of laterally continuous cross sections showing simulated distribution of grain size and sedimentary structures. Invariably field data, when available, are also in the form of sections in a limited number of directions and of limited horizontal extent, or alternatively as a series of discrete sections or boreholes from which a continuous section may be built up. It will be seen in the following discussion that although a reasonable qualitative comparison of the simulated sediments with real world observations can be made, there are many instances where a substantial amount of data is not available or is of unsuitable form.

22 COMPARISON WITH MODERN FREE MEANDERING STREAM DEPOSITS

22.1 Shape of point bar deposits

The experiments indicate that when bank migration is fairly rapid, point bar deposits extend along the length of the valley, but their extent across the width of the valley is limited to the width of the meanders. If there were slow bank migration the deposits would be beaded along the length of the valley. The edges of the deposits have the shape of a channel bank. Their thickness remains approximately constant and corresponds to the depth of the stream measured from bankfull stage to the scoured base of the channel, as is the case in real streams (e.g. Bernard and Major, 1963).

Allen (1965a) reports that the shape of a point bar deposit complex depends on the extent of channel wandering as controlled by channel sinuosity. The point bar deposits are broadly sheet like with rapid migration and low sinuosity and are long, narrow beaded belts which are narrow compared to the floodplain when sinuosity is higher. Presumably the ability to construct a sheet of point bar material depends on the movement of the meander belt continuously or discontinuously (avulsion etc.). Movement of the meander belt cannot be simulated in the model, therefore sheet like deposits cannot be produced at this stage.

In the model the extent of channel wandering, for a given size of stream, is controlled to the extent that the floodplain sediment calibre is supplied as input. Thus if the meanders have low limiting sinuosity the floodplain sediment may be assumed to be sandy in nature. If the meanders have high limiting sinuosity the floodplain sediments may be designated as silt and clay, perhaps corresponding to fine grained channel fills produced with the more frequent cut-off (e.g. Allen, 1965a). The model will respond to these variations in floodplain sediments in a realistic manner.

The geometric nature of point bar and overbank deposits within a thick aggraded sequence of alluvium is only approximately known, and Allen (1965a) has presented some hypothetical alluvial facies models describing this. Detailed quantitative study of the shape of point bar and overbank deposits in thick sequences with relation to rates of aggradation and lateral channel movements is not at hand, and the processes involved with net vertical deposition and such large scale channel movements as avulsion are not fully understood. It has not been possible therefore, to generate thick sequences of alluvial sediment at this stage.

Although not strictly comparable with any recent examples, the model has been able to simulate sections through the meander belt in the mean downvalley direction, and normal to this direction, which show the effects of net aggradation combined with channel migration. The results show a general slope of facies boundaries and scoured basal surfaces upwards in the direction of channel movement, depending on the relative rates of aggradation and migration, and record the effects of increasing amounts of overbank deposits. In general, the slopes involved may be so small that they would not readily be recognised in an alluvial complex. There are some interesting features of the sections in the mean downvalley direction. With no aggradation or degradation the basal scoured surfaces would represent the slope of the valley, assuming negligible downstream changes in channel depth over the section represented. If there were slow and continuous degradation, the slope of the basal surfaces would be greater than the valley slope, and with aggradation the slopes would be less than the valley slope and may even dip in the opposite direction. Clearly many factors would complicate this naive situation. The experiments show a 'stabilisation' effect as thicknesses of fine sediment are deposited on the floodplain with aggradation.

Stabilisation of meander belts is also effected by cut off and subsequent filling of abandoned channels with fine sediment (e.g. Allen, 1965a); such processes cannot be simulated at present, although, as previously indicated, abandoned channel-fills can be defined implicitly at the outset. It is noteworthy that the stabilisation with aggradation would not be simulated if it was assumed that the overbank deposits were sand or gravel grade material.

22.2 <u>Epsilon cross stratification</u>

It is implicit in the model that successive deposits for a given flood event are bounded by sigmoidal boundaries which mark the position of the bar before being filled on falling stages. These surfaces must delineate the epsilon-cross-stratification of Allen (1963a). An important point here is that the maximum angle of the transverse slope of the epsilon-cross stratification must represent the scoured shape of the point bar, when scouring and filling is present. This may go some way to explaining the relatively steep angles of the few examples of epsilon-cross-stratification found in ancient sediments when compared with recent bar <u>surfaces</u> (Allen, 1970b). Recent and ancient examples may therefore be directly comparable. Allen (1970b) also notes that epsilon-cross-stratification may be very difficult to see in rocks unless the transverse slope is reasonably large.

Epsilon-cross-stratification is implied in recent point bar sediments by virtue of their mode of lateral growth, with the units being deposited at discrete periods of time and concomitant with concave bank recession. It would thus appear that the thickness and regularity of development of the units will depend on rate of bank migration, variation in degree of scouring, and variation of the shape of the surface on which sediment is being deposited. In the model the shape of the bar profile is constant and only its maximum slope varies with degree of scouring, therefore the sigmoidal boundaries are very regular, although they may not be exactly parallel at all levels in the bar. In real streams, given sufficient bank migration to develop successive units, a greater degree of irregularity may be expected due to variation in the shape and slope of the point bar profile on which sediment is being deposited. This may or may not be associated with scour and fill. Furthermore, distinct epsilon unit boundaries may be obscured by small scale scouring over the profile, perhaps in the lee of dunes; this feature is not represented in the model sections.

Sundborg (1956) records very regular epsilon-cross-stratification in the point bar deposits of the Klaralven, southern Sweden, at least in the lower parts of the bar. Leopold and Wolman (1960) also note that '...approximate contact surfaces between materials of different textures are more or less parallel to past surface profiles'. Other examples in tidal meandering streams include Van Straaten (1954), Reineck (1958) and Klein (1963).

A final point is that the epsilon-cross-stratification may be visible over the total vertical thickness of the point bar. If this is the case it will represent a vertical thickness measured from about bankfull stage down to the base of the scoured channel.

22.3 Distribution of grain size and sedimentary structure

Attention may be directed to that part of the model which predicts the grain size and sedimentary structure over the point-bar profile, using the conventional hydraulic equations. There are, unfortunately, inadequate experimental observations or data from present day river or tidal meandering channels by which to test this model. The qualitative features of the deposits produced in the model with lateral bar growth (with and without scour and fill) are however consistent with the general characters of lateral deposits formed in comparable tidal systems and streams. In these deposits grain size generally decreases vertically upwards and bed forms change from types indicative of large stream power upwards to forms denoting a small power (e.g. Allen, 1965a; Bernard and Major, 1963; Bernard and LeBlanc, 1965; Evans, 1965; Fisk, 1944, 1947; Klein, 1963; Oomkens and Terwindt, 1960; Reineck, 1958; Sundborg, 1956; Van Straaten, 1954). It was pointed out earlier that the prediction of silt and clay at the tops of the bars was not strictly correct. Qualitative justification is afforded by observations of fine sediment on top of bars to such an extent that they often cannot be distinguished from the overlying levee deposit (e.g. Bernard and Major, 1963; Visher, 1965a; Wolman and Leopold, 1957).

The model does not record the expected variation in size of dunes with flow characteristics, or the scoured bases to the individual cross bedded units. McDowell (1960) describes cross-bedded units in recent point-bar deposits which become on average thinner upwards in the bar. Other structures not simulated include convulute lamination and various types of small scale scours.

Sundborg (1956) and Leopold and Wolman (1960) note that with falling discharge after some flood events, suspended sediment is deposited on bars over the coarser bed load material, thus leading to alternate coarse and fine sediment as individual layers are traced laterally and upward. This variation would be in addition to the general upwards fining in the point bar. Such small scale variation cannot be described within the model (1) by virtue of the scale of variation involved and, probably more significant, (2) because only events at bankfull stage are considered and (3) no explicit account is taken of fine suspended sediment.

Thus when there is little or no scouring and filling, no small scale variation can be simulated. Some vindication lies in the fact that as most sediment is deposited on bars from bed load at high stage, such fine sediment may be insignificant and may be scoured during rising stages of the next flood anyway. Indeed, sometimes the fine sediment is just in the form of mud drapes (e.g. Bluck, 1971: McGowen and Garner, 1970). Fig. 22.1 illustrates the expected variation in grain size in a single natural depositional unit compared with the simulated variation, for the case where no scouring and filling occurs.

When there is no scouring and filling, lateral bar growth in the model produces no relief in the grain size and sedimentary structure facies boundaries or the basal scoured surface. When scouring and filling occurs in conjunction with lateral deposition, small scale variation in grain size and sedimentary structure both within and between individual epsilon units can be simulated, in addition to the general fining upwards of grain sizes and systematic distribution of sedimentary structure. This feature of the model gives rise to a relief, over the whole deposit, in the boundaries separating different grain size classes or sedimentary structure, and may take the form of lensing and interfingering. Obviously scouring and filling is also associated with a degree of relief in the basal erosion surface. The wavelength, amplitude and shape of such relief, and the nature of lensing and interfingering, are important features indicating the amount of scouring and filling relative to the amount of bank migration. In this respect it seems necessary to distinguish the large scale relief in the basal erosion surfaces, as mentioned above, from smaller scale 'within channel' scours. The former are genetically related to processes operating only in meandering streams, whereas the latter may also form, for instance, at the base of levee or crevasse deposits (Allen, 1970c).

In general, there is not enough quantitative information available to test these aspects of the model, but there are many

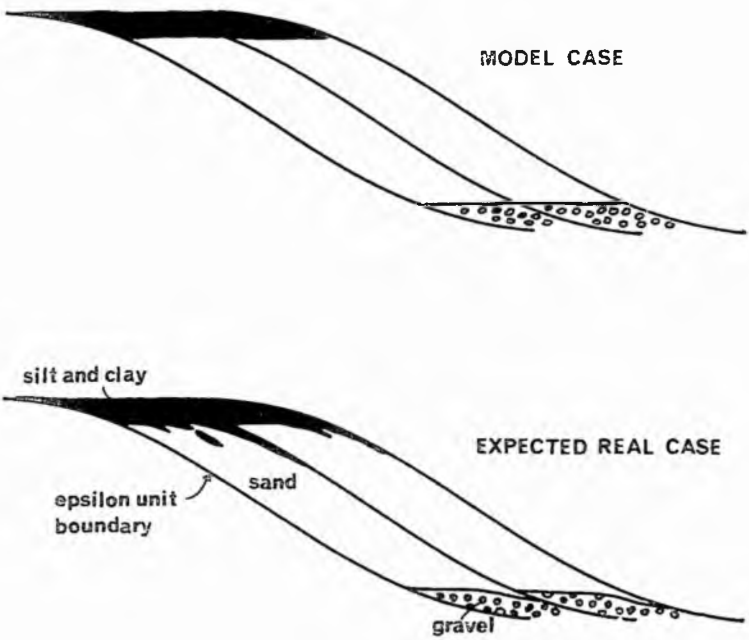

Fig. 22.1 Schematic variation of grain size within single depositional units when no Scour-and-Fill. Expected real world and model cases.

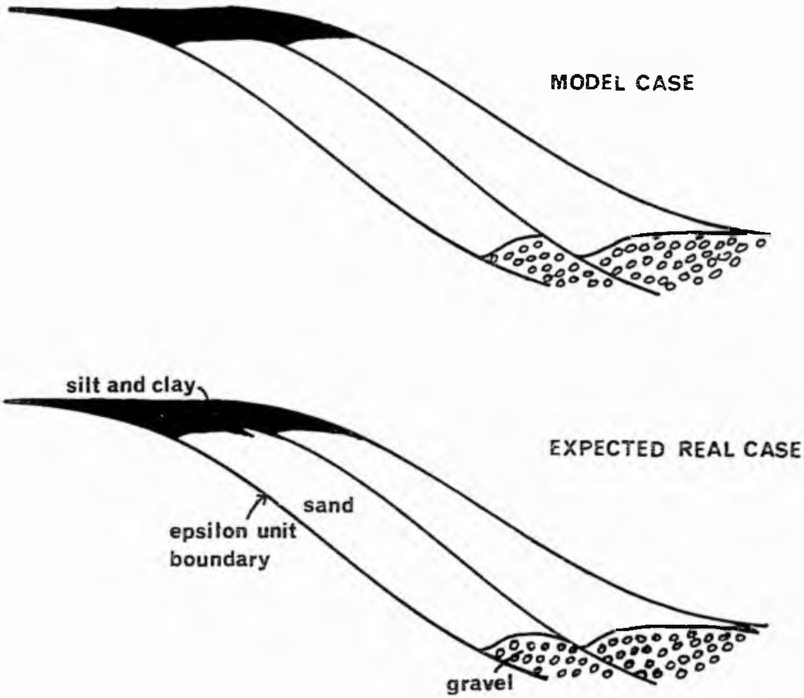

Fig. 22.2 Schematic variation of grain size within single depositional units, with Scour-and-Fill. Expected real world and model cases

examples in recent deposits of large scale relief in basal scoured surfaces and facies boundaries (e.g. Bernard and LeBlanc, 1965; Fisk, 1947; Leopold and Wolman, 1960). Invariably lensing and interfingering of particular types of sedimentary structure and sediment size classes occur (e.g. Allen, 1965a; Frazier and Osanik, 1961; Leopold and Wolman, 1960; Sundborg, 1956).

Fig. 22.2 represents a comparison of the nature of variation in grain size within an individual epsilon unit between the model and that expected in the real situation. It is easy to see from the figure how, for instance, lenses of gravel occur. If there is not significant deposition of fines with falling stages in the real situation or if the fines are subsequently scoured the 'real' example may tend to the simulated situation.

With changes in the slope and radius of curvature of a developing meander in the model there were additional very large-scale variations in grain size and sedimentary structure. In general, grain size decreased and the amount of lower regime forms increased at the expense of upper plane beds as sinuosity increased. Such changes were not simple and an intertonging transition zone was involved. To test this aspect of the model in the light of the assumptions made would require a considerable amount of information over an extensive continuous section. Such information is not forthcoming at present. Furthermore, the variation in all the dependent hydraulic variables in developing meanders needs to be examined in considerably more detail in the field before this aspect of the mathematical model could be used with confidence.

Recent studies have indicated that different processes are acting to give dissimilar sediment deposits in fine and coarse grain point bars (Bluck, 1971; McGowen and Garner, 1970). In coarse grain point bars strong currents develop over the top of the bar during high flood stages in conjunction with those acting in the pool. These currents over the top of the point bar are responsible for localised scouring and deposition of coarse material as bars in this area. Transverse profiles across the point bar become complex and variable along the length of the bar. Sequences produced by bar migration do not always exhibit the general fining upwards as in fine grained point bars. Sequences of sedimentary structures characteristic of particular sub-environments within the bar can be recognised, but may differ from fine grained point bar sequences. Differences will also be expected to exist in the facies geometry. The present study deals essentially with processes operative in fine grained point bars, although there are obvious common features. In general, however, the present model cannot be thought of as truly representing the coarse grained point bar deposition as described by Bluck (1971) and McGowen and Garner (1970).

22.4 Times taken to cut off

No specific experiments were run to test this aspect of the model, although cut-off information is entered in the meander plan figures where relevant. Observations on some of the experiments have shown that the times taken from inception of a meander to cut off is of the order of hundreds of years, which is supported by observational data (see section 10.3). To produce this situation the exponents in the cut off relations must be fairly large, and a realistic value of Q_{volmax} must be specified.

23 COMPARISON WITH ANCIENT FLUVIATILE COARSE MEMBERS

Various aspects of the model can also be compared with the coarse members of the fluviatile 'fining upwards' cycles, known abundantly from ancient sediments, and which are known or strongly believed to have been accumulated through processes of lateral deposition (e.g. Allen, 1963b, 1964, 1965b, c; Allen and Friend, 1968; Beutner et al., 1967; Moody-Stuart, 1966; McGowen and Garner, 1970; Potter, 1967; Visher, 1965a,b). Such interpretation is based on comparison with the textures, sedimentary structures, detailed stratigraphic succession and organic content of recent channel and overbank deposits.

The coarse units are commonly tabular in shape or broadly lens shaped. Epsilon-cross-stratification is only rarely observed, there being only three published occurrences to date (i.e. Allen, 1965b, Beutner et al., 1967; and Moody-Stuart, 1966). This may either be due to lack of preservation, or, as previously mentioned, due to difficulties in recognition. The coarse members exhibit the characteristic vertical patterning of grain size and sedimentary structure, and such vertical patterning has also been recorded from tidal upward fining sequences (e.g. Allen and Friend, 1968; Klein, 1965). Various other obvious recorded and characteristic features which have not been simulated have been the decrease in thickness of cross bedded units upwards, detailed grain fabric and texture, convolute lamination, and the presence of oriented and nonoriented sole structures (i.e. grooves, flutes, pot holes, load structures, etc.).

Relief in grain size class and sedimentary structure boundaries (facies boundaries) is common, although not always present. Lensing of particular sedimentary structures or lithologies is also recorded frequently. Relief of the basal scoured surface is common, although it is not always evident in the literature, whether the relief is due to local small scale scouring, or is genetically related to the processes of scour and fill combined with bar migration. In general, only the amplitude of this relief is recorded but the shape and wavelength is often omitted. The reason for this may be due to lack of exposure, especially when the relief has very long wavelength.

A Downtonian coarse member at Ludlow, Shropshire (Allen, 1964, p. 170) is of uniform thickness, 3.6-3.7 m., and has an essentially flat scoured base, except for scoured hollows with a maximum relief of 15 cm. It would thus appear that scour-and-fill was not prominent in this case. This strongly contrasts with, for example, the high amplitude/wavelength basal scoured surface described by Beutner et al. (1967) in a Pennsylvanian channel sandstone.

The detailed organisation of the grain sizes and structures in the published examples of coarse members is not generally traced laterally in continuous sections. Thus even reasonable qualitative comparison with the simulation model deposits becomes difficult. A rare opportunity to compare the model in detail with ancient sediments occurs when epsilon-cross-stratified units are preserved in extensive outcrops cut perpendicular to the current direction. These structures are the most obvious indicator of the presence of lateral deposition. Allen (1965b) described examples from the Porth-y-Mor beds on the northeast coast of Anglesey. The units average 6' 3" in thickness and were traced for 30 m. or more along the shore. Fig. 23.1 shows Allen's schematic representation of the chief features of lithology and sedimentary structure in the epsilon cross-stratified units. Many of the sigmoidal bedding surfaces are recorded as erosional contacts, indicating scour of the previous bar profile. The cross-stratified units are heterolithic. Although statistically there is an upward decrease of grain sizes with each unit, as well as an upward and lateral decrease in coarseness of beds between major bedding surfaces, the

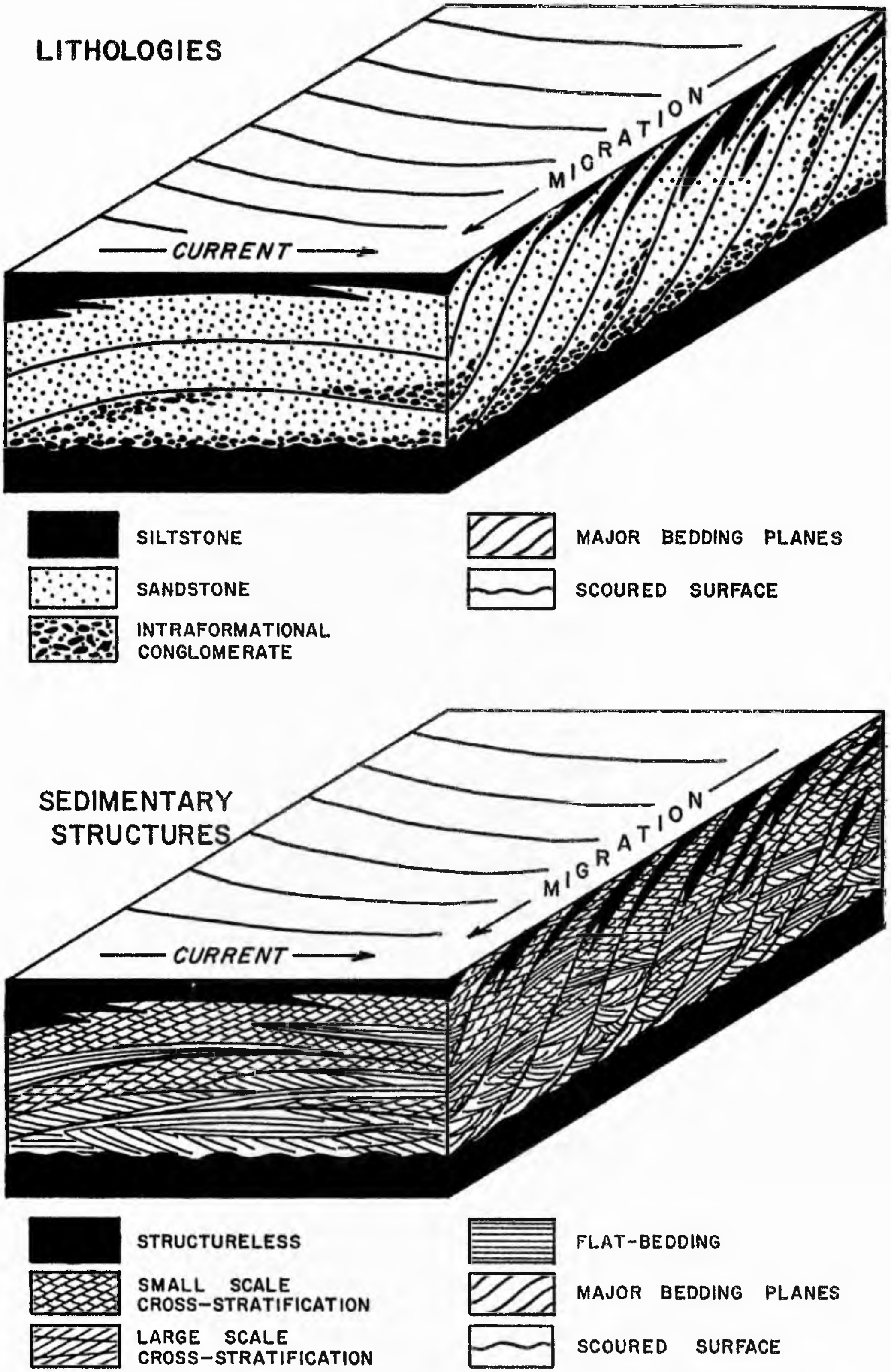

Fig. 23.1. Schematic block diagrams showing the characteristics of epsilon-cross-stratified units in the Old Red Sandstone of Anglesey, North Wales. Unit thickness is from three feet six inches to nine feet. Major bedding surfaces have maximum slopes from four to fourteen degrees. Vertical scale much exaggerated. (from Allen, 1965b).

relationship between lithologies is one of complex intertonging. Sedimentary structures also show complicated spatial relationships with the development of lensing. The nature of these deposits is broadly comparable with simulated deposits, but fig. 23.1 shows up the inability of the model to treat deposition over a range of stages and points to the approximations both in the mathematical model and the computer program. Probably the example of epsilon-cross-stratification that best lends itself to comparison with the model is cited by Beutner et al. (1967). This is discussed more fully in the section dealing with the application of the model to interpretation of ancient fluvial sediments.

Allen (1963b, 1964) described two cases where conglomerate passes laterally gradually into gravel-free rock, despite the underlying basal scoured surfaces persisting laterally for considerable distances. Detailed data unfortunately are not available to determine whether these occurrences represent broad flat lenses of gravel associated with scour and fill of whether they are genetically related to a gradual decrease in load carrying ability of the channel as it moves laterally.

Ancient fluviatile sequences are normally made up of many repeated cyclothems, from which it must be concluded that a channel occupied a given site at successively higher levels relative to an original datum. Such an occurrence can only be attributed to channel migration of continuous or discontinuous nature in conjunction with net vertical deposition, which may also be continuous or discontinuous in nature. The mechanisms responsible for net vertical deposition (aggradation) cannot be simulated at present, however, irrespective of the causative processes involved, a constant rate of aggradation can be simulated. It is only possible to simulate continuous movement of a channel within a meander belt, and not channel abandonment with cut off or meander belt movement in a continuous way or by avulsion. At present therefore it is not possible to simulate repeated channel and overbank sequences. A complex distribution of channel sediments would be expected in a thick alluvial succession (e.g. Allen, 1965a; Potter, 1967), and details of the three dimensional form of the cyclothems would be required before either the controls underlying the cyclicity could be solved or comparison with simulation models is made possible.

24 PRESERVATION OF POINT BAR SEDIMENTS

The experiments show, despite their limitations, that a complete sequence of channel sediments capped by overbank sediments would rarely be preserved in the moving-phase situation, rather that only basal fractions of the total point bar thickness would be preserved (c.f. Bluck, 1971). Clearly the preservation of a 'complete cyclothem' becomes more likely as the section lies out of range of any eroding channel for the sufficient time span. The channel movement may be continuous or discontinuous, and the occurrence of avulsion in particular appears to favour preservation of thick and complete sequences. The experiments suggest that if the general slope of facies boundaries or basal erosion surfaces relative to the land surface is not great and complete bar sequences are preserved, then a process other than purely moving-phase must be responsible.

Complete vertical sequences are rarely preserved in modern and ancient coarse-grained point-bar deposits produced in streams subject to flash floods, because of the rapid channel migration (McGowen and Garner, 1970). Complete vertical sequences are more common in ancient fine-grained point-bar successions of the types described above. Because of the time scales involved in channel movement associated with discontinuous avulsion and cut-off and continuous moving phase, many erosion surfaces would be expected to exist in the lower parts of coarse members; Bluck (1971 states '...many sequences of believed fluvial origin have many erosion surfaces at their base'. In this respect also, the fills of the deeper scoured channels have a greater preservation potential than contemporary shallower ones.

25 APPLICATION OF THE MODEL TO QUANTITATIVE INTERPRETATION OF ANCIENT FLUVIATILE COARSE MEMBERS

Allen (1970a) applies his original 'static' grain size and sedimentary structure model to various Devonian coarse members from Britain and North America, which are strongly believed to have accumulated through processes of lateral deposition. It appears in many cases that the only absolute control on data input used is via the density of the sedimentary particles and the maximum flow depth, which is taken as the thickness of the coarse member. This maximum flow depth must in reality be the maximum scoured flow depth. If scouring and filling has been an important process in the formation of such coarse members the application of this static model invites an additional caution because of the expected lateral variation in member thickness, grain size and bedding geometry. Allen has overcome complications due to major erosion surfaces at the bases of these members by choosing simple coarse members free of evidence of multi-storey character.

Other parameters defining channel geometry were chosen, being consistent with experience of sand-bed rivers, in order to give the closest fit with the observed coarse members. Additional control may have been forthcoming if epsilon cross-stratified units could be traced laterally to the extent that the width of the bar could be discerned (e.g. Moody-Stuart, 1966). Caution is invited here with regard to the definition of the true width when looking at such units as projected in one cross section.

Where exposure limits examination of sections to any great lateral extent the application of the present model will necessarily follow the same general lines as Allen (1970a), thus restricting the use of all aspects of the model. An opportunity to apply substantially more interpretive aspects of the model lies in the Pennsylvanian channel sandstone described by Beutner et al. (1967), which represents some 700 feet in lateral extent of sandy point-bar deposits exposed in a section cut approximately normal to the mean downvalley direction. Directives for use of the model in this application, and a comparison of the simulated and actual section, will follow.

By inspection of the basal scoured surface it seems obvious that channel scouring and filling was continuing with bar migration (see Beutner et al. 1967, p. 913). The unscoured channel depth can be inferred by inspection of the relief of the scoured surface and the shape of the epsilon units. A value of 12 metres was chosen, and thus an idea of the amount of scouring below the talweg could be assessed; average about 4 metres. The width of flow between the inner bank and talweg was approximately 80 metres, by inspection of the width of epsilon units from the top to the bottom of the bar. The individual units actually vary in length and show varying degrees of development, recording variation in the channel direction cutting the section combined with variable scouring. The ratio of partial width to full flow width (at bankfull stage) was arbitrarily taken as 0.8 thus giving a full width of 100 metres. The rate of bar migration can be inferred by measuring the horizontal thickness of certain well developed epsilon units. Average rates of migration are about 10-12 metres per time increment. A value of the exponent n_1 was taken as 1.5 and this provides good agreement with the shape and maximum slope of the epsilon units ($10-20^{o}$). In some runs a straight inner bank profile was used. Parameters for use in the scour and fill and bank migration relations were defined, bearing in mind the required average values of scour and migration required, using an arbitrary flow pattern.

The remaining parameters required for input were defined, being consistent with observations from modern streams, such that the model could best simulate the main features of the section. The sands are medium grained on average but fine upwards. In the basal parts coarse sand and gravel size fragments are found. Most of the deposit is tabular cross bedded and is attributed to deposition by transverse bars migrating over the bar surface. There were a few examples of trough cross-bedding. Occurrences of cross lamination may also be seen towards the top of the section, and lenses of flat bedding sometimes occur in the deepest scours.

Figure 25.1 shows the simulated cross sections which are probably the closest obtainable at present. The grain size distribution section is made up predominantly of sand. Inspection of table 25.1, which shows the variation of various hydraulic parameters over the unscoured bar cross profile for the initial sediment deposition, indicates that the mean grain size is medium sand. The section fines upwards from fine gravel and coarse sand at the base to a small thickness of silt and clay at the top. The correspondence in grain size between the simulated and actual sections appear to be very good.

The correspondence between the simulated sedimentary structure section and the actual section is not as satisfactory. A thick set of cross bedding (due to dunes) is predicted, however, in general, the thicknesses of cross lamination and flat bedding are overemphasised. Furthermore, no flat bedding is predicted in deeper scour hollows. The reason for the discrepancy probably lies in the fact that prediction of bed form was not as readily based on general principles as grain size prediction, and relied heavily on empirical flume data. Not until more rigorous and generalised methods of prediction are developed, which are applicable to natural streams, will this situation be remedied. It has already been pointed out that values of θ_{crit} used are probably too low.

The shape of the basal scoured surfaces agree well

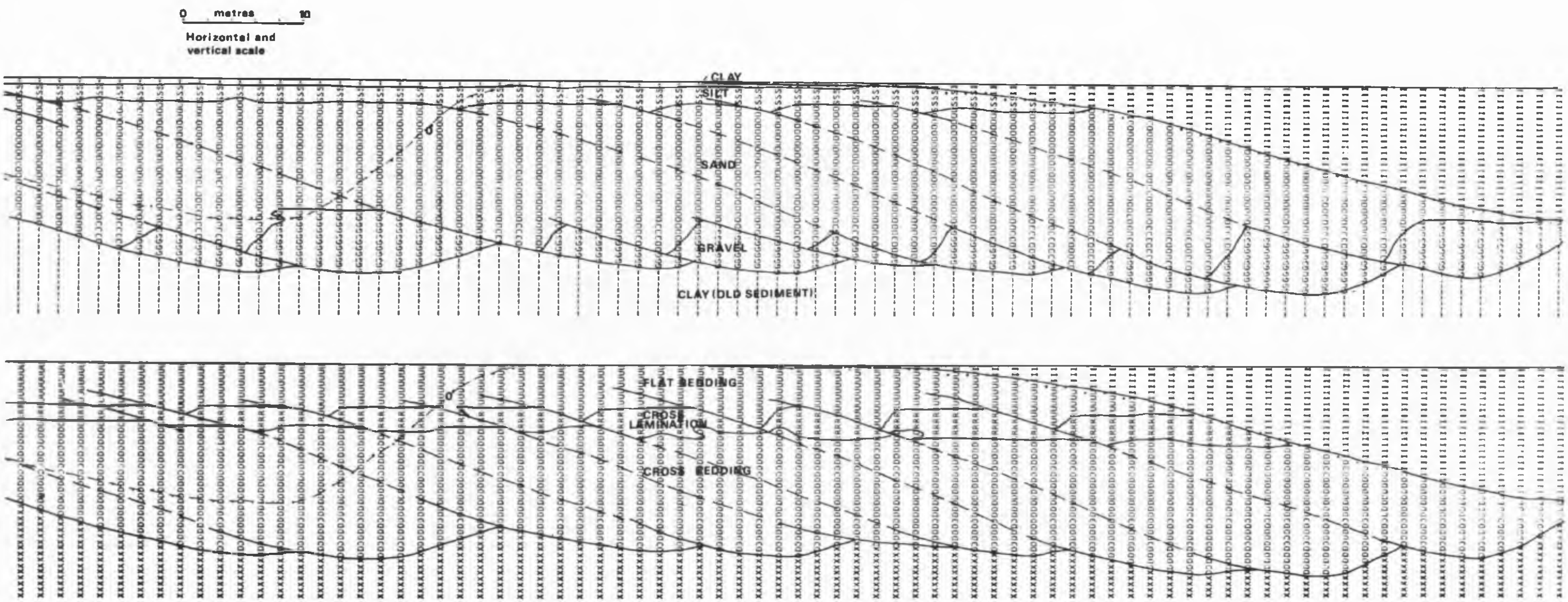

Fig. 25.1. Simulated cross sections comparable with ancient fluviatile coarse member shown in Fig. 25.2.

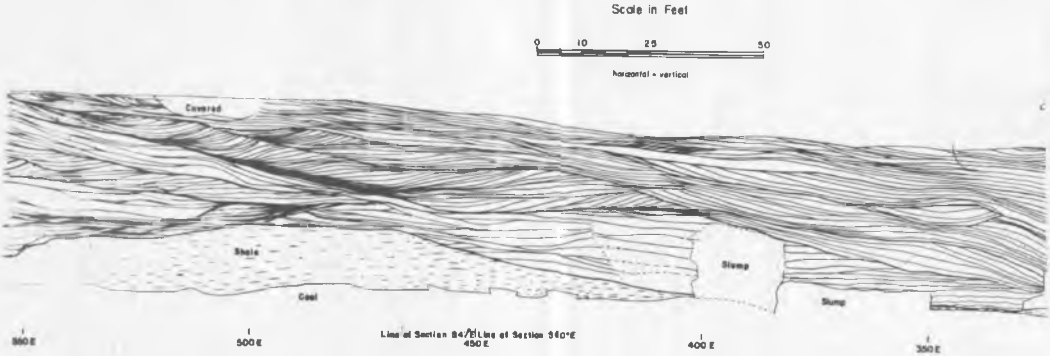

Fig. 25.2. CROSS SECTIONS THROUGH THE PENNSYLVANIAN KITTANNING FORMATION EXPOSED NEAR PHILIPSBURG, PENNSYLVANIA

Upper section, face A; lower section, face B

(after Beutner et al., 1967).

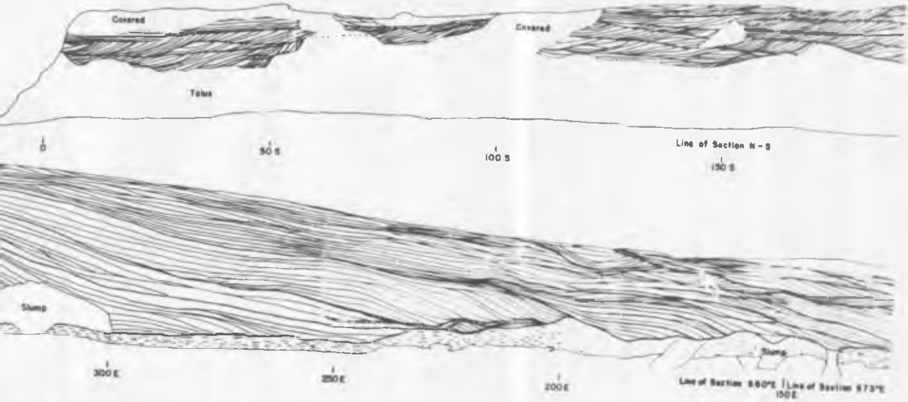

Covered
Covered
Talus
0
50 S
100 S
Line of Section N - S
150 S
Slump
Slump
300 E
250 E
200 E
Line of Section S60°E
Line of Section S73°E
150 E

Table 25.1. Variation of grain size, bed form and various hydraulic parameters over the unscoured bar cross profile for simulated deposits.

FLUVIATILE PROCESS SIMULATION EXPERIMENT X TIME INCREMENT 0

VARIATION OF GRAINSIZE AND BED FORM OVER CHANNEL CROSS PROFILE

DEPTH (M)	GRAINSIZE (CM)		BED FORM	LOCAL MEAN FLOW VELOCITY (CM/SEC)	LOCAL DIMENSIONLESS SHEAR STRESS	LOCAL STREAM POWER (ERGS/CM2/SEC)	LOCAL BED SHEAR STRESS (DYN/CM2)	LOCAL FROUDE NUMBER
0.0002	0.0000	-	U	0.6126	10.7323	0.0006	0.0009	0.1309
0.0018	0.0000	-	U	1.7329	5.4555	0.0130	0.0075	0.1309
0.0060	0.0000	-	U	3.1833	3.6973	0.0806	0.0253	0.1309
0.0143	0.0000	-	U	4.9006	2.8176	0.2942	0.0600	0.1309
0.0279	0.0000	-	U	6.8475	2.2896	0.8027	0.1172	0.1309
0.0482	0.0001	-	U	8.9987	1.9372	1.8217	0.2024	0.1309
0.0764	0.0001	-	U	11.3352	1.6850	3.6411	0.3212	0.1309
0.1139	0.0002	-	U	13.8417	1.4955	6.6300	0.4790	0.1309
0.1620	0.0003	-	U	16.5054	1.3477	11.2414	0.6811	0.1309
0.2218	0.0005	S	U	19.3152	1.2289	18.0150	0.9327	0.1309
0.2947	0.0007	S	U	22.2608	1.1313	27.5779	1.2389	0.1309
0.3816	0.0009	S	U	25.3330	1.0494	40.6444	1.6044	0.1309
0.4838	0.0013	S	U	28.5232	0.9796	58.0140	2.0339	0.1309
0.6022	0.0017	S	U	31.8226	0.9193	80.5649	2.5317	0.1309
0.7377	0.0022	S	U	35.2230	0.8664	109.2499	3.1017	0.1309
0.8913	0.0028	S	U	38.7164	0.8196	145.0859	3.7474	0.1309
1.0637	0.0036	S	U	42.2943	0.7777	189.1414	4.4720	0.1309
1.2554	0.0044	S	U	45.9485	0.7398	242.5242	5.2782	0.1309
1.4671	0.0054	S	U	49.6705	0.7053	306.3630	6.1679	0.1309
1.6989	0.0066	O	U	53.4519	0.6737	381.7937	7.1428	0.1309
1.9512	0.0079	O	U	57.2836	0.6443	469.9277	8.2035	0.1309
2.2240	0.0094	O	U	61.1568	0.6170	571.8396	9.3504	0.1309
2.5171	0.0111	O	U	65.0620	0.5914	688.5310	10.5827	0.1309
2.8302	0.0130	O	U	68.9898	0.5671	820.9077	11.8990	0.1309
3.1627	0.0151	O	U	72.9302	0.5441	969.7542	13.2970	0.1309
3.5140	0.0175	O	U	76.8732	0.5220	1135.7026	14.7737	0.1309
3.8829	0.0201	O	R	40.4041	0.5008	659.5916	16.3249	0.0655
4.2684	0.0231	O	R	42.3623	0.4803	760.2202	17.9457	0.0655
4.6691	0.0263	O	R	44.3057	0.4604	869.7217	19.6300	0.0655
5.0831	0.0299	O	D	46.2287	0.4410	987.9524	21.3710	0.0655
5.5088	0.0339	O	D	48.1255	0.4219	1114.6179	23.1607	0.0655
5.9440	0.0383	O	D	49.9902	0.4030	1249.2634	24.9902	0.0655
6.3863	0.0432	O	D	51.8167	0.3844	1391.2673	26.8498	0.0655
6.8332	0.0485	O	D	53.5991	0.3658	1539.8291	28.7287	0.0655
7.2819	0.0545	O	D	55.3310	0.3473	1693.9739	30.6153	0.0655
7.7295	0.0611	O	D	57.0062	0.3288	1852.5410	32.4972	0.0655
8.1729	0.0685	O	D	58.6184	0.3101	2014.1970	34.3612	0.0655
8.6088	0.0768	O	D	60.1611	0.2913	2177.4502	36.1936	0.0655
9.0337	0.0862	O	D	61.6280	0.2722	2340.6377	37.9801	0.0655
9.4441	0.0970	O	D	63.0125	0.2529	2501.9636	39.7058	0.0655
9.8366	0.1096	O	D	64.3083	0.2332	2659.5139	41.3557	0.0655
10.2073	0.1245	O	D	65.5090	0.2130	2811.2822	42.9144	0.0655
10.5528	0.1425	O	D	66.6084	0.1924	2955.1968	44.3668	0.0655
10.8693	0.1650	O	D	67.5999	0.1711	3089.1436	45.6975	0.0655
11.1534	0.1940	O	D	68.4776	0.1493	3211.0422	46.8919	0.0655
11.4016	0.2337	G	D	69.2354	0.1267	3318.8376	47.9355	0.0655
11.6108	0.2918	G	D	69.8676	0.1034	3410.5774	48.8149	0.0655
11.7778	0.3867	G	D	70.3684	0.0791	3484.4385	49.5171	0.0655
11.8999	0.5738	G	D	70.7323	0.0539	3538.7820	50.0306	0.0655
11.9747	1.1298	G	D	70.9542	0.0275	3572.1873	50.3450	0.0655

FLUVIATILE PROCESS SIMULATION   EXPERIMENT X

CROSS SECTION PARAMETERS	METRES	CELLS
WIDTH OF SECTION	340.000	200
THICKNESS OF SECTION	30.000	60
INITIAL DISTANCE OF INNER CHANNEL BANK FROM L.H.S. OF SECTION	0.0	0
INITIAL BANKFULL STAGE MEASURED FROM SECTION BASE	20.000	40
CELL SIZE IN VERTICAL(Y) DIRECTION	0.500	
CELL SIZE IN HORIZONTAL(Z OR X) DIRECTION	1.700	

CHANNEL PARAMETERS	METRES	CELLS	
TOTAL WIDTH OF CHANNEL(W)	100.000	58	
WIDTH OF FLOW BETWEEN INNER BANK AND TALWEG(W1)	80.000	47	
RATIO OF W1 TO W			0.800
MAXIMUM FLOW DEPTH MEASURED ABOVE TALWEG	12.000		
DENSITY OF SEDIMENTARY PARTICLES			2.650 GM/CM3
FLUID DENSITY			1.000 GM/CM3
DARCY-WEISBACH FRICTION COEFFICIENT FOR DUNES AND RIPPLES			0.080
DARCY-WEISBACH FRICTION COEFFICIENT FOR PLANE BEDS AND ANTIDUNES			0.020
EXPONENT N1			1.500

SYNTHETIC HYDROLOGY PARAMETERS(UNITS NOT NECESSARY)

MEAN OF ALL DAILY MEAN VALUES		543.500					
STANDARD DEVIATION OF DAILY MEAN VALUES		441.000					
MEAN OF YT SERIES		0.0					
STANDARD DEVIATION OF YT SERIES		1.000					
COEFFICIENTS IN AUTOREGRESSIVE MODEL	A1=	0.567	A2=	0.306			
		HARMONICS FROM 1 TO 6					
FOURIER COEFFICIENTS FOR DAILY MEANS(A)		-200.300	145.400	-85.500	58.000	-39.800	7.400
(B)		-112.400	185.000	-79.900	65.600	-72.500	27.800
FOURIER COEFFICIENTS FOR DAILY STD DEVIATIONS(SA)		-123.300	141.600	-66.400	75.700	-47.200	8.600
(SB)		-85.600	105.700	-46.200	31.700	-43.200	4.300
MAXIMUM VALUE OF QVOL		110000.000					

BANK MIGRATION PARAMETERS		
EXPONENT N2		0.500
VALUE OF CONSTANT IN LATERAL MIGRATION RELATION	K2=	0.200E-05
VALUE OF CONSTANT IN DOWNVALLEY MIGRATION RELATION	K3=	0.500E-03
LIMITING PERCENTAGE OF GRAVEL ALLOWABLE IN OUTER BANK		30.000

SCOUR AND FILL PARAMETERS	
CONSTANT K4	0.500E-04
EXPONENT N3	1.000
STANDARD DEVIATION OF ERROR TERM	1.000

CUT-OFF CONTROL PARAMETERS				
LIMITING WIDTH OF MEANDER NECK		200.000 METRES		
EXPONENTS IN NECK CUT-OFF RELATION	EN1=	5.000	EN2=	5.000
LIMITING SINUOSITY		3.000		
LIMITING AMPLITUDE		829.870 METRES		
EXPONENTS IN CHUTE CUT OFF RELATION	EC1=	20.000	EC2=	20.000

A DOWNVALLEY SECTION IS REPRESENTED IN THIS TEST
DISTANCE OF LINE OF SECTION FROM POINT OF INFLECTION OF LOOP IS   0.0   METRES

Table 25.2. Initial data used for simulation.

FLUVIATILE PROCESS SIMULATION EXPERIMENT X

PLANIMETRIC FORM OF MEANDER

WAVELENGTH
AMPLITUDE
SINUOSITY
RADIUS OF CURVATURE AT BEND AXIS
WIDTH OF MEANDER NECK
CHANNEL LENGTH ALONG MEANDER
VALLEY SLOPE
LONGITUDINAL WATER SURFACE SLOPE

SELECTED GEOMETRIC RATIOS

WAVELENGTH TO RADIUS OF CURVATURE
WAVELENGTH TO CHANNEL WIDTH
RADIUS OF CURVATURE TO CHANNEL WIDTH
AMPLITUDE TO CHANNEL WIDTH

FLUVIATILE PROCESS SIMULATION EXPERIMENT X

PLANIMETRIC FORM OF MEANDER

WAVELENGTH
AMPLITUDE
SINUOSITY
RADIUS OF CURVATURE AT BEND AXIS
WIDTH OF MEANDER NECK
CHANNEL LENGTH ALONG MEANDER
VALLEY SLOPE
LONGITUDINAL WATER SURFACE SLOPE

SELECTED GEOMETRIC RATIOS

WAVELENGTH TO RADIUS OF CURVATURE
WAVELENGTH TO CHANNEL WIDTH
RADIUS OF CURVATURE TO CHANNEL WIDTH
AMPLITUDE TO CHANNEL WIDTH

Table 25.3. Various geometric variab
simulation.

TIME INCREMENT 0

METRES

700.000
308.311
1.400
141.032
****
980.000
0.00006000
0.00004286

4.963
7.000
1.410
3.083

TIME INCREMENT 10

METRES

700.000
501.700
1.907
148.890
****
1334.817
0.00006000
0.00003146

4.701
7.000
1.489
5.017

ies at the beginning and end of the

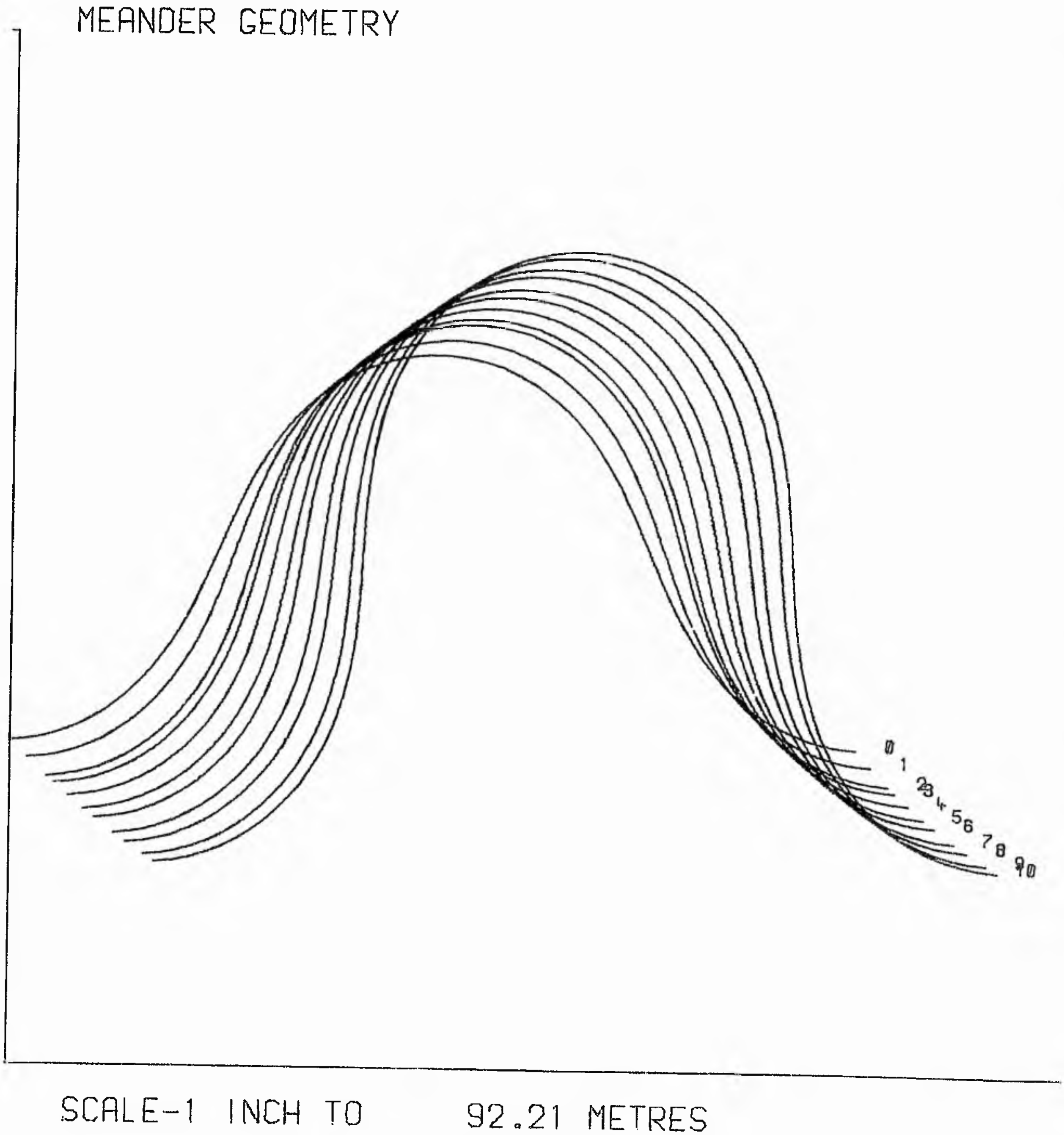

Fig. 25.3. Simulated meander plan forms.

qualitatively with the observed sequence (c.f. fig. 25.2), which indicates that the amounts of bank migration and scour and fill used in the model are appropriate. Where possible approximate outlines of epsilon unit boundaries have been added.

Table 25.2 shows the input data used and various other initial data. Table 25.3 shows various geometric variables at the beginning and end of the simulation, and fig. 25.3 shows the meander movement in plan which produced the deposits. The low valley slope and high sinuosity indicate that the stream was very close to its base level. An estimate of the bankfull discharge can be obtained fairly easily by assuming a realistic value of the friction coefficient for the outer bank; computed values of velocity and the cross sectional area of the channel will then give the discharge. Various other hydrological parameters may be estimated using, for instance, the regression equations developed by Schumm (1972).

26 CONCLUDING REMARKS

As far as the model can be tested against nature it appears to operate realistically. In view of the many simplifications made in its development, the results and implications are encouraging, although no pretence is made to quantitative exactness. Unfortunately the model has not been able to be tested rigorously, and comparison of real examples with solutions produced with the simulation model do not involve any form of optimisation or statistical measure of closeness.

The development of the mathematical model and subsequent experimentation with the computerised version has led to some significant conclusions helpful in the understanding and interpretation of the lateral deposits attributable to meandering streams. The computer simulation model permits, in a matter of minutes computing time, the exploration of the behaviour of the system under a wide variety of physical conditions and over long periods of time. Such data are not easily obtainable from the natural situation by virtue of the time scale involved or the prohibitive costs of field surveys. Scale physical model experiments also have severe limitations on time and often have stringent scaling qualifications.

The model may be used qualitatively as a guide to the recognition of ancient fluviatile sediments which were deposited under conditions of lateral sedimentation on the inside of meander bends. A quantitative picture of certain aspects of the physical environment respsonsible for such deposits may then be built up by comparison with simulated deposits. However, until the model has been tested more rigorously and further developed, any quantitative interpretation must be treated with caution. There are a sufficient number of input variables to provide several solutions in any specific example, and thus any one overall answer cannot always be assumed to be correct in its entirety. Furthermore, at the level of the present study, any 'quantitative' results must be thought of as broad guidelines demarcating a likely physical situation.

Both the mathematical model and computer program provide a framework for the construction of further simulation models of more quantitative validity and embodying more complex and generalised fluvial systems. Obvious improvements would be the development of adequate mathematical models for erosion and deposition over a range of river stages within the channel and over the floodplain. The reasonable treatment of the sequence of events involved with channel abandonment and relocation (cut-off and avulsion) would clearly be valuable. The model is very restrictive in its range of application; riffle deposits, overbank deposits, etc. require attention, and the deposits of coarse-grained point bars and braided rivers must surely merit consideration. Many of the mathematical relationships used in the model are empirical in nature; theoretical relationships will be more desirable in future because of their greater versatility.

As computer simulation models are developed and become more complex, core store requirements may be expected to rise. Fortunately there does not appear to be a problem here in view of the recent advances in computer technology. Associated with further development of such mathematical models will also come a deeper understanding of the processes involved in the natural system. As well as being parasitic on the vast amount of field, laboratory and theoretical information that exists, the models also direct research to areas that are inadequately explored. It should be realised that to test a model adequately, a large amount of data of the appropriate form must be available. The interpretive and predictive potential of computer simulation warrants such further work.

A C K N O W L E D G E M E N T S

This research was carried out whilst under the receipt of a N.E.R.C. research studentship, for which I am grateful.

I would like to express my sincere gratitude to Professor E.K. Walton for his friendly encouragement and guidance during his supervision of this research. Thanks are also due to Dr. B.J. Bluck, Dr. D.G. Farmer and Professor J.R.L. Allen, for their continuing interest and stimulating discussion. My colleagues in the Geology Department, St. Andrews have continued to show a friendly interest and I am indebted in particular to Dr. W. Edryd Stephens for his help in various statistical problems.

Mr. R.W. Benson of the Hydraulics Research Station, Wallingford, kindly allowed me to examine the results of laboratory experiments conducted at Wallingford.

I would like to express my gratitude to Professor A.J. Cole of the St. Andrews University Computing Laboratory for his patient and friendly co-supervision during the early periods of the research. The fine computing facilities at St. Andrews and the invaluable help given by various members of the academic and technical staff of the computing laboratory is gratefully acknowledged.

Thanks are due to Mrs. J. Galloway for painstakingly typing the script and to Mr. J. Allan for producing excellent photographic results.

It has not been possible to give full credit to all the people who have advised, encouraged, criticised, hindered or otherwise shown interest in the research. I would like to extend my gratitude to all those not mentioned specifically above.

LIST OF SYMBOLS USED IN MATHEMATICAL MODEL.

Symbol	Description	*Dimensional formula
a	Cross sectional area of stream.	L^2
a_1, a_2	Coefficients in autoregressive synthetic hydrology model.	-
a(t)	Amplitude of bed wave.	L
A	Meander amplitude.	L
A(t)	Amplitude of surface wave.	L
A_k	Fourier coefficients for cosine terms in harmonic representation of daily mean flows.	-
$_sA_k$	Fourier coefficients for cosine terms in harmonic representation of daily standard deviations about daily means.	
B_k	Fourier coefficients for sine terms in harmonic representation of daily mean flows.	-
$_sB_k$	Fourier coefficients for sine terms in harmonic representation of daily standard deviations about means.	-
$c_1, c_2, ..$	Any constants.	-
C	Chezy C.	$L^{\frac{1}{2}}T^{-1}$
C	Dimensionless parameter from Hayashi (1970).	
C_s	Weight concentration of sediment.	-
d	Mean depth of flow.	L
D	Diameter of sedimentary particle.	L
DSCR	Depth of scour at the talweg.	L
e	Base of naperian logarithms.	-
er	Error term in scour and fill relation.	L
ec_1, ec_2	Exponents in chute cut-off relation.	-
en_1, en_2	Exponents in neck cut-off relation.	-

*M = Mass, L=Length, T=Time.

f	Darcy-Weisbach friction coefficient.	-
f_1	Darcy-Weisbach friction coefficient for ripples and dunes in a straight channel.	-
f_2	Darcy-Weisbach friction coefficient for plane beds and antidunes in a straight channel.	-
f_b	Part of Darcy-Weisbach friction coefficient representing form losses due to addition of a bend.	-
f_s	Darcy-Weisbach friction coefficient in the straight channel that is comparable with a given bend.	-
F	Upslope component of fluid force on a point bar.	MLT^{-2}
F	Width-depth ratio.	-
Fr	Froude number.	-
Fr_1	Maximum Fr for formation of dunes.	-
Fr_2	Maximum Fr for formation of antidunes.	-
Fr_a	Minimum Fr for formation of antidunes.	-
Fr_m	Upper stability limit for 2-D bed waves.	-
Fr_u	Fr at change from transition to upper flow regime.	-
Fr_t	Fr at change from lower flow regime to transition.	-
g	Gravitational acceleration.	LT^{-2}
G	Body force component acting on a particle.	MLT^{-2}
GAP	Width of meander neck.	L
GSI	Grain size index.	-
h	Maximum unscoured flow depth measured above talweg.	L
i	Sediment transport rate (immersed weight per unit width).	$ML^{-1}T^{-1}$

j	Kennedy j factor.	-
k	Wave number ($=2\pi/L$).	L^{-1}
k_1	Ratio of full width to partial width of channel.	-
k_2, k_3	Dimensional constants in bank migration relations.	-
k_4	Dimensional constant in scour and fill relation.	-
l	Meander wavelength.	L
L	Wavelength of sinusoidal bed waves.	L
m	Dimensional coefficient from Hayashi's (1970) sediment transport relation.	-
m_τ	Mean daily flow for day τ, $\tau=1,365$.	L^3T^{-1}
$\bar{m}_\tau$	Mean of all the m_τ.	L^3T^{-1}
m_t	Continuous representation of m_τ using Fourier analysis.	-
M	Weighted mean percentage of silt and clay in channel perimeter.	-
M	Total path length in a meander wavelength	L
n	Exponent in Kennedy's (1963, 1969) transport rate equation.	-
n_1	Exponent in transverse profile shape equation.	-
n_2	Exponent in bank migration relations.	-
n_3	Exponent in scour and fill relation.	-
N	An exponent.	-
NS	Average net scour at a channel cross section.	ML^{-2}
P	A probability.	-
$p(c)$	Probability of chute cut-off.	-
$p(n)$	Probability of neck cut-off.	-
Q	Discharge.	L^3T^{-1}
Q_{vol}	Flood period volume.	L^3
Q_m	Mean annual discharge.	L^3T^{-1}

Q_t	Total sediment load that is sand or bed load at mean annual discharge.	
r	Factor by which f_s may have to be multiplied to account for change in relative roughness (arising from bed features) due to change in hydraulic radius with meandering.	-
r_m	Radius of curvature measured to channel centre lines.	L
r_1	Local radius of curvature.	L
r_L	Lth order serial correlation coefficient of sample Z_t	-
R	Hydraulic radius (= hydraulic mean depth).	L
RMIG	Bank migration rate in specific cross section.	LT^{-1}
RLMIG	Bank migration rate normal to mean downvalley direction.	LT^{-1}
RDMIG	Bank migration rate in mean downvalley direction.	LT^{-1}
s	Distance along meander path.	L
s_τ	Standard deviation of daily flow for day τ.	-
$\bar{s}_\tau$	Mean of all s_τ.	-
s_y	Standard deviation of Y_t series.	-
s_t	Continuous representation of s_τ using Fourier analysis.	-
sn	Sinuosity.	-
stdvn	Standard deviation in error term.	-
S	Longitudinal slope of water surface.	-
S	Distance of channel at bend axis from an assumed equilibrium position (i.e. position of limiting amplitude) - measured normal to mean downvalley direction.	L

S_o	Initial distance from equilibrium position above.	L
S_b	Longitudinal bed slope.	-
t	Time.	T
tan	Dynamic solid friction coefficient.	-
T	Constant value of t in scour and fill analysis.	T
$\bar{T}$	Net forward sediment transport rate for whole stream.	
V	Mean fluid flow velocity for whole stream	LT^{-1}
V_c	Critical velocity for initiation of sediment motion.	LT^{-1}
V_b	Bed form velocity.	LT^{-1}
V_*	Shear velocity.	LT^{-1}
V_{*crit}	Critical shear velocity.	LT^{-1}
w	Full width of flow between inner and outer banks.	L
w_1	Width of flow between inner bank and talweg.	L
w_s	Channel width projected in a specific cross section.	L
W	Meander width.	L
x	Downchannel distance measured parallel to channel centre line.	L
X	Coordinate of reference axis in downvalley direction.	
X_t	Time series.	-
y	Flow depth measured positively downward from water surface at any transverse distance z across channel.	L
Y_t	Standardised fitted series or Fitted series.	-

$\bar{Y}$	Mean of Y_t.	-
z	Perpendicular transverse distance across the water surface measured from edge of water at inner bank.	L
Z	Coordinate for reference axis normal to X axis in horizontal plane.	-
Z_t	Standardised series.	-
Z_{sect}	Normal distance of line of section from line joining points of inflection of loop.	L
α	Angle on bed between channel centre line and tangent to a skin-friction line.	-
α	Angle that line of section makes with normal to mean downvalley direction.	-
β	Slope in degrees of channel cross profile.	-
Γ	Expression in Hayashi's (1970) analysis.	-
δ	Lag distance.	L
Δs	Elemental distance along path of a meander i.e. small change in s.	L
$\Delta \phi$	Small change in ϕ.	-
ϵ_t	Independent residual series.	-
η_t	Standardised independent stochastic variable (primary variable)	-
θ	Dimensionless shear stress.	-
θ_{crit}	Critical dimensionless shear stress.	-
ν	Kinematic viscosity.	L^2T^{-1}
π	Pi, radians.	-
ρ	Fluid density (including suspended sediment).	ML^{-3}
ρ_w	Fluid density of water.	ML^{-3}
ρ_L	Lth order serial correlation coefficient of the population from which Z_t is drawn.	-

σ	Density of sediment particle in bed load.	ML^{-3}
σ_s	Density of suspended sediment.	ML^{-3}
τ_x	Component of bed shear stress parallel to channel centre line.	$ML^{-1}T^{-2}$
τ_s	Bed shear stress parallel to skin friction line.	$ML^{-1}T^{-2}$
ϕ	Deviation angle of meander path from mean downvalley direction.	-
ω	Maximum value of ϕ.	-
ω	Stream power.	MT^{-3}
ω_{crit}	Critical stream power.	MT^{-3}

REFERENCES CITED

ACKERS, P. and CHARLTON, F.G. 1970a. The geometry of small meandering streams. Proc. Instn. Civ. Engrs. Supplement (xii). Paper 7328 S, 289-317.

______________ 1970b. Dimensional analysis of alluvial channels with special reference to meander length. J. Hydraul. Res., 8, 287-314.

______________ 1970c. Meander geometry arising from varying flows. J. Hydrol., 11, 230-252.

______________ 1970d. The slope and resistance of small meandering channels. Proc. Instn. Civ. Engrs. Supplement (xv). Paper 7362 S, 349-370.

ADAMOWSKI, K. 1971. Spectral density of a river flow time series. J. Hydrol., 14, 43-52.

ALBERTSON, M.L. and SIMONS, D.B. 1964. Fluid mechanics. In V.T. Chow (Ed), Handbook of Applied Hydrology, sect. 7. McGraw Hill.

ALLEN, J. 1939. The resistance to flow of water along a tortuous stretch of river and in a scale model of the same. J. Instn. Civ. Engrs., 11, 115.

ALLEN, J. and SHAHWAN, A. 1954. The resistance to flow of water along a tortuous stretch of the river Irwell (Lancashire) - an investigation with the aid of scale-model experiments. Proc. Instn. Civ. Engrs., 25, 144-165.

ALLEN, J.R.L. 1963a. The classification of cross-stratified units with notes on their origin. Sedimentology, 2, 93-114.

______________ 1963b. Depositional features of Dittonian rocks: Pembrokeshire compared with the Welsh Borderland. Geol. Mag., 100, 385-400.

______________ 1963c. Henry Clifton Sorby and the sedimentary structures of sands and sandstones in relation to flow conditions. Geol. Mijnbouw, 42, 223-238.

______________ 1964. Studies in fluviatile sedimentation: six cyclothems from the Lower Old Red Sandstone, Anglo-Welsh Basin. Sedimentology, 3, 163-198.

______________ 1965a. A review of the origin and characteristics of recent alluvial sediments. Sedimentology, 5, 89-191.

______________ 1965b. Sedimentation and palaeogeography of the Old Red Sandstone of Anglesey, North Wales. Proc. Yorks. Geol. Soc., 35, 139-185.

______________ 1965c. Fining upwards cycles in alluvial successions. Liverpool Manchester Geol. J., 4, 229-246.

ALLEN, J.R.L. 1968. Current Ripples. North-Holland Publishing Co., Amsterdam. 433pp.

______________ 1970a. A quantitative model of grain size and sedimentary structures in lateral deposits. Geol. J., 7, 129-146.

______________ 1970b. Studies in fluviatile sedimentation: A comparison of fining upwards cyclothems, with special reference to coarse-member composition and interpretation. J. Sedim. Petrol., 40, 298-323.

______________ 1970c. Physical processes of sedimentation. George Allen and Unwin, London. 248pp.

______________ 1971. Rivers and their deposits. Sci. Prog. Oxf., 59, 109-122.

ALLEN, J.R.L. and FRIEND, P.F. 1968. Deposition of the Catskill facies, Appalachian region: with notes on some other Old Red Sandstone Basins. Spec. Pap. Geol. Soc. Am., 106, 21-74.

ANDERSON, A.G. 1953. The characteristics of sediment waves formed by flow in open channels. Proc. 3rd Midwest. Conf. Fluid Mech., Minneapolis, 379-395.

______________ 1967. On the development of stream meanders. Proc. Int. Ass. Hydraul. Res., 1, 370-378.

ATHAULLAH, M. and SIMONS, D.B. 1970. Prediction of bed forms in alluvial channels. In press.

BAGNOLD, R.A. 1954. Experiments on a gravity free dispersion of large solid spheres in a Newtonian fluid under shear. Proc. R. Soc., 225A, 49-63.

______________ 1956. The flow of cohesionless grains in fluids. Phil. Trans. Roy. Soc. London, Ser. A, 249, 235-297.

______________ 1960. Some aspects of the shape of river meanders. Prof. Pap. U.S. Geol. Surv. No. 282-E, 135-144.

______________ 1966. An approach to the sediment transport problem from general physics. Prof. Pap. U.S. Geol. Surv., No. 422-I, 1-37.

BECKINSALE, R.P. 1969. River regimes. In R.J. Chorley (Ed), Water, Earth and Man, 455-471. Methuen.

BEERBOWER, J.R. 1964. Cyclothems and cyclic depositional mechanisms in alluvial plain sedimentation. Bull. Kansas Geol. Surv., No. 169, 31-42.

BERNARD, H.A. and LeBLANC, R.J. 1965. Resume of the Quaternary geology of the northwestern Gulf of Mexico Province. In The Quaternary of the United States (Ed. H.E. Wright and D.G. Frey). Princeton University Press, Princeton, N.J., 137.

BERNARD, H.A. and MAJOR, C.F. 1963. Recent meander belt deposits of the Brazos River: an alluvial 'sand' model. Bull. Am. Ass. Petrol. Geol., 47, 350.

BEUTNER, E.C., FLUECKINGER, L.A. and GARD, T.M. 1967. Bedding geometry in a Pennsylvanian channel sandstone. Bull. Geol. Soc. Am., 78, 911-916.

BLUCK, B.J. 1971. Sedimentation in the meandering River Endrick. Scott. J. Geol., 7, 93-138.

CALLANDER, R.A. 1969. Instability and river channels. J. Fluid. Mech., 36, 465-480.

CARLSTON, C.W. 1965. The relation of free meander geometry to stream discharge and its geomorphic implications. Am. J. Sci., 263, 864-885.

CHANG, H-Y., SIMONS, D.B., and WOOLHISER, D.A. 1971. Flume experiments on alternate bar formation. J. Waterways, Harbours and Coastal Engrg. Div., Am. Soc. Civ. Engrs., 97, 155-165.

CHANG, T.P. and TOEBES, G.H. 1970. A statistical comparison of meander plan forms in the Wabash Basin. Water Resources Res., 6, 557-578.

CHARLTON, F.G. and BENSON, R.W. 1966. Effect of discharge and sediment charge on meandering of small streams in alluvium. Hydraulics Research Sta., Wallingford, England.

CHITALE, S.V. 1970. River channel patterns. J. Hydraul. Div., Am. Soc. Civ. Engrs., 96, 201-221.

CHORLEY, R.J. and KENNEDY, B.A. 1971. Physical Geography: a systems approach. Prentice Hall, London. 370pp.

CHOW, V.T. 1959. Open Channel Hydraulics. McGraw Hill. 680pp.

__________ 1964. Statistical and probability analysis of hydrologic data. pt. 1. Frequency analysis. In Chow, V.T. (Ed), Handbook of Applied Hydrology, sect. 8.1. McGraw Hill.

__________ 1967. Simulation of the hydrologic behaviour of watersheds, a general report on new ideas and scientific methods in hydrology. Proc. Int. Hydrol. Symp., 50-65. Colorado State University, Fort Collins, Colorado.

__________ and KARELIOTIS, S.J. 1970. Analysis of stochastic hydrologic systems. Water Resources, Res., 6, 1569-1582.

COLBY, B.R. 1964. Scour and Fill in sand bed streams. Prof. Pap. U.S. Geol. Surv., No. 462-D. 32pp.

COLEMAN, J.M. 1969. Brahmaputra River: channel processes and sedimentation. Sediment. Geol., 3, 129-239.

CRAWFORD, N.H. and LINSLEY, R.K. 1966. Digital simulation in hydrology: Stanford Watershed model IV. Stanford Univ. Dept. Civ. Engrg. Tech. Rept. 39.

CRESS, P., DIRKSEN, P. and GRAHAM, J.W. 1970. FORTRAN IV with WATFOR and WATFIV. Prentice Hall.

CULBERTSON, J.K. and DAWDY, D.R. 1964. A study of fluvial characteristics and hydraulic variables, Middle Rio Grande, New Mexico. U.S. Geol. Surv. Water Supply Pap., No. 1498-F, 74pp.

__________ SCOTT, C.H. and BENNETT, J.P. 1972. Summary of alluvial-channel data from Rio Grande Conveyance Channel, New Mexico, 1965-69. Prof. Pap. U.S. Geol. Surv., No. 562-J. 49pp.

DANIEL, J.F. 1971. Channel movement of meandering Indiana streams. Prof. Pap. U.S. Geol. Surv., No. 732-A. 18pp.

DAWDY, D.R. and MATALAS, N.C. 1964. Statistical and probability analysis of hydrologic data. pt. III. Analysis of variance, covariance and time series. In Chow, V.T. (Ed), Handbook of Applied Hydrology, sect. 8-III. McGraw Hill.

ENGELUND, F. 1970. Instability of erodible beds. J. Fluid. Mech., 42, 225-244.

__________ and FREDSOE, J. 1971. Three dimensional stability analysis of open channel flow over an erodible bed. Nordic Hydrology, 2, 93-108.

__________ and HANSEN, E. 1966. Investigations of flow in alluvial streams. Acta Polytech. Scand., Civil Engrg. Bld. Construct. Ser., No. 35, 1-100.

__________ 1967. Comparison between similarity theory and regime formulae. Tech. Univ. Denmark, Copenhagen, Coastal Engrg. Lab. (Hydraulic Lab.), Basic Research Progr. Rep. 13, 14-16.

EVANS, G. 1965. Intertidal flat sediments and their environments of deposition in the Wash. Q.J. Geol. Soc. Lond., 121, 209-245.

FISK, H.N. 1944. Geological investigation of the alluvial valley of the lower Mississippi River. Mississippi River Commission, Vicksburg, Miss. 78pp.

__________ 1947. Fine grained alluvial deposits and their effects on Mississippi river activity. U.S. Waterways Expt. Sta., Vicksburg, Miss. 2 vols.

FRAZIER, D.E. and OSANIK, A. 1961. Point bar deposits, Old River Locksite, Louisiana. Trans. Gulf Coast Assoc. Geol. Soc., 11, 121-137.

FRIEDKIN, J.F. 1945. A laboratory study of the meandering of alluvial rivers. U.S. Waterways Expt. Sta., Vicksburg, Miss.

FUJIYOSHI, Y. 1950. Theoretical treatise on the meandering of river. Japan Sci. Rev., 1, 29-34.

GHOSH, A.K. and SCHEIDEGGER, A.E. 1971. A study of natural wiggly lines in hydrology. J. Hydrol., 13, 101-126.

GRADOWCZYK, M.H. 1968. Wave propagation and boundary instability in erodible-bed channels. J. Fluid Mech., 33, 93-112.

GRAF, W.H. 1971. Hydraulics of sediment transport. McGraw Hill. 513pp.

GUY, H.P, SIMONS, D.B., and RICHARDSON, E.V. 1966. Summary of alluvial channel data from flume experiments, 1956-61. Prof. Pap. U.S. Geol. Surv., No. 462-I. 96pp.

HAMLIN, M.J. 1971. A study of synthetic flow generation techniques using Elan valley data. J. Instn. Water Engrs., 25, 355-370.

HANDY, R.L. 1972. Alluvial cutoff dating from subsequent growth of a meander. Bull. Geol. Soc. Am., 83, 475-480.

HANSEN, E. 1967. On the formation of meanders as a stability problem. Tech. Univ. Denmark, Copenhagen, Coastal Engrg. Lab. (Hydraulic Lab.), Basic Research Progr. Rep. 13, 9-13.

HARBAUGH, J.W. and BONHAM-CARTER, G. 1970. Computer simulation in geology. Wiley.

HARMS, J.C. and FAHNESTOCK, R.K. 1965. Stratification, bed forms and flow phenomena (with an example from the Rio Grande). In Primary Sedimentary structures and their hydrodynamic interpretation (Ed. G.V. Middleton). S.E.P.M. Spec. Publn. 12, 84-115.

HAYASHI, T. 1970. Formation of dunes and antidunes in open channels. J. Hydraul. Div. Am. Soc. Civ. Engrs., 96, 357-366.

HILL, H.M. 1966. Bed forms due to a fluid stream. J. Hydraul. Div. Am. Soc. Civ. Engrs., 92, 127-143.

__________, SRINIVASAN, V.S. and UNNY, T.E. 1969. Instability of a flat bed in alluvial channels. J. Hydraul. Div. Am. Soc. Civ. Engrs., 95, 1545-1558.

IBADE-ZADE, Yu.A. and KIYASBEILI, T.N. 1967. The bed form on rectilinear and curvilinear river and big channel sections. Proc. XII Congress, Int. Ass. Hydraul. Res., 1, 345-353.

IBM 1968. System/360 FORTRAN IV language.

____ 1971. System/360 Scientific Subroutine Package. Version III. Programmers Mannual.

INGLIS, C.C. 1947. Meanders and their bearing on river training. Inst. Civil Engrs. (London). Maritime and Waterways Engrg. Div., Session 1946-47

__________ 1949. The behaviour and control of rivers and canals. Res. Publ. Central Waterpower and Irrigation Navigation Res. Sta., Poona (India), 13, pt. I, 143-157; pt. II, 459-467.

IPPEN, A.T. and DRINKER, P.A. 1962. Boundary shear stresses in curved trapezoidal channels. J. Hydraul. Div. Am. Soc. Civ. Engrs., 88, 143-180.

JAHNS, R.H. 1947. Geologic features of the Connecticut Valley, Massachusetts, as related to recent floods. U.S. Geol. Water Supply Papers, 996, 158pp.

KENNEDY, J.F. 1963. The mechanics of dunes and antidunes on erodible-bed channels. J. Fluid Mech., 16, 521-544.

__________ 1969. The formation of sediment ripples, dunes and antidunes. Annual Review of Fluid Mech., 1, 147-168.

KINOSITA, R. 1961. Study of the channel evolution of the Isikari River. Bureau of Resources, Department of Science and Technology, Japan (In Japanese).

KLEIN, G. de V. 1963. Bay of Fundy intertidal zone sediments. J. Sedim. Petrol., 33, 844-854.

__________ 1965. Dynamic significance of primary structures in the Middle Jurassic Great Oolite Series, southern England. In Primary sedimentary structures and their hydrodynamic interpretation (Ed. G.V. Middleton). S.E.P.M. Spec. Publn., 12, 173-191.

KOLB, C.R. 1963. Sediments forming the bed and banks of the Lower Mississippi River and their effect on river migration. Sedimentology, 2, 227-235.

KONDRATEV, N.G. 1962. River flow and river channel formation. Israel program for scientific translations, Jerusalem.

KREITZBERG, C.B. and SHNEIDERMAN, B. 1972. The elements of FORTRAN style: techniques for efficient programming. Harcourt Brace Jovanovich, Inc.

LANE, E.W. and BORLAND, W.M. 1954. River bed scour during floods. Trans. Am. Soc. Civ. Engrs., 119, 1069-1080.

LANGBEIN, W.B. 1964. Geometry of river channels. J. Hydraul. Div. Am. Soc. Civ. Engrs., 90, 301-312.

LANGBEIN, W.B. and LEOPOLD, L.B. 1964. Quasi-equilibrium states in channel morphology. Am. J. Sci., 262, 782-794.

________________ 1966. River meanders-theory of minimum variance. Prof. Pap. U.S. Geol. Surv., No. 422-H. 15pp.

LATHRAP, D.W. 1968. Aboriginal occupation and changes in river channel on the Central Ucayali, Peru. American Antiquity, 33, 62-79.

LEOPOLD, L.B., BAGNOLD, R.A., WOLMAN, M.G. and BRUSH, L.M. 1960. Flow resistance in sinuous or irregular channels. Prof. Pap. U.S. Geol. Surv., No. 282-D, 111-134.

LEOPOLD, L.B. and LANGBEIN, W.B. 1962. The concept of entropy in landscape evolution. Prof. Pap. U.S. Geol. Surv., No. 500-A, 20pp.

________________ 1966. River meanders. Scientific American, 214, 60-70.

LEOPOLD, L.B. and MADDOCK, T. 1953. The hydraulic geometry of stream channels and some physiographic implications. Prof. Pap. U.S. Geol. Surv., No. 252, 1-57.

LEOPOLD, L.B. and MILLER, J.P. 1956. Ephemeral streams-hydraulic factors and their relationship to the drainage net. Prof. Pap. U.S. Geol. Surv., No. 282-A, 1-36.

LEOPOLD, L.B. and WOLMAN, M.G. 1960. River meanders. Bull. Geol. Soc. Am., 71, 769-794.

LEOPOLD, L.B., WOLMAN, M.G. and MILLER, J.P. 1964. Fluvial processes in geomorphology. W.H. Freeman and Co., San Francisco. 522p.

MATALAS, N.C. 1967. Mathematical assessment of synthetic hydrology. Water Resources Res., 3, 937-946.

MATTHES, G.H. 1941. Basic aspects of stream meanders. Trans. Am. Geophys. Union (1941), 632-636.

MERCER, A.G. 1971. Analysis of alluvial bed forms. In Shen, H.W. (Ed), River Mechanics, 1, ch. 10, 1-26. Fort Collins, Colorado, Water Resources Pubs.

MOODY-STUART, M. 1966. High and low sinuosity stream deposits, with examples from the Devonian of Spitsbergen. J. Sedim. Petrol., 36, 1102-1117.

McDOWELL, J.P. 1960. Cross bedding formed by sand waves in Mississippi River point bar deposits. Bull. Geol. Soc. Am., 71, 1925.

McGOWEN, J.H. and GARNER, L.E. 1970. Physiographic features and stratification types of coarse grained point bars: modern and ancient examples. Sedimentology, 14, 77-111.

McKEE, E.D., CROSBY, E.J. and BERRYHILL, H.L. 1967. Flood deposits, Bijou Creek, Colorado, June 1965. J. Sedim. Petrol., 37, 829-851.

NAGABHUSHANAIAH, H.S. 1967. Meandering of rivers. Bull. Int. Ass. Scient. Hydrol., 12, 28-43.

NEDECO. 1959. River studies and recommendations on improvement of Niger and Benue. North-Holland, Amsterdam, 1000pp.

NORDIN, C.F. 1964. Aspects of flow resistance and sediment transport Rio Grande near Bernalillo, New Mexico. U.S. Geol. Surv. Water Supply Pap., 1498-H. 41pp.

OOMKENS, E. and TERWINDT, J.H.J. 1960. Inshore estuarine sediments in the Haringvleit (The Netherlands). Geol. Mijnbouw, 39, 701-710.

PARTHENIADES, E. 1971. Erosion and deposition of cohesive materials. In Shen, H.W. (Ed), River Mechanics, 2, ch. 25, 1-91. Fort Collins, Colorado, Water Resources Pubs.

PARTHENIADES, E. and PAASWELL, R.E. 1970. Erodibility of channels with cohesive boundary. J. Hydraul. Div. Am. Soc. Civ. Engrs., 96, 755-771.

POKHSRARYAN, M.S. 1957. Non eroding current velocities. Izv. Akad. Nauk. Armyan S.S.R., Ser. Tekh. Nauk., 10,

_______________ 1958. Transverse profiles of natural river channels. Izv. Akad. Nauk. Armyan. S.S.R., Ser. Tekh. Nauk., 11, 31-38.

POTTER, P.E. 1967. Sand bodies and sedimentary environments: a review. Bull. Am. Ass. Petrol. Geol. 51, 337-365.

POTTER, P.E. and BLAKELY, R.F. 1967. Generation of a synthetic vertical profile of a fluvial sand body. J. Petroleum Technology, 7, 243-251.

QUIMPO, R.G. 1967. Stochastic model of daily river flow sequences. Colorado State University, Hydrology Paper No. 18, Fort Collins, Colorado.

QUIMPO, R.G. 1968a. Stochastic analysis of daily river flows. J. Hydraul. Div. Am. Soc. Civ. Engrs. 94, 43-57.

__________ 1968b. Autocorrelation and spectral analysis in hydrology. J. Hydraul. Div. Am. Soc. Civ. Engrs., 94, 363-373.

RAUDKIVI, A.J. 1967. Loose boundary hydraulics. Pergamon Press. 331pp.

REINECK, H.E. 1958. Longitudinale Schragschicht im Watt. Geol. Rdsch., 47, 73-82.

REYNOLDS, A.J. 1965. Waves on the erodible bed of an open channel. J. Fluid Mech., 22, 113-133.

RIPLEY, H.C. 1927. Relation of depth to curvature in channels. Trans. Am. Soc. Civ. Engrs., 90, 207-238.

RODRIGUEZ-ITURBE, I. 1968. A modern statistical study of monthly levels of the Orinoco River. Bull. Int. Ass. Scient. Hydrol., 13, 25-41.

ROESNER, L.A. and YEVDJEVICH, V. 1966. Mathematical models for time series of monthly precipitation and monthly runoff. Colorado State University, Hydrology Paper No. 15. Fort Collins, Colorado.

ROZOVSKII, I.L. 1961. Flow of water in bends of open channels. Israel program for scientific translations, Jerusalem.

RUSSELL, R.J. 1954. Alluvial morphology of Anatolian rivers. Ann. Ass. Am. Geographers, 44, 363-391.

__________ 1967. River and delta morphology. Louisiana State Univ. Press, Coastal Studies Series, No. 20.

SCHEIDEGGER, A.E. 1967. A thermodynamic analogy for meander systems. Water Resources Res., 3, 1041-1046.

__________ 1970. Theoretical geomorphology, 2nd edition. George Allen & Unwin Ltd., London. Springer-Verlag, Berlin, 435pp.

SCHUMM, S.A. 1960. The shape of alluvial channels in relation to sediment type. Prof. Pap. U.S. Geol. Surv., No. 352-B, 17-30.

__________ 1963. Sinuosity of alluvial rivers on the Great Plains. Bull. Geol. Soc. Am., 74, 1089-1100.

__________ 1967. Meander wavelength of alluvial rivers. Science, 157, 1549-1550.

SCHUMM, S.A. 1968. River adjustment to altered hydrologic regimen - Murrumbidgee River and palaeochannels, Australia. Prof. Pap. U.S. Geol. Surv., No.598. 65pp.

________ 1969. River metamorphosis. J. Hydraul. Div. Am. Soc. Civ. Engrs., 95, 255-273.

________ 1971. Fluvial geomorphology. In Shen, H.W. (Ed), River Mechanics, 1, ch. 4, 1-30. Fort Collins, Colorado, Water Resources Pubs.

________ 1972. Fluvial palaeochannels. In Recognition of ancient sedimentary environments, S.E.P.M. Spec. Publ. No. 16, 98-107.

SCHUMM, S.A. and KHAN, H.R. 1972. Experimental study of channel patterns. Bull. Geol. Soc. Am., 83, 1755-1770.

SCHUMM, S.A., KHAN, H.R., WINKLEY, B.R. and ROBBINS, L.G. 1972. Variability of river patterns. Nature, 237, 75-76.

SCHUMM, S.A. and LICHTY, R.W. 1963. Channel widening and floodplain construction along Cimarron River in southwestern Kansas. Prof. Pap. U.S. Geol. Surv. No. 352-D, 71-88.

SELLIN, R.H.J. 1964. A laboratory investigation into the interaction between the flow in the channel of a river and that over the floodplain. La Houille Blanche, No. 7, 793-801.

SHAHJAHAN, M. 1970. Factors controlling the geometry of fluvial meanders. Bull. Int. Ass. Scient. Hydrol., 15, 13-24.

SHUKRY, A. 1950. Flow around bends in an open channel flume. Trans. Am. Soc. Civ. Engrs., 115, 751-779.

SIMONS, D.B. 1971. River and canal morphology. In Shen, H.W. (Ed), River Mechanics, 2, ch. 20, 1-60. Fort Collins, Colorado, Water Resources Pubs.

SIMONS, D.B. and RICHARDSON, E.V. 1966. Resistance to flow in alluvial channels. Prof. Pap. U.S. Geol. Surv., No. 422-J, 1-61.

________________ 1971. Flow in alluvial sand channels. In Shen, H.W. (Ed), River Mechanics, 1, ch. 9, 1-89. Fort Collins, Colorado, Water Resources Pubs.

SIMONS, D.B., RICHARDSON, E.V. and ALBERTSON, M.L. 1961. Flume studies using medium sand (0.45mm). U.S. Geol. Surv. Water Supply Papers, 1498-A. 76pp.

SIMONS, D.B., RICHARDSON, E.V. and NORDIN, C.F. 1965. Sedimentary structures generated by flow in alluvial channels. Spec. Publs. Soc. Econ. Palaeont. Miner., Tulsa, 12, 34-52.

SOUTHARD, J.B. 1971. Representation of bed configurations in depth-velocity-size diagrams. J. Sedim. Petrol., 41, 903-915.

SPEIGHT, J.G. 1965a. Meander spectra of the Angabunga River. J. Hydrol., 3, 1-15.

__________ 1965b. Flow and channel characteristics of the Angabunga River, Papua. J. Hydrol., 3, 16-36.

__________ 1967. Spectral analysis of meanders of some Australasian rivers. In J.N. Jennings and J.A. Mabbutt (Eds), Landform studies from Australia and New Guinea. Cambridge University Press, 48-63.

STALL, J.B. and FOK, YU-SI. 1968. Hydraulic geometry of Illinois Streams. Illinois Univ. Water Resources Centre Res. Rept. 15, 47pp.

SUNDBORG, A. 1956. The River Klaralven: a study of fluvial processes. Geogr. Annlr., 38, 127-316.

SURKAN, A.J. and VAN KAN, J. 1969. Constrained random walk meander generation. Water Resources Res., 5, 1343-1352.

TASK COMMITTEE ON EROSION OF COHESIVE MATERIALS. 1968. Erosion of cohesive sediments. J. Hydraul. Div. Am. Soc. Civ. Engrs., 94, 1017-1049.

THAKUR, T.R. and SCHEIDEGGER, A.E. 1968. A test of statistical theory of meander formation. Water Resources Res., 4, 317-329.

__________ 1970. Chain model of river meanders. J. Hydrol., 12, 25-47.

TOEBES, G.H. and CHANG, T.P. 1967. Planform analysis of meandering river. Proc. 12th Congr. Int. Ass. Hydraul. Res., Fort Collins, Colorado.

TOEBES, G.H. and SOOKY, A.A. 1967. Hydraulics of meandering streams with flood plains. J. Waterways Harbours Div. Am. Soc. Civ. Engrs. (1967), WW2, 213-236.

TURNBULL, W.J., KRINITZSKY, E.L., and WEAVER, F.J. 1966. Bank erosion in soils of the Lower Mississippi Valley. J. Soil Mech. Found. Div. Am. Soc. Civ. Engrs., 92, 121-136.

VAN STRAATEN, L.M.J.U. 1954. Composition and structure of recent marine sediments in the Netherlands. Leid. Geol. Meded., 19, 1-110.

VISHER, G.S. 1965a. Use of vertical profile in environmental reconstruction. Bull. Am. Ass. Petrol. Geol., 49, 41-61.

_____ 1965b. Fluvial processes as interpreted from ancient and recent fluvial deposits. In Primary sedimentary structures and their hydrodynamic interpretation (Ed. G.V. Middleton) S.E.P.M. Spec. Publn. 12, 116-132.

VON SCHELLING, H. 1951. Most frequent particle paths in a plane. Trans. Am. Geophys. Union, 32, 222-226.

_____ 1964. Most frequent random walks. Gen. Elec Co. Rept. 64GL92, Schenectady, N.Y.

WILLIAMS, G.P. 1967. Flume experiments on the transport of a coarse sand. Prof. Pap. U.S. Geol. Surv., No. 562-B. 31pp.

_____ 1970. Flume width and water depth effects in sediment transport experiments. Prof. Pap. U.S. Geol. Surv., No. 562-H. 37pp.

WOLMAN, M.G. 1959. Factors influencing erosion of a cohesive riverbank. Am.J. Sci., 257, 204-216.

WOLMAN, M.G. and EILER, J.P. 1958. Reconnaissance study of erosion and deposition produced by the flood of August 1955 in Connecticut. Trans. Am. Geophys. Union, 39, 1-14.

WOLMAN, M.G. and LEOPOLD, L.B. 1957. River flood plains: some observations on their formation. Prof. Pap. U. S. Geol. Surv., No. 282-C, 87-107.

WOODYER, K.D. 1968. Bankfull frequency in rivers. J. Hydrol., 6, 114-142.

YANG, C.T. 1971a. Potential energy and stream morphology. Water Resources Res., 7, 311-322.

_____ 1971b. On river meanders. J. Hydrol., 13, 231-253.

_____ 1971c. Formation of riffles and pools. Water Resources Res., 7, 1567-1574.

YEN, B.C. 1965. Characteristics of subcritical flow in a meandering channel. Institute of Hydraulic Research, University of Iowa, Iowa City, Iowa.

_____ 1971. Spiral motion of developed flow in wide curved open channels. In Shen, H.W. (Ed), Sedimentation (Einstien), ch. 22, 1-33. Fort Collins, Colorado, Water Resources Pubs.

YEN, C-L. 1970. Bed topography effect on flow in a meander. J. Hydraul. Div. Am. Soc. Civ. Engrs., 96, 57-73.

APPENDIX 1 - MATHEMATICAL METHODS

A1.1 Newton-Raphson iterative formula

This method is used to find approximate values of the real roots of equations. It can be applied to polynomials of any degree and also to nonpolynomial equations. The iterative formula is as follows

$$x_{r+1} = x_r - \frac{f(x_r)}{f'(x_r)} . \qquad (AI.I)$$

Here x_r is the approximate root of function $f(x)=0$. $f(x_r)$ is the value of the function $f(x)$ for $x=x_r$ and $f'(x_r)$ is the first derivative of $f(x)$ for $x = x_r$. Then x_{r+1} is a closer approximation to the real root. The formula is the basis for an iterative process that lends itself to use on a computer. The iterative process is continued until the difference between successive estimates is less than a specified amount. Although the process has the advantage of converging rapidly, an initial estimate is required and sometimes, under exceptional circumstances, convergence may not occur. Difficulties also occur if the equation has two or more nearly equal roots.

The development, geometrical interpretation and reasons for failure of the method can be obtained from any standard text on numerical analysis.

A1.2 Simpson's rule

This is a numerical method for evaluating definite integrals when they cannot be evaluated exactly. The formula is as follows

$$\int_a^b f(x)dx \approx \frac{h}{3} (y_0+4y_1+2y_2+4y_3+ \text{--} + 2y_{n-2}+4y_{n-1}+y_n) \qquad (A1.2)$$

The formula is obtained by dividing the curve y=f(x) into n equal parts between x=a and x=b, of length h = (b-a)/n, where n is always an even integer. Each separate piece of curve, covering an x-subinterval of width 2h is then approximated by an arc of a parabola through its ends and its mid point. These points correspond to values of y=f(x) of y_o, y_1, y_2, then y_1, y_2, y_3, and so on up to y_{n-2}, y_{n-1}, y_n. The areas under each parabolic arc are then added to give the expression above.

On geometrical grounds the smaller the value of h taken, the greater will be the accuracy of the approximation. Thus Simpson's rule may be applied successively, halving the interval on each application, until the difference between successive estimates is less than an arbitrary specified amount.

A1.3 Generation of random samples from specified theoretical distributions

This is usually done by generating uniformly distributed pseudorandom numbers and using these to draw random samples from the specified frequency distribution. This is known as Monte Carlo simulation (Harbaugh and Bonham-Carter, 1970).

The inverse transformation method can sometimes be used to transform the uniform distribution into a specified non-uniform distribution. A random number is simply equated with the cumulative frequency distribution, expressed either discretely or continuously, and a corresponding value from the specified distribution is obtained (see Harbaugh and Bonham-Carter, 1970). The initial step is to define the cumulative frequency distribution, obtained from the specified distribution either by summing over each discrete class (for empirical distributions), or by integration of a continuous distribution, if necessary dividing by the total to scale the range from 0.0 to 1.0.

The normal probability density function cannot be directly integrated to give the cumulative distribution, unless by numerical methods, and so the inverse transformation method cannot be easily used. A much easier way of generating normally distributed random variables is to use the formula derivable from the central limit theorem,

$$y = \frac{\sum_{i=1}^{k} r_i - (k/2)}{\sqrt{k/12}} \qquad (A1.3)$$

where y is a random variable with standard normal distribution with mean=0, standard deviation = 1; r_i is the ith element of a sequence of random numbers from a uniform distribution in the range 0.0 to 1.0; k is the number of values of r_i to be used. As k tends to ∞, y approaches a true normal distribution, but for most applications k=12 is adequate. Thus to generate a normally distributed random variable, x, with mean μ and standard deviation σ, sum 12 random numbers in the range 0.0 to 1.0, subtract 6, and apply the following formula

$$x = y\sigma + \mu \qquad (A1.4)$$

In the mathematical model samples are required to be generated in standardised form, as in equation (A1.3).

For a lognormally distributed random variable we perform the same process but replace the last equation by

$$x = \exp(y\sigma + \mu) \qquad (A1.5)$$

where μ and σ are the mean and standard deviation of logx. Lognormally distributed random variables generated directly from standardised normal distributions, with mean of logarithms of x zero and standard deviation of logarithms of x equal to unity, have an actual mean of 1.65 and standard deviation of 2.15. In order to transform such a variable x into a standardised form x_s the following transformation is necessary

$$x_s = \frac{x - 1.65}{2.15} \qquad (AI.6)$$

A normal standardised deviate, y, can be transformed to be distributed approximately as gamma using the following equation

$$x = \frac{2}{\gamma}\left\{1 + \frac{y\gamma}{6} - \frac{\gamma^2}{36}\right\}^3 - \frac{2}{\gamma} \qquad (AI.7)$$

where x is approximately gamma distributed with zero mean, standard deviation unity and skewness equal to γ (Matalas, 1967).

APPENDIX 2 - STATISTICAL CURVE AND SURFACE FITTING

A2.1 Polynomial regression

The following tables show the relevant results from polynomial regression analyses. Table A2.1 is for the regression of the ratio A/l on sn, as discussed in section 2.2. Table A2.2 refers to the regression of the parameter gD^3/ν^2 on V_*D/ν as discussed in section 5.5.4. Tables A2.3 and A2.4 are for the regression of Kennedy's j factor on Fr discussed in section 5.5.5.

A2.2 Polynomial surface fitting

The accompanying diagram, fig. A2.1, and table A2.5 show the results of fitting polynomial surfaces of degree 1,2 and 3, by least squares, to the solution to the integral given in equation (4.2). The independent variables were sn and ϕ, and 594 points were used.

POLYNOMIAL REGRESSION.....S 005

NUMBER OF OBSERVATIONS 36

POLYNOMIAL REGRESSION OF DEGREE 1

INTERCEPT 0.4529037E 00

REGRESSION COEFFICIENTS
0.2186882E 01

ANALYSIS OF VARIANCE FOR 1 DEGREE POLYNOMIAL

SOURCE OF VARIATION	DEGREE OF FREEDOM	SUM OF SQUARES	MEAN SQUARE	F VALUE	IMPROVEMENT IN TERMS OF SUM OF SQUARES
DUE TO REGRESSION	1	38.33064	38.33064	2510.48682	38.33064
DEVIATION ABOUT REGRESSION	34	0.51912	0.01527		
TOTAL	35	38.84976			

POLYNOMIAL REGRESSION OF DEGREE 2

INTERCEPT 0.8033228E 00

REGRESSION COEFFICIENTS
0.1260494E 01   0.4695846E 00

ANALYSIS OF VARIANCE FOR 2 DEGREE POLYNOMIAL

SOURCE OF VARIATION	DEGREE OF FREEDOM	SUM OF SQUARES	MEAN SQUARE	F VALUE	IMPROVEMENT IN TERMS OF SUM OF SQUARES
DUE TO REGRESSION	2	38.74538	19.37268	6124.40625	0.41473
DEVIATION ABOUT REGRESSION	33	0.10439	0.00316		
TOTAL	35	38.84976			

POLYNOMIAL REGRESSION OF DEGREE 3

INTERCEPT 0.9634151E 00

REGRESSION COEFFICIENTS
0.3370860E 00   0.1674662E 01   -0.4301562E 00

ANALYSIS OF VARIANCE FOR 3 DEGREE POLYNOMIAL

SOURCE OF VARIATION	DEGREE OF FREEDOM	SUM OF SQUARES	MEAN SQUARE	F VALUE	IMPROVEMENT IN TERMS OF SUM OF SQUARES
DUE TO REGRESSION	3	38.82758	12.94252	18667.42576	0.08220
DEVIATION ABOUT REGRESSION	32	0.02219	0.00069		
TOTAL	35	38.84976			

POLYNOMIAL REGRESSION OF DEGREE 4

NO IMPROVEMENT

Table A2.1.

Results of polynomial regression.

POLYNOMIAL REGRESSION.....RIPDUN

NUMBER OF OBSERVATIONS 49

POLYNOMIAL REGRESSION OF DEGREE 1

INTERCEPT 0.6233510E 01

REGRESSION COEFFICIENTS
0.2563132E-01

ANALYSIS OF VARIANCE FOR 1 DEGREE POLYNOMIAL

SOURCE OF VARIATION	DEGREE OF FREEDOM	SUM OF SQUARES	MEAN SQUARE	F VALUE	IMPROVEMENT IN TERMS OF SUM OF SQUARES
DUE TO REGRESSION	1	5069.39062	5069.39062	455.90698	5069.39062
DEVIATION ABOUT REGRESSION	47	522.60937	11.11935		
TOTAL	48	5592.00000			

POLYNOMIAL REGRESSION OF DEGREE 2

INTERCEPT 0.4549340E 01

REGRESSION COEFFICIENTS
0.4167961E-01 -0.1201998E-04

ANALYSIS OF VARIANCE FOR 2 DEGREE POLYNOMIAL

SOURCE OF VARIATION	DEGREE OF FREEDOM	SUM OF SQUARES	MEAN SQUARE	F VALUE	IMPROVEMENT IN TERMS OF SUM OF SQUARES
DUE TO REGRESSION	2	5379.03906	2689.51953	580.94165	309.64844
DEVIATION ABOUT REGRESSION	46	212.96094	4.62959		
TOTAL	48	5592.00000			

POLYNOMIAL REGRESSION OF DEGREE 3

INTERCEPT 0.3577861E 01

REGRESSION COEFFICIENTS
0.6022805E-01 -0.4778238E-04 0.1520497E-07

ANALYSIS OF VARIANCE FOR 3 DEGREE POLYNOMIAL

SOURCE OF VARIATION	DEGREE OF FREEDOM	SUM OF SQUARES	MEAN SQUARE	F VALUE	IMPROVEMENT IN TERMS OF SUM OF SQUARES
DUE TO REGRESSION	3	5451.61719	1817.20557	582.50903	72.57812
DEVIATION ABOUT REGRESSION	45	140.38281	3.11962		
TOTAL	48	5592.00000			

POLYNOMIAL REGRESSION OF DEGREE 4

INTERCEPT 0.3129055E 01

REGRESSION COEFFICIENTS
0.7277495E-01 -0.9190920E-04 0.6242391E-07 -0.1501976E-10

ANALYSIS OF VARIANCE FOR 4 DEGREE POLYNOMIAL

SOURCE OF VARIATION	DEGREE OF FREEDOM	SUM OF SQUARES	MEAN SQUARE	F VALUE	IMPROVEMENT IN TERMS OF SUM OF SQUARES
DUE TO REGRESSION	4	5462.06641	1365.51660	462.41113	10.44922
DEVIATION ABOUT REGRESSION	44	129.93359	2.95304		
TOTAL	48	5592.00000			

POLYNOMIAL REGRESSION OF DEGREE 5

NO IMPROVEMENT

Table A2.2.

Results of polynomial regression.

POLYNOMIAL REGRESSION.....KENDY1

NUMBER OF OBSERVATIONS 13

POLYNOMIAL REGRESSION OF DEGREE 1

INTERCEPT 0.8485743E 00

REGRESSION COEFFICIENTS
0.2577252E-01

ANALYSIS OF VARIANCE FOR 1 DEGREE POLYNOMIAL

SOURCE OF VARIATION	DEGREE OF FREEDOM	SUM OF SQUARES	MEAN SQUARE	F VALUE	IMPROVEMENT IN TERMS OF SUM OF SQUARES
DUE TO REGRESSION	1	0.03022	0.03022	178.87331	0.03022
DEVIATION ABOUT REGRESSION	11	0.00186	0.00017		
TOTAL	12	0.03208			

POLYNOMIAL REGRESSION OF DEGREE 2

INTERCEPT 0.8304257E 00

REGRESSION COEFFICIENTS
0.4557114E-01 -0.3299772E-02

ANALYSIS OF VARIANCE FOR 2 DEGREE POLYNOMIAL

SOURCE OF VARIATION	DEGREE OF FREEDOM	SUM OF SQUARES	MEAN SQUARE	F VALUE	IMPROVEMENT IN TERMS OF SUM OF SQUARES
DUE TO REGRESSION	2	0.03158	0.01579	318.28906	0.00136
DEVIATION ABOUT REGRESSION	10	0.00050	0.00005		
TOTAL	12	0.03208			

POLYNOMIAL REGRESSION OF DEGREE 3

INTERCEPT 0.8377432E 00

REGRESSION COEFFICIENTS
0.2720344E-01 0.4665561E-02 -0.8851467E-03

ANALYSIS OF VARIANCE FOR 3 DEGREE POLYNOMIAL

SOURCE OF VARIATION	DEGREE OF FREEDOM	SUM OF SQUARES	MEAN SQUARE	F VALUE	IMPROVEMENT IN TERMS OF SUM OF SQUARES
DUE TO REGRESSION	3	0.03183	0.01061	379.40259	0.00024
DEVIATION ABOUT REGRESSION	9	0.00025	0.00003		
TOTAL	12	0.03208			

POLYNOMIAL REGRESSION OF DEGREE 4

NO IMPROVEMENT

Table A2.3. Results of polynomial regression.

POLYNOMIAL REGRESSION.....KENDY2

NUMBER OF OBSERVATIONS 13

POLYNOMIAL REGRESSION OF DEGREE 1

INTERCEPT C.3325770E CO

REGRESSION COEFFICIENTS
0.1197C75E 00

ANALYSIS CF VARIANCE FOR 1 CEGREE PCLYNOMIAL

SOURCE OF VARIATION	DEGREE OF FREEDOM	SUM OF SQUARES	MEAN SQUARE	F VALUE	IMPROVEMENT IN TERMS OF SUM OF SQUARES
DUE TO REGRESSION	1	0.65201	0.65201	31.53506	0.652C1
DEVIATION ABOUT REGRESSION	11	0.22743	0.02068		
TOTAL	12	0.87944			

POLYNOMIAL REGRESSION OF DEGREE 2

INTERCEPT 0.1245201E CO

REGRESSION COEFFICIENTS
0.3466788E CO -C.3782854E-01

ANALYSIS CF VARIANCE FCR 2 CEGREE PCLYNCMIAL

SOURCE OF VARIATION	DEGREE OF FREEDOM	SUM OF SQUARES	MEAN SQUARE	F VALUE	IMPROVEMENT IN TERMS OF SUM OF SQUARES
DUE TO REGRESSION	2	0.83106	0.41553	85.88647	C.17905
DEVIATION ABOUT REGRESSICN	10	0.04838	0.00484		
TCTAL	12	0.87944			

POLYNOMIAL REGRESSION OF DEGREE 3

INTERCEPT C.31443C0E-01

REGRESSION COEFFICIENTS
0.5809163E CC -0.1394290E 00 0.1128839E-01

ANALYSIS OF VARIANCE FCR 3 CEGREE PCLYNOMIAL

SOURCE OF VARIATION	DEGREE CF FREEDOM	SUM CF SQUARES	MEAN SQUARE	F VALUE	IMPROVEMENT IN TERMS OF SUM OF SQUARES
DUE TO REGRESSION	3	0.87193	0.29064	347.96606	C.04C86
DEVIATION ABOUT REGRESSICN	9	0.00752	0.00084		
TOTAL	12	0.87944			

POLYNOMIAL REGRESSION OF DEGREE 4

INTERCEPT 0.45C2363E-C2

REGRESSION COEFFICIENTS
0.7150575E CC -0.2493903E 00 0.4049132E-01 -0.2431653E-02

ANALYSIS OF VARIANCE FOR 4 DEGREE POLYNOMIAL

SOURCE OF VARIATION	DEGREE CF FREEDOM	SUM CF SQUARES	MEAN SQUARE	F VALUE	IMPROVEMENT IN TERMS OF SUM OF SQUARES
DUE TO REGRESSION	4	0.87817	0.21954	1384.06030	0.0C625
DEVIATION ABOUT REGRESSION	8	0.00127	0.00016		
TOTAL	12	0.87944			

POLYNOMIAL REGRESSION OF DEGREE 5

NO IMPROVEMENT

Table A2.4. Results of polynomial regression.

TABLE A2.5 Global fit data.

	plane	quadratic	cubic
COEFFICIENTS			
ϕ^3	-	-	0.2804
$\phi^2 sn$	-	-	-0.1713
ϕsn^2	-	-	0.1139
sn^3	-	-	-0.0292
ϕ^2	-	0.4433	0.2244
ϕsn	-	-0.1348	-0.5520
sn^2	-	0.0419	0.2123
ϕ	0.6371	0.2269	0.8895
sn	-0.0505	-0.1993	-0.4651
Intercept	-0.0692	0.2281	0.2668
PERCENTAGE FIT	87.114	96.782	98.568

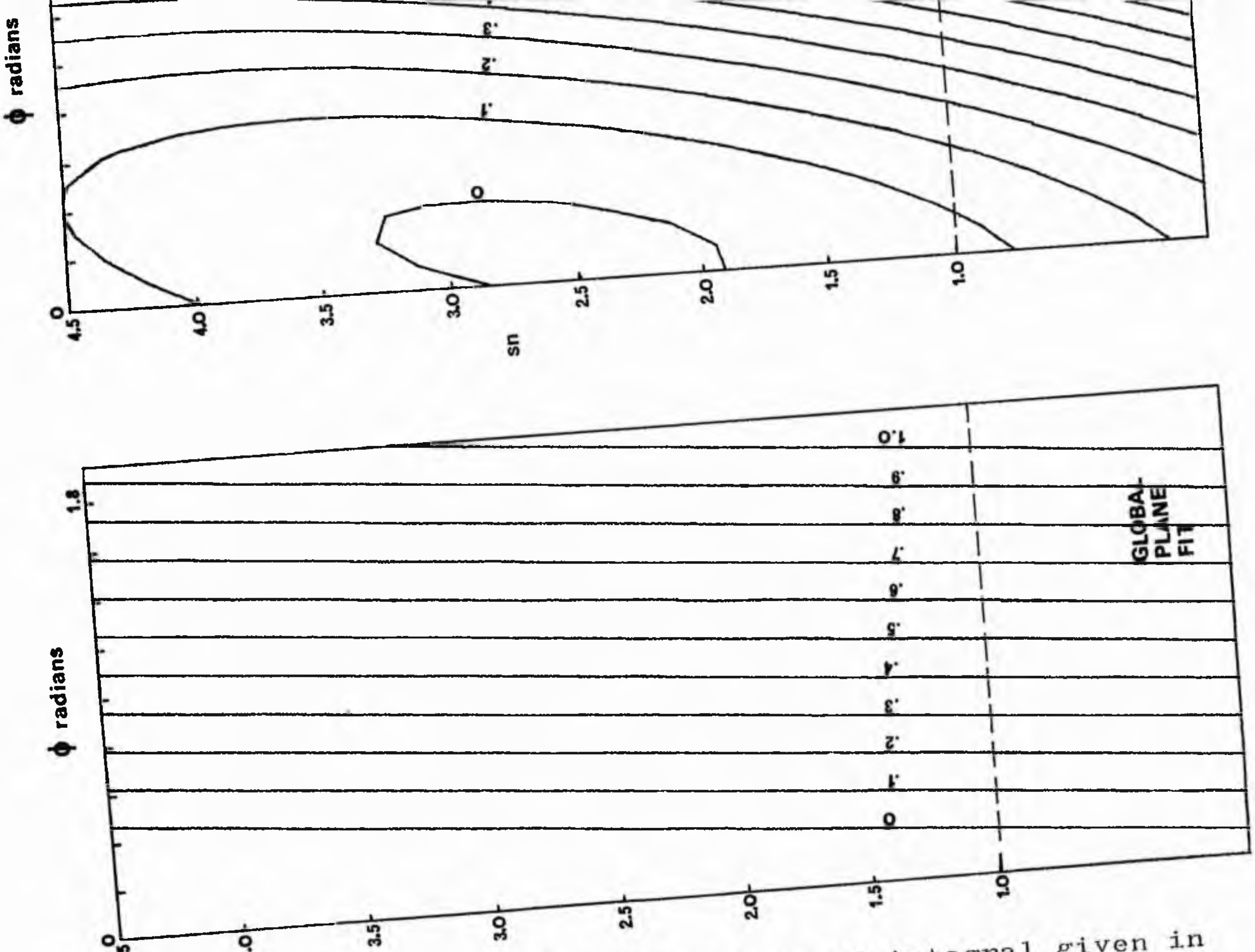

Fig. A2.1. Global fit surface plots of integral given in equation (4.2), with sn and Ø as independent variables. 594 data points were used.

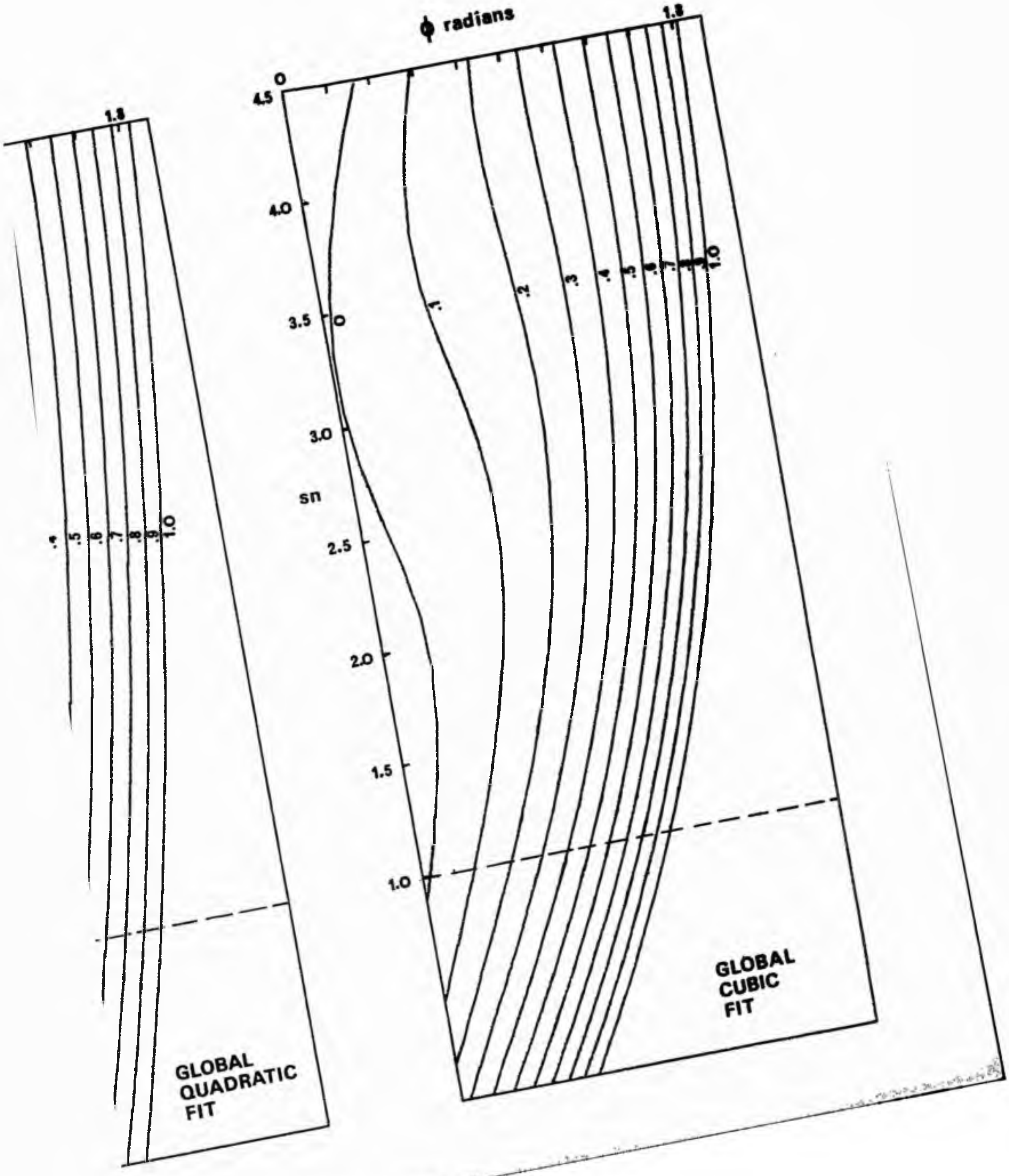

ϕ radians
0
1.8
4.5
4.0
3.5
3.0
sn
2.5
2.0
1.5
1.0
0
.1
.2
.3
.4
.5
.6
.7
.8
.9
1.0
GLOBAL CUBIC FIT
1.8
.4
.5
.6
.7
.8
.9
1.0
GLOBAL QUADRATIC FIT

APPENDIX 3. DATA DECK SET UP FOR EXPERIMENTS.

```
FLUVIATILE PRCCESS SIMULATION   EXPERIMENT 1                81241913 4
 50  10  10  10
200  60  50   1(1X,60A1)
1000.0      60.0          0.0          60.0          0.0          0.0
       2.0          1000.0       0.0001       2CCC.0
   0.000001       0.0001          0.5          3C.C
       50.0          50.0        10.0          1C.0          C.C          2.0
  100.0     20.0       1.0      0.8     0.21     0.15     2.65     1.0
GOS-ULARDXI. F
4     90000.0          1.0
141.2       234.2                   1.0          0.92855      -0.15132
-133.0      -485.0      62.4        -14.3        -7.1         0.C
-135.1      125.3       -9.8        -29.5        1.0          7.4
-49.5       -61.5       9.9         2.8          2.9          1.8
-47.6       81.1        4.9         -31.4        -10.2        5.7
1     0.00001         1.0         0.13
CCCCCCCCCCCCCCCCGCCCODCCCCCCCCCCCOOOCCOCOOGGGGGOOOOCOOOOOOCOSS
```

```
FLUVIATILE PRCCESS SIMULATION   EXPERIMENT 1                81241913 4
 50  10  10  10
200  60  50   1(1X,60A1)
10CC.0      60.0          0.0          60.0          0.0          0.0
       2.0          1000.0       0.0001       2C00.0
   0.000001       0.0001          0.5          3C.0
       50.0          50.0        10.0          1C.C          0.0          2.0
  100.0     20.0       1.0      0.8     0.21     0.15     2.65     1.0
GCS-ULARDXI. F
4     90000.0          1.0
141.2       234.2                   1.0          0.92855      -0.15132
-133.0      -485.0      62.4        -14.3        -7.1         0.0
-135.1      125.3       -9.8        -29.5        1.0          7.4
-49.5       -61.5       9.9         2.8          2.9          1.8
-47.6       81.1        4.9         -31.4        -10.2        5.7
1     0.0001          1.0         1.03
CCCCCCCCCCCCOCCCCCCCCOCCCCCCCOCOOOOOOOOOOOGGGGOOOOOOOOOOOOOOSS
```

```
FLUVIATILE PRCCESS SIMULATION   EXPERIMENT 1                81241913 4
 50  10  10  10
200  60  50   1(1X,60A1)
1000.0      60.0          0.0          60.0          0.0          0.0
       2.0          1000.0       0.0001       2CCC.0


   0.000001       0.0001          C.5          3C.0
       50.0          50.0        10.0          1C.C          C.0          2.0
  1C0.0     20.0       1.0      0.8     0.21     C.15     2.65     1.0
GCS-ULARDXI. F
4     90000.0          1.0
141.2       234.2                   1.0          0.92855      -0.15132
-133.0      -485.0      62.4        -14.3        -7.1         0.0
-135.1      125.3       -9.8        -29.5        1.0          7.4
-49.5       -61.5       9.9         2.8          2.9          1.8
-47.6       81.1        4.9         -31.4        -10.2        5.7
1     0.0002          1.0         2.03
CCCCCCCCCCCCCCCCCCCCCCCCCCCCCGCOOOOOOOOOOOGGGGOOOOOOOOOOOOOOSS
```

```
FLUVIATILE PRCCESS SIMULATION   EXPERIMENT 1                81241913 4
 30  10  10  10
200  60  50   1(1X,60A1)
1000.0      60.0          0.0          60.0          0.0          0.0
       2.0          1000.0       0.0001       2C00.0
   0.000005       0.0005          0.5          30.0
       50.0          50.0        10.0          10.0          0.0          2.0
  100.0     20.0       1.0      0.8     0.21     C.15     2.65     1.0
GCS-ULARDXI. F
4     90000.0          1.0
141.2       234.2                   1.0          0.92855      -0.15132
-133.0      -485.0      62.4        -14.3        -7.1         0.0
-135.1      125.3       -9.8        -29.5        1.0          7.4
-49.5       -61.5       9.9         2.8          2.9          1.8
-47.6       81.1        4.9         -31.4        -10.2        5.7
1     0.00001         1.0         0.13
CCCCCCCCCCCCCCCCCCCCCCCCCCCCCCOCOOOOCOOOOOGGGGGOOOOOOOOOOOOOOSS
```

```
FLUVIATILE PRCCESS SIMULATICN   EXPERIMENT 1                81241913 4
 30  10  10  10
200  60  50   1(1X,60A1)
1000.0      60.0          0.0          60.0          0.0          0.0
       2.0          1000.0       0.0001       2CC0.0
   0.000005       0.0005          0.5          3C.0
       50.0          50.0        10.0          1C.0          C.0          2.0
  100.0     20.0       1.0      0.8     0.21     0.15     2.65     1.0
GCS-ULARDXI. F
4     90000.0          1.0
```

```
141.2         234.2                       1.0          C.92855       -C.15132
-133.0        -485.0       62.4           -14.3        -7.1          C.0
-135.1        125.3        -9.8           -29.5        1.0           7.4
-49.5         -61.5        9.9            2.8          2.9           1.8
-47.6         81.1         4.9            -31.4        -10.2         5.7
1      0.0001          1.0           1.03
CCCCCCCCCCCCCCCCCCCCCCCCCCCCCCCCCCCOOOCCCCCOOGGGGGGOCOOCOOCOOCCOSS

 FLUVIATILE PROCESS SIMULATICN    EXPERIMENT 1                      81241913 4
  30  10  10  10
 2C0  60  50    1(1X,60A1)
10C0.0        60.0          0.0           60.0         0.0           C.0
        2.0          1000.0       0.0CC1       2CCC.0
    0.000005      0.0005          0.5          3C.0
         50.0          50.0          1C.0         1C.C           C.0          2.0
   100.0     20.0       1.0      0.8     0.21     C.15     2.65     1.0
GCS-ULARCXI. F
4     90000.0          1.0
141.2         234.2                       1.0          C.92855       -0.15132
-133.0        -485.0       62.4           -14.3        -7.1          C.0
-135.1        125.3        -9.8           -29.5        1.0           7.4
-49.5         -61.5        9.9            2.8          2.9           1.8
-47.6         81.1         4.9            -31.4        -10.2         5.7
1      0.0002          1.0           2.03
CCCCCCCCCCCCCCCCCCCCCCCCCCCCCCCCCCCOOOOCCCCOOGGGGGGOOOOCOCOOOCCOSS

 FLUVIATILE PRCCESS SIMULATICN    EXPERIMENT 1                      81241913 4
  10   5   5   5
 2C0  60  50    1(1X,60A1)
1CC0.0        60.0          0.0           60.0         0.0           0.C
         2.0          1000.0      0.00C1       2CCC.C
    0.00002       0.002           C.5          3C.0
         20.0          10.0          10.C         1C.C           C.C          2.0
   100.0     20.0       1.0      0.8     0.21     C.15     2.65     1.C
GCS-ULARCXI. F
4     90000.0          1.0
141.2         234.2                       1.0          C.92855       -0.15132
-133.0        -485.0       62.4           -14.3        -7.1          0.C
-135.1        125.3        -9.8           -29.5        1.0           7.4
-49.5         -61.5        9.9            2.8          2.9           1.8
-47.6         81.1         4.9            -31.4        -10.2         5.7
1     0.00001          1.0           C.13
CCCCCCCCCCCCCCCCCCCCCCCOCOCCCCOCOOOOOCOOOOGGGGOOOOOOOOOOOCOOSS


 FLUVIATILE PRCCESS SIMULATION    EXPERIMENT 1                      81241913 4
  10   5   5   5
 2C0  60  50    1(1X,60A1)
10C0.0        60.0          0.0           60.C         C.0           C.0
        2.0          1000.0       0.00C1       2CCC.C
    0.00002       0.002           C.5          3C.C
         20.0          10.0          10.C         1C.C           C.C          2.0
   100.0     20.0       1.0      0.8     0.21     0.15     2.65     1.C
GCS-ULARCXI. F
4     90000.0          1.0
141.2         234.2                       1.0          C.92855       -0.15132
-133.0        -485.0       62.4           -14.3        -7.1          0.C
-135.1        125.3        -9.8           -29.5        1.0           7.4
-49.5         -61.5        9.9            2.8          2.9           1.8
-47.6         81.1         4.9            -31.4        -10.2         5.7
1      0.0001          1.0           1.C3
CCCCCCCCCCCCCCCCCCCCCCCCCCCCCCCCCCCCOCOCCCOOOGGGGGOOOOOOOOOOOOCOOSS

 FLUVIATILE PROCESS SIMULATION    EXPERIMENT 1                      81241913 4
  10   5   5   5
 2C0  60  50    1(1X,60A1)
1000.0        60.0          0.0           60.0         0.0           0.0
        2.0          1000.0       0.00C1       2CCC.C
    0.00002       0.002           0.5          3C.0
         20.0          10.0          10.C         1C.0           C.0          2.0
   100.0     20.0       1.0      0.8     0.21     C.15     2.65     1.0
GCS-ULARCXI. F
4     90000.0          1.0
141.2         234.2                       1.0          0.92855       -0.15132
-133.0        -485.0       62.4           -14.3        -7.1          0.0
-135.1        125.3        -9.8           -29.5        1.0           7.4
-49.5         -61.5        9.9            2.8          2.9           1.8
-47.6         81.1         4.9            -31.4        -10.2         5.7
1      0.0002          1.0           2.03
COCCCCCCCCCCCCCCCCCCCCCCCCCOCOCOOCOOOOOGGGGGOOOOOOOOOOOOCOOSS
```

```
FLUVIATILE PRUCESS SIMULATICN  EXPERIMENT 2                 81241913
11C  20  20  20
350  60   2  1750.0    60.0      0.0     30.0   0.C01          (1X,60A1)
        2.0       1C0C.0      0.0001      2000.0
   0.C0CCC1     0.0CC1          0.5        30.0
      100.0       10C.0        10.0        10.0          0.0          2.0
  100.0    20.0     1.0     0.8     0.21     0.15     2.65     1.0
GOS-ULARDXI. F
4    13CCC0.0          1.0
543.5        441.0                     1.0          0.56671     0.30560
-2CC.3       145.4       -85.5         58.0         -39.8       7.4
-112.4       185.0       -79.9         65.6         -72.5       27.8
-123.3       141.6       -66.4         75.7         -47.2       8.6
-85.6        105.7       -46.2         31.7         -43.2       4.3

COCCOCCOOCCCCOCCCCCCCCCCCCCCCCSS

FLUVIATILE PROCESS SIMULATION  EXPERIMENT 2                 81241913
12C  20  20  20
350  6C   2  1750.0    60.0      0.0     3C.0    0.01          (1X,60A1)
        2.0       1000.0      0.0001      2000.0
   0.C00C01     0.0001          0.5        30.0
      1C0.0       100.0        10.0        10.0          0.0          2.0
  100.0    20.0     1.0     0.8     0.21     0.15     2.65     1.0
GOS-ULARDXI. F
4    130000.0          1.0
543.5        441.0                     1.0          0.56671     0.3056C
-2CC.3       145.4       -85.5         58.0         -39.8       7.4
-112.4       185.C       -79.9         65.6         -72.5       27.8
-123.3       141.6       -66.4         75.7         -47.2       8.6
-85.6        105.7       -46.2         31.7         -43.2       4.3

000C0000CC00000000C00CCCCCCOSS

FLUVIATILE PROCESS SIMULATICN  EXPERIMENT 2                 81241913
1C0  20  20  20
35C  60   2  175C.0    60.0      0.0     30.0     0.1          (1X,60A1)
        2.0       1CC0.0      0.0001      2C00.0
   0.C00001     0.C001          0.5        30.0
      1C0.0       1CC.0        10.0        10.0          0.0          2.0
  100.0    20.0     1.C     0.8     0.21     0.15     2.65     1.0


GOS-ULARDXI. F
4    130CC0.0          1.0
543.5        441.0                     1.0          0.56671     0.30560
-2CC.3       145.4       -85.5         58.0         -39.8       7.4
-112.4       185.C       -79.9         65.6         -72.5       27.8
-123.3       141.6       -66.4         75.7         -47.2       8.6
-85.6        105.7       -46.2         31.7         -43.2       4.3

OOCCOCCCOOCOCCCCCCCCCCCCCCCCSS

FLUVIATILE PROCESS SIMULATICN  EXPERIMENT 2                 81241913
110  20  20  20
350  60   2  1750.0    60.0      0.0     30.0   0.C01          (1X,60A1)
        2.0       1000.C      0.0001      2000.0
   0.C00C05     0.0005          0.5        30.0
      100.0       100.C        10.0        10.0          0.0          2.0
  100.0    20.0     1.C     0.8     0.21     0.15     2.65     1.0
GOS-ULARDXI. F
4    130000.0          1.0
543.5        441.0                     1.0          0.56671     0.30560
-200.3       145.4       -85.5         58.0         -39.8       7.4
-112.4       185.0       -79.9         65.6         -72.5       27.8
-123.3       141.6       -66.4         75.7         -47.2       8.6
-85.6        105.7       -46.2         31.7         -43.2       4.3

000000C000000000C0C00000CCCOSS

FLUVIATILE PROCESS SIMULATICN  EXPERIMENT 2                 81241913
11O  20  20  20
35C  60   2  1750.0    60.0      0.0     30.0    0.01          (1X,60A1)
        2.0       1C00.0      0.0001      20C0.0
   0.C00005     0.0005          0.5        30.0
      1C0.0       100.0        10.0        10.0          0.0          2.0
  100.0    20.0     1.C     0.8     0.21     0.15     2.65     1.0
GOS-ULARDXI. F
4    1300C0.0          1.0
543.5        441.0                     1.0          0.56671     0.30560
-2C0.3       145.4       -85.5         58.0         -39.8       7.4
-112.4       185.0       -79.9         65.6         -72.5       27.8
-123.3       141.6       -66.4         75.7         -47.2       8.6
-85.6        105.7       -46.2         31.7         -43.2       4.3
```

```
OOCCCOCOOOOOCCCCCCCOOCCCCCCCCSS

 FLUVIATILE PROCESS SIMULATION  EXPERIMENT 2                 81241913
 110  20  20  20
 350  60   2  1750.0    60.0     0.0     30.0     0.1          (1X,60A1)
          2.0       1000.0      0.0001      2000.0
    0.000005      0.0005         0.5          30.0
         100.0        100.C       10.0        10.0          0.0         2.0
   100.0     20.0      1.0     0.8     0.21     0.15    2.65     1.0
GOS-ULARDXI. F
4    130000.0        1.0
543.5        441.0                     1.0          0.56671      0.30560
-200.3       145.4        -85.5        58.0         -39.8        7.4
-112.4       185.0        -79.9        65.6         -72.5        27.8
-123.3       141.6        -66.4        75.7         -47.2        8.6
-85.6        105.7        -46.2        31.7         -43.2        4.3

OOCOOOOOOOCCOCOCOCOCOCCCCCCCCOSS

 FLUVIATILE PROCESS SIMULATION  EXPERIMENT 2                 81241913
 11C  20  20  20
 350  60   2  175C.0    60.0     0.0     30.0   0.C01          (1X,60A1)
          2.0       1CCC.C      0.0001      2C00.0
    0.C0002       C.C02          0.5          30.0
         1CC.C        1CC.C       10.0        10.0          0.0         2.0
   1CC.0     20.0      1.C     0.8     0.21     0.15    2.65     1.0
GOS-ULARDXI. F
4    13CCC0.0        1.C
543.5        441.C                     1.0          0.56671      0.3056C
-2C0.3       145.4        -85.5        58.0         -39.8        7.4
-112.4       185.C        -79.9        65.6         -72.5        27.8
-123.3       141.6        -66.4        75.7         -47.2        8.6
-85.6        1C5.7        -46.2        31.7         -43.2        4.3

OCCCCCCOOCCOCCCCCCCCCCCCCCCCCOSS

 FLLVIATILE PRCCESS SIPULATICN  EXPERIPENT 2                 81241913
 11C  20  2C  20
 35C  60   2  175C.C    60.0     0.0     30.0     0.01         (1X,60A1)
          2.C       1CCC.C      0.0001      2C00.0
    0.CCC02       C.CC2          0.5          30.0



         1CC.0        10C.C       10.0        1C.0          C.0         2.C
   10C.0     2C.C      1.C     0.8     0.21     0.15    2.65     1.C
GOS-LLARDXI. F
4    13CCC0.0        1.0
543.5        441.C                     1.0          0.56671      0.3056C
-2CC.3       145.4        -85.5        58.0         -39.8        7.4
-112.4       185.C        -79.9        65.6         -72.5        27.8
-123.3       141.6        -66.4        75.7         -47.2        8.6
-85.6        105.7        -46.2        31.7         -43.2        4.3

COCCOCCCCCCCCOCCCCCCCCCCCCCCCCSS

 FLLVIATILE PRCCESS SIPLLATICN  EXPERIPENT 2                 81241913
 11C  2C  2C  2C
 35C  60   2  175C.0    6C.0     0.0     30.0     0.1          (1X,60A1)
          2.C       1CCC.C      0.0001      2CC0.0
    0.CCC02       C.C02          0.5          30.0
         1CC.C        1CC.C       10.0        10.0          0.0         2.0
   1CC.0     20.C      1.C     0.8     0.21     0.15    2.65     1.0
COS-LLARDXI. F
4    13CCC0.0        1.0
543.5        441.C                     1.0          0.56671      0.3056C
-2CC.3       145.4        -85.5        58.0         -39.8        7.4
-112.4       185.C        -79.9        65.6         -72.5        27.8
-123.3       141.6        -66.4        75.7         -47.2        8.6
-85.6        105.7        -46.2        31.7         -43.2        4.3

OCCCCOCOCOOOOCCCCCCCCCCCCCCCCSS
```

```
 FLUVIATILE PROCESS SIMULATION   EXPERIMENT 4A                   81241913 4
 100  10  10  10
 200  60  50   1(1X,60A1)
1000.0      60.0        0.0         60.0        0.0         0.0
         1.1        1000.0      0.0001      2000.0
   0.000003       0.0001        0.5         30.0
        20.0        20.0        5.0         5.0        100.0        3.0
   100.0    20.0    1.0     0.8     0.21    0.15    2.65    1.0
GCS-ULARDXI. F
4   110000.0         1.0
543.5       441.0                   1.0         0.56671     0.30560
-200.3      145.4       -85.5       58.0        -39.8       7.4
-112.4      185.0       -79.9       65.6        -72.5       27.8
-123.3      141.6       -66.4       75.7        -47.2       8.6
-85.6       105.7       -46.2       31.7        -43.2       4.3
1      0.0001        1.0         1.03
CCCCCCCCCCCCCCCCCCCCCCCCCCCCC0CCC0CCC0000GGGG0000C00000CC0SS

 FLUVIATILE PROCESS SIMULATION   EXPERIMENT 4A                   81241913 4
 100  10  10  10
 200  60  50   1(1X,60A1)
1000.0      60.0        0.0         60.0        0.0         0.0
         1.1        1000.0      0.0001      2000.0
   0.0000003      0.0001        0.5         30.0
        20.0        20.0        5.0         5.0        100.0        3.0
   100.0    20.0    1.0     0.8     0.21    0.15    2.65    1.0
GCS-ULARDXI. F
4   110000.0         1.0
543.5       441.0                   1.0         0.56671     0.30560
-200.3      145.4       -85.5       58.0        -39.8       7.4
-112.4      185.0       -79.9       65.6        -72.5       27.8
-123.3      141.6       -66.4       75.7        -47.2       8.6
-85.6       105.7       -46.2       31.7        -43.2       4.3
1      0.0001        1.0         1.03
CCCCCCCCCCCCCCCCCCCCCCCCCCCCC0C00CCC0000GGGGC0000000000C00SS

 FLUVIATILE PROCESS SIMULATION   EXPERIMENT 4A                   81241913 4
 100  10  10  10
 200  60  50   1(1X,60A1)
1000.0      60.0        0.0         60.0        0.0         0.0
         1.1        1000.0      0.0001      2000.0

   0.0000009      0.0001        0.5         30.0
        20.0        20.0        5.0         5.0        100.0        3.0
   100.0    20.0    1.0     0.8     0.21    0.15    2.65    1.0
GCS-ULARDXI. F
4   110000.0         1.0
543.5       441.0                   1.0         0.56671     0.30560
-200.3      145.4       -85.5       58.0        -39.8       7.4
-112.4      185.0       -79.9       65.6        -72.5       27.8
-123.3      141.6       -66.4       75.7        -47.2       8.6
-85.6       105.7       -46.2       31.7        -43.2       4.3
1      0.0001        1.0         1.03
CCCCCCCCCCCCCCCCCCCCCCCCCCCCCCC00C000000GGGG00000000000000SS
```

```
FLUVIATILE PROCESS SIMULATION   EXPERIMENT 4B                    81241913
100  10  10  10
200  60   0  1000.0    60.0     0.0     60.0     0.0     0.0(1X,60A1)
          1.1        1000.0       0.0001       2000.0
  0.000003          0.0001        0.5          30.0
         20.0         20.0        5.0           5.0       100.0        3.0
  100.0    20.0     1.0     0.8     0.21    0.15    2.65    1.0
GOS-ULARDXI. F
4    110000.0          1.0
543.5        441.0                      1.0          0.56671      0.30560
-200.3       145.4        -85.5         58.0         -39.8        7.4
-112.4       185.0        -79.9         65.6         -72.5        27.8
-123.3       141.6        -66.4         75.7         -47.2        8.6
-85.6        105.7        -46.2         31.7         -43.2        4.3
1      0.0001          1.0          1.03
0000000000000000000000000000000000000000GGGGG0000000000000SS

FLUVIATILE PROCESS SIMULATION   EXPERIMENT 4B                    81241913
100  10  10  10
200  60   0  1000.0    60.0     0.0     60.0     0.0     0.0(1X,60A1)
          1.1        1000.0       0.0001       2000.0
  0.0000003         0.0001        0.5          30.0
         20.0         20.0        5.0           5.0       100.0        3.0
  100.0    20.0     1.0     0.8     0.21    0.15    2.65    1.0
GOS-ULARDXI. F
4    110000.0          1.0
543.5        441.0                      1.0          0.56671      0.30560
-200.3       145.4        -85.5         58.0         -39.8        7.4
-112.4       185.0        -79.9         65.6         -72.5        27.8
-123.3       141.6        -66.4         75.7         -47.2        8.6
-85.6        105.7        -46.2         31.7         -43.2        4.3
1      0.0001          1.0          1.03
0000000000000000000000000000000000000000GGGGG0000000000000SS

FLUVIATILE PROCESS SIMULATION   EXPERIMENT 4B                    81241913
100  10  10  10
200  60   0  1000.0    60.0     0.0     60.0     0.0     0.0(1X,60A1)
          1.1        1000.0       0.0001       2000.0
  0.0000009         0.0001        0.5          30.0
         20.0         20.0        5.0           5.0       100.0        3.0
  100.0    20.0     1.0     0.8     0.21    0.15    2.65    1.0


GOS-ULARDXI. F
4    110000.0          1.0
543.5        441.0                      1.0          0.56671      0.30560
-200.3       145.4        -85.5         58.0         -39.8        7.4
-112.4       185.0        -79.9         65.6         -72.5        27.8
-123.3       141.6        -66.4         75.7         -47.2        8.6
-85.6        105.7        -46.2         31.7         -43.2        4.3
1      0.0001          1.0          1.03
0000000000000000000000000000000000000000GGGGG0000000000000SS
```

```
FLUVIATILE PROCESS SIMULATION  EXPERIMENT 5                  81241913
200  20  20  20
200  60   0  1000.0     60.0      0.0     30.0   0.001          (1X,60A1)
          1.1        1000.0     0.0001      2000.0
  0.0000003       0.0001         0.5         30.0
        50.0         50.0        5.0          5.0         100.0          3.0
  100.0     20.0       1.0      0.8     0.21     0.15    2.65      1.0
GOS-ULARDXI. F
4   120000.0           1.0
543.5         441.0                     1.0           0.56671     0.30560
-200.3        145.4        -85.5        58.0          -39.8       7.4
-112.4        185.0        -79.9        65.6          -72.5       27.8
-123.3        141.6        -66.4        75.7          -47.2       8.6
-85.6         105.7        -46.2        31.7          -43.2       4.3

000000000000000000000000000000SS
```

```
FLUVIATILE PROCESS SIMULATION  EXPERIMENT 5                  81241913
200  20  20  20
200  60   0  1000.0     60.0      0.0     30.0     0.01         (1X,60A1)
          1.1        1000.0     0.0001      2000.0
  0.0000003       0.0001         0.5         30.0
        50.0         50.0        5.0          5.0         100.0          3.0
  100.0     20.0       1.0      0.8     0.21     0.15    2.65      1.0
GOS-ULARDXI. F
4   120000.0           1.0
543.5         441.0                     1.0           0.56671     0.30560
-200.3        145.4        -85.5        58.0          -39.8       7.4
-112.4        185.0        -79.9        65.6          -72.5       27.8
-123.3        141.6        -66.4        75.7          -47.2       8.6
-85.6         105.7        -46.2        31.7          -43.2       4.3

000000000000000000000000000000SS
```

```
FLUVIATILE PROCESS SIMULATION  EXPERIMENT 5                  81241913
200  20  20  20
200  60   0  1000.0     60.0      0.0     30.0     0.1          (1X,60A1)
          1.1        1000.0     0.0001      2000.0
  0.0000003       0.0001         0.5         30.0
        50.0         50.0        5.0          5.0         100.0          3.0
  100.0     20.0       1.0      0.8     0.21     0.15    2.65      1.0



GOS-ULARDXI. F
4   120000.0           1.0
543.5         441.0                     1.0           0.56671     0.30560
-200.3        145.4        -85.5        58.0          -39.8       7.4
-112.4        185.0        -79.9        65.6          -72.5       27.8
-123.3        141.6        -66.4        75.7          -47.2       8.6
-85.6         105.7        -46.2        31.7          -43.2       4.3

000000000000000000000000000000SS
```

```
FLUVIATILE PROCESS SIMULATION  EXPERIMENT 5                  81241913
200  20  20  20
200  60   0  1000.0     60.0      0.0     30.0   0.001          (1X,60A1)
          1.1        1000.0     0.0001      2000.0
  0.0000009       0.0001         0.5         30.0
        50.0         50.0        5.0          5.0         100.0          3.0
  100.0     20.0       1.0      0.8     0.21     0.15    2.65      1.0
GOS-ULARDXI. F
4   120000.0           1.0
543.5         441.0                     1.0           0.56671     0.30560
-200.3        145.4        -85.5        58.0          -39.8       7.4
-112.4        185.0        -79.9        65.6          -72.5       27.8
-123.3        141.6        -66.4        75.7          -47.2       8.6
-85.6         105.7        -46.2        31.7          -43.2       4.3

000000000000000000000000000000SS
```

```
FLUVIATILE PROCESS SIMULATION  EXPERIMENT 5                  81241913
200  20  20  20
200  60   0  1000.0     60.0      0.0     30.0     0.01         (1X,60A1)
          1.1        1000.0     0.0001      2000.0
  0.0000009       0.0001         0.5         30.0
        50.0         50.0        5.0          5.0         100.0          3.0
  100.0     20.0       1.0      0.8     0.21     0.15    2.65      1.0
GOS-ULARDXI. F
4   120000.0           1.0
543.5         441.0                     1.0           0.56671     0.30560
-200.3        145.4        -85.5        58.0          -39.8       7.4
-112.4        185.0        -79.9        65.6          -72.5       27.8
-123.3        141.6        -66.4        75.7          -47.2       8.6
-85.6         105.7        -46.2        31.7          -43.2       4.3
```

```
OOOOOOOOOOOOOOOOOOOOOOOOOOOOSS

 FLUVIATILE PROCESS SIMULATION  EXPERIMENT 5                      81241913
 200  20  20  20
 200  60   0   1000.0    60.0      0.0     30.0     0.1            (1X,60A1)
          1.1       1000.0      0.0001      2000.0
   0.0000009      0.0001         0.5         30.0
        50.0         50.0         5.0          5.0        100.0         3.0
   100.0      20.0       1.0      0.8     0.21     0.15     2.65      1.0
GOS-ULARDXI. F
4    120000.0          1.0
543.5         441.0                       1.0            0.56671     0.30560
-200.3        145.4          -85.5        58.0           -39.8       7.4
-112.4        185.0          -79.9        65.6           -72.5       27.8
-123.3        141.6          -66.4        75.7           -47.2       8.6
-85.6         105.7          -46.2        31.7           -43.2       4.3

OOOOOOOOOOOOOOOOOOOOOOOOCCCOOSS

 FLUVIATILE PROCESS SIMULATION  EXPERIMENT 5                      81241913
 200  20  20  20
 200  60   0   1000.0    60.0      0.0     30.0   0.001            (1X,60A1)
          1.1       1000.0      0.0001      2000.0
    0.000003      0.0003         0.5         30.0
        50.0         50.0         5.0          5.0        100.0         3.0
   100.0      20.0       1.0      0.8     0.21     0.15     2.65      1.0
GOS-ULARDXI. F
4    120000.0          1.0
543.5         441.0                       1.0            0.56671     0.30560
-200.3        145.4          -85.5        58.0           -39.8       7.4
-112.4        185.0          -79.9        65.6           -72.5       27.8
-123.3        141.6          -66.4        75.7           -47.2       8.6
-85.6         105.7          -46.2        31.7           -43.2       4.3

OOOOOOOOOOOOOOOOOOOOOCOCOCCOOSS

 FLUVIATILE PROCESS SIMULATION  EXPERIMENT 5                      81241913
 200  20  20  20
 200  60   0   1000.0    60.0      0.0     30.0     0.01           (1X,60A1)
          1.1       1000.0      0.0001      2000.0
    0.000003      0.0003         0.5         30.0

        50.0         50.0         5.0          5.0        100.0         3.0
   100.0      20.0       1.0      0.8     0.21     0.15     2.65      1.0
GOS-ULARDXI. F
4    120000.0          1.0
543.5         441.0                       1.0            0.56671     0.30560
-200.3        145.4          -85.5        58.0           -39.8       7.4
-112.4        185.0          -79.9        65.6           -72.5       27.8
-123.3        141.6          -66.4        75.7           -47.2       8.6
-85.6         105.7          -46.2        31.7           -43.2       4.3

OOOOOOOOOOOOOOOOOOOOOOOOCCOOSS

 FLUVIATILE PROCESS SIMULATION  EXPERIMENT 5                      81241913
 200  20  20  20
 200  60   0   1000.0    60.0      0.0     30.0     0.1            (1X,60A1)
          1.1       1000.0      0.0001      2000.0
    0.000003      0.0003         0.5         30.0
        50.0         50.0         5.0          5.0        100.0         3.0
   100.0      20.0       1.0      0.8     0.21     0.15     2.65      1.0
GOS-ULARDXI. F
4    120000.0          1.0
543.5         441.0                       1.0            0.56671     0.30560
-200.3        145.4          -85.5        58.0           -39.8       7.4
-112.4        185.0          -79.9        65.6           -72.5       27.8
-123.3        141.6          -66.4        75.7           -47.2       8.6
-85.6         105.7          -46.2        31.7           -43.2       4.3

OOOOOOOOOOOOOOOOOOOOOOOOOOOOSS
```